

HISTORICAL INFORMATION

TABLE 2.4-1

Security-Related Information
Text Withheld Under 10 CFR 2.390

HISTORICAL INFORMATION

HISTORICAL INFORMATION

TABLE 2.4-1

Security-Related Information
Text Withheld Under 10 CFR 2.390

HISTORICAL INFORMATION

HISTORICAL INFORMATION

TABLE 2.4-1

Security-Related Information
Text Withheld Under 10 CFR 2.390

HISTORICAL INFORMATION

HISTORICAL INFORMATION

TABLE 2.4-1

Security-Related Information
Text Withheld Under 10 CFR 2.390

HISTORICAL INFORMATION

HISTORICAL INFORMATION

TABLE 2.4-1

Security-Related Information
Text Withheld Under 10 CFR 2.390

HISTORICAL INFORMATION

HISTORICAL INFORMATION

TABLE 2.4-2

Security-Related Information
Text Withheld Under 10 CFR 2.390

HISTORICAL INFORMATION

HISTORICAL INFORMATION

TABLE 2.4-3

Security-Related Information
Text Withheld Under 10 CFR 2.390

HISTORICAL INFORMATION

SSES-FSAR
TABLE 2.4-4

HISTORIC FLOODS IN THE VICINITY OF THE SUSQUEHANNA STEAM ELECTRIC STATION

Flood Date	Danville ^(a)		Susquehanna SES		Wilkes-Barre ^(b)	
	Elevation ^(c) (ft-msl)	Discharge (cfs)	Elevation ^(d) (ft-msl)	Discharge (cfs)	Elevation ^(e) (ft-msl)	Discharge (cfs)
June 24, 1972	463.6	363000	516.6	349000	552.7	345000
March 9, 1904 ^(f)	462.0	-	-	-	-	-
Sept. 27, 1975	458.8	257000	510	252000	547.2	251000
March 20, 1936	458.6	250000	510	236000	545.2	232000

- (a) 31 Miles Downstream of Susquehanna SES
- (b) 22 Miles Upstream of Susquehanna SES
- (c) Danville Flood Stage 451.3 Feet, MSL
- (d) Susquehanna SES Flood Stage 670 Feet, MSL
- (e) Wilkes-Barre Flood Stage 534.1 Feet, MSL
- (f) High Stage Due to Ice Jam Flooding

SSES-FSAR

TABLE 2.4-5

ALL-SEASON 24-HOUR PROBABLE MAXIMUM PRECIPITATION

Time (Hour)	Precipitation Increment (Inches)
0 - 9	2.52
9.5	1.24
10.0	1.24
10.5	1.49
11.0	1.74
11.5	1.74
12.0	2.73
12.5	6.70
13.0	1.98
13.5	1.74
14.0	1.49
14.5	1.49
15.0	1.24
15 - 24	2.38
Total	29.72

SSPS-FSAR

TABLE 2.4-6

PROBABLE MAXIMUM PRECIPITATION FOR DURATIONS LESS THAN
30 MINUTES

Duration (Minutes)	Accumulated PMP (Inches)
5	2.48
10	3.82
15	4.82
30	6.70

SSES-FSAR

TABLE 2.4-7

Security-Related Information
Text Withheld Under 10 CFR 2.390

SSES-FSAR

TABLE 2.4-8

ADOPTED 4-HOUR UNIT HYDROGRAPHS AND CHARACTERISTICS

<u>STATION NO.</u>	<u>DRAINAGE AREA (sq. mi.)</u>	<u>R*</u>	<u>Tc*</u>	<u>Cp*</u>	<u>tp**</u>
101	351	48.31	27.99	.423	27.30
102	164	14.79	11.83	.471	11.49
103	118	11.46	16.02	.630	13.42
104	43	2.70	2.00	.423	3.46
105	108	16.14	12.81	.500	13.07
106	102	9.60	8.60	.579	8.00
107	98	5.71	5.62	.499	5.59
108	196	18.46	19.85	.579	18.60
109	94	4.67	7.04	.578	6.22
110	79	5.96	4.04	.426	4.53
111	121	12.00	7.00	.430	9.00
112	28	10.03	2.00	.402	5.30
113	116	7.36	6.03	.479	6.34
114	622	28.30	22.39	.483	20.34
1261	40	7.38	5.95	.477	6.29
115	264	16.04	7.06	.334	7.81
116	58	11.04	2.03	.374	5.76
117	84	11.78	2.03	.364	5.87
118	192	14.78	7.23	.352	7.79
119	36.4	11.31	4.52	.376	6.03
120	27.8	9.91	2.00	.389	5.57
121	231.8	16.69	7.70	.354	8.37
122	255	15.09	16.06	.579	14.48
123	184	24.67	12.17	.357	12.00
124	95	13.60	7.66	.382	7.92
125	64	9.30	3.94	.396	5.44
126	118	7.46	5.99	.470	6.33
127	70	5.32	4.86	.486	4.75
128	113	13.00	7.50	.485	7.11
129	186	11.82	10.10	.405	4.70
130	151	12.10	10.50	.405	8.00
131	370	20.05	14.81	.477	14.19
132	30	4.52	6.15	.539	5.52
133	56	4.48	6.18	.541	5.53
134	96	4.79	6.19	.539	5.68
135	160	6.35	7.22	5.260	6.74
136	114	4.94	5.04	.554	5.43
137	72	3.66	5.82	.510	4.73
138	402	5.59	10.51	.601	8.03
139	298	8.47	6.91	.457	6.95
140	70	6.74	5.08	.460	5.49

SSES-FSAR

TABLE 2.4-8 (Continued)

<u>STATION NO.</u>	<u>DRAINAGE AREA (sq. mi.)</u>	<u>R*</u>	<u>Tc*</u>	<u>Cp*</u>	<u>tp**</u>
141	72	8.85	5.97	.441	6.55
142	66	19.00	5.50	.276	7.05
143	254	35.00	9.06	.258	10.89
144	75	19.20	4.34	.270	6.55
145	77	20.90	2.00	.260	6.52
146	44	9.64	4.93	.410	6.05
147	127	12.61	4.83	.359	6.35
148	80	18.39	9.71	.405	10.42
149	67	10.92	6.40	.396	6.99
150	143	13.00	7.00	.531	6.50
151	227	10.60	7.16	.403	7.26
152	193	16.00	8.40	.738	9.00
153	144	9.60	10.00	.480	9.60
154	150	6.18	5.33	.479	5.51
155	215	8.11	7.68	.469	7.19
156	101	6.48	5.27	.472	5.56
157	223	15.96	13.50	.475	12.06
158	159	14.47	13.87	.505	12.11
159	114	14.00	7.00	.556	6.50
160	114	12.00	8.00	.738	7.70
161	383	2.50	28.00	.860	13.70
163	37	5.44	5.63	.502	5.49
165	41	5.11	5.30	.481	5.02
168	97	6.89	6.43	.498	6.47
171	157	6.94	7.43	.507	6.94
172	116	12.80	8.10	.738	7.90
173	206	11.04	9.93	.505	9.28

* Clark coefficients

** Snyder coefficients

Security-Related Information
Text Withheld Under 10 CFR 2.390

SSES-FSAR

TABLE 2.4-10
MANNING "N" VALUES
COMPUTED FROM 1936 FLOOD

<u>Section</u>	<u>Elevation</u>	<u>River Mile</u>	<u>Reach Length</u>	<u>Channel</u>	<u>"n"</u> <u>Overbank</u>	
1	493.2	157.2	10,050	0.041	0.100	Berwick Bridge
2	497.1	159.0	6,900	0.035	0.100	
3	500.0	160.31	4,400	0.037	0.100	
4	502.0	161.15	8,970	0.032	0.100	
5	506.0	162.85	3,960	0.027	0.100	
6	507.6	163.6	5,808	0.046	0.100	
7	511.0	164.7	7,650	0.052	0.100	
8	514.3	166.15				
Site		165.64				

SSES-FSAR

TABLE 2.4-11

SUSQUEHANNA RIVER FREEZE OVER AT HARRISBURG
(1870-1955)

<u>Number Days Frozen</u>	<u>Number of Freeze Overs</u>
1-14	36
15-30	33
31-60	20
61-90	8
91+	1

<u>Month</u>	<u>Number of Years River Frozen</u>
Nov.	2
Dec.	36
Jan.	54
Feb.	49
Mar.	22
Apr.	1

SSES-FSAR

TABLE 2.4-12

ICE JAM FLOODING

Danville (Flood Stage = 20 ft.)

<u>DATE</u>	<u>STAGE</u>	<u>ELEVATION</u>
Jan. 25, 1904	26.2	457.5
Feb. 10, 1904	24.6	455.9
Mar. 9, 1904	30.7	462.0

Wilkes Barre (Flood Stage = 22 ft.)

Mar. 11, 1893	28.7	540.8
Mar. 3, 1895	27.0	539.1
Jan. 16, 1898	21.8	533.9
Jan. 7, 1899	25.0	537.1
Feb. 9, 1900	17.8	529.9
Mar. 12, 1901	21.5	533.6
Jan. 23, 1902	18.2	530.3

TABLE 2.4-13

SUMMARY OF FLOOD ROUTING STUDIES - SPRAY POND

Case	Condition	Maximum Water Elevation (ft)	Outflow Through Conduit @ ESSW (cfs)	Outflow Over Emergency Spillway* (cfs)	Total Outflow from the Pond* (cfs)
1	Normal operation (10,000 gpm blowdown into pond)	679.0	13.8	0	13.8
2	10,000 gpm blowdown into pond + 50% PMF + PMF 72 hr later	682.3	41	150	191
3	10,000 gpm blowdown into pond + PMF + 50% PMF 72 hr later	682.3	41	150	191
4	10,000 gpm blowdown into pond + 1/2 PMF + 1/2 PMF 72 hr later and failure of discharge conduit at ESSW	681.8	0	105	105
5	10,000 gpm blowdown into pond + 25-yr flood and failure of discharge conduit at ESSWP	681.4	0	65	65
6	10,000 gpm blowdown into pond + 10-yr flood	679.6	33	0	33
* Spillway discharge and total discharge shown to nearest 5 cfs, except for those under normal operating conditions.					

TABLE 2.4-14			
RESULTS OF WIND WAVE COMPUTATION			
Wind speed (mph)	40	65	80
Static water level (ft, msl)	682.3	681.8	679.6
Wave height (ft)			
Significant	0.7	1.3	1.7
1%	1.2	2.2	2.9
Runup elevation from 1% wave (ft, msl)			
at ESSW pumphouse	684.3	684.8	683.3
at side of spray pond	683.8	684.6	683.4

TABLE 2.4-15

MAXIMUM LOADINGS RESULTING FROM WIND-WAVE ACTIVITIES

Structure	Wind Speed (mph)	Static Water Level (El. ft)	1% Wave Height (ft)	Maximum Resultant Forces (kips)	Maximum Moment at Base of Structure (ft-kips)
Pipe Supports	40	682.3	1.2	0.2	2.4
	65	681.8	2.2	0.3	3.0
	80	679.6	2.9	0.5	4.2
ESSW Pumphouse	40	682.3	1.2	33	218
	65	681.8	2.2	62	679
	80	679.6	2.9	76	642

TABLE 2.4-16

MAXIMUM HYDRODYNAMIC LOADING RESULTING FROM EARTHQUAKE

Structure	Earthquake Type	Direction	Maximum Resultant Forces (kips)	Maximum Moment at Base of the Structure (ft-kips)
Pipe Support	SSE	E-W & N-S	0.6	5.0
	OBE	E-W & N-S	0.3	2.4
ESSW Pumphouse	SSE	N-S	263.3	2250
		E-W	140.6	1910
	OBE	N-S	145.7	1271
		E-W	77.5	1062

SSES-FSAR

TABLE 2.4-17

THIS TABLE HAS BEEN INTENTIONALLY LEFT BLANK

Security-Related Information
Text Withheld Under 10 CFR 2.390

Security-Related Information
Text Withheld Under 10 CFR 2.390

TABLE 2.4-19

THIS TABLE HAS BEEN INTENTIONALLY LEFT BLANK

Table 2.4-20

This Table Has Been Deleted

SSES-FSAR

HISTORICAL INFORMATION

TABLE 2.4-21

REGIONAL HYDROGEOLOGIC SECTION (within 20-mile radius of Susquehanna SES)

Era	Period	Epoch	Group or Formation	Lithologic Character	Estimated Range of Thickness in Region (ft)	Groundwater Yield Characteristics
Cenozoic	Quaternary	Pleistocene	Stratified glacial drift	Primarily outwash sediments or kame terraces consisting of sand and gravel deposits, with occasional layers of clay.	0 to 300	Yield per well ranges from 6 to 1300 gallons per minute (gpm), with a median yield of 100 gpm. Where sufficient saturated thickness occurs, properly constructed wells should yield more than 250 gpm.
Paleozoic	Pennsylvanian		Llewellyn Formation	Sandstone, conglomerate, shale, fire clay, slate and numerous anthracite coal beds.	700 to 2200	Yield per well ranges from 2 to 80 gpm, with a median yield of 10 gpm. Highly acidic water is common because of proximity to coal mining operations.
			Pottsville Formation	Generally a hard quartzose unit consisting of gray conglomerate and white, gray or brownish sandstone.	150 to 850	Yield per well ranges from 5 to 160 gpm, with a median yield exceeding 50 gpm.
	Mississippian	Middle Mississippian	Mauch Chunk Formation	Red, green, yellow or brown shale, with some sandstones.	200 to 2000	Yield per well ranges from 4 to 375 gpm, with a median yield of 22 gpm, based on 101 wells for which data were available.
		Lower Mississippian	Pocono Formation	Hard massive gray sandstone and conglomerate, including some shale layers.	600 to more than 1000	Yield per well ranges from 3 to 133 gpm, but the median yield for 8 wells for which data were available is only 6 gpm.

HISTORICAL INFORMATION

SSSES-FSAR

HISTORICAL INFORMATION

TABLE 2.4-21

REGIONAL HYDROGEOLOGIC SECTION
(within 20-mile radius of Susquehanna SES)

Era	Period	Epoch	Group or Formation	Lithologic Character	Estimated Range of Thickness in Region (ft)	Groundwater Yield Characteristics
Paleozoic	Devonian	Upper Devonian	Catskill Formation	Red to brownish shales, red and gray crossbedded sandstone, and gray to green sandstone tongues.	1000 to 3000	Yield per well ranges from 2 to 325 gpm, and the median yield is 12 gpm.
			Marine beds consisting essentially of Trimmers Rock Formation	Hard gray to greenish-gray massive to flaggy sandstone, containing little shale.	1500 to 3000	Yield per well ranges from 1 to 15 gpm, with a median yield of 5 gpm.
		Middle Devonian	Mahantango Formation	Bluish-gray to brownish sandy shale with interbedded sandstones, and locally thin limestone.	~1100	Yield per well ranges from 2 to 21 gpm in nine wells for which data were available.
			Marcellus Formation	Black, gray or dark blue fissile shale.	~400	
	Silurian	Middle to Lower Devonian	Onondaga Formation	Non-cherty limestone overlying a gray calcareous shale.	~150	No well yield data are available. Not believed to be high yielding in the region.
		Silurian	Keyser Formation	Alternating beds of sandy limestone and calcareous sandstone, some conglomeritic sandstone and a bed of soft shaly limestone.	?	Yield per well ranges from 16 to 250 gpm, with three out of the four wells for which data were available yielding 125 gpm, or more.
			Tonoloway Formation	Play, laminated and argillaceous limestones, with thick beds occurring locally at the top.	100 to 150	
Paleozoic	Silurian	Middle Silurian	Wills Creek Formation	Alternating limestone, limy shales and fissile shales.	~300	
			Bloomsburg Formation	Dark-red sandy shale, with a few thin layers of bright-green shale, and a few beds of red sandstone.	~800	Yield per well ranges from 5 to 20 gpm. One well is reported to give a "large", although unmeasured supply.
			Clinton Formation	Units of the Clinton Formation in the region consist to a large extent of hard ferriferous red sandstone and yellowish green and olive-green shale.	600 to 700	No wells tapping units of the Clinton Formation are recorded, as they form a high ridge in the outcrop area.

HISTORICAL INFORMATION

HISTORICAL INFORMATION

TABLE 2.4-22

Security-Related Information
Text Withheld Under 10 CFR 2.390

HISTORICAL INFORMATION

HISTORICAL INFORMATION

TABLE 2.4-22

Security-Related Information
Text Withheld Under 10 CFR 2.390

HISTORICAL INFORMATION

HISTORICAL INFORMATION

TABLE 2.4-22

Security-Related Information
Text Withheld Under 10 CFR 2.390

HISTORICAL INFORMATION

HISTORICAL INFORMATION

TABLE 2.4-22

Security-Related Information
Text Withheld Under 10 CFR 2.390

HISTORICAL INFORMATION

HISTORICAL INFORMATION

TABLE 2.4-22

Security-Related Information
Text Withheld Under 10 CFR 2.390

HISTORICAL INFORMATION

HISTORICAL INFORMATION

TABLE 2.4-22

Security-Related Information
Text Withheld Under 10 CFR 2.390

HISTORICAL INFORMATION

HISTORICAL INFORMATION

TABLE 2.4-22

Security-Related Information
Text Withheld Under 10 CFR 2.390

HISTORICAL INFORMATION

HISTORICAL INFORMATION

TABLE 2.4-22

Security-Related Information
Text Withheld Under 10 CFR 2.390

HISTORICAL INFORMATION

HISTORICAL INFORMATION

TABLE 2.4-22

Security-Related Information
Text Withheld Under 10 CFR 2.390

HISTORICAL INFORMATION

HISTORICAL INFORMATION

TABLE 2.4-22

Security-Related Information
Text Withheld Under 10 CFR 2.390

HISTORICAL INFORMATION

HISTORICAL INFORMATION

TABLE 2.4-22

Security-Related Information
Text Withheld Under 10 CFR 2.390

HISTORICAL INFORMATION

HISTORICAL INFORMATION

TABLE 2.4-22

Security-Related Information
Text Withheld Under 10 CFR 2.390

HISTORICAL INFORMATION

HISTORICAL INFORMATION

TABLE 2.4-22

Security-Related Information
Text Withheld Under 10 CFR 2.390

HISTORICAL INFORMATION

HISTORICAL INFORMATION

TABLE 2.4-22

Security-Related Information
Text Withheld Under 10 CFR 2.390

HISTORICAL INFORMATION

HISTORICAL INFORMATION

TABLE 2.4-22

Security-Related Information
Text Withheld Under 10 CFR 2.390

HISTORICAL INFORMATION

HISTORICAL INFORMATION

TABLE 2.4-22

Security-Related Information
Text Withheld Under 10 CFR 2.390

HISTORICAL INFORMATION

HISTORICAL INFORMATION

TABLE 2.4-22

Security-Related Information
Text Withheld Under 10 CFR 2.390

HISTORICAL INFORMATION

HISTORICAL INFORMATION

TABLE 2.4-22

Security-Related Information
Text Withheld Under 10 CFR 2.390

HISTORICAL INFORMATION

HISTORICAL INFORMATION

TABLE 2.4-22

Security-Related Information
Text Withheld Under 10 CFR 2.390

HISTORICAL INFORMATION

HISTORICAL INFORMATION

TABLE 2.4-23

Security-Related Information
Text Withheld Under 10 CFR 2.390

HISTORICAL INFORMATION

HISTORICAL INFORMATION

TABLE 2.4-23

Security-Related Information
Text Withheld Under 10 CFR 2.390

HISTORICAL INFORMATION

HISTORICAL INFORMATION

TABLE 2.4-23

Security-Related Information
Text Withheld Under 10 CFR 2.390

HISTORICAL INFORMATION

HISTORICAL INFORMATION

TABLE 2.4-23

Security-Related Information
Text Withheld Under 10 CFR 2.390

HISTORICAL INFORMATION

HISTORICAL INFORMATION

TABLE 2.4-24

Security-Related Information
Text Withheld Under 10 CFR 2.390

HISTORICAL INFORMATION

HISTORICAL INFORMATION

TABLE 2.4-24

Security-Related Information
Text Withheld Under 10 CFR 2.390

HISTORICAL INFORMATION

HISTORICAL INFORMATION

TABLE 2.4-24

Security-Related Information
Text Withheld Under 10 CFR 2.390

HISTORICAL INFORMATION

HISTORICAL INFORMATION

TABLE 2.4-24

Security-Related Information
Text Withheld Under 10 CFR 2.390

HISTORICAL INFORMATION

HISTORICAL INFORMATION

TABLE 2.4-24

Security-Related Information
Text Withheld Under 10 CFR 2.390

HISTORICAL INFORMATION

HISTORICAL INFORMATION

TABLE 2.4-24

Security-Related Information
Text Withheld Under 10 CFR 2.390

HISTORICAL INFORMATION

HISTORICAL INFORMATION

TABLE 2.4-24

Security-Related Information
Text Withheld Under 10 CFR 2.390

HISTORICAL INFORMATION

HISTORICAL INFORMATION

TABLE 2.4-25

Security-Related Information
Text Withheld Under 10 CFR 2.390

HISTORICAL INFORMATION

HISTORICAL INFORMATION

TABLE 2.4-25

Security-Related Information
Text Withheld Under 10 CFR 2.390

HISTORICAL INFORMATION

HISTORICAL INFORMATION

TABLE 2.4-25

Security-Related Information
Text Withheld Under 10 CFR 2.390

HISTORICAL INFORMATION

HISTORICAL INFORMATION

TABLE 2.4-25

Security-Related Information
Text Withheld Under 10 CFR 2.390

HISTORICAL INFORMATION

HISTORICAL INFORMATION

TABLE 2.4-25

Security-Related Information
Text Withheld Under 10 CFR 2.390

HISTORICAL INFORMATION

HISTORICAL INFORMATION

TABLE 2.4-25

Security-Related Information
Text Withheld Under 10 CFR 2.390

HISTORICAL INFORMATION

HISTORICAL INFORMATION

TABLE 2.4-25

Security-Related Information
Text Withheld Under 10 CFR 2.390

HISTORICAL INFORMATION

HISTORICAL INFORMATION

TABLE 2.4-25

Security-Related Information
Text Withheld Under 10 CFR 2.390

HISTORICAL INFORMATION

HISTORICAL INFORMATION

TABLE 2.4-25

Security-Related Information
Text Withheld Under 10 CFR 2.390

HISTORICAL INFORMATION

HISTORICAL INFORMATION

TABLE 2.4-25

Security-Related Information
Text Withheld Under 10 CFR 2.390

HISTORICAL INFORMATION

HISTORICAL INFORMATION

TABLE 2.4-25

Security-Related Information
Text Withheld Under 10 CFR 2.390

HISTORICAL INFORMATION

HISTORICAL INFORMATION

TABLE 2.4-25

Security-Related Information
Text Withheld Under 10 CFR 2.390

HISTORICAL INFORMATION

HISTORICAL INFORMATION

TABLE 2.4-25

Security-Related Information
Text Withheld Under 10 CFR 2.390

HISTORICAL INFORMATION

HISTORICAL INFORMATION

TABLE 2.4-25

Security-Related Information
Text Withheld Under 10 CFR 2.390

HISTORICAL INFORMATION

HISTORICAL INFORMATION

TABLE 2.4-25

Security-Related Information
Text Withheld Under 10 CFR 2.390

HISTORICAL INFORMATION

HISTORICAL INFORMATION

TABLE 2.4-25

Security-Related Information
Text Withheld Under 10 CFR 2.390

HISTORICAL INFORMATION

HISTORICAL INFORMATION

TABLE 2.4-25

Security-Related Information
Text Withheld Under 10 CFR 2.390

HISTORICAL INFORMATION

HISTORICAL INFORMATION

TABLE 2.4-25

Security-Related Information
Text Withheld Under 10 CFR 2.390

HISTORICAL INFORMATION

HISTORICAL INFORMATION

TABLE 2.4-25

Security-Related Information
Text Withheld Under 10 CFR 2.390

HISTORICAL INFORMATION

HISTORICAL INFORMATION

TABLE 2.4-25

Security-Related Information
Text Withheld Under 10 CFR 2.390

HISTORICAL INFORMATION

HISTORICAL INFORMATION

TABLE 2.4-25

Security-Related Information
Text Withheld Under 10 CFR 2.390

HISTORICAL INFORMATION

HISTORICAL INFORMATION

TABLE 2.4-26

ESTIMATED GROUNDWATER WITHDRAWAL IN 1976
WITHIN TWO MILES OF THE STATION

Geological Unit	Rate, in gpd		
	From Wells	From Springs	Total
Mahantango Formation	27,800	1,060	28,860
Trimmers Rock Formation	10,790	11,310	22,100
Catskill Formation	0	300	300
Pleistocene Sand & Gravel	2,070	1,550	3,620
Recent Alluvium	210	0	210
Residual Soil	300	0	300
TOTALS	41,170	14,220	55,390

Note: gpd - gallons per day

Metric Conversion Factor: 1 gallon = 3.785 liters

HISTORICAL INFORMATION

HISTORICAL INFORMATION

TABLE 2.4-27

**PROJECTIONS OF FUTURE GROUNDWATER WITHDRAWAL
WITHIN 2 AND 20 MILES OF THE STATION**

Area	Year				
	1980	1990	2000	2010	2020
For area within 2-mile radius of station, in mgd	0.060	0.063	0.064	0.066	0.066
For area within 20-mile radius of station, in mgd	11.7	12.1	12.1	11.5	10.9

Notes:

Groundwater Withdrawal Projections were based on population projections, as found in Tables 2.1-7 through 2.1-16.

mgd - million gallons per day

Metric Conversion Factor: 1 gallon = 3.785 liters

HISTORICAL INFORMATION

HISTORICAL INFORMATION

TABLE 2.4-28

**MAJOR GROUNDWATER WITHDRAWAL, AND POPULATION SERVED
BY WATER SUPPLY COMPANIES WITHIN 20-MILE AREA**

GROUNDWATER USER OR WATER SUPPLY COMPANY	APPROXIMATE POPULATION SERVED WITHIN 20-MILE RADIUS IN 1970*	ESTIMATED AVERAGE GROUNDWATER WITHDRAWAL IN 1975* (GPD)
Keystone Water Company (Berwick Water Company)	16,982	2,900,000 +
Bloomsburg Water Co.	14,768	0
Benton Water Co.	1,022	60,300
Catawissa Municipal Authority	1,701	175,000
Orangeville Municipal Water Company	431	19,400
Pennsylvania Gas and Water Company	159,705	0
Dallas Water Company	4,292	390,000
Freeland Municipal Water Authority	6,102	316,400
Hazleton City Authority:		
1) Derringer Division	209	27,668 +
2) Lattimer Division	378	62,767 +
3) Ebervale Division	610	116,644 +
4) Tomhicken Division	101	6,748 +
5) Delano Division	518	0 +
6) Buck Mountain Division	969	0 +
7) Hazleton Division	42,501	423,296 +
Williams and Son Water Co.	75	0
Conyngham Water Company	1,556	120,600
Citizens Water Company	200	8,200 +
Mocanaqua Water Company	1,151	0
Indian Springs Water Company	150	9,500
Beaver Brook Water Co.	232	10,000
Garbush Water Company	16	700
John Fielding	137	12,000
Shavertown Water Co.	1,212	268,300
Midway Manor Water Co.	263	30,000
Trucksville Water Co.	553	0
Shaverstown-Kingston Township Water Co.	158	22,000
Hillcrest Water Co.	53	9,600
Meadowcrest Water Co.	369	72,000
William A. Still, Estate Water Company	106	12,000
Oakhill Water Supply Co.	444	50,000

HISTORICAL INFORMATION

HISTORICAL INFORMATION

TABLE 2.4-28

**MAJOR GROUNDWATER WITHDRAWAL, AND POPULATION SERVED
BY WATER SUPPLY COMPANIES WITHIN 20-MILE AREA**

GROUNDWATER USER OR WATER SUPPLY COMPANY	APPROXIMATE POPULATION SERVED WITHIN 20-MILE RADIUS IN 1970*	ESTIMATED AVERAGE GROUNDWATER WITHDRAWAL IN 1975*(GPD)
Village Water Company	44	2,800
Shickshinny Water Co.	1,832	0
Warden Place Water Co.	~30	2,000
Whitebread Water Co.	37	11,200
Harvey's Lake Water Co.	60	5,500
Honey Brook Water Co.	6,133	720,000
Oneida Water Co.	319	23,000
Nuremburg Water Co.	486	33,300
Ringtown Boro Water Co.	909	38,400
Shenandoah Boro Municipal Authority	10,311	0
Keystone Water Company, Frackville Div.	357	0
Mahanoy Township Authority	7,538	4,000
Weatherly Municipal Authority	1,916	146,700
Beaver Meadows Municipal Authority	1,057	0
Wilbar Realty Company: 1) Forest Park Division 2) Penn Lake Division	146 36	10,000 2,000
White Haven Municipal Authority	1,323	~0
Native Textiles, Dallas, Pa.	0	3,150
White Haven State School	--	22,460
Pennsylvania Institution For Def. Delinquents	--	167,650
TOTALS	289,498	6,315,283
<p>* Information taken from Reference 2.4-70</p> <p>+ Information obtained from the local water department and from Reference 2.4-70</p> <p>Note: gpd - gallons per day</p> <p>Metric Conversion Factor: 1 gallon = 3.785 liters</p>		

HISTORICAL INFORMATION

HISTORICAL INFORMATION

TABLE 2.4-29

ESTIMATION OF TOTAL GROUNDWATER WITHDRAWAL IN 1975
WITHIN 20-MILE RADIUS OF THE STATION

1.	Total Estimated 1970 population within 20-mile radius *	352,852
2.	Estimated Population within 20-mile radius served by water companies or municipal water departments in 1970 +	<u>289,498</u>
3.	Estimated population using private wells or springs to supply water needs in 1970	63,354
4.	Estimated population using private wells or springs in 1975: Approximate ratio of 1975 to 1970 population in area = 1.022** Therefore, $63,354 \times 1.022 =$	64,748
5.	Estimated withdrawal from private wells and springs in 1975 (for domestic and livestock use): $64,748 \times 80 \text{ gpd/person} =$	5,179,840 gpd
6.	Estimated total withdrawal from public supply and industrial wells and from major springs within 20-mile radius, in 1975 +	<u>6,315,283 gpd</u>
7.	Total Estimated Groundwater Withdrawal in region in 1975	<u>11,495,123 gpd</u>
<p>* Based on Reference 2.4-72 (U.S. Bureau of the Census, <u>1970 Census of Population, Number of Inhabitants Pennsylvania</u> PC(1)-A40, U.S. Govt. Printing Office, Washington, D.C.)</p> <p>** Based on Tables 2.1-3 and 2.1-5</p> <p>+ Source is unpublished records and computer printouts from the Division of Comprehensive Resources and Planning of the Pennsylvania Department of Environmental Resources (Reference 2.4-70).</p> <p>Note: gpd = gallons per day</p> <p>Metric Conversion Factor: 1 gallon = 3.785 liters</p>		

HISTORICAL INFORMATION

HISTORICAL INFORMATION

TABLE 2.4-30

DETAILS OF THE CONSTRUCTION OF OBSERVATION WELLS AT THE SUSQUEHANNA SES

Observation well no.	Casing, internal diam. & type of material	Approx. depth interval of any screen or slotted casing (ft)	Original depth of boring (ft)	Present plumbable depth (ft)	Depth to top of bedrock (ft)	Static water level in late April '77 (ft below ground)	Probable geologic zone(s) in hydraulic connection with well
2	1.8", PVC	*	160.	54.4	60.	15.9	Lower Overburden (silty sand and gravel)
8	1.6", PVC	+	264.	>200.	75.	9.4	Lowermost overburden and bedrock
11	1.5", PVC	*	80.	46.5	60.	9.0	Lower overburden (coarse sand and silty gravel layers)
19	1.6", PVC	*	80.	42.6	53.	9.2	Lower overburden (coarse sand and gravel)
109	1.7", PVC	-70 - 90	176.	116.3	81.	16.2	Lower overburden and upper bedrock
124	1.6", PVC	-18 - 38	168.	46.	40.	19.5	Lower overburden and bedrock (sandy gravel)
1111	1.8", PVC	-75 - 95	109.	104.	99.	70.5	Lower overburden (sandy gravel with boulders)
1113	1.8", PVC	-60 - 80	97.	85.8	83.	60.6	Lower overburden (gravel, boulders and sand)
1114	1.9", PVC	-40 - 60	74.	64.2	63.	57.6	Lower overburden (boulders, gravel and sand)
B-1	8", steel	84.5 - 89.5	96.	87.5	>96.	5.4	Lower overburden (sand with fine gravel)
CPW	12", steel	42 - 57	82.	54.5	80.	4.5	Lower overburden (gravel and sand)
1200A	3", PVC	20 - 32	32.	32.	30.	31.2 ¹	Lower overburden and upper two feet of bedrock
1201	4", steel	+	69.	69.	34.	19.5 ¹	Upper 35 feet of bedrock
1204	4", PVC	42 - 54	54.8	54.	52.5	13.5 ¹	Lower overburden and upper two feet of bedrock
1208	3", PVC	26 - 38	38.	38.	36.	26.6 ¹	Lower overburden and upper two feet of bedrock
1209A	4", steel	+	60.	60.	26.	15.9 ¹	Upper 34 feet of bedrock
1210	4", PVC	26 - 38	39.5	38.	35.5	31.2 ¹	Lower overburden and upper three feet of bedrock
<p>* Not known</p> <p>+ Only blank casing used</p> <p>¹ Measured in September 1977</p> <p>Metric Conversion Factor: 1 foot = 0.3048 meters</p>							

HISTORICAL INFORMATION

SSSES-FSAR

HISTORICAL INFORMATION

TABLE 2.4-31

GROUNDWATER LEVEL DATA TAKEN AT SUSQUEHANNA SES 1972 THROUGH 1975

Boring or Well	Depth (ft)	Probable zone(s) in hydraulic connection with boring or well	Date of measurement	Depth of water level below ground surface (ft)	Elevation of groundwater level (ft above m.s.l.)	Estimated height of groundwater level above top of bedrock (ft)
7	75	Overburden and upper bedrock	6-30-72	8.7	497.3	42
			8-18-72	19.0	487.0	32
			7-25-72	23.0	626.2	0
104	122	Bedrock	8-18-72	31.1	618.1	0
107	208	Overburden and bedrock	8-16-72	54.5	608.8	46
			8-18-72	54.3	609.0	46
111	110	Overburden and bedrock	6-30-72	10.6	672.8	23
			8-18-72	14.7	668.7	19
116	95	Overburden and bedrock	7-10-72	15.0	663.1	6
			8-18-72	15.8	662.3	5
202	57	Overburden and upper bedrock	7-10-72	24.8	640.2	6
			8-11-72	26.0	639.0	5
205	46	Overburden and upper bedrock	7-10-72	18.7	646.3	8
			8-16-72	20.5	644.5	7
206	116	Overburden and bedrock	7-18-72	19.5	645.5	7
			8-16-72	21.1	643.9	6
209	30	Overburden and upper bedrock	7-18-72	7.7	661.3	2
			8-18-72	9.4	659.6	1
			7-10-72	7.2	696.8	0
211	38	Bedrock	8-18-72	9.7	694.3	0
215	44	Overburden and upper bedrock	7-10-72	25.0*	644.0*	0*
			8-18-72	19.0	650.0	3
301	42	Overburden and upper bedrock	6-30-72	13.7	666.3	2
			7-18-72	15.2	664.8	1
			6-30-72	18.2	659.8	0
305	70	Bedrock	8-1-72	25.7	652.3	0
312	62	Overburden and upper bedrock	6-30-72	5.2	698.8	4
			8-18-72	9.9	694.1	0
317	50	Overburden and upper bedrock	6-30-72	19.3	696.7	5
			8-01-72	23.7	692.3	0
319	60	Overburden and upper bedrock	6-30-72	3.7	688.3	18
			8-18-72	15.0	677.0	7
410	73	Overburden and upper four feet of bedrock	7-18-72	57.0	626.1	12
			8-18-72	65.3	617.8	4
411	70	Overburden and upper three feet of bedrock	7-18-72	58.5	629.4	9
			8-01-72	60.4	627.5	7
413	67	Overburden and upper four feet of bedrock	7-18-72	48.4	640.5	15
			8-18-72	48.7	640.2	14
			7-21-72	25.5	672.8	33
415	59	Overburden	8-18-72	36.0	662.3	23
422	24	Overburden and upper four feet of bedrock	7-26-72	7.2	509.7	17

HISTORICAL INFORMATION

SSES-FSAR

HISTORICAL INFORMATION

TABLE 2.4-31

GROUNDWATER LEVEL DATA TAKEN AT SUSQUEHANNA SES 1972 THROUGH 1975

Boring or Well	Depth (ft)	Probable zone(s) in hydraulic connection with boring or well	Date of measurement	Depth of water level below ground surface (ft)	Elevation of groundwater level (ft above m.s.l.)	Estimated height of groundwater level above top of bedrock (ft)
444	15	Overburden and upper four feet of bedrock	8-08-72	4.2	719.7	7
605	25	Overburden and upper six feet of bedrock	8-08-72	6.0	689.1	13
606	10	Bedrock	8-08-72	4.2	691.2	0
1002	18	Overburden	4-08-74	3.3	505.7	>15
1006	24	Overburden	4-08-74	6.1	504.9	>18
1008	22	Overburden	4-08-74	10.8	501.2	>11
1010	15	Overburden	4-08-74	12.8	501.7	>2
1111	109	Overburden	7-31-74	74.7	610.7	22
			11-07-74	78.7	608.7	20
			1-17-75	77.7	609.7	21
			5-15-75	73.7	613.7	25
1113	97	Overburden	7-31-74	69.0	633.1	14
			11-08-74	73.0	629.1	10
			1-17-75	70.0	632.1	13
			5-15-75	70.0	632.1	13
1114	74	Overburden and upper 11 feet of bedrock	7-31-74	64.0	647.7	-1
			11-14-74	65.0	646.7	-2
			1-10-75	64.0	647.7	-1
			5-15-75	64.0	647.7	-1

* Reading in doubt

Metric Conversion Factor: 1 foot = 0.3048 meters

HISTORICAL INFORMATION

HISTORICAL INFORMATION

TABLE 2.4-32

GROUNDWATER LEVEL DATA TAKEN AT SUSQUEHANNA SES 1976 THROUGH 1977

Observation Well	Zone(s) Tapped By Well	Date of Measurement	Depth of Water Level Below Ground Surface (ft)	Elevation of Groundwater Level (ft above m.s.l.)	Height of Groundwater Level Above Top of Bedrock (ft)
2	Lower Overburden	11-09-76	17.1	495.3	43
		01-04-76	21.2	491.2	39
		04-14-77	16.2	496.2	44
		07-26-77	23.0	489.4	37
		08-16-77	22.9	489.5	37
		09-20-77	22.0	490.3	38
4	Lower Overburden and Bedrock	11-10-76	10.4	495.7	65
		01-05-76	13.5	492.6	62
		04-14-77	8.5	497.5	67
		07-26-77	14.9	491.1	60
		08-16-77	14.9	491.1	60
		09-20-77	13.5	492.6	62
11	Lower Overburden	04-14-77	7.8	500.6	52
		07-26-77	12.9	495.5	47
		08-16-77	12.9	495.5	47
		09-20-77	12.7	495.6	47
19	Lower Overburden	11-10-76	12.0	493.1	41
		01-05-76	15.1	490.0	38
		04-14-77	11.2	493.9	42
		07-26-77	16.7	488.4	36
		08-16-77	16.4	488.8	37
		09-20-77	13.1	492.1	40
109	Lower Overburden and Upper Bedrock	11-09-76	16.3	593.0	65
		01-04-77	21.8*	587.5	59*
		04-14-77	15.5	593.9	65
		07-26-77	26.3*	583.0	55*
		08-16-77	30.1*	583.0	51*
		09-20-77	37.6**	579.2	43**
				571.7	
124	Lower Overburden and Bedrock	11-08-76	19.7	523.7	20
		01-04-77	22.7	520.7	17
		04-14-77	17.5	625.9	23
		07-26-77	27.5	615.9	13
		08-16-77	28.4	615.0	12
		09-20-77	28.7	614.7	11
		1111	Lower Overburden	11-08-76	71.2
01-04-77	16.0			612.1	24
04-14-77	68.5			619.5	31
04-27-77	70.5			617.6	29
1113	Lower Overburden	11-09-76	60.2	634.1	15
		01-04-77	61.4	634.9	14
		04-14-77	59.8	634.5	15
		04-27-77	60.6	633.7	15
1114	Lower Overburden	11-09-76	57.2	644.7	-4
		01-04-77	58.1	643.8	-5
		04-14-77	57.3	644.6	-4
		04-27-77	57.6	644.3	-4

* Pump in well TW-2 (170 feet from observation well 109) was on during measurement.

** Pumps in wells TW-1 (31 feet from observation well 109) and TW-2 were on during measurement.

HISTORICAL INFORMATION

SSSES-FSAR

HISTORICAL INFORMATION

TABLE 2.4-33

SUMMARY OF PERMEABILITY TESTS OF OVERBURDEN AND UPPER BEDROCK AT THE SUSQUEHANNA SES
PERFORMED DURING PREVIOUS INVESTIGATIONS

Type of Test	Location of test or sample collection	Geologic material tested	Value(s) of hydraulic conductivity obtained (ft/day)		Reference
			Horizontal (Kh)	Vertical (Kv)	
Pumping Tests	Wells TW-1 & TW-2	Lower 40 feet of Kame terrace deposits	3.3 to 15.0	--	25
	Well C	Lower 43 feet of Kame terrace deposits	200.**	--	21
	Well CPW	37 feet of permeable materials within Kame terrace deposits	194.**	--	22
Falling-head Laboratory Permeability Test	Approximately 1500 ft. northeast of plant center	Upper silty soils	--	0.028	20
Open-End Tests in Borings+	Prospective retention pond areas	Kame terrace deposits	5.7 (Tests performed in 29 borings)	13. to 63. (Tests performed in 29 borings)	27
	Spray pond area (borings 1111, 1112, 1115, 1122, 1123, 1124, & 1125)	Kame terrace deposits	0.022 to greater than 11.8	--	29
	Spray pond area (borings 1113 & 1114)	Kame terrace deposits and underlying few feet of siltstone	1.0 to 3.8	--	29
	Spray pond area (boring 1117)	Mahantango siltstone in interval 12-22' below top of rock	2.5	--	29
Packer Tests in Borings+	Near railway bridge over Rt. 11 (borings 929-935, and 937-940)	Mahantango siltstone and black shale, upper 50 feet of rock	0.013 to 0.76 (Median of 41 tested intervals = 0.22)	--	29
	Reactor area and prospective retention pond areas	Mahantango siltstone upper 20 feet	0.85	--	27
		Mahantango siltstone below 20 feet	1.0×10^{-5}	--	27
<p>** Based on specific capacity data, assuming wells were 85 percent efficient.</p> <p>+ Performed in accordance with designations E-18 and E-19 of the U.S. Bureau of Reclamation's <u>Earth's Manual</u>.</p> <p>Metric Conversion Factor: 1 foot = 0.3048 meters.</p>					

HISTORICAL INFORMATION

SSS-FSAR

HISTORICAL INFORMATION

TABLE 2.4-34

SUMMARY OF PERMEABILITY TESTS OF OVERBURDEN AND UPPER BEDROCK AT THE SUSQUEHANNA SES PERFORMED FOR THIS INVESTIGATION

Type of Test	Location of Test or Soil Sample Collection	Geological Material Tested	Average Thickness of Saturated Zone Tested (ft)	Depth of Interval Below Top of Bedrock (ft)	Values of Hydraulic Conductivity Obtained (ft/day)	
					Horizontal (K _h)	Vertical (K _v)
Constant-head Laboratory Permeability Test	Boring 1200A at 27-foot depth	Kame terrace deposits	-	-	-	2.3
Slug Tests	Well 1208	Saturated Kame terrace deposits and upper 2 to 3 feet of bedrock	11.5	-	1.8	-
	Well 1210	Saturated Kame terrace deposits and upper 2 to 3 feet of bedrock	6.8	-	6.6	-
6-Hour Pumping Tests	Well 1210	Saturated Kame terrace deposits and upper 2 to 3 feet of bedrock	6.8	-	7.8	-
	Well 1204	Saturated Kame terrace deposits and upper 2 to 3 feet of bedrock	19.3*	-	21.7 to 29.2	-
Packer Tests	Boring 305+	Mahantango siltstone bedrock	-	7 to 12 12 to 17 17 to 52	0.41 0.048 0.0061	- - -
	Well 1201	Mahantango siltstone bedrock	-	6.7 to 15 15 to 25.3 25 to 35.3	0.063 0.0021 0	- - -
	Well 1209A	Mahantango siltstone bedrock	-	5.7 to 14 14 to 24 24 to 34	0.0012 0.028 0	- - -
* Average thickness for the confined aquifer between wells 1204 and 11. + Only the analysis was performed for this investigation. Metric Conversion Factor: 1 foot = 0.3048 meters						

HISTORICAL INFORMATION

TABLE 2.4-35

RADIONUCLIDE CONTENT OF THE TANK POSTULATED TO RUPTURE
 - REACTOR WATER CLEANUP (RWCU) PHASE SEPARATOR TANKS -
 SUSQUEHANNA SES

RADIONUCLIDE OF CONCERN FOR ACCIDENT ANALYSIS	HALF LIFE	HALF LIFE (DAYS)	TOTAL CURIES IN TANK (Ci)	CONCENTRATION ON BASIS OF 80% OF TOTAL TANK VOLUME OF 7400 GAL (μ Ci/ml)
Mn-54	312 d	312	38.6	1.72E+00
Fe-55	2.7 y	986.18	719.0	3.21E+01
Co-60	5.272 y	1,925.60	307.0	1.37E+01
Sr-90	29 y	10,592.25	5.68	2.53E-01
I-131	8.04 d	8.04	46.0	2.05E+00
Cs-137	30.17 y	11,019.59	16.2	7.23E-01
Pu-239	2.411E+4 y	8.8062E+06	0.0015	6.87E-05

NOTE: Liquid volume of 5,920 gallons x 3.785 liters/gal x 1000 ml/liter = 2.24072E+7 ml

SSSES-FSAR

Table 2.4-36

GROUNDWATER PARAMETER VALUES USED FOR SLUG3D SIMULATIONS
ACCIDENT ANALYSIS FOR SUSQUEHANNA SES

Flow Path Segment	Description	Geologic Unit In Which Flow Occurs	Travel Distance (ft)	Horizontal Hydraulic Conductivity (ft/day)	Hydraulic Gradient	Total Porosity	Effective Porosity	Dispersivities (ft)			Kd values (ml/g)				
								aL	aT	aV	Mn-54	Fe-55	Co-60	Sr-90	Cs-137
FLOWPATH 1															
1	RWCU Tank North To Buried Valley	Upper 15 ft of Bedrock	805	0.5	0.0600	0.02	0.02	10.0	0.5	0.001	0.0	0.0	0.0	0.0	0.0
2	Along Buried Valley To Well TW-2	Lower Pleistocene Deposits	725	18.0	0.0240	0.30	0.27	10.0	0.5	0.001	8.7	13.5	10.0	7.0	18.0
3	TW-2 To Stream Just East Of RR Tracks	Lower Pleistocene Deposits	860	8.0	0.0420	0.30	0.27	10.0	0.5	0.001	8.7	13.5	10.0	7.0	18.0
4	From Point In Stream To Lake Took-A-While	Lower Pleistocene Deposits	1420	20.0	0.0388	0.30	0.27	10.0	0.5	0.001	8.7	13.5	10.0	7.0	18.0
5	From Lake Took-A- While To River	Lower Pleistocene Deposits	1720	60.0	0.0081	0.30	0.27	30.0	2.0	0.050	8.7	13.5	10.0	7.0	18.0
FLOWPATH 2															
1	RWCU Tank East To North Stream Just East Of RR Tracks	Upper 15 ft of Bedrock	1865	0.5	0.0550	0.02	0.02	10.0	0.5	0.001	0.0	0.0	0.0	0.0	0.0
2	From Point In Stream To Lake Took-A-While	Lower Pleistocene Deposits	1420	20.0	0.0388	0.30	0.27	10.0	0.5	0.001	8.7	13.5	10.0	7.0	18.0
3	From Lake Took-A- While To River	Lower Pleistocene Deposits	1720	60.0	0.0081	0.30	0.27	30.0	2.0	0.050	8.7	13.5	10.0	7.0	18.0

Table 2.4-37

RANGE OF PARAMETER VALUES USED IN CALIBRATED NUMERICAL MODEL OF BURIED
VALLEY AQUIFER NORTHERN SIDE OF SUSQUEHANNA SES

PARAMETER	UNITS	VALUE
FLOW MODEL (MODFLOW)		
HEAD IN CONSTANT-HEAD CELLS		
Upgradient Boundary	ft (msl)	648.0 - 649.0
Downgradient Boundary	ft (msl)	562.0 - 564.0
HOR. HYDRAULIC CONDUCTIVITY		
	ft/day	4.0 - 50.0
RECHARGE		
	ft/day	0.0003 - 0.0085
SPECIFIC STORAGE		
	1/ft	1.15E-05
SPECIFIC YIELD		
	-	0.20
TOTAL POROSITY		
	-	0.30
EFFECTIVE POROSITY		
	-	0.27
TRANSPORT MODEL (MT3D)		
INITIAL CONCENTRATIONS		
At cell (17,8)		
Mn-54	μCi/ml	0.0765
Fe-55	μCi/ml	2.290
Co-60	μCi/ml	1.080
Sr-90	μCi/ml	0.0219
Cs-137	μCi/ml	0.0625
Pu-239	μCi/ml	6.01E-06
elsewhere	μCi/ml	0
CONSTANT CONCENTRATION CELL		
At cell (17,8) first 500 days		
Mn-54	μCi/ml	0.0765
Fe-55	μCi/ml	2.290
Co-60	μCi/ml	1.080
Sr-90	μCi/ml	0.0219
Cs-137	μCi/ml	0.0625
Pu-239	μCi/ml	6.01E-06
At cell (17,8) after 500 days	μCi/ml	0.0
AQUIFER BULK DENSITY		
	(lb/cu.ft.)	115.75
TRANSPORT MODEL (MT3D) - cont		

Table 2.4-37

RANGE OF PARAMETER VALUES USED IN CALIBRATED NUMERICAL MODEL OF BURIED
VALLEY AQUIFER NORTHERN SIDE OF SUSQUEHANNA SES

PARAMETER	UNITS	VALUE
DISPERSIVITIES		
I_L	ft	10.0
I_T	ft	0.5
I_V	ft	0.001
DISTRIBUTION COEFFICIENTS (kd)		
Mn-54	ml/g	8.7
Fe-55	ml/g	13.5
Co-60	ml/g	10.0
Sr-90	ml/g	7.0
Cs-137	ml/g	18.0
Pu-239	ml/g	0.0
DECAY CONSTANTS		
Mn-54	1/day	2.2212E-03
Fe-55	1/day	7.0272E-04
Co-60	1/day	3.5989E-04
Sr-90	1/day	6.5425E-05
Cs-137	1/day	6.2888E-05

Table 2.4-38

ESTIMATED PEAK CONCENTRATION OF RADIONUCLIDES IN GROUNDWATER
 RESULTING FROM POSTULATED RUPTURE OF RWCU PHASE SEPARATOR TANK
 - RESULTS OF SIMULATIONS WITH SLUG3D MODEL -
 SUSQUEHANNA SES

Radionuclide	At Well TW-2		At Biology Lab Well		At Susquehanna River		10 CFR 20 Appendix B Table 2 Effluent Concentration Limit (μCi/ml)
	Time of Peak Since Accident (days)	Peak Concen. (μCi/ml)	Time of Peak Since Accident (days)	Peak Concen. (μCi/ml)	Time of Peak Since Accident (days)	Peak Concen. (μCi/ml)	
FLOWPATH 1							
Mn-54*	10,350	7.70E-15	-	< 1.0E-30	-	< 1.0E-30	3.0E-05
Fe-55*	18,660	4.27E-08	-	< 1.0E-30	79,100	< 1.0E-30	1.0E-04
Co-60*	15,850	1.38E-04	-	< 1.0E-30	73,870	9.16E-16	3.0E-06
Sr-90*	12,010	5.34E-04	-	< 1.0E-30	59,720	5.60E-07	5.0E-07
I-131	360	5.83E-18	-	< 1.0E-30	-	< 1.0E-30	1.0E-06
Cs-137*	28,240	2.08E-04	-	< 1.0E-30	141,770	3.34E-09	1.0E-06
Pu-239	560	6.75E-06	-	< 1.0E-30	1,570	2.86E-07	2.0E-08
FLOWPATH 2							
Mn-54*	np	np	-	< 1.0E-30	22,030	1.54E-29	3.0E-05
Fe-55*	np	np	-	< 1.0E-30	39,480	1.69E-16	1.0E-04
Co-60*	np	np	-	< 1.0E-30	33,760	6.56E-09	3.0E-06
Sr-90*	np	np	-	< 1.0E-30	25,400	7.49E-06	5.0E-07
I-131	np	np	-	< 1.0E-30	630	3.33E-30	1.0E-06
Cs-137*	np	np	-	< 1.0E-30	59,900	8.55E-07	1.0E-06
Pu-239	np	np	-	< 1.0E-30	900	3.00E-07	2.0E-08
<div>* Adsorption through cation exchange on Pleistocene deposits included in simulation</div> <div>+ 10CFR20 Appendix B (2007)</div> <div>np not on flow path</div>							

Table 2.4-39

ESTIMATED PEAK CONCENTRATION OF RADIONUCLIDES IN GROUNDWATER IN BURIED VALLEY AQUIFER
 RESULTING FROM POSTULATED RUPTURE OF RWCU PHASE SEPARATOR TANK
 - RESULTS OF SIMULATIONS WITH SLUG3D MODEL -
 SUSQUEHANNA SES

Radionuclide	At Entry Point to Aquifer Cell (17,8)		At Well TW-2 Cell (27,6)		At Downgradient Boundary Cell (36,1)		10 CFR 20 Appendix B Table 2 Effluent Concentration Limit ($\mu\text{Ci/ml}$)
	Time of Peak Since Accident** (days)	Peak Concen.** ($\mu\text{Ci/ml}$)	Time of Peak Since Accident (days)	Peak Concen. ($\mu\text{Ci/ml}$)	Time of Peak Since Accident (days)	Peak Concen. ($\mu\text{Ci/ml}$)	
Mn-54*	281	1.78E-01	3,100	3.33E-09	4,050	1.25E-27	3.0E-05
Fe-55*	300	5.10E+00	7,020	3.97E-06	11,180	2.09E-20	1.0E-04
Co-60*	300	2.41E+00	8,140	1.03E-04	28,210	7.24E-13	3.0E-06
Sr-90*	300	4.87E-02	8,540	5.78E-05	46,140	3.59E-08	5.0E-07
I-131	190	1.49E-09	ns	ns	ns	ns	1.0E-06
Cs-137*	300	1.39E-01	19,140	3.14E-05	92,110	8.70E-10	1.0E-06
Pu-239	300	1.34E-05	708	4.97E-07	1,740	1.20E-08	2.0E-08

- * Adsorption through cation exchange on Pleistocene deposits included in simulation
 ** Computed from SLUG3D simulations of migration from ruptured tank to buried-valley aquifer
 + 10CFR20 Appendix B (2007)
 ns Simulation not run because of low I-131 concentration at entry point to aquifer

NOTE: These simulations were performed with Well TW-2 pumping continuously at 31 gpm

THIS FIGURE HAS BEEN
DELETED

FSAR REV. 65

SUSQUEHANNA STEAM ELECTRIC STATION UNITS 1 & 2 FINAL SAFETY ANALYSIS REPORT

Figure Deleted

FIGURE 2.4-1, Rev. 55

AutoCAD Figure 2_4_1.doc

THIS FIGURE HAS BEEN
DELETED

FSAR REV. 65

SUSQUEHANNA STEAM ELECTRIC STATION UNITS 1 & 2 FINAL SAFETY ANALYSIS REPORT

Figure Deleted

FIGURE 2.4-2, Rev. 55

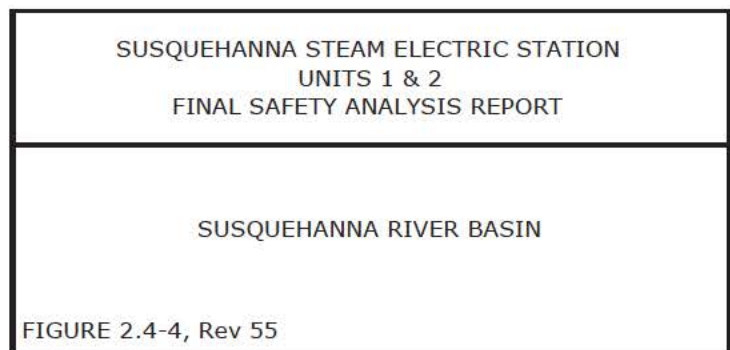
AutoCAD Figure 2_4_2.doc

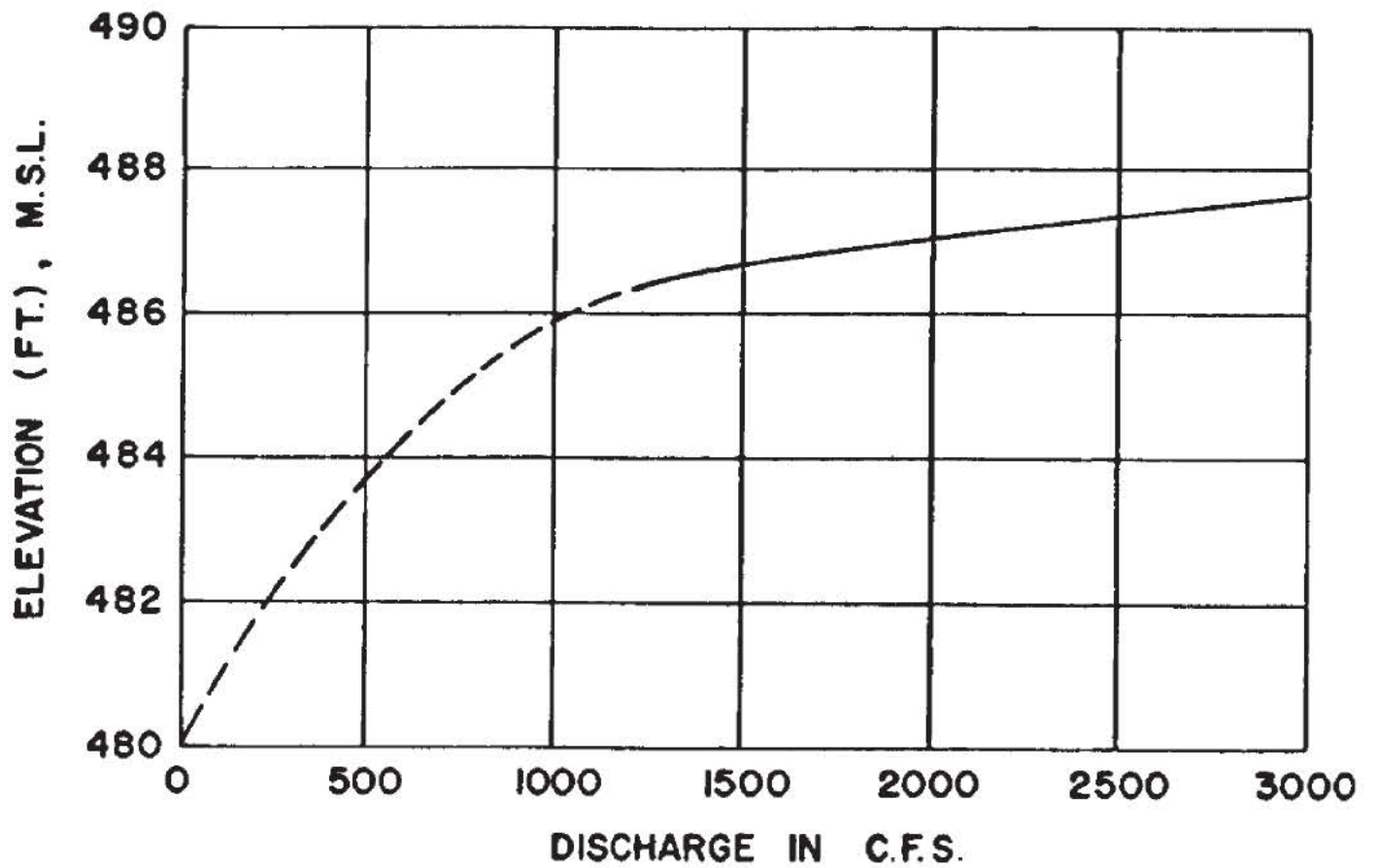
Security-Related Information

Figure Withheld Under 10 CFR 2.390

Security-Related Information

Figure Withheld Under 10 CFR 2.390





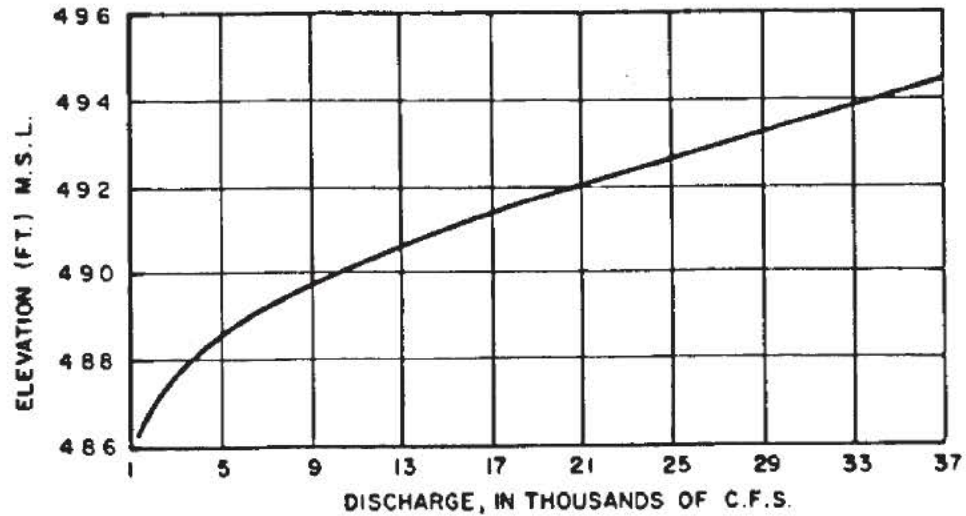
FSAR REV. 65

SUSQUEHANNA STEAM ELECTRIC STATION
UNITS 1 & 2
FINAL SAFETY ANALYSIS REPORT

STAGE DISCHARGE CURVE
AT LOW FLOWS

FIGURE 2.4-5, Rev 47

AutoCAD: Figure Fsar 2_4_5.dwg



NOTES: ELEVATIONS MEASURED BY GAGE AT SUSQUEHANNA SITE
 FLOWS MEASURED AT WILKES-BARRE AND DANVILLE. FLOW
 AT SITE OBTAINED BY INTERPOLATION ON BASIS OF
 DRAINAGE AREA.

DRAINAGE AREAS :

WILKES-BARRE 9960 SQ MILES (25795 SQ KM)
 SUSQUEHANNA SITE 10200 SQ MI (26416 SQ KM)
 DANVILLE 11220 SQ MI (29058 SQ KM)

FSAR REV. 65

SUSQUEHANNA STEAM ELECTRIC STATION
 UNITS 1 & 2
 FINAL SAFETY ANALYSIS REPORT

STAGE DISCHARGE CURVE,
 DISCHARGE RANGE
 1000 - 37000 CFS

FIGURE 2.4-6, Rev 47

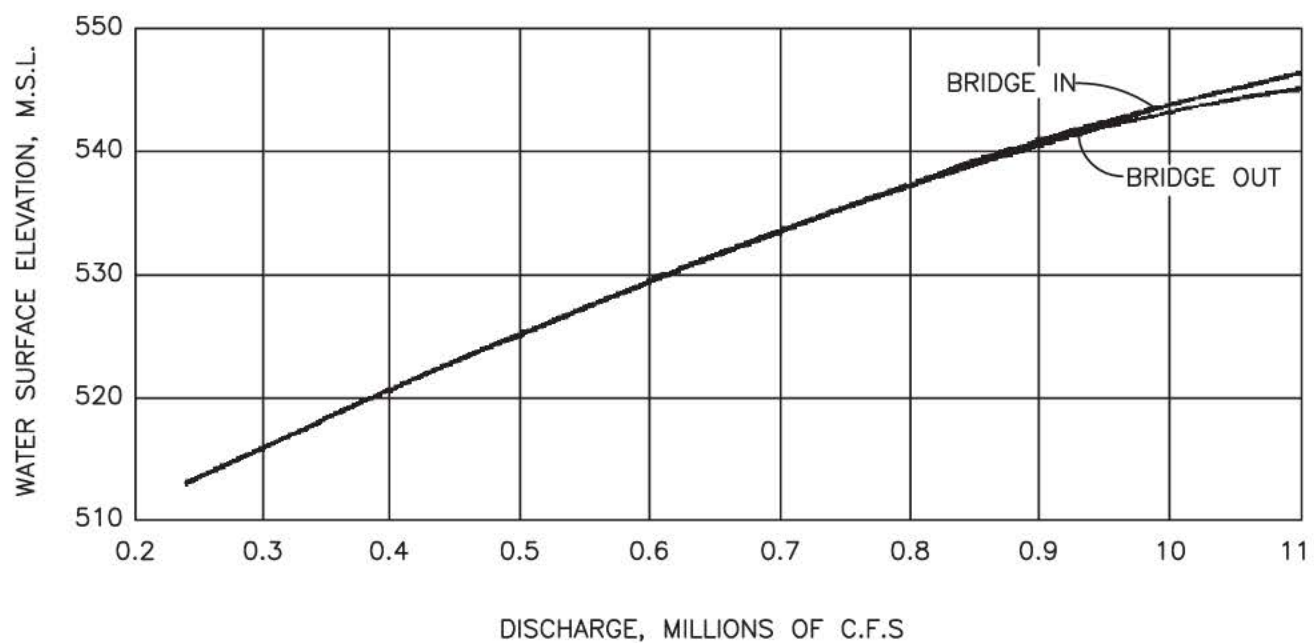
AutoCAD: Figure Fsar 2_4_6.dwg

Security-Related Information

Figure Withheld Under 10 CFR 2.390

SUSQUEHANNA STEAM ELECTRIC STATION UNITS 1 & 2 FINAL SAFETY ANALYSIS REPORT	
WATER USERS ON THE SUSQUEHANNA RIVER	
FIGURE 2.4-7, Rev 55	

AutoCAD: Figure Fsar 2_4_7.dwg



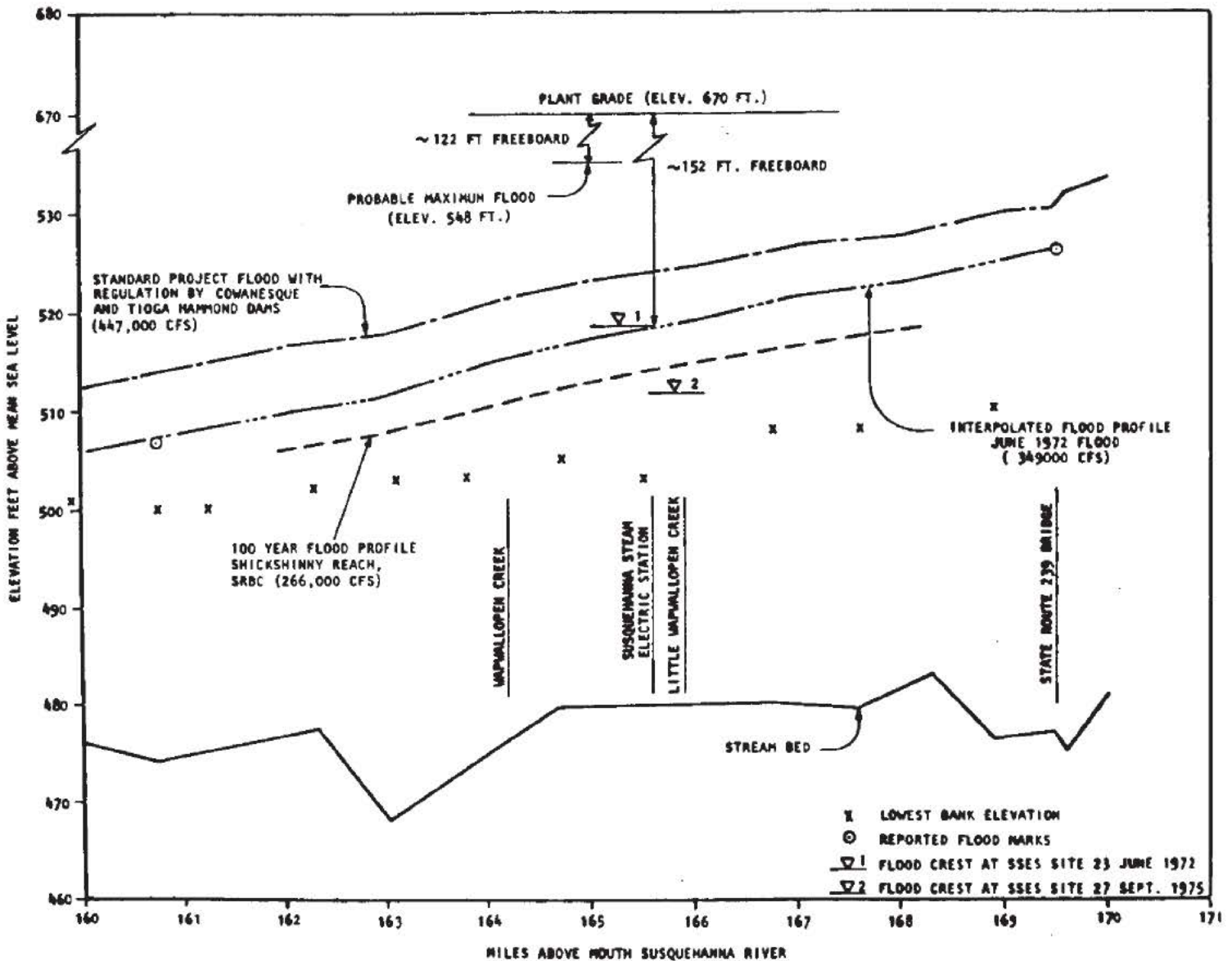
FSAR REV. 65

SUSQUEHANNA STEAM ELECTRIC STATION
UNITS 1 & 2
FINAL SAFETY ANALYSIS REPORT

STAGE DISCHARGE CURVES
AT PLANT SITE

FIGURE 2.4-8, Rev 47

AutoCAD: Figure Fsar 2_4_8.dwg



DATA SOURCE:
BALTIMORE DISTRICT CORPS OF ENGINEERS 1974.

DATA SOURCE FOR THE 100 YEAR FLOOD PROFILE:
FEDERAL INSURANCE ADMINISTRATION, TYPE 15,
FLOOD INSURANCE STUDY, OBTAINED FROM
SUSQUEHANNA RIVER BASIN COMMISSION (SRBC)

FSAR REV. 65

SUSQUEHANNA STEAM ELECTRIC STATION
UNITS 1 & 2
FINAL SAFETY ANALYSIS REPORT

FLOOD PROFILES ON THE
SUSQUEHANNA RIVER
AT THE SITE

FIGURE 2.4-9, Rev 47

AutoCAD: Figure Fsar_2_4_9.dwg

Security-Related Information
Figure Withheld Under 10 CFR 2.390

Security-Related Information

Figure Withheld Under 10 CFR 2.390

SUSQUEHANNA STEAM ELECTRIC STATION UNITS 1 AND 2 FINAL SAFETY ANALYSIS REPORT
SITE DRAINAGE LOCATIONS A & B
FIGURE 2.4-11, Rev. 47

Auto Cad: Figure Fsar 2_4_11.dwg
Created from Land Studies Dwg.

Security-Related Information

Figure Withheld Under 10 CFR 2.390

SUSQUEHANNA STEAM ELECTRIC STATION UNITS 1 AND 2 FINAL SAFETY ANALYSIS REPORT
SITE DRAINAGE LOCATIONS C & D
FIGURE 2.4-12, Rev. 47

Auto Cad: Figure Fsar 2_4_12.dwg
Created from Land Studies Dwg.

Security-Related Information

Figure Withheld Under 10 CFR 2.390

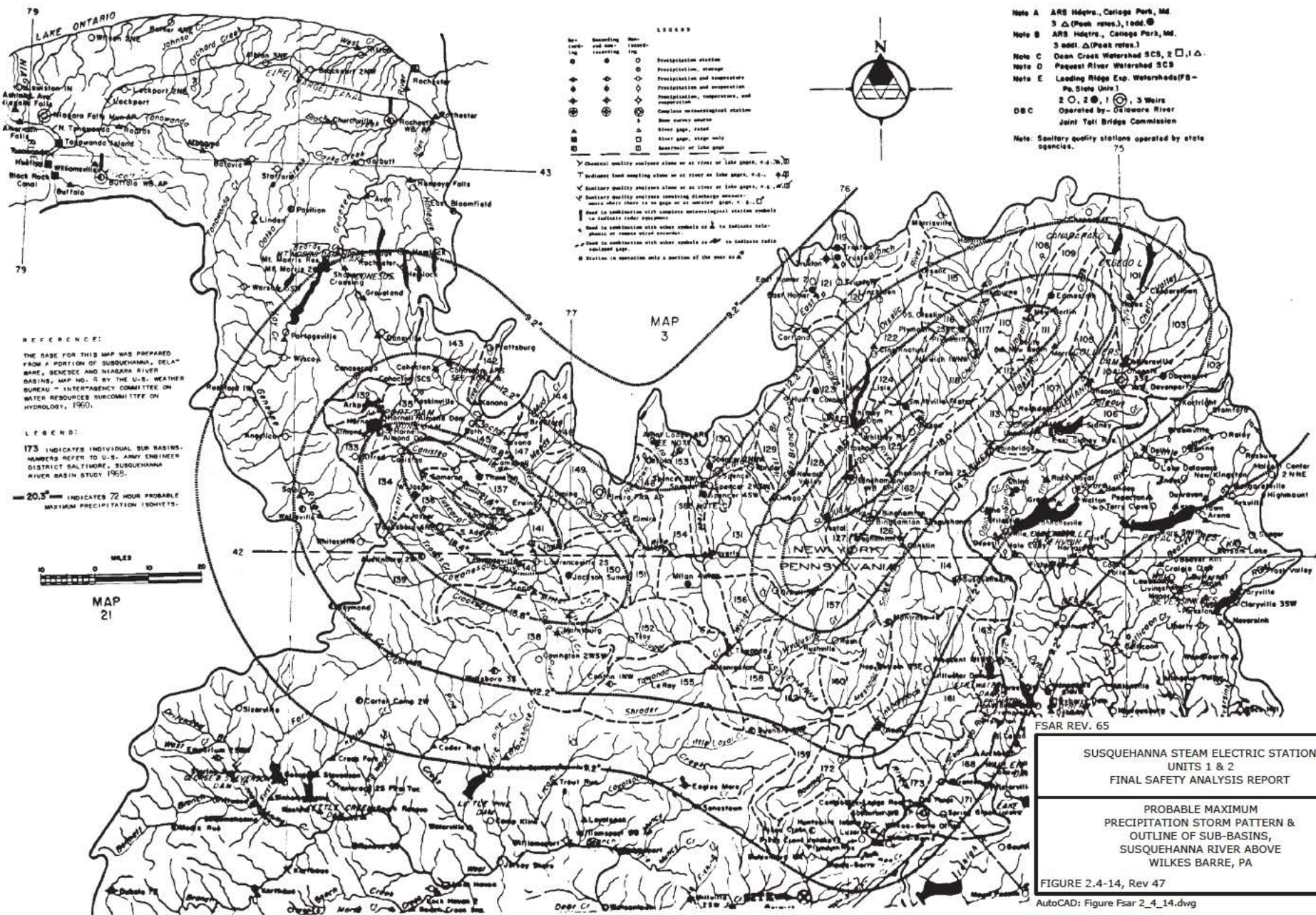
FSAR REV. 65

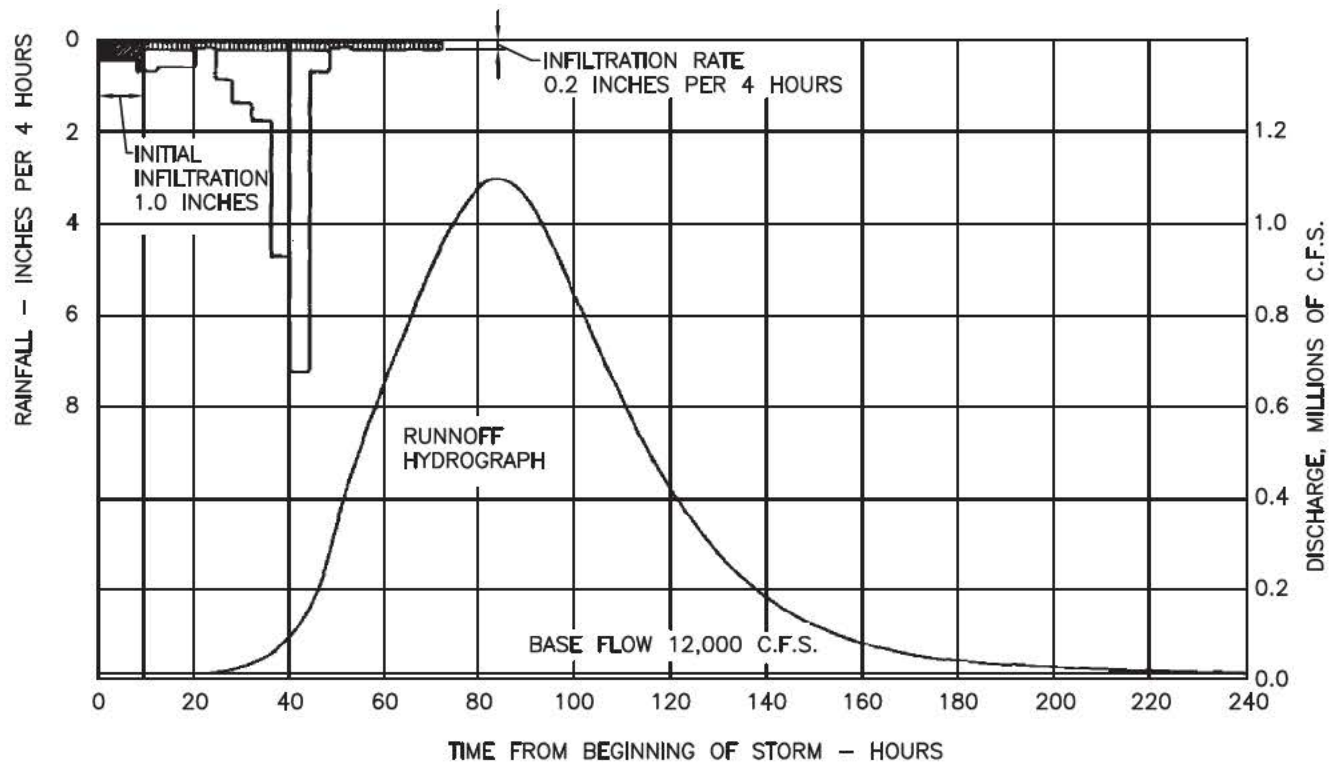
SUSQUEHANNA STEAM ELECTRIC STATION
UNITS 1 AND 2
FINAL SAFETY ANALYSIS REPORT

SITE DRAINAGE
LOCATIONS E & F

FIGURE 2.4-13, Rev. 47

Auto Cad: Figure Fsar 2.4.13.dwg
Created from Land Studies Dwg.





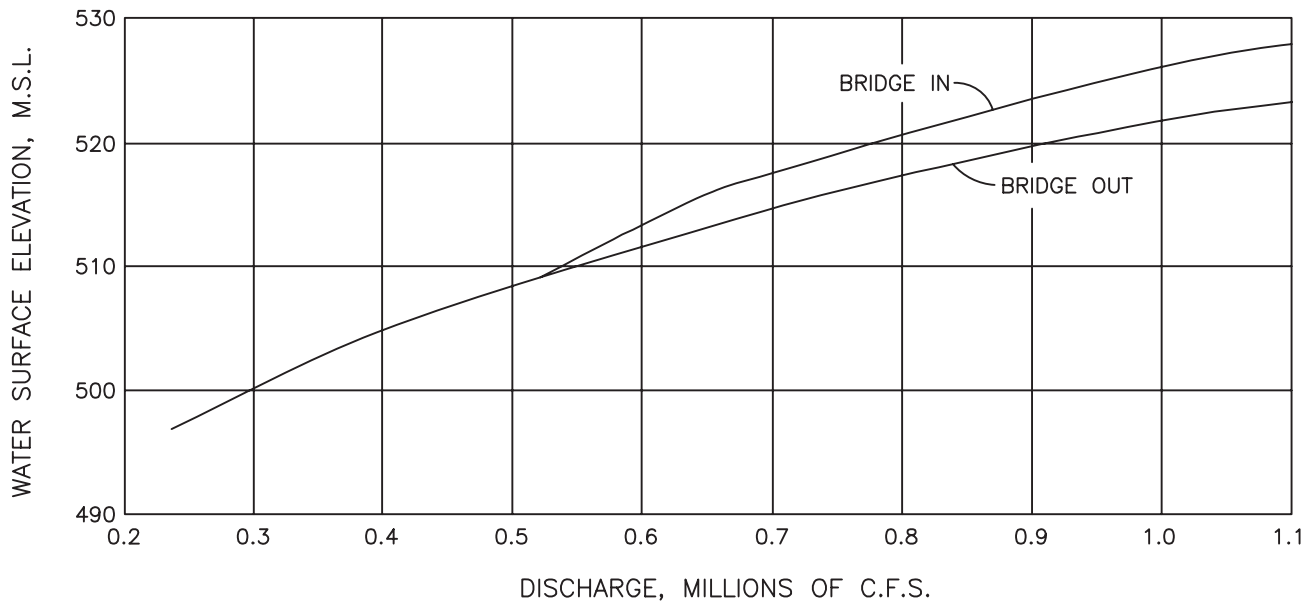
FSAR REV. 65

SUSQUEHANNA STEAM ELECTRIC STATION
UNITS 1 & 2
FINAL SAFETY ANALYSIS REPORT

PROBABLE MAXIMUM
PRECIPITATION ON SUSQUEHANNA
RIVER BASIN & PROBABLE
MAXIMUM FLOOD HYDROGRAPH
AT WILKES BARRE, PA

FIGURE 2.4-15, Rev 47

AutoCAD: Figure Fsar 2_4_15.dwg



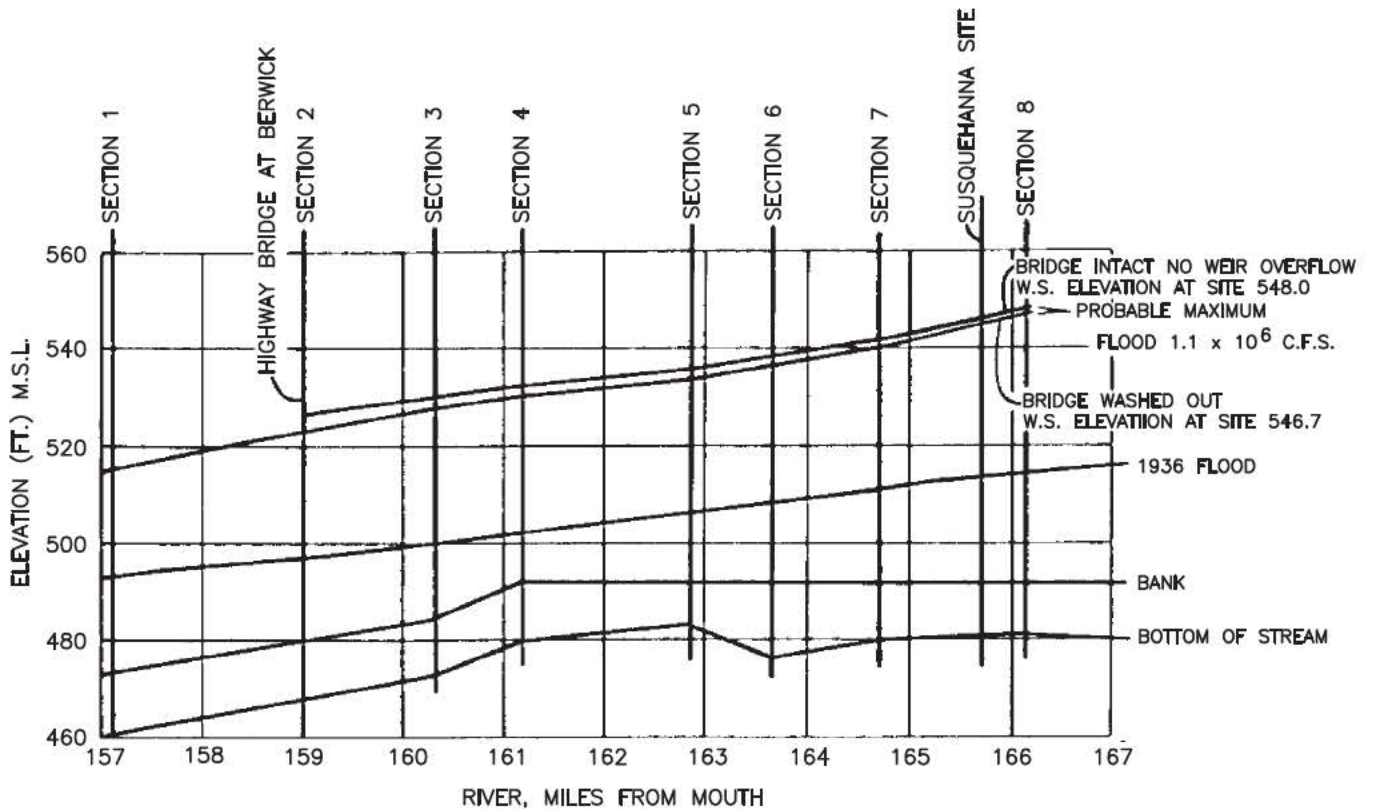
FSAR REV. 65

SUSQUEHANNA STEAM ELECTRIC STATION
UNITS 1 & 2
FINAL SAFETY ANALYSIS REPORT

STAGE DISCHARGE CURVE AT
SECTION 2 -
BERWICK BRIDGE

FIGURE 2.4-17, Rev 47

AutoCAD: Figure Fsar 2_4_17.dwg



NOTE:

W.S. ELEVATIONS REFLECT
ADJUSTMENT OF +2.3 FT.
FOR WIND-WAVE RUNUP

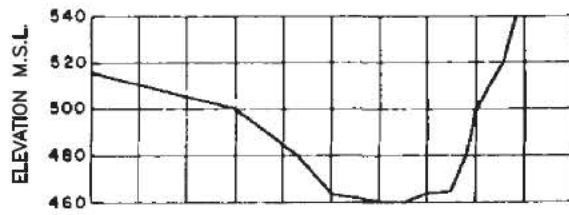
FSAR REV. 65

SUSQUEHANNA STEAM ELECTRIC STATION
UNITS 1 & 2
FINAL SAFETY ANALYSIS REPORT

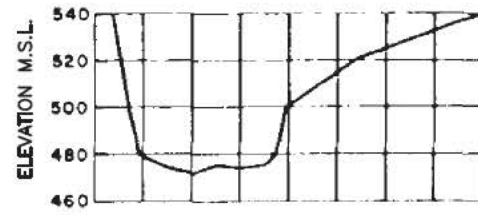
RIVER AND WATER SURFACE
PROFILES OF SUSQUEHANNA
RIVER IN VICINITY OF SITE

FIGURE 2.4-18, Rev 47

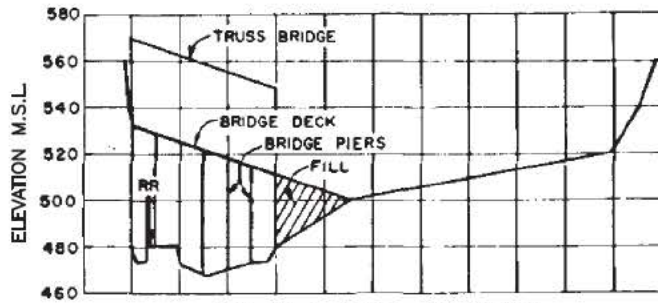
AutoCAD: Figure Fsar 2_4_18.dwg



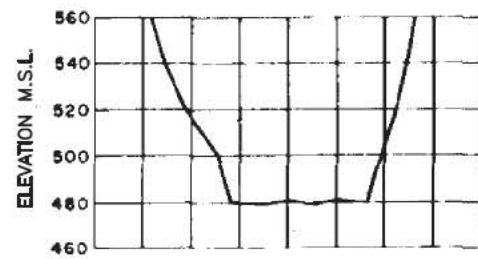
SECTION 1 - MILE 157.05



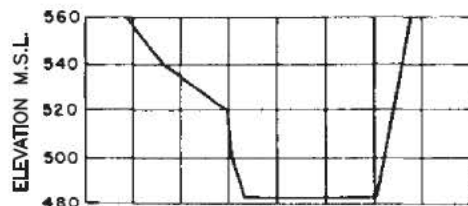
SECTION 3 - MILE 160.31



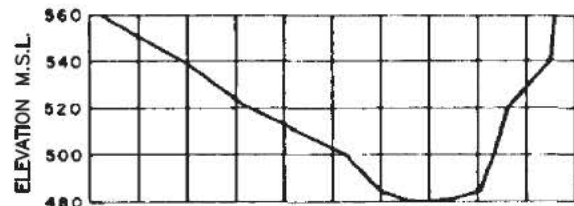
SECTION 2 - BRIDGE AT BERWICK



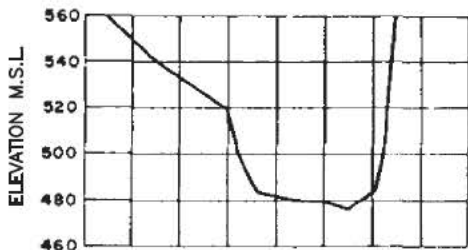
SECTION 4 - MILE 161.15



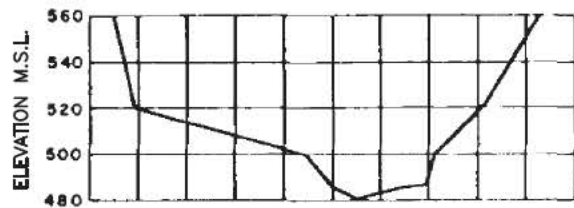
SECTION 5 - MILE 162.85



SECTION 7 - MILE 164.70



SECTION 6 - MILE 163.60



SECTION 8 - MILE 166.15

CROSS SECTIONS LOOKING UPSTREAM
SCALE - HORIZONTAL- 1"=2000FT.
VERTICAL- 1"= 80FT.

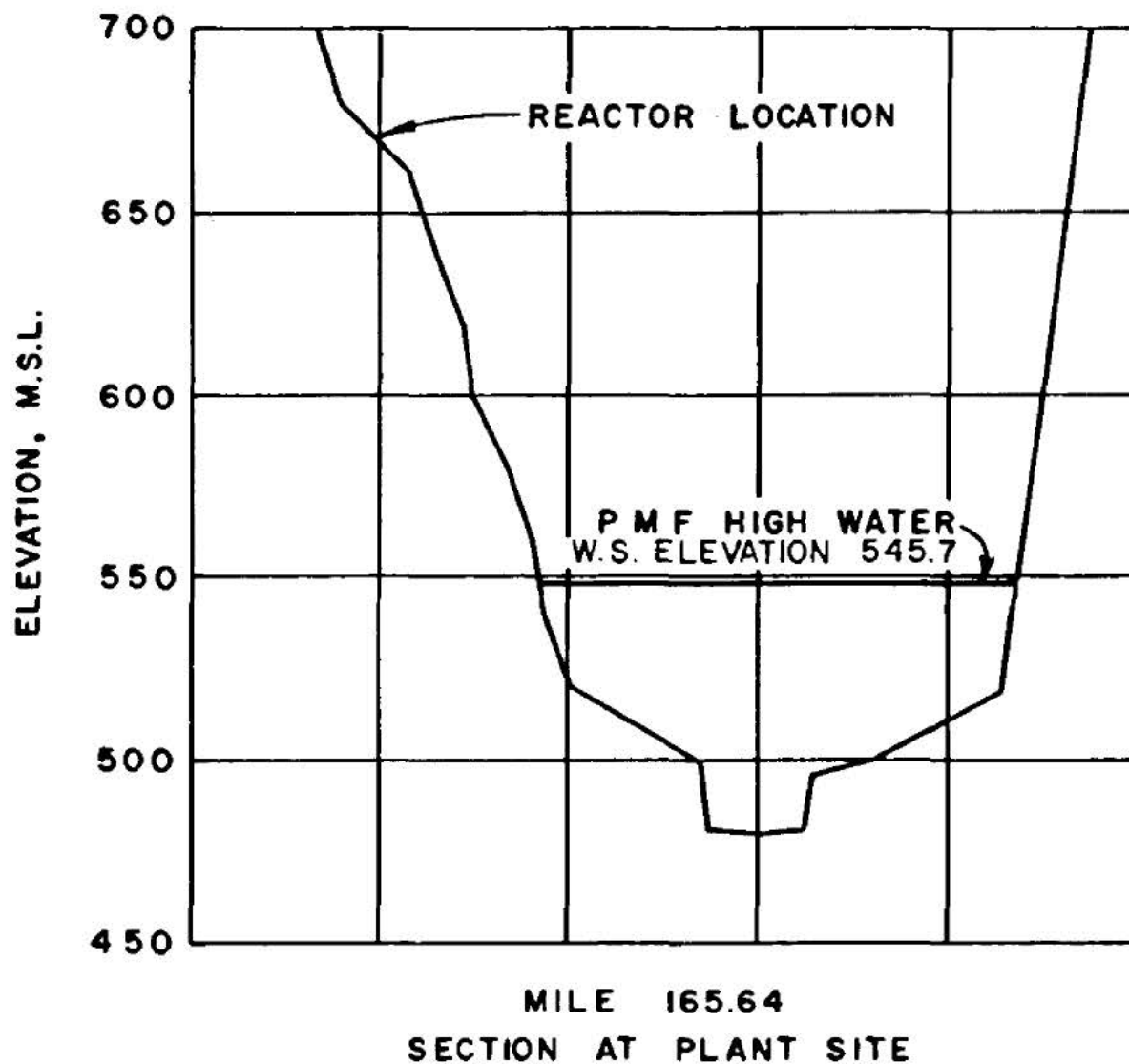
FSAR REV. 65

SUSQUEHANNA STEAM ELECTRIC STATION
UNITS 1 & 2
FINAL SAFETY ANALYSIS REPORT

CROSS SECTIONS AT THE
EIGHT RIVER SECTIONS
NEAR THE SITE

FIGURE 2.4-19, Rev 47

AutoCAD: Figure Fsar 2_4_19.dwg



CROSS SECTIONS LOOKING UPSTREAM
SCALE - HORIZONTAL : 1" = 2000 FT.
VERTICAL : 1" = 50 FT.

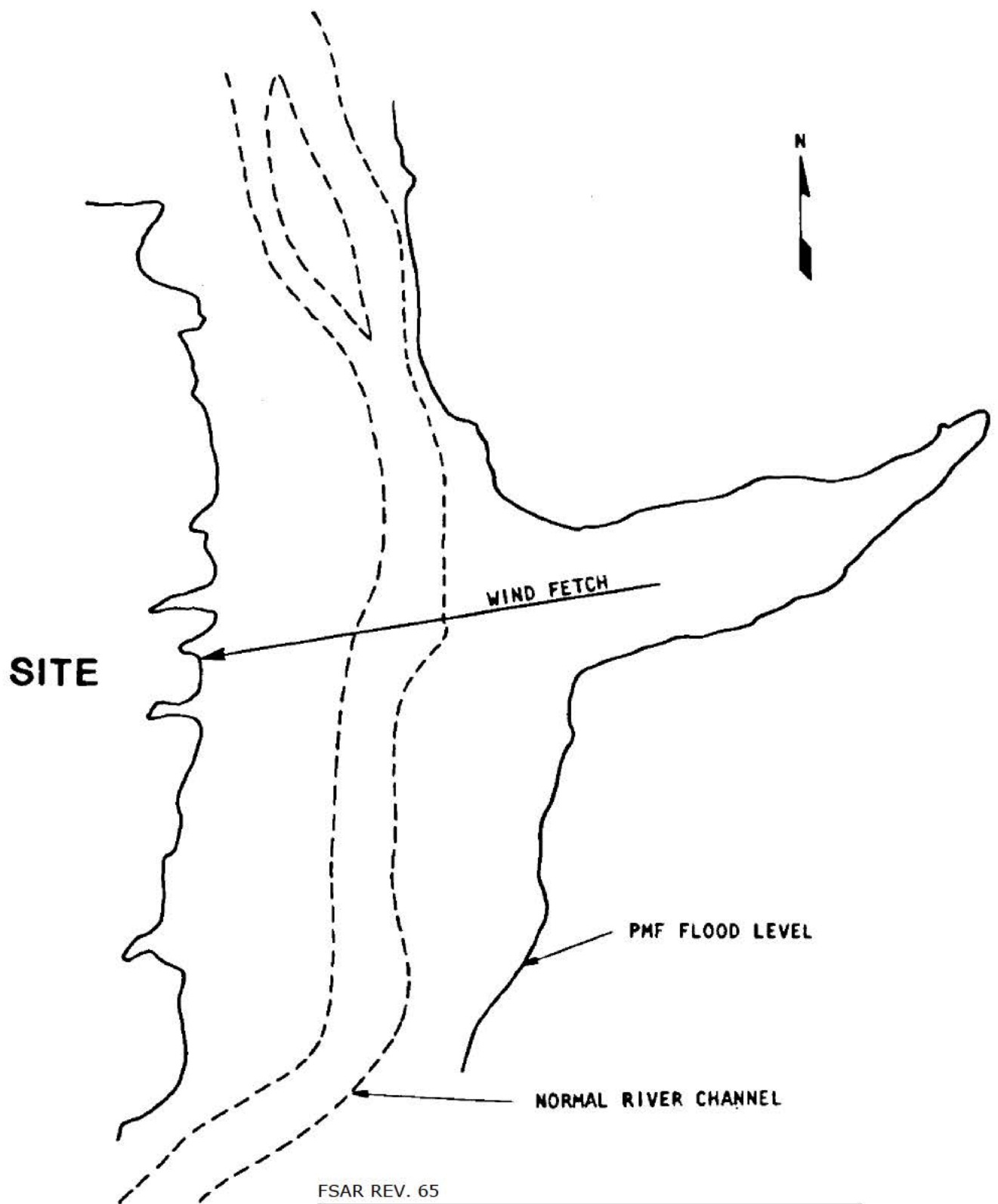
FSAR REV. 65

SUSQUEHANNA STEAM ELECTRIC STATION
UNITS 1 & 2
FINAL SAFETY ANALYSIS REPORT

CROSS SECTION
OF RIVER AT
THE PLANT SITE

FIGURE 2.4-20, Rev 47

AutoCAD: Figure Fsar 2_4_20.dwg



FSAR REV. 65

SUSQUEHANNA STEAM ELECTRIC STATION
UNITS 1 & 2
FINAL SAFETY ANALYSIS REPORT

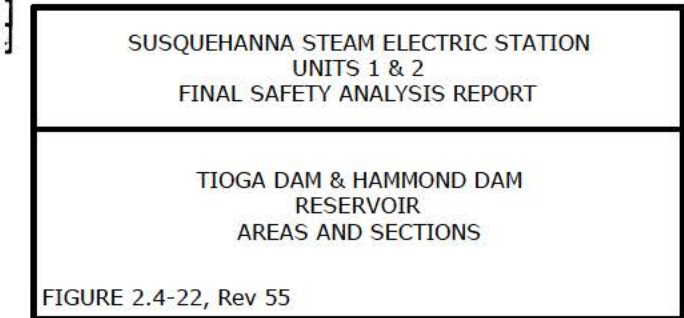
WIND FETCH,
SUSQUEHANNA RIVER PMF

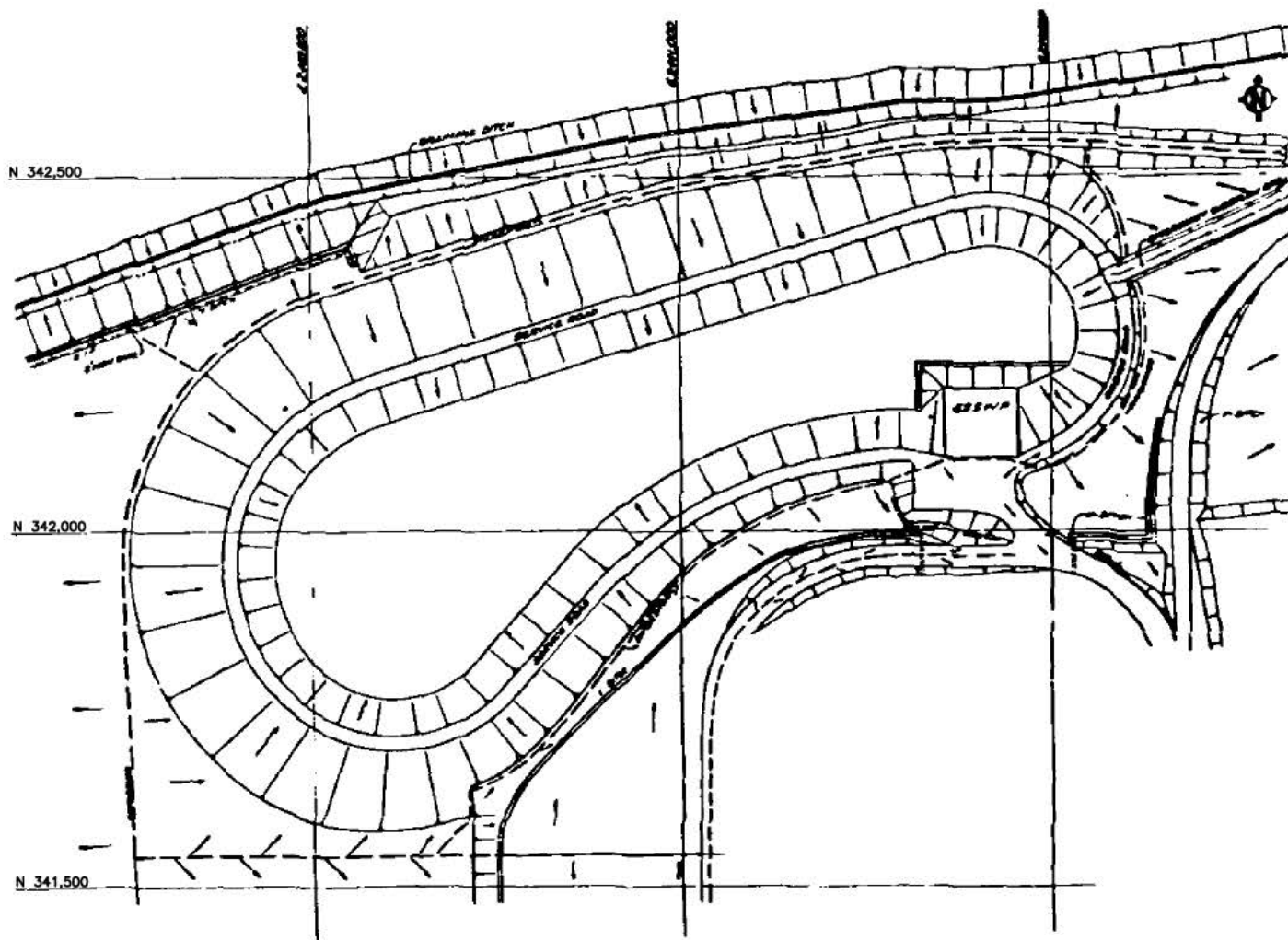
FIGURE 2.4-21, Rev 47

AutoCAD: Figure Fsar 2_4_21.dwg

Security-Related Information

Figure Withheld Under 10 CFR 2.390





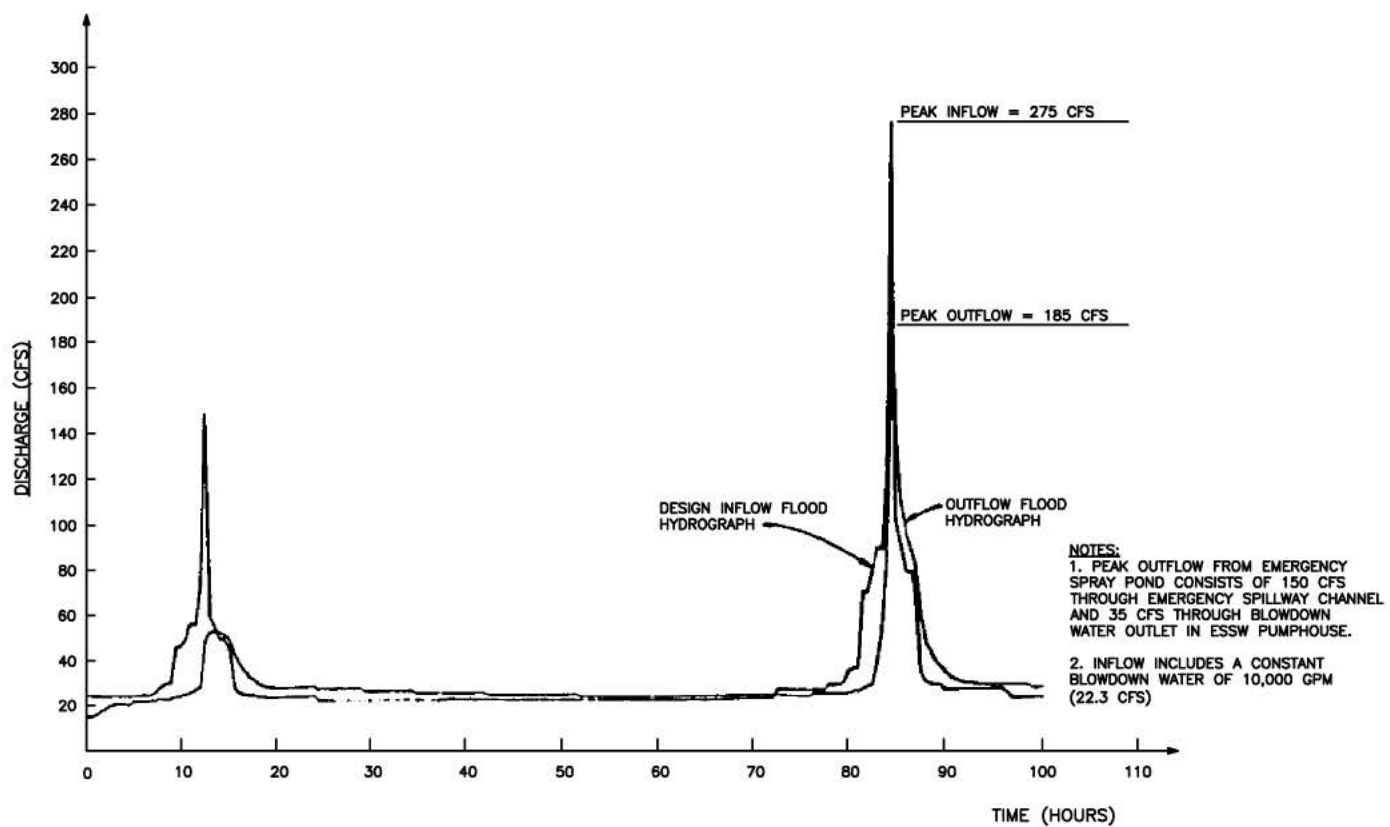
FSAR REV. 65

SUSQUEHANNA STEAM ELECTRIC STATION
UNITS 1 & 2
FINAL SAFETY ANALYSIS REPORT

SURFACE DRAINAGE PATTERNS
AROUND THE SPRAY POND

FIGURE 2.4-23, Rev 47

AutoCAD: Figure Fsar 2_4_23.dwg



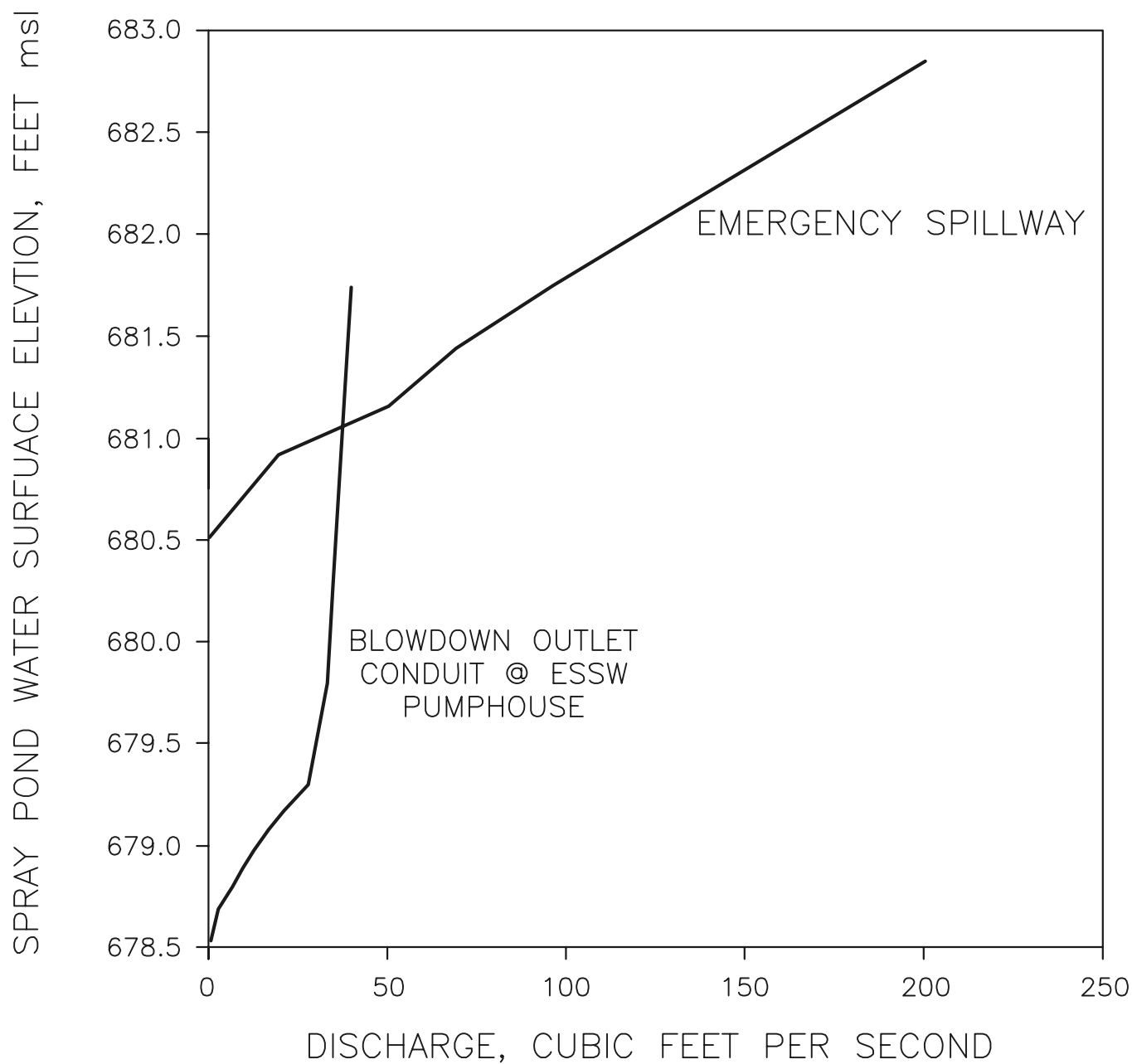
FSAR REV. 65

SUSQUEHANNA STEAM ELECTRIC STATION
UNITS 1 & 2
FINAL SAFETY ANALYSIS REPORT

SPRAY POND INFLOW
AND
OUTFLOW HYDROGRAPH

FIGURE 2.4-24, Rev 47

AutoCAD: Figure Fsar 2_4_24.dwg



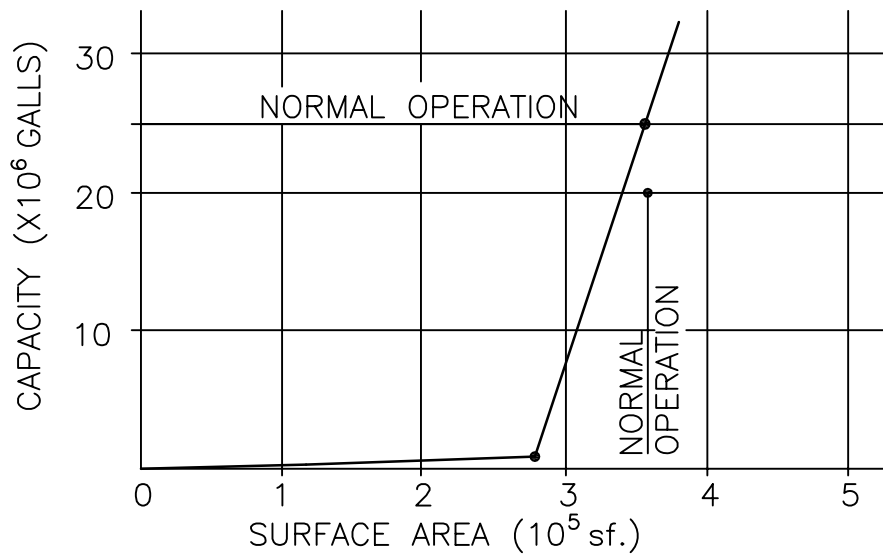
FSAR REV. 65

SUSQUEHANNA STEAM ELECTRIC STATION
UNITS 1 & 2
FINAL SAFETY ANALYSIS REPORT

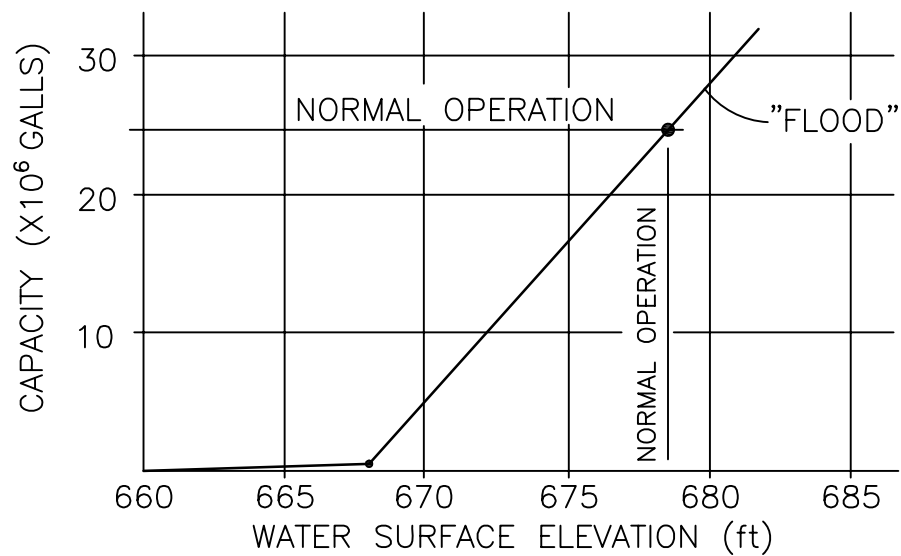
SPRAY POND OUTLET
RATING CURVES

FIGURE 2.4-25, Rev 49

AutoCAD: Figure Fsar 2_4_25.dwg



CAPACITY VS WATER
SURFACE AREA CURVE



CAPACITY VS WATER ELEVATION CURVE

FSAR REV. 65

SUSQUEHANNA STEAM ELECTRIC STATION
UNITS 1 & 2
FINAL SAFETY ANALYSIS REPORT

SPRAY POND ELEVATION AREA
STORAGE CAPACITY CURVES

FIGURE 2.4-26, Rev 47

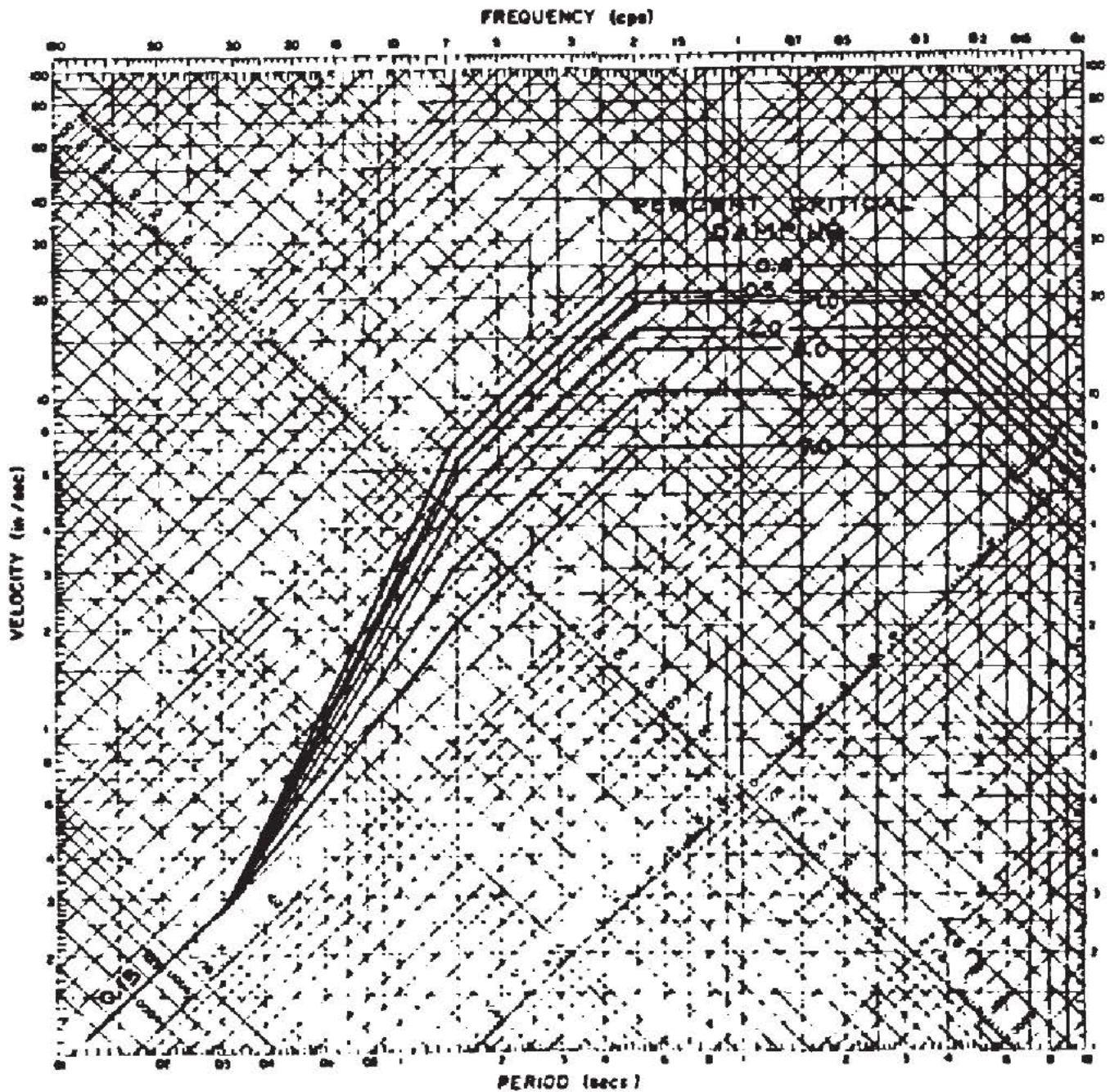
AutoCAD: Figure Fsar 2_4_26.dwg

Security-Related Information

Figure Withheld Under 10 CFR 2.390

SUSQUEHANNA STEAM ELECTRIC STATION UNITS 1 & 2 FINAL SAFETY ANALYSIS REPORT
SPRAY POND EMERGENCY SPILLWAY WATER SURFACE PROFILE
FIGURE 2.4-27, Rev 48

AutoCAD: Figure Fsar 2_4_27.dwg



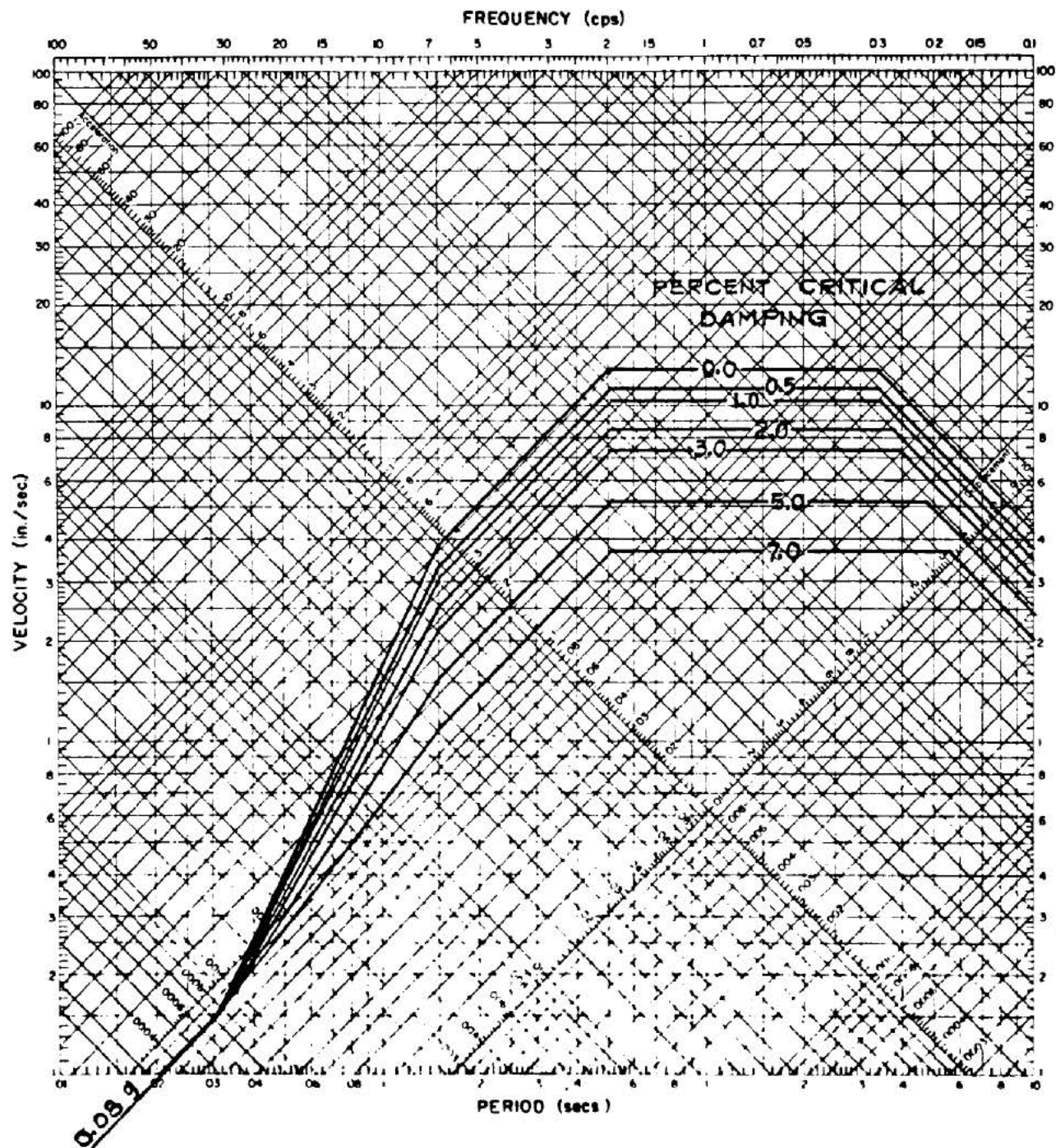
FSAR REV. 65

SUSQUEHANNA STEAM ELECTRIC STATION
UNITS 1 & 2
FINAL SAFETY ANALYSIS REPORT

SPRAY POND
DESIGN SPECTRUM
FOR SSE

FIGURE 2.4-28, Rev 47

AutoCAD: Figure Fsar 2_4_28.dwg



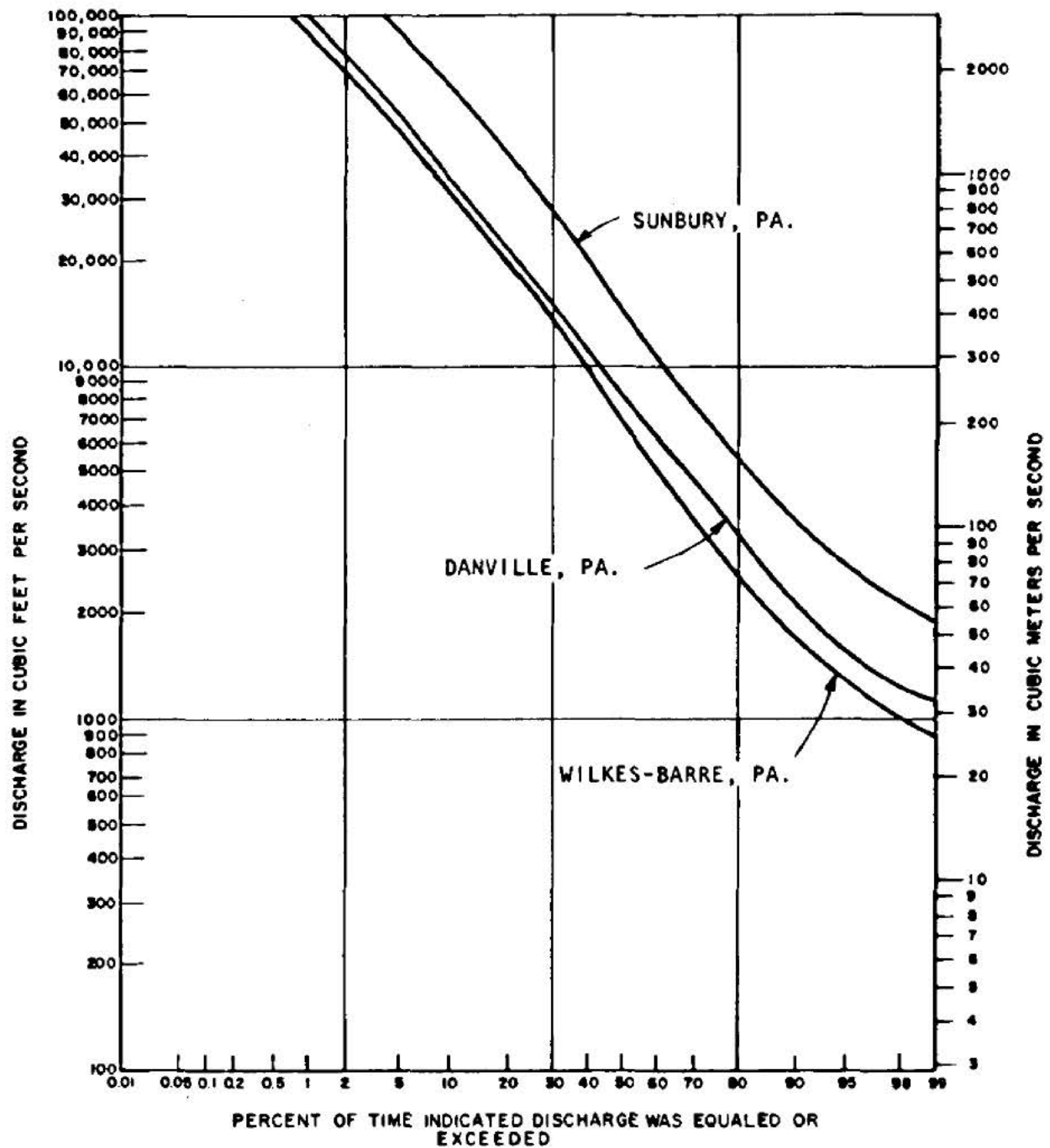
FSAR REV. 65

SUSQUEHANNA STEAM ELECTRIC STATION
UNITS 1 & 2
FINAL SAFETY ANALYSIS REPORT

SPRAY POND
DESIGN SPECTRUM
FOR OBE

FIGURE 2.4-29, Rev 47

AutoCAD: Figure Fsar 2_4_29.dwg



SOURCE : USGS OPEN FILE REPORT 76-247 , 1976

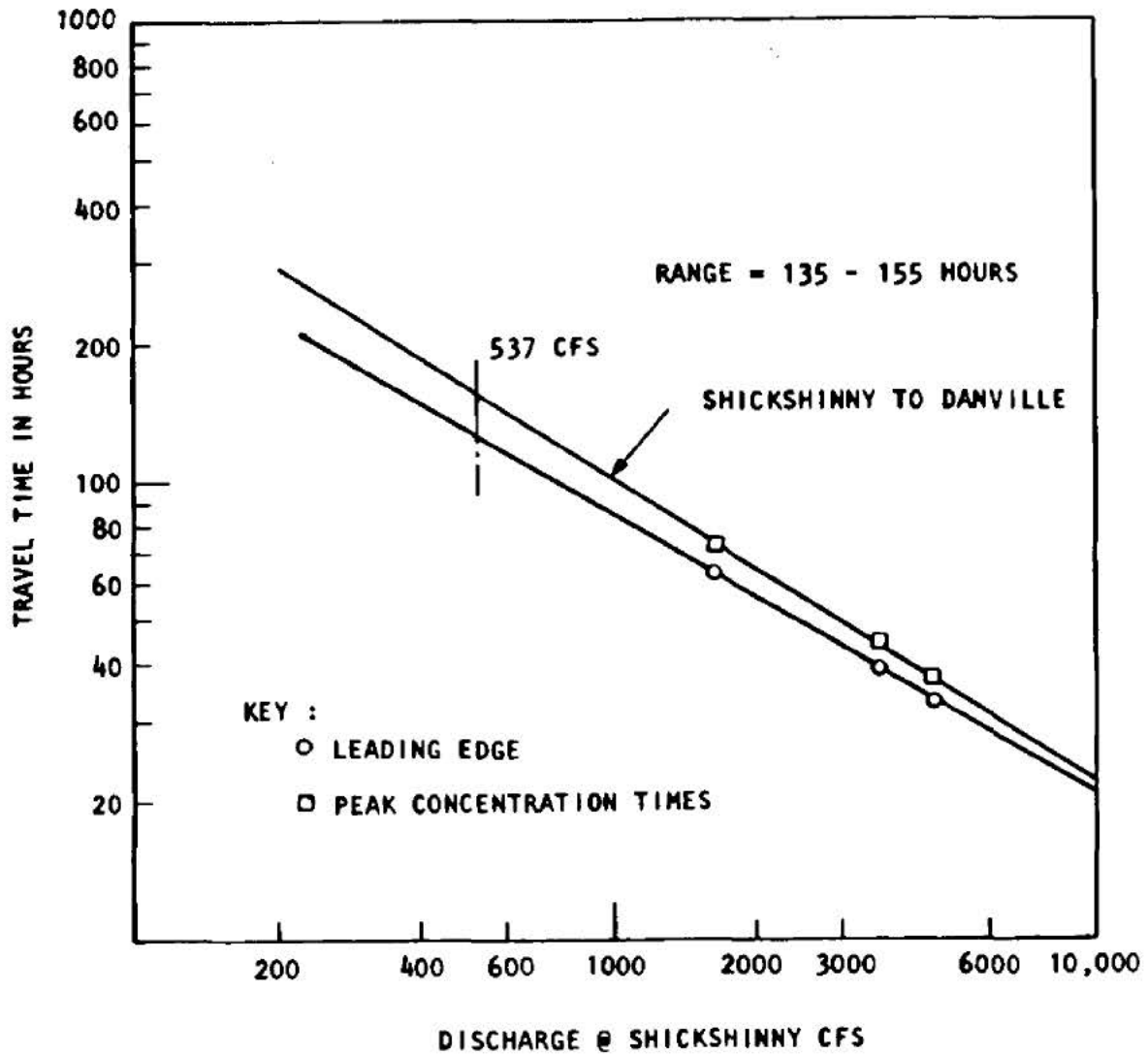
FSAR REV. 65

SUSQUEHANNA STEAM ELECTRIC STATION
UNITS 1 & 2
FINAL SAFETY ANALYSIS REPORT

DURATION CURVES OF
DAILY DISCHARGE

FIGURE 2.4-30, Rev 47

AutoCAD: Figure Fsar 2_4_30.dwg



FSAR REV. 65

SUSQUEHANNA STEAM ELECTRIC STATION
UNITS 1 & 2
FINAL SAFETY ANALYSIS REPORT

TIME OF TRAVEL
SUSQUEHANNA RIVER
SHICKSHINNY TO DANVILLE

FIGURE 2.4-31, Rev 47

SOURCE: USGS, 1976

AutoCAD: Figure Fsar 2_4_31.dwg

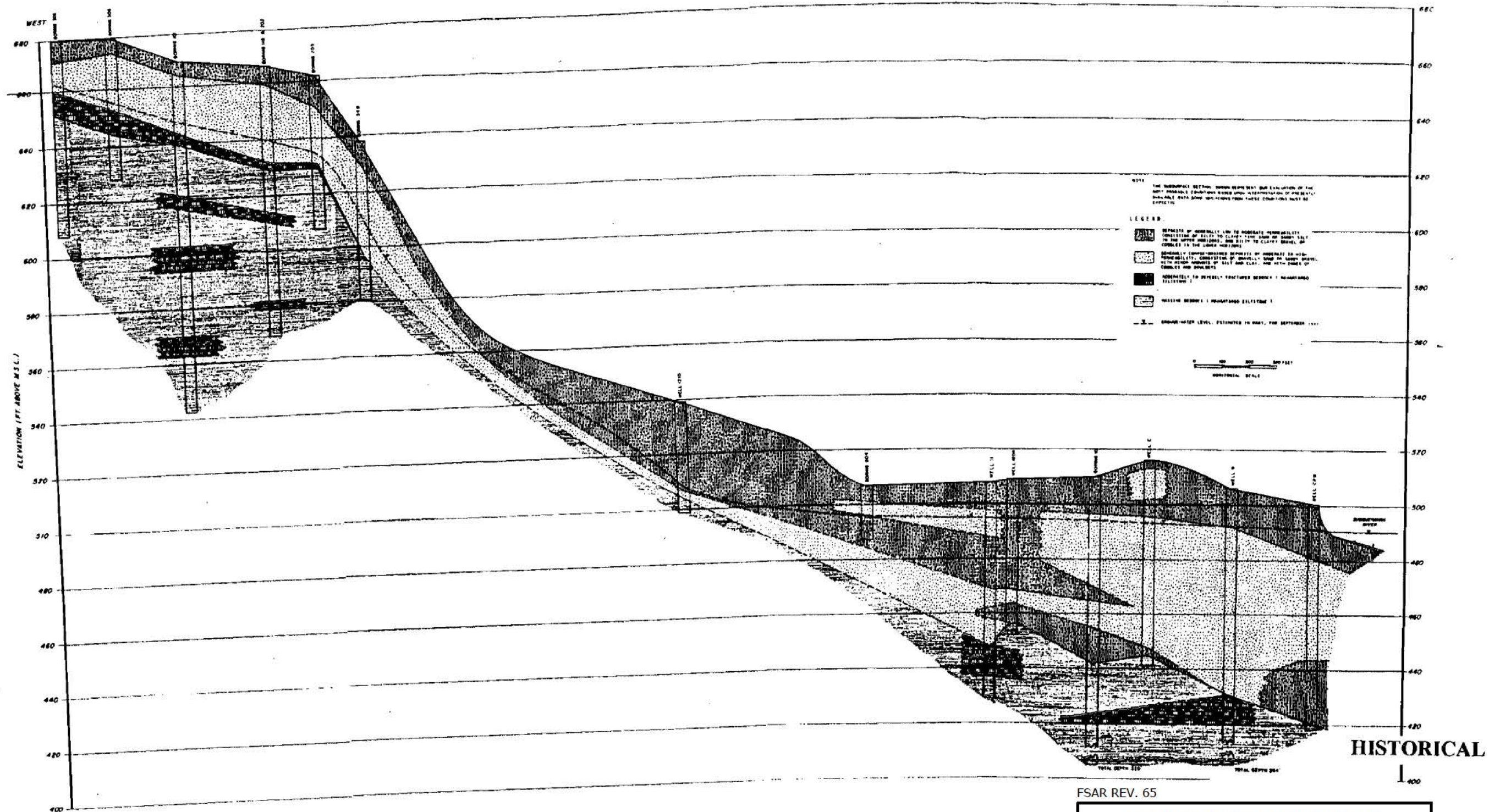
Security-Related Information
Figure Withheld Under 10 CFR 2.390

SUSQUEHANNA STEAM ELECTRIC STATION
UNITS 1 & 2
FINAL SAFETY ANALYSIS REPORT

MAP AT SUSQUEHANNA SES
SHOWING GROUNDWATER
CONTOURS IN SEPTEMBER 1977

FIGURE 2.4-32, Rev 55

AutoCAD: Figure Fsar 2_4_32.dwg

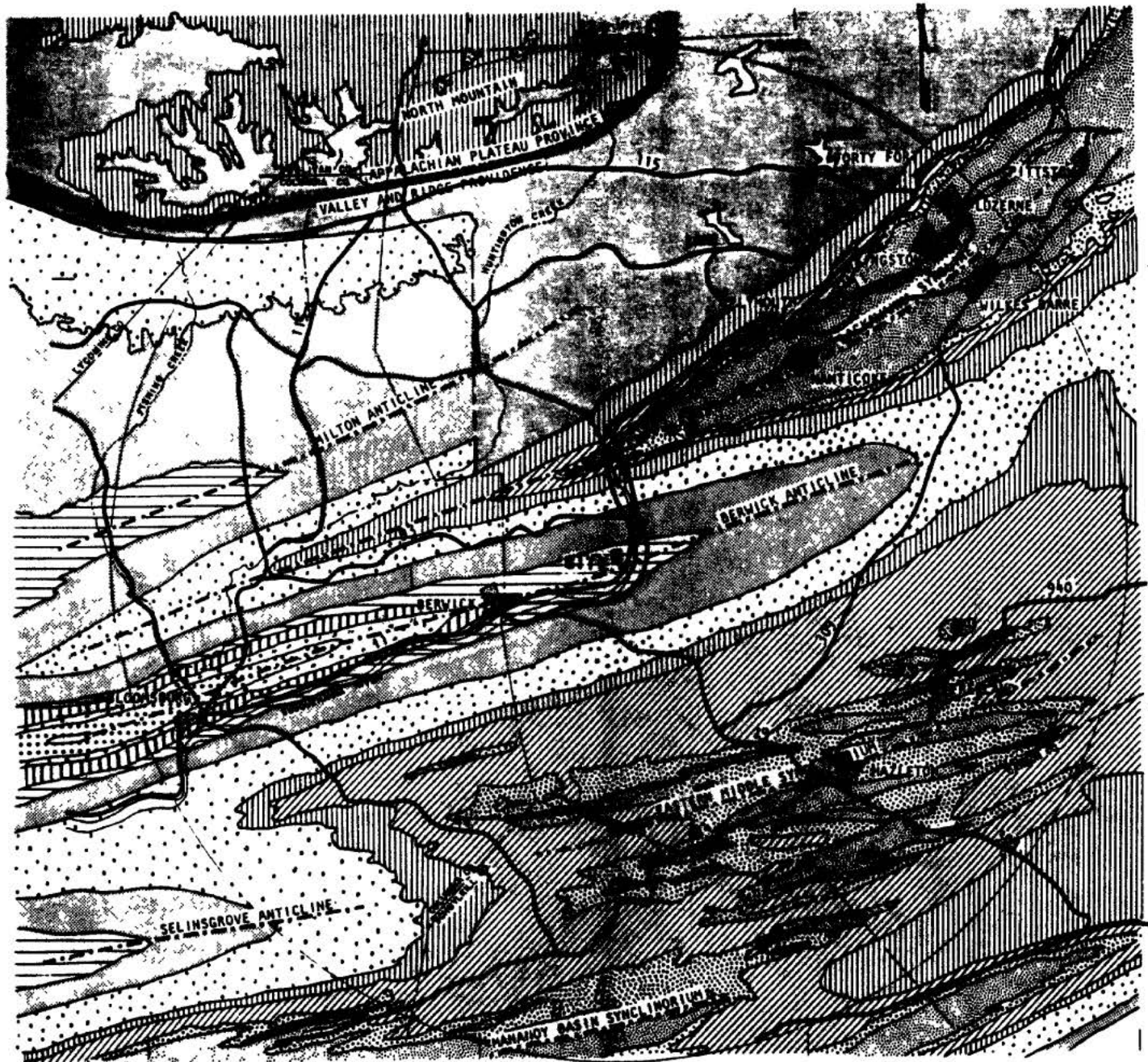


SUSQUEHANNA STEAM ELECTRIC STATION
UNITS 1 & 2
FINAL SAFETY ANALYSIS REPORT

HYDROLOGIC CROSS SECTION
FROM WEST TO EAST ALONG
GROUNDWATER FLOW PATH
AT THE SUSQUEHANNA SES

FIGURE 2.4-33, Rev 55

AutoCAD: Figure Fsar_2_4_33.dwg



LEGEND:

PENNSYLVANIAN

- LLEWELLYN FORMATION
- POTTSVILLE FORMATION

MISSISSIPPIAN

- MAUCH CHUNK FORMATION
- POCONO FORMATION

DEVONIAN

- CATSKILL FORMATION
- MARINE BEDS
- MANANTANGO, MARCELLUS AND ONONDAGA FMS (UNDIFFERENTIATED)

SILURIAN

- KEYSER, TOMOLOWAY AND WILLS CREEK FORMATIONS
- BLOOMSBURG FORMATION
- CLINTON FORMATION
- MAJOR ANTICLINAL OR SYNCLINAL AXIS
- DIVISION BETWEEN PHYSIOGRAPHIC PROVINCES



BASED ON:
C. SHAW, V.C. SHAW, AND OTHERS, GEOLOGIC MAP OF PENNSYLVANIA,
1:250,000, HARRISBURG, PA. PA. DEPARTMENT OF ENVIRONMENTAL
RESOURCES, TOPOGRAPHIC AND GEOLOGIC SURVEY, MAP 1, (1960),
WITH CERTAIN MODIFICATIONS BASED ON FIELD WORKING WITHIN 5
MILES OF STATION PERFORMED BY BAKER AND ROBE IN SPRING OF 1977.

HISTORICAL

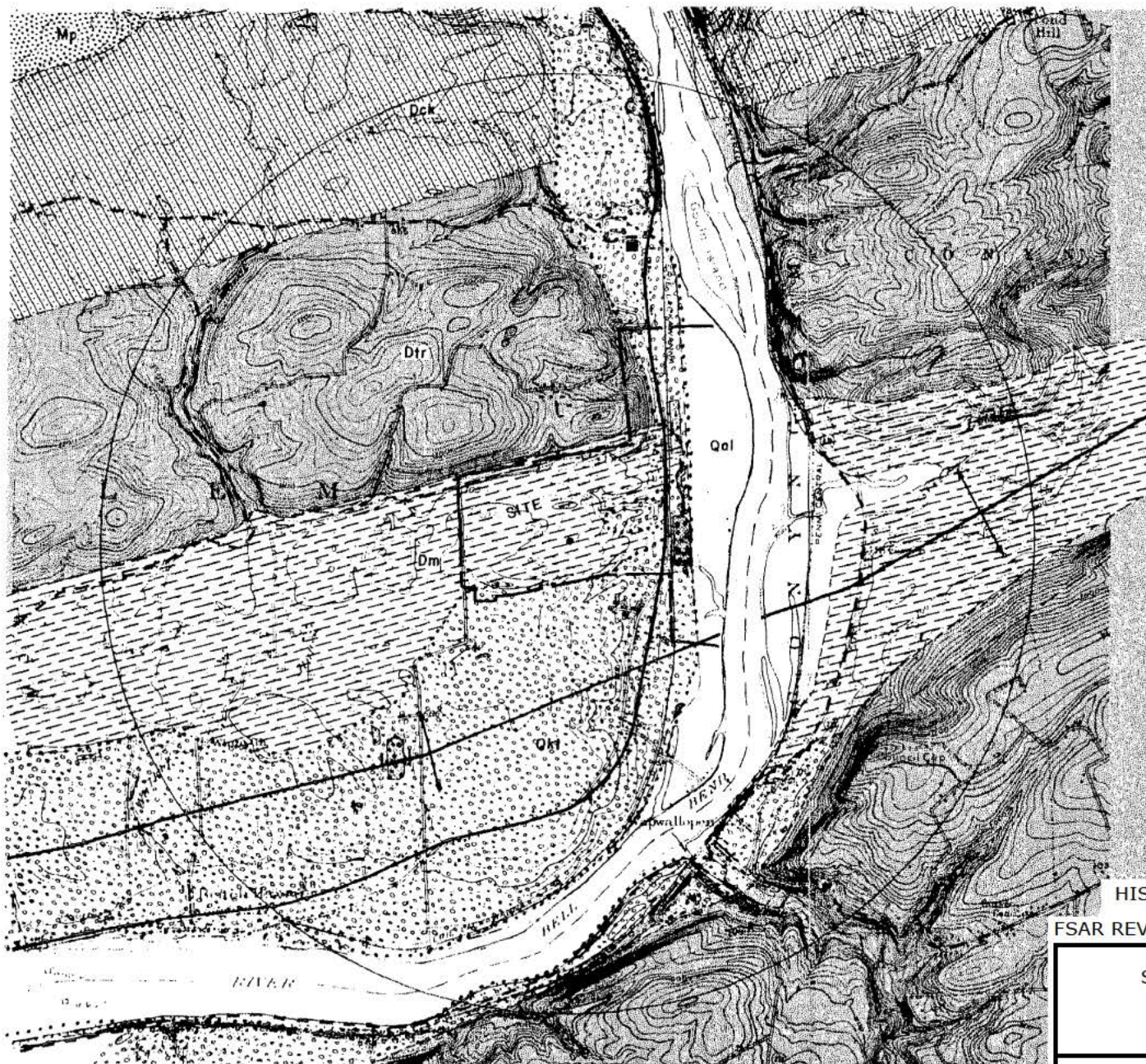
FSAR REV. 65

SUSQUEHANNA STEAM ELECTRIC STATION
UNITS 1 & 2
FINAL SAFETY ANALYSIS REPORT

BEDROCK GEOLOGIC MAP OF AREA
WITHIN 20 MILES OF
SUSQUEHANNA SES

FIGURE 2.4-34, Rev 55

AutoCAD: Figure Fsar 2_4_34.dwg



REFERENCE :

THE BASE FOR THIS MAP WAS PREPARED FROM THE FOLLOWING 7.5 MINUTE U.S.G.S. TOPOGRAPHIC QUADRANGLES: BERWICK PA., 1969; HIFFLINVILLE, PA., 1969; SYBERTSVILLE, PA. 1969. CONTACTS WERE DETERMINED DURING FIELD MAPPING PERFORMED BY DAMES & MOORE IN SPRING OF 1977.

SYMBOL :

- STATION PROPERTY BOUNDARY
- - - APPROXIMATE STRATIGRAPHIC CONTACT
- + BERWICK ANTICLINE

LEGEND :

- Qal QUATERNARY ALLUVIUM
- Qkt PLEISTOCENE KAME TERRACE
- MISSISSIPPIAN
- Mp POCONO FORMATION
- DEVONIAN
- Dck CATSKILL FORMATION
- Dtr TRIMMERS ROCK FORMATION
- Dm MAHANTANGO FORMATION



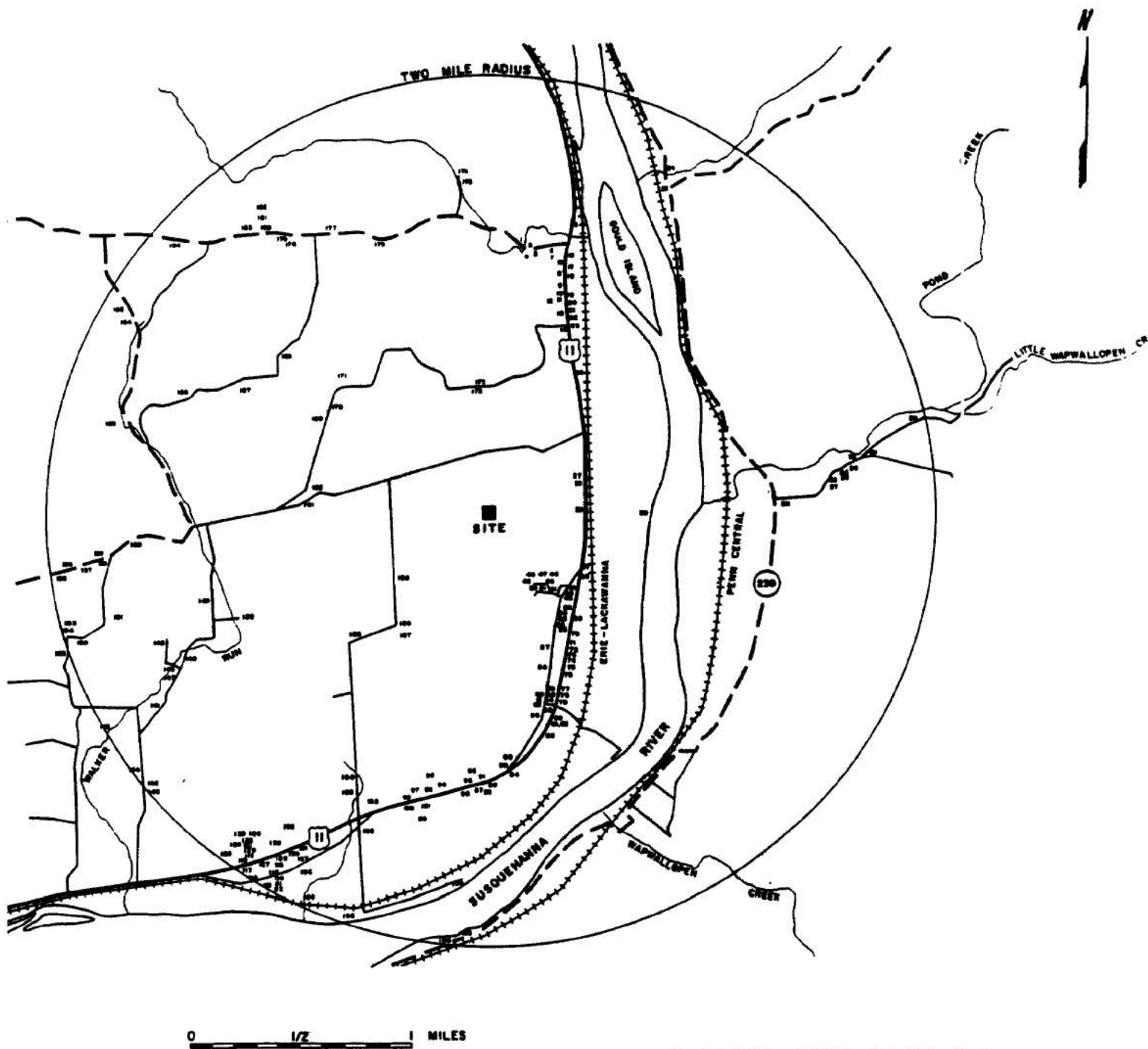
HISTORICAL

FSAR REV. 65

SUSQUEHANNA STEAM ELECTRIC STATION
UNITS 1 & 2
FINAL SAFETY ANALYSIS REPORT

GEOLOGIC MAP OF AREA
WITHIN TWO MILES
OF THE STATION

FIGURE 2.4-36, Rev 55



NOTE:
NUMBERS INDICATE APPROXIMATE LOCATION OF WELLS

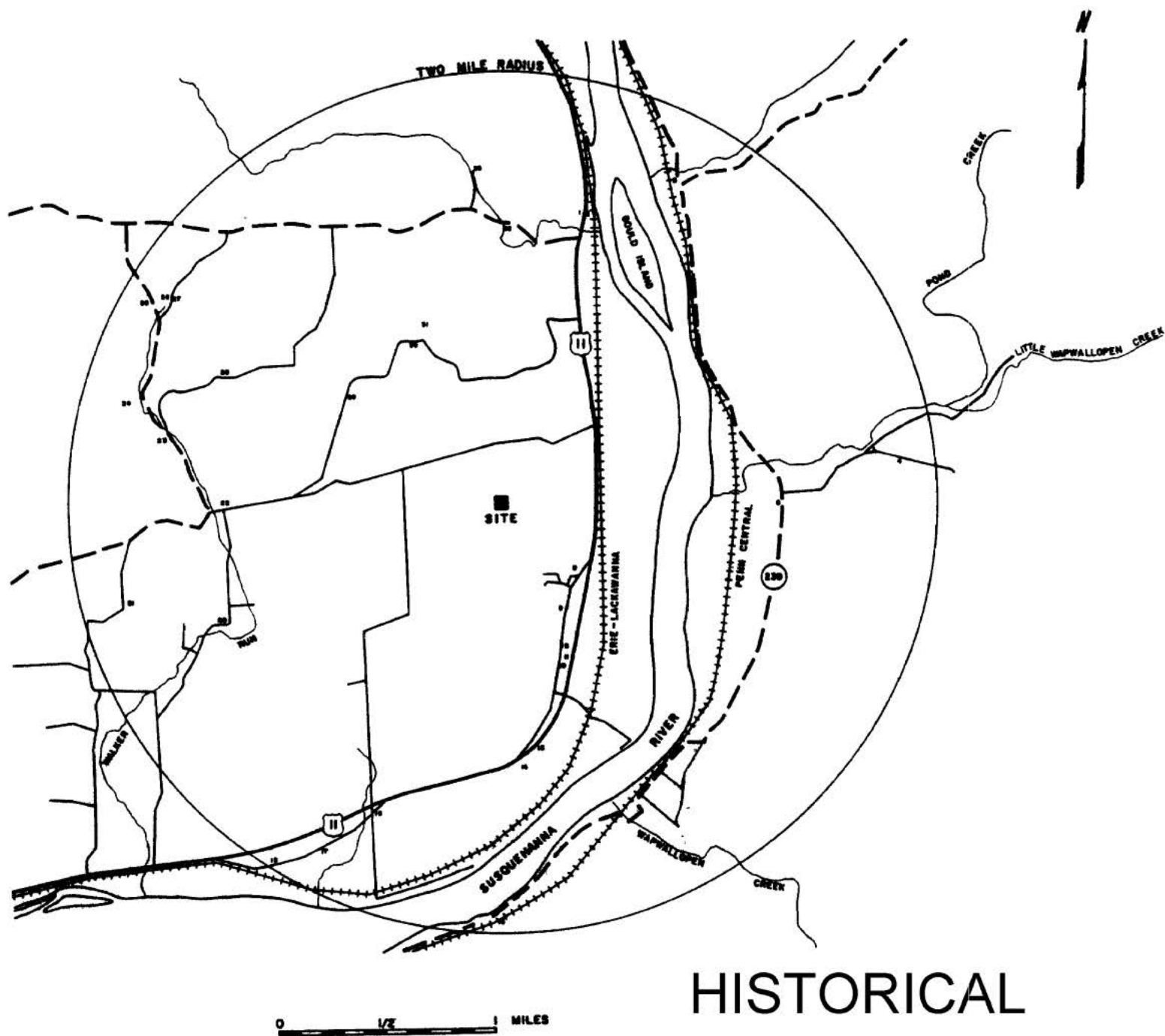
HISTORICAL

FSAR REV. 65

SUSQUEHANNA STEAM ELECTRIC STATION
UNITS 1 & 2
FINAL SAFETY ANALYSIS REPORT

WATER WELLS
WITHIN TWO MILES
OF THE STATION

FIGURE 2.4-37, Rev 55



HISTORICAL

NOTE:
NUMBERS INDICATE APPROXIMATE LOCATION OF SPRINGS

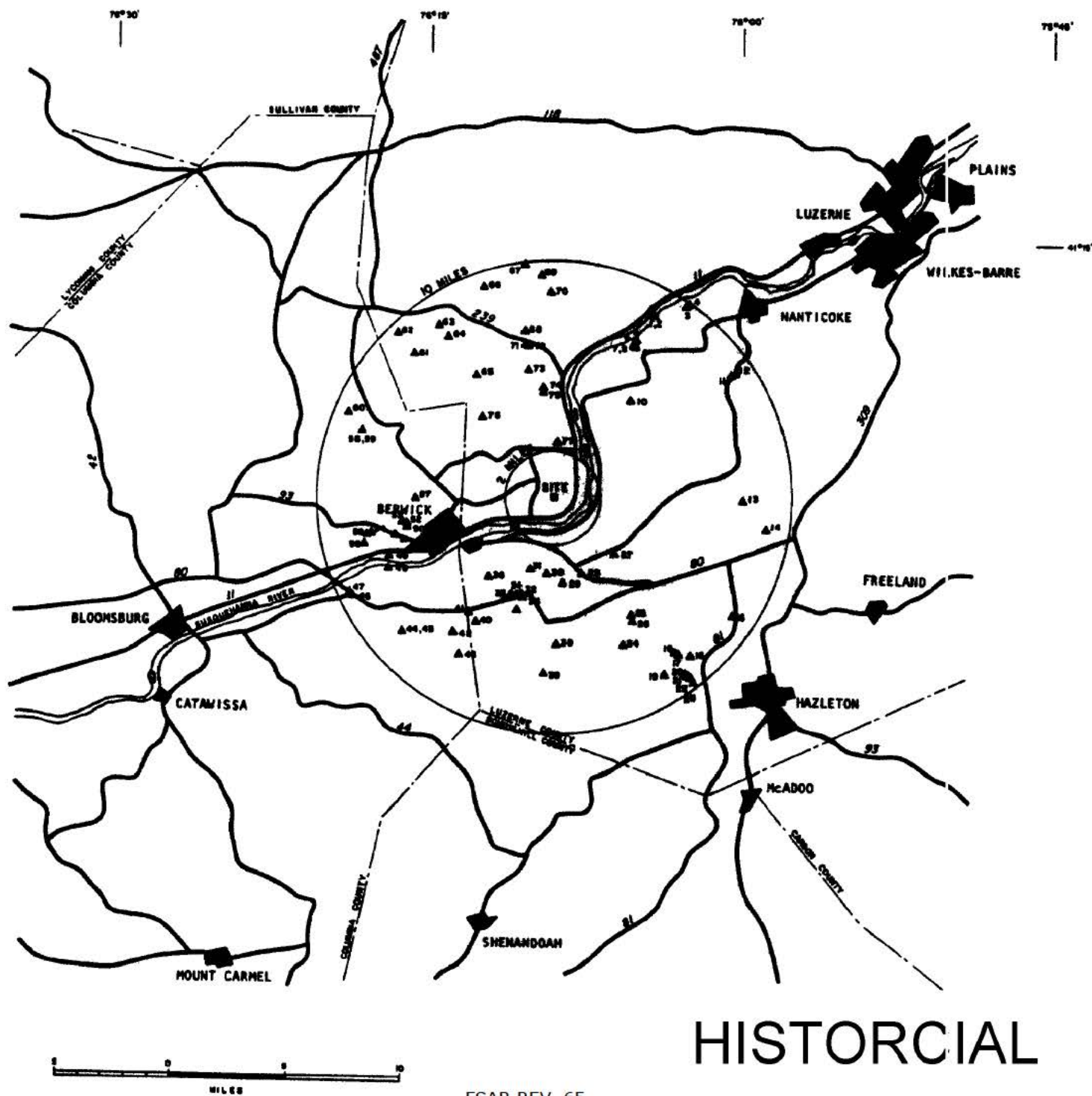
FSAR REV. 65

SUSQUEHANNA STEAM ELECTRIC STATION
UNITS 1 & 2
FINAL SAFETY ANALYSIS REPORT

SPRINGS USED FOR WATER SUPPLY
WITHIN TWO MILES OF
THE STATION

FIGURE 2.4-38, Rev 55

AutoCAD: Figure Fsar 2_4_38.dwg



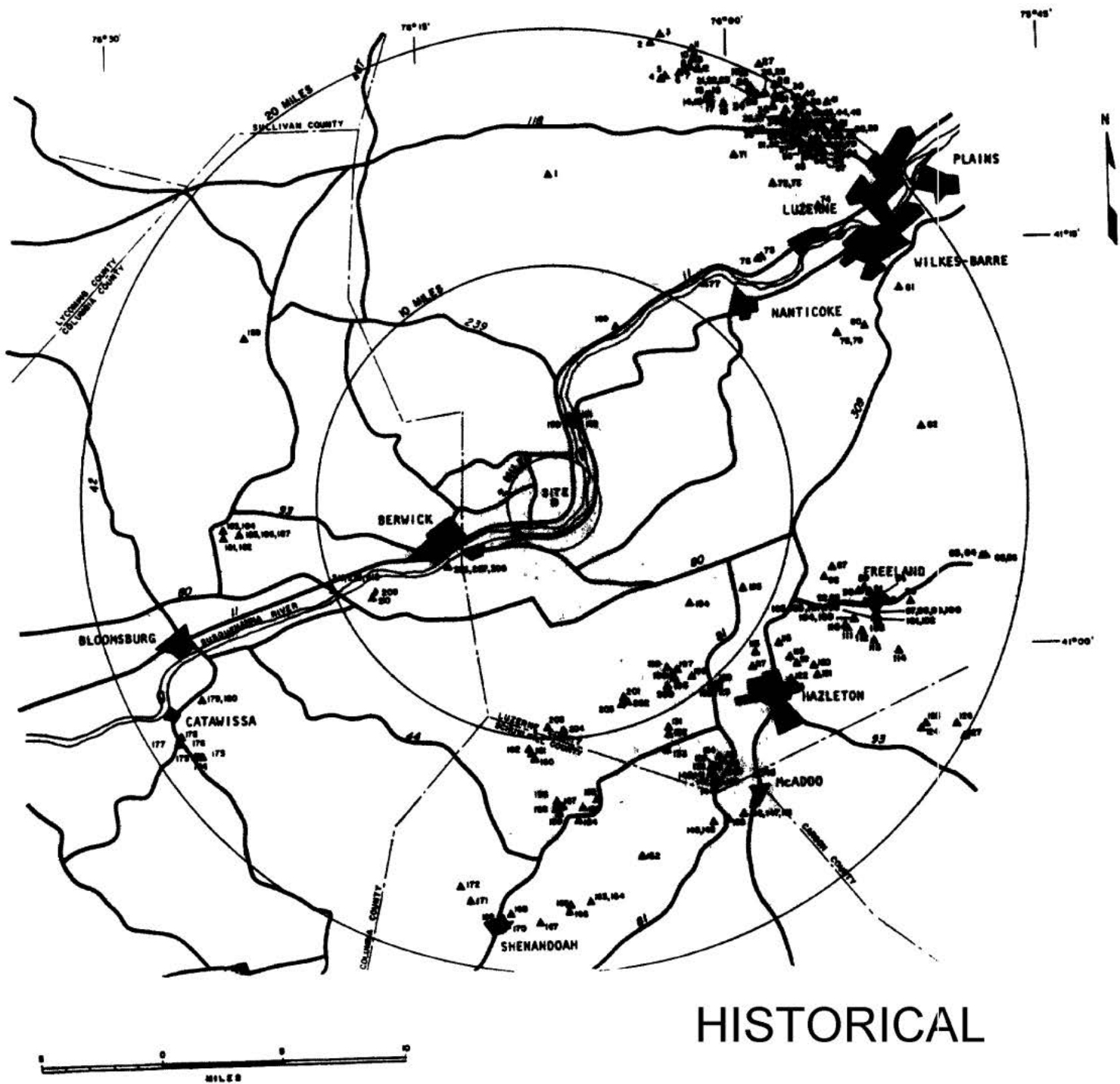
FSAR REV. 65

SUSQUEHANNA STEAM ELECTRIC STATION
UNITS 1 & 2
FINAL SAFETY ANALYSIS REPORT

MAJOR WATER WELLS
TWO TO TEN MILES FROM
THE STATION
EXCEPTING PUBLIC SUPPLY WELLS

FIGURE 2.4-39, Rev 55

AutoCAD: Figure Fsar 2_4_39.dwg



HISTORICAL

FSAR REV. 65

SUSQUEHANNA STEAM ELECTRIC STATION
UNITS 1 & 2
FINAL SAFETY ANALYSIS REPORT

PUBLIC SUPPLY WELLS
TWO TO TWENTY MILES
FROM THE STATION

FIGURE 2.4-40, Rev 55

AutoCAD: Figure Fsar 2_4_40.dwg

Security-Related Information
Figure Withheld Under 10 CFR 2.390

SUSQUEHANNA STEAM ELECTRIC STATION UNITS 1 & 2 FINAL SAFETY ANALYSIS REPORT
MAP OF SUSQUEHANNA SES SHOWING ISOPACH CONTOURS OF OVERBURDEN THICKNESS
FIGURE 2.4-41, Rev 55

Security-Related Information
Figure Withheld Under 10 CFR 2.390

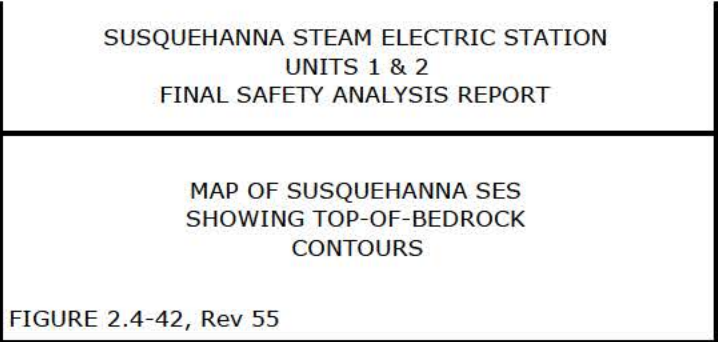
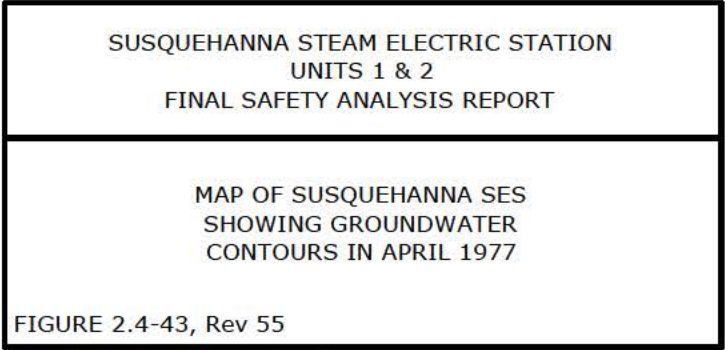
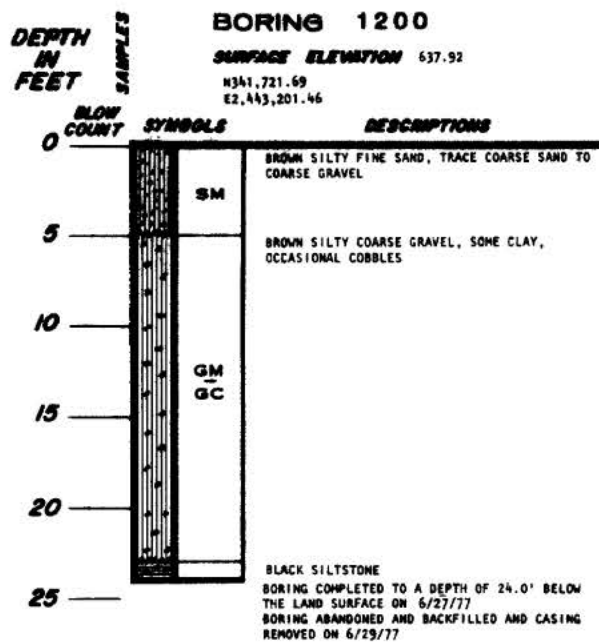


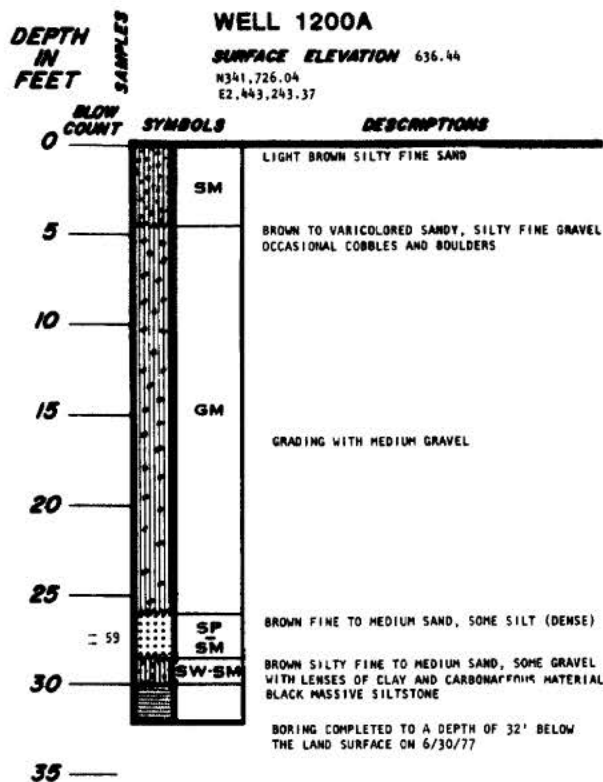
FIGURE 2.4-42, Rev 55

Security-Related Information
Figure Withheld Under 10 CFR 2.390



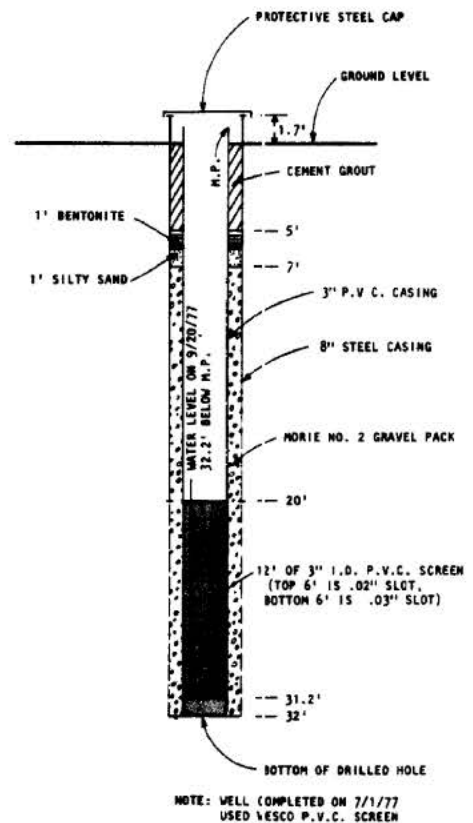


LOG OF BORING 1200



LOG OF WELL 1200A

HISTORICAL



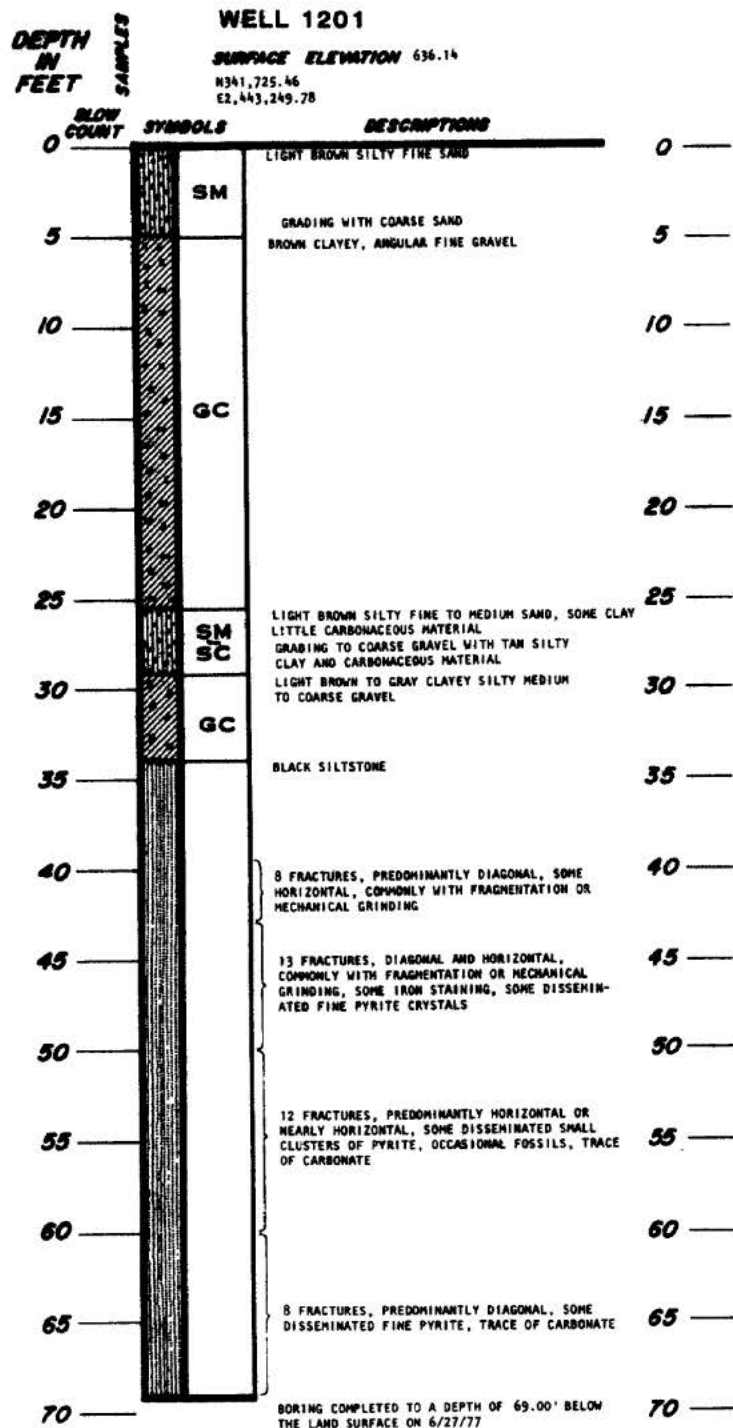
FSAR REV. 65

SUSQUEHANNA STEAM ELECTRIC STATION
UNITS 1 & 2
FINAL SAFETY ANALYSIS REPORT

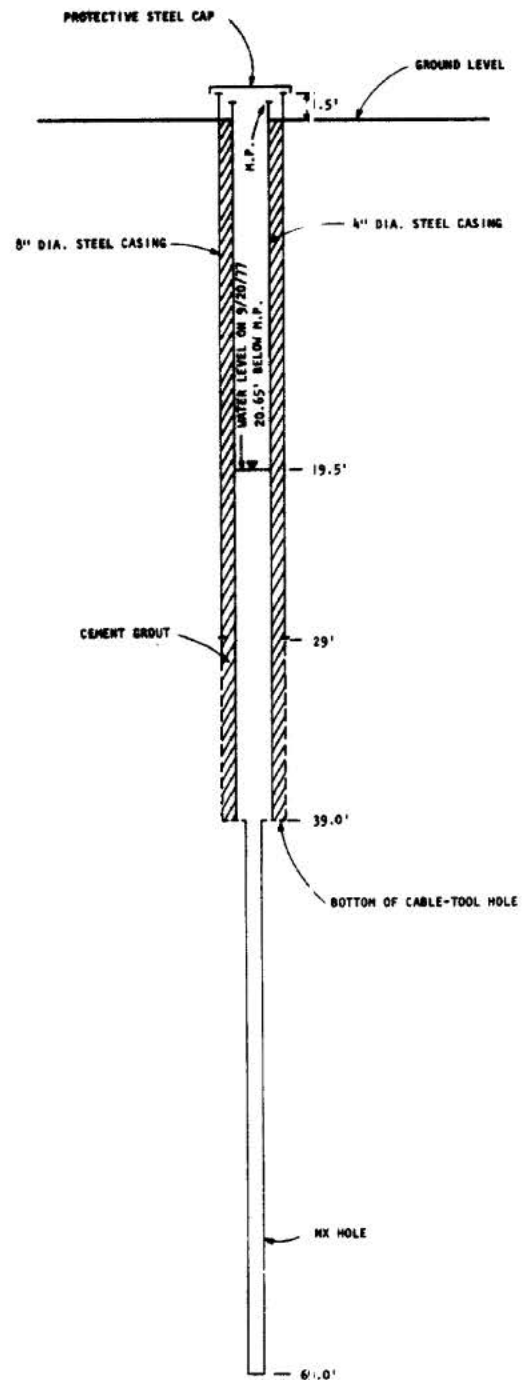
LOG OF BORING AND OBSERVATION WELL
CONSTRUCTION DETAILS - 1200, 1200A

FIGURE 2.4-44, Rev 55

AutoCAD: Figure Fsar 2_4_44.dwg



LOG OF WELL 1201



NOTE: WELL COMPLETED ON 6/27/77

CONSTRUCTION DETAILS
 OF WELL 1201

FSAR REV. 65

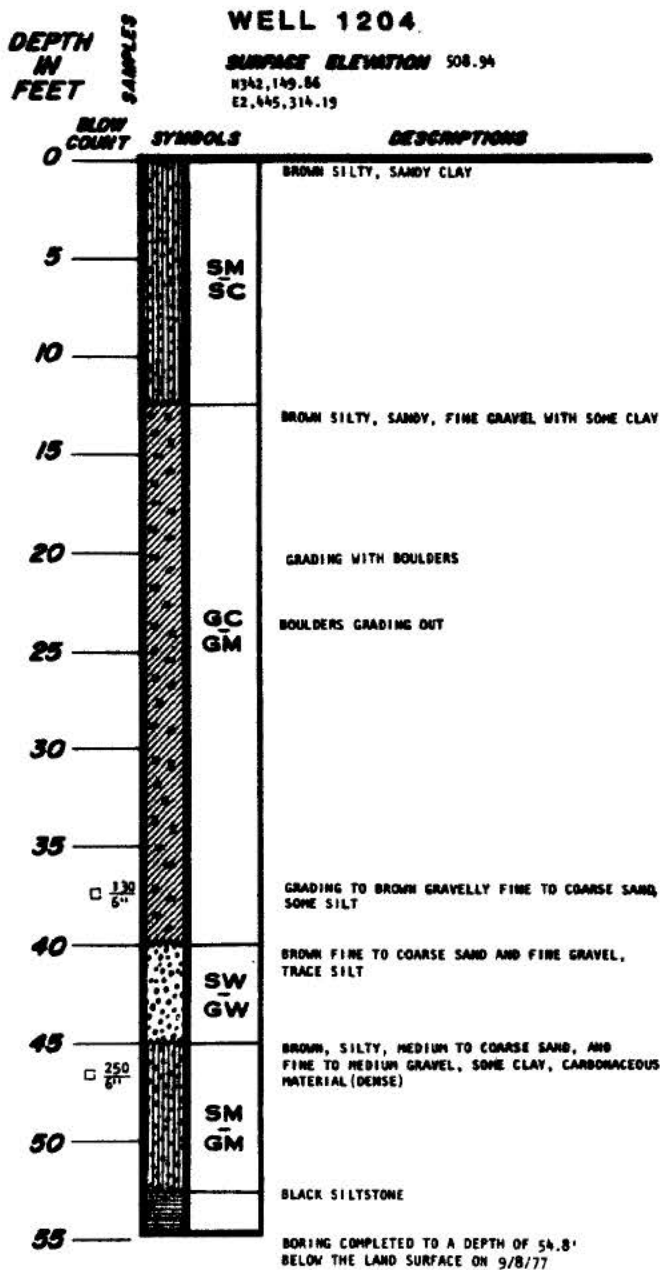
SUSQUEHANNA STEAM ELECTRIC STATION
 UNITS 1 & 2
 FINAL SAFETY ANALYSIS REPORT

LOG OF BORING AND OBSERVATION WELL
 CONSTRUCTION DETAILS - 1201

FIGURE 2.4-45, Rev 55

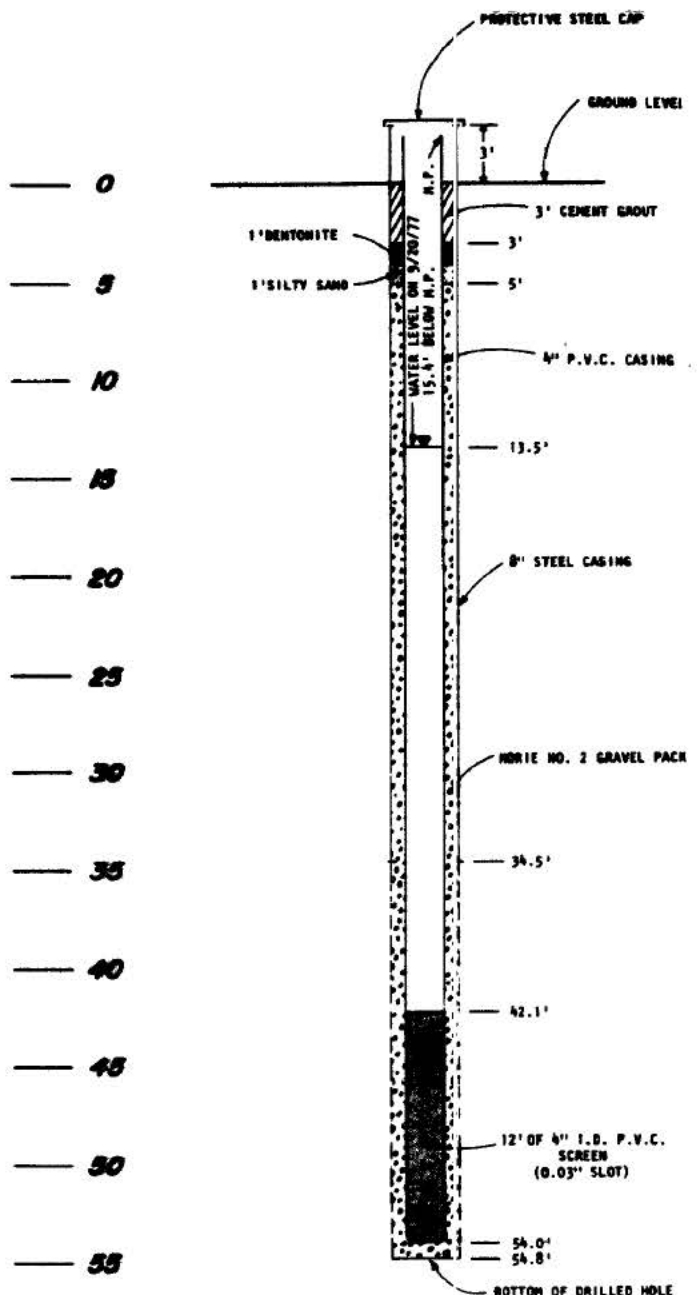
AutoCAD: Figure Fsar 2_4_45.dwg

HISTORICAL



LOG OF WELL 1204

HISTORICAL



CONSTRUCTION DETAILS
 OF WELL 1204

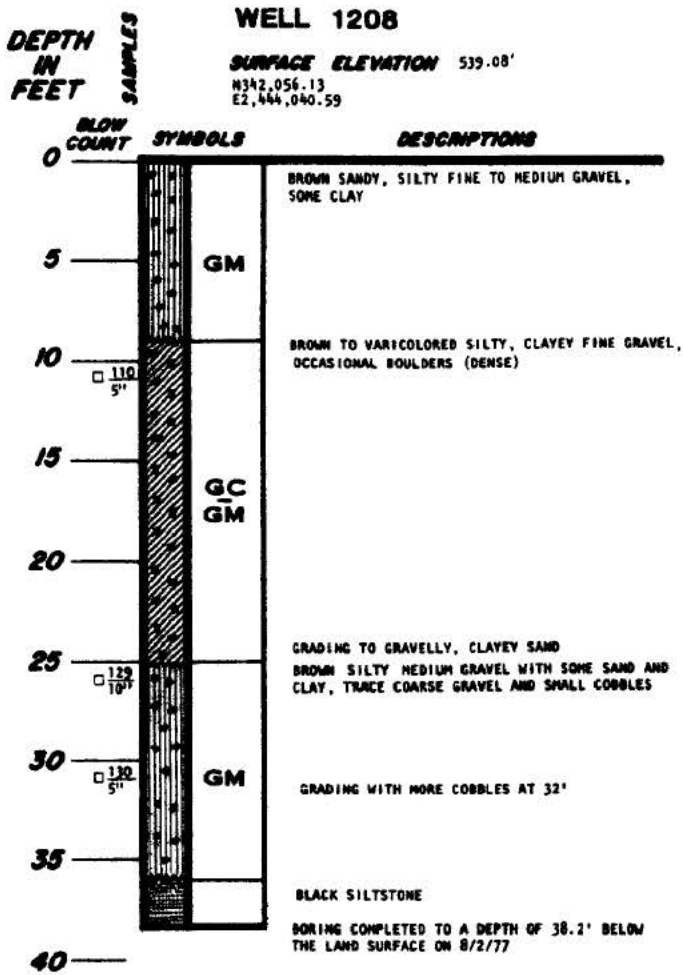
FSAR REV. 65

SUSQUEHANNA STEAM ELECTRIC STATION
 UNITS 1 & 2
 FINAL SAFETY ANALYSIS REPORT

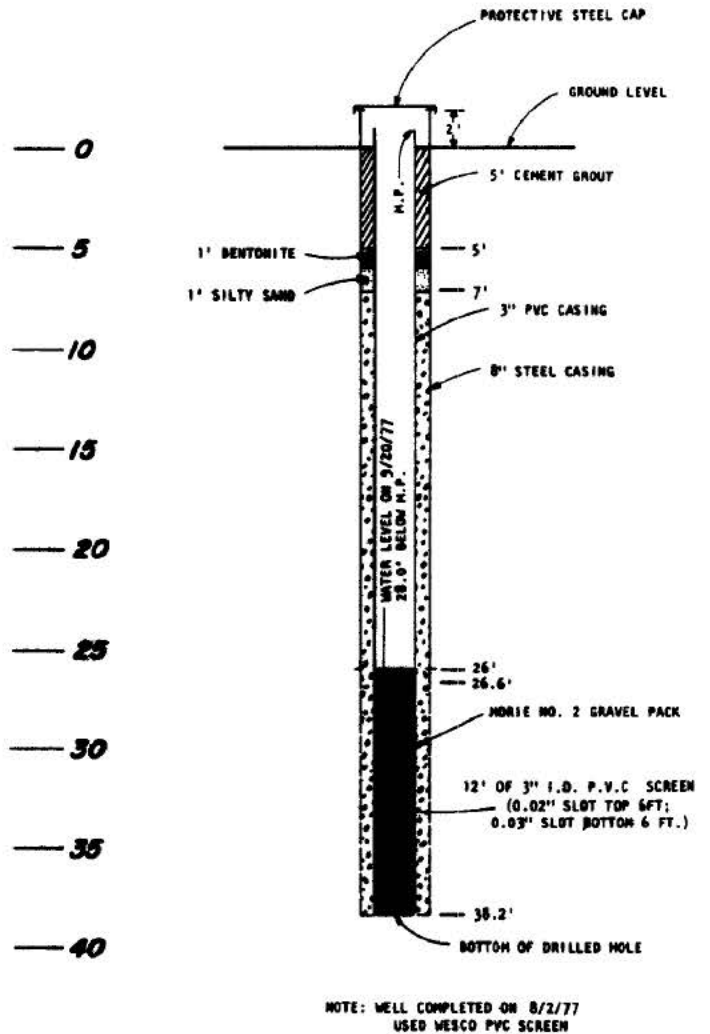
LOG OF BORING AND OBSERVATION WELL
 CONSTRUCTION DETAILS - 1204

FIGURE 2.4-46, Rev 55

AutoCAD: Figure Fsar 2_4_46.dwg



LOG OF WELL 1208



CONSTRUCTION DETAILS
OF WELL 1208

HISTORICAL

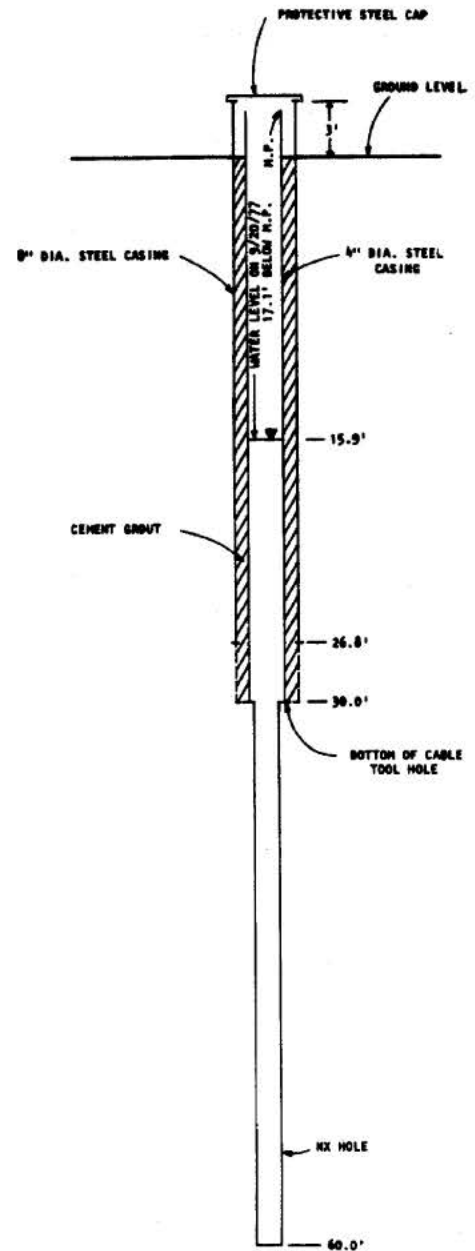
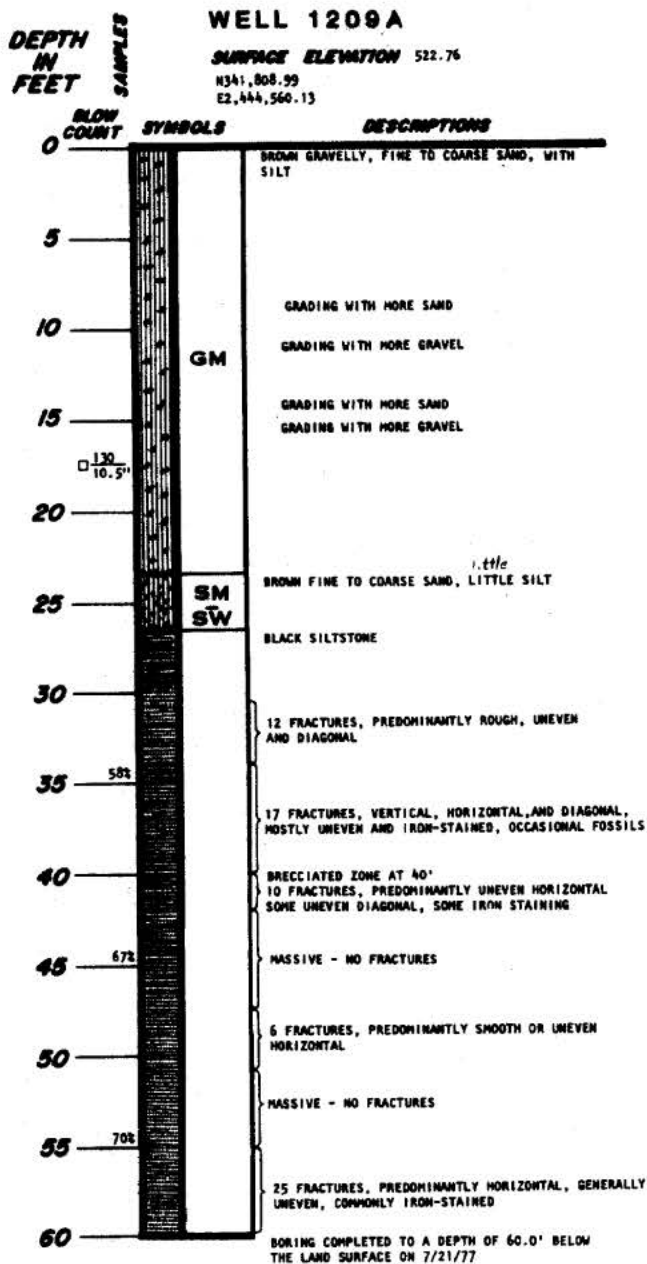
FSAR REV. 65

SUSQUEHANNA STEAM ELECTRIC STATION
UNITS 1 & 2
FINAL SAFETY ANALYSIS REPORT

LOG OF BORING AND OBSERVATION WELL
CONSTRUCTION DETAILS - 1208

FIGURE 2.4-47, Rev 55

AutoCAD: Figure Fsar 2_4_47.dwg



NOTE: WELL COMPLETED ON 7/22/77

LOG OF WELL 1209A

HISTORICAL

CONSTRUCTION DETAILS OF WELL 1209A

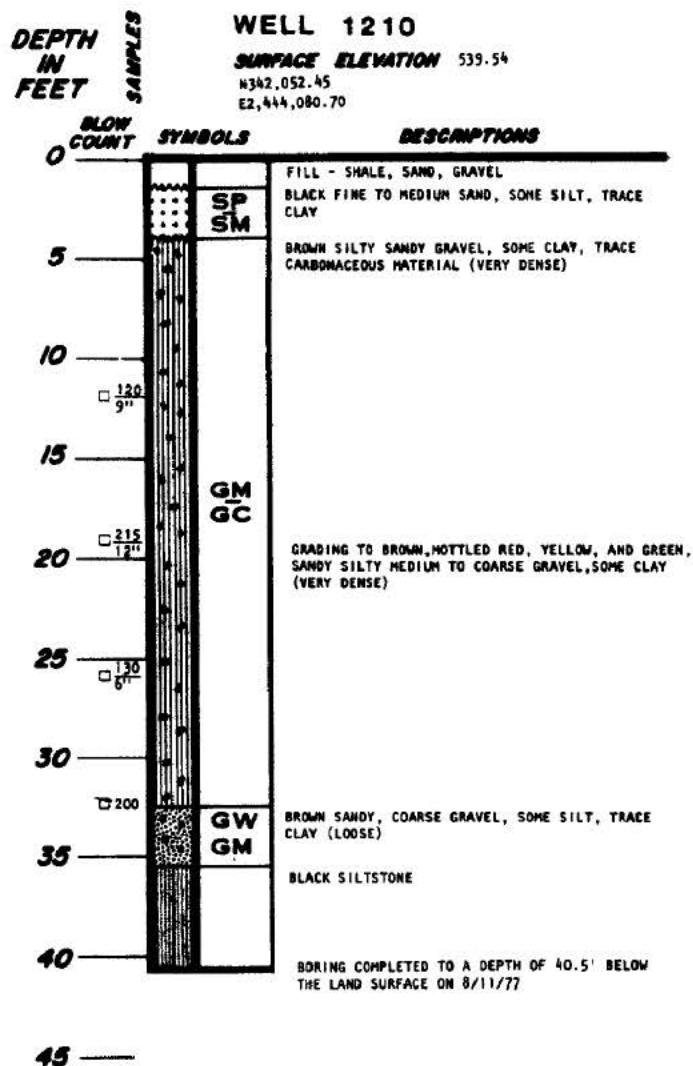
FSAR REV. 65

SUSQUEHANNA STEAM ELECTRIC STATION
UNITS 1 & 2
FINAL SAFETY ANALYSIS REPORT

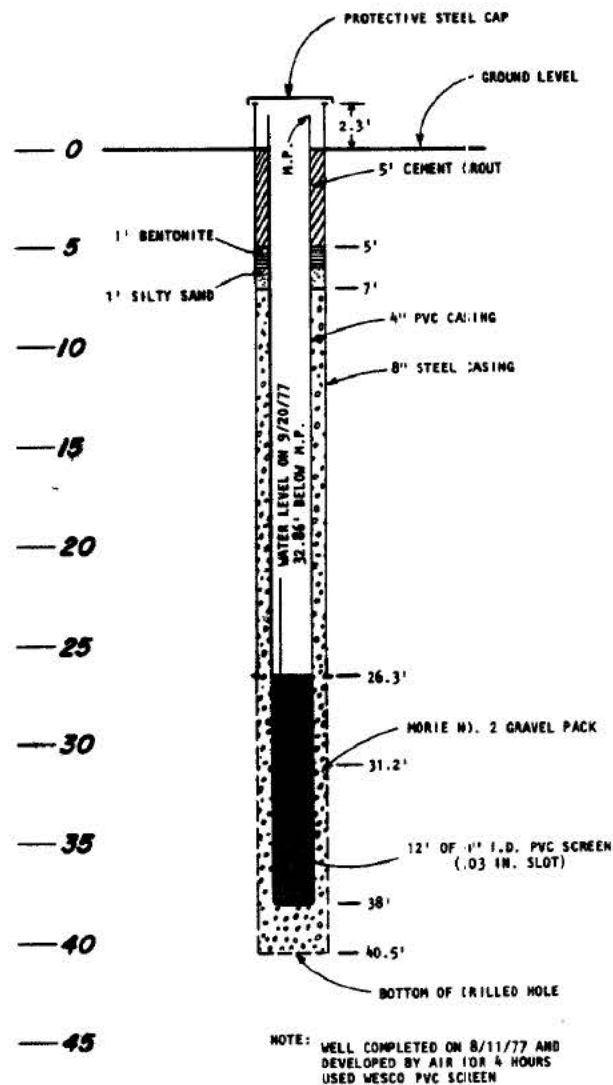
LOG OF BORING AND OBSERVATION WELL
CONSTRUCTION DETAILS - 1209A

FIGURE 2.4-48, Rev 55

AutoCAD: Figure Fsar 2_4_48.dwg



LOG OF WELL 1210



CONSTRUCTION DETAILS OF WELL 1210

HISTORICAL

FSAR REV. 65

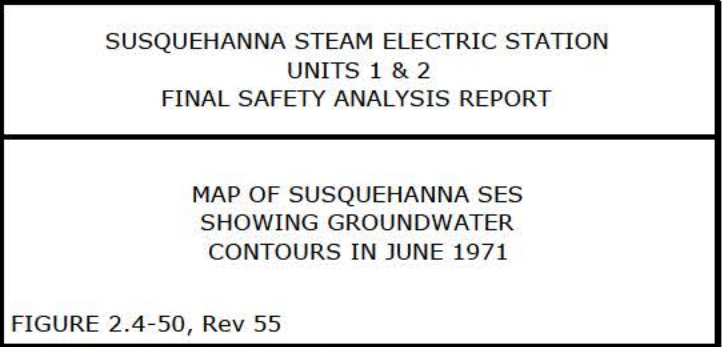
SUSQUEHANNA STEAM ELECTRIC STATION
 UNITS 1 & 2
 FINAL SAFETY ANALYSIS REPORT

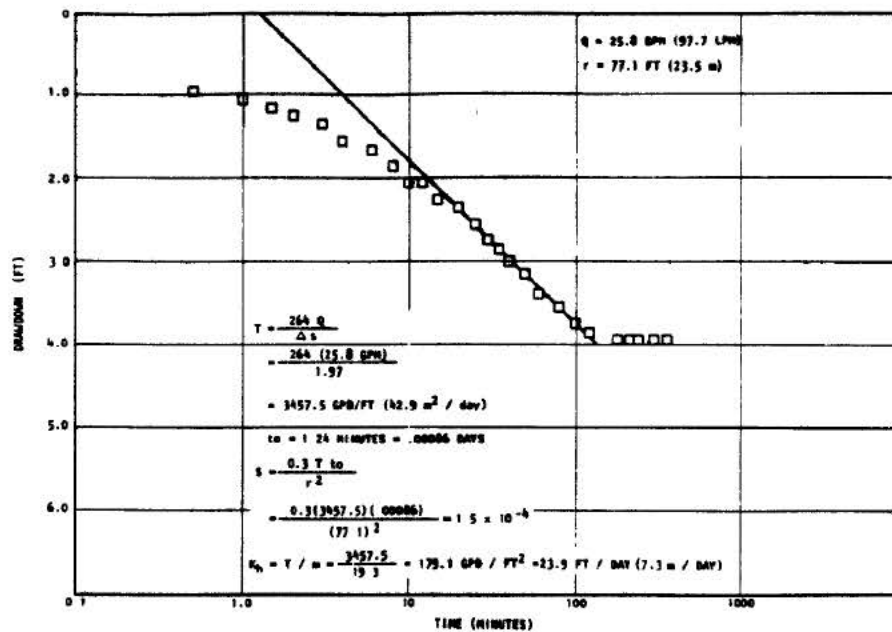
LOG OF BORING AND OBSERVATION WELL
 CONSTRUCTION DETAILS - 1210

FIGURE 2.4-49, Rev 55

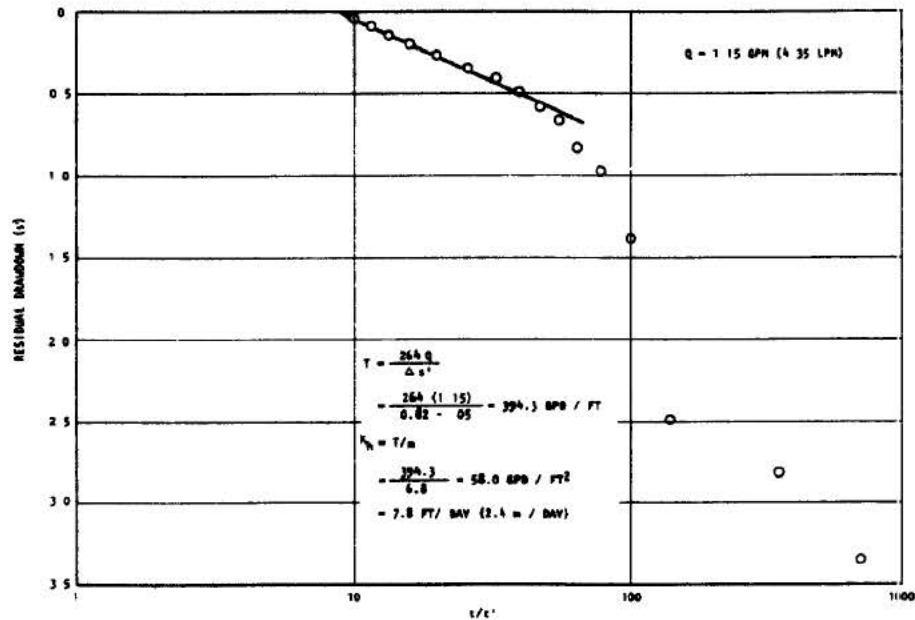
AutoCAD: Figure Fsar 2_4_49.dwg

Security-Related Information
Figure Withheld Under 10 CFR 2.390





**TIME-DRAWDOWN CURVE AT WELL 11
DURING PUMPING OF WELL 1204 - SUSQUEHANNA SES**



**RESIDUAL DRAWDOWN CURVE AT WELL 1210
FOLLOWING 348 MINUTES OF PUMPING WELL 1210
SUSQUEHANNA SES**

FSAR REV. 65

SUSQUEHANNA STEAM ELECTRIC STATION
UNITS 1 & 2
FINAL SAFETY ANALYSIS REPORT

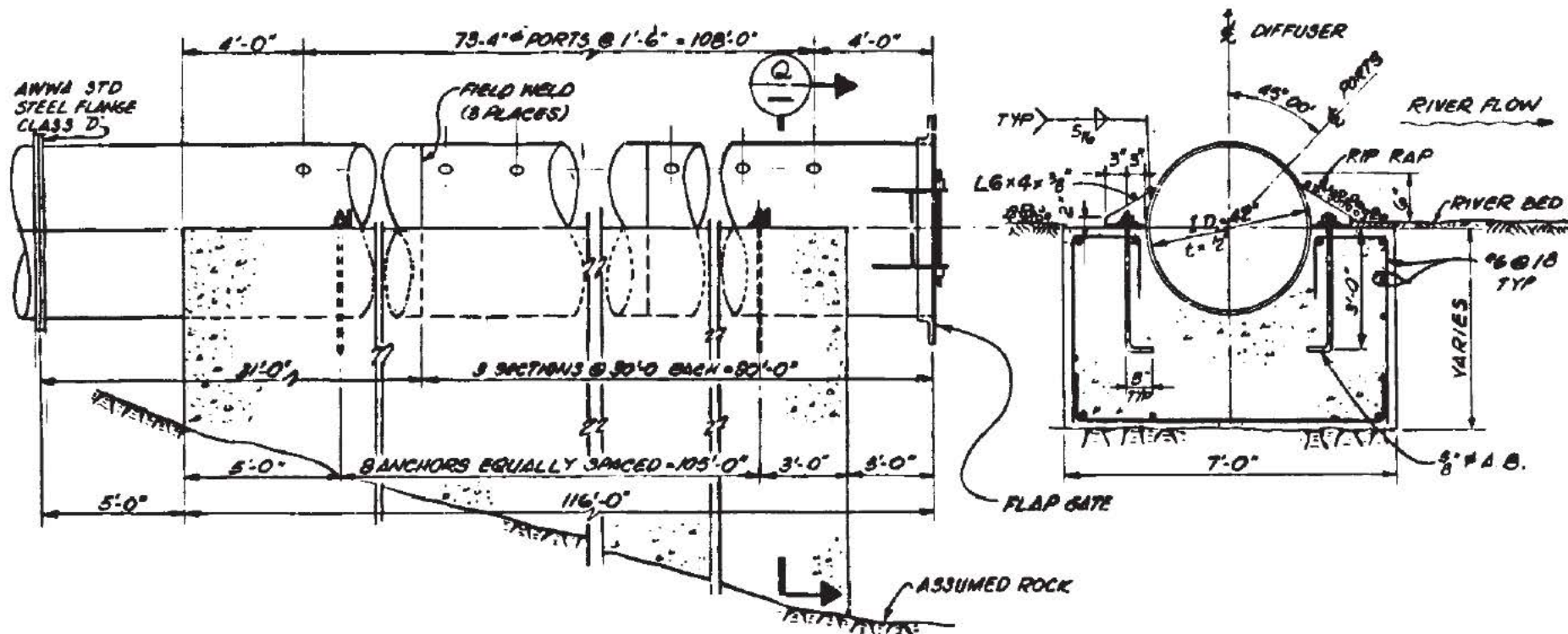
DRAINDOWN CURVES FROM
PUMPING TESTS OF OBSERVATION
WELLS 1204 AND 1210

FIGURE 2.4-51, Rev 55

AutoCAD: Figure Fsar 2_4_51.dwg

HISTORICAL

Security-Related Information
Figure Withheld Under 10 CFR 2.390



FSAR REV. 65

SUSQUEHANNA STEAM ELECTRIC STATION
UNITS 1 & 2
FINAL SAFETY ANALYSIS REPORT

RIVER DISCHARGE DIFFUSER

FIGURE 2.4-53, Rev 47

AutoCAD: Figure Fsar 2_4_53.dwg

THIS FIGURE HAS BEEN
REPLACED BY DWG.
A-12, Sh. 1

FSAR REV. 65

SUSQUEHANNA STEAM ELECTRIC STATION UNITS 1 & 2 FINAL SAFETY ANALYSIS REPORT

Figure 2.4-54 replaced by dwg. A-12, Sh. 1

FIGURE 2.4-54, Rev. 57

AutoCAD Figure 2_4_54.doc

THIS FIGURE HAS BEEN
REPLACED BY DWG.
FF62005, Sh. 1

FSAR REV. 65

SUSQUEHANNA STEAM ELECTRIC STATION UNITS 1 & 2 FINAL SAFETY ANALYSIS REPORT

Figure 2.4-55 replaced by dwg. FF62005, Sh. 1
--

FIGURE 2.4-55, Rev. 55

AutoCAD Figure 2_4_55.doc

THIS FIGURE HAS BEEN
DELETED

FSAR REV. 65

SUSQUEHANNA STEAM ELECTRIC STATION UNITS 1 & 2 FINAL SAFETY ANALYSIS REPORT

Figure Deleted

FIGURE 2.4-54a, Rev. 54

AutoCAD Figure 2_4_54a.doc

2.5 GEOLOGY, SEISMOLOGY, AND GEOTECHNICAL ENGINEERING

2.5.1 BASIC GEOLOGIC AND SEISMIC INFORMATION

2.5.1.1 Regional Geology

2.5.1.1.1 Physiography and Geomorphology

The site is located (Figure 2.5-1) in the Valley and Ridge Physiographic Province which is bordered on the southeast by the Reading Prong and on the northwest by the Appalachian Plateau Physiographic Province (Figure 2.5-2).

The Valley and Ridge Province is characterized by folded Paleozoic sedimentary rocks of varying erosional resistance. These strata form a series of level ridges and intervening valleys which trend generally northeast to southwest. Higher ridges are formed on the more resistant, inclined sandstone whereas lower ridges are underlain by other competent formations. The valleys occur in less resistant limestone and shale.

The Valley and Ridge Province attains a maximum width of about 80 miles along a line drawn northwest through Harrisburg, Pennsylvania. In Pennsylvania, folds generally plunge away from this line to the northeast and to the southwest. Because of the folding, resistant strata form broad, zig-zag outcrop patterns across the province. These strata form steep slopes, that flank anticlinal valleys, and canoe-shaped synclinal valleys. Lithology and structure control the drainage pattern, the principal direction of which is to the southeast. Major drainage generally follows the strike of less competent strata and crosses the strike at water gaps where transverse structures, such as a high concentration of fractures, exist. Minor drainage trends normal to the regional strike or along major fracture sets, and usually intersects major streams at right angles to form a trellis pattern.

The Great Valley Section, in the southeastern third of the province, consists of broad, rolling valleys of low relief formed in Paleozoic soft limestones and calcareous shales. To the southeast, the Reading Prong exposes the oldest rocks (Precambrian) within 50 miles of the site (Figures 2.5-2 and 2.5-3). In general, the Reading Prong consists of high grade metasedimentary and metavolcanic rocks along with dominantly acidic plutonic rocks. These rocks experienced deformation commencing with the Grevillian orogeny about 1 billion years ago which imparted the dominant structural fabric, i.e., foliations, lineations and polyphase folds, present today. Succeeding tectonism during the Paleozoic and Mesozoic eras, and possibly even more recently, have also affected these rocks. According to Drake (Ref. 2.5-1) the rocks of the Reading Prong are allochthonous. The Triassic Lowlands of the Piedmont Province lie to the east and southeast of the Reading Prong, and contain the youngest rocks in eastern Pennsylvania (Figures 2.5-2 and 2.5-3). The rocks in the lowlands are dominantly red clastic sediments with associated basic intrusives and flows. Diabase dikes near Pottstown, Pennsylvania yielded K/Ar whole rock ages of 151 to 198 million years (Ref. 2.5-2, p. 3-25).

Northeast of the site, folds are broader and more open and give way to the gentle synclinal Pocono Plateau Section which is underlain by Devonian sandstone and shale. To the northwest, the Valley and Ridge Province terminates abruptly at the Allegheny Structural Front.

Beyond the front lies the Appalachian Plateaus (Figure 2.5-2), a gently rolling highland formed on broad folds of low structural relief that plunge gently to the southwest. The strata consist predominantly of an upper Paleozoic cyclic sequence of sandstone, shale, limestone and coal.

The Susquehanna River, which flows past the site, has two important features associated with it. First the river makes several sharp bends along its length with the closest being adjacent to the site. East of the site the river maintains a west-southwest course which parallels the regional tectonic fabric. However at Shickshinny, Pennsylvania, about 5 miles north of the site, it makes a sharp right-angle bend and flows in a south-southeast direction for about 5 miles. Just below the site it again swings sharply and resumes its west-southwest flow direction. This phenomenon has been cogently explained by Iltter (Ref. 2.5-). He noted that this area was submerged during the Cretaceous and coastal plain sedimentation ensued. Sedimentation completely covered the pre-existing drainage pattern. Following coastal plain sedimentation, the area underwent broad uplift while the North Branch of the Susquehanna River apparently flowed southeastward, across the Pocono Plateau to Trenton, New Jersey (Ref. 2.5-3, p. 12-13). Tributaries must also have developed on this coastal plain. Following downcutting of the coastal plain sediments the streams encountered bedrock. Of these downcutting streams the present-day Susquehanna River, south of the confluence of the North and West Branches, apparently was able to incise more rapidly than other major streams. This resulted in stream capture and the pronounced bends seen along the river today.

The second feature of import is the buried valley of the Susquehanna. This buried valley occurs in bedrock overlain by a broad, flat plain across which the present-day Susquehanna flows (Ref. 2.5-3, p. 26). It extends upstream as a series of elongate basins, for about 15 miles, from near Nanticoke, Pennsylvania (approximately 10 miles northeast of the site) to just above West Pittston (Ref. 2.5-4, p. 8). This valley is filled with alternating layers of water laid gravel, sand and clay. The development of this valley is attributed to the erosive action of the Wisconsin ice sheet which must have flowed diagonally across the valley (Ref. 2.5-3, p. 27 and 2.5-4, p. 7). Subsequently, this valley was filled with sediment deposited by streams which emanated from this melting ice.

Most of the region, north and east of the site, has been scoured by at least three periods of glaciation in the last 150,000 years (Ref. 2.5-5, p. 15 and 2.5-6). The three major directions of ice advance were postulated as follows: 1) south and southeast from central Ontario, 2) south and southwest from approximately the Adirondack region, and 3) south and southwest from the Hudson Valley by way of the Catskills (Ref. 2.5-5, p. 18). Effects of glacial scouring are most notable on the Pocono Plateau.

At the present time, there is no positive evidence that any pre-Illinoian glaciation occurred in northeastern Pennsylvania although elsewhere in the eastern United States, such evidence does exist for pre-Illinoian glaciation. It is thus suggested that it should also have occurred here (Ref. 2.5-6). The recorded glacial events include the Illinoian and two stages of the Wisconsinan, the Altonian which spans the interval from about 70,000 years to about 28,000 years B.P., and the Woodfordian which lasted from about 21,000 years to approximately 13,000 years B.P.

In earlier literature (Ref. 2.5-5) the terms Altonian and Woodfordian were not utilized. Instead the Wisconsinan was divided into the Binghamton, Olean, Valley Heads and Mankato substages. However, it is not precisely known how the Altonian and Woodfordian subdivisions

relate to the older terms except that the Mankato is somewhat younger than the Woodfordian (Ref. 2.5-6).

In the site region a lobe of Illinoian ice extended down the valley of the Susquehanna River from just above Berwick to the West Branch of the Susquehanna at Northumberland, Pennsylvania. The exposed length of deposits left by this lobe is about 40 miles whereas the maximum width does not exceed 8 miles. Illinoian drift is present on the slopes to within 60 feet of the present river level suggesting that only moderate deepening of the Susquehanna Valley has occurred since deposition of the Illinoian drift (Ref. 2.5-7, p. 24-25).

Valley trains of Wisconsinan gravel were examined along the Susquehanna River and its tributaries by Leverett (Ref. 2.5-7). He noted that from just east of Berwick downstream (westward) to the West Branch at Northumberland, the surface of a Wisconsinan gravel train is well defined and generally occurs at about 40 to 60 feet above the river.

Moderately eroded terraces underlain by freshly appearing gravels mark the upper level attained by waters derived from the Wisconsinan ice sheet along the Susquehanna River and its tributaries. These terraces occur at lower elevations than those exposing Illinoian gravel and have also been much less extensively eroded than Illinoian gravel (Ref. 2.5-7, p. 16). In general the relative heights of the terrace levels representing each of the four Wisconsinan sub-stages are fairly constant. For example, in the site vicinity relative heights for the Mankato, Valley Heads, Binghamton and Olean are 9, 15, 30 and 45 feet respectively (Ref. 2.5-5, p. 77). The surfaces of most of the terraces have been eroded subjecting the observed height of any terrace to an error of as much as 30 percent. However, no evidence is presented indicating differential vertical offset of these terraces.

At Berwick several well developed kame terraces and terrace remnants of frontal kames which formed at the end of marginal kames occur (Ref. 2.5-, p. 91). The four lowest marginal kames were identified by Peltier as the First Olean, Second Olean, Third Olean, and Fourth Olean kame terraces which are respectively 86, 98, 110, and 158 feet above the river.

2.5.1.1.2 Stratigraphy and Lithology

2.5.1.1.2.1 The Appalachian Basin

The Valley and Ridge Province, in which the site is located, is part of a structural entity known as the Appalachian Basin. As defined by Colton (Ref. 2.5-8, p. 6-7), the Appalachian Basin is not a physiographic province. Rather, it is an elongate feature extending from the Canadian Shield in southern Quebec and Ontario, southwestward to central Alabama (Figure 2.5-4). It is bounded on the west by the Findlay Arch and on the south by the boundary between Paleozoic and Cretaceous strata. The eastern edge is marked by the surface contact between slightly-to-unmetamorphosed Paleozoic rocks on the west and more intensely metamorphosed Paleozoic and Precambrian rock on the east. In Pennsylvania this boundary coincides with the boundary between the Valley and Ridge and Piedmont Physiographic Provinces.

Isopach maps and stratigraphic columns show the respective thicknesses and relationships of the Cambrian through Pennsylvanian sequences in the Appalachian Basin (Figures 2.5-5 and 2.5-6).

In the Appalachian Basin, as outlined by Colton (Ref. 2.5-8), the Lower Cambrian clastic sequence is a wedge-shaped mass which is thickest along the eastern margin of the basin and thinnest along the northern and western margins. The rocks along the eastern margin are dominantly Early Cambrian whereas the rocks along the northern and western margins are mainly Late Cambrian. The Lower Cambrian sequence is conformably overlain in most of the Appalachian Basin by a suite of dominantly carbonate rocks with lesser amounts of quartz sandstone. This overlying suite consists mainly of rocks ranging in age from Middle and Late Cambrian to Early and Middle Ordovician and was designated by Colton (Ref. 2.5-8, p. 19) as the Cambrian-Ordovician carbonate sequence. This sequence ranges in thickness from about 600 ft. in northern New York State to a little more than 10,000 ft. in southeastern Tennessee. A belt of maximum thickness extends along, and approximately parallel to, the eastern edge of the Appalachian Basin from southeastern New York State to northern Alabama (Ref. 2.5-8, p. 23).

This carbonate sequence is conformably overlain in most of the basin by dominantly non-calcareous clastic rocks, the majority of which are Late Ordovician in age. These Upper Ordovician clastic rocks are thickest along the northeastern margin of the basin in Pennsylvania and show a generally uniform thinning to the north, west and southwest. An exception to this generally uniform pattern of thinning occurs in Pennsylvania and adjacent New York State where the sequence thins more abruptly against the southwestern extension of the Adirondack axis (Ref. 2.5-8, p. 23).

Although the boundary between these rocks and the older Cambrian-Ordovician sequence is conformable, the boundary with the overlying Silurian clastics is marked by an unconformity in the northeast and southwest portions of the Appalachian Basin. "Volumetrically the unconformity is greatest in eastern Pennsylvania and contiguous parts of New Jersey" (Ref. 2.5-8, p. 23). This unconformity was considered by Colton as evidence of Late Ordovician or Early Silurian diastrophism.

The Early Silurian rocks are mainly clastic and extend across most of the Appalachian Basin. These rocks are thickest (2,600 ft.) and coarsest in the northeastern part of the basin where they are composed mainly of sandstone and conglomerate.

Carbonate rocks, classified by Colton (Ref. 2.5-8, p. 31) as the Silurian-Devonian carbonate sequence, range in age from Middle Silurian to early Middle Devonian and occur throughout much of the basin. They, like the older sequences, are thickest in the east and thinnest in the west. The thickest section is found in northeastern Pennsylvania where it is about 3300 ft. thick. In northeastern Pennsylvania the lower half of this sequence actually consists of a thick wedge of red clastic rocks comprising, among others, the Bloomsburg Red Beds. West, northwest and southwest of this area the red beds grade into an alternating suite of variegated shale and siltstone, carbonates and evaporites. The margins of this suite are predominantly dolomite and limestone.

Rocks of Middle and Late Devonian age consist of a moderately thick sequence of shale, mudrock, siltstone and sandstone and extend throughout most of the basin. In most areas these Middle to Upper Devonian clastic rocks rest conformably on the strata of the Silurian-Devonian carbonate sequence. Like the underlying rocks this Devonian suite is wedge-shaped with the thickest part near the eastern margin of the basin and the thinnest part near the western periphery. The northeastern part of the basin, which includes east-central Pennsylvania, contains the thickest accumulation (more than 10,000 ft.) dominated by coarse-grained sedimentary rocks (including red beds). As the thickness decreases the average grain

size of the rocks shows a corresponding diminution, being medium-grained where the rocks are of intermediate thickness and fine-grained where the section is thinnest (Ref. 2.5-8, p. 34).

The Middle to Upper Devonian clastic suite is conformably overlain by Mississippian rocks in most of the basin, but the contact is slightly disconformable along much of the eastern margin. However, in parts of northeastern Pennsylvania the entire Mississippian is missing. This anomalous unconformity is probably due to erosion prior to Pennsylvanian sedimentation (Ref. 2.5-9, p. 35). Generally the Mississippian sequence defines a crudely wedge-shaped mass. The greatest accumulation occurs in southeastern Virginia (6800 ft.), but Wood (Ref. 2.5-10, p. C39) reported a thickness exceeding 6,000 ft. in eastern Pennsylvania.

Pennsylvanian rocks overlie those of Mississippian age with the basal boundary, in much of the basin, marked by a sudden change from older, thinly-bedded, relatively fine-grained rocks to younger, massively-bedded, conglomeratic quartz sandstone. The Pennsylvanian sequence is commonly thickest and coarsest-grained along the eastern periphery. In eastern Pennsylvania, where only the lower half of the Pennsylvanian is preserved, a thickness of 4600 ft. of principally sandstone, conglomeratic sandstone and conglomerate was recorded (Ref. 2.5-10).

2.5.1.1.2.2 The Valley and Ridge Province

The Valley and Ridge is a physiographic province which is situated within the Appalachian Basin and consists of a nearly continuous sequence of rocks extending from the Cambrian to the Pennsylvanian. Within this sequence are two major clastic intervals, the Cambrian-Silurian Taconic cycle and the Devonian-Pennsylvanian Appalachian cycle (Ref. 2.5-11, pg. 231). Each cycle consists of pre-orogenic carbonates and orthoquartzites overlain by turbidite flysch deposits which are, in turn, succeeded by molasse. The first phase of the older cycle is represented by Cambrian to Middle Ordovician carbonates (Ref. 2.5-12, p. 4). The flysch phase is represented by siltstone, silty-shale and gray sandstone of the Upper Ordovician Reedsville. The molasse phase comprises the Upper Ordovician Bald Eagle and Juniata Formations and the Lower Silurian Tuscarora Formation. The transition from the molasse phase to the renewal of marine conditions is delineated by the successively younger Rose Hill, Keefer, Mifflintown and Bloomsburg Formations of Middle Silurian age. Upper Silurian to Lower Devonian carbonates (Wills Creek to Onondaga) identify the first phase of the Appalachian cycle (Ref. 2.5-12, p. 4). Within this younger cycle direct passage from the carbonate phase to the turbidite phase was interrupted by deposition of a local sub-aqueous delta identified in central Pennsylvania as the Mahantango Formation. Following sedimentation of the Mahantango, the turbidite beds of the Upper Devonian Trimmers Rock Formation, constituting the second phase of the Appalachian cycle, were laid down. The molasse phase was initiated by the Upper Devonian Catskill Formation which, at an outcrop along the Lehigh River (Figure 2.5-7), is in gradational contact with the underlying Trimmers Rock (Ref. 2.5-13, p. 8). The molasse phase culminated twice, first in the Mississippian Pocono Formation and later in Pennsylvanian rocks (Ref. 2.5-12, p. 4).

2.5.1.1.2.3 Stratigraphic Units Within the Site Vicinity

Stratigraphic nomenclature used throughout this FSAR follows the recent usage of the Pennsylvania Geologic Survey who have not recently used the terms Susquehanna Group, Hamilton Group or Fort Littleton Formation in the site vicinity (See for example Ref. 2.5-12 and 2.5-17).

Middle Silurian to Pennsylvanian rocks within 10 miles of the site have been folded on the Berwick Anticlinorium. The units exposed across the fold are:

- The Middle Silurian Bloomsburg
- Upper Silurian Wills Creek
- Upper Silurian Tonoloway
- Middle Devonian Marcellus
- Middle Devonian Mahantango
- Upper Devonian Trimmers Rock
- Upper Devonian Catskill
- Upper Devonian-Lower Mississippian Pocono
- Middle Mississippian-Pennsylvanian Mauch Chunk
- Pennsylvanian Pottsville and "Post-Pottsville" (Llewellyn) Formations

In central Pennsylvania the Bloomsburg Formation was deposited in a brackish, shallow water, marine environment which is transitional between fluvial, continental sediment to the east and marine carbonates, shale and marl of the interfingering Wills Creek Formation to the west (Ref. 2.5-14, p. 119). It is a thick-to massive-bedded, dominantly grayish-red silty claystone with two sandstone intervals which occur both at the base and near the top (Ref. 2.5-14, p. 119). The sandstone intervals are medium-to-thin-bedded, poorly sorted hematitic sub-graywacke. The Bloomsburg is highly calcareous in the vicinity of Lewisburg, Pennsylvania, approximately 40 miles southwest of the site.

In central Pennsylvania the Bloomsburg is separated from the Marcellus Formation by about 1770 ft. of dominantly limestone and calcareous shale. These lithologies belong, in stratigraphically higher order, to the Wills Creek (Upper Silurian), Tonoloway (Upper Silurian), Keyser (Upper Silurian to Lower Devonian), Old Port (Lower Devonian) and Onondaga (Lower to Middle Devonian) formations (Ref. 2.5-12, Table 1).

The Wills Creek Formation gradationally overlies the Bloomsburg and consists of interlayered dark gray to greenish shale, red siltstone, light gray-green to olive siltstone and silty shale (all calcareous) and light gray dolomite to argillaceous dolomite. Medium gray limestone may be present.

The Tonoloway Formation gradationally overlies the Wills Creek and is composed of medium to dark gray, thinly laminated to thinly bedded limestone with some thin beds of medium gray calcareous shale. The Tonoloway is dolomitic at several locations.

The Upper Silurian to Middle Devonian Keyser, Old Port and Onondaga Formations were not mapped north of, nor east of Bloomsburg, Pennsylvania. The Keyser, therefore, does not appear to occur within ten miles of the site but was mapped further southwest (Subsection 2.5.1.1.3.3).

The lower Keyser is dominantly medium gray, fossiliferous, "pseudo-nodular" limestone which is cobbly when weathered. The upper Keyser contains laminated to thin bedded limestone similar to the underlying Tonoloway.

The Old Port and Onondaga Formations do not occur in the site vicinity but do crop out north of Bloomsburg (Subsection 2.5.1.1.3.3). The Old Port consists of dark gray, whitish weathering

chert, underlain by calcareous shale and thin gray limestone. The chert is locally overlain by gray to buff, medium to coarse grained fossiliferous sandstone.

The lower Onondaga is medium gray, highly fissile shale which is calcareous toward the top. The upper Onondaga is medium to dark gray, dense, fossiliferous argillaceous, locally carbonaceous, microcrystalline limestone.

The Marcellus, in central New York State, where it was defined, is about 350 ft. thick and consists predominantly of black shale with lesser amounts of black limestone (Ref. 2.5-15, p. 103). In east-central Pennsylvania, between Harrisburg and Williamsport, the Marcellus is a uniformly massive black, carbonaceous shale with several thin to thick bedded fine grained sandstone units (Ref. 2.5-16, p. 156). According to Faill (Ref. 2.5-17) the Marcellus refers exclusively to black shale overlying the Onondaga Formation.

The Mahantango Formation, which underlies most of the site, consists primarily of silty mudrock, shale, siltstone and sandstone with local occurrences of conglomerate, limestone and ironstone (Ref. 2.5-18, p. 13-14). In eastern Pennsylvania the Mahantango overlies the Marcellus shale and is, in turn, overlain by the Harrell Shale (Ref. 2.5-19, p. 18), a feature corroborated by Kaiser (Ref. 2.5-18, p. 6) who indicated that the Mahantango is defined by black shale, both at its base and its top.

Kaiser (Ref. 2.5-18, p. 18) informally divided the Mahantango into lower, middle and upper members. The basal member consists of an olive-gray shale with a basal sandstone and the middle member contains siltstone and shale, but where it is sandy it is identified as the Montebello. The upper member comprises an olive-colored shale, siltstone and sandstone with the sandstone locally highly ferruginous, finer grained, darker colored and more argillaceous than the underlying Montebello. Faill (Ref. 2.5-17, p. 23-24) divided the Mahantango into five members which are, in stratigraphically higher order, the Turkey Ridge, Dalmatia, Fisher Ridge, Montebello and Sherman Creek. According to Wells and Faill (Ref. 2.5-12, Table 1) the Turkey Ridge is a light to olive-gray, fine to coarse-grained sandstone and the Fisher Ridge is predominantly a laminated olive gray to medium-gray silty shale. The Montebello is an olive-gray, medium-light gray to dusky yellow, fine to medium-grained, locally conglomeratic, fossiliferous sandstone with interbedded siliceous siltstone and silty claystone which display cycles of reverse graded bedding. The Sherman Creek (Ref. 2.5-17) or Sherman Ridge (Ref. 2.5-12) comprises olive-gray, fossiliferous, silty claystone with two interbedded siltstone and fine sandstone units which coarsen upward.

Faill (Ref. 2.5-17, p. 23-24) noted that the Middle Devonian rocks are cyclic with each cycle marked by black to dark gray, silty claystone at the base and displaying an upward increase in grain size to conglomeratic sandstone. Immediately overlying the coarsest rock units there is a marked decrease in grain size with claystone or siltstone marking the base of the overlying cycle.

The cyclic nature of the Middle Devonian strata is reflected within the Mahantango. These internal cycles are asymmetric and are smaller scale reflections of the cyclicity recorded throughout the entire Middle Devonian. That is, they commence with black to dark or olive-gray silty claystone which grades upward into argillaceous siltstone, silty sandstone and fine to medium-grained, locally conglomeratic, silty sandstone. The cycles within the Mahantango are repetitive and range, in thickness, from approximately 7 to 250 ft. The thicker cycles can usually be traced over distances of from 5 to 35 miles. (Ref. 2.5-20, p. 113).

The average thickness of the Mahantango is about 1650 ft. with respective maximum and minimum thicknesses of about 2900 ft. at McCullochs Mills, Pennsylvania and 840 ft. at Riverside which is northeast of McCullochs Mills and about 20-22 miles west of the site (Figure 2.5-7). Overall the Mahantango shows a general thinning to the north, a feature reflected in the Montebello sandstone member which is thickest just west-northwest of Harrisburg and thins to the west, north and east. North of the 41st parallel, which lies just south of the site, the Montebello has totally disappeared (Ref. 2.5-18, p. 13-14).

In the Anthracite region of Pennsylvania the Mahantango and the Marcellus were combined to form a lithotectonic unit. As defined by Wood and Bergin (Ref. 2.5-21, p. 151) this lithotectonic unit actually includes the Marcellus, Harrell and Brallier Shales and the Tully Limestone. However, the Brallier overlies the Mahantango at about the Tully horizon (Ref. 2.5-19, p. 18). The Tully, in this area, has been incorporated into the Mahantango. Thus, in this report, the lithotectonic unit of Wood and Bergin is considered as containing the Marcellus, Mahantango, Tully and Harrell. In the southwestern and western parts of the Anthracite region this unit is $1100 \pm$ ft. thick whereas in the central and eastern parts it is about $3000 \pm$ ft. thick; the average thickness is $2000 \pm$ ft. (Ref. 2.5-21, p. 148). However, a greatly thickened section of this unit occurs in the P. Good No. 1 Well (Figure 2.5-7) on the crest of the Berwick Anticlinorium, east of the site. This excess thickness is believed to be due to faulting and disharmonic folding (Ref. 2.5-21, p. 148).

At the site the Mahantango consists of a lower, gray, calcareous siltstone (120-150 ft. thick) overlain by a dark gray, locally fossiliferous siltstone which is intermittently calcareous. These two members are lithologically similar to and occur within the same stratigraphic interval as the Harrell Shale and the underlying Tully Limestone; thus, the latter two units were incorporated into the Mahantango.

In the site vicinity, the Mahantango is represented only by the uppermost member, the Sherman Creek which is dominantly a dark gray to blue gray, olive gray to brown weathering mudrock. Siltstone and fine grained sandstone units crop out locally. Both calcareous and non-calcareous strata occur at several localities.

In the site vicinity an interval of light, medium-gray argillaceous limestone, near or at the top of the Mahantango, was recognized as a Tully Limestone equivalent and was included within the Mahantango. Calcareous silty mudrocks which may be Tully equivalents also occur (Subsection 2.5.1.2.2). Faill (Ref. 2.5-17, p. 24) also included the Tully as part of the Mahantango because of its lithologic similarity to the Sherman Creek Member. The overlying Harrell Formation, a poorly exposed, dark silty shale which appears to be in gradational contact with the Mahantango was incorporated into this map unit (Subsection 2.5.1.2.2).

Fossils are relatively abundant within the Sherman Creek member of the Mahantango Formation and include various genera of brachiopods, bryozoa, pelecypods, coral, trilobites and crinoid fragments. Fossil casts are abundant with occasional molds and rare preservation of internal structure and original shell material.

Concretions (commonly rusty weathering), spheroidal weathering and prominent closely spaced steeply dipping cleavage, which may quite easily be mistaken for primary bedding fissility, are other features characteristic of the Mahantango. Due to its predominantly argillaceous nature and cleavage, the Mahantango is fairly easily eroded and is thus topographically expressed as a relatively low area.

In the general area marked by the confluence of the Susquehanna and Juniata Rivers, the Trimmers Rock Formation comprises an interlayered assemblage (about 2000 ft. thick) of thin to medium-bedded, medium gray siltstone and medium gray, slightly silty and somewhat fissile shale. Thin layers of fine-grained sandstone occur in the upper part (Ref. 2.5-12, Table 1). Graded bedding, along with groove and flute casts, occur in some of the siltstone beds indicating deposition by turbidity currents. Load casts or ball and pillow structures are also present in some siltstone layers. These lithologies and sedimentary structures are also present in the Trimmers Rock at an outcrop along the Lehigh River about 16 miles southeast of the site (Ref. 2.5-13, p. 8) (Figure 2.5-7). At this exposure both bedding thickness and grain size increase upward in this formation which is about 1165 ft. thick.

In the site area the Mahantango and Harrell grade upward into the Trimmers Rock (Subsection 2.5.1.2.2). The Trimmers Rock is dominantly interbedded, medium to olive gray, thinly laminated siltstone, silty shale and fine grained, laminated to massive sandstone. These rocks weather to brownish gray color. Sedimentary structures include fining-upward sequences, groove casts, current lineations, load casts, ball and pillow and flow roll structures. Ripple marks were also locally identified. These structures indicate deposition by turbidity currents in a marine environment. Fossils are often restricted to relatively thin layers of brachiopods. Other fossils include pelecypods and crinoid fragments.

The upper Trimmers Rock Formation consists of light to medium grayish green silty shale and micaceous, dark greenish gray siltstone (both of which weather to a dark reddish brown color), a reddish brown silty fine to medium grained sandstone to siltstone and an olive green vitreous, fine grained sandstone to siltstone. The uppermost units of the Trimmers Rock Formation grade upward into the basal Catskill Formation. This gradation between the Trimmers Rock and the Catskill has apparently caused problems concerning the placement of the contact between them. However, Faill and Wells (Ref. 2.5-22) have placed this contact at the base of a thick sandstone unit which is the lowest occurrence of upward fining cycles, a feature characteristic of the Catskill. This unit was selected by Faill and Wells because it is easily mappable. Glaeser (Ref. 2.5-13, p. 4) evidently concurred with Faill and Wells for he considered the base of the Catskill to lie at the first occurrence of distinctive sandstone units which are found above or near the top of the turbidite suite which constitutes the bulk of the Trimmers Rock Formation.

The Catskill Formation at the Lehigh River outcrop is about 7675 ft. thick and consists mainly of siltstone and sandstone with some conglomerate and shale. Upward fining cycles were recognized at various intervals throughout the entire formation both at Lehigh River (Ref. 2.5-13, Figure 2) and near Halifax, Pennsylvania (Figure 2.5-7), (Ref. 2.5-22, p. 107).

Complete or nearly complete sections of Upper Devonian rocks are preserved, both in outcrop and in the subsurface, at the Lehigh River outcrop, the Richards Well and the Hudson Realty Well (Figure 2.5-7). Based on these occurrences Glaeser (Ref. 2.5-13, p. 35) estimated the original thickness of the Upper Devonian section at various locations in northeastern Pennsylvania. He then compared these estimates to the amount of section preserved today and ultimately estimated the amount of section lost. The amount of missing section ranges from 0 ft. to about 6125 ft. (Ref. 2.5-13, p. 38) a variation due mainly to the location of the sections with respect to structure. For example, in the P. Good Well, which occurs on the nose of the Berwick Anticlinorium, about 8 miles east of the site (Figure 2.5-7), about 5203 ft. are missing. Glaeser (Ref. 2.5-13, p. 36) assumed that these sections were lost due to erosion.

In the site area, the contact between the Catskill and the underlying Trimmers Rock was drawn at the base of the first relatively thick reddish brown to maroon sandstone or brownish red siltstone and more massive reddish brown (maroon) micaceous fine grained sandstone. This mappable contact appears to occur at or near the lowest fining upward sequences. The lower Catskill Formation contains sedimentary structures such as intraformational clasts of green shale within light gray fine sandstone, oscillation ripple marks and roots which are indicative of the marine to non-marine transition zone.

The Pocono Formation which overlies the Catskill, consists typically of medium and coarse grained light gray to white, rusty weathering quartz sandstone with thin layers of quartz pebble conglomerate. Olive gray, fine grained sandstone, reddish gray medium to fine grained sandstone and siltstone and greenish gray medium grained, cross bedded sandstone also occur within this formation. Cross bedding is common.

Grayish red sandstone layers occur near the base of the Pocono. These were recognized along the east side of the Susquehanna River South of Mocanaqua and along the road between Aldean and Folstown. North of the site, the Pocono consists of an interlayered sequence of predominantly medium gray, thick, well laminated, gray weathering quartz sandstone and subordinate, red, flaggy quartz sandstone. Near Folstown, well laminated red sandstone is interlayered with, but decidedly subordinate to, well laminated, rusty weathering, light gray, coarse grained sandstone and fine grained gray sandstone. Coarse to medium grained, mainly grayish to greenish gray sandstone featuring rather subtle cross bedding dominate the upper portion of the exposure. These strata, along with an underlying thin zone of light greenish gray sandstone, in turn, underlain by green shale and mudrock, has been selected as marking the basal Pocono. Beneath all of these units, is a red, well laminated, argillaceous siltstone which is interpreted as marking the top of the Catskill. Red shale, which marks the base of the outcrop underlies cross bedded medium, light gray, olive gray weathering quartz sandstone. The lower (topographically and stratigraphically) portion of the outcrop is dominated by red lithologies in contrast to the upper part in which no red lithologies were exposed. Besides the obvious color change the sandstone above the inferred contact is coarser grained and more subtly cross bedded than sandstone which occurs between the red units near and at the base of the outcrop. Thus, contrary to other interpretations the Catskill-Pocono contact appears to be gradational in the site area rather than unconformable.

The upper Pocono Formation in the vicinity of Shickshinny consists of medium to light gray conglomeratic sandstone with rounded to sub-rounded quartz pebbles and shale fragments and rusty weathering, fine to medium grayish green, micaceous siliceous sandstone and finely laminated greenish gray, rusty weathering, siliceous quartz sandstone. Rusty weathering, medium light gray, medium to coarse grained quartz sandstone is interbedded with thin layers of dark gray silt. Shale and medium gray quartz lithic sandstone fills channels.

The overlying Mauch Chunk Formation is generally bright red in color and consists of mudrock, silty shale, siltstone and fine to medium grained cross bedded, well laminated sandstone. In the southern part of the Anthracite region, this sequence of red beds is $2,400 \pm$ feet thick and is overlain by a sequence of alternating red sandstone and shale beds and gray conglomerate and sandstone beds 300 to 600 feet thick. This upper sequence represents a transition zone in which red beds typical of the underlying Mauch Chunk are interbedded with gray beds typical of the overlying Pottsville Formation (Ref. 2.5-10). Detailed stratigraphic studies indicate that the beds of the transition zone (upper Mauch Chunk) intertongue with and laterally replace the

lower beds of the Pottsville Formation from south to north. The upper Mauch Chunk is, therefore, late Mississippian and Early Pennsylvanian in age (Ref. 2.5-10).

Both lower and upper members of the Mauch Chunk Formation are exposed in the site area. The lower member is exposed immediately above the conformable contact with the underlying Pocono Formation at several locations. The upper part of the formation along the south limb of the Lackawanna Synclinorium is marked by interlayered red and olive gray sandstone, siltstone, and silty shale. Locally the siltstone contains layers of rounded, circular to elliptical calcite filled voids. Elsewhere the Mauch Chunk contains greenish gray to grayish green medium to coarse grained, locally micaceous sandstone, thinly laminated gray, fine grained sandstone and siltstone and massive medium grained sandstone.

The Pottsville and Llewellyn formations represent the coal bearing zones of the Anthracite Region and have, for the purpose of this report, been combined and treated as a single formation. The Pottsville is composed of coarse pebble conglomerate, quartzose sandstone, subgraywacke, siltstone, shale and anthracite. This formation ranges in thickness from about 1,400 feet in the southern Anthracite field to about 600 feet in the Western Middle Anthracite field (Ref. 2.5-10).

Strata overlying the Early to Middle Pennsylvanian Pottsville have been informally termed "Post-Pottsville" rocks (Ref. 2.5-24). "Post-Pottsville rocks" in the Southern and Western Middle Anthracite fields were named the Llewellyn Formation by Wood (Ref. 2.5-10). This name is informally used for the grayish and brownish conglomeratic sandstones, quartz sandstones, subgraywackes, and siltstones overlying, but not subdivided from, the Pottsville Formation in the site area. Usage of the name Llewellyn for "Post-Pottsville" rocks in the Northern Anthracite field is consistent with Bergin (Ref. 2.5-23).

Within five miles of the site, the Pottsville and Llewellyn, collectively consist of quartz pebble conglomerate in a quartz sandstone matrix, quartz pebble conglomerate in a carbonaceous quartz sandstone matrix, coarse grained dark to medium gray, massive and flaggy, carbonaceous sandstone and shale, dark gray to black siltstone and coal. The non-carbonaceous quartz pebble conglomerate displays cross beds.

2.5.1.1.3 Regional Tectonics

2.5.1.1.3.1 Tectonic Provinces

The Appalachian orogen in the northeastern United States was divided into two parts, the mobile belt and the craton (Ref. 2.5-25 and Subsection 2.5.2.2). The mobile belt in this area lies along the east coast with its western edge parallel to, and west of, the eastern limit of North America (Figures 2.5-8A and 2.5-8B). In general the mobile belt is underlain partly by Precambrian crustal rocks and partly by presumably mafic crust. However, in the Maritime Provinces of Canada as well as in southeastern Massachusetts it is underlain by a volcanic-sedimentary sequence which formed less than 600 million years ago. These three grossly-grouped lithologies, i.e. Precambrian crustal rocks, mafic crust and volcanic-sedimentary rocks of the Avalon Platform provided the basis for dividing the mobile belt into the 1) eastern cratonic margin, 2) the Central New England tectonic province and 3) the Avalon Platform tectonic province respectively (Ref. 2.5-25). In the eastern cratonic margin the Precambrian basement is overlain by 1) Late Precambrian clastic rocks and associated mafic

dikes and volcanics, 2) a miogeosynclinal assemblage and 3) a eugeosynclinal assemblage (Ref. 2.5-25). The eastern cratonic margin is marked by a zone of faulting, contrasting structural styles and contrasting metamorphic facies. The Central New England province is bounded on the east by the Avalon platform and on the west by the Inner Piedmont. It features a thick, dense, presumably mafic crust overlain by eugeosynclinal sediments. It is also marked by intense deformation and Lower Paleozoic metamorphism. The Avalon Platform province is characterized by crystalline, continental crust (Late Precambrian) intruded by Ordovician to Devonian age plutons. In juxtaposition with, and to the west of the mobile belt, lies the craton which is underlain by Precambrian crystalline rocks that were deformed during the Grenvillian orogeny, about 1 billion years ago. Based on gross geologic structure the craton was divided into an eastern belt and a western basin. The eastern belt is coincidental with the Highlands Tectonic Province (Figures 2.5-8A and 2.5-8B) which is characterized by Grenvillian (Precambrian) rocks deformed during Paleozoic crustal convergence. The western portion, which is subdivided into the Fold and Thrust Belt and the stable interior is characterized by the absence of basement involvement during Paleozoic crustal convergence (Ref. 2.5-25). The Fold and Thrust Belt, in which the site is located, is in contact with the Highlands Province of the eastern craton and exposes tightly folded and faulted Paleozoic sedimentary rocks. To the west of, and in sharp contact with, the Fold and Thrust Belt lies the Stable Interior which is underlain by very gently folded, shelf delta type deposits. The Fold and Thrust Belt and the Stable Interior coincide approximately with the Valley and Ridge (including the Great Valley) and Appalachian plateaus Physiographic provinces respectively.

2.5.1.1.3.2 Structural Elements within the Craton

The site is situated upon the Scranton gravity high (Figure 2.5-9) which extends southwestward from Albany, New York to Harrisburg, Pennsylvania where it abruptly terminates (Ref. 2.5-26, p. 198; Ref. 2.5-27, p. 711). To the west of this termination, regional gravity patterns suggest a northwest trending Precambrian fault with left lateral displacement of several tens of miles (Ref. 2.5-27, p. 711).

The high, itself, is located in both the Fold and Thrust Belt and the Stable Interior. The maximum Bouguer anomaly values associated with this feature occur in northeastern Pennsylvania and adjacent New York State where the overlying sedimentary section is at least 39,370 ft. thick (Ref. 2.5-28, p. 52 and 2.5-26, p. 201). Of all the models (which include tensionally induced rifting) proposed to explain this feature (see Ref. 2.5-26, p. 203-209) the favored one involves warping of the mantle with the anomaly due to an extensively broad mass occurring deep within or at the base of the crust. This structure is apparently related to the tectonic evolution of the Appalachian system (Ref. 2.5-26, p. 213 and 218-219).

Principally the Fold and Thrust Belt contains deformational features indicative of regional crustal compression (Figure 2.5-8A and 2.5-8B). In the area northeast of Roanoke, Virginia the structural style, at the surface, is dominated by folding with faulting subordinate, whereas southwest of Roanoke reverse faults predominate over folding at the surface (Ref. 2.5-29, p. 125). Another feature present in this belt, and indeed in the entire Appalachian Orogen, is an arcuate configuration which is especially well expressed in central Pennsylvania.

The largest folds in the Fold and Thrust Belt exceed 125 miles in length but folds of microscopic to hand specimen scale have also been recognized. The largest folds, with wave lengths ranging from 6 to 11 miles, were classified by Nickelsen (Ref. 2.5-30, p. 16) as first order folds, whereas the hand specimen and microscopic size folds were classified as fifth order folds.

Second through fourth order folds are intermediate in size. The largest folds are not restricted to the Fold and Thrust Belt for they also occur in the adjacent Stable Interior (Ref. 2.5-30).

Generally these folds do not display an ideally parallel form, rather their hinges are usually narrow relative to their wave lengths. They are somewhat akin to similar folds yet they lack the characteristic features of similar folds which include attenuated limbs, with correspondingly thickened axial regions, and a sinusoidal form (Ref. 2.5-31, p. 10). Thus, according to Faill, the fold geometry is neither parallel, similar nor intermediate for it shows features that are not associated with either geometric type, i.e., the bedding in the limbs is planar and the hinges are narrow (Ref. 2.5-30, p. 19).

Although the folds lack the characteristic geometry of parallel folds, they are flexural slip in nature for they display wedge faults, uniform bed normal thickness across the fold and slickensides on bedding surfaces (Ref. 2.5-32, p. 1289 and 2.5-31, p. 11). In addition to these flexural slip folds, kink bands, a few inches to hundreds of feet wide, are visible in outcrop. Kinematically and geometrically the kink bands and the flexural slip folds are congruent and, therefore, related (Ref. 2.5-32, p. 1289).

Kink bands are usually considered to be small scale structures, however they occur on a much larger scale in the Fold and Thrust Belt with smaller kink bands and folds present in the limbs of the larger-scale structures. Faill attributed the existence of large scale kink bands to the wide spacing between bedding surfaces.

From southeast to northwest across the Fold and Thrust Belt, and westward into the Stable Interior, the folds become progressively less tightly appressed. This gradual change from tight to more open folds is illustrated by changes in the inter-limb angle which is about 50°-70° on the east side of the Great Valley and approximately 80° on the west side. In the central Valley and Ridge (Fold and Thrust Belt) the limbs subtend an angle of about 100° and in the Appalachian Plateaus (Stable Interior) this angle is nearly 180° (Ref. 2.5-32, p. 348). This change is also expressed by differences in structural relief which diminishes from possibly 35,000 ft. on the South Mountain Anticlinorium on the southeast (Ref. 2.5-33, p. 348) to 7,000-9,000 ft. in the central Valley and Ridge to about 4,500 ft. in the western Valley and Ridge. In the eastern Plateaus area 2,500 to 3,000 feet of structural relief occur. Across the Plateaus area this relief continues its progressive decrease with the most westerly folds showing less than 300 ft. (Ref. 2.5-33, p. 349). In fact in the Plateaus region the folds are so broad and gentle that structural contour maps are required in order to analyze them. Between the Valley and Ridge (Fold and Thrust Belt) and the Appalachian Plateaus (Stable Interior) there is an abrupt decrease in structural relief. This area has been termed the Appalachian Structural Front (Ref. 2.5-34).

LANDSAT images of an area along the west branch of the Susquehanna River at Lewisburg, Pennsylvania suggested the presence of a nearly northwest trending cross or tear fault. This structure shows about one mile of left lateral separation of a prominent ridge underlain by the Tuscarora Formation. However, geological reconnaissance mapping confirms that this left lateral topographic offset is caused by a kink fold as shown on the Geologic Map of Pennsylvania (Ref. 2.5-24).

Faults, like the folds, occur on all scales within the Fold and Thrust Belt and show displacements ranging from inches to hundreds of feet. The largest faults range in length from about 7 miles to 200 miles (Ref. 2.5-33, p. 349).

According to Faill and Nickelsen (Ref. 2.5-31, 20) most faults seen at the surface can be classified as wedge faults or cross faults. Root (Ref. 2.5-33, p. 349) stated that all major faults in the Fold and Thrust Belt and the Stable Interior are moderate to steep thrusts with dips ranging from 40°-70° to the southeast. However, in the southern Great Valley (affecting part of the Fold and Thrust Belt), he also identified steeply dipping, west facing thrust faults and tear or cross faults (Ref. 2.5-34). Wood and Bergin (Ref. 2.5-21) noted that in the southeastern part of the Anthracite region (of the Valley and Ridge Province) there are hundreds of reverse, tear and bedding faults, whereas in the northern part faults are far more scarce with only reverse faults, showing minor displacements, having been recognized. Glass (Ref. 2.5-36, p. 9) identified at least eighty major, essentially vertical faults in the Appalachian Plateaus Province. Generally these faults are normal to the regional tectonic grain although variations between N05W and N89W were observed. Wedge, splay and reverse (thrust) faults are categorized together because they all result in crustal shortening and duplication of strata. Faill (Ref. 2.5-32, p. 1298) indicated that splay off decollements and wedge faults are identical. However, Root (Ref. 2.5-35) distinguished between thrusts dipping steeply to the west and those dipping steeply to the east with the former equated to wedge faults and the latter to splay faults off decollements. The Hunting Valley-Cream Valley Faults and the Sweet Arrow Thrust (Figure 2.5-7) appear to fit into this category.

Wedge faults intersect bedding at a low angle (10°-30°) and terminate in bedding planes (Ref. 2.5-32, p. 1295), although a number of them terminate in folds (Ref. 2.5-32, p. 1298). Commonly they occur as isolated structures on the limbs of folds but they have also been observed in fold hinges. In outcrop wedge faults generally occur in interlayered sequences displaying contrasting mechanical properties and only cut across beds of sandstone or siltstone that are surrounded by shale (Ref. 2.5-32, p. 1297 and 2.5-31, p. 23). This same relationship also holds on a much larger scale, since most of the large, mappable faults occur in interlayered sequences of contrasting lithologies.

Root (Ref. 2.5-35, p. 105-106) identified faults in the southern Great Valley which presently dip steeply to both the east and west. The steeply inclined, east dipping reverse faults generally parallel the trace of anticlinal hinges and cut the vertical to overturned, west facing anticlinal limbs. These faults developed as steeply dipping schuppen structures which splayed off subhorizontal reverse faults (decollements) (Ref. 2.5-37, Figure 5, 2.5-33, P. 350 and 2.5-35, Figure 5). Reverse faults, which dip steeply to the west, are also present in the west-facing subvertical to overturned limbs and parallel the structural fabric. However, some have been rotated during folding and now display the geometry of east-dipping normal faults.

In the Anthracite region, faults (akin to the steeply east-dipping splays described by Root) are inferred to occur in the cores of anticlines (Ref. 2.5-21). Wood and Bergin interpreted that many of these faults were folded along with the rock units, however folded splay faults have not been depicted in other publications (e.g. Ref. 2.5-37 and 2.5-33).

Cross (transverse) faults are commonly vertical to nearly vertical structures which are approximately perpendicular to the regional tectonic grain. They are less common than wedge faults although they have been mapped in the southeastern part of the Anthracite region, in the Great Valley and in the Appalachian Plateaus region (Ref. 2.5-21, p. 149, 2.5-35 and 2.5-36). They are also evident in the Cambro-Ordovician rocks of the Conestoga Valley near York and Lancaster, Pennsylvania (Ref. 2.5-24). Commonly cross faults display strike-slip separation and, in fact, have been described in the Appalachian Plateaus Province as wrench faults (Ref. 2.5-36). According to the verbal description provided by Glass (Ref. 2.5-36, p. 6) at least some of these

faults could be identified as paired conjugate wrench faults, for those that strike nearly north show left lateral separation whereas those which strike in a more westerly direction display right lateral separation. Despite his verbal description the map pattern shows a general pattern of anastomosing fault traces which are more or less subparallel to each other and normal to the trend of the Allegheny Structural Front (Ref. 2.5-36, p. 8). It is conceivable that both wrench faults and cross faults occur in the Appalachian Plateau but attempting to distinguish them is of little import for both are predictable cogenetic products of regional horizontal compression. Two cross faults in the southern Great Valley have lateral movements associated with them (Ref. 2.5-35, p. 104), and the map pattern in the Conestoga Valley shows lateral separations of lithologic units along the cross faults there (Ref. 2.5-24). Another feature common to most cross faults is that reverse or wedge faults frequently terminate against them. According to Root (Ref. 2.5-35, p. 103), however, their most distinctive feature is that the rocks on either side of these faults have experienced different amounts of horizontal shortening.

2.5.1.1.3.3 Structural Elements in the Site Vicinity

The site rests on the easterly plunging nose of the Berwick Anticlinorium. Across this folded structure, at depths of 17,500-25,000 ft \pm 3,500 ft, the strata (based on seismic reflections) are nearly horizontal to slightly north dipping (Ref. 2.5-38, p. 134). According to Wood and Bergin (Ref. 2.5-21) either a major decollement or a series of decollements probably exists within the Marcellus Shale throughout most of the Anthracite region. Although not seen at the surface the presence of decollements is inferred based upon the existence of disturbed outcrops "differing styles, wavelengths and amplitudes of folds above and below the Marcellus, and by wells that penetrated either duplicated sections or greatly thickened sections" (Ref. 2.5-21, p. 151).

It is worthy to note, however, that neither this fault nor any other fault appears as a surface feature associated with the Berwick Anticlinorium in either Wood and Bergin's paper (Ref. 2.5-21, Figure 2) or Gwinn's paper (Ref. 2.5-38, Figure 1). The 1960 edition of the Pennsylvania Geologic Map (Ref. 2.5-24) does indicate a fault along part of the north limb of the Berwick Anticlinorium just north of Bloomsburg. This fault approximately 8 miles long, separates the undifferentiated Wills Creek, Tonoloway and Keyser Formations from undifferentiated Onondaga, Marcellus and Mahantango Formations (Ref. 2.5-24, map unit Skw from map unit Dho, respectively). According to the state map, the missing interval between these two sets of units includes the Mandata and Oriskany Formations. Recent mapping indicates that the Tonoloway Formation is juxtaposed to the Marcellus Formation (Figure 2.5-10, Stations DJ-4B, -33 and -34). The fault on the geologic map of Pennsylvania was probably postulated to explain the missing stratigraphic interval on the north limb of the Berwick anticlinorium, which includes dominantly carbonate rocks of the Keyser, Old Port and Onondaga Formations; these units are present west of the indicated fault. The south limb of the Berwick anticlinorium shows the same relationships occur on the north limb; that is, that the Keyser, Old Port, and Onondaga Formations are missing along the more western portion. However, no fault has been indicated to account for the missing section along the south limb (Ref. 2.5-24).

Mapping on a scale of 1:24,000 (Figure 2.5-10) indicates that west of the confluence of Fishing Creek and Little Fishing Creek (and also west of the interpreted fault), the Tonoloway, Old Port, Onondaga and Marcellus Formations were recognized but no limestone of the Keyser Formation was identified. Thus, one of the units (the Keyser Formation) which is interpreted as missing due to faulting is absent from the stratigraphic section about 4,000 feet west of the postulated fault, despite the fact that the Old Port and Onondaga are present there.

Field investigations at two locations along the trace of the proposed fault (Stations DJ-4A, DJ-4B, DJ-32, DJ-33, and DJ-34; Figure 2.5-10) failed to reveal any evidence of cataclasis except for dip slip slickensides associated with a small flexural slip fold in the Marcellus Formation at DJ-4B. In both cases the Tonoloway limestone and Marcellus shale were exposed within 100 feet of the hypothesized fault. In the former case, however, at DJ-4A and DJ-4B the Tonoloway and Marcellus are separated by less than 20 feet. Consideration was given to the difficulty of detecting faulting within argillaceous units; however, where faulting was recognized within the study area, all lithologies (i.e., limestone, shale, mudrock, siltstone, and sandstone) showed some evidence of cataclasis. While continuous exposure across the postulated trace was not available, no positive evidence for faulting was observed and thus, at best, the fault can only be inferred. The only location along or near the trace of the postulated fault where significant cataclasis occurs is at Station DJ-31 (Figure 2.5-10) about 1,500 feet north of the "fault trace" where shale of the Mahantango Formation is exposed. Here the strata show noticeable variations in both strike and dip directions. For example, at the west end of the exposure strata swing from an attitude of N45°E: 35°SE to N40°W: 15°SW. In the center the attitude changes from N20°E: 30°SE to N10°W: 35°E back to N15°E: 45°SE, and at the eastern end, strata are oriented about N60°E: 40°NW and N35°E: 45°SE. At the western end of the outcrop the change in orientation represents a fairly smooth continuum whereas at the eastern end both continuous and discontinuous changes in orientation occur. The discontinuous changes are marked by oblique slip faults with slickensides displaying rakes of about 60° to 70°. Three such faults trend N55°E: 35°NW, N80°E: 35°NW, and N88°E: 29°NW. No unequivocal movement plan was identified, but structures recognized elsewhere in the Valley and Ridge Province, as well as the area within five miles of the site, show that reverse faults form in response to the release of stored strain energy in tightly appressed kink bands; thus, these faults are interpreted as relatively small scale accommodating reverse faults. This exposure (DJ-31) occurs within an area in which there is map scale folding producing deflections in the lithologies which is not unlike patterns seen elsewhere in the Valley and Ridge Province.

In the P. Good Well, located on the Berwick Anticlinorium east of the site (Figure 2.5-7), faulting has been interpreted at an approximate depth of 5,800 feet which is well above the depth range (17,000 to 25,000 ft) at which a major decollement is implied (Ref. 2.5-38). Thus, the decollement alluded to by Wood and Bergin (Ref. 2.5-21) as well as the fault seen on the Geologic Map of Pennsylvania (Ref. 2.5-24) 12 miles west of the site may actually be a splay fault(s) off a more deeply buried decollement. This suggested splay fault may also be, in part, responsible for the excess thickness seen in the P. Good Well of lithotectonic Unit 2, as defined by Wood and Bergin (Ref. 2.5-21).

In summary, no direct unequivocal evidence exists to either postulate or refute the existence of the fault which has been mapped on the north limb of the Berwick Anticlinorium west of the site (Ref. 2.5-24). However (1) the absence of the Keyser Formation on the north limb, west of the western limit of the inferred fault, and (2) the map pattern in which the units missing from the north limb of the anticlinorium are also absent from the south limb, yet the fault restricted to the north limb suggests that the missing section of the north limb is perhaps better explained by an unconformity than by faulting. Regardless of whether or not a fault is interpreted, data from the P. Good Well show that the limestone sequence missing from both the north and south limbs of the Berwick Anticlinorium is absent from the nose of the fold as well. Thus, if a fault is postulated, it pre-dates the formation of the Berwick Anticlinorium and does not pose a safety-related problem to the site.

Flanking the Berwick Anticlinorium on the north and south respectively, are the Lackawanna and Eastern Middle synclinoria. The Lackawanna Synclinorium, the axis of which passes about 3-1/2 miles north of the site, is about 120 miles long and displays a wavelength of 8 to 9 miles and an average amplitude of 4,000-5,000 ft (Ref. 2.5-21, Table 2). Near the axis of this fold the Mocanaqua decollement is exposed. The axis of the Eastern Middle Synclinorium is approximately 3-4 miles south of the site. This fold is about the same size as the Lackawanna Synclinorium (Ref. 2.5-21, Table 2).

The Nittany Anticlinorium is a large structure which is located just to the west of the Berwick Anticlinorium about 50 miles west of the site. Based on seismic records garnered from longitudinal and traverse profiles, there exists a series of well defined, subhorizontal velocity interfaces which are correlative with similar velocity contrasts in the Cambrian sequence and at the top of the Precambrian basement (Ref. 2.5-38, p. 134). The deepest interface was estimated to occur at a depth of about $25,000 \pm 3,000$ ft.

The Birmingham Fault is located in the core of the Nittany Anticlinorium and is the only fault in Pennsylvania associated with a major, well-exposed decollement known as the Sinking Valley Fault (Ref. 2.5-33, p. 350). This fault is a steeply, east dipping splay (thrust) which is about 33 miles long.

2.5.1.1.3.4 Relationship Among Structural Elements

In the opinion of all previous workers all of the structural elements encountered in the Valley and Ridge Province are genetically related, a feature which is clearly demonstrated in several instances. First, cross faults and reverse faults are generally spatially related with the reverse (or wedge) faults commonly terminating against the cross faults. In fact, there are instances where one passes into the other. A prime example of this is in the Carbaugh-Marsh Creek Fault in the southern Great Valley. This fault is composed of two segments, an east dipping reverse fault which parallels the regional grain and passes continuously into a nearly east trending, subvertical cross fault across which right lateral separation has occurred (Ref. 2.5-37, p. 8, 9 and 822 and 2.5-35, p. 102-103). Rock units across this cross, or transverse, fault segment have shortened independently of one another. Because of this independent behavior of rock units across the transverse portion of this fault, Root (Ref. 2.5-35, p. 103) concluded that this segment existed prior to most of the regional deformation.

Faill and Nickelsen (Ref. 2.5-31) and Faill (Ref. 2.5-32) pointed out that slickenside orientations on: 1) bedding surfaces associated with flexural slip folding, 2) wedge faults, and 3) cross faults are similar) indicating kinematic compatibility among these three structural elements. Furthermore, the lines of intersection of the wedge faults and bedding are subparallel to the fold axes. Splay faults with large displacements occur in the hinges of anticlines which possess a kink band geometry suggesting that these folds were produced by the splays which originate at depth along unexposed decollements (Ref. 2.5-38, 2.5-37 and 2.5-33, p. 349). Faill (Ref. 2.5-32, p. 1298) also conceded that possibly all major anticlinoria are underlain by splay faults. Prior to Gwinn's work, the existence of major decollements and thin skinned tectonics in the Appalachian orogen was somewhat debatable but the results of his latest study (Ref. 2.5-38) indicate clearly that these subsurface structures exist.

In the southern Great Valley, Root (Ref. 2.5-35) deduced the sequential development of folding and faulting. He suggested that the cross faults existed prior to, or at the initiation of, most of

the regional deformation, although he indicated that their origin is not understood. Nonetheless, he concluded (Ref. 2.5-35, p. 109) that the cross faults which are subvertical and normal to the regional grain were, during folding, equivalent to ac fractures. This is logical since the orientation of cross faults with respect to the other structural elements is not consonant with having originated as shear fractures; rather it is likely that they formed early in the tectonic history of this area as extension (ac) fractures which were subsequently utilized as strain discontinuities (tear faults) during the same protracted period of stress application. This interpretation is supported by Nickelsen and Hough (Ref. 2.5-39) who stated that systematic extension fractures in shales are grossly transverse to northeast-trending fold axes, and formed early and independently of folding and faulting. Root continued (Ref. 2.5-35, p. 111) by indicating that the earliest folds were broad and open and as horizontal shortening continued and the folds became more appressed; west dipping steep thrusts (wedges) formed in the upper strata. Continued shortening resulted in the development of subsidiary folds, east dipping thrusts (splay faults) and the rotation of the earlier formed, west dipping thrust to a steeper inclination. In the case of the Carbaugh-Marsh Creek Fault the east dipping splay fault linked up with a portion of the cross faults to form the Carbaugh-Marsh Creek Fault system.

Fail and Nickelsen (Ref. 2.5-31, p. 37) noted that deformation was initiated by vertical compaction during sedimentation. Regional horizontal compression followed, while the strata were still horizontal, with the earliest stage marked by microfolding in shales and limestones. Major decollements probably also occurred during this early stage and were followed by buckling and kink band folding. As the folds tightened, faults in the hinge along with some wedge and cross faults, developed. These faults were accompanied by tightly spaced fractures (fracture cleavage) which formed parallel to the axial planes of the folds. Fail and Nickelsen further concluded that with time the deformed materials passed progressively from a ductile stage to a more brittle stage.

2.5.1.1.3.5 Age of Deformation

Root (Ref. 2.5-35) concluded that all the structural elements in the craton developed during a single orogenic event (Alleghenian) about 230 million years ago. This age is based on an inferred episodic lead loss about 230 million years ago recorded by Rankin (Ref. 2.5-40) in zircons from the Catoctin Formation. However, Fail and Nickelsen (Ref. 2.5-36, p. 19) implied that the deformation occupied a greater time span, possibly commencing prior to complete lithification of Silurian age sediment (e.g., the Lower Silurian Tuscarora Formation). Despite this apparent difference concerning the age of the onset of deformation, there is general agreement that the major structural elements in the Fold and Thrust Belt and the Stable Interior are no younger than Late Permian to Middle Triassic in age (Ref. 2.5-37, 2.5-33, 2.5-35, 2.5-32, 2.5-31, 2.5-38, 2.5-41, 2.5-34, and 2.5-21).

There is considerable disagreement as to the age, nature and method of formation of the curvature that is so prominent along the entire Appalachian Chain. Drake and Woodward (Ref. 2.5-42, p. 49) concluded that this arcuation in central Pennsylvania is truly a rounded structure which formed in response to right lateral slip along the east trending Cornwall-Kelvin Fault, perhaps around Late Devonian time (Ref. 2.5-42, p. 29). Fail (Ref. 2.5-32, p. 1305-1306) noted that it is not smooth and continuous, as it appears, but instead is composed of straight segments, the joining of which marks the boundary between the northern and southern Appalachians. Furthermore, he concluded that this "curvature" and the major folds were contemporaneous. Root (Ref. 2.5-37, p. 825) noted the same observations as Fail and

indicated that these rectilinear elements oriented N17°E south of the Carbaugh-Marsh Creek Fault and about N40°-50°E north of the fault, assume their present position by rotation across the fault. He also added that all structural elements seen in the Piedmont to the southeast would be more compatible if the Piedmont were arcuate by the Early Paleozoic. This appears to be a contradiction since on the one hand, Root suggested that rotation across the Carbaugh-Marsh Creek Fault (presumably during the Late Paleozoic Alleghenian event) was responsible for this curvature, whereas on the other hand, he suggested that the curvature already existed by Early Paleozoic time. Fleming and Sumner (Ref. 2.5-42, p. 58) suggested that an embayment associated with the Late Precambrian-Early Paleozoic proto-Atlantic was responsible for this arcuation in central Pennsylvania. Rankin (Ref. 2.4-40) and Rodgers (Ref. 2.5-44) stated that Appalachian salients and recesses formed during the initial breakup of a continental mass which commenced about 820 million years ago. Thus, at present, although there is no unique hypothesis concerning the age and origin of this curvature there is general agreement that it is pre-Mesozoic in age.

Evidence of younger tectonics is confined to the mobile belt. The southern border of the Newark-Gettysburg basin is obscured in New Jersey by the overlap of Coastal Plain sediments; however, in Pennsylvania and Maryland, the Triassic sedimentary rocks lie unconformably upon lower Paleozoic quartzites and carbonates and, in a few areas, upon Precambrian gneisses, granites and metabasalts. Residual gravity anomalies indicate that southern "border faults" are covered by the younger Triassic sediments (Ref. 2.5-45).

The northern edge of the basin, in the area east of the Schuylkill River, borders on the granitic-gneissic complex of the New Jersey Highlands and its southwest extension, the Reading Prong. West of the Schuylkill River, rocks north of the border are Cambrian and Ordovician carbonates. Triassic rocks unconformably overlie adjacent older rocks along much of the northern border suggesting that this margin is not continuously faulted (Ref. 2.5-2). In Pennsylvania, only 35 percent of the margin is known to be faulted (Ref. 2.5-46). The northern border faults are characterized as an echelon fault zones that gives a crenelated appearance to the northern margin. Where overlap has occurred the contact dips approximately 20% to the south (Ref. 2.5-46).

The Ramapo Fault System, a continuation of the northeast trending system of border faults, crosses the New York-New Jersey State boundary north of New York City. No evidence of surface rupture, warping or offset of geomorphic features has been observed along its member fault zones (Ref. 2.5-47).

Several faults of apparently large displacement occur within the center of the Newark-Gettysburg basin (Figure 2.5-11). These are the Chalfont and Furlong Faults in Pennsylvania and the Flemington and Hopewell Faults in New Jersey. Orientation and direction of movement of these faults are not known. Although generally considered to be steeply south dipping normal faults (Ref. 2.5-48 and 2.5-49), Sanders (Ref. 2.5-50) has suggested predominant strike slip movement and Fail (Ref. 2.5-46) indicates they may be high angle reverse faults resulting from intersection of two different axes of monoclinical folding within the basin.

Smaller Triassic faults cross cut the basin margins and extend well into the surrounding rocks, but usually show less than 3,000 feet of displacement. Associated with these faults are local concentrations of small faults of constant attitude and sense of displacement (Ref. 2.5-2).

The Triassic basins and associated faulting are located in the mobile belt, whereas the site is situated on the craton which includes the Fold and Thrust Belt. No tectonic structures of Mesozoic or younger age have been recognized in the Fold and Thrust Belt.

Analysis of lineaments observable on LANDSAT imagery yielded data consistent with these observations. The greatest number of lineaments plotted in the Valley and Ridge Province within the Appalachian salient strike N10-25°W (Figure 2.5-11). This is roughly normal to fold axes in the area and thus the cluster of lineaments parallels the direction of extension fractures and cross faults. The fold axes and bedding are well expressed as a cluster of east-northeast trending lineaments.

Secondary trends oriented north-northeast and northeast may indicate jointing of Mesozoic age. These are the dominant lineament trends expressed in the Newark-Gettysburg Basin.

2.5.1.1.3.5.1 Relationship of Lineaments to Regional Geology

The remote sensing work for the Susquehanna SES FSAR utilized landsat satellite imagery. The imagery was obtained from the EROS Data Center, Sioux Falls, South Dakota. Analysis of the five frames was performed on 20" x 20" black-and-white prints at a scale of 1/500,000 (Imagery Access Nos. 1495-15222, 1079-15124, 1440-15172, 1403-15123, and 5359-14433).

Images from the Landsat satellite comprise individual frames recorded in different bands of the electromagnetic spectrum. For this analysis, two bands (5 and 7) for each frame were analyzed. These bands were utilized because band 7 (0.8 to 1.1 micrometer) shows drainage much better than the other bands while band 5 (0.6 to 0.7 micrometer) emphasizes cultural features. Each frame covers an area of approximately 13,225 square miles. This investigation encompassed the area within a 100 mile radius about the Susquehanna SES.

In the analysis of satellite imagery an acetate overlay was initially prepared showing all of the lineaments observed on band 7 of each frame. These overlays were then registered to band 5 of their corresponding frames, and any additional lineaments observed on these frames were then added to the overlays. It was possible to observe much of the study area (approximately 25 to 30 percent) in stereo due to the overlap of the adjacent frames. Using a mirror stereoscope corresponding bands of the adjacent frames with their previously analyzed overlays were studied. This added three dimensional view of the lineaments provided a means by which spurious, apparently culturally controlled lineaments (e.g. roads and transmission lines) could be eliminated.

A base map was prepared from the 1/250,000 topographic map series (Army Map Service), that covered the study area. This map was reduced to 1/500,000 scale to match the imagery scale and to facilitate transfer of data from the analyzed satellite imagery. A separate overlay was prepared from the geologic maps of New York, New Jersey and Pennsylvania, delineating the fold axes, intrusives, faults and physiographic provinces of the region. This overlay was brought to the common scale of the imagery and topographic base maps. Having all data at the same scale facilitated comparison and interpretation and also permitted elimination of other cultural lineaments.

Comparison of FSAR Figures 2.5-7 and 2.5-11 reveals that within the Valley and Ridge Province lineament trends strongly reflect the structural grain of the Appalachian Salient.

The greatest number of lineaments are roughly normal 75° - 105° (to the fold axes and consistent with the directions along which cross faults and extension fractures occur (FSAR Subsection 2.5.1.1.3.2). The next greatest number of lineaments trend parallel to the fold axes indicating their control by bedding, foliation, thrust faults, and wedge faults. Secondary trends, particularly evident within the Appalachian Salient, are $N10^{\circ}$ - 15° E, $N20^{\circ}$ - 25° E and $N25^{\circ}$ - 35° E. These are the dominant trends observed in the Newark-Gettysburg Basin and probably reflect jointing developed under the early Mesozoic stress regime. Conversely the dominant $N40^{\circ}$ E trend observed in the Precambrian rock of the New England Uplands is virtually non-existent in the Valley and Ridge Province (except where fold axes trend near $N40^{\circ}$ E).

Within the Appalachian Plateau Province the dominant trends are also parallel or near normal to the fold axes. Secondary trends oriented north-northeast and northeast which may indicate jointing Mesozoic age are also evident in the Plateaus Province, particularly in the eastern portion of the study area which is nearest to the Newark-Gettysburg Basin.

Thus, the linear features observed during this investigation which may be of structural origin can be ascribed either to Paleozoic tectonics or the early Mesozoic stress regime. No evidence of younger (Cenozoic-Recent) structural elements was observable.

The relationships between the results of this analysis and the work of Saunders and Hick, 1976 are not geometrically direct. The problem is one of both scale and concept. Saunders and Hick worked with features traceable for hundreds of miles which they feel are reflective of fundamental crustal tectonics. The analysis for Susquehanna SES was, relatively speaking, local in both scope and approach. The greatest part of this study area encompasses allochthonous rocks which contain structural elements derived from "thin-skinned" tectonics as opposed to fundamental basement tectonics. Saunders and Hick have related the major geomorphic lineaments of the United States to the currently accepted theories of plate tectonics and hypothesized that these lineaments have been of primary importance in controlling crustal tectonics. It may be stated that their work dealt with the cause while the Susquehanna SES analysis, due to the allochthonous nature of the terrain, dealt with the effect of plate tectonics. Whether or not their postulated mechanisms for the cause are accurate, it is generally accepted that the Atlantic Ocean has opened and closed at least twice in the geologic past. The analysis summarized in the FSAR Subsection 2.5.1.1.3.5 and Figures 2.5-7 and 2.5-11) revealed that the significant lineaments of the Valley and Ridge and Appalachian Plateaus provinces in the region of the Susquehanna SES are the effect of the Paleozoic closing of Iapetus (proto-Atlantic Ocean). Secondary lineaments of these provinces can be related to the initial opening of the Atlantic in early Mesozoic time.

2.5.1.1.4 Regional Uplift and Subsidence

Several investigators have presented evidence for present day crustal movement in the Atlantic Coastal Plain, the Fold and Thrust Belt and exposed shield areas (Ref. 2.5-51, 2.5-52, 2.5-53 and 2.5-54). Based on the accumulation of an eastward facing clastic wedge of sediments along the coastal plain, Owens (Ref. 2.5-52) concluded that post-Triassic diastrophism has affected the entire central and southern Appalachians with the latest recorded upwarping having occurred in the Pliocene to Quaternary. Brown and Oliver (Ref. 2.5-54) concluded that the "Appalachian Highlands are presently rising relative to the Atlantic Coast at rates of up to 6 mm/yr" with the elongate zones of relative movement paralleling either the major Appalachian Structural trend or the Appalachian drainage divide. Superimposed on this broader uplift are local zones marked by a slightly greater rate of vertical crustal movement. One of these, known

as the Harrisburg feature, occurs near the eastern limit of the Valley and Ridge Province along a line which extends northward from the eastern edge of the Blue Ridge Province (Ref. 2.5-54, p. 26). They further suggested that the entire thickness of the lithosphere is involved in these movements.

No instances of faulting due to tectonism have been associated with this regional scale activity. The only known instance of surficial displacements in the Fold and Thrust Belt occurs in New York (about 120 miles east of the site) and New England where small scale (less than one inch of vertical separation), high angle reverse faults that parallel the regional tectonic fabric offset glacial striations. Oliver and others (Ref. 2.5-51) have considered glacial rebound and surficial effects such as thermal changes, hydration or a chemical process in the shales as well as tectonic stresses as possible causes of these faults. While admitting the available data are inconclusive, they appear to favor the hypothesis that the faults are the result of expansion due to hydration or the release of continuing pressure by melting of overlying ice or other causes. They further suggest that if the faults are of tectonic origin, an apparently poor correlation between fault locations and modern seismicity indicates that episode of deformation is already completed (Ref. 2.5-51, p. 587). No structures of this nature have been found in Pennsylvania.

As discussed further in Subsection 2.5.1.2.3, the available data do not indicate that regional uplift is of significance to the Susquehanna SES.

2.5.1.1.5 Natural Hazards

A natural hazard has been defined by Burton and Kates as "those elements of the physical environment that are potentially harmful to man and his works". Thus, geological natural hazards would be potentially harmful geological elements of the physical environment. The geologic hazards to be considered are: subsidence due to coal mine collapse, subsidence due to karst collapse, and landslides.

The coal (anthracite) of northeastern Pennsylvania is located in the Northern, Middle, and Southern Anthracite fields. The southwest end of the Northern Field is the closest to the site being about 4 miles to the northeast (Figure 2.5-7). Within this Northern Field there are many well documented incidences of subsidence, particularly in the cities of Scranton, Wilkes-Barre, Nanticoke, and Pittstown (Ref. 2.5-55). There have also been incidences of subsidence in the Middle and Southern Fields, which at their closest points, are about 10 miles southeast of the site (Fig. 2.5-7). Thus, the site will not be affected directly by subsidence due to coal mine collapse.

The nearest major carbonate units are the Silurian Keyser and Tonoloway Formations which are composed of gray to dark gray, thick to thin bedded, crystalline to argillaceous limestones (Ref 2.5-24). These formations are not major cavern producers (Ref. 2.5-56) especially in this portion of Pennsylvania, and thus do not pose a hazard of collapse. As mapped, these two formations occur as relatively thin beds on both limbs of the Berwick Anticlinorium which come together in the town of Berwick, Pennsylvania. This location is about 5 miles west of the site; thus, these units would pose no subsidence problems at the site. Miller (Ref. 2.5-57) stated that Onondaga limestone crops out along road and railroad cuts near Beach Haven, Pennsylvania. Examination of these outcrops indicates that the rock is dark gray, brownish weathering calcareous silty mudrock interbedded with thin layers of silt to clay shale or with siltstone.

Lithology and fossil fauna indicates that these rocks belong to the Mahantango Formation (Subsection 2.5.1.2.2) which does not pose a subsidence problem at the site.

Radbruch-Hall (Ref. 2.5-58) placed the site in a region of moderate landslide incidence with a high susceptibility to landsliding. Moderate incidence means that generally less than 15 percent, but more than 1.5 percent, of the underlying rock or earth material is estimated to be involved in landsliding. A high susceptibility means that natural or artificial cutting, loading of slopes or anomalously high precipitation may cause landsliding involving more than 15 percent of the rock or soil. On this regional basis no specific statement can be made on local susceptibility to landsliding. However, some general statements can be made. Although moderate to steep, natural slopes of the local formations (Marcellus, Manhatango, which is stratigraphically equivalent to the Hamilton, and Trimmers Rock) are stable, cut slopes generally have only poor to fair stability due to rapid disintegration of the shales upon exposure to weathering. Much of the surface area in the vicinity of the site is covered with glacial till and outwash. The stability of this material in cut slopes needs to be carefully analyzed. Slope stability and landslide potential at the site are discussed in greater detail in Subsection 2.5.1.2.5.

2.5.1.2 Site Geology

2.5.1.2.1 Site Physiography

The Susquehanna Steam Electric Station is located in the Valley and Ridge Physiographic Province which is described in Subsection 2.5.1.1.1. The site is situated within a broad undulating valley developed in mudrock, shale and siltstone of the Devonian Mahantango Formation along the axis of the Berwick Anticlinorium (Figure 2.5-12).

Lee Mountain (about 2-1/2 miles north) and Nescopeck Mountain (about 4-1/2 miles south of the site, are held up by the more resistant sandstone and conglomerate of the Mississippian Pocono Group. Lesser ridges formed by sandstone of the Trimmers Rock Formation occur at the north end of the site and along the south bank of the Susquehanna River (about 2 miles south of the site).

Topography and drainage of the area is controlled to a large degree by the lithologic and structural characteristics of the bedrock. Ridges and valleys generally trend east-northeast parallel to the strike of the Paleozoic strata. The site fronts on the south flowing Susquehanna River which here flows perpendicular to the east-northeast trending axis of the fold, resuming its west-southwest flow about 1-1/2 miles south of the site, to follow the strike of the shale valley. The north-northwest segment of the Susquehanna River which flows normal to the strike appears to have been inherited from the course of the Ancient Little Schuylkill River (Ref. 2.5-3) (Refer to Subsection 2.5.1.2.4).

Topographic elevations in the site vicinity range from 500 to 1,100 feet above sea level. Higher elevations occur in the more rugged terrain further north and west of the site. The site itself contains generally gentle to moderately sloping hills and well developed drainage patterns. Existing surface elevations vary from about +750 feet in the western portion to about +500 feet in the east. Portions of the area were formerly cultivated. In those areas not cultivated, heavy to moderate woodlands and scrub brush are found. A steep sandstone ridge borders the north side of the site. A narrow east-west trending interior bedrock ridge, rising some 60 feet above the surrounding ground surface, is located just north of the center of the site. A rounded

bedrock knoll about 80 feet high occurs at the western edge of the site in the southwest quadrant.

The site is well-drained by eastward trending depressions near the north and south edges of the site. Plant grade at 650 feet above sea level (about 150 feet above the flood plain of the Susquehanna River) is at about the level of the Fourth Olean Kame Terrace (Ref. 2.5-5) which is well preserved southward between the site and the Susquehanna River.

The irregular bedrock surface underlying the site is the result of a combination of preglacial weathering and stream erosion, glacial scour, later erosion by glacial melt waters, and the varying resistance of the lithologic units to erosion. The maximum thickness of the overburden is on the order of 40 feet in the southern half of the site, with bedrock occasionally cropping out at the surface. North of the east-northeast bedrock ridge that is located near the center of the site just north of the reactor and turbine buildings, glacial deposits fill a bedrock valley to a depth exceeding 100 feet.

During excavation at the site, abundant evidence of glacial and glacio-fluvial scour of the bedrock surface was found in the form of channels, potholes, grooves, striations and fluted rock. A large, buried pothole over 30 feet wide and more than 30 feet deep was exposed in the Unit 1 turbine building excavation (Figure 2.5-13). Similar large buried potholes have been documented farther north along the Susquehanna River Valley (Ref. 2.5-3, p. 23-27 and 2.5-59, p. 195). At the site, numerous other smaller potholes and rounded pits and channels in unweathered bedrock were observed in the excavations. Smooth, east-northeast trending linear channels about 6 to 8 feet deep eroded in unweathered bedrock were observed north of the radwaste building. Similarly, somewhat larger features were excavated in the northeast and west rims of the Unit I cooling tower. This fluting of the rock surface observed in a number of places at the site was either gouged by ice, eroded by water or both, and apparently served as flumes for torrential glacial meltwater runoff which evidently at one time cascaded across much of the site area. Undoubtedly many steep or even undercut surfaces of the bedrock at the site are attributable to ice scour and intense fluvial erosion that was associated with the Olean and earlier glaciations. These features are discussed in Subsection 2.5.1.2.3.3.

As indicated in Subsection 2.5.1.2.5, landslide potential, surface or subsurface subsidence, uplift or collapse are not of concern at the site.

2.5.1.2.2 Site Lithology and Stratigraphy

2.5.1.2.2.1 Lithology and Stratigraphy in the Site Vicinity

Figure 2.5-12 illustrates the distribution of the geologic units within at least 5 miles of the site. The stratigraphic relationships of the various formations are shown on the site geologic column (Figure 2.5-14). Silurian and Devonian formations occur throughout the Valley and Ridge Province. Silurian and lower and middle Devonian strata consist of marine shale, mudrock, siltstone, sandstone and limestone. The upper Devonian strata are generally non-marine sandstone and shale.

A northeast trending fold, referred to as the Berwick Anticlinorium, completely encompasses the site area. This feature has been breached by erosion, exposing rocks of Silurian and Devonian age along the core and at the flanks of the anticlinorium. As it plunges to the east, progressively

younger formations are exposed. Silurian formations present west of the site include, from oldest to youngest: the Tuscarora sandstone, the Clinton ferruginous sandstone, the McKenzie greenish shale with limestone, the Bloomsburg red shale, the Wills Creek shale and the Tonoloway limestone. The Tuscarora sandstone caps Montour Ridge along the axis of the Berwick Anticlinorium in the vicinity of the West Branch of the Susquehanna River. Here as elsewhere in the Valley and Ridge Province, the Tuscarora is a prominent ridge former. The Clinton Formation contains a fossil iron ore which was formerly mined along Montour Ridge. The Bloomsburg Formation supports the eastern extension of Montour Ridge. The Wills Creek and Tonoloway Formations occur in the flanks of the Anticlinorium west of Berwick (Figure 2.5-10).

The basal Devonian formations are the Keyser limestone and Old Port sandstone. These formations crop out along the flanks of the Berwick anticlinorium. East of Bloomsburg they are no longer exposed having presumably been removed from the section by erosion or faulting (Subsections 2.5.1.1.3 and 1.5.1.2.3).

Stratigraphic units exposed in the map area are from oldest to youngest: the Devonian Mahantango (which includes the Marcellus Shale, Trimmers Rock and Catskill Formations), the Mississippian Pocono Formation, the Mississippian to Pennsylvania Mauch Chunk Formation, and the Pennsylvania Pottsville and post-Pottsville Formations.

Above the Marcellus, the Mahantango Formation is represented only by the uppermost member, the Sherman Creek which is dominantly a dark gray to blue gray, olive gray to brown weathering mudrock. Siltstone and fine grained sandstone units crop out locally, including at the site and at certain outcrop locations both calcareous and noncalcareous strata coexist (Figure 2.5-12, Stations DF-2, DF-3, and DF-6).

An interval of light, medium gray argillaceous limestone near the top of the Mahantango, was recognized as correlative with the Tully Limestone and was mapped as part of the Mahantango (Figure 2.5-12, Stations DF-53 and DF-45). The overlying Harrel Shale, a poorly exposed, dark silty shale which appears to gradationally overlie the Mahantango (Figure 2.5-12, Stations DF-30, DF-31, DF-43, and DF-44b) was also mapped as part of the Mahantango Shale.

Fossils are relatively abundant within the Sherman Creek member of the Mahantango Formation and include various genera of brachiopods, bryozoa, pelecypods, coral, trilobites, and crinoid fragments. Fossil casts are abundant with occasional molds and rare preservation of internal structure and original shell material.

Concretions (commonly rusty weathering), spheroidal weathering, and prominent, closely spaced steeply dipping cleavage, which may quite easily be mistaken for primary bedding fissility, are other features characteristic of the Mahantango.

The Mahantango grades upward into the Trimmers Rock (Figure 2.5-12, Stations DF-30 and DF-33). The Trimmers Rock Formation is dominantly interbedded, medium to olive gray, thinly laminated siltstone, silty shale and fine grained, laminated to massive sandstone. These rocks weather to a brownish gray color. Sedimentary structures include fining-upward sequences (Figure 2.5-12, DF-7, DF-8, and JW-10); groove casts, current lineations, load casts, ball and pillow structure, and flow rolls (Figure 2.5-12, JW-7B, JW-10, and JW-11). Ripple marks were also locally identified. These structures indicate deposition by turbidity currents in a marine environment. Fossils are often restricted to relatively thin layers of brachiopods (spirifers DF-9).

Other fossils include pelecypods and crinoid fragments (DF-17b). Channels were observed at DF-25.

The upper Trimmers Rock Formation consists of light to medium grayish green silty shale and micaceous, dark greenish gray siltstone, both of which weather to a dark reddish brown color, a reddish brown silty fine to medium grained sandstone to siltstone, and olive green vitreous fine grained sandstone to siltstone (DF-26, DF-27, DF-28, DF-32, DF-36, DF-37 and DF-68).

The Catskill Formation rests conformably upon lithologically similar interlayered rocks of the upper Trimmers Rock but is predominantly red colored. It is this dominantly red color as well as sedimentary structures (roots, oscillation ripple marks; Station DF-68) which distinguishes the Catskill from the Trimmers Rock. The contact between the Catskill and the underlying Trimmers Rock was mapped therefore, at the base of the first relatively thick reddish brown to maroon sandstone (Figure 2.5-12, Station DF-68) or brownish red siltstone and more massive reddish brown (maroon) micaceous, fine grained sandstone (Figure 2.5-12, Station DF-37c). At Station JW-65 (Figure 2.5-12), the upper Trimmers Rock consists of fine grained, medium gray sandstone overlain by a thin band of green mudrock which is, in turn, overlain by a fine grained, green, well laminated sandstone. The green sandstone grades upward into a fine grained, red, well laminated sandstone which marks the basal unit of the Catskill.

The basal red unit at Station DF-37c (Figure 2.5-12) is overlain by greenish gray, fine grained sandstone and olive green shale and at DF-68 it is overlain by thinly laminated, light green, silty shale and siltstone. These units are succeeded, upward, by interbedded maroon and light olive gray to greenish gray sandstone, siltstone, and shale (Figure 2.5-12, Stations DF-37c and DF-68). Stratigraphically younger units within the Catskill include: (a) reddish brown mudrock and silty mudrock, (b) brownish red medium grained sandstone, (c) reddish brown to maroon micaceous, fine grained sandstone, and (d) greenish gray micaceous, fine to medium grained sandstone. Sedimentary structures include intraformational clasts of green shale, oscillation ripple marks, roots, and prominent cross bedding. The Pocono Formation, which overlies the Catskill, consists typically of medium and coarse grained light gray to white, rusty weathering quartz sandstone with thin layers of quartz pebble conglomerate. Olive gray, fine grained sandstone, reddish gray medium to fine grained sandstone and siltstone (Figure 2.5-12, Station DF-14) and greenish gray medium grained, cross bedded sandstone (Figure 2.5-12, Station DF-67) also occur within this formation. Cross bedding is common.

Near the base of the Pocono, grayish red sandstone layers occur. These were recognized along the east side of the Susquehanna River south of Mocanaqua (Stations JW-1 and JW-64) and along the road between Alden and Folstown (Stations JW-28 and JW-29). At JW-1 and JW-64, the Pocono consists of an interlayered sequence of predominantly medium gray, thick, well laminated, gray weathering quartz sandstone and subordinate, red, flaggy quartz sandstone. At JW-28 well laminated red sandstone is interlayered with, but decidedly subordinate to, well laminated, rusty weathering, light gray, coarse grained sandstone and finer grained gray sandstone. Coarse to medium grained, mainly grayish to greenish gray sandstone featuring rather subtle cross bedding dominate the upper portion of the exposure at JW-29. This, along with an underlying thin zone of light greenish gray sandstone, in turn, underlain by green shale and mudrock, has been selected as marking the basal Pocono. Beneath all of these units at JW-29, is a red, well laminated, argillaceous siltstone which we have interpreted as marking the top of the Catskill. This red siltstone rests upon a green shale which overlies a cross bedded, medium light gray, olive gray weathering quartz sandstone. Red shale, which marks the base of the outcrop, underlies the quartz sandstone. The lower (topographically and

stratigraphically) portion of the outcrop is dominated by red lithologies in contrast to the upper part in which no red lithologies were exposed. Besides the obvious color change the sandstone, above the inferred contact, is coarser grained and more subtly cross bedded than the sandstone which occurs between the red units near and at the base of the outcrop. Thus, contrary to other interpretations (e.g. Ref. 2.5-16) we suggest that the Pocono-Catskill contact is gradational in this area, rather than unconformable.

The upper Pocono Formation in the vicinity of Shickshinny consists of medium to light gray conglomeratic sandstone with rounded to sub-rounded quartz pebbles and shale fragments, and rusty weathering, fine to medium grayish green micaceous siliceous sandstone (DF-56) and finely laminated greenish gray, rusty weathering, siliceous quartz sandstone (DF-57, DF-58). Rusty weathering, medium light gray, medium to coarse grained quartz sandstone is interbedded with thin layers of dark gray silty shale and medium gray quartz-lithic sandstone fills channels at DF-59.

The Mauch Chunk Formation is generally bright red in color and consists of mudrock, silty shale, siltstone and fine to medium grained, cross bedded, well laminated sandstone. The upper part of the formation along the south limb of the Lackawanna Synclinorium (Figure 2.5-12, Stations JW-22 to JW-24) is marked by interlayered red and olive gray sandstone, siltstone, and silty shale. Locally the siltstone contains layers of rounded, circular to elliptical calcite filled voids. Elsewhere the Mauch Chunk consists of greenish gray to grayish green medium to coarse grained, locally micaceous sandstone, thinly laminated gray, fine grained sandstone and siltstone (Figure 2.5-12, Station DF-54) and massive medium grained sandstone (Station DF-55).

The Pottsville and Llewellyn Formations represent the coal bearing zones of the Anthracite Region and have, for the purpose of this report, been combined and treated as a single formation. Collectively, the Pottsville and Llewellyn (formerly post-Pottsville) consist of quartz pebble conglomerate in a quartz sandstone matrix, quartz pebble conglomerate in a carbonaceous quartz sandstone matrix, coarse grained dark to medium gray, massive and flaggy, carbonaceous sandstone and shale, dark gray to black siltstone and coal. The non-carbonaceous quartz pebble conglomerate displays cross beds.

Pleistocene unconsolidated deposits of glacial drift blanket most of the region north of the site. They extend approximately 10 miles to the south and 50 miles to the west of the site. Deposits of various glacial advances are recognized in the region. The drift materials include glacial till and stratified waterlain deposits consisting of poorly sorted mixtures of clay, silt, sand, gravel and boulders. The youngest and best preserved deposits are those of the Wisconsinan glacial stage.

The site lies just behind the Pleistocene terminal moraine of Olean drift, deposited between 55,000 and 60,000 years ago (Ref. 2.5-60, Figure 4; 2.5-61, plate 3; and 2.5-5, p. 25). The Olean drift represents an early glacial substage of late Pleistocene, or Wisconsinan time and has been correlated with the Altonian substage by Sevon (Ref. 2.5-62) to distinguish it from the later Wisconsinan, or Woodfordian, drift farther north. The Olean drift is an assemblage of contemporaneous drifts deposited by several ice lobes that occurred from New Jersey westward to Indiana, believed to represent a regional glacial advance in early Wisconsinan time. A correlation chart of deposits of early and middle Wisconsinan age by Dreimanis and Goldthwait (Ref. 2.5-60, Figure 4) utilizing available geomorphic, lithologic, paleontologic and radiocarbon data, shows the Olean drift to be between about 55,000 and 60,000 years old; conservatively,

the Olean drift may therefore be considered to be in excess of 50,000 years old according to this correlation. Drifts recording later ice advances in Wisconsinan time are not present in northeastern Pennsylvania (Ref. 2.5-61, plate 4), so in this area evidence of the earlier Wisconsinan drift is preserved (Ref. 2.5-62 and 2.5-63).

The leading edge of the Olean terminal moraine is depicted by Denny and Lyford (Ref. 2.5-61, plate 4) as occurring in the Susquehanna Valley about three miles southwest of the site, just west of the village of Beach Haven. Ahead of (downstream from) this moraine are deposits left by an earlier Illinoian glaciation (Ref. 2.5-7, p. 24); however, no Illinoian deposits have been recognized north of the Wisconsinan terminal moraine in Pennsylvania (Ref. 2.5-5, p. 26), indicating that Olean ice overrode and reworked apparently all of the pre-existing Illinoian drift. Nevertheless, it is possible that some buried drift at the site and elsewhere, particularly that located in bedrock depressions, may represent unrecognized remnants of overridden Illinoian or earlier deposits.

The glacial deposits near the Susquehanna site have been studied in some detail by Peltier (Ref. 2.5-5). He describes (Ref. 2.5-5, p. 25) the various features and processes associated with the terminal moraine near Beach Haven. He characterizes the morainic material as "a gravel moraine... composed largely of poorly sorted, coarse kame gravel, medium-grained valley train gravel, and sand... During the early stages of kame terrace development, the marginal channels flowed at a level which was high above the valley... Continued ablation of the ice in the valley probably caused the marginal streams to flow at successively lower levels. These streams, where they flowed along the ice, both eroded the earlier deposits and filled in their channels... In this manner any till deposited at the ice front became buried or eroded." This description of erosion and deposition near the site by ice-margin streams at elevations above the valley floor is consistent with the development of large potholes and steep or even undercut erosional contacts at the site. Evidently waterfalls and large-volume torrential streams occurred at the site during retreat of the early Wisconsinan ice. (Additional discussion of the origin and features of glacial deposits at the site is presented in Subsection 2.5.1.2.3.3).

Peltier (Ref. 2.5-5, Figure 33) profiles discontinuous kame terraces along a 25-mile stretch of the Susquehanna River including the site. The highest such terrace formed by a stream marginal to Olean ice is indicated to occur at about 650 ft. msl at the site (about mile 165), or about 160 ft. above the river. Glacial deposits at elevations higher than this, which would include the glacial deposits in most of the site area, would be part of either the Olean terminal moraine or the ground moraine behind it.

The moraine in the Berwick-Beach Haven area is noncalcareous (Ref. 2.5-5, p. 24). Sedimentary rocks, mostly gray and red sandstone and siltstone, constitute over four-fifths of the material in the moraine (Ref. 2.5-5, Table 3). Peltier (Ref. 2.5-5, p. 24) considers that the remaining igneous and metamorphic types in the moraine indicate it was derived from the Mohawk tongue of an Olean ice lobe originating from the Adirondack area or east of it (Ref. 2.5-60, p. 83).

Unconsolidated sediments mantle most of the Susquehanna River Valley within 5 miles of the site. The valley deposits consist of glacio-fluvial deposits (outwash alluvial terraces, kame terraces), alluvium and colluvium. Unconsolidated deposits were examined at Stations DF-4, DF-15, DF-16, DF-37, DF-42, DF-44a, DF-44b, DF-52, DF-64, and DF-66 at all DJU stations. Thin deposits were noted at various other localities (Figure 2.5-12).

Station DJU-1 is located at a currently (Spring, 1977) operating gravel quarry exhibiting excellent exposures. This quarry contains well layered, brownish gray, very coarse sand to medium gravel interlayered with gray, medium, well sorted gravel with medium to coarse gravel and cobble layers. This is overlain by pebble to cobble gravel with coal and rare boulders interlayered with coarse sand to medium gravel with little coal. The dip of bedding tends to decrease or flatten toward the south. The middle level contains medium to coarse, well rounded, gravel with coarse sand containing lenses of cobbles and gravel below fine to medium gravel and coarse sand with some coal rich laminae. The overlying unit is generally finer grained and dominantly fine to medium sand, some silt with fine laminae of coal. This unit contains layers of cobbly gravel, silt plus fine sand, and coarse to medium finely laminated gravel and coarse sand. Local coarse sand to medium gravel plus cobble layers have steeper dipping beds which appear to flatten southward. On the uppermost level, tan cobbly gravel with rare boulders under tan fine grained sand with coal exhibiting possible load casts is exposed above slumped material. This is overlain by medium yellow brown silt with little fine sand. This silt contains rare sub-angular cobbles. Feint layering is visible in the thickly bedded silt.

The deposit described above is the largest good exposure of unconsolidated sediments observed during this mapping program. Based on sedimentology (well sorted, rounded gravels in contact with well sorted sands or well sorted silts which appear to indicate rapidly changing hydraulic regimes; gravels with interstitial silt) sedimentary structure (steeply dipping bedding whose dip flattens southward or downstream) and geographical location (against the valley wall); these sediments are interpreted as a kame terrace deposit. No faults were observed cutting this layered sequence.

Kame terrace deposits were observed at the other DJU stations. Ice contact deformation was observed at several locations (refer to Subsection 2.5.1.2.3).

A yellow-brown silt with some fine sand, occasional to rare pebbles or cobbles was observed at several locations (DJU-1 at Elevation 665 feet; DJU-2 at Elevation 600 feet; DJU-3 at Elevation 580 feet; DJU-4 at Elevation 595 feet; possibly at DJU-7 at Elevation 640 feet overlain by cobbly gravel; and DF-15 at Elevation 1040 feet). These deposits have been interpreted as loess (Ref. 2.5-5) but may represent relatively quiet fluvial conditions. Well rounded cobbly gravels observed at DF-52 and DJU-5 may represent either valley train or kame terrace deposits.

2.5.1.2.2.2 Lithology and Stratigraphy at the Site

At the site, the thickness of the surficial materials occurring south of coordinate line N342,000, which includes all of the principal plant structures except the spray pond facilities, ranges from zero to about 40 feet. These materials consist of till and kame outwash, typically grading upward from a basal gravelly boulder zone to a surface layer of silty fine sand and sandy silt. The surface layer may represent reworked loess. Rock fragments in the gravelly outwash are well rounded and are composed mainly of hard, well-cemented, white to brown or red sandstones of various textures. No calcareous fragments were noted. In places, the sands and gravels contain minor amounts of anthracite grains and rounded anthracite pebbles up to a foot in diameter. These anthracite fragments cannot have been transported less than 3-1/2 miles from Shickshinny, the nearest occurrence of coal beds.

In the spray pond area in the northern part of the site, permeable, gravelly outwash and alluvial material fill an east-west bedrock valley to depths in excess of 100 feet. Cobble and boulder

pockets were encountered at various depths in most of the boreholes drilled in this locality. The deposit is glacial in origin, possible in part pre-glacial and overridden by ice, and reworked by water derived from ablation of the ice mass in the manner described by Peltier. It consists of sequences of sand, gravel and boulders, overlain by sand and gravel, overlain in turn by sand and silty sand. A geologic map of the surficial materials excavated in the spray pond area is presented on Figure 2.5-15.

Bedrock at the site is in the upper part of the Middle Devonian Mahantango Formation, except for a strip along the northern margin of the site. The uppermost member of the formation, which forms the top of rock in the east-west bedrock valley north of about N342,000, is a dark gray, noncalcareous siltstone in which bedding is generally delineated by thin, inconsistent, light-gray, fine-grained sandstone stringers. Upward and with increasing sand content the Mahantango Formation grades into the Trimmers Rock Formation, which occurs north of about N342,500 at the northern edge of the site. The Trimmers Rock, a gray fine-grained sandstone which caps the high, northeast-trending ridge north of the site, is massive to flaggy and exhibits well-developed joint systems.

Beneath its uppermost member, the Mahantango is comprised of 120 to 150 feet of hard, dark gray calcareous siltstone. It is harder and more resistant to erosion than the uppermost member, forming the east-west trending bedrock ridge just north of the reactor location and underlying the site to past the southern limit of the site area. The principal plant structures are founded on it.

These two upper members of the Mahantango Formation are similar in lithology and occur at the same stratigraphic position as the Harrell shale and underlying Tully limestone. However, the characteristic fossils of the Tully are not present in the site area which require these members to be assigned to the Mahantango Formation.

As exposed in the foundations, the unweathered bedrock is a dark gray, massive to thick bedded slaty siltstone, homogeneous in appearance and lacking the bedding plane fissility that is normally associated with less well indurated shaly rocks. The rock also exhibits a variably developed slaty cleavage or fracture cleavage, further indication of its indurated nature. Typically the rock is slightly calcareous and has intermittent fossiliferous zones which display impressions of brachiopods, crinoids, corals, bryozoa and trilobites. Scattered veinlets and joint fillings consist of white, crystalline calcite or a mixture of calcite and quartz.

The rock weathers to a brown color, with iron oxide stains on joint and cleavage surfaces. Weathering progresses initially by dissolution of calcite from joint and fracture fillings, followed by more pervasive weathering of the rock mass and refilling of joints and veinlets with clay and other weathered material. Advanced weathering on exposed, natural surfaces evidently proceeded mainly along cleavage planes, so that on well weathered outcrops the platy cleavage fabric dominates greatly over jointing or bedding. Lack of significant weathering of the rock surface is often associated with areas where there is evidence of considerable glacial scour or fluvial erosion of the rock. Additional information on the engineering characteristics of the bedrock at the site is given in Subsection 2.5.1.2.5.

2.5.1.2.3 Structural Geology

2.5.1.2.3.1 Major Geologic Structures in Site Vicinity

The major structural features in the vicinity of the site are the Berwick Anticlinorium and the Lackawanna and Eastern Middle synclinoria which are discussed in Subsection 2.5.1.1.3. Structurally the site is situated slightly north of the axis of the Berwick Anticlinorium. The term "anticlinorium" as used herein is defined as a series of minor, intermittent anticlinal structures so arranged that they form a general arch or anticline.

Virtually all structural elements in the site area are related to Paleozoic crustal compression. These elements include kink bands which occur on all scales (Ref. 2.5-31 and 2.5-32) and most likely account for the Berwick and Lackawanna folds, contraction (reverse and bedding-plane) faults, and small scale flexural slip folds. These structures occur on all scales (e.g., Ref. 2.5-30 and 2.5-31). Where exposed it can generally be inferred that the small scale kink bands, contraction faults, and flexural slip folds are cogenetic, developed early in the tectonic history and were rotated by later, larger scale, genetically related folds. For example, at Station JW-3 (Figure 2.5-12) bedding strikes $N70^{\circ}-75^{\circ}E$ and dips $70^{\circ}-75^{\circ}NW$. A reverse fault strikes $N80^{\circ}E$, dips $70^{\circ}NNW$, and displays slickensides which rake 85° in the direction $S80^{\circ}W$. The axis of the associated drag fold plunges 15° in the direction $N85^{\circ}E$. The enveloping bedding on a small kink fold at this same exposure is oriented $N70^{\circ}E$: $70^{\circ}NW$ and the kink band is oriented $N68^{\circ}E$: $60^{\circ}SE$. Similarly, at Stations DF-34 and DF-55 the geometric relations among cleavage, faulting and folding strongly suggest these structures are all coeval.

Like the folds, contraction faults also occur at different scales. At least some of the larger faults appear to have developed in response to a space problem created by the development of tightly appressed folds. An example of this is noted at Station JW-30, where the strain energy associated with a tight kink fold was released along one fairly large reverse fault (which parallels bedding on the hanging wall and cross cuts bedding on the foot wall) and several smaller faults which strike parallel to the larger one yet dip in the opposite direction. At JW-30 bedding, the kink fold and the associated faults all show nearly parallel trends; slickensides on the faults and bedding surfaces deformed by the kink band rake approximately 90° . Similar observations have been made elsewhere in the Fold and Thrust Belt (Valley and Ridge Province) and, as described by Faill and Nickelsen (Ref. 2.5-31), all of these structures are kinematically congruent, i.e., cogenetic.

Besides the aforementioned structures, local evidence of lateral movement was recognized along the north-south segment of the Susquehanna River at Stations JW-3 and JW-60. At JW-3, slickensides rake 20° in the direction $S05^{\circ}E$ on a surface striking $N05^{\circ}W$ and dipping $70^{\circ}W$. At JW-60, slickensides rake 20° in the direction $S10^{\circ}W$ on a surface striking $N10^{\circ}E$ and dipping $50^{\circ}E$.

This movement appears to be related to cross faulting in which case it, too, would be cogenetic with the other structures (Subsection 2.5.1.1.3). In any case lateral movement along this segment of the river was too small to produce any perceptible displacement on the map scale of 1:24,000.

As indicated in Subsection 2.5.1.1.3, all of these structural elements developed during the Late Paleozoic. No evidence was observed in outcrops within five miles of the site which would suggest that they have been active since that time.

Minor structural features were observed in Pleistocene sediment at a few locations in the site vicinity. Two small faults (exhibiting 18 inches and 2.5 inches of vertical separation) were observed at the margin of an apparent ice melt collapse feature in kame or kame terrace deposits at station DF-47. Asymmetric, reclined folds in unconsolidated sand and silt were observed at stations DJU-3, DJU-7, DF-7 and DF-47 (Figure 2.5-12). A small scale fault oriented N30-35E: 73-75SE with approximately 2 mm of dip slip separation occurs at DJU-9. This apparent reverse fault dies out upward. A coal bearing sand which lies about 6 cm above the observed displacement is not disturbed. Similar features at the site have been related to syndepositional slump, differential compaction and ice contact phenomena (Subsection 2.5.1.2.3.3).

2.5.1.2.3.2 Geologic Structures at the Site

During preconstruction exploration at the site, geologic structures in the bedrock at the site were defined and evaluated. Since bedrock exposures at the site were scarce (see Figure 2.5-17), most of this information was obtained from borehole cores, supplemented by geophysical logging of boreholes, seismic refraction surveys, cross-hole and down-hole measurements, test pits and trenches, and geologic mapping of the surface. Presented herein is a summary discussion of the geologic structures at the site as defined from the preconstruction exploration, followed by a description and discussion of the geologic structures that were observed in the excavations for the principal plant facilities.

The principal structural features in bedrock beneath the site are shown on Figure 2.5-18. The axis of a minor anticline crosses the site generally along the east-west base line (approximately N341,700). To the north of this base line, the strata dip to the north at between 20 degrees and 35 degrees. South of the base line, dips are to the south at between 5 degrees and 15 degrees. The predominant strike of the strata is N75E.

The prominent joint directions are parallel and perpendicular to the strike of the strata. The major joints strike parallel to bedding. This joint set is nearly perpendicular and dips opposite in direction to the dip of the bedding. A more open but less frequent series of vertical joints strikes parallel to the direction of dip of the strata. High angle joints healed by secondary calcite and quartz mineralization are present in the vicinity of minor shear zones.

The most prevalent type of rock displacements occurring in the region generally are low angle thrust faults. It has been indicated (Ref. 2.5-21) that many low angle thrusts shear upward through competent rocks utilizing incompetent strata as glide zones. Small shear planes that step stratigraphically from one shale-siltstone layer to another by shearing across intervening sandstone or conglomerate strata have been reported exposed in numerous road cuts and strip pits (Ref. 2.5-21).

Based on interpretation of initial data obtained for the PSAR from 100 and 200 series borings, particularly those located near coordinate line E2,442,400 (location of Section A-B, Figure 2.5-22), two areas of minor shearing were recognized at the site; namely, one in the vicinity of N341,200, slightly east of the reactor facilities and the other in the vicinity of N342,700. The

evidence of shearing is manifested by the presence of slickensides, calcite-healed gash fractures, and breccia zones.

The shears are of the low-angle type generally parallel to the bedding and are mechanically associated with the forces that acted to produce the folding of the strata.

The shear zone which occurs to the north of N342,600 is characterized by a series of bedding plane slips associated with breccia, slickensides, thin clay seams, and numerous fractures. The shear zone is contained within the less competent upper member of the Mahantango Formation and the lower portion of the Trimmers Rock Formation. The shear zone probably terminates at depth in the more competent calcareous member of the Mahantango.

No evidence of displacement was encountered in the main body of the more competent strata of the calcareous member of the Mahantango Formation between N341,950 and N342,600. The stresses that acted on these strata were taken up by the development of joints and fracture cleavage. Detailed inspection of the rock cores extracted from this area reveals microshear offsets along the cleavage planes. The net effect of this mechanism is to thicken the strata as revealed by the stacking and shortening of sandy stringers. The cleavage planes are generally healed by secondary lithification of the rock matrix.

The contact between the top of the Mahantango Formation and the base of the Trimmers Rock Formation was encountered in borings 117, 108, 122 and 126, all located north of N342,550. Detailed examination of bedding planes observed in the rock cores from these borings indicated that the dip of the strata increases with increasing depth. This is confirmed by borehole geophysical data. The numerous breccia, slickensides, thin clay seams and fractures encountered in borings 122 and 126, and to a lesser extent in boring 108, represent a zone of en echelon shear planes, both parallel and subparallel to the bedding. These shears are related to the original tectonic stresses which produced the regional folding.

A petrographic examination of the clay and rock encountered in some of these borings in the northern part of the site was conducted by Dr. Charles Thornton of Pennsylvania State University. The examination indicated that the rock and clay in the broken zones were mineralogically similar to the intact rock obtained from the core above and below the broken zones. Since no secondary mineralization was encountered in association with the clay and broken rock, it appears that this condition was mechanically induced and is not a result of chemical alteration and/or weathering.

In the second area of minor shearing identified above, evidence of structural adjustment which may be called a shear zone is present as slickensides and healed breccia at various depths in borings 125, 127, 132 and 103 as indicated on the subsurface section (Figures 2.5-21A and 2.5-21B), and in borings 100, 217 and to a minor extent in 105 perpendicular to the section. These borings are in the area adjacent to and immediately east of the reactor facilities. Based on this evidence, this zone of structural adjustment strikes east-northeast and dips southerly at approximately 10 degrees. If this zone of structural adjustment extended northward beyond boring 102, it has been subsequently removed by erosion.

Detailed inspection of the microstructure in the rock core extracted from the borings at the site reveal shear-fold structural relationships similar to those encountered on a larger scale across the site. The displacements observed in the rock core are completely healed by secondary calcite and quartz mineralization.

It is probable that the bedrock at the site served as an intervening buffer or adjustment zone during the regional folding of the strata.

Stresses that formed the Berwick Anticlinorium and synclinal structures appear to have been absorbed within the rocks of Mahantango and underlying Marcellus formations, as flexural slip, disharmonic folding and glide thrusting. The stresses that were necessary to produce these structural features were compressional from the southeast. These structural features were formed no later than the close of the Paleozoic Era, approximately 200 million years ago. Based on thorough consideration of all the information provided by the pre-construction foundation exploration, it was concluded that the minor structural conditions observed at the site are not of significance with respect to siting or design for the use of the site for its intended purpose. An evaluation of subsequent data assembled from additional boring exploration and from geologic mapping of the foundations, confirms the initial conclusion.

During excavation and clean-up of the rock at Unit 1 reactor and turbine foundations, at the circulating water pumphouse, and along the trench for the hot water intake pipeline to Unit 1 cooling tower, a bedding plane shear showing strong slickensides was uncovered. This bedding plane shear is the same shear plane that was identified in the early phases of the site exploration and is herein referred to as "bedding plane shear A" (refer to Figures 2.5-18 and 2.5-19).

In the northeast corner of the Unit 1 reactor foundation, bedding plane shear "A" strikes N85°E and dips 7°SE. The surfaces of the bedding plane contain 1/4-inch to 3/4-inch thick laminae of calcite, siltstone and some quartz. The calcite laminae are approximately 1/16-inch thick, alternating with thinner siltstone laminae. The entire exposed area of this bedding plane contains prominent slickensides trending N30° to 40°W, with a 6° to 7°SE plunge. Up-dip and closer to top of rock, the bedding plane contains a 1/2 to 1-inch wide, iron-stained zone, and it also shows extensive leaching of the minerals filling the shear.

In places, the adjacent rock is weathered to a granular sandy soil. The calcite which fills the bedding plane shows no sign of crushing. The weathering and staining on the bedding plane shear occurs only near top of rock where surface water and groundwater could penetrate along the plane; at foundation grade which is well below the weathered zone, the unweathered laminae have the properties of firm rock. In places the bedding plane shear is apparently not a prominent feature in the unweathered rock. For example, it was identified only as a slickenside surface with associated jointing in boring 105 and as horizontal jointing planes in boring 351 (geologic section E-E', on Figure 2.5-19).

A second essentially parallel bedding plane shear striking N75°E and dipping 7°SE was exposed in the trench for the circulation pipe, at the intersection of column lines 19 and G. Slickensides trending N30°W with a 7°SE plunge are also exposed on this plane. The surface is coated with a 1/8 to 1/4-inch-thick layer of unweathered calcite. This shear plane is designated "bedding plane shear B" on Figure 2.5-18. Although similar in appearance to bedding plane shear A at this location, apparently this shear is more restricted in a real extent, because it was not recorded on the logs of nearby bore holes nor was it mapped in the radwaste foundation area where it should have been exposed if it had continued that far north.

It proved possible to collect intact samples from the sheared portion of bedding plane shear "A" for more detailed analysis, including petrographic thin sectioning. The mineralization along the bedding plane consists of thin, parallel bands of intergrown calcite and quartz. The bands, 0.5

to 5.0 mm wide, are separated by thin films of dark shaly material on which slickensided striations caused by shearing have formed. Within the bands, the majority of quartz grains shows recrystallization into interlocking, strain-free grains up to 5 mm long, but becoming cryptocrystalline in the thinner bands. These relationships suggest that the quartz-calcite mineralization was not a late, post-tectonic occurrence, but rather was probably introduced in association with shearing, which is known to have taken place at the end of the Paleozoic (refer to discussion at the end of this Subsection 2.5.1.2.3.2). Undeformed microscopic veinlets of calcite can be observed to cut across the bands at nearly right angles. These veinlets are not themselves offset, and therefore constitute mineralization that has not been crushed or deformed since its deposition. Similar instances of undeformed calcite veinlets crossing slickensided bedding planes are observed on a megascopic scale in the site excavation. Figures 2.5-20a through 2.5-20g illustrate such occurrences.

Bedding plane shear "A" was mapped in the excavations westward from the northeast corner of the Unit 1 reactor foundation to the west slope of the circulating water pump house excavation (Figure 2.5-18). It was also exposed in the trench for the Unit 1 cooling tower hot water intake piping and in two pedestal (No. 6 and No. 7) excavations for the tower itself. Although it displays minor undulations, the average strike of the bedding plane shear is close to N85°E eastward from the turbine and reactor foundations, approximately parallel to the axis of the minor anticline at the site and to the regional structural trend. Near the Unit 1 cooling tower, the bedding plane shear strikes about N70°E, consistent with measured bedding attitudes in that area. Representative dip measurements on the shear plane in the foundations were between 5° and 8°S, which is parallel to the dip of bedding. The trend of the slickenside lineation on this bedding plane shear across the foundation area ranges between S10°E and S40°E, most between S20°E and S30°E, a direction consistent with regional north-northwest compression during folding.

Drill hole data were utilized to project bedding plane shear "A" down-dip. Geologic sections E-E' and F-F' on Figure 2.5-19 show profiles of the shear through the reactor and turbine foundations. The source of data for these profiles is from foundation geologic mapping and elevation surveys, supplemented by subsurface data from the boring logs. It is evident that the foundation mapping and boring log data are in very good agreement, and that the minor shear zone originally identified in this area from exploratory borings is identical to the bedding plane shear "A" identified during construction (see Figures 2.5-21A and 2.5-21B, which was prepared before excavation for the plant structures began). Although this figure suggests that bedding plane shear "A" may not be completely parallel to bedding, no evidence was found during later exploration and excavation to indicate that the shear plane transects bedding.

Bedding plane shear "A" can be traced updip along the Unit 1 hot water intake pipeline trench to the excavation for Unit 1 cooling tower pedestals 6 and 7, where the shear plane crosses the axis of the minor anticline that trends through the site. At pedestal 6 which was excavated to Elevation 667 feet, the weathered bedding plane shear was exposed and dips gently south, conformable to bedding (Figure 2.5-18). At the adjacent pedestal 7 which was excavated to elevation 668 feet, the same weathered bedding plane shear was again exposed, but here it dips gently north, again conformable to bedding. At these locations the weathered shear is two to three inches thick. Where unweathered, the shear is tightly healed with calcite and quartz mineralization; where weathered, these minerals have been partially removed and replaced with claylike material. A roller-bit probe made during the Unit 1 cooling tower foundation exploration recorded a thin seam of soft rock in the vicinity of pedestals 8 and 9 at about elevation 662 feet,

which was probably a penetration of bedding plane shear "A", and, together with measured bedding attitudes, reveals a continuation of the northward dip of the shear plane. West and south of the circulating water pumphouse, undulations in the bedding are evidenced by local northward dips of 5 to 10 degrees. Elevations at which shears were intersected by boreholes 318, 321 and B-5 suggest that bedding plane shear "A" closely parallels the undulations of the strata in this area. These structural relationships are shown in profile in geologic section G-G' on Figure 2.5-19. The fact that the shear plane is folded in conformance to local structure demonstrates that the shear plane originated before or during the time of folding and effectively dates its formation at 200 million years ago or earlier, which is the minimum age of Appalachian deformation in the region (Refer to Subsection 2.5.1.1.3 and the discussion at the end of this Subsection 2.5.1.2.3.2).

Other slickensides were recorded on many joint planes at the site, particularly on low-angle joint planes. Most of these slickensides plunge southeast. The geologic map (Figure 2.5-18) shows these measurements. Numerous slickensided joint planes had been recorded in bedrock cores in the early stages of the site exploration see boring logs, holes 100-132 and 210-219, Figures 2.5-23a through 2.5-23t); they were also observed in rock removed during foundation excavation. Many of these low-angle slickensided joint planes are calcite-coated, and some are undulatory in form rather than planar. They were noted in some instances to splay out from the more prominent bedding-plane shears described above. Evidently, differential movement which occurred principally along bedding planes was transmitted laterally to the encompassing bedrock mass along these bifurcating slickensided joints or shear planes. Such slickensides and shears should be expected in view of the tectonic history and the nature of deformation which the region has undergone.

Significantly, regardless of the orientation of the planes on which slickensides occur (whether they dip north or south), the trend of the slickenside lineation is almost invariably in the northwest-southeast quadrant, clustering N20-35°W (or S20-35°E). This direction is completely consistent with the northwesterly-directed tectonic compressive stress that produced the regional folding and thrust faulting during the Appalachian orogeny, and is further evidence that the slickensides that occur at the site are geologically old; that is, they originated over 200 million years ago. Their consistent orientation suggests deformation during a single tectonic episode, rather than recurrent deformation at different times in geologic history.

Bedding plane shear "A" intersects the top of bedrock surface in the diesel generator and Unit 1 turbine and reactor area. During excavation, two exposures of this intersection were examined to determine the nature of this contact (exposures at intersections of grid line N341,400 with column line G and with column line N (Figure 2.5-18), and photographs (Figures 2.5-20b through 2.5-20e) were taken. Glacial deposits overlay the rock at these points. In each case the eroded rock surface was continuous across the trace of the bedding plane without displacement or offset. If displacement had occurred subsequent to erosion of the rock surface, this would be apparent as an angular, sharp projection of rock into the overlying glacial deposits; instead, the rock surface across the trace of the bedding plane is smoothed by erosion. Figures 2.5-20b through 2.5-20d show this relationship. In the area north of this intersection, the bedding plane shear had been eroded away, thus confirming the original evaluation based on exploratory borings (compare geologic section E-E', Figure 2.5-19 with geologic section B-C, Figures 2.5-21A and 2.5-21B). The erosion of the rock surface would necessarily have occurred prior to the deposition of the overlying glacial deposits, which have been established as being more than 50,000 years old (refer to Subsection 2.5.1.2.2.1). Consequently, this relationship shows that any displacement along bedding plane shear "A"

occurred more than 50,000 years ago. Actually, regional relationships plus the fact the plane is folded indicate that any displacements are a result of the tectonic forces which occurred prior to the late Triassic, over 200 million years ago.

Thus, the original preconstruction appraisal of shears which occur at the site as reported in the PSAR remains the same. These minor shears and structural conditions are consistent with the mode of deformation which occurred during the Appalachian orogeny, over 200 million years ago. They are not significant to the plant site or to the operation of the plant.

Cleavage. Secondary cleavage is variably as developed in the rock exposed at the site; in some places, such in the slopes of the ESSW pipe trench north of the circulation water pumphouse and in parts of the cooling tower areas, it forms the dominant structural feature of the rock, both on fresh and on weathered exposures. The strike of the cleavage is oriented east-northeast, approximately parallel to the trend of the major fold axes, and dips with variable steepness to the south, but generally in the range of 40-80°. Where the dip of the cleavage locally becomes fairly shallow, such as along the eastern perimeter of the south cooling tower, it is sometimes difficult to distinguish cleavage planes from bedding planes. The fact that the cleavage is oblique to bedding demonstrates its secondary origin, apparently during the episode of regional tectonic deformation, 200 million or more years ago.

Joints and Fractures. Jointing in the rock excavated for foundations is fairly well developed. Figure 2.5-18 maps the principal joints encountered at foundation grade, which is at a sufficient depth below top of rock to be in essentially unweathered material. Here joints are tight and either uncoated or coated with calcite or a mixture of quartz and calcite. Relatively few joints at foundation level contained significant iron staining; some iron-stained joints are mapped in the radwaste foundation area. Toward the surface these joints generally become more heavily iron-stained with greater degree of weathering, and calcite coatings tend to be leached out, resulting in open joints, in joints partly coated with quartz or in clay-filled joints in the zone of weathering.

The most abundant joint set in the principal foundations area (Figure 2.5-18) strikes east-northeast (N60°-85°E), roughly parallel to the major regional fold axes and to the secondary fold axis at the site. North of the anticlinal axis at N341,300, these joints strike N70-85°E and dip, with some scatter about the vertical, 75°S-75°N, most 85°S- 85°N. South of N341,100 similar but more numerous joints, shown diagrammatically on Figure 2.5-18, strike N50°-60°E, dip uniformly 50°-60°SE, and appear to comprise a distinguishable set. Less numerous but quite prominent joints with a similar east to east-northeast trend dip gently northward at 10°-18° and are best represented along the vicinity of coordinate line N341,200.

Other dominant joint sets are steeply dipping to vertical north-northwest to northwest joints, and north-south joints. Dips in both sets are usually greater than 70° with both east and west dips represented although the majority of those measured dip toward the west.

Many joints are filled with white calcite or a mixture of calcite and quartz, but there appears to be no preferential orientation for these filled joints. The low-angle joints are commonly slickensided (discussed above). In the turbine building excavation, two vertical, calcite-filled joints cut across bedding plane "B". The calcite in these vertical joints is continuous across the bedding plane with no offset, showing that the joints were formed and the calcite was deposited

in the joints subsequent to the development of the slickensides on the bedding plane. Photographs were taken of this exposure (Figures 2.5-20e through 2.5-20f).

In addition to these principal joints, high-angle, discontinuous, white calcite and quartz-calcite veinlets are typically exposed locally throughout principal plant foundations. These veinlets probably represent fractures that originated during Late Paleozoic tectonic deformation. They tend to occur most abundantly in the vicinity of bedding plane shears (discussed below) and as such may have arisen as gash fractures, as for example the veinlets mapped in the vicinity of N341,350-E2, 441,550 (Figure 2.5-18). At this same location is a singular occurrence of numerous west-dipping open vugs and seams up to several inches wide containing undeformed, euhedral quartz crystals up to 2 inches long. These seams were here exposed several feet above a bedding plane shear (see description above). Chunks of loose, coarsely crystalline white calcite also occur in the vugs. It is evident that these vugs had originally been relatively wide (up to 5 inches) gash fractures containing a coarsely crystalline quartz-calcite mineral filling; later the rock weathered and the calcite was selectively dissolved by circulating ground water (Refer to Subsection 2.5.1.2.5.1).

Bedrock Configuration at the Site. Figure 2.5-17, a map showing top of rock contours at the site, illustrates the general original configuration of the bedrock surface. It is evident that the major erosional feature of this surface is a buried, east-west bedrock valley in the northern part of the site, including the spray pond location. Here glacial or pre-glacial erosion has incised the bedrock surface approximately 100 feet below the general top of rock elevations to the south. In detail, the bedrock surface is very irregular due to the action of glacial plucking and subsequent glacio-fluvial erosion. The large pothole over 30 feet deep and 30 feet wide was found in the Unit 1 turbine building excavation; other smaller ones also occur at the site. Additional discussion of erosional features in bedrock at the site is presented in Subsections 2.5.1.2.1 and 2.5.1.2.3.3.

Relation of Site Geologic Structure to Regional Structure. Geologic mapping at the foundation excavations for the plant structures, together with subsurface borehole data, shows that bedding plane shear "A", the only shear plane traceable across a significant part of the foundations area is, within the accuracy of the data, parallel to bedding and follows the folds which the bedding defines, indicating that the bedding plane shear was either formed prior to folding, or, more likely, developed in conjunction with folding (refer to geologic section G-G' on Figure 2.5-19). Therefore, knowledge of the age of folding would provide a minimum date of origin of the bedding plane shears exposed at the site. With that objective in mind, the literature was examined first to determine whether or not the structures of the site are consistent with the regional structure, and second to date as accurately as possible the age of deformation.

The attitude of the sheared bedding planes and the trend of the slickensides on the planes may be compared to the nearest major tectonic structure (The Berwick Anticlinorium) to the site that is an obvious and consistent member of the pattern of regional deformation in the Valley and Ridge province. The strike of the sheared bedding planes (N75°-85°E) are essentially parallel to the axis of the Berwick Anticlinorium (N75°-80°E) immediately south with compressive forces from the southeast which caused the folding in the region, and of the Berwick Anticlinorium in particular. The Berwick Anticlinorium is one of a series of folds in the Pennsylvania Valley and Ridge Province. It is located in the northwestern part of the province near the Allegheny plateau. Rocks involved in this deformation within the Valley and Ridge province range as recent as Permian in age, and the intensity of deformation increases toward the southeast -- from broad,

gentle open folding at the Allegheny front to overturned, recumbent folds and nappes complicated by thrust faulting at the Blue Ridge.

Arndt and Wood (Ref. 2.5-64) have classified this progressive deformation resulting from compressive stresses originating to the southeast into a number of stages, each stage being categorized by effects of successively more intense deformation. Thus, the effects of deformation were transmitted with time northwestward over an increasingly greater distance, and deformation acted at any one locality with increasingly greater intensity with time. It follows that "the areas of most complex structures to the southeast underwent each of the first four stages of deformation, whereas the least intensively deformed area to the northwest was subjected only to the last orogenic force and contains features characteristic of only the first stage of deformation" (Ref. 2.5-64).

The first stage of deformation is characterized by horizontal strata cast into broad, open folds without significant thrust faulting. The second stage, which characterizes the area in which the Berwick Anticlinorium is located, exhibits low-angle thrusting and imbricate faulting followed by formation of subsidiary folds on the larger folds to develop anticlinoria and synclinoria. Structures in the vicinity of the site are consistent with this categorization. Subsidiary flexures at the site are broad, open features (refer to geologic section G-G', Figure 2.5-19), and low-angle thrust faulting is represented by the decollement in the site vicinity as discussed in Subsection 2.5.1.1.3. Subsequent stages, in which the folds are overturned and then additionally folded and faulted, are absent from the Berwick anticline area. Arndt and Wood (Ref. 2.5-64, p. B134) state, "the process of structural evolution appears to have been continuous and the result of a single orogeny that was not necessarily punctuated by pulsations.... The orogeny began after rocks of Pennsylvanian age were consolidated and prior to deposition of rocks of Late Triassic age." It is obvious from this model of deformation that thrust faulting was a logical and integral accompaniment to folding, rather than being part of some separate tectonic episode subsequent to folding.

In this process of deformation, "rocks of the more competent units characteristically folded into generally concentric, symmetric to asymmetric anticlines and synclines broken variably by faults. The rocks of the less competent units developed disharmonic folds broken by decollements, low angle thrust and bedding faults, and commonly separate discordant folds in the more competent rocks" (Ref. 2.5-21, p. 160). As a result, it is expected that rocks least able to withstand great shear pressures, such as shales, would display evidence not only of large magnitude differential movement as is found near the major thrust zones, but also of lesser but more prevalent minor structural adjustments, such as shears, incipient bedding plane faults, zones of closely spaced joints or fractures, slickensides, slaty cleavage, and so on. Thus, it would be surprising if the Mahantango Formation which occurs at the site did not show at least some of these features produced during Appalachian deformation.

"Northwestward-directed stresses of the late Paleozoic Appalachian orogeny were largely responsible for the development of the tectonic framework of the Anthracite region and the remainder of the Valley and Ridge province in Pennsylvania" (Ref. 2.5-21). There is general agreement that the time of the Valley and Ridge deformation, which is equated with the "Appalachian Revolution" (Ref. 2.5-28, p. 645), also termed the "Alleghany" or "Allegheny orogeny" (Ref. 2.5-65), ended before late Triassic time over 200 million years ago, but there is surprisingly little evidence to indicate a more exact dating of the events. As Rodgers (Ref. 2.5-34, p. 34) states, "traditionally...the deformation has been dated at the end of the Paleozoic, and in fact for generations American students were taught that it was the event that marked the end

of the era." The youngest known deformed strata are lower Permian in age (in the Georges Creek syncline just west of the province boundary in Maryland) (Ref. 2.5-34, p. 64). Therefore, typical Valley and Ridge folding and faulting occurred in the Permian and perhaps continued into the early Triassic; apparently it formed most if not all the major structural features of the province (Ref. 2.5-34, p. 64).

According to Woodward (Ref. 2.5-65, p. 2320), "there is no tangible evidence regarding the time of this deformation save that part of it must have occurred after the Pennsylvanian (or after the early Permian) and all of it before the late Triassic...Nothing fixes its appearance specifically at the end of the Permian; even its latest movements could have ceased by Middle Permian. They could also have continued through the Middle Triassic for any evidence to the contrary." The Upper Triassic shale and red bed deposits in their tilted and downfaulted basins provide an upper age limit for the Allegheny orogeny (Ref. 2.5-34, p. 115) because it is thought that the pervasive northwest-southeast compressive force field required for the northwest-directed thrust faulting and folding during the Allegheny orogeny could not have been present during the formation of the Upper Triassic basins, which required essentially extensional or tensional stress acting in the east-west or northwest-southeast direction.

In several places undeformed Triassic features are directly superimposed on Valley and Ridge structures, establishing an upper limit for Valley and Ridge deformation, of which the Berwick anticline is a part. Between the Schuylkill and Susquehanna Rivers, Triassic basin sediments rest directly on and truncate the recumbent folds and nappes (Ref. 2.5-66) developed in the southeast part of the Valley and Ridge province. These upper Triassic sediments were deposited on a peneplained surface; thus, the Valley and Ridge structures had become inactive and were exposed and eroded to near base level before upper Triassic time over 200 million years ago. Late Triassic diabase dikes are shown on the Tectonic Map of the United States (Ref. 2.5-67) crossing Appalachian fold structures about 20 miles northwest of Harrisburg near the mouth of the Juniata River. Since these dikes are neither deformed nor offset by Valley and Ridge faults, they also establish a pre-late Triassic age for Valley and Ridge tectonism.

According to Dr. Gordon H. Wood of the U. S. Geological Survey (verbal communication, 1974) there are no local specific field relationships in the Anthracite basin which could be used to supply a definite date for faulting and folding in the Anthracite basin. The only known date for Appalachian structures is supplied by regional relationships such as the Triassic events. However, Dr. Wood stated that all faulting related to Appalachian structures, except possibly for some very minor Triassic faulting, is Paleozoic in age.

On the basis of the foregoing discussion, it is concluded that thrust faulting, shearing, bedding plane faults and other similar features in the area near the site, and the slickensides and striations in the foundation rock underlying the site, were formed during the "Allegheny orogeny" or "Appalachian Revolution" which produced the folds and thrusts of the Valley and Ridge province, of which the Berwick Anticline is a part; thus, these events became tectonically inactive before upper Triassic time or over 200 million years ago. The slickensides and shearing which are evident on various bedding planes and joint planes in the foundation rock at the Susquehanna Site are therefore of no significance to the plant structures.

2.5.1.2.3.3 Geologic Features in Surficial Materials at the Site

Surficial material in the site vicinity consists of glacial drift deposited near the Olean terminal moraine (refer to Subsection 2.5.1.2.2.1). The glacial deposits near the Susquehanna site have been studied in some detail by Peltier (Ref. 2.5-5, p. 25). He describes the various features and processes associated with the terminal moraine near Beach Haven (3 miles southwest of the site) as follows:

(The Moraine) is a gravel moraine and is composed largely of poorly sorted, coarse kame gravel, medium-grained valley train gravel, and sand. These gravels were deposited in marginal channels between a stagnant tongue of ice, which lay in the center of the valley, and the valley walls... During the early stages of kame terrace development, the marginal channels flowed at a level which was high above the valley, and, at the front of the ice, fell sharply to the valley floor. At the ice front a steep alluvial deposit, composed largely of coarse gravel, was formed. Continued ablation of the ice in the valley probably caused the marginal streams to flow at successively lower levels. These streams, where they flowed along the ice, both eroded the earlier deposits and filled in their channels; where they crossed the "terminal moraine" they cut channels in the previously deposited alluvium and laid down sand and gravel on more gently sloping gradients toward the river valley beyond it. In this manner any till deposited at the ice front became buried or eroded.

At the site, little till was exposed in the excavations for the principal plant structures, in conformance with Peltier's nearby observations. Essentially all of the glacial material excavated consist of stratified drift in the form of kame delta and terrace deposits, alluvial outwash and stream gravels, much of it probably reworked in the manner described by Peltier. Indeed, the scoured and fluted bedrock surface, large potholes, and steep and even undercut contacts between bedrock and glacial drift attest to the torrential flow of water which at one time evidently cascaded across the site; and the coarse boulder gravels and erosion channels within the outwash indicate energetic reworking of the materials. In keeping with this glacio-fluvial mode of deposition, contemporaneous sedimentary features, such as those resulting from slumps at undercut or eversteepened stream banks, from differential compaction of materials deposited on irregular surfaces, and from other adjustments during deposition, may be expected (see for example (Ref. 2.5-68, p. 184-185). A few minor features such as sedimentary creep or small slumps were observed in the stratified drift, as for example north of the radwaste building, where they are associated with an undulating, fluted rock surface. Apparently these features, which terminate above the rock surface, arose through differential compaction across the irregular bedrock surface.

None of the sedimentary features exposed in the glacial materials were observed to extend downward to intersect the bedrock surface. It is concluded that all such features observed in the surficial materials at the site are consistent with their known mode of origin by glacio-fluvial process that occurred near the terminal moraine of the Olean glaciation.

2.5.1.2.3.4 Hazards from Storage in Local Geologic Structures

The unconsolidated Quaternary deposits in the vicinity of the Susquehanna SES are unsuitable for storage or disposal. While storage in unconsolidated strata is feasible, the thickness and extent of the Quaternary strata in the site area is insufficient. For example, with regard to aquifer storage of natural gas, the minimum depth of overburden necessary to maintain

adequate deliverability at the well head is about 500 ft., while depths in excess of 1500 ft. are desirable for an efficient operation.

As discussed in Subsection 2.4.13, none of the bedrock formations in the site vicinity have a high primary transmissivity. Both the primary porosity and permeability of these well consolidated rocks are generally low. Ground water utilization is dependent upon secondary permeability developed through tectonic fracturing and jointing or solution processes. Thus, while the anticlinal structure in the site vicinity may provide geometry suitable for aquifer storage or disposal, no suitable reservoir strata are known to be present.

Deep well injection into fracture porosity zones in impermeable rock might be considered as a potentially feasible method of waste disposal in the site vicinity. However, based on existing literature and considering current technology, this method of disposal is the least desirable. Reservoir strata with some degree of primary permeability are preferred (Ref. 2.5-116).

It is believed that the Precambrian basement, at depths in excess of 30,000 feet in the vicinity of the Susquehanna SES, does not contain the Fold and Thrust Belt Fracture System (Subsection 2.5.1.1.3). The nature and extent of any fracturing in these rocks is unknown. Recent advances in drilling technology suggest that the technical capability to construct a disposal well at depths in excess of 30,000 feet may be available in the near future. In the U.S. there has been at least one instance of disposal of chemical waste into Precambrian age crystalline rock (Ref. 2.5-117). However, rocks of this type with transmissibilities dependent solely on fracture porosity are not generally considered to be suitable storage or disposal reservoirs (Refs. 2.5-118, 2.5-119 and 2.5-120).

A discussion of the potential hazard resulting from a subsurface storage facility would be dependent upon the type of facility and the type of material being stored. In view of the low potential for the development of such a facility in the near vicinity of the Susquehanna SES, a discussion of potential hazard is unwarranted.

2.5.1.2.4 Site Geologic History

The geologic history of this region can be traced from Precambrian times. Rocks beneath the Paleozoic strata at the site form the Grenvillian cratonic basement, approximately 1 billion years old. The sediments that were deposited to form the Precambrian rocks in the region were subjected to magmatic intrusion, metamorphism and erosion before the onset of Cambrian time.

Paleozoic sedimentary strata in the site vicinity are estimated to be on the order of 30,000 feet thick (Ref. 2.5-28 and 2.5-38). The deposition and deformation of these strata is related to the opening and closing of the Proto-Atlantic Ocean (Ref. 2.5-69).

Although deformation in the Appalachian Orogen culminated three times in the Paleozoic -- the Taconic, the Acadian, and the Alleghenian (Appalachian) orogenies -- the effects of the first two orogenies in the folded Appalachians in which the site occurs were mainly sedimentologic rather than structural, being evidenced as unconformities and as changes in provenance, lithology and in sedimentation characteristics, in contrast to the intense folding, faulting, volcanism and metamorphism which occurred at these times on the Mobile Belt during the Taconic and Acadian events. The Alleghenian orogeny, on the other hand, resulted in the structural

configuration at the site today. The structural evolution of the Fold and Thrust belt is described in Subsection 2.5.1.1.3.

Crustal divergence in Late Precambrian, Cambrian and Early Ordovician time allowed the accumulation of a thick sequence of miogeosynclinal sediment in the Appalachian Basin (Subsection 2.5.1.1.2). The Taconic Orogeny beginning in Middle Ordovician time signifies convergence and uplift in the Mobile Belt.

The highly deformed early Paleozoic strata are unconformably overlain by less deformed, coarser grained clastic sediment which is in turn overlain by the Siluro-Devonian carbonate sequence. This sequence is thickest in the east and thins westward.

Northeastward from the site the carbonate strata interfinger with clastic detritus. Late Paleozoic strata are clastic through most of the Appalachian Basin (Subsection 2.5.1.1.2).

These strata reflect the closing of the Proto-Atlantic Ocean. At the peak of the Taconic Orogeny along the cratonic margin to the east, ophiolitic rocks (presumably oceanic crust) were obducted from the eugeosyncline, and the miogeosynclinal strata (carbonate and detrital alike) were thrust onto the craton. The geologic setting at the site is the result of this activity. Folding and thrust faulting occurred through mechanical detachment from rigid basement rocks along decollements in shaly strata near the base of the Paleozoic section (Ref. 2.5-38). The site rests on the northern limb of one such fold, the Berwick Anticlinorium. The deformation progressively increased in intensity toward the southeast, from broad, gentle open folding northwest of the Allegheny front to overturned, recumbent folds and nappes complicated by thrust faulting at the Blue Ridge. The effects of final convergence and translation during the Late Paleozoic appear to be limited to the Mobile Belt (Subsection 2.5.1.1.3 and 2.5.2.2).

The Appalachians appear to have undergone erosion through most of the Mesozoic Era. Tectonic activity related to the opening of the Atlantic Ocean appears to have had no significant structural effect in the Fold and Thrust Belt and Stable Interior (Subsections 2.5.1.1.3 and 2.5.2.2) until the Cretaceous Period. At that time, subsidence of the Atlantic continental margin allowed transgression of the sea well inland of the site vicinity.

During Cenozoic uplift, major drainage in the area followed relatively straight southeastward courses through the Cretaceous sedimentary strata to the Atlantic. The Ancient Little Schuylkill River flowed past the site toward the present day Delaware Bay. The ancient north branch of the Susquehanna River flowed through Wilkes-Barre, Pennsylvania toward Trenton, New Jersey. As the Appalachians were exhumed, the east-northeast structural fabric began to exhibit control of the drainage pattern. The present course of the north branch of the Susquehanna River resulted from stream capture of the Ancient Little Schuylkill and ancient north branch through their east-northeast tributaries by the main branch of the Susquehanna River (Ref. 2.5-3).

Northeastern Pennsylvania has undergone at least three glaciations during the last 150,000 years and possibly one or more prior to that date. Till at the site was deposited during the Olean substage about 55,000 to 60,000 years ago (Ref. 2.5-5 and 2.5-6). Older Illinoian drift occurs in the valley of the Susquehanna River between the Olean terminal moraine at Beach Haven (about 3 miles southwest of the site) and the confluence of the north and west branches of the Susquehanna River. Post-Olean advances did not reach the site vicinity (Ref. 2.5-5 and 2.5-6).

Peltier (Ref. 2.5-5) mapped discontinuous kame terraces along the Susquehanna River in the site vicinity. The highest such terrace formed by ice marginal streams occurs at about 650 feet above sea level at the site. Refer to Subsections 2.5.1.2.2 and 2.5.1.2.3.3 for further discussion of Pleistocene erosion and deposition at the site.

Since the retreat of the Wisconsin ice sheets from the region, broad regional uplift appears to have occurred, probably at least in part as a result of crustal rebound subsequent to the removal of ice load. Erosion has continued and soil profiles have formed.

2.5.1.2.5 Engineering Geology Evaluation

Site subsurface exploration is described and discussed in Subsection 2.5.4.3.

Laboratory tests of foundation materials, and in situ geophysical tests of the foundation materials are discussed in Subsections 2.5.4.2 and 2.5.5.

Geologic mapping of the final foundations is described in Subsections 2.5.1.2.2, 2.5.1. and 2.5.4.1.3. It was concluded from these studies and evaluations that the site geologic and foundation conditions are entirely suitable for the construction and operation of the plant.

2.5.1.2.5.1 Geologic Conditions Under Category 1 Structures

All Seismic Category 1 plant facilities, except the spray pond, Engineered Safeguard Service Water (ESSW) pumphouse and pipeline, and the diesel generator 'E' fuel tank are founded on bedrock. The ESSW pipeline trench is excavated partly in soil and partly in rock. The location of these facilities is shown on Figure 2.5-24.

The foundation rock is a hard, indurated siltstone, a member of the Devonian Mahantango Formation. In the foundations area it is quite massive and lithologically homogeneous, with bedding generally not well defined, and lacking the bedding plane fissility usually associated with less well indurated shaly siltstones and silty shales. In places the rock exhibits a slaty cleavage, further evidence of its indurated nature. All Category 1 rock foundations were excavated to unweathered bedrock. Geologic maps and sections of the Category 1 excavations in rock are shown in Figures 2.5-18 and 2.5-19. More detailed discussion of the foundation geologic conditions is contained in Subsections 2.5.1.2.2 and 2.5.1.2.3. Engineering properties of the foundation rock are described in Subsection 2.5.4.

The spray pond is situated over a glacial or preglacial, east-west trending bedrock valley as outlined by contours on top of bedrock (Figure 2.5-17). The valley is filled with dense gravelly and sandy glacial outwash and till deposits which attain a maximum thickness of about 110 feet adjacent to the spray pond area. They were deposited no later than the Olean substage (early Wisconsinan) of the Wisconsinan glaciation which occurred over 50,000 years ago. In general, the deposits are permeable and consist of a sequence of sand, gravel, and boulders overlain by sand and gravel, overlain in turn by silty sand. The entire sequence is highly variable in grain size distribution and sorting, and contains discontinuous pockets of similar materials. As a rule, grain size decreases and sorting increases toward the top of the sequence.

The southwestern tip of the spray pond is cut into bedrock while the remainder was excavated in these permeable glacial materials. The thickness of the glacial deposits beneath the bottom of the spray pond ranges from zero at the rock contact to 93 feet at the eastern end of the pond. The spray pond is lined to minimize seepage losses to the underlying permeable glacial deposits. The foundation of the pumphouse structure located at the southeastern corner of the pond is underlain by 35 to 60 feet of glacial material. The ESSW circulation pipelines between the pumphouse and the plant intersect bedrock at an elevation of 668 feet, approximately 260 feet southeast of the pumphouse (refer to Figure 2.5-17A). A geologic map of the spray pond area is presented on Figure 2.5-15. Further discussion of conditions at the ESSW pumphouse and spray pond are contained in Subsections 2.5.1.2.2, 2.5.3 and 2.5.5.

The area underlying the diesel generator 'E' fuel tank consists of a dense to very dense glacial outwash and till deposit. The deposit consists of a sequence of sand, gravel, cobbles, and boulders overlain by sand and gravel, overlain in turn by crushed stone.

2.5.1.2.5.2 Landslide Potential

Natural slopes adjacent or close to the principal plant structures are relatively flat. Most of these slopes are composed of soil; few rock slopes occur (Figure 2.5-17 shows areas of rock outcrops).

North of the spray pond the Trimmers Rock Formation forms a relatively steep ridge rising approximately 380 ft. above the pond. The south-facing slope of this ridge is essentially a rock slope underlain by flaggy, resistant sandstone thinly mantled with soil and rock fragments. The closest approach of this slope to the spray pond is along the northern perimeter of the pond; the toe of the slope, at elevation 710-720 feet, is 250 feet or more from the edge of the pond (at elevation 679 feet). The maximum slope along the ridge is about 2 horizontal to 1 vertical, with an overall slope of 3-1/2 horizontal to 1 vertical, a relatively flat slope for competent rock. Figure 2.5-56 shows a typical profile along the steepest portion of this slope north of the spray pond area. Bedding in the rock dips approximately 30° to the north into the slope; thus, it is favorably oriented for slope stability. Data of McGlade, et al. (Ref. 2.5-56, p. 147) indicate that natural slopes eroded on Trimmers Rock strata are "steep and stable."

No old landslides, rock slips, or landslide scars have been noted near the plant structures. It is concluded that the natural slopes present no significant hazards to plant structures.

Stability of excavated and fill slopes is discussed in Subsection 2.5.5.

2.5.1.2.5.3 Areas of Potential Subsidence, Uplift, or Collapse

Potential sources of subsidence or collapse in the Pennsylvania Valley and Ridge region include coal mines and karst terrain; however, neither of these conditions are known to occur within several miles of the site and therefore they are not significant to the site.

No coal beds are present beneath the site; the nearest coal measures are about 3-1/2 miles north of the site near Shickshinny, which is at the extreme western end of the anthracite producing belt in the Lackawanna syncline (Figures 2.5-25 and 2.5-26). The nearest underground coal workings are about 2 miles east of Shickshinny (Ref. 2.5-70); the nearest that

have been associated with surface settlement are near Nanticoke, Pennsylvania, approximately 10 miles northeast of the site. Rocks in the site area have no known potential for oil or gas production. The nearest oil or gas field is located 25 miles northeast of the site.

The shallowest carbonate rock that may be present beneath the site occurs below the Marcellus-Manhantango sequence as limy beds within the Upper Silurian, Tonoloway and Wills Creek Formations and the Lower Devonian, Keyser, Old Port, and Onondaga Formations (refer to Subsection 2.5.1.1.2.3 and Figure 2.5-14). Some of these units crop out on the flank of the Berwick anticlinorium north of Bloomsburg about 10 miles west-southwest of the site, but most are absent nearer than this to the site having been removed by erosion or faulting (Subsection 2.5.1.1.2.3). None have been mapped within five miles of the site (Figure 2.5-12). The Onondaga may occur in the subsurface near Berwick, five miles west-southwest of the site, inasmuch as mud-filled caves have been encountered during well drilling operations at Berwick; however, since the secondary porosity along joints and bedding planes in the Onondaga has been characterized as of only "medium" magnitude (Ref. 2.5-56), such cavities would be expected to be neither large in size nor extensively developed. If the Onondaga does extend eastward beneath the site, it would be at a depth probably exceeding 1,000 feet and beneath the Marcellus-Mahantango shale and siltstone sequence (Figure 2.5-14). At this depth of burial beneath the site, carbonate beds possibly present would have no significant potential for subsidence or collapse at ground surface.

The site is not known to be in an area experiencing localized doming or subsidence. Relative rates of regional uplift or subsidence are not well defined for this area, but some recent studies have been presented in the literature. Brown and Oliver (Ref. 2.5-54, Figures 5 and 7) show a releveling profile across the Appalachians at the latitude of Harrisburg about 60 miles south of the site. This profile suggests that the Valley and Ridge province at the latitude of Harrisburg is rising uniformly at the rate of about 5 mm per year. They find in general that "the Appalachian Highlands are being uplifted with respect to the Atlantic Coast at rates up to 6 mm per year" (Ref. 2.5-54, p. 31). Because the measurements are referenced to a given station, it is not possible to determine absolute vertical crustal velocities. Since Brown and Oliver (Ref. 2.5-54, p. 31) also state the "Atlantic Coastal Plain... is tilting away from the continental interior" the data may indicate simply that the Appalachian Highlands are nearly stationary, or that they are subsiding more slowly than the coastal region. Inasmuch as differential rates of this magnitude are greater than the geologic record suggests could be sustained over geologic time, the authors presume an oscillatory mode of continental interior uplift or coastal depression with time on the order of 106 years per oscillation.

Superimposed on these broad, regional differentials are smaller, secondary variations in the rate of vertical movement within the Appalachian Highland on the order of 1 to 3 mm per year total amplitude (Ref. 2.5-54, Figures 7 and 8). The location of some of these secondary maxima or minima appear to correlate spatially with seismicity; others do not. The wave length between such secondary maxima is on the order of 300 km, a distance suggestive of origin in "large scale movements of the earth's crust" (Ref. 2.5-54, p. 27). Although the authors speculate there may be, in some areas, a possible association of these secondary peaks in the vertical velocity profiles with seismicity, they acknowledge (Ref. 2.5-54, p. 30) that "without further data it is impossible to demonstrate that the relationship is more than coincidental." In any event, flexure of a very few millimeters over hundreds of kilometers is very broad indeed and is not significant to structures.

In eastern New York, post-glacial offsets in shales and slates are documented by Oliver, et al. (Ref. 2.5-51). The nearest locality listed by Oliver, et al. (Ref. 2.5-51) is near Hyde Park, New York, about 120 miles east of the site. The authors wonder whether the cause of these offsets "might stem from crustal rebound following removal of the ice load or from still more broadly based tectonic or orogenic forces" (Ref. 2.5-51, p. 586). However, it is significant that these high-angle reverse offsets of the glacial striations in bedrock are on the order of only one inch or less of displacement. The authors also mention other possible mechanisms such as "...thermal changes, hydration, or a chemical process in the shales," and conclude the data "do not seem adequate to resolve this point" (Ref. 2.5-51, p. 569). Another assessment of the same data concluded the offsets arise from either frost heave or glacial rebound. If related in some way to frost action or the severity of frost, then one might expect the effects of heave, such as on precise leveling monuments, to be more pronounced with altitude. Precisely such a correlation of secondary velocity maxima with elevation was noted and discussed by Brown and Oliver (Ref. 2.5-54, p. 27).

Additional independent evidence on the magnitude of general Appalachian uplift, or lack thereof, in the Pliocene and Quaternary is provided by Owens (Ref. 2.5-52), who based his assessment on the assumption that uplift in the source area is accompanied by erosional transport of clastic material to adjacent basins. He found that Pliocene and Quaternary sediments of the Atlantic coastal plain from New Jersey southward are only 50 feet or less in thickness, indicating no great intensity of uplift through this period; and moreover that there are no marked accumulations of sediment in centers of deposition, suggesting a general, uniform uplift, or even static conditions, of the entire Appalachians.

Therefore, the total geologic record strongly suggests that unusual regional crustal instability has not recently occurred in the Appalachians. Brown and Oliver (Ref. 2.5-54, p. 31) conclude, "Although the rates of relative vertical movements determined from leveling seem large by comparison with rates deduced from some forms of geological evidence...these velocities do not seem unreasonable in terms of other types of geological information." Further, "the rates of vertical crustal movement presented . . . compare very favorably with those found in other portions of the world." Relative rates of vertical uplift observed for the site region therefore appear to be quite typical compared to observations elsewhere, and accordingly do not seem to be reflective of abnormal conditions.

The balance of evidence favors Appalachian crustal activity restricted to generally uniform uplift, probably differing slightly in local areas, and perhaps having an oscillatory character with time. Little if any evidence has been presented to demonstrate that these may be significant to engineering planning or seismic risk evaluation. No faulting has been shown to be involved in this recent activity, and correlation with seismicity is likewise not established. In areas adjacent to the Appalachians, small-scale post-glacial offsets have not been correlated with seismicity and tectonic origin of the offsets has not been established.

It is concluded that the available data do not indicate that existing or future uplift or subsidence, as from man's activities or from geologic conditions such as regional warping, will be significant to the site.

2.5.1.2.5.4 Behavior of Site During Prior Earthquakes

There is no evidence at the site of any effects, such as landslides, fissuring or subsidence, which could be attributed to the occurrence of prior earthquakes.

No Pennsylvania earthquakes have been reported as felt in the site vicinity. Within historical times, approximately fourteen earthquakes originating outside Pennsylvania could have been felt at the site, with the probable maximum intensity of IV on the Modified Mercalli Scale. The nearest of these earthquakes occurred 90 to 100 miles from the site (Wilmington, Delaware, 1871, epicentral Intensity VII). Ground motion at this intensity (IV) would have had no effect on the site.

2.5.1.2.5.5 Zones of Deformation or Structural Weakness

As reported in the PSAR, the preconstruction investigation defined a number of structural features at the site such as folds, joints, fractures, cleavage, slickensided joint planes, and bedding plane shears. The PSAR stated (p. 2.5-16),

The prominent joint directions are parallel and perpendicular to the strike of the strata. The major joints...(strike) parallel to bedding. This joint set dips nearly perpendicular and opposite in direction to the dip of the bedding. A more open but less frequent series of vertical joints strikes parallel to the dip of the strata. High angle joints healed by secondary calcite and quartz mineralization are present in the vicinity of minor shear zones. The observed fractures, while relatively numerous in the upper 20 feet of rock, decrease with depth. At a depth of about 20 feet into rock, the fractures are tight (generally healed with calcite filling) and would not adversely affect foundation performance.

Minor bedding plane slips at depth have been observed in the site area, both north and south of the interior ridge. Those slips have not experienced movements in more than 200 million years. A minor slip of this nature could be exposed in any large excavation anywhere in the area; however, it would not affect the structural design of the facilities.

Excavation during construction confirmed the PSAR evaluation and supplied additional data. During excavation, numerous slickensided joint planes were exposed and mapped (Figure 2.5-18). Thin, slickensided bedding plane shears, well healed with laminar quartz and calcite mineralization, were also exposed in the foundations. The field data indicate these shear planes are folded in the same manner as the bedding (Figure 2.5-19). They are, moreover, cut by vertical, calcite-filled joints which are continuous across the shears with no offset. In addition, where the shears can be traced to an intersection with a smooth, glacially eroded surface forming the top of rock, the eroded surface displays no displacement or offset across the shear plane. Since the erosion of the rock surface would necessarily have occurred prior to the deposition of the overlying glacial deposits, which have been established as being more than 50,000 years old (refer to Subsection 2.5.1.2.2.1), this relationship shows that any displacement along the shearing occurred more than 50,000 years ago. In reality, the most probable age of the shearing is pre-Triassic, or over 200 million years ago. This is indicated by regional relationships plus the fact that the shear plane is folded (A detailed presentation and analysis of the relationship between site and regional structure is presented at the end of Subsection 2.5.1.2.3.2).

All features arising from tectonic deformation at the site are geologically old. In the foundation rock, all shears and joints are tight or are fully healed with calcite and quartz mineralization; accordingly, they do not adversely affect the strength, bearing capacity or compressibility of the foundation rock. They are therefore not significant to the plant structures. The conclusion stated in the PSAR (P. 2.5-18) that "the minor structural conditions observed at the site are not of significance with respect to siting or design for the use of the site for its intended purpose," has been confirmed.

2.5.1.2.5.6 Zones of Alteration or Irregular Weathering

Bedrock beneath the seismic Category I structures is a dark gray, indurated, massive siltstone. It is not susceptible to rapid weathering; no appreciable slaking of fresh rock exposures was observed in the foundations. Depth of weathering below original top of rock varies from zero to about 20 feet. The rocks occupying depressions in the bedrock surface are generally unweathered. However, open fractures were encountered to a depth of about 20 feet. Below that depth, fractures are not common but where they do occur, they are generally "healed" with calcite filling.

Weathering appears to have progressed initially downward by dissolution of calcite from calcite-coated joints, seams and shear planes, and refilling by clay or other weathered material. In one exceptional case, weathering along joints and fractures, as distinguished from weathering of the rock itself, was observed nearly 70 ft. below original top of rock. In this instance, which was between the circulating water pumphouse and the Unit 1 cooling tower, the bedrock originally formed a knoll and contained numerous low angle, slickensided, calcite and quartz-filled joint planes and abundant vertical, calcite-filled fractures, forming an intersecting, permeable network of channels through which water readily percolated downward, dissolving the soluble carbonate joint and fracture fillings. Notwithstanding the depth of weathering here, the design elevation of the bottom of the circulating water pumphouse is below the depth to which this zone is weathered, and this structure was founded on sound unweathered bedrock.

2.5.1.2.5.7 Potential for Unstable or Hazardous Rock or Soil Conditions

Foundation rock at the site is hard, indurated, unweathered siltstone, a member of the Middle Devonian Mahantango Formation. Similar materials underlie the site to a depth of over 1,000 feet. This rock does not contain unstable minerals; it provides highly stable foundation conditions and does not constitute a source of potential hazard to the plant.

Soils at the site are, except for the uppermost few feet, glacial in origin and consist of resistant fragments of rock that were transported from the region north of the site. Most were deposited by flowing melt water from the glaciers under torrential flow conditions, and some of the soils probably have been overridden by ice sheets. These glacial soils are noncalcareous and over four-fifths of the rock in them consists of sandstone (Ref. 2.5-5).

The origin and mineralogy of the soils is such that they present no hazardous conditions. Detailed engineering characteristics of soils in regard to slope stability, bearing capacity, stability under dynamic loads and consolidation characteristics under structural loads are discussed in Subsections 2.5.4 and 2.5.5.

All foundations for the Category 1 plant structures that are founded on rock are excavated to or into essentially unweathered material. No significant irregular alteration or weathering, or zones of structural weakness due to weathering, shearing or fracturing were encountered at the bearing elevation for those structures designed to rest on unweathered rock.

2.5.1.2.5.8 Unrelieved Residual Stress on Bedrock

No indications were found during excavation and construction at the site of the presence of significant stress in bedrock. No popping or spalling rock was observed. There were no indications of heave at the base of rock slopes or in the bottom of excavations. Some vertical joints close to and subparallel to vertical excavated slopes opened very slightly, but this was attributed to gravity forces, not in situ stresses. If significant in situ stresses did in fact exist in the rock, evidence of this should have been noted in the excavation; no such indications were noted. For example, a thin mudmat was routinely placed on the rock after evacuation to foundation grade. If significant heave had occurred, it would have been readily detected by cracking of the mudmat. No such cracking was observed.

2.5.1.2.5.9 Conclusions and Summary

Consideration of all engineering geologic factors at the Susquehanna site leads to the conclusion that the site is well suited for the construction and operation of the plant. There is no geologic feature or condition at the site or in the surrounding area which precludes the use of the site for a nuclear generating facility. The bedrock in the construction area is competent and provides satisfactory foundation support for all major structures.

2.5.1.2.6 Site Groundwater Conditions

The groundwater table beneath the site generally occurs within 35 feet of the ground surface. The notable exception is in the deep, easterly sloping, buried bedrock valley present about 1000 feet north of the center of the plant, where a water table depth of as much as 79 feet was recorded. Generally, the lower part of the overburden deposits is saturated, although over portions of the upland area on the site, the groundwater level is found only in the underlying bedrock. Depth to bedrock is variable and ranges from zero to over 100 feet. The groundwater level contours shown in Figure 2.4-31 appear to be controlled to a large extent by the top of bedrock contours (Figure 2.5-17).

Groundwater movement on the site is generally in an easterly direction. With the exception of a few springs on site. Most of the groundwater is believed to discharge ultimately to the Susquehanna River. The average groundwater velocity is estimated to be between 1.5 and 2.0 feet per day along flow paths from the station to the Susquehanna River.

The site is not located in a recharge zone for any aquifer. However, groundwater recharge to the unconsolidated sand and gravel does occur over the site area. The predominantly siltstone strata of the Mahantango Formation beneath the site constitutes a source of limited domestic water supply. Because of its relatively low transmissibility characteristics, the Mahantango cannot be considered to be an aquifer.

From a hydrologic standpoint, there are two general types of aquifers in the region. The first type consists of sandstone and occasional limestone strata which occur within the predominantly shale sections of the Paleozoic age bedrock. The second type is unconsolidated Quaternary deposits which consist for the most part of Pleistocene stratified drift, till, or kames which are often overlain by a thin recent soil cover. From a survey of domestic water supplies within two miles of the station, it was found that nearly all of the wells are completed in shale bedrock.

Detailed information on groundwater conditions and movement on the site and in the region is given in Subsection 2.4.13.

2.5.2 VIBRATORY GROUND MOTION

A discussion and evaluation of the seismotectonic characteristics of the Susquehanna SES site and the surrounding region is presented in this section. The purpose of this investigation is to present the seismic design criteria for major structures at the station in conformance with guidelines as outlined in Standard Format and Content of the Safety Analysis Reports for Nuclear Power Plants, and Appendix A of 10 CFR, Part 100.

A description and results of the field investigation and laboratory testing program, which provided background information for this investigation, is presented in detail in Subsection 2.5.1.

2.5.2.1 Seismicity

The station is situated in a region which has experienced only a minor amount of moderate earthquake activity in historic time. The record of earthquake occurrences in the region dates back to the middle 16th century. Many earthquakes have been reported since that time and minor structural damage has been associated with several of the events; however, none of these earthquakes were considered to be of major or catastrophic proportion. Because this region has been fairly heavily populated since the early 18th century, it is quite certain that any significant earthquake activity (MM Intensity VII or greater as defined by the Modified Mercalli Intensity Scale, 1931, see Table 2.5-1) would have been reported in local newspapers, private journals or diaries. The lack of any such documentation is indicative of the absence of significant major earthquake activity in the region during this period.

Structural damage is the primary rating criterion for larger shocks. The effects of earthquakes on the rather large variety of construction materials used in older structures such as chimneys, rock walls, etc., are highly variable, making intensity evaluations based on such reports imprecise. The rather long period of record, however, and the evenly distributed population provide a reasonable basis for estimates of future activity.

Table 2.5-2 lists all events within 200 miles of the station with magnitudes (Richter) greater than 3.0 or MM intensities greater than III, and all seismic events within 50 miles of the station. Figures 2.5-8A and 2.5-8B displays these events on the regional structure of the area around the station, along with the significant earthquakes (MM Intensity V and greater) which have occurred outside the 200-mile radius.

The largest events to have occurred in the immediate station vicinity were the Wilkes-Barre disturbances of February 21 and 23, 1954 (local dates), with assigned intensities of VII and VI, respectively. These intensities were based on the damage inflicted upon a very small area, about 0.15 square miles of the city. These disturbances occurred only 16 miles from the station; however, they are considered to have resulted from mine collapse as discussed in detail in Appendices 2.5A and 2.5B. Thus, these shocks need not be considered in the analysis of earthquake risk as regards the station.

The largest event to have occurred within 200 miles of the station was the Intensity VII-VIII shock at Attica, New York, on August 12, 1929, some 150 miles northwest of the station. This earthquake imposed some moderate damage at Attica and villages in the immediate vicinity of the epicenter, but was not reported as felt in the Berwick area (Ref. 2.5-71).

Four Intensity VII earthquakes have occurred at a distance of about 100 miles from the station: two (1737 and 1884) were near New York City, one (1927) near Asbury Park, New Jersey and one (1871) near Wilmington, Delaware.

The closest of these Intensity VII events was the shock which occurred in the vicinity of Wilmington, Delaware on October 9, 1871, approximately 100 miles to the south of the station. Based on damage reports and intensities felt, the epicenter has been located near Wilmington, whereas the shock was felt from near Chester, Pennsylvania on the north to Middletown, Delaware, on the south and from Salem, New Jersey on the east to Oxford, Pennsylvania on the west. The initial shock was followed by a much smaller shock just after midnight on October 10. A contemporary newspaper account indicates that the initial shock was felt at Wilmington "with greater distinctness." Buildings were shaken severely and a number of chimneys were damaged in the surrounding towns of Oxford, Pennsylvania, and New Castle and Newport, Delaware. An interesting aspect of this earthquake is the fact that it was accompanied by a very loud sound, as of an explosion. This loud noise, in fact, led to the belief that the shock was caused by an explosion, probably at the powder mill of the E.I. DuPont de Nemours Company, near Wilmington. This possibility was carefully investigated at the time and it was concluded that the shock was a legitimate earthquake. Existing reports, however, do not report the shock being felt in the Berwick area.

The two events near New York City, about 118 miles from Berwick, may have been felt at the station, but with an intensity certainly no greater than III. The 1884 shock affected an area extending from Portsmouth, N.H., to Burlington, Vt., southwest to Binghamton, N.Y., Williamsport, Pa., southeast to Baltimore, Md., and Atlantic City, N.J. At Bradford, Pennsylvania, reports were made of panes of glass broken in a large hotel, and other moderate damage was sustained. All hotels in Brooklyn, New York were shaken violently. In 1927, a similar shock listed as Intensity VII was centered near Asbury Park, New Jersey. Several successive waves, described as seeming to travel from west to east, caused homes near Asbury Park to shake and oscillate perceptibly.

Several Intensity VI earthquakes have occurred less than 100 miles from the station. On May 31, 1908, 48 miles from the site, Allentown, Pennsylvania was shaken by what was believed to be a mild earthquake. The shock lasted about a second and was described as a rumbling sound followed quickly by a report which "sounded like the falling of chimneys of a building" (The Lehigh Register June 3, 1908). The Philadelphia Inquirer adds, "The only other place where the shock was felt was Catasauqua, three miles away. At first it was thought that a battery of boilers in some local industry might have exploded, but no such accident was

reported. The quake was accompanied by a low rumbling noise and lasted about two seconds but was only felt over an area of some 50 square miles. On January 7, 1954, an Intensity VI shock occurred approximately 54 miles from the station. This was the first of a series of minor shocks in Berks County. The Reading Times reported on January 8, 1954, that a "minor" earthquake shook Berks County communities, and succeeding tremors of lesser intensity were experienced mainly by residents in West Reading, Wyomissing, West Louve, West Wyomissing, Wyomissing Hills and Sinking Spring. Continued mild aftershocks shook the downtown area of Sinking Spring which appeared to be the epicentral area for these disturbances. The damage was described (Ref. 2.5-72) as minor: broken chimneys, breaks in brick and plaster walls, and broken dishware. Similar damage, including broken windows, was reported in other communities west of the Schuylkill River. The main shock was recorded by seismograph stations at Fordham, Palisades (Columbia University) and the U.S. Coast & Geodetic Survey at Washington, D.C. Dr. Jack Oliver of Columbia University described the initial tremor as "a typical east coast earthquake."

According to the Philadelphia Inquirer, as of January 8, 1954, the earth tremors which had been recorded in Berks County since 1900 were:

- August 30, 1902
- June 6, 1915
- February 28, 1925
- November 1, 1935
- June 8, 1937
- February 18, 1938
- September 4, 1944

The events of 1902, 1915 and 1938 are not reported in the standard catalogues and are, therefore, considered as very small, localized disturbances for which there is only local record. The shocks of 1925 and 1944 were large events in the St. Lawrence River near Quebec, Canada and Massena, New York which were felt with intensities of less than III at the station.

Shocks on January 24, 1954 and on August 11, 1954 affected Sinking Hole, Pennsylvania, according to the Reading Times (August 11, 1954). These shocks were attributed by the U.S.G.S. to the caving of solution cavities. Similar conclusions about the "sinking of the earth in general" were reached by Penn State University scientists after the event on September 24, 1954 which was assigned an Intensity II at Sinking Spring Borough, 5 miles west of Reading, Pennsylvania.

Another shock of Intensity VI occurred 63 miles southeast of the station, near Cornwall, Pennsylvania, on May 12, 1964. Coffman and Von Hake (Ref. 2.5-72) report a cracked wall, fallen plaster, and small landslides. The Lebanon Daily News reported: "...the tremor was so mild that many persons slept right through it." However, Dr. B.F. Howell, Jr., Chairman of the Geophysics Department at Penn State University, reported that the quake was the most intensive to hit the state in 10 years.

On September 1, 1895, an event of Intensity VI near Philadelphia, 76 miles from the station, was felt from Sandy Hook, New Jersey to Brooklyn, New York to Darby, Pennsylvania, and Wilmington, Delaware. Another shock of Intensity VI occurred on March 23, 1957 in the same general vicinity, 79 miles southeast of the station. These shocks were not reported felt in the Berwick area.

Five shocks (Intensity VI, III, V, III, and IV) occurred in central and southern New Jersey on August 23, 1938, 116 to 128 miles from the station. The largest shock was felt from northern New Jersey to Wilmington, Delaware.

Although it is indicated that several of the large, distant shocks listed above were probably felt at the station, no damaging effects were experienced. No Pennsylvania earthquakes have been reported as felt in the area of the Susquehanna SES.

In summary, there are no reports from the Berwick area of Pennsylvania which would indicate that ground motions from any historical earthquake in the east have exceeded (or even equalled) an intensity as great as IV on the competent rock on which the station is located.

2.5.2.2 Geologic Structures and Tectonic Activity

2.5.2.2.1 Tectonic Provinces

The area within a 200 mile radius of the Susquehanna SES includes parts of six tectonic provinces (Figures 2.5-8A and 2.5-8B). The provinces are, from west to east, Stable Interior, Fold and Thrust Belt, Blue Ridge-Highlands, Conestoga Valley, Inner Piedmont, and Coastal Plain.

The tectonic province concept used to define these provinces is based on an evolutionary model of the Appalachian orogen (Ref. 2.5-73) and derived from early studies in the region (Ref 2.5-74). This concept was used in this study to provide the province boundaries of significance to the station.

2.5.2.2.2 Tectonic Differentiation of the Appalachian Orogen

The outline and discussion presented below summarizes the relationships and derivations of tectonic provinces of the Appalachian orogen, as displayed in Figures 2.5-8A and 2.5-8B any parts of which occur within 200 miles of the station.

1. Craton
 - a. Eastern Belt
 - (1) Blue Ridge-Highlands
 - b. Western Basin
 - (1) Stable Interior
 - (2) Fold and Thrust Belt
2. Mobile Belt
 - a. Eastern Cratonic Margin
 - (1) Conestoga Valley
 - (2) Inner Piedmont
 - (3) Coastal Plain

Considering the tectonic evolution of the Appalachian orogen, it is subdivided as above into two fundamental areas; the part affected only by convergent diastrophism (craton), and the part affected by initial divergent, convergent, translational, and final divergent diastrophisms (mobile belt). The mobile belt, as defined in this report, is situated east of the great anticlinoria cored by Grenvillian rocks; i.e., east of the Long Range (Nova Scotia), the Green Mountains, the Berkshire Highlands, the Hudson-New Jersey Highlands-Reading Prong, and the Blue Ridge Mountains. The mobile belt thus corresponds to the Appalachian eugeosyncline and includes the quasi-cratonic margins. The western edge of the mobile belt parallels and lies to the west of what was originally the eastern edge of the North American continent during Cambro-Ordovician time as defined by Rodgers (Ref. 2.5-74).

2.5.2.2.3 Tectonic Differentiation of the Craton

The cratonic portion of the Appalachian Highlands is underlain by continental crust composed of 1000 million-year-old crystalline rocks which were deformed during the Grenvillian orogenic cycle. On the eastern edge of the craton, these rocks crop out at the surface as great anticlinoria. West of these elevated anticlinoria lies an elongated, downwarped segment of the continental crust forming the asymmetric Appalachian basin. The floor of this basin is formed of Grenvillian rocks greatly depressed in the east (up to 40,000 feet below sea level) and gradually rising toward the west. The basin is filled with largely unmetamorphosed sedimentary rocks (both clastic and carbonate) ranging in age from Early Cambrian to Carboniferous. These rocks form a sedimentary wedge, thickening to the southeast, reflecting the asymmetry of the basin floor.

Blue Ridge - Highlands Tectonic Province

The eastern portion, termed here the Blue Ridge - Highlands, constitutes a tectonic province and is characterized by Grenvillian rocks deformed during the Paleozoic convergent stage.

Characteristically, the terrain is mountainous and exhibits exposure of some of the oldest rocks in the eastern U.S. (1000-1100 million years). Earthquakes no greater than Intensity VI are characteristic of this tectonic regime, and none have been related to specific structures.

Stable Interior Tectonic Province

The Stable Interior Tectonic Province of the western basin is characterized by the absence of intense deformation and the presence of shelf-delta type Paleozoic sediments.

The rocks display gentle folding as opposed to the intensely folded and faulted rocks of the Fold and Thrust Belt immediately to the southeast. The largest significant earthquake to have occurred in this province (within the regional scope of this study) was the 1929 Attica, New York, event (initially cataloged as Intensity VII-VIII) approximately 168 miles from the station. This shock and an accompanying concentration of lesser events has been spatially related to the Clarendon-Linden Fault, an anomalous structure in the essentially untectonized rocks making up this portion of the Stable Interior. A small concentration of activity, apparently related to doming of the Adirondak massif, occurs 150 to 200 miles northeast of the station. With the exception of these moderately active areas, the province is virtually aseismic.

Fold and Thrust Belt Tectonic Province

The Fold and Thrust Belt tectonic province is characterized by tightly folded and thrust-faulted Paleozoic sedimentary strata deposited as flysch or molasse. The northwestern boundary of this province generally marks a transition between gently folded strata on the northwest (Stable Interior) and intensely folded and faulted strata on the southeast, thus marking the western limit of Paleozoic thrusting (Ref. 2.5-75).

The largest earthquake which has been recorded in the Fold and Thrust Belt tectonic provinces was the Giles County, Virginia, Intensity VIII shock of 1897, over 350 miles from the station, and in the southerly division of the Fold and Thrust Belt. Other earthquakes in this province are widely scattered with only two events as large as Intensity VI occurring within 200 miles of the station.

2.5.2.2.4 Tectonic Differentiation of the Mobile Belt

The mobile portion of the northern Appalachian orogen within the region of interest for this study includes the eastern cratonic margin, which is underlain by continental crust of predominantly Grenvillian age (Inner Piedmont and Conestoga Valley tectonic provinces).

The eastern cratonic margin is bounded on its western side by the Blue Ridge - Highlands tectonic province and on its eastern side by the eastern most extent of Grenvillian basement.

This eastern boundary is interpreted principally from a line of gneiss domes of one billion year-old continental crust including the Pine Mountain belt, the Sauratown Mountains anticlinorium, the Baltimore Gneiss domes, and, possibly, the Chester dome of Vermont. This boundary corresponds to the eastern limit of the ancient continental margin of North America (Ref. 2.5-76 and 2.5-77). It also coincides with several significant geological and geophysical changes (Ref. 2.5-76). First, it parallels the main gravity high of the Appalachians (Ref. 2.5-78). Second, it is marked by contrasting seismic refraction profiles that reflect deep crustal contrast. Finally, it is a zone of faulting, contrasting structural style and contrasting metamorphic facies.

This cratonic margin is divided into two tectonic provinces north of Virginia, the Conestoga Valley province and the Inner Piedmont province. The boundary between these provinces corresponds to the Martic Line in Pennsylvania (Ref. 2.5-79) and the southward extension of Cameron's Line in western Connecticut.

Conestoga Valley Tectonic Province

The Conestoga Valley tectonic province is characterized by a miogeosynclinal assemblage overlapping an older clastic assemblage. Triassic Basins of the Newark Group are characteristic of the Conestoga Valley province (and, to a lesser extent, the Inner Piedmont and Coastal Plain) and are found in the area between Massachusetts and North Carolina. Triassic rocks have been encountered in borings at Bowling Green and Edgehill, Virginia and near Brandywine, Maryland.

These basins were formed during Triassic time as downfaulted and folded elongate graben structures. Non-marine arkosic sediments and intercalated lava flows filled these basins as they were down-faulted and tilted. At the close of the period, the processes of erosion continued to

modify the topography of the eastern section to form the base for the position of Coastal Plain sediments. In the Triassic Basins and associated down-faulting, intrusions of Triassic-Jurassic age are cut and displaced, indicating a post-Triassic-Jurassic age for some of the faulting.

Similar intrusions in the Inner Piedmont are not disrupted or offset in this manner. Earthquakes no larger than Intensity VI have been noted in the Conestoga Valley province, although some small events, up to Intensity VI, are reported and have been tentatively associated with Triassic basin border faults.

Inner Piedmont Tectonic Province

The Inner Piedmont Tectonic Province is characterized by a eugeosynclinal assemblage over an older clastic assemblage, which is characterized in this region by a northeast-southwest trending belt of Precambrian to early Paleozoic schists, gneisses, slate, metaconglomerates and some igneous intrusions. These rocks are interrelated in a complex manner by faulting and folding.

Earthquakes ascribed to the Inner Piedmont should include the boundary (Inner Piedmont-Coastal Plain) Intensity VII events at Wilmington, Delaware (1871) and Asbury Park, New Jersey (1927) as well as several Connecticut valley events of Intensity VII which occurred over 200 miles from the station, albeit, in the Inner Piedmont Province (Ref. 2.5-73). No larger events have been recorded in this province and none of the historical shocks can be satisfactorily related to specific structures. The Inner Piedmont is, in general, apparently the most seismically active portion of the area within 200 miles of the station. Concentrations of moderate events are apparent in the New York City area and the Central Virginia seismic zone near Charlottesville as described by Bollinger (Ref. 2.5-80). Both of these zones are characterized by low to moderate seismic activity. Seismicity elsewhere in the province is relatively rare and apparently random.

Coastal Plain Tectonic Province

The Coastal Plain tectonic province is characterized by the development of a miogeosynclinal wedge during the advanced phases of the final crustal divergence. In the region south and east of the station, this province is characterized by a stratigraphic sequence of interbedded sands, gravels, clays and silty sands of both marine and continental origin. These materials were deposited on the downwarped basement complex from Early Cretaceous to Quaternary time. The strata wedge out at the Fall Zone to form a wedge-shaped mass that thickens to the southeast. The average dip of these strata varies from 75 feet per mile within the Cretaceous sediments to approximately 10 feet per mile in the upper Tertiary formations.

Few geologic structures are known in the Coastal Plain Province. The Salisbury Embayment is a structural low in the basement rocks between Newport News, Virginia and Atlantic City, New Jersey. The Embayment is marked by a deep accumulation of Mesozoic and Cenozoic sediments, which approach a thickness of 3,500 to 7,500 feet at the Maryland coastline. The feature is fairly prominent in the basement rocks but loess form in the younger sedimentary sequences, suggesting that it is predominately a pre-Tertiary feature. The Coastal Plain underwent regional epeirogenic movements from Pliocene to Quaternary time, which lifted a portion of the continental terrace above sea level. The significant seismic activity in the Coastal Plain includes the Intensity X event at Charleston, South Carolina, and, for the sake of conservatism, the Wilmington, Delaware event of Intensity VII.

2.5.2.3 Correlation of Earthquake Activity with Geologic Structures or Tectonic Provinces

Only a few of the historical earthquakes in the northeastern United States can be satisfactorily related to specific structures at this time. Therefore, a consideration of the significant events which could influence the seismic design for the Susquehanna SES will rely, for the most part, on an approach based on the tectonic settings discussed above. To augment the tectonic province approach, the concept of the seismic zones within the provinces as discussed by Bollinger (Ref. 2.5-80) and Hadley and Devine (Ref. 2.5-81) will be addressed.

Those events which constitute the largest earthquakes of record in the Eastern United States and which embrace all significant considerations for the Safe Shutdown Earthquake for the station, are listed below:

- 1) The large events (maximum Intensity IX) such as those in the St. Lawrence Valley and Ottawa-Bonnechere Graben area
- 2) The large events such as those (maximum MM Intensity VIII) which occurred in the Cape Ann Massachusetts area
- 3) The (originally categorized as Intensity VII-VIII) Attica shock (1929) in western New York State
- 4) The Intensity (IX to X) Charleston, South Carolina earthquake in the Coastal Plain
- 5) The Intensity VIII Giles Co., Virginia earthquake of 1897
- 6) The Intensity VII events such as those shocks which have been recorded in and around New York City, Wilmington, Delaware, Asbury Park, New Jersey, and Lake George, New York, and
- 7) The Intensity VI events which occur only infrequently in the general region

St. Lawrence Valley

The St. Lawrence Valley and the Ottawa-Bonnechere Graben area are contained in the Ottawa Basin tectonic province (Ref. 2.5-73). Earthquakes as large as Intensity IX are reported in this region. The structural interpretation shows that this area is the extension of a transverse trough and mobile zone into the stable interior (Ref. 2.5-73).

Because of the obvious historical confinement of seismic activity to this region marked by an intraplate weakness, recurrence of such large shocks are expected to remain in the area and are thus not translatable to the station.

Boston-Cape Ann

The large (Maximum Intensity VIII) events in the Boston-Cape Ann area were formerly historically associated with the Boston-Ottawa trend of earthquake activity (Ref. 2.5-82) which included the Ottawa-Bonnechere Graben area. However, a recent re-evaluation (Ref. 2.5-73) has resulted in the identification of tectonic regimes which separate the former "Boston-Ottawa

trend" into specific tectonic provinces. On the basis of this, the Cape Ann Intensity VIII event, being the largest event to have occurred in the Avalon Platform province (Ref. 2.5-73) would be restricted to a distance from the site of no less than 250 miles. Moreover, according to Ballard and Uchupi (Ref. 2.5-83), it is possible that the significant Boston-Cape Ann seismic activity is associated with the faulted northwestern boundary of the Avalon Platform.

For these reasons it is not deemed necessary to translate this activity (Maximum VIII) out of the Avalon Platform.

Western New York

The shock of 1929 near Attica, New York is anomalous with respect to the exceedingly sparse seismicity of this portion of the Stable Interior. It does mark, however, a noted concentration of earthquakes which are spatially related to the well-recognized feature of the immediate area, the Clarendon-Linden Structure (Ref. 2.5-114). It is generally accepted that any recurrence of a similar event would be confined to the Attica area. Therefore, the postulation of a recurrence of this shock at the closest approach of Stable interior to the station is not warranted. A recurrence of the largest event at any location along the Clarendon-Linden Structure could result in only minimal ground motion at the station (less than Intensity IV).

Charleston, South Carolina

The largest events to occur in the eastern United States were the events of approximately Intensity X at Charleston, South Carolina in 1886.

The concentration of seismic activity (over 400 events) in the immediate vicinity of Charleston is unique to the Atlantic Coastal Plain; moreover, such a confined density of epicenters is unmatched anywhere in the central and eastern United States, with the possible exception of the New Madrid, Missouri region. On the strength of this areal distribution alone, it would be concluded that a specific tectonic anomaly is responsible for this localized activity. Independent lines of investigation have recently suggested a structural regime which may be responsible for the observed seismicity. On the basis of seismic reflection profiles parallel to the coast of South Carolina, Dillon (Ref. 2.5-84) has reported evidence of northwest-trending faults in the continental shelf along the South Carolina coast, and states that this would seem to be the only zone of active faulting in the United States south of Cape Hatteras and east of the Appalachians. Possible evidence of faulting is noted in the basement rocks offshore and in the Tertiary rocks of the continental margin. This possible faulting aligns with the northwest-trending seismic zone (Ref. 2.5-80) and has been postulated to be the extension of an active oceanic fracture zone into the continental block (Ref. 2.5-84, and 2.5-82).

More locally, a mild, breached fold in the shallow sediments several miles west-southwest of Charleston has been identified by Colquhoun and Comer (Ref. 2.5-85) as the Stono Arch. The axis of this arch trends west-northwest and has possible associated faulting. The trend of this structure is aligned with, and grossly parallel to, the seismic zone and the offshore structure discussed above, and represents the only known deformation in the immediate vicinity of Charleston. Thus, it may be a near-surface expression of the more regional (and deeper) anomaly suggested by offshore reflection surveys and magnetic anomaly trends (Ref. 2.5-86).

Transverse to the strike of these structural features are the northeast-trending axes of two structural highs which are identified along the coast, from Savannah, Georgia to just south of

Charleston, as the Beaufort-Burton High and the Yamacraw Ridge (Ref. 2.5-84). According to Dillon et al. (2.5-84), the Beaufort-Burton High may be a shallow expression of the deeper lying Yamacraw Ridge. The intersection of these structures with the suggested northwest trends in the vicinity of Charleston may, at least, be an expression of deeper basement complexity in the area, and lends support to a definition of structure responsible for the well-defined cluster of seismic activity in the Charleston area. No other structural anomalies of significance are known in this area of the Coastal Plain. Therefore, the unique density of earthquake activity in the Charleston area is considered to be associated with localized structure, the character and extent of which are only grossly suggested at the present time. In this respect, an earthquake similar to the largest Charleston shock would be expected to recur in the same locale, and would not be subject to translation throughout the Atlantic Coastal Plain tectonic province.

Giles County, Virginia

The Giles County, Virginia earthquake of 1897 is the largest shock to have occurred in the southern Appalachian region. It is listed (Ref. 2.5-72) as Intensity VIII, and occurred in the Southern Appalachian Seismic Zone near its intersection with the Central Virginia Seismic Zone (Ref. 2.5-80), more than 350 miles from the station. This intersection is marked by a definite break in the continuity of the activity of the northeast-trending Southern Appalachian Seismic Zone and lies well to the south of an area of apparent differentiation of the system of tectonic stresses along the Appalachians called the Central Appalachian Salient in southern Pennsylvania.

This salient was probably initiated during early crustal divergence in late Precambrian time (Ref. 2.5-73 and 2.5-87) resulting in a profound difference between the northern and southern portions of the Appalachian orogen as evidenced by three stages of the orogen's development:

1. In late Precambrian the initial rifting stage developed with a bend, offsetting the northern and southern portions of the continental margin.
2. During the end of the convergent stage (middle to late Paleozoic), the Alleghenian orogeny was pronounced only in the south and translation was restricted to the northern Appalachians.
3. In the Jurassic during the final rifting stage, different stress regimes prevailed in the northern and southern portions (Ref. 2.5-88).

The Central Appalachian Salient occurs where the NNE to NE trends, common to the Appalachians, change to EW in the vicinity of 40°N latitude. The EW trend has been interpreted to be a major crustal structure by several authors (Ref. 2.5-89 and 2.5-90) based largely on circumstantial evidence of interpreted offsets of geophysical anomalies, isopach contours, and geologic map patterns. Drake and Woodward (Ref. 2.5-90) have suggested that 80-90 miles of dextral offset has occurred on this feature and that no evidence of post-Cretaceous movement has been found. Figures 2.5-8A and 2.5-8B shows the approximate location of this structure as defined by Woodward (Ref. 2.5-89).

Even though its surficial expression cannot be well-defined, the Central Appalachian Salient clearly divides the northern and southern portions of the orogen. This is borne out by inspection of the historical seismicity shown on Figures 2.5-8A and 2.5-8B, wherein consistent changes in the seismicity within the described provinces are noted from north to south. The virtually

aseismic character of that portion of the Fold and Thrust province containing the station has been noted by the Nuclear Regulatory Commission (Ref. 2.5-91).

Thus, in consideration of the tectonic development, the inferred geological and geophysical evidence, and seismicity, the existence of a fundamental boundary between the northern and southern orogen is herein considered and illustrated as a zone on Figures 2.5-8A and 2.5-8B.

This change of seismotectonic style is further corroborated by Hadley and Devine (Ref. 2.5-81, Sheet 3) who have shown a seismotectonic province generally recognizing the earthquake activity of Bollinger's (Ref. 2.5-80) Southern Appalachian Seismic Zone within the Fold and Thrust Belt. At its northern extent, their boundary stops at the southern Pennsylvania border about 125 miles from the station. They describe the zone as an area where epicentral distribution or relation to known structure indicated a limiting structural factor, and where at least one earthquake of Intensity VII or VIII (Giles County event, 1897) has been recorded.

Because of (1) the notable change in tectonic style in the Fold and Thrust Belt in Province South of the Pennsylvania border, (2) the reduction in seismicity north of the Central Appalachian Seismic Zone, (3) the assignment of a different seismotectonic character to the Fold and Thrust Belt south of Pennsylvania, and (4) the historical record which shows a sparsity of earthquakes in Pennsylvania, we consider that a translation of an Intensity VIII event (Giles County recurrence) closer than 100 miles to the Susquehanna SES is not warranted.

Intensity VII Events

Consideration must be given to the likelihood of Intensity VII events which are known to occur occasionally in this region of the northeast. Within 200 miles of the station, nine shocks of Intensity VII have been documented. Five of these are early reports (1568, 1574, 1584, 1592, and 1791 - See Table 2.5-2) of concentrated activity in the Connecticut Basin about 200 miles from the site. This area lies within the Inner Piedmont Tectonic Province. The other four occurred within the Piedmont province, or at its (eastern) boundary with the Coastal Plain near New York City and northern Delaware. The closest approach to the station of the tectonic province containing these events would be 50 miles. Such an event would attenuate to about Intensity V even on unconsolidated materials at the station, according to conservative central U.S. attenuation characteristics (Ref. 2.5-92), and would be less on competent rock.

The Intensity VII event at Lake George in northern New York, although over 200 miles from the station, is spatially associated with a general concentration of smaller earthquakes. Hadley and Devine (Ref. 2.5-81, Plate C) confine this Lake George event to (1) a tectonic province whose nearest approach to the Susquehanna SES is greater than 150 miles, and (2) a bounded area of seismic activity "in which known faults are associated with epicentral alignments or distribution in such a way as to indicate that movements on the known faults or closely related faults have been the source of recorded earthquakes." This seismic area boundary approaches no closer than 150 miles to the station.

It is seen, then, that Intensity VII events can be confined to approaches of tectonic provinces, seismic zones, and/or structure which are no closer than 50 miles to the Susquehanna SES.

Intensity VI Events

Within 200 miles of the station, a few scattered Intensity VI events are noted (Figures 2.5-8A and 2.5-8B). The two closest events occur about 48-60 miles due south at the closest approach of their tectonic province and are, at least spatially, related to Triassic border faults (Ref. 2.5-81). Several others are concentrated in the immediate vicinity of the Clarendon-Linden structure in northwestern New York State. It should be noted that in the station province (Fold and Thrust Belt) no Intensity VI events occur north of the Central Appalachian Salient in southern Pennsylvania, a distance of over 100 miles from the station. In the Stable Interior, an Intensity VI event in northern New York, 180 miles north of the station, is not related to known structure, and could conservatively be translated to the closest approach of its province to the station, a distance of about 40 miles.

2.5.2.4 Maximum Earthquake Potential

The previous section defined the maximum potential earthquake in terms of the closest postulated approach of maximum historical events to the Susquehanna SES. Consideration was given in each case to a conservative utilization of tectonic province models, recognized seismic zones, and/or any associated tectonic structure. The resulting candidates for the Safe Shutdown Earthquake (SSE) are:

<u>Intensity (MM)</u>	<u>Closest Approach to Site</u>	<u>Maximum Site Intensity</u>
X	450 miles	V
IX	300 miles	V
VIII	100 miles	V-VI
VII	50 miles	V-VI
VI	40 miles	IV-V

In deriving the maximum Intensity to be felt at the station from the above candidates, the attenuation curves developed for the central United States (Ref. 2.5-92) were used. These curves are the most conservative available for the United States in that both western (California) and eastern (Canada, New York, Charleston, S.C.) data show a greater attenuation of Intensity with distance than does the central United States experience. It should be noted, also, that such attenuation relations are based on isoseismal maps which tend to record the maximum Intensity felt in a given locale, usually on poor soil conditions. It is likely, then, that the Intensities (damage potential) actually experienced on solid foundation material of the Susquehanna SES would be somewhat less than those levels specified in the foregoing table which are used in the Safe Shutdown Earthquake derivation in Subsection 2.5.2.6 below.

From inspection of the above candidates, a station intensity of less than VI is the maximum consistent with the tectonic model seismic zones, and/or associated structure. This is entirely in keeping with the historical earthquake record which shows that the area of the station is virtually aseismic. Moreover, there are no known faults which appear capable of generating other than minor disturbances well below damaging levels of ground motion.

2.5.2.5 Seismic Wave Transmission Characteristics

The static and dynamic properties of the subsurface materials at the station are presented in Subsection 2.5.4.2. The analyses presented in this referenced section are based on characteristic ground motion and significant frequencies generated by the maximum potential earthquake described above and quantified below.

2.5.2.6 Safe Shutdown Earthquake (SSE)

As a result of the derivations discussed above, an SSE of less than Intensity VI is the maximum earthquake consistent with tectonic models and historical evidence presented for the site. However, an SSE generating a horizontal ground acceleration of 10 percent of gravity (g) has been selected in compliance with the minimum design requirement of the regulatory agencies.

To justify the conservative nature of this design level as an anchor for design response spectra, the acceleration/intensity correlations which have been developed for an Intensity of VI are discussed, although this Intensity is not expected to be felt at the station on the basis of the discussions above.

Recent correlations between Intensity and peak horizontal ground acceleration have made use of currently available data for the western United States (Ref. 2.5-113) and worldwide (Ref. 2.5-93). The results of these current studies do not differ greatly from prior parallel studies, but are generally more conservative. Therefore, these investigations can be used as a general guide for an expected value of acceleration (from an Intensity VI event) on which to anchor design response spectra. These studies show an expected acceleration level of about 6 to 7 percent of gravity as a result of a Intensity VI event. On the basis of these relationships, the design acceleration for the Susquehanna SES for structures founded on rock is conservatively selected as the required minimum of 10 percent g in accordance with 10CFR100, Appendix A. This level is used to anchor the design response spectra shown on Figure 2.5-27. For structures founded on soil, the NRC required that the SSE be increased 50 percent or to 0.15 g in order to accommodate any amplification of ground motion in the soil overlying the bedrock. It should be noted, however, that the maximum earthquake for the station is less than Intensity VI, which correlates with an acceleration of no more than 0.06 g. If this value were increased by 50% to accommodate amplification due to soils, the resulting SSE for structures founded on soil would not be more than 0.10 g. Thus, the selected value of 0.15 g provides a large margin of safety. The 0.15g value is applied at foundation level.

The duration of strong motion from the SSE is not expected to exceed 5 seconds (Ref. 2.5-95 and 2.5-96) and in all probability, would be considerably less at frequencies critical to design. Duration of motion from a larger, more distant event such as the Charleston, South Carolina event (X) would be relatively longer than that from the design event, but the low accelerations which are characteristics of long period motion from distant large events will be adequately enveloped by response spectra anchored at the minimum level of 10 percent g.

2.5.2.7 Operating Basis Earthquake (OBE)

On the basis of the historical seismicity described above wherein a maximum Intensity felt at the station from historical earthquakes was no larger than IV, an Operating Basis Earthquake (OBE) which would, during the life of the facility, generate a ground acceleration at the station no

higher than 5 percent g (1/2 SSE) has been selected. This level of acceleration will not be exceeded by the occurrence of even an Intensity V shock adjacent to the station or a recurrence of large, regional events at a distance. According to Trifunac and Brady (1975), a felt Intensity of V will result in acceleration levels below 4 percent g. Return periods for such ground motion at the station are of an extremely low order of probability, as evidenced by the fact that no local (Pennsylvania) shocks have been reported as felt at the station. Figure 2.5-28 is the design spectra anchored at the OBE level of 5 percent g. For structures founded on soil, an OBE of 0.08 g was used for design.

2.5.3 SURFACE FAULTING

Based on the data contained in Subsections 2.5.1 and 2.5.2 and the interpretations and conclusions therein, there is no capable fault (Appendix A, 10 CFR, Part 100) within at least five miles of the Susquehanna Steam Electric Station.

A detailed description of the lithologic, stratigraphic and structural conditions at the site and the surrounding region is contained in Subsection 2.5.1. All historical reported earthquakes within 50 miles of the site, and all earthquakes within 200 miles of the site with magnitudes (Richter) greater than 3.0 or MM intensities greater than III are detailed in Subsection 2.5.2.

The above referenced information clearly indicates that surface faulting is not of significance to the Susquehanna Steam Electric Station.

2.5.4 STABILITY OF SUBSURFACE MATERIALS AND FOUNDATIONS

2.5.4.1 Geologic Features

General. The upper bedrock at the site area includes the Middle Devonian Mahantango Formation. The upper part of the Mahantango is a dark gray siltstone, with bedding generally delineated by thin, consistent, light gray, fine-grained sandstone stringers. Beneath the upper member, the Mahantango is comprised of 120 to 150 ft of dark gray, hard calcareous siltstone, typically having bedding obscure to absent and displaying cleavage. This member which supports the power block structures is harder, more massive, and more resistant to erosion than the upper member.

The irregular bedrock surface underlying the site is the result of a combination of preglacial weathering and stream erosion, glacial scour, later erosion by glacial melt waters, and the varying resistance of the rock units to erosion. The bedrock is blanketed by till and glacial outwash which grades upward from a gravelly boulder zone to a surface layer of silty fine sands and sandy silt. The surface layer is believed to be reworked loess. The maximum thickness of overburden is around 40 ft in the southern half of the site, with bedrock occasionally cropping out at the surface. North of the east-west bedrock ridge situated just north of the reactors, the glacial deposits fill a valley eroded into bedrock to a depth exceeding 100 ft.

Structurally, the site is situated on the north limb of the Berwick Anticlinorium; its axis passes just south of the site. The anticlinorium trends east-northeast and plunges gently to the northeast. As with the regional picture, folding is the most characteristic feature of the site area. Minor faulting in the form of small bedding-plane slips and intraformational shear zones occur,

but they are of no significance to the site. They apparently developed during the Paleozoic (more than 200 million years ago) during the Appalachian orogeny. The zones are typically healed with calcite and quartz (Additional description of site geologic conditions is presented in Subsection 2.5.1.2).

All Seismic Category I plant structures except the spray pond, the Engineered Safeguard Service Water (ESSW) pumphouse and pipeline are founded on bedrock. The ESSW pipeline trench is excavated partly in soil and partly in rock. Most of the other major plant structures, including the cooling towers, are also founded on bedrock.

Site geologic and foundation conditions are entirely suitable for the construction and operation of the Susquehanna SES.

2.5.4.1.1 Areas of Potential Subsidence, Uplift, or Collapse

The potential for significant uplift or subsidence at the site, due to man's activities or geologic conditions such as regional warping, is negligible.

The shallowest carbonate rock that may be present beneath the site is the Onondaga Formation, above which occurs more than 2,000 ft of Middle Devonian shales and siltstones (Figure 2.5-14). At that depth the Onondaga Formation, if present, would not be expected to have a significant potential for subsidence or collapse even if it contained solution cavities. No coal beds are present beneath the site; the nearest coal measures are about 3-1/2 miles north of the site near Shickshinny. Rocks in the site area have no known potential for oil or gas production. The nearest oil or gas field is located 25 miles northeast of the site. Precise leveling surveys and other data in the literature provide no indication that the Site is in an area experiencing any abnormal regional warping, uplift, or subsidence. More detailed discussion of the potential for uplift or subsidence at the site is presented in Subsection 2.5.1.2.5.3.

2.5.4.1.2 Previous Loading History of the Foundation Materials

Bedrock at the site had been buried and deformed during the Appalachian orogeny (over 200 million years ago) with sufficient intensity to impose secondary cleavage in places and to mobilize calcite and to some extent quartz, resulting in a hard, indurated rock lacking the bedding-plane fissility normally associated with less well indurated silty shales and shaly siltstones. During Quaternary time, at least two ice lobes advanced over the site; the only direct effect this additional load might have on the bedrock at the site would be a tendency to scour loose or weathered rock from the rock-soil interface. Any pre-existing surficial deposits not removed by the glaciers would have been preconsolidated and thereby strengthened by ice loading.

Surficial material at the site consists of glacial drift largely, if not wholly, deposited by the Olean advance of the Wisconsin ice sheet. These deposits, which are described in Subsection 2.5.4.1, would be expected to have varying consolidation or preloading characteristics depending on local depositional history. Soils in the spray pond excavation (including the ESSW pumphouse excavation) and in the pipeline excavations leading to the spray pond are of particular interest because they support Seismic Category I facilities in these areas. Here geologic mapping shows that these soils consist of well stratified outwash sands and gravels,

together with poorly stratified to unstratified kame-like gravels (refer to geologic maps, Figures 2.5-15 and 2.5-18). They evidently were deposited during or subsequent stagnation of the final ice advance in the site area, since they are not overlain by a till blanket, nor do the strata show structural evidence of having been overridden by ice. Geologic evidence, therefore, indicates that the stratified surficial materials exposed in the excavations for the soil-supported Seismic Category I facilities are likely to be normally consolidated and not preloaded by ice during or subsequent to deposition.

As the overburden soils in the area were not preloaded, no correction is necessary for the influence of preloading on the SPT or on the relative density shown in Figure 2.5-32, and the cyclic shear stress ratio at failure as shown on Table 2.5-14. The lateral earth pressures shown on Figure 2.5-39 refer to pressures due to compacted backfill and are not influenced by the previous loading history of the site soils.

2.5.4.1.3 Structures and Zones of Weathering, Disturbance, or Weakness in Foundation Materials

Foundation materials consist of two basic types; namely, glacial till and outwash in the spray pond area, and siltstone or indurated slaty shale in the remainder of the principal plant foundations.

A geologic map of the foundation rock for the principal plant structures is presented on Figure 2.5-18. It shows joints, shears, attitudes of bedding and other features. All foundations shown were excavated so that structures are founded on firm bedrock, the Devonian Mahantango Formation. Geologic sections through the foundations are shown on Figure 2.5-19. A geologic map for the spray pond is presented on Figure 2.5-15.

The southwestern tip of the spray pond is cut into bedrock while the remainder is excavated in glacial materials. The thickness of the glacial deposits beneath the bottom of the spray pond ranges from zero at the rock contact to 93 ft at the eastern end of the pond. The foundation for the pumphouse structure, located at the southeastern corner of the pond, is underlain by 35 to 60 ft of glacial material. The water circulation pipelines, between the pumphouse and the plant, intersect bedrock at an elevation of 668 ft, approximately 260 ft southeast of the pumphouse.

The vicinity of the spray pond is situated over a glacial or preglacial, east-west trending bedrock valley as outlined by contours on top of bedrock (Figure 2.5-17). Total relief of the bedrock surface is about 130 ft. The valley is filled with dense, permeable gravelly and sandy glacial outwash and till deposits that attain a maximum thickness of about 110 ft in the spray pond area. They were deposited during the Olean substage (early Wisconsinan) of the Wisconsin glaciation which occurred at least 50,000 years ago, and there is a possibility that at least some of the bedrock erosion and overlying glacial deposits are the result of an earlier Illinoian glaciation (refer to Subsection 2.5.1.2). In general, the deposits consist of a sequence of sand, gravel, and boulders overlain by sand and gravel, overlain in turn by silty sand. The entire sequence is highly variable in grain size distribution and sorting, and contains discontinuous pockets of similar materials. As a rule, grain size decreases and sorting increases toward the top of the sequence. The glacial materials in the deposit are noncalcareous; most of the rock particles consist of indurated sandstones. The origin and composition of the deposit are such that it is not susceptible to significant weathering or alteration.

In the power block and cooling tower foundations, the principal structural feature is a minor anticline, the axis of which trends about N85° E and was exposed in the radwaste and Unit 1 cooling tower foundations (Figure 2.5-18). South of this feature, bedding generally dips gently south with minor undulations; to the north, beds dip more steeply north. Bedding, which generally strikes N70 to 85°E, is obscure in the foundations; the foundation rock is quite massive and is not characterized by weak zones developed along bedding or cleavage planes. Where observed, the bedding planes as a rule are smooth and unconforted with only minor undulations. In the turbine and reactor building foundations, the bedding dips 5 to 10 degrees to the south, while north of the circulating water pumphouse the dips are in places up to 5 to 8 degrees north to northeast, reflecting this minor undulatory variability of bedding. Small-scale folds a few feet in dimension occur but are not prevalent in the site area; one such small anticlinal fold was recognized at the north edge of the circulating water pumphouse excavation. Cleavage is variably developed, strikes generally parallel to the strike of bedding, and dips steeply south. Jointing in the rock excavated for foundations is fairly well developed. Figure 2.5-18 shows the principal joints encountered at foundation grade, which is at sufficient depth below the top of the rock to be in essentially unweathered material. Here joints are tight and either uncoated, or coated with calcite or a mixture of quartz and calcite. Few joints at foundation level contained significant iron staining; some iron-stained joints are mapped in the radwaste foundation area. Toward the surface these joints generally become more heavily iron-stained with greater degree of weathering, and calcite coatings tend to be leached out, resulting in open joints, in joints partly coated with quartz, or in clay-filled joints in the zone of weathering. The major joint set strikes east-northeast (N60-85°E), and dips vertically (within 15° of vertical). Other steeply dipping to vertical joint sets strike northwest to north-northwest, and north-south. Less steeply dipping joints generally have an east-northeast strike; one group dips gently northward at 10-18°, and another, in the southern part of the excavation, dips 50-60°SE. Some of the joint surfaces, particularly the low-angle joints, are slickensided. In addition to these principal joints, high-angle, discontinuous, white calcite and quartz-calcite veinlets are typically exposed locally throughout principal plant foundations.

A few minor shear planes, originally recognized in the cores obtained during the early phase of site exploration, were exposed during foundation excavation and are mapped on Figure 2.5-18. One shear plane, traced from the northeast corner of the Unit 1 reactor foundation northward to the Unit 1 cooling tower, was found to be oriented parallel to bedding and is denoted "bedding plane shear A" on Figure 2.5-18. The surfaces of the bedding plane shear are healed with 1/4 to 3/4 in. thick laminae of calcite, siltstone and some quartz. The calcite laminae are approximately 1/16 in. thick, alternating with thinner siltstone laminae. The entire exposed area of this bedding plane contains prominent slickensides trending N30° to 40°W, with a 6° to 7°SE plunge. Updip and closer to the top of the rock, the bedding plane contains a 1/2 to 1 in. wide, iron-stained zone, and it also shows extensive leaching of the minerals filling the shear. In places the adjacent rock is weathered to a granular sandy soil. The calcite which fills the bedding plane shows no sign of crushing. It should be emphasized that the weathering and staining on the bedding plane shear occurs only near the top of the rock where surface water and groundwater could penetrate along the plane; at foundation grade which is well below the weathered zone, the unweathered laminae have the properties of firm rock. In places the bedding plane shear is apparently not a prominent feature in the unweathered rock. For example, it was identified only as a slickensided surface with associated jointing in boring 105 and as horizontal jointing planes in boring 351 (shown in profile on Figure 2.5-19).

Foundation mapping reveals that the bedding plane shear is warped in conformance to the folding of bedding. The shear can be traced northward to the excavation for the Unit 1 cooling

tower (Figure 2.5-18). Measured attitudes of bedding show that the axis of the minor anticline described above occurs near the foundations for pedestals 6 and 7 of the cooling tower. South of pedestal 7, the bedding plane shear dips gently south; north of pedestal 6, the bedding plane shear dips gently north. Additional subsurface data from bore holes farther south and north strongly suggest that the configuration of the bedding plane closely follows the undulations in bedding (Figure 2.5-19). No evidence was found at the site to indicate that the shear plane substantially deviates from bedding planes.

During excavation, this bedding plane shear was traced updip to its intersection with the top of rock at a steep, glacially eroded contact. The eroded rock surface was continuous across the trace of the bedding plane, without displacement or offset (Figures 2.5-20a through 2.5-20g). Since the erosion of the rock surface would necessarily have occurred prior to the deposition of the overlying glacial deposits, which have been established as being more than 50,000 years old (refer to Subsection 2.5.1.2.2.1), this relationship shows that any displacement along bedding plane shear A occurred more than 50,000 years ago. In reality, the most probable age of the shearing is pre-Triassic or over 200 million years ago. This is indicated by regional relationships plus the fact that the shear plane is folded (A detailed presentation and analysis of the relationship between site and regional structure is presented at the end of Subsection 2.5.1.2.3.2).

A second bedding plane shear (Shear B), a few feet below and parallel to the first bedding plane shear, was exposed near the northwest corner of the Unit 1 turbine building foundation. It is similar in appearance but apparently more restricted in a real extent than the first. Two vertical, calcite-filled joints cut across this second bedding plane (Figures 2.5-20a through 2.5-20g). The calcite in these vertical joints is continuous across the bedding plane with no offset, showing that the joints were formed and the calcite was deposited in the joints, subsequent to development of the slickensides on the bedding plane.

The conclusion stated in the PSAR (p. 2.7-2) regarding the significance of these shear planes is still appropriate and deserves restatement: "Minor bedding plane slips at depth have been observed in the site area, both north and south of the interior ridge. Those slips have not experienced movements in more than 200 million years. A minor slip of this nature could be exposed in any large excavation anywhere in the area; however, it would not affect the structural design of the facilities."

All deformational features observed in rock at the site are geologically old and are not significant to plant structures. In unweathered rock, minor shears that do occur are tightly healed with calcite and quartz mineralization, and joints are likewise tight and unweathered. All foundations for plant structures designed to rest on sound rock were excavated to, or into, unweathered bedrock. No structurally weak zones were encountered in these foundations (Refer to Subsection 2.5.1.2.5.5).

Further description of depth of weathering and geologic structures at the site and in the foundations is presented in Subsections 2.5.1.2.3.2 and 2.5.1.2.5.6.

2.5.4.1.4 Unrelieved Residual Stresses in Bedrock

No indications were found during excavation and construction at the site of the presence of any significant stress in bedrock (refer to Subsection 2.5.1.2.5.8 for additional discussion).

2.5.4.1.5 Potential for Unstable or Hazardous Rock or Soil Conditions

Foundation rock at the site is a hard, indurated, unweathered siltstone, a member of the Middle Devonian Mahantango Formation. Similar materials underlie the site to a depth of at least 1,000 ft. This rock contains no unstable minerals and provides highly stable foundation conditions.

Soils at the site are glacial in origin, deposited mostly by flowing glacial meltwater, much under torrential conditions. The soil is noncalcareous. Most of the rock fragments consist of indurated sandstones. The origin and mineralogy of these soils is such that they present no hazardous conditions (refer to Subsection 2.5.1.2.5.7).

2.5.4.2 Properties of Subsurface Materials

A few of the safety-related principal plant structures are founded on soil. These structures consist of the Engineered Safeguard Service Water (ESSW) pumphouse, the spray pond, and portions of the Seismic Category I pipeline linking the reactor building to the spray pond and the diesel generator 'E' fuel tank. Most other plant structures are founded on rock. The location of these structures is shown on Figure 2.5-24; soil and rock foundations are identified on Figure 2.5-17A.

The static and dynamic engineering properties of the site bedrock and overburden soils were determined by field investigation and laboratory testing. The results of laboratory testing of the materials sampled from the project site are covered in two reports (Ref. 2.5-97 and 2.5-98).

A detailed study of the soil properties at the site of the spray pond and ESSW pumphouse is given in Subsection 2.5.5.

2.5.4.2.1 Properties of Foundation Rock

The Category I reactor buildings and diesel generator buildings, as well as the non-Category I turbine and radwaste buildings (see Figure 2.5-24) are founded on unweathered siltstone bedrock. The siltstone, a member of the Mahantango Formation of Devonian age, is hard and indurated, and in the foundations area is lithologically homogeneous with bedding generally not well defined, and lacking the bedding plane fissility usually associated with less well indurated shaly siltstones and silty shales. In places the rock exhibits cleavage, further evidence of its indurated nature.

In the area of the principal plant structures, bedrock bedding where observed generally dips gently (less than 10°) south; locally, such as north of the circulating water pumphouse, beds dip slightly north. At the north end of the radwaste building and the north side of the Unit 1 cooling tower, bedding dips more steeply north. The cleavage is steeply inclined to the south. Minor slickensided bedding plane shears and joint planes occur in the foundations as described in Subsections 2.5.4.1 and 2.5.1.2.3. All such shears beneath the principal plant foundations are fully healed with unweathered calcite and quartz mineralization and do not adversely affect the strength and competence of the foundation rock. Further evidence of the healed nature of these shears is furnished by the RQD values and core recovery rates in borings that penetrated bedding plane shear A (refer to Figure 2.5-18 and discussion in Subsection 2.5.4.1) at elevations below the bottom of the foundation of the principal plant structures, such as in

borings 302, 309, and 314. In all cases RQD values are above 35 percent through the shear plane; in most cases, RQD values exceed 80 or 90 percent and core recovery was close to 100 percent (Further information on foundation geologic conditions is presented in Subsection 2.5.4.1).

Typical values of unconfined compressive strength of unweathered siltstone underlying the principal plant foundations range from 3,650 to 16,000 psi (see Table 2.5-3). The modulus of deformation determined from these laboratory tests on core samples ranges from 3.1×10^6 to 9.4×10^6 psi. These values indicate strong, competent rock.

P-wave measurements were made by Dames and Moore in the laboratory on individual core specimens. The cores were from borings 303, 314, and 315 which are located, respectively, near the Unit 1 turbine building condensate pump pit at the center of the Unit 1 reactor, and at the center of the Unit 2 reactor. The average seismic P-wave velocity determined for 10 samples at or below foundation grade beneath power block structures is 13,236 fps. For three samples from boring 303 in the Unit 1 turbine building, the average Vp value is 14,272 fps, or approximately 14,000 fps. These determinations are listed in Tables 2.5-4 and 2.5-5.

Rock quality designation (RQD) measurements made by Dames and Moore on rock cores from below the foundation elevations in the reactor, turbine, radwaste, diesel generators, and circulating water pumphouse foundations exceed 80 percent (refer to boring logs, Ref. 2.5-97 and 2.5-121).

In the reactor area, cross-hole and down-hole measurements of in situ seismic velocities show high values. The measurements were made by Weston Geophysical Engineers, Inc., June 8 - August 6, 1971 using boreholes 105, 303, 307, 314, 315, and 316 (refer to Figure 2.5-29). Values obtained from the cross-hole array for the elevation interval 550-640 ft MSL are 16,000 fps for the P-wave velocity and 7500 fps for the S-wave velocity in the reactor area (design elevation of bottom of reactor foundations, 639 ft MSL). The results of the down-hole measurements yield values that are slightly lower, by a factor of about 15 percent; that is, a Vp value of about 14,000 fps and Vs of about 6,200 fps. These in site results are in good agreement with the laboratory determinations. Additional cross-hole and up-hole in situ seismic velocity measurements were made in the spray pond area (Ref. 2.5-99). Results of the cross-hole explorations at the site are further discussed in Subsections 2.5.4.2.2 and 2.5.4.4.

Plate load tests were carried out on sound rock near the center of the Units 1 and 2 reactor building excavation in the vicinity of boring 105 (refer to Figure 2.5-18). Plates 24, 13.5, and 8 in. in diameter were subjected to successively increasing total loadings of 7, 22, and 60 tons per square foot (tsf), respectively. A total deflection of .062 in. occurred when the 24 in. plate was loaded to a maximum of 7 tsf. An additional deflection of 0.036 in. was recorded on subsequent loading to 22 tsf, and another 0.036 in. of deflection on application of the 60 sf maximum load, producing a total settlement of 0.134 in. for the three-stage loading to 60 tsf. Recovery of the rock by elastic rebound upon release of these loads was substantial: 68, 75, and 80 percent repeatable elastic recovery of the total deflections were recorded after release of the 7, 22, and 60 tsf loadings, respectively. Additional deflections due to cyclic loading were small. Application of 14 cycles of load at 7, 15, and 30 tsf resulted in additional settlements of only 0.012, 0.003, and 0.002 in., respectively, over the corresponding single loadings. These results are consistent with the high modulus values and seismic velocities of the foundation rock, and indicate structurally strong, competent material for foundations in unweathered rock.

It is concluded from the engineering properties of the unweathered bedrock of the Mahantango Formation that the rock provides adequate support for the major plant structures under both static and dynamic conditions. Settlement of structures under static loading is insignificant. It consists of pseudo-elastic compression of the underlying rocks and occurs essentially upon load application. Moreover, the bedrock will undergo no loss of strength and will experience negligible additional settlement under earthquake loading.

A summary of the properties of the foundation rock is compiled in Table 2.5-5.

2.5.4.2.2 Properties of Foundation Soils

The results of detailed exploration of the soils in the spray pond area are given in Subsection 2.5.5. Only information on the properties of the pumphouse and diesel generator 'E' fuel tank foundation soils is given in this subsection.

The natural soils at the pumphouse and diesel generator 'E' fuel tank sites are normally consolidated and consist predominantly of sand, gravel, cobbles, and boulders. The soils are poorly stratified, starting as sand or sandy gravel at the surface and grading to mostly cobbles and boulders near bedrock. The depth of the soil deposit below foundation grade ranges from about 35 ft at the south end of the pumphouse to about 60 ft at the north end. About eight (8) feet and twenty (20) feet of sand, gravel and boulders are below the foundation grade of diesel generator 'E' fuel tank at north end and south end respectively. A subsurface cross-section through the pumphouse site is shown on Figure 2.5-30, cross-section D-D. The soils below the foundation level are predominantly sandy gravels with large amounts of cobbles and boulders. The properties of these sandy and gravelly soils are as follows:

a) Grain Size Distribution

Grain size distribution tests were made on most of the split spoon samples for classification purposes. Sieve and hydrometer analyses were performed according to ASTM Procedure D-422. The range of grain size curves is shown on Figure 2.5-31. The mean grain size (D50) of the gravelly soils, which are the predominant material below the pumphouse and diesel generator 'E' fuel tank was found to be in the range of 4.5 to 25.0 mm. Wherever the sand is present below the pumphouse, the D50 size is in the range of 0.14 to 3.0 mm.

b) Relative Density

Relative density data were derived from standard penetration test results using the Gibbs and Holtz procedure (Ref. 2.5-100). This procedure is valid for normally consolidated sands.

Values of relative density obtained in this way are summarized on Figure 2.5-32. A direct comparison of relative density from 'N' values given in Figure 2.5-32 and from undisturbed samples and/or in site density tests cannot be made because no relative density tests were made. The soil deposits are glacial in nature. The deposits are quite variable in particle size and sorting and contain discontinuous sand pockets and gravel pockets. Grain size in general increases with depth. At

the foundation level of the pumphouse and diesel generator 'E' fuel tank, the maximum sizes of the particles are in the range of 3 to 12 inches. Undisturbed tube samples could not be obtained in the gravelly soils. The gravel also will influence the results of in site density tests so that they may not represent the in site condition as a whole. The Standard Penetration resistance versus elevation is given on Figure 2.5-33. The 'N' values will be influenced by gravel. Because of this the higher blowcounts were not considered representative of site conditions. A value of $N = 40$ was selected for design. Of the 49 standard penetration tests made beneath the foundation level at the ESSW Pumphouse and 2 standard penetration tests beneath the diesel generator 'E' fuel tank, 45 exceeded 40 blows per foot. Of the 6 values that were less than 40 blows per foot only one was less than 30 blows per foot.

c) Static and Dynamic Shear Strength

Undisturbed sampling of gravelly soils was not possible. Therefore, shear strength testing was conducted only on the sands. The shear strength of the gravelly soils was then conservatively assumed to be equal to that of the sands.

The details of the testing procedures and selection of design strengths are given in Subsection 2.5.5. The effective angle of internal friction was selected from the test data to be 35° (Figure 2.5-34). The cyclic shear stress ratios at the two effective consolidation pressures 1.0 ksf and 6.0 ksf were determined to be 0.320 and 0.260, respectively, for 5 loading cycles (Figure 2.5-35, Subsection 2.5.5). A linear relationship was assumed in computing cyclic shear stress ratios at other effective consolidation pressures.

d) Shear Wave Velocity and Shear Moduli

Cross-hole shear wave velocity measurements were performed by Weston Geophysical Engineers, Inc. (Ref. 2.5-99). Compressional and shear wave velocities obtained from the measurements are given on Figure 2.5-36.

Shear moduli were computed from the values of shear wave velocity:

$$G = \frac{\gamma}{g} V_s^2$$

Where:

G = shear modulus, psf

γ = unit weight, pcf

g = gravitational acceleration, ft/sec²

V = shear wave velocity, fps

A discussion on how the shear modulus is influenced by the confining pressure, the strain amplitude, and the relative density is given in Subsection 2.5.5.2.

2.5.4.3 Exploration

The location of all field explorations is shown on the plot plan, Figure 2.5-22.

A total of approximately 250 exploratory borings was made in soil and rock at the site. Borings were logged in detail; boring logs are contained in Ref.s. 2.5-97, 2.5-98 and 2.5-99 and Appendix 2.5C. The soils were classified in accordance with the Unified Soil Classification System. Rock logs include RQD (rock quality designation) values. Coring in rock was performed using NX double-tubed coring equipment.

Drilling was conducted in late 1970 (100 and 200 series borings) to establish general geologic relationships over the site area and to determine general soil and rock conditions at the site. A more intensive program (300 series borings) was conducted in the Spring of 1971 to define foundation conditions in the principal plant structures area. Four 45-degree angle holes were drilled in the reactor area. Additional exploration drilling was necessary to locate the site for the Susquehanna River intake and discharge structures (700-800 series borings), to define soil and rock conditions at the spray pond and ESSW pumphouse site (1100 series and some 400 series borings), and to investigate foundation conditions for the cooling towers (borings B1 to B10) and the railroad spur and bridge over State Highway 11 (borings 417 to 455 and 929 to 940). An investigation program (borings 1 through 7) was conducted in 1983 to determine soil and rock conditions in the area of the diesel generator 'E' building. Boring logs are contained in Appendix 2.5C. Because of the safety-related (Category I) function of the spray pond and ESSW pumphouse, the exploration program for these facilities was comprehensive and included split spoon and undisturbed samples, laboratory testing, hydrologic surveys, permeability tests, and seismic cross-hole and up-hole surveys. Split spoon sample laboratory testing, hydrologic surveys, and permeability tests were also performed in the area of the diesel generator 'E' fuel tank. After completion of geologic borings, static water levels were measured in some of the borings drilled on the site. Perforated plastic pipes were installed in a number of the borings to allow collection of future water level data. These borings are denoted on the plot plan, Figure 2.5-22.

Forty-seven test pits were excavated by backhoe at selected locations to observe soil and rock conditions. Two north-south trenches totalling over 700 ft in length were excavated to obtain information on physical properties, structure, and variability of the near-surface materials at the site. Logs of the test pits and trenches are compiled in Appendix 2.5C.

A geologic map of the Category I and other principal plant foundations is presented on Figure 2.5-18. A geologic map of the excavation for the spray pond is shown on Figure 2.5-15. Geologic profiles are identified on Figures 2.5-18, 2.5-22, 2.5-30 and shown on Figures 2.5-19, 2.5-21A, 2.5-21B, 2.5-30, 2.5-40 and 2.5-56.

Photographs depicting significant features in the principal plant foundation excavations are shown on Figures 2.5-20a through 2.5-20g.

2.5.4.4 Geophysical Surveys

Seismic refraction profiles and cross-hole, up-hole and down-hole measurements were conducted at the site during the Fall of 1970, Summer of 1971, and Summer of 1974. The

seismic refraction lines totalled over 40,000 lf of coverage. They are identified on Figure 2.5-29. The refraction profiles collected in Appendix 2.5C.

As interpreted from refraction measurements, overburden at the site consists of a surficial layer of unconsolidated, unsaturated material up to 15 ft thick, constituting at least in part the soil horizon, underlain by more consolidated, partly or fully saturated till and compact outwash, which extend to the bedrock surface. Compressional (P-wave) velocity of the surficial material is typically about 1500 fps. Velocities in the lower till and outwash material generally range between 3,000 and 4,500 fps, although in some places velocities attain 6,000 fps (north-south baseline at boring 107).

The refraction survey obtained a persistent P-wave value of 12,000 to 14,000 fps for unweathered bedrock, which in many places is coincident with the top of rock. Frequently, however, lower velocities were recorded in a zone 0 to 20 ft thick near the top of rock. These lower compressional velocities are in the range of 6,000 to 9,000 fps, and are indicative of the zone of surficial weathering near the top of rock. At the site, material having a P-wave velocity of 4,000 to 6,000 fps may represent either dense soil or more thoroughly weathered or fractured bedrock; construction experience at the site indicates that here such material is generally correlative with dense soil.

Seismic cross-hole velocity measurements were performed in the reactor and spray pond areas, the principal sites of the Category I structures. Two arrays were employed in the spray pond area; namely, a north-south array across the location of the ESSW pumphouse, and an east-west array over the approximate location of lowest top of rock elevations in the spray pond. Both latter arrays provided data from which were calculated values for the dynamic moduli of the soil materials. In addition, down-hole measurements were made in the reactor area and up-hole measurements in the spray pond area. Figure 2.5-29 shows the borings that were used for the cross-hole arrays.

In the spray pond area, the seismic characteristics of the subsurface materials as measured in each array are similar. The material overlying bedrock has a P-wave velocity ranging from 4,200 to 4,800 fps and an S-wave velocity ranging from 1,600 to 1,900 fps. It is overlain by lower velocity material at about elevation 658 at the ESSW pumphouse location and at about elevation 643 farther west in the spray pond. At the ESSW pumphouse, this upper material has P-wave and S-wave velocity ranges of 2,300 to 2,400 fps and 1,300 to 1,350 fps, respectively, while farther west beneath the pond the materials between approximate elevations 643 and 673 have P-wave and S-wave velocity ranges of 3,000 to 3,300 fps and 1,450 to 1,500 fps, respectively. Table 2.5-6 summarizes the results of the seismic velocity measurements in the spray pond area and lists dynamic moduli computed from these data.

In the reactor area, cross-hole measurements were made on material above and below foundation grade. Above foundation grade the bedrock was weathered to a depth of about 10 ft below original top of rock. P-wave velocity of this weathered material was 7,600 fps and S-wave velocity, 3,600 fps. A P-wave velocity of 14,800 fps for the interval 640 to 660 ft MSL indicates the top of unweathered rock is at about 660 ft. At and below foundation grade in the reactor area high seismic velocities were recorded ($V_p = 16,000$ fps, $V_s = 7,500$ fps) indicating the presence of strong, competent foundation rock. Table 2.5-7 lists the results of the in situ cross-hole velocity measurements made in the reactor area; Table 2.5-5 lists the moduli values. Further discussion of the properties of the underlying soils and bedrock are given in Subsections 2.5.4.2 and 2.5.5.

2.5.4.5 Excavations and Backfill

2.5.4.5.1 Extent of Seismic Category I Excavations, Fills, and Slopes

Figure 2.5-37 shows the location and limits of excavations, fills, and backfills associated with Seismic Category I structures at the site. Typical foundation sections for seismic Category I structures are shown.

2.5.4.5.2 Excavation Methods and Dewatering

2.5.4.5.2.1 Excavations in Rock

All Seismic Category I rock foundations were carried to or well below unweathered bedrock. Rock foundations for the turbine and radwaste buildings, although they are not Seismic Category I structures, were prepared according to the same general procedures and criteria used in preparing the Seismic Category I rock foundations.

Excavation of rock proceeded by initial ripping of any weathered surficial rock material followed where necessary by line blasting and presplitting in holes drilled to provide slopes of 1 horizontal to 4 vertical. Essentially vertical slopes in unweathered rock proved stable throughout the duration of construction and no special protective measures were required. Weathered rock was cut on slopes of 1 horizontal to 2 vertical. In a few places, wire mesh was used for protection of higher weathered rock slopes that were exposed for extended periods.

The surface of the excavated foundation rock was scaled to remove loose debris and jetted with water or air to remove loose fragments and to prepare the surface for concrete. Before placement of structural concrete or concrete backfill to design elevation, all Seismic Category I foundations were inspected by an engineering geologist to verify the suitability of the rock and its proper surface preparation to receive concrete. All foundation rock bearing a Seismic Category I structure was geologically mapped (see Figure 2.5-18) or geologically cross sectioned (see Figures 2.5-19 and 2.5-30A).

Foundations for each of the cooling towers (nonseismic-Category I structures) consist of 40 individual pedestals supporting the columns and extended to bedrock. Excavation proceeded by cutting a ring trench and preparing for each pedestal a suitable surface in unweathered or partly weathered bedrock by ripping or blasting as necessary, followed by scaling and jetting.

During construction of principal plant structures founded on rock, excavations extended below the water table and some dewatering was required. Due to the low permeability of the rock, groundwater inflow was small. Dewatering was accomplished by surface drains and sumps.

2.5.4.5.2.2 Excavations in Soil

The excavation for the spray pond, ESSW Pumphouse and diesel generator 'E' fuel tank was predominantly in soils. Excavation proceeded initially by using large earth moving equipment, then finished by using more refined procedures. On completion of excavation, the surface layer of the natural soil formation was recompacted as follows:

- a) For soils having not more than 12 percent passing the No. 200 sieve size, 80 percent relative density as determined by ASTM D2049
- b) For all other soils, 95 percent of maximum dry density as determined by ASTM D1557

Test Results are included in Appendix 2.5C. The location of test specimens with respect to the spray pond is shown on Figure 2.5-59. A statistical analysis of the test results was made and is summarized on Figure 2.5-60. The required compaction was met or exceeded.

A protective concrete mat was immediately placed over the compacted soil under the ESSW Pumphouse and a minimum of 5 in. thick reinforced concrete liner placed over the entire spray pond area.

All temporary slopes in soil were formed at a maximum slope of 1 1/2 horizontal to 1 vertical. The temporary slopes in the vicinity of the ESSW Pumphouse were protected with a 3 in. layer of concrete to maintain the natural soil formation intact. All permanent slopes in soil were formed at a slope of 3 horizontal to 1 vertical.

The excavation for the Seismic Category 1 pipelines in soil was carried out similarly. All slopes were cut at a maximum of 1 1/2 horizontal to 1 vertical. The minimum clearances were 1 ft beneath the pipe and 2 ft to the sides.

The excavation for diesel generator 'E' building was carried to unweathered bedrock by using soldier beams and laggings. All timber laggings were treated with preservative by pressure process. The soldier beams and laggings were left in place. The disturbed soils adjacent to the soldier beams and laggings were densified by compaction grouting. The results of compaction grouting were verified by standard penetration tests. The results of standard penetration tests indicate that the blow count numbers are equal to or exceed those of original soils.

The excavation for diesel generator 'E' fuel tank was carried out to open cut. All slopes were cut at a maximum of 1 1/2 horizontal to 1 vertical.

2.5.4.5.3 Backfill and Compaction

Generally, the excavated area, for a minimum distance of 10-ft surrounding the major structures, was backfilled with a non-corrosive lean mix concrete known as sand-cement-flyash backfill. A minimal amount of backfilling has taken place using granular backfill, with the exception of the spray pond and vicinity addressed later in this section.

The excavated area for the diesel generator 'E' fuel tank was backfilled with sand-cement-flyash to two (2) feet below finished grade.

The Seismic Category I pipelines were generally backfilled with the sand-cement-flyash; otherwise granular material was used.

All category I structures and a portion of the ESSW pumphouse (below approximately elevation 676 feet) was backfilled with sand-cement-flyash. The backfill was placed a minimum of 10 feet

in width all around the building structures. There is no concern with differential settlement at the interface between structure-supported and ground-supported parts of pipelines and conduits.

Buried Seismic Category I electrical ductbanks are composed of reinforced concrete encasements around plastic or metal ducting; the concrete encasement being cast directly against the excavated grade. Granular or sand-cement-flyash backfill was used the same as for buried pipes. The properties of these respective backfills were as follows:

a) Sand-Cement-Flyash

Weight -	110 lb/cu ft minimum
Slump -	3 in. minimum
Slump -	6 in. maximum
Strength -	40 psi minimum at 28 days

Sand-cement-flyash used on the Susquehanna SES project has been obtained from two sources, namely as follows:

- a) Metropolitan Edison, Portland Plant, Reading, Pennsylvania
- b) Michigan Ash Sales, Essexville, Michigan.

The sand-cement-flyash backfill that was mixed on-site used flyash furnished by Michigan Ash Sales. The sand-cement-flyash backfill that was furnished by an off-site supplier (Galli Ready Mixed Concrete) used flyash from Metropolitan Edison.

During January 1979, the pH value of each source of flyash and the pH value of the fresh sand-cement-flyash mix was investigated. The results are as follows:

a) Metropolitan Edison Flyash

pH flyash = 4.36 to 4.42
pH sand-cement-flyash mixture = 11.7 to 12.8

b) Michigan Ash Sales Flyash

pH flyash = 4.2 to 8.2
pH sand-cement-flyash mixture = 12.2

The above tests adequately demonstrated that the sand-cement-flyash backfill used on the Susquehanna SES project is not corrosive.

b) Granular

Granular backfill was well-graded, sound, dense, and durable material. It consisted of sand, gravel or crushed rock and did not contain any topsoil, humus, brush, roots, peat, sod, cinders, shale, rubbish or other perishable materials, or portions of clay, waste concrete, trash, or frozen material. No more than five percent by weight passed the No. 200 sieve. The maximum size of the material was 4 in. in confined areas where hand tamping was required and 6 in. in other areas.

The placement specification of these respective backfills was as follows:

a) Sand-Cement-Flyash

Sand-cement-flyash backfill was either mixed at the batch plant or obtained from an offsite source, conveyed to the point of placement by truck, and placed in lifts not exceeding 30 in. in height. The maximum rate of pour did not exceed 4 ft/hr. It was vibrated in place with approved equipment. It was protected from freezing temperatures for a minimum of 3 days.

b) Granular

Granular backfill was placed in maximum 8 in. loose horizontal layers, moisture conditioned, and compacted to at least 80 percent relative density as determined by ASTM D2049.

Backfill material within 2 ft of structures and in areas where large construction equipment could not be used or where there was a danger of damage to structures was compacted to the specified density by hand operated equipment.

Small areas resulting from dental excavation beneath the spray pond concrete liner received a shallow leveling course. The material and placement specification for this type of fill (arbitrarily designated Fill Type A) was as follows:

Fill Type A, Material

The maximum size of this material was 4 inches and no more than 5 percent by dry weight passed the No. 200 sieve.

Fill Type A, Placement

Fill Type A was placed in maximum 6 inch uncompacted layers, moisture conditioned, and compacted to at least 80 percent relative density as determined by ASTM D2049.

The area to the south and south-east of the spray pond was filled in a controlled manner. The material and placement specification for this type of fill (arbitrarily designated Fill Type 'B') was as follows:

Fill Type B, Material

The maximum size of this material was 12 inches and no more than 35 percent by dry weight passed the No. 200 sieve.

Fill Type B, Placement

Fill Type B was placed in a 15 inch maximum uncompacted layer thickness, moisture conditioned, and compacted to satisfy both of the following requirements:

- a) At least 80% relative density as determined by ASTM D2049 for material having not more than 12% passing the No. 200 sieve or 90% of maximum dry density as determined by ASTM D1557 for all other material.
- b) Irrespective of the compacting effort required to satisfy part a) above, the fill was compacted in one of the following manners as a minimum effort:
 - i) Using a crawler tractor having a weight at least equal to that of a D8 Caterpillar tractor with bulldozer blade. Each track overlapped the preceding track by not less than four inches. When the tractor has made one entire coverage of an area in this manner, it was considered to have made one pass. Each fill lift was compacted with four passes.
 - ii) Using a vibratory roller of minimum weight 20,000 pounds having a rolled width of approximately 60 inches. The roller had a vibrator frequency range of between 1100 and 1600 vibrations per minute and had a minimum vibratory dynamic force of 40,000 pounds. The roller speed did not exceed 3 mph and each track overlapped the preceding one by a least 4 inches. When the roller had made one entire coverage of an area in this manner, it was considered to have made one pass. Each fill lift was compacted with four complete passes.
 - iii) Using a hand controlled vibratory compactor in locations inaccessible by tractor or vibratory compactors was on the basis of the demonstrated ability of the compactor to compact the material to the same density as the continuous backfill.

Test results are included in Appendix 2.5C. The location of test specimens with respect to the spray pond is shown on Figure 2.5-59. A statistical analysis of the test results was made and is summarized on Figure 2.5-60. The required compaction was met or exceeded.

To compute the lateral pressures acting on subterranean walls, all backfill was conservatively assumed to be granular. The static and dynamic engineering properties of this granular backfill was assumed as follows:

Bulk unit weight,	=	135 pcf
Saturated unit weight,	=	140 pcf
Coefficient active earth pressure, K_A	=	0.30
Coefficient earth pressure "at-rest", K_o	=	0.70

The computation of static and dynamic lateral soil pressures acting on subterranean walls is addressed in Subsection 2.5.4.10.2.

A statistical analysis for the sand-cement-flyash backfill is shown in Fig. 2.5-61.

Figure 2.5-61 shows the distribution for the majority of test reports falls within the specification requirement of 40 PSI minimum at 28 days and 100 psi maximum at 90 days. There are

however a sufficient quantity of tests that fall outside these limits and therefore justification is required. The reasons for acceptability are as follows:

- 1) Slump - The slump requirements of 3 inch minimum and 6 inch maximum were for reasons of workability during field pouring operations and as one of the measurements to ensure that a sufficient compressive strength would be obtained. Therefore a deviation from the specification requirement does not constitute unacceptability, since the only basis would be an altered compressive strength and these items have their own acceptability limits.
- 2) 90 day compressive strength - The requirement for the 100 psi (150 psi maximum strength for the diesel generator 'E' facility) maximum strength was a convenience item only. The purpose for this upper limit was to facilitate ease of excavation in an area previously backfilled with sand-cement-flyash material. A deviation from the specification requirement in this area in no way limits the intended use of the material.
- 3) 28 day compressive strength - the requirement for minimum compressive strength was chosen such that the compressive strength would be in the same range as the bearing value of compacted granular backfill. The 40 psi strength converts to 5,760 lb./ft² whereas compacted granular backfill has bearing values on the order of 3,000 to 6,000 lb./ft². However, on SSES the sand-cement-flyash material has not been used for fill beneath any structure. Therefore, the higher bearing value is not required. The sand-cement-flyash backfill has been used only as general backfill for pipes, conduits, and along the sides of buildings. It has therefore been determined that the 20 psi (2,880 lb/ft²) minimum value that may be found in some areas is completely adequate to satisfy the conditions for which the fill is being used.

Strength and Slump tests were conducted every 100 cu. yds, placed or every placement, whichever occurred first.

Slump and Compressive strength samples of sand-cement flyash were taken at the Batch Plant, or in the case of samples taken from an offsite source, from the concrete mixer agitator truck.

2.5.4.5.4 Bedding Material for Seismic Category I Pipes and Electrical Duct Banks

The bedding material was sand-cement-flyash as defined in Section 2.5.4.5.3 of the FSAR.

The excavation was made to original ground or in sand-cement-flyash backfill to required bedding subgrade. The bedding subgrade was inspected and verified to be sound and dense meeting visual requirements for backfill adequate for support of bedding material, thus meeting specification intent. The subgrade was also inspected for unsuitable material such as water, frozen, organic or deleterious material. Such material, when found, was removed.

The sand-cement-flyash bedding material was either mixed at the batch plant or obtained from an approved offsite source. The sand-cement-flyash was then placed in lifts not exceeding 30 inches in height nor 4 feet per hour. For pipes the pour was brought to the pipe spring line and

was allowed to set. For duct banks the bedding was not placed until the duct bank concrete reached the required strength. Sand-cement-flyash was then poured to the top of the duct bank and allowed to set.

Analysis of the relevant field tests for bedding material is included in the summary given in Figure 2.5-61.

2.5.4.6 Groundwater Conditions

Special measures for control of groundwater levels beneath Seismic Category I plant structures founded on rock are not required. However, control of groundwater levels and seepage is needed at the spray pond; discussion of design criteria for stability of the spray pond is presented in Subsection 2.5.5.

Periodic water level readings were obtained in the vicinity of the principal plant (power block) structures between December 1970 and August 1972. Groundwater fluctuations ranged from 1.5 ft in drill holes 209, 311, to 6.2 ft in drill hole 213.

The maximum groundwater level measured in the plant structures area during this preconstruction period ranged from approximately 690 ft at the west edge of the site of the turbine building, to about 655 ft at the east edge of the site of the reactor buildings (refer to Figure 2.5-55). These levels were obviously influenced by the topographic high of 749 ft just west of the site of the power block structures. However, subsequent excavation and grading in these areas preclude water levels from rising to this height in the future.

During construction, the area just west of the power block structures was graded to elevation 710 ft or less. Excavations for the foundations of the principal plant structures extended below the water table and some minor dewatering was required. Due to the low permeability of the rock, groundwater inflow was small and was confined to seepage from fractures. Dewatering was accomplished by pumping from low areas and sumps. Where seeps were noted issuing from fractures in the rock, holes were drilled into the fractures and pipes caulked in the holes to control water while the mudmat was placed. In the foundation for the reactor building (elevation 639 ft) and in the turbine condensate pump pit (at elevation 635 ft), hydrostatic pressure caused lifting of small areas of the 3 inch thick concrete mudmat that had been placed over the impervious membrane. Approximately 20 relief wells drilled through the mudmat released the pressure and allowed the mat to settle back to its original position. The weight of the structural concrete slab subsequently placed on this mudmat was more than sufficient to resist any uplift pressures.

The highest seeps noted in the foundation rock during construction were at elevation 642 ft in the radwaste building excavation and at about the same elevation in the pipe trench in the southern part of the Unit 2 turbine building. Some seeps were also noted in the foundation rock for the reactor buildings at elevation 639 ft and in sumps below this. To the west of the turbine building in the circulating water pumphouse excavation, water was noted to enter the excavation to an elevation of approximately 660 ft. Hydrostatic lifting (described above) of the impervious membrane did not occur at foundation elevations above 640 ft.

Excavation for diesel generator 'E' building extended below the water table and some minor dewatering was required. The groundwater which seeped into the excavation area was diverted to a sump at a low point and was removed by pumping.

Additional information with regard to groundwater monitoring and water table fluctuations in the principal plant structures area is provided in Subsection 2.4.13 and Tables 2.4-31 and 2.4-32.

At the spray pond, water level information taken between July 29, 1974 and August 4, 1975, and from January through March 1977, indicate a minimum water level fluctuation of 4.0 ft recorded at observation wells 1111 and 1113, and a maximum fluctuation of 7.0 ft in 1115. Additional discussion of groundwater fluctuations in the spray pond area can be found in Subsection 2.5.5. Because groundwater levels at the pond will be higher than the maximum projected flood elevation (refer to Figure 2.5-38 and Subsection 2.4.3, respectively), flooding conditions will not significantly affect the groundwater levels.

Local wells within two miles of the plant site were inventoried and the information is given in Table 2.4-22.

Groundwater flows away from the principal plant structures area to the north, east, and south. However, the predominant direction of flow is to the east and southeast at gradients of 0.05 and 0.06, respectively. The flow rate in bedrock is estimated to be less than 1 ft per day as discussed in Subsection 2.4.13. Groundwater contours at the site are shown on Figure 2.5-38.

Permeability of the intact bedrock at the site is less than 1 ft/year. The average permeability of the glacial materials at the spray pond is 2,000 ft/year; however, this value has been considerably exceeded in some tests. For a complete description of permeability at the spray pond and plant structures areas, consult Subsections 2.5.5 and 2.4.13, respectively. Measured permeability values may be found in Tables 2.4-33 and 2.4-34.

2.5.4.7 Response of Soil and Rock to Dynamic Loading

2.5.4.7.1 Response of Rock to Dynamic Loading

Rock at the site would be unaffected by dynamic loading from earthquakes. During historical time, no Pennsylvania earthquakes have been felt at the site. Approximately 14 earthquakes originating outside Pennsylvania could have been felt at the site, but with a probable maximum intensity of only IV on the Modified Mercalli Scale. Ground motion at this intensity would have had no effect on the site.

The compressional and shear wave velocities of sound, unweathered foundation rock in the reactor area ($V_p = 14,000$ to $16,000$ fps; $V_s = 6,200$ to $7,500$ fps) indicate that the rock possesses a high rigidity and provides effective resistance against dynamic loads for all structures founded upon it (refer to Table 2.5-5). Such rock will not be subject to any loss of strength under earthquake loadings.

2.5.4.7.2 Response of Soil to Dynamic Loading

The analysis of earthquake-induced soil strain and settlement of the spray pond and ESSW pumphouse are given in Subsection 2.5.5. Evaluation of potential soil settlement under the diesel generator 'E' fuel oil storage tank is provided in Reference 2.5-121. If the sands at the site behave like dry sand during an earthquake, the settlement will be less than 0.05 in. If the sand deposits are saturated and excess pore pressures develop, they will reconsolidate following the earthquake and settlements up to 1.2 in. at the east end of the pond and up to 1.0 in. at the ESSW pumphouse may be expected. Settlement under the diesel generator 'E' fuel tank will be minor and will take place as soon as the loads are applied. There will be no long term settlement.

The bearing capacity of the pumphouse mat footing was evaluated by the following equation (Ref. 2.5-115):

$$q'_d = 1/2 B \gamma N_\gamma + D_f (N_q - 1)$$

where:

q'_d = ultimate bearing capacity

B = width of the footing

γ = unit weight of the soil

D_f = depth of surcharge

N_γ, N_q = bearing capacity factors

This equation was derived for the static condition; however, a conservative evaluation of the bearing capacity for the dynamic condition can be made by assuming that, during dynamic loading, the footing has an effective width equal to 1/3 of the actual footing (Ref. 2.5-115). Substituting all values given in Subsection 2.5.4.10.2 into the equation but using B=21.3 ft instead of 64 ft, the ultimate bearing capacity was calculated to be 52 kips/sq ft. The corresponding factor of safety against bearing failure is 17.

2.5.4.7.3 Soil Structure Interaction

Soil structure interaction has been addressed in Subsection 3.7.2.4. The analysis and design of buried pipelines has been addressed in Subsection 3.7.3.12.

2.5.4.8 Liquefaction Potential

For the soil supported spray pond, ESSW pumphouse, diesel generator 'E' fuel oil storage tank and Seismic Category I pipelines, the liquefaction potential was evaluated. The soil underneath these structures is predominantly sand, gravel, cobbles, and boulders.

The liquefaction potential of the soils beneath the spray pond and the ESSW pumphouse is discussed in detail in Subsection 2.5.5. The minimum factor of safety against liquefaction for these structures was found to be 1.26, which is larger than the minimum acceptable factor of safety of 1.20.

The soil supported diesel generator 'E' fuel oil storage tank and Seismic Category I pipelines are underlain by the same glacial deposits as the spray pond area and the maximum predicted water level below the pipelines is lower than that under the pond. Hence, liquefaction potential of the soils beneath the diesel generator 'E' fuel oil storage tank and seismic Category I pipelines is no greater than that of soils beneath the spray pond.

2.5.4.9 Earthquake Design Bases

The design bases for the SSE and OBE are addressed in Subsections 2.5.2.6 and 2.5.2.7.

2.5.4.10 Static Stability

2.5.4.10.1 Static Stability of Safety-Related Structures Supported on Rock

The reactor buildings, control structure, and the diesel generator buildings, all of which are Seismic Category I structures, are founded on sound, unweathered siltstone bedrock. The Seismic Category I pipelines linking the reactor buildings with the spray pond are trenched partly in soil and partly in bedrock.

The strength of the unweathered bedrock amply accommodates the loads of the plant providing highly stable foundation conditions. As measured in the Seismic Category I reactor area, compressional velocities are in the range of 14,000 to 16,000 fps; shear wave velocity ranges between 6,200 and 7,500 fps. Static deformational moduli as measured on rock cores vary between 3.1 to 9.4×10^6 psi (refer to Table 2.5-3). Measurements of unconfined compressive strength of unweathered foundation rock from the vicinity of the principal plant structures were between 3,650 and 16,000 psi (Table 2.5-3). Static properties of the foundation rock are summarized in Table 2.5-5. Loads induced by the plant structures are less than the allowable bearing pressure of the rock and far below the ultimate bearing capacity. The structural loads will produce no significant total or differential settlement of the foundations.

Safety-related structures founded on rock were designed for a hydrostatic groundwater loading caused by a maximum groundwater level of 665 ft. This is higher than the expected maximum water level, as discussed in Subsection 2.4.13.

2.5.4.10.2 Static Stability of Safety-Related Structures Supported on Soil

The mat footing of the ESSW pumphouse is 112 ft long, 64 ft wide, and 3 ft thick. The total dead and live loads are 20,000 kips and 2,100 kips, respectively. The corresponding unit pressures are 2.80 ksf and 0.30 ksf, respectively. The bottom of the mat is at elevation 657 ft.

The ultimate bearing capacity of the mat foundation was found to be 158 kips/sq ft. The factor of safety was computed to be 51, which indicates no danger in overstressing the supporting

granular soil. Therefore, the allowable bearing pressure and settlement of the mat footing were evaluated by the method of limiting settlements suggested by Peck, Hanson, and Thornburn (Ref. 2.5-116). The allowable bearing pressure for a maximum settlement not to exceed 2 in. was computed by the formula:

$$q_a = 0.22 C_n C_w N$$

Where:

q_a = allowable bearing pressures, tsf

N = number of blows per foot in the standard penetration test

C_n, C_w = correction factors for "N", for the effects of overburden pressure and location of groundwater surface

A conservative N value of 40 was selected to represent the soils below the mat foundation (Elevation 657 ft, Figure 2.5-38). The Standard Penetration Tests below the foundation level were made at an average overburden pressure of about 6,000 psf (Figure 2.5-39); the corresponding correction factor C was obtained from Figure 19.6 of Ref. 2.5-115 to be 0.63. Assuming that the groundwater surface is at 7 ft below the mat and no surcharge, the correction factor C_w was computed to be 0.55 by equation 19.4 of Ref. 2.5-115.

The allowable bearing pressure was computed to be 6.0 kips/sq ft based on the values of N , C_n , and C_w given above. At this bearing pressure, the settlement of the mat foundation should be less than 2 in. and the differential settlement should be less than 3/4 in. Therefore, by proportion, for a design total pressure of 3.1 kips/sq ft, the corresponding maximum and differential settlements would be less than 1 in. and 1/2 in., respectively. Settlement in sand and gravel deposits occurs almost simultaneously with the application of load. Since more than 80 percent of the total load is dead load, then less than 0.2 in. of settlement is expected after the completion of the construction.

The same equations and procedures can be applied to compute the ultimate bearing capacity of the foundation soils and the allowable bearing pressure for a maximum settlement not to exceed 2 inches.

The foundation mat for the diesel generator 'E' fuel tank is 17 feet wide, 57 feet long and 5 feet thick. The total dead and live loads are 111.4 kips and 684.8 kips respectively. The corresponding unit pressures are 0.12 ksf and 0.71 ksf respectively. The bottom of the foundation mat is at elevation 645.0 feet.

The ultimate bearing capacity of the foundation soils was found to be 42.0 ksf. The factor of safety against shear failure was computed to be 50 which indicates that there is no danger of shear failure.

The allowable bearing pressure was found to be 12.0 ksf for a maximum settlement not to exceed 2 inches. By proportion, the maximum and differential settlement corresponding to a design total pressure of 0.83 ksf would be less than 1/8 in. and 1/16 in. respectively.

The structural stability of the ESSW pumphouse is discussed in Subsection 3.8.4 and 3.8.5.

The sustained load from the spray pond is less than the weight of overburden removed; therefore, there is an adequate factor of safety against overstressing the underlying soil. Soil rebound during excavation in granular soils of the type found at the spray pond is insignificant.

The maximum predicted elevation of the water table is below the base of the spray pond and ESSW pumphouse; therefore, hydrostatic water loadings were not considered in the design of these structures. A full discussion of the water table in this vicinity is in Subsection 2.5.5.

The lateral earth pressure acting on subterranean walls of Seismic Category I structures was computed assuming granular backfill having the properties stated in Subsection 2.5.4.5.3. The coefficient of earth pressure "at-rest" was used. Additionally, the walls were designed for surcharge loadings and dynamic soil pressures as appropriate. The typical pressure diagrams and combinations are shown on Figure 2.5-39.

Water levels in the spray pond area are discussed in Subsection 2.5.5.1.2. Contours of the groundwater table in the spray pond area are shown on Figure 2.5-38. Profiles of measured and projected profiles of the groundwater table beneath the spray pond are shown on Figure 2.5-40.

2.5.4.11 Design Criteria

2.5.4.11.1 Design Criteria of Safety-Related Structures on Rock

The plant structures founded on rock are designed for a maximum acceleration of 0.10g from an occurrence of the SSE event. From consideration of its engineering properties, it is evident that the foundation rock will not be measurably affected by seismic loadings, and negligible additional foundation settlement will accompany these maximum potential dynamic loads. The maximum contemplated total static and dynamic loads of 40 tsf are only a fraction of the bearing capacity of the rock, thus ensuring an ample margin of safety.

2.5.4.11.2 Design Criteria of Safety-Related Structures on Soil

The spray pond slopes are designed for a maximum acceleration of 0.15g from an occurrence of the SSE event at the site. The spray pond riser pipe columns, the Seismic Category 1 buried pipes, and the ESSW pumphouse are designed for a maximum acceleration of 0.15g from an occurrence of the SSE event at the site.

The allowable bearing pressure under both static and dynamic conditions satisfies these conditions:

- a) Sustained dead load plus live load with a minimum factor of safety of 3
- b) Sustained dead load plus maximum live load with a minimum factor of safety of 2
- c) Sustained dead load plus live load keeping settlement within tolerable limits.

At the spray pond, a liner has been designed to restrict the seepage rate from the pond in order to limit buildup of a groundwater mound in the glacial materials underlying the pond. The pond has been designed for a maximum groundwater elevation of 665 ft. Detailed description of

design criteria for control of groundwater levels and seepage at the spray pond and the stability of the pond are in Subsection 2.5.5.

2.5.4.12 Techniques to Improve Subsurface Conditions

2.5.4.12.1 Foundations in Rock

No special treatment was required to improve foundation conditions beneath the Seismic Category I structures bearing on rock. During construction, high loads were carried by the gantry crane rails, one of which was adjacent to the top of the temporary vertical slope on the east side of the reactor building excavation. As a precautionary measure to ensure stability of this slope during construction, tensioned rock bolts were installed in the slope. One large pothole was encountered in the Unit 1 turbine building area, necessitating over excavation of some 23 ft below design base elevation. The resulting hole, which was in fresh, unweathered rock, was backfilled with 574 cubic yards of concrete ($f'_c = 2,000$ psi) to foundation grade.

2.5.4.12.2 Foundations in Soil

No improvement of the natural soil formation at this site was required.

2.5.4.13 Subsurface Instrumentation

2.5.4.13.1 Instrumentation for Rock Foundations

Since settlements are negligible for the safety-related facilities founded on rock (refer to Subsections 2.5.4.7 and 2.5.4.10), no instrumentation to monitor such settlements is necessary.

2.5.4.13.2 Instrumentation for Soil Foundations

The foundation design for the ESSW pumphouse was based on measured soil parameters obtained by field and laboratory testing. The actual settlement should not exceed tolerable limits for the structure and its piping connections. A systematic monitoring program was therefore instituted to study the settlement performance of the structure. The following instrumentation program was carried out:

- a) Permanent Bench Marks: Two permanent bench marks were installed as reference points for measurements.
- b) Settlement Pins: A total of six settlement pins were cast into the structural mat and 5 settlement pins were installed in the pumphouse floor at Elev. 685'-6". Details are shown on Figure 2.5-41 and Figure 2.5-62. A survey reading was taken on each pin at approximately monthly intervals. The total settlement and differential settlement of the mat foundation was therefore deduced.

Survey readings will be taken on the five pins located at ESSW pumphouse floor elevation 685'-6". These readings will be recorded until 1983. This will give

recordings of at least 4 years from the pumphouse completion. In addition to the a survey of these pins shall be conducted after any of the following events:

- 1) Earthquake
- 2) 100 year storm
- 3) Major leakage or break in a water pipe in the pumphouse fill area.

Initial results are shown on Table 2.5-8. Subsequent results are retained in the appropriate SSES records file. All results are within the projections described in FSAR Section 2.5.4.10.2.

2.5.4.14 Construction Notes

During the construction phase excavated material was temporarily stored at the spray pond area which was used for approximately two years as a laydown area for construction materials. This material was then excavated under specification C36 and since the material was unable to meet the requirements of fill type "A" or "B" as outlined in Specification C36 it was removed from the spray pond area. Such removal was ensured as the excavation line for the pond was below the original ground contour.

During construction of the spray pond liner, cracking was observed in several areas, the most extensive being the area along the southwest edge of the spray pond. The remainder of the cracking was distributed between areas just north and south of the spillway and two small areas located along the north and south central portions. The cracks along the southwest and spillway area were approximately 50 feet in length while the cracks along the central area averaged 7 to 10 feet in length. The cracks in all areas ranged from 1/2" to 1 1/2" in depth. The cracks located above elevation 676'-6" and the cracks wider than 1/16" below elevation 676'-6' were "V" grooved to a depth of 1/2" and sealed with Horn Flex L sealant A manufactured by W. R. Grace Co. Cracks below elevation 676'-6" and having widths smaller than 1/16" were left as is.

The hairline cracking which is predominant in the southwest section of the pond is coincident with the concrete liner being placed directly on bedrock. Since the liner in contact with the bedrock is more restrained during the initial concrete curing and shrinkage period it has been determined that these shrinkage forces were the major cause for cracks in this area. In addition two slabs in this area were displaced by hydrostatic uplifting forces causing some additional cracking. This uplift occurred during the construction phase when the pond was empty of water. The hydrostatic uplift pressure was relieved by means of 2-inch diameter core drills through the liner. These relief holes were then filled with grout just prior to filling the pond with water.

A slab located south of the spray pond spillway was displaced by means of frost heave and resulted in cracking. This action also took place during the construction phase when the pond was empty of water. The displaced section was removed and repaired in accordance with section 7.14 of specification C36. The cracks were repaired as described above.

Uplift due to hydrostatic pressure up to design elevation and frost heave are of no design concern when the pond is filled with water as required during plant operation.

In areas where the liner was placed on soil very little hairline cracking has occurred. As a result there has been no indication of cracks being caused by soil settlement.

2.5.5 STABILITY OF SLOPES

Natural slopes at the site are depicted in the site topographic map, Figure 2.4-1. Final plant grades are shown on Figure 2.5-24.

Few rock slopes are present at the site that need to be considered with respect to possible adverse effects on the safety-related operation of the plant. Within the area impounded by the spray pond, bedrock forms a portion of the southwest slope, cut on a gradient of 3 horizontal to 1 vertical. North of the spray pond, a natural slope formed on Trimmers Rock sandstone rises at a maximum gradient of 2 horizontal to 1 vertical to a height of approximately 380 ft above the bottom of the pond (refer to Figure 2.5-56). As discussed in Subsection 2.5.5.2.3.1, such rock slopes would present no significant hazard to safety related plant structures.

The soil slopes to be considered are those forming and surrounding the spray pond.

2.5.5.1 Slope Characteristics

The slopes analyzed include the cut slopes of the spray pond and the slopes of the railroad embankment adjacent to the spray pond. The failure of either slope could affect the normal operation of the spray pond. The stability of these slopes is also dependent upon the stability of the spray pond itself. Therefore, the safety analyses of the slopes and the stability of the spray pond are investigated and discussed together in this section.

The cut slopes of the spray pond consist of two portions separated by a 20 ft service road; both were made at 3 horizontal to 1 vertical (Figures 2.5-42 and Dwg. C-63, Sh. 1). The lower portion is a 17.5 ft slope between the service road (Elevation 685.5) and the pond bottom (Elevation 668). The upper portion extended from the service road to daylight, the height of the slopes varies from 0 ft at the east end to about 40 ft at the west end of the pond. Except for a few cut slopes that are made in bedrock, the majority of the slopes are made of granular material.

The slopes of the railroad embankment adjacent to the spray pond were made of shot-rock. The slopes are at 3 horizontal to 1 vertical with a maximum height of 30 ft.

2.5.5.1.1 Geologic Conditions

The vicinity of the spray pond is situated over a glacial, or preglacial, east-west trending bedrock valley as outlined by contours on top of bedrock (Figure 2.5-17). These contours indicate that the bedrock surface of the valley was eroded about 100 ft below the average elevation of bedrock to the south and considerably more than that below bedrock elevations to the north. Total relief of the bedrock surface is about 130 ft. The valley is filled with dense gravelly and sandy glacial outwash and till deposits which attain a maximum thickness of about 110 ft in the spray pond area. They were deposited during the Olean substage (early Wisconsinan) of the Wisconsin glaciation, which occurred approximately 50,000 years ago, and there is a possibility that some of the bedrock erosion and overlying glacial deposits are the result of an earlier Illinoian glaciation known to have occurred here (refer to Subsection 2.5.1.2). In general, the

deposits are normally consolidated and consist of a sequence of sand, gravel, and boulders overlain by sand and gravel, overlain in turn by silty sand. The entire sequence is highly variable in grain size distribution and sorting, and contains discontinuous pockets of similar materials. As a rule, grain size decreases and sorting increases toward the top of the sequence. Topsoil of variable thickness, consisting of brown sandy silt and organic matter, overlies the glacial drift.

Bedrock beneath the spray pond is correlated with the uppermost strata of the Middle Devonian Mahantango Formation. Strata of the overlying Trimmers Rock Formation crop out along the ridge north of the spray pond; the contact between these two formations is buried by glacial material, but has been inferred from drill hole data to occur immediately north of the spray pond along the buried south-facing bedrock slope (refer to Subsection 2.5.1.2.2.2 and Figures 2.5-40 and 2.5-56). The strata, which consist of dark gray, noncalcareous siltstone with fine sandstone stringers in the upper Mahantango grading to more sandy material in the Trimmers Rock Formation, strike N75°E and dip 15° to 40° north.

The southwestern tip of the spray pond is cut into bedrock while the remainder is excavated in glacial materials. The thickness of the glacial deposits beneath the bottom of the spray pond range from zero at the rock contact to 93 ft at the eastern end of the pond. The ESSW pumphouse structure located at the southeastern corner of the pond is underlain by 40 to 80 ft of glacial material. The water circulation pipelines between the pumphouse and the plant overlie glacial material having a maximum depth of 65 ft. They intersect bedrock at an elevation of 668 ft, approximately 260 ft southeast of the pumphouse (refer to Figure 2.5-17A).

North of the spray pond, the Trimmers Rock Formation forms a steep ridge rising approximately 380 ft above the spray pond. The south-facing slope of this ridge is essentially a rock slope underlain by resistant sandstone thinly mantled with soil and rock fragments. The sandstone is massive to flaggy and exposures exhibit well developed joint systems. The lower portions of the Trimmers Rock are less sandy and occur beneath the surface from the base of this high ridge southward to the northern part of the spray pond area (Figure 2.5-56).

Geologic conditions elsewhere at the site are reviewed in Subsection 2.5.4.1.

2.5.5.1.2 Groundwater Conditions

The groundwater table elevations and contours shown on Figure 2.5-38 are based on water level measurements made June 30, 1971 in the vicinity of the major plant structures, and on measurements made August 6, 1974 in the spray pond area. Water level measurements in the plant structures area were discontinued before the observation wells in the spray pond area were installed, and the wells were destroyed during construction of the plant. The water level data show that the groundwater table is in bedrock beneath the major plant structures, whereas beneath most of the spray pond it is in the glacial drift. Modification (lowering) of the water table by excavation in the major plant structures area is described in Subsection 2.4.13.5. However, some movement of groundwater from the plant structures area toward the spray pond to the north can still be expected, even though the major direction of movement is toward the Susquehanna River to the east. The direction of groundwater movement from the spray pond is also easterly toward the Susquehanna River. The undisturbed groundwater table elevation beneath the southwest end of the spray pond is about 670 ft where it is in bedrock. At the east end of the pond, it is in soil at an elevation of 615 ft.

The observation wells installed in the spray pond area have not been monitored long enough to allow a close determination of a maximum high water level. Monitoring of the observation points was discontinued in August 1975 and was resumed in January 1977. The recorded measurements suggest that, in some cases, up to 11 ft of fluctuation has occurred. However, the measurements taken during October 1974 are considered to be incorrect; therefore, they are not included in the evaluation. Eliminating those measurements, the maximum fluctuation is 7 ft (Table 2.5-9). Intermittent measurements of water levels at observation wells in the area of the principal plant structures were taken by Dames & Moore over a period of 11 months (1970 through 1971). These data indicate fluctuation of less than 10 ft. Using these limited data, it is estimated that the maximum rise of groundwater levels beneath the spray pond will not be greater than 10 ft above those on August 6, 1974.

2.5.5.1.3 Field Sampling and Testing

The field exploration for the spray pond was carried out from June 27, 1974 through August 15, 1974. The drilling subcontractor was American Drilling and Boring Company of Providence, Rhode Island. The boring locations are shown on Figure 2.5-44.

At the time of the investigation, the spray pond area had been used as a spoil area for excavation from the plant site. As much as 33 ft of soil and rock was dumped above natural ground. The majority of this was in the east half of the spray pond area. At the west end of the spray pond, a railroad fill consisting in large part of shot rock skirted the spray pond. The railroad fill was 30 ft deep at Boring 1120. The area between Borings 1110 and 1107 was the only area without any spoil.

Underlying the spoil material is glacial drift which in turn overlies siltstone bedrock. The depth of glacial material varies from 0 ft at Borings 1118 and 1121 to 108 ft at Boring 1104. The bedrock surface generally slopes to the east. At the southwest end of the site, bedrock is exposed at ground surface. The natural soils consist predominantly of sand, gravel, cobbles, and boulders. The soils are poorly stratified, starting as sand or sandy gravel at the surface and grading to mostly cobbles and boulders near bedrock. However, cobbles and boulders were encountered at various depths in most of the borings. Some of the sands and gravels were silty. Generalized sections through the pond area are given on Figure 2.5-30.

Twenty-five test borings were drilled. Ten holes were completed for the geophysical survey, ten for permeability and five as groundwater observation wells. Also shown on Figure 2.5-44 are borings in the 300 and 400 series made in 1971 and 1972 (Ref. 2.5-97 and 2.5-98). Information provided by these early borings was used for preparing the generalized sections given on Figure 2.5-30. The details of the drilling and sampling program are included in Subsection 2.5.5.3 along with logs of borings.

Permeability tests, using either packers or driven casing to isolate zones to be tested, were conducted in nine holes in the spray pond site. The method of analysis used is described in US Bureau of Reclamation Earth Manual, Designation E-18. One hole (1124) was constructed for permeability testing using the field permeameter method, as described in the US Bureau of Reclamation Earth Manual, Designation E-19. Locations of these test holes are shown on Figure 2.5-44, and results of the tests are listed in Table 2.5-10.

The tests were conducted primarily to determine permeability characteristics of the glacial drift and the contact zone between the glacial drift and the bedrock (siltstone of the Mahantango formation). Permeability testing of the Mahantango Formation was performed during investigation of the railroad bridge (Table 2.5-11). The siltstone beneath the spray pond is similar to that tested at the railroad bridge, and these data are taken as representative of the intact bedrock beneath the spray pond.

One of the test sections in the spray pond was isolated in the weathered and fractured siltstone (Boring 1117) immediately below the contact with the glacial drift. The calculated average permeability of that test (Table 2.5-10) is markedly higher than any of the tests performed in the intact bedrock, as would be expected. The exploratory holes in the spray pond area penetrated no more than 10 ft of the more permeable weathered bedrock. Three of the tests (Borings 1112, 1113, and 1114) measured permeability of the contact zone (including from 5 to 10 ft of the weathered bedrock with overlying glacial drift in the test section), and the balance of tests in the spray pond measured permeability of different materials in the glacial drift.

The boring logs indicate that the glacial drift is primarily outwash deposits consisting of permeable sands and gravels, with some discontinuous lenses of less permeable silty sands. The materials tend to be coarser and, presumably, more permeable toward the base of the deposits filling the small valley. The tests summarized in Table 2.5-10 indicate that the permeability of these materials varies considerably. Permeability of the predominant sand and gravel deposits is greater than 2,000 ft/yr (Borings 1111 and 1115). The silty sand lenses are much lower in permeability (Boring 1122 through 1125).

These data indicate that the average permeability of the glacial drift is considerably higher than that of the intact bedrock. The range of permeability in the glacial drift is greater, with permeability of some silty sands as low as some of the bedrock.

The maximum measured permeability of intact bedrock is 277 ft/yr, and the median value of the 41 tested intervals (Table 2.5-11) is 81 ft/yr. Assigning an average permeability of 200 ft/yr to the bedrock appears conservative. For purposes of seepage analysis, it can be assumed that bedrock is impermeable and groundwater movement occurs in the glacial drift.

The high permeability of the glacial outwash deposits is indicated by the two tests in which the capacity of the measuring equipment was exceeded. Also, during drilling of eight of the exploratory holes, there was considerable difficulty because of loss of drilling fluid (see Table 2.5-12). Commonly, it was necessary to drive casing to seal off highly permeable zones. The coarse nature of these lost-circulation zones precluded attempts to perform meaningful permeability tests. Further, the permeable nature of the glacial drift is demonstrated by the performance of the two plant site water wells for construction use (Figure 2.5-38). Each of these wells has a capacity of 150 gpm, and at least one is operating continuously. These wells draw from a maximum of 60 ft of saturated glacial drift. From the relationship of specific capacity of a water well to the thickness of the aquifer, the permeability of the aquifer can be estimated (Ref. 2.5-101). This method indicated 4,000 ft/yr as the apparent minimum average permeability at these wells.

An average permeability of 2,000 ft/yr for the glacial drift was used in the seepage analysis. Considering the evidence that highly permeable materials are present, the results of the permeability tests, and the yield from the wells, assumption of an average permeability of 2,000

ft/yr is conservative in relating seepage losses to groundwater levels and safety against liquefaction.

In the seepage analyses, the possible differences of vertical and horizontal permeabilities must be considered. The vertical permeability of glacial outwash deposits can be as small as one-fifth the horizontal permeability. Because groundwater in the saturated zone moves in a predominantly horizontal direction, the effective permeability is the horizontal permeability. In analyzing seepage through the unsaturated zone, however, movement of groundwater may be predominantly vertical; thus, the possibly lower vertical permeabilities were considered. Beneath the spray pond lenses of materials with low permeability are thin and discontinuous and therefore do not appear to cause a significantly lower permeability in the vertical direction. This is confirmed by the fact that no perched water has been detected in the area.

2.5.5.1.4 Laboratory Testing

2.5.5.1.4.1 General

In general, the granular deposits underlying the spray pond consist of silty sand at shallow depth, underlain by sandy gravel with boulders and cobbles. The test program was conducted only on the sands because of difficulties in collecting undisturbed gravel samples. The undisturbed samples were obtained in sand zones which had lower standard penetration blow counts than in the coarser material. The relative locations of soil samples for which the tests were made are shown on the generalized cross sections E and F, on Figure 2.5-45.

The laboratory test results are summarized in Table 2.5-13. For detailed information on test procedures and results, see Ref. 2.5-102.

2.5.5.1.4.2 Grain Size Distribution

Grain size determinations were made on most of the split spoon samples and on Shelby tube samples for classification purposes and to determine the D50 size that can be used as an index for evaluating the potential susceptibility of granular soils to liquefaction.

Sieve and hydrometer analyses were performed according to ASTM Procedure D 422-63, 1972. The range of grain size curves for the granular deposits is shown on Figure 2.5-31. The mean grain sizes (D50) of the samples of sand and gravel were found to be in the range of 0.14 to 3.0 mm and 4.5 to 25.0 mm, respectively.

2.5.5.1.4.3 Unit Weight

Unit weights were obtained for all undisturbed Shelby tube samples on which strength tests were performed. The undisturbed samples were obtained by cutting the Shelby tubes into approximately 7 in. lengths by a tube cutter. The length and weight of each sample section was determined while in the tube for unit weight computations. The unit weight is required to determine the relative density of the site soils.

2.5.5.1.4.4 Maximum-Minimum Densities

Maximum dry density values were obtained using two procedures; namely, impact compaction and vibratory compaction. Both tests were performed on samples obtained by mixing bulk samples from Test Pit No. 1.

The impact compaction tests were performed using ASTM Procedure D 1557-70, method D, modified so that each of the five layers was compacted with 20 blows of a 10 lb hammer dropping 18 in., i.e., a total compaction energy equal to 20,000 ft.lb/ft³ of soil. The vibratory compaction test was performed according to ASTM Procedure D 2049-69 using a 0.1 cu ft mold and the wet method.

The maximum dry density obtained from these two tests were 106.1 pcf and 108.2 pcf, respectively.

The minimum dry density was also performed on bulk samples obtained from Test Pit No. 1 according to ASTM Procedure D 2049-69. The minimum dry density obtained was 91.5 pcf.

The relative density of the in site soils was determined using the maximum and minimum densities.

2.5.5.1.4.5 Relative Density

Relative density data were obtained from two sources: densities of the undisturbed Shelby tube samples were correlated to the maximum-minimum dry densities, and correlations were made with standard penetration test results obtained during the drilling operations using the Gibbs and Holtz procedure (Ref. 2.5-100).

The relative densities based on maximum-minimum dry densities were determined using the relationship:

$$D_d = \frac{\gamma^{\max}(\gamma - \gamma^{\min}) \times 100}{\gamma(\gamma^{\max} - \gamma^{\min})}$$

as given in ASTM Procedure D 2049-69, where

D_d	=	relative density, percentage
γ^{\max}	=	maximum dry density, pcf
γ^{\min}	=	minimum dry density, pcf
γ	=	dry density of undisturbed samples, pcf

There was insufficient data to directly determine the relative density of each of the samples of in site soils. Therefore, the relative density of undisturbed samples was not used in the analyses. The design engineering properties of the site soils were based on tests on undisturbed samples. During drilling operation, a Standard Penetration Test was performed every 3 ft in each of the

drill holes. From these data and the values of effective overburden pressure at the location of each Standard Penetration Test, the relative densities were determined from the correlation between standard penetration resistance, effective overburden pressure, and relative density of granular soils given by Gibbs and Holtz (Ref. 02.5-100). The Gibbs and Holtz procedure is valid for normally consolidated sands. Values of relative density obtained in this way are summarized on Figure 2.5-46.

Relative density determinations of well stratified outwash sands and gravels, together with poorly stratified to unstratified kame-like gravels by currently available test procedures is not meaningful as the maximum and minimum density values will not be representative of the maximum and minimum density values of individual strata or lenses. Therefore no attempt was made to measure relative density directly. Furthermore, for the same reasons it is not possible in deposits such as those at the spray pond site, to select "the most appropriate maximum and minimum density values."

In deposits like these an indication of the relative density can be obtained from a conservative evaluation of the Standard Penetration test data. This was done by estimating the relative density from the lower bound values of the blowcounts by using the Gibbs and Holtz procedure (Ref. 2.5-100). Since the deposit is normally consolidated the Gibbs and Holtz procedure can be used to estimate relative density.

A direct comparison between measured relative density and Standard penetration test results cannot be presented as relative density was not measured directly.

2.5.5.1.4.6 Static Triaxial Shear Test

Eight static consolidated-drained triaxial tests were performed on undisturbed samples. The purpose of the test was to obtain the strength data required to evaluate the static stability of the cut slopes.

The tests were carried out in triaxial cells and the test specimens were saturated by the back pressure method. The saturation was checked by determining the value of Skempton's B coefficient (Ref. 2.5-103). Specimens were considered to be saturated when the B coefficient was 0.95 or higher. The specimens were obtained by cutting the 3 in. Shelby tubes into 7 in. lengths. They were then extruded and trimmed. The specimens were consolidated isotropically under effective consolidation pressures ranging from 0.50 to 6.0 ksf. These confining pressures represent the range of effective overburden pressures at the site. The results of these tests are presented on Figure 2.5-34 which also shows the selected design parameters.

2.5.5.1.4.7 Cyclic Triaxial Shear Tests

Twenty-five cyclic loading triaxial shear tests (CR) were performed to determine the cyclic shear strength of the soils. Sixteen tests were performed on undisturbed samples. Nine tests were performed on remolded samples. Undisturbed specimens were prepared in the same manner as for static triaxial tests. After completion of the tests on selected undisturbed specimens, they were oven dried, broken down, and compacted by vibration to the same dry density as the original undisturbed specimen. Test specimens were saturated as in the case of the static triaxial tests and consolidated under an isotropic pressure equal to either 1.0 ksp or 6.0 ksf.

During the cyclic shear tests, a symmetrical cyclic deviator stress was applied at a constant frequency ranging between 1 cycle per 2 to 3 seconds while measuring axial deformation, axial load, and pore pressure continuously by means of electric transducers and a chart recorder. The results of all CR tests including the number of cycles to reach a total strain of 5 percent are given in Table 2.5-14. The undisturbed specimens were generally found to be more resistant to cyclic loading than the corresponding remolded specimens prepared at the same dry density. The loss of shear resistance may be due to changes in the original soil structure and destruction of slight cementation which exists in the soil in the undisturbed state. The test results on undisturbed samples are shown on Figure 2.5-35.

Also shown on Figure 2.5-35 are the results of four cyclic triaxial tests reported by Dames & Moore (Ref. 2.5-98). In general, the Dames & Moore samples yielded higher cyclic strength. The reason for the difference may be due to the difference in the method of sampling. The undisturbed samples tested by GEI (Ref. 2.5-102) were sampled with a thin-walled Shelby tube sampler which was pushed by hydraulic pressure in accordance with ASTM D1587-67. However, the undisturbed samples tested by Dames & Moore were obtained with the "Dames & Moore" sampler. The area ratio of the "Dames & Moore" sampler is large compared to the thin-walled Shelby tube sampler, and the greater area ratio may result in greater disturbance to the sample. Since the amount of disturbance could not be evaluated and since the GEI samples yielded lower cyclic strength, the Dames & Moore results were not used in the liquefaction analysis for conservatism.

2.5.5.2 Design Criteria and Analyses

2.5.5.2.1 Design Criteria for Spray Pond

The design criteria adopted for the analysis of the spray pond and the slopes surrounding the spray pond include criteria for ground surface acceleration, liquefaction, and slope stability.

2.5.5.2.1.1 Ground Surface Acceleration

The horizontal ground accelerations used for design of the spray pond are 0.15g for the Safe Shutdown Earthquake (SSE) and 0.08g for the Operating Basis Earthquake (OBE).

2.5.5.2.1.2 Liquefaction

For the most adverse water level conditions at the spray pond site, the factor of safety provided against liquefaction should not be less than 1.2 for the SSE condition.

2.5.5.2.1.3 Slope Stability

The slopes in the area of the spray pond must be designed to provide a minimum factor of safety of 1.5 for the static condition and 1.1 when subjected to an SSE event.

2.5.5.2.2 Design Analyses for Spray Pond

The design analyses, including the seepage analysis, liquefaction potential of the spray pond, stability of slopes, and the earthquake induced settlement, are given in the following four Subsections.

2.5.5.2.2.1 Spray Pond Seepage Analysis

The total inventory that determines the spray pond capacity includes sufficient water to compensate for losses that could occur over the 30 day shutdown period. Additionally, seepage losses must be controlled during normal operation so that the groundwater table is not artificially elevated to a level that would aggravate the safety margin against liquefaction. Seepage analyses were made to determine what design parameters are required for the spray pond to meet these restrictions. It was first determined that seepage from an unlined pond does not meet these restrictions, and that a lining of the pond is required. The second case determines the design parameters for a lining that will sufficiently control the quantity of seepage to satisfy liquefaction requirements.

To maintain the groundwater level below the levels necessary to ensure an adequate factor of safety against liquefaction, an unsaturated zone must be maintained beneath the spray pond. A liner must be designed that will sufficiently restrict seepage and prevent groundwater levels from rising above the design levels. Seepage from the pond will increase the total groundwater underflow beneath the pond and develop a groundwater mound. That is: Total Underflow = Pond Seepage and Base Flow (the present underflow).

The groundwater flow path from the pond is eastward along the trough in bedrock which is filled with glacial deposits. The downstream discharge point of the groundwater mound is assumed to be at the surface at elevation 600 near a present spring. The quantity of underflow, Q , beneath the pond may be calculated using Darcy's law:

$$Q = KIA$$

Where:

Q = quantity of underflow (ft³/yr)

K = permeability (ft/yr)

I = average hydraulic gradient (ratio)

A = cross sectional area of flow path (sq ft)

The controlling permeability for this case is the average permeability of the glacial drift, 2,000 ft/yr. The average hydraulic gradient may be taken as the difference in elevation between the elevation of the assumed discharge point, 600 ft, and the elevation of the water table beneath the center of the pond over the distance between the two points, 1,850 ft. Gradients were determined for several assumed elevations beneath the pond. The average cross-sectional area of saturated glacial drift along the flow path was determined for each assumed elevation of the groundwater mound beneath the pond.

An average base underflow of $4.3 \times 10^5 \text{ ft}^3/\text{yr}$ was calculated for the undisturbed groundwater conditions, represented by water levels shown on Figure 2.5-38. The amount of total underflow was then calculated for several assumed groundwater elevations beneath the center of the pond. The seepage which is producing the groundwater mound can be determined by subtracting the base flow of $4.3 \times 10^5 \text{ ft}^3/\text{yr}$ from the total underflow. Then, by using a form of Darcy's Law (Ref. 2.5-105):

$$q = k \frac{p + d}{d} \text{ and } Q = qa$$

Where:

q	=	quantity of seepage through one square foot of liner assumed to be saturated
K	=	effective liner permeability (ft/yr)
p	=	head of water in pond (ft)
d	=	liner thickness (ft)
Q	=	effective seepage losses through the liner (ft^3/yr)
A	=	area of the spray pond (sq ft)

The seepage loss as related to maximum groundwater level beneath the pond can be calculated. Then, the liner thickness and permeability that would restrict the amount of seepage sufficiently to maintain the selected groundwater elevation can be calculated. This provides a relationship between liner parameters and the elevation of the groundwater mound. The groundwater elevations beneath the pond that would be maintained by specific liner parameters are listed in Table 2.5-15 and shown on Figures 2.5-38 and 2.5-40. The relationship between seepage losses and the groundwater elevation beneath the pond is shown on Figure 2.5-47. To maintain the groundwater level below the maximum allowable level determined by the liquefaction analysis, 665 ft, a reinforced concrete liner has been constructed. The concrete liner has expansion, contraction and construction joints at appropriate spacing to control cracking. Both expansion and construction joints have impermeable rubber waterstops incorporated.

The relationship between the thickness of the liner, permeability of the liner and seepage loss is shown on Figure 2.5-57. The permeability of reinforced concrete is conservatively 1×10^{-2} feet per year. The minimum thickness of liner provided over the entire pond is 5 inches. Therefore, during normal operation, the seepage loss from the spray pond is estimated to be 5.9×10^4 gallons per 30 days. More than 5 times this amount is required to raise the groundwater level to the design value of 665 feet which was used for the liquefaction analysis.

Accident conditions and their possible effect on the integrity of the liner and on seepage losses have also been examined.

Should a tornado-generated missile having a frontal area of 20 square feet puncture the liner, the additional leakage would be

1.6×10^4 gallons per 30 days. This volume of water would not be sufficient to elevate the water table to an unacceptable level.

In the event of an SSE, the soils analysis covering slope stability, discussed in Subsection 2.5.5.2.2.3.2, shows that the cut slopes will remain stable. No credit is taken in the analysis for the presence of the concrete liner. Subsection 2.5.5.2.2.4 discusses the settlement which might result from an earthquake induced motion. The relative settlement across the pond would be very small, less than 1 inch in 500 ft. It is therefore anticipated that the liner will not undergo any significant displacement as a result of an SSE. Some additional cracking could occur. However, since a very conservative approach has been taken in providing a liner with a permeability well below that required to establish liquefaction potential, the additional cracking can be tolerated.

2.5.5.2.2.1.1 Spray Pond Seepage Monitoring

A total of six (6) permanent observation wells in soil along the perimeter of the spray pond are used to monitor seepage from the spray pond. These piezometer installations consist of two inch (2") minimum diameter well point casings with base elevations of 645' along the west section of the spray pond to a low elevation of 625' east of the pond. Every six months readings of these wells will be taken to monitor the elevation of the ground water table beneath the concrete liner. A seventh well (piezometer number 2) is located in bedrock and therefore cannot be used to assess the possibility of liquefaction of the soil.

Seepage from the spray pond was documented by measuring pond levels, precipitation and evaporation. Meteorology and evaporation data was collected. Data collected included the following: Pan evaporation, air temperature relative humidity, wind speed, precipitation, solar radiation and cloud cover. Measurements were taken on a daily basis for a period of 33 days from 4/25/81 to 5/27/81 to perform the seepage study of the spray pond liner. Data collected as a result of this study is included in the quality assurance files.

Groundwater levels will be monitored every six months using the six (6) permanent piezometer wells (located in soil) discussed above. When it has been determined that the actual groundwater level has reached EL 663 feet at any one (1) of the six (6) piezometer locations, the following actions will be taken:

- (1) NRC will be notified of the high (EL 663') groundwater condition;
- (2) Steps will be taken to identify the cause of the rise in the water level;
- (3) An assessment of the safety impact of the occurrence will be performed;
- (4) Appropriate action(s) will be taken based on the findings of the safety impact analysis.

2.5.5.2.2.2 Liquefaction Potential

2.5.5.2.2.2.1 Method of Analysis

The evaluation of the liquefaction potential of the soils at the site was made by comparing the shear strength of the soils under cyclic loading conditions to the dynamic shear stress induced in the soils by the vibratory motion associated with the SSE. The ratio of shear strength to induced shear stress is termed the factor of safety against liquefaction. Since both the shear strength of the soils and the induced shear stresses are dependent on depth below ground surface, determinations of the factor of safety against liquefaction were made at various depths.

Soil profiles and the corresponding groundwater levels representative of the site conditions were chosen for the study. The SSE was applied at the ground surface and deconvolved downward to bedrock using the SHAKE 3 Computer Program (Ref. 2.5-106).

The soil profiles used in the analyses were conservatively assumed to consist only of sand even though they included gravel, boulders, and cobbles in places as discussed in Subsection 2.5.5.1. Based on limited information available (Ref. 2.5-107), the resistance to liquefaction of gravel, boulders, and cobbles is equal or better than that of sand. For instance Kishida (Ref. 2.5-112) has indicated that soils with D_{60} less than 2 mm and with uniformity coefficients less than 10 are most susceptible to liquefaction (Ref. 2.5-98). The saturated unit weight of the sand was taken to be 130 pcf and the buoyant unit weight to be 67.5 pcf. The spray pond was simulated as a material with a low shear modulus value of 1.0 ksf. Because water does not transmit shear waves, the simulation was necessary so that the computer program SHAKE 3 could be used to compute the shear stresses induced by the earthquake. Use of this small modulus has an insignificant influence on the induced shear stresses.

2.5.5.2.2.2.2 Soil Profiles and Positions of Groundwater Table

As disclosed by the field investigation, the thickness of overburden varies at the site of the spray pond. The bedrock contours are shown on Figure 2.5-17. At the southwest end, bedrock was exposed at the ground surface and over 90 ft of granular deposits were encountered at the northeast end. Therefore, to evaluate the liquefaction potential, three soil profiles were chosen to represent three thicknesses of overburden. The depths from the bottom of the pond (Elevation 668 ft) to the bedrock for the three soil profiles were 93 ft (Profile 1 - east end of spray pond), 57 ft (Profile 2 - central section, and pumphouse), and 20 ft (Profile 3 - west end of spray pond). The predicted maximum groundwater levels that will occur beneath a lined pond as discussed in Subsection 2.5.5.2.2.1 were used at each profile.

To evaluate the liquefaction potential at other locations in the spray pond, the same soil profiles were used and the groundwater table was varied in accordance with the predicted maximum water table elevations given on Figure 2.5-40.

Figure 2.5-48 shows the soil profiles and the maximum groundwater levels used at Profiles 1, 2, and 3 in the analyses.

2.5.5.2.2.2.3 Shear Moduli

Cross-hole shear wave velocity measurements were performed during August and September 1974 (Ref. 2.5-99). Compressional and shear wave velocities were measured in situ to depths of about 100 ft by the cross-hole procedure. The average shear wave velocities obtained from the measurement are presented on Figure 2.5-36. As shown on the figure, the shear wave velocity increases linearly with depth. The average shear wave velocities used for soil and rock in the liquefaction analyses are also shown.

The shear moduli of sand were computed from the values of shear wave velocity as follows:

$$G = \frac{\gamma}{g} V_s^2$$

Where:

G	=	shear modulus, psf
γ	=	unit weight, pcf
g	=	gravitational acceleration, ft/sec ²
V_s	=	shear wave velocity, fps

The shear modulus is influenced by the confining pressure, the strain amplitude, and the relative density and, in general, these can be related by the equation:

$$G = 1000 K_s (\bar{\sigma}_m)^{1/2} \quad (\text{Ref. 2.5-108})$$

Where:

G	=	shear modulus, psf
k	=	a variable parameter, dependent on relative density, shear wave velocity, and strain amplitude
$\bar{\sigma}_m$	=	mean principal effective stress, psf

In the liquefaction analysis, the shear modulus values at the corresponding effective confining pressures obtained from the above equation, were used as initial values at very small strains. The strain-compatible shear moduli were then determined from the curve of shear modulus-shear strain relationship as given by Seed and Idriss (Ref. 2.5-108).

2.5.5.2.2.2.4 Cyclic Shear Strength

The results of cyclic triaxial shear tests are given in Table 2.5-14 and on Figure 2.5-35. The results are given in terms of the cyclic shear stress ratio $(\sigma_1 - \sigma_3)_{cy}/2 \bar{\sigma}_c$ and the number of loading cycles required for the test specimen to reach a total axial strain of 5 percent, where:

$(\sigma_1 - \sigma_3)_{cy}$ = cyclic deviator stress

$\bar{\sigma}_c$ = effective consolidation pressure

The selected design cyclic shear strength is given on Figure 2.5-35. Based on results of the site seismicity study and on the SSE having a magnitude less than 6, the cyclic shear strength at 5 equivalent uniform load cycles was considered appropriate and this was used in evaluating the liquefaction potential at the pond (Ref. 2.5-96). The cyclic tests were performed at two effective consolidation pressures, 1.0 and 6.0 ksf. These pressures were selected to envelope the actual field conditions. However, the 1.0 ksf was selected as a lower limit for the testing pressure. Testing of sand samples at very low pressure may not be relative. From the test results, the cyclic shear stress ratios at these two effective consolidation pressures were determined to be 0.320 and 0.260, respectively, for 5 loading cycles. A linear relationship was assumed in computing cyclic shear stress ratios at other effective consolidation pressures. The cyclic triaxial testing conditions differ from field conditions and to account for these differences, and also to permit the use of effective vertical pressures instead of effective consolidation pressures, a correction factor, C, must be applied to the test results before using them in liquefaction analyses. The correction factor is a function of relative density and values have been published by Seed and Idriss (Ref. 2.5-108). A value of 0.57 was used in the analyses. This corresponds to an average field relative density of 50 percent for normally consolidated sands at the site. Using the above data, the following relationship was established between field cyclic shear strength, and the effective vertical pressure:

$$\text{Cyclic Shear Strength, } \tau = 0.57 \bar{\sigma} (0.32 - 0.012 \bar{\sigma}_N)$$

or

$$\tau = \bar{\sigma} (0.189 - 0.0068 \bar{\sigma})$$

(τ and $\bar{\sigma}$ in ksf)

The above expression permits the calculation of the cyclic shear strength at any depth down to bedrock.

2.5.5.2.2.2.5 Determination of Dynamic Shear Stresses

The vibratory motion of the SSE was applied at the ground surface and deconvolved downward to the bedrock; thus, inducing shear stresses into the soil. The synthetic time history of ground surface acceleration during the SSE was used with a maximum acceleration of 0.15g as discussed in Subsection 2.5.2.6.

The maximum shear stresses developed at various depths within the soil during the SSE were calculated using the computer program SHAKE 3 developed by Schnabel, Lysmer, and Seed (Ref. 2.5-106). In addition to the SSE time history and maximum ground acceleration, the computer program uses the following parameters:

- a) Unit weights of the subsurface strata and depth to the groundwater table

- b) Damping ratios of the subsurface strata and the variation of these damping ratios with shear strain
- c) Shear moduli of the subsurface strata and the variation of these moduli with shear strain

The output of the SHAKE 3 computer program provides values of the peak shear stresses induced in the various strata during an SSE event. However, for the liquefaction potential analysis, the equivalent uniform average shear stress is required. The average shear stress during the SSE has been taken to be equal to 0.65 times the peak shear stress (Ref. 2.5-107).

The results of the average shear stress determinations for the various cases analyzed are compared with the cyclic shear strength.

2.5.5.2.2.6 Design Earthquake

The synthetic acceleration time history as discussed in Subsection 3.7b.1.2 was used in the evaluation of liquefaction potential.

Based on the site seismicity studies discussed in Subsection 2.5.5.1.2, the ground acceleration of 0.15g was adopted for the SSE for structures founded on soil.

2.5.5.2.2.7 Results of Liquefaction Analyses

2.5.5.2.2.7.1 Liquefaction Potential Under the Design SSE

The average shear stresses induced by the SSE of 0.15g and the corresponding shear strengths and factors of safety, for three different profiles and various groundwater levels, are given in Table 2.5-16. The factors of safety are also shown on Figure 2.5-49.

Based on these values, it was possible to obtain and to interpolate the factor of safety at any particular location in the pond for the predicted maximum groundwater elevation as shown on Figure 2.5-38. On Figure 2.5-50 the factors of safety at seven selected locations are shown along with the information on the elevation of maximum predicted water table and bedrock. The minimum factor of safety was found to be 1.26, which is larger than the minimum acceptable factor of safety of 1.20, as given in Subsection 2.5.5.2.1.

As indicated by the results shown on Figure 2.5-50, the factor of safety decreases as the groundwater table rises, and at the same water level the factor of safety decreases as the depth to bedrock increases.

2.5.5.2.2.7.2 Variations of Shear Moduli and Damping Ratios for Evaluation of Liquefaction Potential

As mentioned in Subsection 2.5.5.2.2.5, the "standard" relationship between the effective strain and the dynamic properties (shear moduli and damping ratios) given by Seed and Idriss (Ref. 2.5-108) was used in the liquefaction analysis for estimating induced cyclic stresses. To

evaluate the effects of possible variations of these relationships, liquefaction studies were made initially in which the values of shear moduli and damping ratios were varied by ± 30 percent.

A plot of damping ratio versus shear strain, used in the liquefaction analysis for the sandy deposits, is shown on figure 2.5-58. The plot is similar to the average curve of damping ratio versus strain presented by Seed and Idriss (Reference 2.5-108). In the liquefaction analysis, the curve was digitized and represented by a set of points connected by straight lines. No damping tests were made on samples from the site. However, the Seed and Idriss curves represent a summary of laboratory damping values determined for a wide range of granular materials and the data are given in Reference 2.5-108.

In the liquefaction analyses variation of damping does not have a very significant effect on the magnitude of induced stresses. For example, reducing the damping ratio by 30%, changes the average shear stress from 553 psf to 556 psf which is less than 1% (Table 2.5-17). The effect on Factor of Safety (F.S.) of change in the damping ratio is shown on Figure 2.5-50A. The trend established indicates that if the damping ratio was varied beyond 30%, the Factor of Safety would still be larger than the acceptable value of 1.2. Also shown on Figure 2.5-50A is a line representing the F.S. vs. change of damping ratio if the shear modulus was varied by 50%. This line was projected based on data in Table 2.5-17. As shown by this line, the minimum acceptable F.S. of 1.2 will still be satisfied by the combined variation of $\pm 50\%$ shear modulus and -50% damping ratio.

The most critical soil profile (Profile 2) with the maximum predicted water table at 665 ft was used in the study.

The study included the following cases:

- a) Varying shear moduli ± 30 percent, damping ratios remain unchanged
- b) Varying damping ratios by ± 30 percent, shear moduli remain unchanged
- c) Change both shear moduli and damping ratios by ± 30 percent

The average induced cyclic shear stresses, shear strengths, and factors of safety, along with the results using the standard relationship, are summarized in Table 2.5-17. The maximum change of shear stress is found to be about 3 percent. This reduces the minimum factor of safety to 1.23, but it is still larger than the acceptable value of 1.2 (Subsection 2.5.5.2.1). The results of this study indicate that the effects of variations of moduli and damping are small and do not change the conclusion that there is an adequate factor of safety against liquefaction.

A subsequent review of the results in Table 2.5-17 were made to determine the effect of varying the damping ratio by $\pm 50\%$ and the shear modules by $\pm 50\%$. The review was made by projecting the results. A plot showing the effect on the factor of safety is given on Figure 2.5-50A.

2.5.5.2.2.2.7.3 Results of Liquefaction Analyses Using Real Earthquake Records

All the results of the liquefaction study, presented in the previous sections, were based on the design SSE of 0.15g at the ground surface. Some real earthquake records obtained at sites with comparable geologic conditions and in the same range of magnitude were available and were used to check the liquefaction potential. Three rock records: Golden Gate (M = 5.3, 1957), Helena (M = 6.0, 1935), and Parkfield (temblor Station, M = 5.6, 1966) were used for this purpose.

Liquefaction studies were made using these records applied at rock outcropping for obtaining cycle shear stresses in the soil.

The resulting factors of safety along with the factor of safety for the design SSE (Bechtel synthetic) are summarized on Table 2.5-18 and Figure 2.5-51. The minimum factors of safety obtained from the real records were larger than the ones obtained from the synthetic earthquake. The stresses induced by both the design SSE and the real earthquakes are also shown on Figure 2.5-52.

2.5.5.2.2.3 Slope Stability Analyses

2.5.5.2.2.3.1 Stability of Rock Slopes

The southwestern tip of the spray pond is cut into bedrock. However, since the cut slope is 3 horizontal to 1 vertical, the slope will obviously be stable, considering the engineering properties of the bedrock as discussed in Subsection 2.5.4. A detailed analysis of the stability of such a slope in rock is therefore not required.

North of the spray pond, the Trimmers Rock Formation forms a steep ridge rising approximately 380 ft above the bottom of the spray pond. The south-facing slope of this ridge is essentially a rock slope underlain by flaggy, resistant sandstone thinly mantled with soil and rock fragments. The closest approach of this slope to the spray pond is along the northern perimeter of the pond; the toe of slope at elevation 710-720 ft is at least 150 ft from the top of the north slope of the pond at elevation 700-727 ft (Refer to Figure 2.5-24 for final site grades in this area). The maximum slope along the ridge is about 2 horizontal to 1 vertical, and an overall slope of 3-1/2 horizontal to 1 vertical, a relatively flat slope for rock. Bedding in the rock dips approximately 30° to the north into the slope; thus, it is favorably oriented for slope stability. Data of McGlade (Ref. 2.5-56, p. 108) indicate that natural slopes eroded on Trimmers Rock strata are "steep and stable". In consideration of the competency of the rock forming the slope and the favorable orientation of rock structure, together with the fact that such gentle rock slopes are normally stable in this region, it is concluded that there is an ample margin of safety against failure of the slope north of the spray pond.

2.5.5.2.2.3.2 Stability of Slopes in Soil

Stability analyses were performed for the spray pond cut slopes and the fill slopes of the railroad embankment that are immediately adjacent to the pond. Both cut and fill slopes are constructed at 3 horizontal to 1 vertical. Except a small portion of cut slopes that are made in bedrock, the majority of cut slopes and all the fill slopes are made of granular materials. The granular materials range from sand and sandy gravel for the cut slope to the shot rocks for the embankment slopes. The shot rocks were obtained from the main plant excavation.

To evaluate the stability of the slopes, the effective angle of internal friction of the sand deposits was found to be 35° from the test data shown on Figure 2.5-34. For the sandy gravel and the shot rock, the effective angle of internal friction was conservatively assumed to be the same as that of the sand.

The pond is lined and the maximum predicted groundwater level is below the bottom of the slopes. Therefore, the infinite slope analysis and the yield acceleration analysis by Seed and Goodman (Ref. 2.5-109) are considered appropriate for evaluating the stability of the slopes.

For static conditions, the infinite slope analysis was used to determine the factor of safety of soil slopes:

$$FS = \frac{\tan \phi}{\tan i}$$

Where:

ϕ = friction angle of sand

i = inclination of slope

Therefore, for $\phi = 35^\circ$ and $i = \tan^{-1} (1/3)$, the factor of safety under static condition is found to be 2.10.

For the dynamic condition the yield acceleration analysis was used. The yield acceleration is defined as the acceleration at which sliding will begin to occur. The yield acceleration coefficient (k_y) is defined as:

$$k_y g = \tan (\phi - i) g$$

where ϕ and i were defined in the previous paragraph. For $\phi = 35^\circ$ and $i = \tan^{-1} (1/3)$, k_y is found to be 0.297. Compared to the SSE of 0.15g, the factor of safety for the dynamic condition would be:

$$FS = \frac{0.297}{0.150} = 1.98$$

Consequently, the railroad embankment slopes and the cut slopes will be stable under both the static and dynamic conditions.

2.5.5.2.2.4 Earthquake-Induced Soil Strain and Settlement

Two methods were used for estimating the earthquake induced settlement. Seed and Silver have proposed a method for determining settlement of sands that are sufficiently free draining in the field such that excess pore pressure cannot develop during an earthquake (Ref. 2.5-110). Lee and Albaisa have proposed a method that accounts for the reconsolidation settlement that results from dissipation of excess pore pressure following the earthquake (Ref. 2.5-111).

Following the procedure suggested by Seed and Silver (Ref. 2.5-110), the distributions of average induced shear strain as a function of depth for the soil profiles shown on Figure 2.5-48 were plotted and are shown on Figure 2.5-53.

It was conservatively assumed that the relationship between vertical strain and cyclic shear strain for sand at 60 percent relative density, as shown on Figure 8b of Ref. 2.5-110, was applicable for the sand deposits at the site. The corresponding values of vertical strain were then interpolated based on the values of shear strain as shown on Figure 2.5-53. The settlement of each layer was obtained by multiplying the layer thickness and the vertical strain. The total settlement was then obtained by summing up the settlements of all layers. By this approach, the vertical settlements at three Profiles 1, 2, and 3 shown on Figure 2.5-48 were found to be 0.05, 0.03, and 0.01 in., respectively. The results of these computations are summarized in the first half of Table 2.5-19.

To estimate the vertical settlement resulting from dissipation of excess pore pressure following the earthquake, the procedure proposed by Lee and Albaisa (Ref. 2.5-111) was followed. The results of cyclic triaxial shear tests carried out by GEI (Ref. 2.5-99) and an analysis using the SHAKE 3 computer program were used in addition to the experimental data shown on Figures 6 and 7 of Ref. 2.5-111.

The stress ratio causing liquefaction is related to field conditions by the equation (Ref. 2.5-104):

$$\frac{\sigma_{dc}}{2\sigma_a} = \frac{1}{C_r} \left(\frac{\tau}{\sigma'_o} \right)$$

in which

$$\frac{\sigma_{dc}}{2} = \text{stress ratio}$$

and C_r = correction factor

τ = shear stress induced

σ'_o = effective overburden pressure

The stress ratios developed at various depths can be computed when the shear stress induced during an earthquake and the effective overburden pressure are known. The stress ratios

developed at various depths were computed based on the values of induced shear stress given in Table 2.5-16, the computed effective overburden pressure, and a correction factor $C = 0.57$. Entering these stress ratios on Figure 2.5-35, the corresponding number of cycles (N_1) to reach a total axial strain of 5 percent are obtained. A nondimensional cycle ratio (N/N_1) is computed for each depth with N equal to 5.

Figure 2.5-54 was prepared to show the relationship between the peak excess pore pressure and cycle ratio. The correlation was based on the data obtained from the cyclic triaxial shear tests on undisturbed samples (Ref. 2.5-99). This figure is similar to Figure 9 of Ref. 2.5-111. The peak excess pore pressure ratio ($\Delta\mu/\sigma'_{3c}$) that will occur during an earthquake can be estimated from Figure 2.5-54 using the cycle ratio (N/N_1) obtained previously.

The volumetric strains were estimated from Figures 6 and 7 of Ref. 2.5-110 using the peak excess pore pressure data in Figure 2.5-54. Figure 6 of Ref. 2.5-110 was used first to obtain the volumetric strains for sand at 50 percent relative density. These strains were then corrected to correspond to strains in sand at 60 percent relative density by multiplying by a factor of 0.8 obtained from the curve shown on Figure 7 of Ref. 2.5-110.

Lee and Albaisa assumed in their paper (Ref. 2.5-110) that vertical strain is equal to the measured volumetric strain in triaxial tests. However, when lateral movement is restricted as is the case of the soil deposit at the Susquehanna site, the vertical strain is one-half of such volumetric strain. Therefore, the volumetric strains obtained by the procedure of Lee and Albaisa were divided by two to obtain the appropriate vertical strains for the site conditions. The vertical settlement of each layer was then determined by multiplying the thickness of each layer by the vertical strain in the layer. The total settlement was obtained by summing up the settlements of each layer. The results of these computations are summarized in the second part of Table 2.5-19.

The values of total vertical settlement are also summarized below:

	Resulting from Compaction of Dry Soils (Inches)	Resulting from Reconsolidation of Saturated Soils (Inches)
PROFILE 1 (East End of Pond)	0.05	0.1-1.2
PROFILE 2 (Central Section, Pumphouse, etc.)	0.03	0.1-1.0
PROFILE 3 (West End of Pond)	0.01	0.01-0.2

Based on the results given above, it is apparent that if the sands at the site behave like dry sand during an earthquake, then the settlement will be less than 0.05 in. However, if the sand deposits are saturated and excess pore pressures develop, they will reconsolidate following the earthquake and settlements up to 1.2 in. at the east end of the pond and up to 1.0 in. at the ESSW pumphouse may be expected.

The settlements given above were based on soil profiles consisting of sand deposits (Figure 2.5-48); the imposed dead and live loads on the mat footing of the pumphouse were not considered. The imposed weight will increase the confining pressure of the soil, resulting in a higher reconsolidation volumetric strain. However, according to Lee and Albaisa (Ref. 2.5-111), the influence of confining pressure is not strong and is only significant for developed excess pore pressure ratios greater than about 0.6. As shown on Table 2.5-19, the only soil that may develop a pore pressure ratio greater than 0.6 is at a depth below 43 ft near the bedrock of Profile 2. The soil at that depth, however, has a higher relative density than the 60 percent used for estimating the settlement. Since the volumetric strain decreases rapidly as the relative density increases (Ref. 2.5-111), the net combined effects of a larger pore pressure ratio developed and a higher relative density would result in a smaller volumetric strain. Therefore, the results given above are still valid for the additional imposed weight at the surface.

2.5.5.3 Logs of Borings

Logs of 25 test borings and two test pits are presented in Appendix 2.5C.

Standard Penetration Tests were made in 16 of these holes at 3 ft intervals. Undisturbed samples were taken in five of the split spoon holes where soil conditions permitted. Ten holes were completed for the geophysical survey, 10 for permeability and five as groundwater observation wells. The locations of borings and test pits are shown on Figure 2.5-44. Holes 1118, 1119, and 1121 were planned but not drilled.

Based on the results of the Standard Penetration Test borings, six borings (1106A, 1107A, 1110A, 1112A, 1113A, and 1115A) were drilled immediately adjacent to six of the Standard Penetration Test borings for undisturbed sampling of strata in which, based on classification of the split spoon samples, it was believed undisturbed samples could be obtained. Two test pits were dug with a Case backhoe to a depth of 12 ft to obtain bulk samples.

Due to the large amounts of oversize material encountered, drilling operations were slow and difficult. Frequent mud losses hampered drilling operations in spite of using additives in the drilling fluid. The additives included walnut shells, sawdust, cotton waste and Quick-gel. In some holes, it was necessary to case the hole in order to continue drilling.

Soil sampling consisted of both split spoon (Standard Penetration Test) and undisturbed sampling. The split spoon sampling was carried out in accordance with ASTM D1586-67. The undisturbed sampling was conducted in accordance with ASTM D1587-67. The undisturbed sampling was carried out using both Shelby tube and pitcher barrel sampler methods. In both cases, the sample tubes were 3 in. outside diameter, 3 ft long and the tubes were of 16 gage steel.

Undisturbed samples were difficult to obtain due to the large amount of gravel, cobbles, and boulders in the glacial drift. The majority of undisturbed samples were obtained from Borings 1106, 1106A, 1107A, 1113A, and 1122. Where possible, every attempt was made to obtain samples below the proposed bottom elevation of the spray pond (Elevation 668 ft).

All undisturbed samples were handled in the same manner. The top end of the tube was cleaned out; a piece of plastic followed by damp paper towels was inserted and a plug was then formed with microcrystalline wax. The bottom end of the tube was trimmed and an expandable

packer was installed. The packers were perforated with a 1/16 in. diameter hole for drainage of free water from the sample. Both ends of the tube were capped and dipped in wax. The samples were stored vertically with the expandable packer on the bottom in the subcontractor's equipment trailer in special boxes supplied for this purpose. The temperatures were well above freezing during the time they were stored so no provisions for heating were necessary.

Soil samples selected for the laboratory testing are indicated on the boring logs. The following symbols were used on the boring logs to indicate the type of laboratory test conducted.

CR - Cyclic Consolidated - Undrained Triaxial Test

S - Consolidated - Drained Triaxial Test

Gs - Specific Gravity Determination

Grain Size - Grain Size Determination

2.5.5.4 Compacted Backfill

Compacted fill is placed at the southeast corner of the spray pond to satisfy freeboard requirements. This fill has been placed with a maximum slope of 3 horizontal to 1 vertical. The material, placement, and testing specifications were as follows:

a) Material

Well graded, sound, dense, durable material. It does not contain any topsoil, roots, brush, logs, trash or waste material, ice, or snow. The maximum size of the material is 12 in. and no more than 35 percent by weight passed the No. 200 sieve.

b) Placement

The material was placed in uniform horizontal layers so that when compacted it was free from lenses, pockets, and layers of material differing substantially in grading from surrounding material. It was not placed on frozen ground. Placement for which moisture conditioning was required was suspended whenever the ambient temperature reached 34°F and falling.

The compaction requirements were specified as follows:

Fill shall be placed in a 15 in. maximum uncompacted layer thickness, moisture conditioned to obtain the required compaction, and compacted to satisfy both of the following requirements:

- a) At least 80 percent relative density as determined by ASTM D2049 for material having not more than 12 percent passing the No. 200 sieve or 90 percent of maximum dry density as determined by ASTM D1157 for all other material.

- b) Irrespective of the compacting effort to satisfy part a) above the fill shall be compacted in one of the following manners as a minimum effort:
 - i) Using a crawler tractor having a weight at least equal to that of a D8 Caterpillar tractor with bulldozer blade. Each track shall overlap the preceding track by not less than 4 in. When the tractor has made one entire coverage of an area in this manner, it will be considered to have made one pass. Each fill lift shall be compacted with four passes.
 - ii) Using a vibratory roller of minimum weight 20,000 lb having a roller width of approximately 78 in. and a diameter of approximately 60 in. The roller shall have a vibrator frequency range of between 1,100 and 1,600 vibrations per minute and have a minimum vibratory dynamic force of 40,000 lb. The roller speed shall not exceed 3 mph and each track shall overlap the preceding one by at least 4 in. When the roller has made one entire coverage of an area in this manner, it shall be considered to have made one pass. Each fill lift shall be compacted with four complete passes.
 - iii) Using a hand controlled vibratory compactor in locations inaccessible by tractor or vibratory roller. Approval to use hand controlled vibratory compactors will be on the basis of the demonstrated ability of the compactor to compact the material to the same density as the contiguous backfill.
- c) Testing

The testing requirements were specified as follows:

The in site density of the fill shall be determined in accordance with ASTM D1556 and performed at a frequency of at least one test per lift and every 10,000 sq ft on plan.

Tests in accordance with ASTM D2049 or ASTM D1557, as appropriate, shall be carried out on the same material extracted for the ASTM D1556 test. The frequency of this testing shall be once in every 10 ASTM D1556 tests.

Gradation tests in accordance with ASTM D422 shall be carried out at least twice in each 8 hours during placing operations.

The railroad embankment to the north of the spray pond was constructed out of rock, obtained from the main plant area excavation.

The material and placement specifications were as follows:

- a) Material

Fill shall consist of rock derived from Class B and C excavation having a maximum size of 20 in. Class B and C excavations are defined as follows:

1) Class B Excavation

Rock that cannot be excavated except by systematic ripping.

Ripping shall not be judged necessary when the material can be cut by a bulldozer in the following manner: A fifty-three and one-half (53 1/2) inch high bulldozer blade with standard rock or corner bits mounted on a caterpillar D-8 or equal tractor having 270 net flywheel horsepower moved through forty (40) feet of travel shall fill even with the top with a minimum angle of repose of forty-five (45) degrees, or a volume of ten (10) cubic feet per one linear foot of width of the blade.

2) Class C Excavation

Rock that cannot be excavated except by systematic drilling and blasting.

Blasting shall not be judged necessary if the rock can be ripped by a tractor rated at not less than 385 net flywheel horsepower, equipped with a single shank beam, parallelogram type (72" for deep arrangement), and weighing not less than 40 tons fully equipped; i.e., with dozer blade, ripper and other accessories. Drawbar pull will not be less than the following ratios:

1st gear - 95,000 lbs at 1 mph
 2nd gear - 48,000 lbs at 2 mph
 3rd gear - 30,000 lbs at 3 mph.

Fill shall be placed in lifts not exceeding 24 in. in uncompacted thickness and in such a manner so as to produce a well graded matrix.

b) Placement

Fill shall be compacted in one of the following manners:

- 1) Using a crawler tractor having a weight at least equal to that of a D8 Caterpillar tractor with bulldozer blade. Each track shall overlap the preceding track by not less than 4 in. When the tractor has made an entire coverage of an area in this manner, it will be considered to have made one pass. Each fill lift shall be compacted with four passes.
- 2) Using a vibratory roller of minimum weight 20,000 lb having a roller width of approximately 78 in. and a diameter of approximately 60 in. The roller shall have a vibrator frequency range of between 1,100 and 1,600 vibrations per minute and have a minimum vibratory dynamic force of 40,000 lb. The roller speed shall not exceed 3 mph and each track shall overlap the preceding one by at least 4 in. When the roller has made one entire coverage of an area in this manner, it shall be considered to have

made one pass. Each fill lift shall be compacted with four complete passes.

- 3) Using a hand controlled vibratory compactor in locations inaccessible by tractor or vibratory roller. Approval to use hand controlled vibratory compactors will be on the basis of the demonstrated ability of the compactor to compact the material to the same density as the contiguous backfill.

2.5.6 REFERENCES

- 2.5-1 Drake, A.A., Jr., 1970, Structural Geology of the Reading Prong: in Fisher, G.W., and others (eds.), Studies of Appalachian Geology: Central and Southern, Interscience, New York, p. 271-291.
- 2.5-2 Dames & Moore, 1974, Geologic Report - Limerick Generating Station, Limerick, Pennsylvania.
- 2.5-3 Itter, H.A., 1938, The Geomorphology of the Wyoming-Lackawanna Region: Pennsylvania Topographic and Geologic Survey, Bulletin G9, p. 21-23.
- 2.5-4 Ash, S.H., 1950, Buried Valley of the Susquehanna River: Anthracite Region of Pennsylvania, U.S. Bur. Mines Bulletin 494, p. 27.
- 2.5-5 Peltier, L.C., 1949, Pleistocene Terraces of the Susquehanna River, Pennsylvania, Penna. Geol. Survey, 4th Ser., Bull. G23, p. 158.
- 2.5-6 Sevon, W.D., and others, 1975, The Late Wisconsinan Drift Border in Northeastern Pennsylvania, in Guidebook, 40th Annual Field Conference of Pennsylvania Geologists., p. 108.
- 2.5-7 Leverett, Frank, 1934, Glacial Deposits Outside the Wisconsin Terminal Moraine in Pennsylvania, Pennsylvania Topographic and Geologic Survey, 4th Ser., Bull. G7, p. 123.
- 2.5-8 Colton, G.W., 1970, The Appalachian Basin - Its Depositional Sequences and Their Geologic Relationships: in Fisher, G.W., et al.(eds.), Studies of Appalachian Geology: Central and Southern, Interscience, New York, p. 5-47.
- 2.5-9 Sevon, W.D., 1970, Mississippian Unconformity in Northeastern Pennsylvania (abs.): Geol. Soc. America Abs. with Programs, V. 2, No. 1, p. 35-36.
- 2.5-10 Wood, G.H. Jr., et al., 1962, Pennsylvanian Rocks of the Southern Part of the Anthracite Region of Eastern Pennsylvania, U.S. Geol. Survey Prof. Paper 450-C, p. C39-C42.
- 2.5-11 Potter, P.E., and Pettijohn, F.J., 1963, Paleo Currents and Basin Analyses, Academic Press Inc., New York, p. 362.

- 2.5-12 Wells, R.B. and Faill, R.T., 1973, Stratigraphy: in Faill, R.T. (ed.), Guidebook for the 38th Annual Field Conference of Pennsylvania Geologists, p. 4-8.
- 2.5-13 Glaeser, J.D., 1974, Upper Devonian Stratigraphy and Sedimentary Environments in Northeastern Pennsylvania, Pennsylvania Geol. Surv., Gen. Geol. Report 63, p. 89.
- 2.5-14 Nickelsen, R.P., 1973, Deformational Structures in the Bloomsburg Formation, Cowan, Pa.: in Faill, R.T. (ed.) Guidebook for the 38th Annual Field Conference of Pennsylvania Geologists, p. 119-129.
- 2.5-15 Chute, N.E. and Brower, J.C., 1964, Stratigraphy of the Hamilton Group in the Syracuse Area: in Prucha, J.J. (ed.), New York State Geological Association Guidebook, 36th Annual Meeting, p. 102-108.
- 2.5-16 Hoskins, D.M., 1973, Dalmatia Quarries: in Faill, R.T. (ed.), Guidebook for the 38th Annual Field Conference of Pennsylvania Geologists, p. 156-161.
- 2.5-17 Faill, R.T., and others, 1974, Middle Devonian Stratigraphy in Central Pennsylvania, A Revision (abs.): Geol. Soc. America Abs. with Programs, V. 6, No. 1, p. 23-24.
- 2.5-18 Kaiser, W.R., 1972, Delta Cycles in the Middle Devonian of Central Pennsylvania, Unpub. doctoral dissert., The Johns Hopkins Univ., p. 183.
- 2.5-19 Dennison, J.M., and Hasson, K.O., 1974, Lithostratigraphic Nomenclature Recommendations for Devonian Hamilton Group in Southern Pennsylvania, Maryland and the Virginias (abs.): Geol. Soc. America Abs. with Programs, V. 6, No. 1, p. 18.
- 2.5-20 Wells, R.B., 1973, Field Trip Stop No. VII: in Faill, R.T. (ed.), Guidebook for the 38th Annual Field Conference of Pennsylvania Geologists, p. 112-115.
- 2.5-21 Wood, G.H., Jr., and Bergin, M.J., 1970, Structural Controls in the Anthracite Region, Pennsylvania, in: Fisher, G.W. and others (eds.), Studies of Appalachian Geology: Central and Southern: Interscience Publishers, New York, p. 147-160.
- 2.5-22 Faill, R.T. and Wells, R.B., 1973, Girtys Notch Section: in Faill, R.T. (ed.), Guidebook for the 38th Annual Field Conference of Pennsylvania Geologists, p. 105-110.
- 2.5-23 Bergin, M.J., 1976, Bedrock Geologic Map of the Anthracite-Bearing Rocks in the Wilkes-Barre West Quadrangle, Luzerne County, Pennsylvania, U.S. Geological Survey, Misc. Invest. Map I-838.
- 2.5-24 Gray, C., and others, 1960, Geologic Map of Pennsylvania.
- 2.5-25 Dames & Moore, 1975b, Report - Tectonic Provinces in the Northeastern United States and the Relationships of Historic Earthquakes to the Indian Point Site.

- 2.5-26 Revetta, F.A., 1970, A Regional Gravity Survey of New York and Eastern Pennsylvania, Unpub. doctoral dissert., Univ. of Rochester, p. 229.
- 2.5-27 Diment, W.H., and others, 1975, Speculations about the Precambrian Basement of New York and Pennsylvania from Gravity and Magnetic Anomalies (abs.): Geol. Soc. America Abs. with Programs, V. 6, No. 7, p. 711.
- 2.5-28 King, P.B., 1950, Tectonic Framework of Southeastern United States, Amer. Assoc. Petrol. Geologist Bull., V. 34, No. 4, p. 635-671.
- 2.5-29 Weaver, K.N., 1970, Introduction: in Fisher, G.W., and others, (eds.) Studies of Appalachian Geology, Central and Southern, Interscience, New York, p. 125-126.
- 2.5-30 Nickelsen, R.P., 1963, Fold Patterns and Continuous Deformation Mechanisms of the Central Pennsylvania Folded Appalachians: in Tectonics and Cambrian-Ordovician Stratigraphy in the Central Appalachians of Pennsylvania, Pittsburgh Geol. Soc. Appalachian Geol. Soc. Guidebook, p. 13-29.
- 2.5-31 Faill, R.T. and Nickelson, R.P., 1973, Structural Geology: in Faill, R.T. (ed.), Guidebook for the 38th Annual Field Conference of Pennsylvania Geologists, p. 9-38.
- 2.5-32 Faill, R.T., 1973, Kink-Band Folding, Valley and Ridge Province, Pennsylvania, Geol. Soc. America Bull., V. 84, p. 1289-1314.
- 2.5-33 Root, S.I., 1973a, Structure, Basin Development and Tectogenesis in the Pennsylvania Portion of the Folded Appalachians: in DeJong, K.A. and Scholten, R. (eds.), Gravity and Tectonics, J. Wiley and Sons, New York, p. 343-360.
- 2.5-34 Rodgers, John, 1970, The Tectonics of the Appalachians: Wiley-Interscience, New York, p. 271.
- 2.5-35 Root, S.I., 1973b, Sequence of Faulting, Southern Great Valley of Pennsylvania, Am. J. Sci., V. 273, p. 97-112.
- 2.5-36 Glass, G.B., 1971, Wrench Faulting in the Appalachian Plateaus of Pennsylvania, Penn. Geology, V. 2, No. 3, p. 7-11.
- 2.5-37 Root, S.I., 1970, Structure of the Northern Terminus of the Blue Ridge in Pennsylvania, Geol. Soc. America Bull., V. 81, p. 815-830.
- 2.5-38 Gwinn, V.E., 1970, Kinematic Patterns and Estimates of Lateral Shortening, Valley and Ridge and Great Valley Provinces, Central Appalachians, South-Central Pennsylvania: in Fisher, G.W., and others (eds.), Studies of Appalachian Geology, Central and Southern, Interscience Publishers, New York, p. 127-146.
- 2.5-39 Nickelsen, R.P. and Hough, V.D., 1967, Jointing in the Appalachian Plateau of Pennsylvania, Geol. Soc. America Bull., V. 78, p. 609-630.

- 2.5-40 Rankin, D.W., 1976, Appalachian Salients and Recesses: Late Precambrian Continental Breakup and the Opening of the Iapetus Ocean, *J. Geophys. Res.* V. 81, p. 5605-5619.
- 2.5-41 Alterman, I.B., 1973, Tectonic Events in and Around the Eastern End of the Hamburg Klippe, East-Central Pennsylvania (abs.): *Geol. Soc. America Abs. with Programs*, V. 5, No. 2, p. 133-134.
- 2.5-42 Drake, C.L., and Woodward, H.P., 1963, Appalachian Curvature, Wrench Faulting and Offshore Structures, *Trans. N.Y. Acad. Sci.*, V. 26, p. 48-63.
- 2.5-42 Fleming, R.S., Jr., and Summer, J.R., 1975, Interpretation of Geophysical Anomalies over the Arcuate Appalachians (abs.): *Geol. Soc. America Abs. with Programs*, V. 7, No. 1, p. 58.
- 2.5-44 Rogers, John, 1975, Appalachian Salients and Recesses, *GSA Abstracts*, 10th Annual Meeting, Syracuse, March, 1975, Vol. 7, No. 1, p. 111-112.
- 2.5-45 Summer, J.R., 1976, Residual Gravity Anomaly Map of the Newark-Gettysburg Triassic Basin (abs.): *Geol. Soc. Amer., Abstr. with Prog.*, V. 8, N. 2, p. 280.
- 2.5-46 Faill, R.T., 1973b, Tectonic Development of the Triassic Newark-Gettysburg Basin in Pennsylvania, *Geol. Soc. America Bull.*, V. 84, p. 725-740.
- 2.5-47 Dames & Moore, 1977, Geotechnical Investigation of the Ramapo Fault System in the Region of the Indian Point Generating Station, Consolidated Edison of New York, Inc., 2 Vols.
- 2.5-48 Kummel, H.B., 1897, *N.J. Geol. Survey, Ann. Rept. State Geologist for 1896*.
- 2.5-49 Zetz, I. and Gray, C., 1960, Geophysical and Geological Interpretation of a Triassic Structure in Eastern Pennsylvania, *U.S. Geol. Surv., Prof. Paper 400-B*, p. 174-178.
- 2.5-50 Sanders, J.E., 1962, Strike-Slip Displacement on Faults in Triassic Rocks in New Jersey, *Science*, V. 136, p. 40-112.
- 2.5-51 Oliver, J.E., and others, 1970, Post-Glacial Faulting and Seismicity in New York and Quebec, *Can. Jour. Earth Science*, V. 7, p. 579-590.
- 2.5-52 Owens, J.P., 1970, Post-Triassic Tectonic Movements in the Central and Southern Appalachians as Recorded by Sediments of the Atlantic Coastal Plain: in Fisher, G.W., and others (eds.), *Studies of Appalachian Geology, Central and Southern*, Interscience Publishers, New York, p. 417-427.
- 2.5-53 Isachsen, Y.W., 1975, Possible Evidence for Contemporary Doming of the Adirondack Mountains, New York and Suggested Implications for Regional Tectonics, and Seismicity, *Tectonophysics*, V. 29, p. 169-181.

- 2.5-54 Brown, L. D., and Oliver, J. C., 1976, Vertical Crustal Movements from Leveling Data and their Relation to Geologic Structure in the Eastern United States, Review Geophys. and Space Phys., V. 14, p. 13-35.
- 2.5-55 Dames & Moore, 1976, The Dimensions of the Natural Hazard Phenomena in the Appalachian Region, p. 20-25, 55, 57, 59.
- 2.5-56 McGlade, W.G., Geyer, A.R., and Wilshusen, J.P., 1972, Engineering Characteristics of the Rocks of Pennsylvania, Pennsylvania Topographic and Geologic Survey, 4th Ser., Bull. EGI.
- 2.5-57 Miller, B.L., 1934, Limestones of Pennsylvania, Pennsylvania Topographic and Geologic Survey, Bulletin M20, p. 112-125, 320-328, 526-527.
- 2.5-58 Radbruch-Hall, D.H., et al., 1976, Preliminary Landslide Overview Map of the Conterminous United States, U.S. Geological Survey, Miscellaneous Field Studies Map MF-771.
- 2.5-59 Lobeck, A. K., 1939, Geomorphology, McGraw-Hill Book Co., p. 731.
- 2.5-60 Dreimanis, A., and Goldthwait, R.P., 1973, Wisconsin Glaciation in the Huron, Erie and Ontario Lobes: in Black, R.F., Goldthwait, R.P., and Willman, H.B. (eds.), The Wisconsinan Stage, Geol. Soc. Amer., Mem. 136, p. 71-106.
- 2.5-61 Denny, C.S., and Lyford, W.H., 1963, Surficial Geology and Soils of the Elmira-Williamsport Region, New York and Pennsylvania, U.S. Geol. Survey, Professional Paper 379.
- 2.5-62 Sevon, W.D., 1974, Relative Age and Sequence of Glacial Deposits in Carlson and Monroe Counties, Pennsylvania (abs.): Geol. Soc. Amer., Abs. with Prog. (Northeastern Sect.), V. 6 (Mistitled V. 5), No. 1, p. 71.
- 2.5-63 Sevon, W.D., 1973, "Early" Wisconsinan Drift in Lycoming County, Pennsylvania (abs.): Geol. Soc. Amer., Abs. with Prog. (Northeastern Section), V. 5, No. 2, p. 218.
- 2.5-64 Arndt, H.H., and Wood, G. H., Jr., 1960, Late Paleozoic Orogeny in Eastern Pennsylvania Consists of Five Progressive Stages, U.S. Geol. Survey, Professional Paper 400-B, p. B182-B184.
- 2.5-65 Woodward, H.P., 1957, Chronology of Appalachian Folding: Amer. Assoc. Petrol. Geologists Bull., V. 41, No. 10, p. 2312-2327.
- 2.5-66 Gray, Carlyle, 1959, Nappe Structures in Pennsylvania (abs.): Geol. Soc. Amer. Bull., v. 70, p. 1611.
- 2.5-67 Cohee, G.F. (Chairman), 1962, Tectonic Map of the United States Exclusive of Alaska and Hawaii, U.S. Geol. Survey and Amer. Assoc. Petrol. Geologists, Washington, D.C. (Scale 12,500,000).

- 2.5-68 Flint, R.F., 1971, *Glacial and Quaternary Geology*, John Wiley and Sons, New York, 892.
- 2.5-69 Bird, J.M., and Dewey, J.F., 1970, Lithosphere Plate-Continental Margin Tectonics and the Evolution of the Appalachian Orogen, *Geol. Soc. Amer. Bull.*, V. 81, 1031-1060.
- 2.5-70 Darton, N.H., 1940, Some Structural Features of the Northern Anthracite Coal Basin, Pennsylvania, U.S. Geol. Survey, Prof. Paper 193-D.
- 2.5-71 Heck, N.H. and Bodle, R.R., 1929, United States Earthquakes: 1929, U.S.C.&G.S., U.S. Dept. of Commerce.
- 2.5-72 Coffman, J.L. and Von Hake, C.A., 1973, Earthquake History of the United States, N.O.A.A., Publication 41-1, Revised thru 1970.
- 2.5-73 Dames & Moore, 1976, Indian Point Seismic Proceedings before the Atomic Safety & Licensing Appeal Board on Behalf of Consolidated Edison of New York, 1976.
- 2.5-74 Rodgers, J., 1968, The Eastern Edge of the North American Continent during the Cambrian and Early Ordovician, in: Zen, E-an, White, W.S., Hadley, J.B., and Thompson, J.B. (eds.), *Studies of Appalachian Geology: Northern and Maritime*, Wiley, 141-149.
- 2.5-75 Bryant, B. and Reed, J.C., Jr., 1970, Structural and Metamorphic History of the Southern Blue Ridge, in: Studies of Appalachian Geology: Central and Southern, ed. by Fischer, G.W., Peitijohn, F.J., Reed, J.C., and Weaver, K.N., Interscience, N.Y., 213-225.
- 2.5-76 Williams, H. and Stevens, R.K., 1974, The Ancient Continental Margin of Eastern North America, 781-796, in: Burk, C.A. and Drake, C.L. (eds.), *The Geology of Continental Margins*, Springer-Verlag, 781-796.
- 2.5-77 Rakin, D.W., 1975, The Continental Margin of Eastern North America in the Southern Appalachians, *American Journal of Science*, V. 275-A, 298-330.
- 2.5-78 Mayhew, M.A., 1974, Geophysics of Atlantic North America, 409-427, in: Burk and Drake (eds.).
- 2.5-79 Wise, D.U., 1970, Multiple Deformation, Geosynclinal Transitions and the Martic Problem in Pennsylvania, in: Fisher, et al. (eds.), 1970, 317-334.
- 2.5-80 Bollinger, G.A., 1973, Seismicity of the Southeastern United States, *Bull. Seism. Soc. Amer.*, V. 63, October, 1973.
- 2.5-81 Hadley, J.B. and Devine, J.F., 1974, Seismotectonic Map of the Eastern United States: Misc. Field Studies, Map MF-620, U.S. Geological Survey, in: Harrison, C.G.A. and M.H. Ball, 1973, The Role of in Sea Floor Spreading, *Jour. Geophys. Res.*, 7785.

- 2.5-82 Sbar, M.L. and Sykes, L.R., 1973, Contemporary Compressive Stress and Seismicity in Eastern North America, An Example of Intra Plate Tectonics, Geological Society of America Bulletin, V. 84, 1861-1882.
- 2.5-83 Ballard, R. and Uchupi, E., 1975, Triassic Rift Structure in Gulf of Maine; Amer. Assoc. Pet. Geol. Bull., V. 59, No. 7., p. 1041-1072.
- 2.5-84 Dillon, W.P., 1974, Faults Related to Seismicity off the Coast of South Carolina, U.S.G.S. Open File Report No. 74-145.
- 2.5-85 Colquhoun, D.J. and Comer, C.D., 1973, The Stono Arch, A Newly Discovered Breached Anticline near Charleston, South Carolina, Geologic Notes, South Carolina State Dev. Board, V. 17, No. 4.
- 2.5-86 Zietz, Isadore, Popenoe, Peter, and Higgins, Brenda B., 1976, Regional Structure of the Southeastern United States as Interpreted from New Aeromagnetic Maps of Part of the Coastal Plain of North Carolina, South Carolina, Georgia and Alabama. Abs. S.E. Section Mtg. of Geol. Soc. Amer., March 25-27, 1976, Arlington, Va., p. 307.
- 2.5-87 Wise, D.U. and Werner, M.L., 1969, Tectonic Transport Domains and the Pennsylvania Elbow of the Appalachians, (abs.): Progr. Amer. Geophys. Union Mtgs.
- 2.5-88 DeBoer, J., 1967, Paleomagnetic-Tectonic Study of Mesozoic Dike Swarms in the Appalachians, Journal Geophys. Res. V. 72, No. 8, p. 2237-2250.
- 2.5-89 Woodward, H.P., 1968, A Possible Major Fault Zone Crossing Central New Jersey: Bull. New Jersey Acad. Sci., V. 13, n. 1., p. 40-46.
- 2.5-90 Drake, C.L. and Woodward, H.P., 1963, Appalachian Curvature, Wrench Faulting, and Offshore Structures: Trans. New York Acad. Sci., Ser. II, V. 26, p. 48-63.
- 2.5-91 NRC, 1975, Safety Evaluation Report by the Division of Reactor Licensing, U.S. Nuclear Regulatory Commission, in the matter of Delmarva Power & Light Co., Summit Power Station, Units 1 and 2, Docket Nos. 50-450 and 50-451.
- 2.5-92 Earthquake Data Listing, 1974, New York State Museum and Science Service, Geological Survey (Preliminary), Gupta, I.N. and O.W. Nuttli, 1976, Spatial Attenuation of Intensities for Central U.S. Earthquakes, B.S.S.A., V. 66, No. 3, June, 1976, p. 748-752.
- 2.5-93 O'Brien, L., Murphy, J., and Lahoud, J., 1977, The Correlation of Peak Ground Acceleration Amplitude with Seismic Intensity and other Physical Parameters, Computer Science Corp. for U.S. Nucl. Reg. Comm. Report NUREG-043, March, 1977.

- 2.5-94 Coulter, H.W., Waldron H.H., and Devine J.F., 1973, Seismic and Geologic Siting Considerations for Nuclear Facilities, Proceedings of the World Conference on Earthquake Engineering, 5th, Rome, Italy, 1973.
- 2.5-95 Donovan, N.C., 1974, Earthquake Hazards for Buildings, Engineering Bulletin No. 46, Dames & Moore, December, 1974.
- 2.5-96 Seed, H.B., Idriss, I.M., Makdisi, F., and Banerjee, N., 1975, Representation of Irregular Stress Time Histories by Equivalent Uniform Stress Series in Liquefaction Analyses, Report No. EERC 75-29, Univ. of Calif., Berkeley, Calif., October, 1975.
- 2.5-97 Dames & Moore, Foundation Investigation Report, Proposed Susquehanna Steam Electric Station, Units 1 and 2, May 12, 1972.
- 2.5-98 Dames & Moore, Supplemental Foundation Investigation Report, Susquehanna Steam Electric Station, Units 1 and 2, September 24, 1973.
- 2.5-99 Weston Geophysical Engineers, Inc., Seismic Velocity and Elastic Moduli Measurements, Spray Pond, Susquehanna Steam Electric Station, October 18, 1974.
- 2.5-100 Gibbs, H.J., and Holtz, W.G., "Research on Determining the Density of Sand by Spoon Penetration Test," Proc. 4th Int. Conf. on Soil Mechanics and Foundation Engineering, London, Vol. 1, 1957, p. 35-59.
- 2.5-101 Lohman, S.W., 1972, "Groundwater Hydraulics," U.S.G.S. Professional Paper 708.
- 2.5-102 Geotechnical Engineers, Inc., Report on Soil Testing, Susquehanna Steam Generating Station, October 11, 1974.
- 2.5-103 Skempton, A.W., 1954, "The Pore Pressure Coefficients A and B," Geotechnique, Vol. 4, p. 143.
- 2.5-104 Davis, S.N., and DeWiest, R.J.M., 1966, Hydrogeology, John Wiley & Sons, Inc.
- 2.5-105 Kisch, M., "The Theory of Seepage from Clay Blanketed Reservoirs," Geotechnique, Vol. 9, No. 1, March 1959, p. 9-12.
- 2.5-106 Schnabel, P.B., Lysmer, J., and Seed, H.B., "SHAKE, A Computer Program for Earthquake Response Analysis of Horizontally Layered Sites," Report No. EERC 72-12, University of California, Berkeley, December 1972.
- 2.5-107 Seed, H.B., and Idriss, I.M., "Simplified Procedure for Evaluating Soil Liquefaction Potential," Journal of the Soil Mechanics and Foundations Div., ASCE, Vol. 97, No. SM9, September 1971, p. 1249-1273.

- 2.5-108 Seed, H.B. and Idriss, I.M., "Soil Moduli and Damping Factors for Dynamic Response Analysis," Report No. EERC 70-10, University of California, Berkeley, December 1970.
- 2.5-109 Seed, H.B., and Goodman, R.E., "Earthquake Stability of Slopes of Cohesionless Soils," Journal of Soil Mechanics and Foundation Div., ASCE, Vol. 90, No. SM6, November 1964, p. 43-72.
- 2.5-110 Seed, H.B., and Silver, M.L., "Settlement of Dry Sands During Earthquakes," Journal of Soil Mechanics and Foundations Div., ASCE, Vol. 98, No. SM4, April 1972, p. 381-397.
- 2.5-111 Lee K.L., and Albaisa A., "Earthquake Induced Settlements in Saturated Sands," Journal of Geotechnical Engineering Div., ASCE, Vol. 100, No. GT4, April 1974, p. 287-406.
- 2.5-112 Kishida, H., "Characteristics of Liquefied Sands during Mino-Owari Tohnankai and Fukui Earthquakes," Soils and Foundation, Japan, Vol. 9, No. 1, March 1969.
- 2.5-113 Trifunac, M.D., and Brady, A.G., 1975, On the Correlation of Seismic Intensity Scales with Peaks of Recorded Strong Ground Motion, Bull. Seis. Soc. Amer., Vol. 65, No. 1, February 1975.
- 2.5-114 Pomeray, P.W., and Fahunding, R.H., 1976, Seismic Activity and Geologic Structure in New York and Adjacent Areas, Map and Chart Series, No. 27, New York State Museum and Science Service, Albany, New York.
- 2.5-115 Peck, R.B., Hanson, W.E., and Thronburn, T.H., 1974, Foundation Engineering, 2nd Ed., John Wiley & Sons, Inc.
- 2.5-116 Donaldson, E. C., 1972, Injection Wells and Operations Today; Cook, T. D., (Ed.) Underground Waste Management and Environmental Implications, A.A.P.G. Mem. 18, pp. 24-46.
- 2.5-117 Healy, J. H., Rubey, W. w., Griggs, D. T., and Raleigh, C. B., 1968, The Denver Earthquakes, Science, V. 161, N. 3848, pp. 1301-1310.
- 2.5-118 Galley, J. E., 1968, Economic and Industrial Potential of Geologic Basins and Reservoir Strata; Galley, J. E., (Ed.), Subsurface Disposal in Geologic Basins - A Study of Reservoir Strata, A.A.P.G. Mem. 10, pp. 1-10.
- 2.5-119 Galley, J. E., 1972, Geologic Framework for Successful Underground Waste Management; Cook, T.D., (Ed.) Underground Management and Environmental Implications, A.A.P.G. Mem. 18, pp. 119-125.
- 2.5-120 Warner, D. L., 1968, Subsurface Disposal of Liquid Industrial Wastes by Deep Well Injection; Galley, J. E., (Ed.), Subsurface Disposal in Geologic Basins - A Study of Reservoir Strata, A.A.P.G. Mem. 10, pp. 11-20.

- 2.5-121 Gibbs & Hill, Inc., Report on Subsurface Investigation for New Emergency Diesel Generator Facility, Susquehanna Steam Electric Station Units 1 and 2, January, 1984.
- 2.5-122 Dames & Moore, Geologic Map of the Emergency Diesel Generator Foundation, Susquehanna Steam Electric Plant, August, 1984.

SSBS-FSAR

TABLE 2.5-1

MODIFIED MERCALLI INTENSITY (DAMAGE) SCALE -
(Abridged)

- I. Not felt except by a very few under especially favorable circumstances. (I Rossi-Forel Scale.)
- II. Felt only by a few persons at rest, especially on upper floors of buildings. Delicately suspended objects may swing. (I to II Rossi-Forel Scale.)
- III. Felt quite noticeably indoors, especially on upper floors of buildings, but many people do not recognize it as an earthquake. Standing motorcars may rock slightly. Vibration like passing of truck. Duration estimated. (III Rossi-Forel Scale.)
- IV. During the day felt indoors by many, outdoors by few. At night some awakened. Dishes, windows, doors disturbed; walls make creaking sound. Sensation like heavy truck striking building. Standing motorcars rocked noticeably. (IV to V Rossi-Forel Scale.)
- V. Felt by nearly everyone, many awakened. Some dishes, windows, etc., broken; a few instances of cracked plaster; unstable objects overturned. Disturbances of trees, poles, and other tall objects sometimes noticed. Pendulum clocks may stop. (V to VI Rossi-Forel Scale.)
- VI. Felt by all, many frightened and run outdoors. Some heavy furniture moved; a few instances of fallen plaster or damaged chimneys. Damage slight. (VI to VII Rossi-Forel Scale.)
- VII. Everybody runs outdoors. Damage negligible in buildings of good design and construction; slight to moderate in well-built ordinary structures; considerable in poorly built or badly designed structures; some chimneys broken. Noticed by persons driving motorcars. (VIII Rossi-Forel Scale.)
- VIII. Damage slight in specially designed structures; considerable in ordinary substantial buildings with partial collapse; great in poorly built structures. Panel walls thrown out of frame structures. Fall of chimneys, factory stacks, columns, monuments, walls. Heavy furniture overturned. Sand and mud ejected in small amounts. Changes in well water. Person driving motorcars disturbed. (VIII+ to IX Rossi-Forel Scale.)

SSES-PSAR

TABLE 2.5-1 (Continued)

- IX. Damage considerable in specially designed structures; well-designed frame structures thrown out of plumb; great in substantial buildings, with partial collapse. Buildings shifted off foundations. Ground cracked conspicuously. Underground pipes broken. (IX+ Rossi-Forcl Scale.)
- X. Some well-built wooden structures destroyed; most masonry and frame structures destroyed with foundations; ground badly cracked. Rails bent. Landslides considerable from river banks and steep slopes. Shifted sand and mud. Water splashed (slopped) over banks. (X Rossi-Forcl Scale.)
- XI. Few, if any, (masonry) structures remain standing. Bridges destroyed. Broad fissures in ground. Underground pipelines completely out of service. Earth slumps and land slips in soft ground. Rails bent greatly.
- XII. Damage total. Waves seen on ground surface. Lines of sight and level distorted. Objects thrown upward into the air.

SSES - PSAR
TABLE 2.5 -2
EARTHQUAKE LIST

DATE	H	M	S	LAT (NORTH)	LONG (WEST)	INTEN* (MM)	MAGNITUDE*	REF*	DISTANCE (MILES)
1568				41.5	72.5	VII		ANY	193
1574				41.5	72.5	VII		ANY	193
1584				41.5	72.5	VII		ANY	193
1592				41.5	72.5	VII		ANY	193
1698				41.4	73.5	IV		ANY	140
1702				41.4	73.5	IV		ANY	140
1711				41.4	73.5	IV		ANY	140
6 AUG 1729				41.4	73.5	IV		ANY	140
19 DEC 1737	4	0	0.0	40.8	74.0	VII		EQH	115
25 APR 1758	2	30	0.0	38.9	76.5			EQH	151
30 NOV 1783	2	0	-0.0	41.0	74.5			PAG	87
30 NOV 1783	3	50	-0.0	41.0	74.5	VI		PAG	87
30 NOV 1783	7	0	-0.0	41.0	74.5			PAG	87
16 MAY 1791	3	0	0.0	41.5	72.5	VII		WGP	193
29 AUG 1792	3	0	0.0	41.5	72.5	IV		ANY	193
24 OCT 1792	6	0	0.0	41.5	72.5	IV		ANY	193
11 JAN 1793	13	0	0.0	41.5	72.5	IV		ANY	193
6 JUL 1793	11	0	0.0	41.5	72.5	IV		ANY	193
6 MAR 1794	19	0	0.0	41.5	72.5			EQH	193
9 MAR 1794	19	0	0.0	41.5	72.5	IV		EPA	193
9 MAY 1794	19	0	0.0	41.5	72.5	IV		ANY	193
12 AUG 1805				41.5	72.4	IV		ANY	198
30 DEC 1805	11	0	0.0	41.5	72.4	IV		ANY	198
28 DEC 1813	21	0	0.0	41.5	72.4	IV		ANY	198
12 APR 1837				41.7	72.7	V		EPB	185
9 AUG 1840	20	30	0.0	41.5	72.9	V		EQH	172
26 OCT 1845				41.0	73.8	V		WGP	123
9 SEP 1848	4	0	0.0	40.8	74.0	V		NYS	115
12 MAR 1853	7	3	0.0	43.7	75.5	VI		EQH	183
7 FEB 1855	4	30	0.0	42.0	74.0	V		WGP	129
13 MAR 1856	3	0	0.0	41.4	72.6	IV		WGP	187
23 OCT 1857	20	15	0.0	43.2	78.6	VI		EQH	192
1 JUL 1853	3	45	0.0	41.3	73.0	V		WGP	165
3 FEB 1862	1	0	0.0	41.5	72.5	IV		ANY	193
9 OCT 1871	14	40	0.0	39.7	75.5	VII		EQH	101
11 JUL 1872	10	25	0.0	40.9	73.8	V		EQH	124
11 DEC 1874	3	25	0.0	40.9	73.8	V		WGP	124
28 JUL 1875	9	10	0.0	41.8	73.2	V		EQH	161
10 SEP 1877	14	59	0.0	40.3	74.9	V		EQH	85
5 FEB 1878	16	20	0.0	40.7	73.7	V		WGP	131

*See Notes and Reference Key at end of Table.

SSSES - FSAR
TABLE 2.5 - 2 (CONT.)
EARTHQUAKE LIST

DATE	H	M (GMT)	S	LAT (NORTH)	LONG (WEST)	INTEN (MM)	MAGNITUDE	REF	DISTANCE (MILES)
4 OCT 1878	7	30	0.0	41.5	74.0	V		EQH	116
25 MAR 1879	24	30	0.0	39.2	75.5	V		EQH	134
9 AUG 1880	20	30	0.0	41.5	72.9	V		ANY	172
11 MAR 1883	23	57	0.0	39.5	76.4	V		EQH	109
12 MAR 1883	6	0	0.0	39.5	76.4	V		EQH	109
31 MAY 1884				40.6	75.5	V		ANY	48
10 AUG 1884	19	7	0.0	40.6	74.0	VII		EQH	118
3 JAN 1885	2	16	0.0	39.2	77.5	V		EQH	147
5 SEP 1886				41.5	72.5	IV		ANY	193
8 MAR 1889	23	40	0.0	40.0	76.0	V		EQH	75
9 MAR 1893	5	30	0.0	40.6	74.0	V		EQH	118
10 APR 1894				41.6	72.5	IV		ANY	194
1 SEP 1895	11	9	0.0	40.7	74.8	VI		EQH	76
5 SEP 1897				41.5	72.5	IV		ANY	193
17 MAY 1899	1	15	0.0	41.5	72.5	V		ANY	193
8 MAY 1906	17	41	0.0	38.7	75.7	V		EQH	166
8 MAY 1906	13	30	0.0	41.5	72.5	IV		ANY	193
10 JAN 1907	9	45	0.0	41.3	77.0	IV		ANY	45
24 JAN 1907	11	30	0.0	42.8	74.0	V		EQH	162
5 FEB 1908	8	20	0.0	41.4	73.2	IV		ANY	156
31 MAY 1908	17	42	0.0	40.6	75.5	VI		EQH	48
2 APR 1909	7	25	0.0	39.4	78.0	VI		EQH	151
23 APR 1910				41.0	73.0	IV		NJS	165
2 FEB 1916	16	26	0.0	42.9	74.0	V		EPB	167
8 JUN 1916	21	15	0.0	41.0	73.8	V		EQH	123
2 NOV 1916	2	32	0.0	43.3	73.7	V		EQH	198
16 FEB 1917	9	0	0.0	41.5	72.5	IV		ANY	193
6 SEP 1919	2	46	0.0	38.8	78.2	VI		EQH	191
19 JAN 1921	10	0	0.0	43.3	73.7	IV		NYS	198
26 JAN 1921	23	40	0.0	40.0	75.0	V		EQH	96
27 JAN 1921				43.3	73.7	IV		NYS	198
29 OCT 1925				41.5	72.5	IV		ANY	193
14 NOV 1925	13	4	0.0	41.5	72.5	V		WGP	193
16 NOV 1925	6	20	0.0	41.8	72.7	IV		ANY	186
26 JAN 1926	23	40	0.0	40.0	75.0	V		ANY	96
12 MAY 1926	3	30	0.0	40.9	73.9	V		EQH	119
30 MAR 1927				41.7	72.8	IV		ANY	180
1 JUN 1927	12	20	0.0	40.3	74.0	VII		EQH	126
12 AUG 1929	11	24	48.0	42.9	78.3	VIII		EPB	168
2 DEC 1929	22	14	0.0	42.8	78.3	IV		EPB	161

SSES - FSAR
TABLE 2.5-2 (CONT.)
EARTHQUAKE LIST

DATE	H	M (GMT)	S	LAT (NORTH)	LONG (WEST)	INTEN (MM)	MAGNITUDE	REF	DISTANCE (MILES)
3 DEC 1929	12	50	0.0	42.8	78.3	IV		NYS	161
1 NOV 1930	6	34	0.0	39.2	76.5			USE	131
22 APR 1931				42.9	78.9	IV	3.6	EPB	188
1 JUL 1931	2	45	0.0	41.6	73.4	IV	3.6	EPB	148
25 JAN 1933	2	0	0.0	40.2	74.7	V	4.3	EPB	98
29 OCT 1933				43.0	74.7	IV		NYS	152
30 JAN 1934	10	30	0.0	41.8	72.6	IV	3.6	EPB	191
19 JUL 1937	3	51	0.0	40.7	73.7	IV		USE	131
15 JUL 1938	22	45	0.0	40.4	78.2	V		USE	119
2 AUG 1938	10	2	0.0	41.1	73.7	IV		USE	128
23 AUG 1938	3	36	34.0	40.2	74.2	V	4.6	EPB	116
23 AUG 1938	5	4	55.0	40.2	74.2	VI	4.8	EPB	116
23 AUG 1938	7	3	29.0	40.2	74.2	V	4.6	EPB	116
23 AUG 1938	11	11	6.0	40.2	74.2	IV	3.7	EPB	120
15 NOV 1939	2	53	48.0	39.6	75.2	V		CGS	114
18 NOV 1939	2	33	0.0	39.5	76.5			USE	110
24 OCT 1942	17	27	3.6	41.0	75.2	IV	3.4	EPB	48
1943				41.1	74.2	V		NJS	102
5 FEB 1944	16	22	.5	40.8	76.2	IV	3.7	EPB	19
14 DEC 1944	3	15	0.0	41.6	72.8	IV	3.6	EPB	178
28 OCT 1946	20	36	6.0	41.5	76.6	IV	3.6	EPB	36
10 NOV 1946	11	41	23.1	42.9	77.4	III	3.1	EPB	139
4 JAN 1947	18	51	4.0	41.0	73.6	V	4.3	EPB	135
20 MAR 1950	22	55	11.5	41.5	75.8	III	3.3	EPB	34
29 MAR 1950	14	43	2.0	41.0	73.6	IV	3.6	EPB	134
26 JAN 1951	3	27	0.0	41.5	72.5	III	3.3	EPB	193
3 SEP 1951	21	26	24.5	41.2	74.2	V	4.4	EPB	100
23 NOV 1951	6	45	36.0	40.6	75.5	IV	3.6	EPB	48
25 AUG 1952	0	7	0.0	43.0	74.5	V	4.3	EPB	157
8 OCT 1952	21	40	0.0	41.7	74.0	V	4.3	EPB	120
27 MAR 1953	8	50	0.0	41.1	73.5	V	4.3	EPB	139
17 AUG 1953	4	22	50.0	41.0	74.0	IV	3.7	EPB	113
7 JAN 1954	7	25	0.0	40.3	76.0	VI	5.0	EPB	54
1 FEB 1954	0	37	50.0	43.0	76.7	IV	3.3	NYS	135
21 FEB 1954*	20	0	0.0	41.2	75.9	VII	5.7	EPB	15
24 FEB 1954*	3	55	0.0	41.2	75.9	VI	5.0	EPB	16
31 MAR 1954	21	25	0.0	40.2	74.0	IV	3.6	EPB	127
11 AUG 1954	3	40	0.0	40.3	76.0	IV	3.6	EPB	55
20 JAN 1955	3	0	0.0	40.3	76.0	IV	3.6	EPB	54
21 JAN 1955	8	40	0.0	43.0	73.8	V	4.3	EPB	179

* See text (mine collapse).

SSES - FSAR
TABLE 2.5-2 (CONT.)
EARTHQUAKE LIST

DATE	H	M	S	LAT (NORTH)	LONG (WEST)	INTEN (MM)	MAGNITUDE	REF	DISTANCE (MILES)
16 AUG 1955	7	35	0.0	42.9	78.3	V	4.3	EPB	165
23 MAR 1957	19	2	0.0	40.6	74.8	VI	4.8	ANY	79
6 MAY 1958	19	0	0.0	42.7	73.8	IV	3.6	EPB	162
22 AUG 1958	14	25	5.0	43.0	79.0	IV	3.6	EPB	196
13 APR 1959	21	20	19.0	41.9	73.3	IV	3.4	EPB	161
22 JAN 1960	20	53	22.0	41.5	75.5	IV	3.4	EPB	45
15 SEP 1961	2	16	56.0	40.6	75.4	V		ANY	52
27 DEC 1961	17	6	0.0	40.1	74.8	V		ANY	98
6 MAR 1962				41.1	74.6			NJS	81
11 AUG 1962				41.1	74.6			NJS	81
7 SEP 1962	14	0	45.9	39.7	78.2			CGS	143
3 MAR 1963	1	24	32.0	41.5	75.8	IV*	3.4	ANY	34
19 MAY 1963	19	14	18.0	43.5	75.2	IV	3.5	EPB	173
20 MAY 1963	0	14	18.0	43.5	75.2	IV*	3.5	NYS	174
24 JUN 1963				41.1	74.6			NJS	81
1 JUL 1963	19	59	12.0	42.4	73.8	III	3.3	EPB	153
10 OCT 1963	14	59	52.5	39.8	78.2	IV	3.6	EPB	139
12 MAY 1964	6	45	14.1	40.2	76.5	VI	4.5	CGS	63
17 NOV 1964	17	8	0.0	41.2	73.7	V	4.3	EPB	128
16 JUL 1965	11	6	55.0	43.2	78.5	IV	3.5	EPB	189
28 AUG 1965	1	57	0.0	42.9	78.2	IV		NYS	163
29 SEP 1965	20	57	39.5	41.4	74.4	IV		NYS	94
1 JAN 1966	13	23	38.0	42.9	78.2	VI	4.7	CGS	163
1 JAN 1966	13	23	38.0	42.9	78.2	VI	4.7	EPB	163
21 MAY 1966	7	30	55.0	41.2	74.0		1.3	NYS	113
13 JUN 1967	19	8	54.4	42.9	78.2	VI	3.9	USE	163
22 NOV 1967	22	10	0.0	41.2	73.8	V		NYS	123
3 NOV 1968	8	33	52.5	41.4	72.5	V		ANY	192
10 DEC 1968	9	12	44.9	39.7	74.6	V	2.6PAL	USE	126
13 AUG 1969	2	42	0.0	42.9	78.2	IV		NYS	163
6 OCT 1969				41.0	74.6	IV		NJS	82
8 DEC 1972	3	0	32.6	40.1	76.2	IV		ERL	64
28 FEB 1973	8	21	32.3	39.7	75.4	VI	3.8SLM	ERL	101
27 APR 1974	14	45	39.1	41.0	76.0	III*	3.0GS	GS	12
7 JUN 1974	19	45	36.8	41.6	73.9	III*	3.3PAL	PAL	120
11 MAR 1976	21	7	20.2	41.0	74.4	IV	2.5PAL	D-M	94
13 APR 1976	15	39	13.0	40.8	74.1	V	3.0PAL	PAL	112

SSES - FSAR
TABLE 2.5-2 (CONT.)

NOTES:

1. The magnitude listed on the printout is chosen in the following order: Local ML, CGS MS, Other MS, black if no magnitude information.
2. When maximum intensity is not given, an estimated intensity is calculated by using the relation: $M = 1 + 2/3 I$. The calculated intensity is indicated by an asterisk. However, a large percentage of our data cards were obtained from - Earth Physics Branch, Dept. of Energy, Mines and Resources, Canada (EPB), which converted the original intensity values, for earthquakes occurring before 1899, into Local Magnitude (ML), by using the above relation. Many magnitudes for earthquakes after 1899 were also converted from intensity values. However, because on the cards received from EPB, no distinction is made between Local Magnitude, ML, determined instrumentally and those estimated from intensity, the calculated intensities in this situation are not indicated by the asterisk.
3. The following abbreviations are used in Table C-1:

ANY Earthquakes adjacent to New York State (N.Y. State Geological Survey)
CGS Coast and Geodetic Survey
D-M Dames & Moore (1969), proposed North Anna Power Station
EEC Earthquakes in Eastern Canada, Smith (1962)
EPB Earth Physics Branch, Dept. of Ener. Mines and Res., Canada
EQH Earthquake History of the United States, Coffman and Von Hake (1973)
ERL Environmental Research Laboratories (NOAA)
G-R Gutenberg and Richter (1953)
GS U.S. Geological Survey
NJS New Jersey State Geological Survey, Dombroski (1973)
NOS National Ocean Survey (NOAA)
NUT NUTTLI (1974)
NYS Earthquakes within New York State (N.Y. State Geological Survey)
PAG Page et al. (1968)
PAL Lamont Doherty Geological Observatory, Palisades
USE U.S. Earthquakes, Yearly Publication (NOAA)
WGP Weston Geophysical

TABLE 2.5-3

UNCONFINED COMPRESSIVE STRENGTHS OF FOUNDATION ROCK (MAHANTANGO FORMATION)

BORING	PLANT STRUCTURE	SAMPLE ELEVATION (FT)	DEPTH (FT)	DEPTH BELOW TOP OF ROCK (FT)	COMPRESSIVE STRENGTH (LBS/SQ. IN.)	YOUNG'S MODULUS (LBS/SQ. IN.)
101	(a)	620	49	23	12,500	-
105	Reactor #1	618	63	61	14,400	-
110	(a)	494	183	73	3,650	-
114	(a)	608	31	19	11,600	-
204	(a)	612	35	29	910(b)	-
210	(a)	652	37	14	12,000	9.4×10^6
303	Turbine #1	657	38	28	16,000	4.45×10^6
307	Reactor #1	632	42	29	14,150	4.12×10^6
311	Reactor #2	629	46	41	14,300	3.1×10^6
320	Clg. Twr. #1	680	28	20	8,240	6.8×10^6
321	Clg. Twr. #2	643	36	14	6,940	5.2×10^6
323	Clg. Twr. #2	648	28	6	8,150	5.4×10^6

Notes:

(a) Boring location not contained within principal plant structure foundation. See Plot Plan Figure for location.

(b) Fractured on recemented joint.

SSES-FSAR

TABLE 2.5-4

LABORATORY MEASUREMENTS OF P-WAVE SEISMIC VELOCITIES ON ROCK CORES
TAKEN FROM REACTOR AND TURBINE BUILDING AREAS

<u>Boring No.</u>	<u>Depth</u> (feet)	<u>Elevation</u> (feet above MSL)	<u>P-Wave Velocity, V_p</u> (feet per second)
303	45	650	14,130
303	65	630	13,773
303	95	600	14,912
314	44	638	11,737
314	61	621	12,061
314	90	592	14,754
315	40	640	15,432
315	61	619	12,785
315	68	612	11,111
315	90	590	11,666

TABLE 2.5-5

REPRESENTATIVE ENGINEERING PROPERTIES OF UNWEATHERED FOUNDATION ROCK FOR PRINCIPAL PLANT STRUCTURES

<u>PROPERTY</u>	<u>RANGE</u>	<u>AVERAGE VALUE</u>
Density	-	170 lb/cu. ft.
Unconfined compressive strength	3,650 - 16,000 lb/sq. in.	11,080 lb/sq. in.
Static modulus of deformation	3.1×10^6 - 9.4×10^6 lb/sq. in.	5.5×10^6 lb/sq. in.
Compressional wave velocity (on core)(1)	11,111 - 15,432 ft/sec.	13,236 ft/sec.
Compressional wave velocity (in situ)(2)	14,000 - 16,000 ft/sec.	14,670 ft/sec.
Shear wave velocity (in situ)(2)	6,200 - 7,500 ft/sec.	6,730 ft/sec.

Notes:

- (1) From laboratory "Shockscope" measurements on core samples (refer to Table 2.5-4).
- (2) From cross-hole and down-hole measurements in reactor area (below elevation 670 ft. MSL).

TABLE 2.5-6

P-WAVE AND S-WAVE VELOCITIES AND COMPUTED DYNAMIC MODULI, ⁽¹⁾ SPRAY POND AREA

ELEVATION (FT ABOVE MSL)	AVERAGE "P" WAVE VELOCITY (FT/SEC)	AVERAGE "S" WAVE VELOCITY (FT/SEC)	POISSON'S RATIO	YOUNG'S MODULUS (PSI)	SHEAR MODULUS (PSI)	BULK MODULUS (PSI)
ESSW PUMPHOUSE ARRAY ⁽²⁾						
683 to 658	2,350	1,320	.270	1.24×10^5	4.9×10^4	9.0×10^4
658 to 606	4,340	1,710	.408	2.31×10^5	8.2×10^4	4.19×10^5
606 to 603	13,300	6,400	.349	4.06×10^6	1.50×10^5	4.49×10^6
SPRAY POND ARRAY ⁽³⁾						
678 to 673±	2,600	1,300	.333	1.26×10^5	4.7×10^4	1.26×10^5
673± to 643±	3,200	1,480	.364	1.68×10^5	6.1×10^4	2.05×10^5
643± to 606	4,775	1,800	.417	2.58×10^5	9.1×10^4	5.19×10^5
606 to 588	12,400	5,850	.357	3.41×10^6	1.26×10^6	3.97×10^6

Notes:

- (1) Computations are based on unit weights of 130 lbs/cu. ft. for soil and 170 lbs/cu. ft. for rock.
 (2) ESSW array is a north-south alignment utilizing boreholes 1101 to 1105.
 (3) Spray pond array is an east-west alignment utilizing boreholes 1106 to 1110.

SSES-FSAR

TABLE 2.5-7

CROSS-HOLE SEISMIC VELOCITIES, REACTOR AREA⁽¹⁾

ELEVATION (FT. ABOVE MSL)		COMPRESSIONAL WAVE (FT/SEC)	SHEAR WAVE (FT/SEC)
FROM	TO		
680	670	1,500	700
670	660	7,600	3,600
660	640	14,000	6,500
640	550	16,000	7,500

(1) Utilizing boreholes 105, 303, 307, 314, 315 and 316 for the seismic array.

SSES-FSAR

TABLE 2.5-8

RESULTS OF SETTLEMENT MEASUREMENTS
TAKEN ON ESSW PUMPHOUSE BASEMAT

Date	Elevation (Ft. MSL)					
	Pin #1	Pin #2	Pin #3	Pin #4	Pin #5	Pin #6
8-30-77	659.839	659.833	659.812	659.832	659.848	659.845
9-30-77	659.84	659.83	659.81	659.83	659.85	659.85
10-28-77	659.84	659.83	659.81	659.83	659.85	659.85
12-2-77	659.84	659.83	659.81	659.83	659.85	659.85
12-30-77	659.84	659.83	659.81	659.83	659.85	659.85
2-2-78	659.83	659.83	659.80	659.82	659.84	659.84
3-7-78	659.82	659.82	659.79	659.81	659.83	659.83
4-3-78	659.84	659.83	659.81	659.83	659.85	659.84
4-28-78	659.84	659.83	659.81	659.83	659.85	659.84
5-30-78	659.84	659.83	659.81	659.83	659.85	659.84
7-5-78	Backfilled	659.83	659.81	659.83	659.85	Backfilled
8-3-78	Backfilled	659.83	659.81	659.83	659.85	Backfilled
9-5-78	Backfilled	659.83	659.81	659.83	659.85	Backfilled
10-3-78	Backfilled	659.83	659.80	659.82	659.85	Backfilled
11-1-78	Backfilled	659.83	659.80	659.82	659.85	Backfilled
12-1-78	Backfilled	659.83	659.80	659.82	659.85	Backfilled
1-4-79	Backfilled	Inaccessable Due to Ice & High water				Backfilled
2-6-79	Backfilled	Inaccessable Due to Ice & High water				Backfilled
3-2-79	Backfilled	Inaccessable Due to Ice & High Water				Backfilled

NOTE: Pin Locations are given on Figure 2.5-41

SSES-PSAR

TABLE 2.5-8 (Page 2)

RESULTS OF SETTLEMENT MEASUREMENTS
TAKEN ON ESSW PUMPHOUSE BASEMAT

Date	Elevation (Ft. MSL)				
	Pin #7	Pin #8	Pin #9	Pin #10	Pin #11
6-5-78	685.53	685.54	685.51	685.49	685.49
7-5-78	685.53	685.54	685.51	685.49	685.49
8-3-78	685.53	685.54	685.51	685.49	685.49
9-5-78	685.52	685.53	685.51	685.49	685.49
10-3-78	685.52	685.53	685.51	685.49	685.48
11-1-78	685.52	685.53	685.51	685.49	685.48
12-1-79	685.52	685.53	685.50	685.49	685.48
1-4-79	685.52	685.53	685.50	685.49	685.48
2-6-79	685.51	685.53	685.50	685.48	685.48
3-2-79	685.51	685.53	685.50	685.48	685.48
4-4-79	685.51	685.53	Temp. Inaccess.	685.48	685.48
5-3-79	685.51	685.53	"	685.48	685.47
6-4-79	685.50	685.52	"	685.47	685.46
7-2-79	685.50	685.52	"	685.47	685.47
8-1-79	685.50	685.52	"	685.47	685.47
9-4-79	685.51	685.53	"	685.48	685.48
10-2-79	685.51	685.53	"	685.48	685.47
11-9-79	685.51	685.53	"	685.48	685.48
12-4-79	685.50	685.52	"	685.48	685.47
1-8-80	685.51	685.53	"	685.48	685.47

SSIS-PSAP

TABLE 2.5-8 (Page 3)

RESULTS OF SETTLEMENT MEASUREMENTS
 TAKEN ON ESSW PUMPHOUSE BASEMAT

Date	Elevation (Pt. MSL)				
	Pin #7	Pin #8	Pin #9	Pin #10	Pin #11
* 4-3-80	685.51	685.53	"	685.48	685.48
6-30-80	685.50	685.52	685.50	685.48	685.47
10-2-80	685.51	685.52	685.50	685.48	685.48

* Time interval for survey measurements revised to 3 months.

SSES - FSAR

TABLE 2.5-9

SPRAY POND
WATER LEVEL ELEVATIONS

<u>OBSERVATION WELL NO.</u>	<u>1111</u>	<u>1112</u>	<u>1113</u>	<u>1114</u>	<u>1115</u>
<u>GROUND SURFACE</u> <u>ELEVATION</u>	687.4	708.2	702.1	711.7	708.0
7-29-74	613.0	626.0	632.5	647.0	640.5
7-30-74	613.0	625.5	633.0	647.0	639.5
7-31-74	611.0	625.0	632.0	648.0	640.5
8-2-74	612.5	626.0	633.0	648.0	640.5
8-5-74	611.5	626.0	632.5	648.0	640.5
8-6-74	612.0	626.0	632.0	649.0	641.5
8-7-74	612.0	626.0	631.0	649.0	640.5
8-9-74	611.5	625.8(1)	632.0	648.0	640.2(1)
8-12-74	611.5	626.0	632.2(1)	645.5	640.5
8-14-74	612.0	626.0	633.0	644.0	640.5
8-16-74	612.0	626.0	633.0	645.0	640.0
8-19-74	612.0	626.0	632.2(1)	645.0	638.7(1)
8-21-74	611.5	626.0	632.5	645.0	640.5
8-22-74	612.0	626.0	633.0	645.0	640.5
8-27-74	611.0	625.0	631.5	644.0	638.5
9-3-74	610.5	625.0	632.0	644.5	638.5
9-4-74	611.0	625.5	632.5	644.5	638.5
9-8-74	611.2(1)	626.0	633.0	645.0	639.0
9-10-74	611.5	626.0	633.0	645.0	639.0
9-12-74	611.0	626.0	632.5	645.0	638.5
9-17-74	611.5	625.5	632.5	645.5	638.5
9-18-74	611.0	630.0	635.0	647.0	637.5
9-23-77	611.0	626.0	632.5	645.0	638.5
9-30-74	-	(2)	-	647.0	637.5
10-23-74	602.0(3)	-	628.1(3)	646.0(3)	630.5(3)
10-25-74	602.0(3)	-	628.1(3)	646.0(3)	630.5(3)
10-30-74	602.0(3)	-	629.1(3)	646.0(3)	630.5(3)
11-6-74	610.0	-	-	648.0	634.5
11-7-74	609.0	-	-	648.0	634.5
11-8-74	611.0	-	629.0	648.0	638.5
11-12-74	609.0	-	633.0	648.0	636.5
11-14-74	609.0	-	631.0	647.0	637.5
11-18-74	610.0	-	632.0	647.0	637.5
11-22-74	610.0	-	632.0	648.0	638.5
11-26-74	610.0	-	632.0	648.0	638.5

SSES - FSAR

TABLE 2.5-9 (CONTINUED)

<u>OBSERVATION WELL NO.</u>	<u>1111</u>	<u>1112</u>	<u>1113</u>	<u>1114</u>	<u>1115</u>
<u>GROUND SURFACE</u> <u>ELEVATION</u>	687.4	708.2	702.1	711.7	708.0
11-29-74	610.0	-	632.0	648.0	638.5
12-2-74	608.0	-	632.0	648.0	638.5
12-6-74	610.2(1)	-	633.0	648.0	638.5
12-10-74	610.0	-	633.0	648.0	638.5
12-12-74	610.0	-	633.0	648.0	637.5
12-18-74	610.0	-	633.0	648.0	637.5
12-24-74	609.0	-	633.0	648.0	637.5
12-31-74	610.0	-	633.0	648.0	637.5
1-10-75	610.0	-	633.0	648.0	637.5
1-17-75	610.0	-	632.0	646.5	637.5
1-22-75	610.0	-	632.0	647.0	637.5
1-30-75	610.0	-	632.0	647.0	638.5
27-75	612.0	-	632.0	648.0	637.5
2-13-75	612.0	-	632.0	648.0	637.5
2-21-75	612.0	-	632.0	648.0	637.5
2-26-75	612.0	-	632.0	648.0	637.5
3-5-75	612.0	-	632.0	648.0	637.5
3-13-75	612.0	-	632.0	648.0	638.5
3-18-75	613.0	-	632.0	648.0	639.5
3-24-75	613.0	-	632.0	648.0	640.5
4-2-75	613.0	-	632.0	648.0	640.5
4-11-75	613.0	-	632.0	648.0	639.5
4-17-75	613.0	-	632.0	647.0	639.5
4-28-75	613.0	-	632.0	648.0	639.5
5-15-75	614.0	-	632.0	648.0	638.5
529-75	614.0	-	632.0	647.0	638.5
6-4-75	614.0	-	631.5	647.0	638.5
6-12-75	613.5	-	631.5	647.0	638.5
6-18-75	613.5	-	631.5	647.0	638.5
6-30-75	614.0	-	631.5	647.0	638.5
7-1-75	613.5	-	631.5	646.2(1)	637.5
7-9-75	613.0	-	631.0	647.0	638.0
7-28-75	612.3(1)	-	632.5	647.6(1)	638.5
8-4-75	611.9(1)	-	632.5	648.0	638.1(1)

SSSES - FSAR

TABLE 2.5-9 (CONTINUED)

Notes: Water level measurements made to the nearest half a foot except where noted.

- (1) Water level measurements made to the nearest .1 foot.
- (2) Well No. 1112 destroyed after 9-23-74.
- (3) Readings believed to be anomalous due to use of incorrect reference point by new monitor.

SSEE - FSAR

TABLE 2.5-10

PERMEABILITIES
MEASURED IN SPRAY POND¹

Hole	Ground Surface Elevation (ft)	Depth Interval Tested (ft)	Material	Average Permeability of Tested Interval (ft/yr)
1111	687.4	89-99 (35-97) (97-99)	glacial drift siltstone	>2900 ²
1112	708.2	73-111(est.) (96.-100.5) (100.5-106.)	glacial drift siltstone	560
1113	702.1	77-87 (77-83) (83-87)	glacial drift siltstone	1400
1114	711.2	47-74 (47-63) (63-74)	glacial drift siltstone	350
1115	708.0	65-75	glacial drift	>4300 ²
1117	706.8	21-31	siltstone	900
1122	685.0	33-35	glacial drift	30
1123	707.4	53-55	glacial drift	8
1125	705.3	53.5-55	glacial drift	16
1124 ¹	705(est.)	36-40	glacial drift	50

1. Constant-head tests in bore holes were performed in accordance with Designation E-18 of the U.S.B.R. Earth Manual for all tested intervals, except for boring 1124. Testing of 1124 was performed in accordance with Designation E-19.
2. These are minimum values. These holes accepted water in quantities greater than could be pumped with available equipment (30 gpm). The minimum value was calculated by assuming the gravity head (H) is equal to three-fourths of the depth to the water table, and using the maximum pump-in rate (Q). Hole 1111 took over 30 gpm and hole 1115 took over 50 gpm.

SSES-FSAR

TABLE 2.5-11

PERMEABILITIES

MEASURED NEAR THE RAILROAD BRIDGE

HOLE	GROUND SURFACE ELEVATION (FT)	INTERVAL TESTED (FT)	MATERIAL	PERMEABILITY (FT/YR)
929	530.1	48 - 53	Rock	-
		38 - 53	Rock	5.7
		33 - 53	Rock	4.6
		28 - 53	Rock	29.2
		23 - 53	Rock	20.6
		18 - 53	Rock	104.6
930	531.2	35 - 40	Rock	127.5
		30 - 40	Rock	81.8
		25 - 40	Rock	67.2
		20 - 40	Rock	52.0
		15 - 40	Rock	175.8
931	521.7	40 - 47	Rock	36.3
		40 - 47	Rock	55.9
		36 - 47	Rock	100.3
		36 - 47	Rock	107.5
		30 - 47	Rock	95.4
		30 - 47	Rock	81.4
932	516.8	38 - 43	Rock	129.0
		32 - 43	Rock	40.4
		27 - 43	Rock	36.2
		22 - 43	Rock	257.0
933	519.9	36 - 41	Rock	48.7
		31 - 41	Rock	253.7
		27 - 41	Rock	276.6
934	519.4	32 - 38	Rock	43.7
		28 - 38	Rock	46.6
		22 - 38	Rock	60.6
935	526.1	36 - 41	Rock	187.9
		31 - 41	Rock	134.1
		26 - 41	Rock	123.4
		21 - 41	Rock	110.8
937	540.4	39 - 44	Rock	-
		30 - 44	Rock	25.7
		25 - 44	Rock	24.2
		20 - 44	Rock	31.2

SSES-PSAR

TABLE 2.5-11

HOLE	GROUND SURFACE ELEVATION (FT)	INTERVAL TESTED (FT)	MATERIAL	PERMEABILITY (FT/YR)
938	538.3	41 - 46	Rock	-
		36 - 46	Rock	33.4
		31 - 46	Rock	96.1
		26 - 46	Rock	140.5
939	514+	35 - 38	Rock	23.7
		30 - 38	Rock	201.9
		25 - 38	Rock	158.5
940	514+	38 - 43	Rock	-
		33 - 43	Rock	109.2
		28 - 43	Rock	194.4

NOTE: These permeability values were obtained assuming the water table is 38 feet below the ground surface in this area and that the gauge was 2.0 feet above the ground surface, unless otherwise specified.

SSES-FSAR

TABLE 2.5-12CIRCULATION LOSSES IN
DRILL HOLES IN SPRAY POND

<u>Hole No.</u>	<u>Depth (ft) Below Surface</u>	<u>Elevation (ft)</u>	<u>Geologic Material</u>
1102	88	613	sand and gravel
1105	62	639	coarse sand and gravel
1110	73	616	coarse-fine sand, coarse- fine gravel, cobbles & boulders
1111	88	599	sand & gravel - boulders
1114	60 66	651 645	fine-coarse silty sand, little gravel, cobbles
1116	43 84	658 617	sand & gravel, boulders sand & gravel, boulders
1123	22	685	silty gravely sand
1127	46	659	sand & gravel, cobbles and boulders

SOIL TEST RESULTS SUMMARY (continued)

DATE Jan. 10, 1975

 $\bar{\sigma}_c$ = CONFIRMED PRESS. KSF



SOIL TEST RESULTS SUMMARY

JOB NO. 8856 PROJECT: Susquehanna Unit 1 & 2 FEATURE: Spray Pond DATE: Jan. 9, 1975

HOLE, TEST PIT, OR TRENCH NO.	SAMPLE NO.	DEPTH FT.		LABORATORY CLASSIFICATION	MECHANICAL ANALYSIS			ATTERBERG LIMITS			SPECIFIC GRAVITY	NATURAL			COMPACTION		SHEAR DATA						CONSOLIDATION TEST	REMARKS	
		FROM	TO		GRAVEL %	SAND %	FINES %	LL	PL	PI		G	WATER CONTENT %	TOTAL UNIT WEIGHT PCF	DRY UNIT WEIGHT PCF	OPTIMUM WATER %	MAXIMUM DRY DENSITY PCF	TEST	INITIAL WATER %	INITIAL DRY DENSITY PCF	C KSF	Ø DEG			CF PSF
1104	UD-2	41		GM-SW	55	38	7																		
	UD-4	56.5	58.2	SW	38	53	9					8.4	142.8	131.9											Sample disturbed
	UD-5	69		GM	56																				Grain size curve stops at #10 sieve
1106	UD-6B	15.5	17.2	SP	0	95	5					11.4	113.5	101.6			CR	11.7	99.0			6.0	4	.28E	
	UD-8A	19.5	21.1	SP	3	93	4				2.71	9.2	108.3	99.2			CR	9.2	98.3			6.0	2	.32	
	UD-8A	19.5	21.1	SP	0	99	1				2.71	9.2	108.3	99.2			CR	12.9	97.9 98.1			1.0	45 16	.21 .18	2nd sample remolded
	UD-8B	19.5	21.1	SP	1	95	4					12.9	113.7	100.7											
	UD-9A	21.5	23.1	SP	0	94	6					7.8	110.8	102.8											
	UD-9B	21.5	23.1	SP	0	95	5					10.7	112.7	101.8			CR	10.7	100.2 99.9			1.0 1.0	108 39	.13E .12	2nd sample remolded
	UD-10A	23.5	26.1	SM	15	76	9				2.70	12.5	123.4	109.7			CR	12.5	107.7			6.0	23	.15E	
	UD-10B	23.5	26.1	SM	5	79	16					14.1	127.7	111.9			CR	14.1	109.5			1.0	40	.214	
	UD-11A	26.5	29.0	SM	5	78	17					18.1	127.9	108.3			CR	18.1	106.3			6.0	20	.175	
	UD-11A	26.5	29.0	SM	3	90	7					18.1	127.9	108.3											
	UD-11B	26.5	29.0	SP	0	89	11					22.1	129.7	106.2			CR	22.1	105.7 106.0			1.0 1.0	48 12	.26 .23	Remolded sample for CR Test
1106A	UD-2B	9.5	11.4	SP	2	80	18					12.9	109.6	97.1			CD	12.9	97.5	0	43				
	UD-5B	15.0	16.6	SP	0	86	14					11.9	112.0	100.1			CD	11.9	99.2	0	43				
	UD-6B	17.0	18.5	SP	0	95	5					10.9	113.3	102.2			CR	10.9	102.8			2.0	55	.167	
	UD-7A	18.5	21.0	SP	0	92	8				2.70	12.5	109.5	97.3											
	UD-7B	18.5	21.0	SM	0	77 0	23 95					19.2	118.5	99.4			CR	19.2	97.0 99.6			1.0	6 Th	.28C .27E	2nd sample remolded

VISUAL CLASSIFICATION
 (a) - GRAVEL NO. 4
 (b) - PLUS NO. 4
 (c) - SAND NO. 60
 (d) - FINE SAND NO. 200
 (e) - CLAY NO. 200
 (f) - OTHER (SEE TEST)

COMPACTION
 (1) - ASTM D 1557
 (2) - ASTM D 1557
 (3) - ASTM D 1557
 (4) - ASTM D 1557
 (5) - OTHER (SEE TEST)

TRIAxIAL COMPRESSION TESTS
 UC UNCONSOLIDATED UNCONFINED
 UU UNCONSOLIDATED UNCONFINED
 CU CONSOLIDATED UNCONFINED
 EU CONSOLIDATED UNCONFINED
 CD CONSOLIDATED DRAINED
 CU CYCLIC CONSOLIDATED UNCONFINED
 (NOTE: PRESSURE MEASUREMENTS)

OTHERS
 G_c - CONFIRMED PRESS. KSF

BSIS - PSAR
TABLE 2.5 - 13



SOIL TEST RESULTS SUMMARY (Continued)

JOB NO. 8856

PROJECT Susquehanna Unit 1 A 7

FEATURE SPRAY POND

DATE Jan. 10, 1975

HOLE, TEST PIT, OR TRENCH NO.	SAMPLE NO.	DEPTH FT.		LABORATORY CLASSIFICATION	MECHANICAL ANALYSIS			ATTERBERG LIMITS			SPECIFIC GRAVITY G	NATURAL			COMPACTION		SHEAR DATA							CONSOLIDATION TEST	REMARKS		
		FROM	TO		GRAVEL %	SAND %	FINES %	LL	PL	PI		WATER CONTENT %	TOTAL UNIT WEIGHT PCF	DRY UNIT WEIGHT PCF	OPTIMUM WATER %	MAXIMUM DRY DENSITY PCF	TEST	INITIAL		C KSF	φ DEG	σ _c KSF	CYCLE			SYMBOL #1-10	
																		WATER %	DRY DENSITY PCF								
1111	SS-13	39		SW	45																						Grain size curve stops at #10 sieve
	SS-14	42		SW	65	26	9																				
	SS-22	66		SW	37																						Grain size curve stops at #10 sieve
	SS-23	69		SW-GW	42	46	12																				
1112	SS-14	57		GW	70	22	8																				
	SS-15	60		SW	20																						Grain size curve stops at #10 sieve
	SS-25	90		SW	15	66	19																				
	SS-26	93		SM	11																						Grain size curve stops at #10 sieve
1112A	UD-5	26.0	28.6	SW-GW	44	50	6					17.6															
1113	SS-13	41		SW-GW	47	47	6																				
	SS-19	58		SW	35	57	8																				
1113A	UD-3B	25.0	27.5	SW	10	80	10					3.9	110.8	106.7			CD	3.9	110.0	0	36						
	UD-4A	28.0	30.5	SW	13	82	5					10.6	117.7	106.4													Sample disturbed
	UD-4B	28.0	30.5	SW	13	79	8					9.1	121.1	111.0													Sample disturbed
	UD-6A	33.5	35.4	SP	7	87	6					9.8	125.6	114.4			CD	9.8	117.3	0	46						
1115	SS-12	45		GM-SW	61	32	7																				
	SS-15	55		GM-SW	50	37	13																				

* VISUAL CLASSIFICATION

SPECIFIC GRAVITY

(a) MINUS NO. 4
(b) PLUS NO. 4

COMPACTION

(1) ASTM D998
(2) ASTM D1557
(3) 20,000 FT. LB. / CFT
(4) BASHORE - MODIFIED
(5) OTHER (SEE TEST)

TRIAxIAL COMPRESSION TESTS

UC UNCONSOLIDATED UNDRAINED
UU UNCONSOLIDATED UNDRAINED
CU CONSOLIDATED UNDRAINED
CD CONSOLIDATED DRAINED (PORE PRESSURE MEASUREMENTS)
CB CONSOLIDATED DRAINED
CC CYCLIC CONSOLIDATED UNDRAINED (PORE PRESSURE MEASUREMENTS)

OTHERS

σ_c * CONFINING PRESS. KSF

8828 - FBAR
TABLE 2.5 - 13



SOIL TEST RESULTS SUMMARY (Continued)

JOB NO. 8856 PROJECT Susquehanna Unit 1 & 2 FEATURE Spray Pond DATE Jan. 10, 1975

HOLE, TEST PIT, OR TRENCH NO.	SAMPLE NO.	DEPTH FT.		LABORATORY CLASSIFICATION	MECHANICAL ANALYSIS			ATTERBERG LIMITS			SPECIFIC GRAVITY	NATURAL			COMPACTION		SHEAR DATA							CONSOLIDATION TEST	REMARKS		
		FROM	TO		GRAVEL %	SAND %	FINES %	LL	PL	PI		G	WATER CONTENT %	TOTAL UNIT WEIGHT PCF	DRY UNIT WEIGHT PCF	OPTIMUM WATER %	MAXIMUM DRY DENSITY PCF	TEST	WATER %	INITIAL DRY DENSITY PCF	C KSF	Ø DES	OC KSF			CYCLE	STP-33 RA-10
1115A	UD-2	35		GM-SW	52	38	10																				
1116	SS-16	57		SW	23	59	18																				
	SS-19	66		SW	29	58	13																				
1120	UD-4A	52.0	53.5	SM	0	90	10					13.1	114.2	101.1			CD	13.1	102.4	0	36						
	UD-4B	52	53.5	SM	0	87	13					15.6	116.9	101.2													
	SS-10	69		GM-SW	47	42	11																				
	SS-14	83		GM	53	36	11																				
1122	UD-2A	8.0	9.8	SP	0	92	8					10.1	112.8	102.5			CD	10.1	105.4	0	43						
	UD-2B	8.0	9.8	SP	0	96	4					11.4	117.6	105.6													
	UD-4B	16.0	17.5	SM	2	68	30					8.7	108.7	100.0			CD	8.7	99.4	0	40						
1128	UD-4B	26.0	28.0	SW	8	84	8					14.1	139.4	122.2			CD	14.1	119.9	0	50						
	SS-12	50		SW	35	53	12																				
	SS-14	60		GM-SW	48	42	10																				
Test Pit	TP-1			SP	0	90	10																				

* VISUAL CLASSIFICATION

SPECIFIC GRAVITY
(a) = MINUS NO. 4
(b) = PLUS NO. 4

COMPACTION
(1) = ASTM D 698
(2) = ASTM D 1557
(3) = 20,000 FT. LB. / CU. FT.
(4) = MAXIMUM - MINIMUM
(5) = OTHER (SEE TEXT)

UNCONSOLIDATED COMPRESSION
UNCONSOLIDATED UNDRAINED
CONSOLIDATED UNDRAINED
CONSOLIDATED UNDRAINED
(Pore Pressure Measurements)

TRIAXIAL COMPRESSION TESTS

CD CONSOLIDATED DRAINED
CU CYCLIC CONSOLIDATED UNDRAINED
(Pore Pressure Measurements)

OTHERS

FC = CONFIRMED PRESS. KSF

TABLE 2.5-14

SPRAY POND

SUMMARY OF CYCLIC

CONSOLIDATED-UNDRAINED TRIAXIAL (CR) TESTS

Test† Number	Sample* Condition	Dry Unit Weight, pcf	Relative ** Density, % (ASTM D-2049)	Consolidation Pressure, $\bar{\sigma}_c$ ksf	Number of Cycles To 5% Strain	Stress Ratio $(\sigma_1 - \sigma_3)_{cy} / 2\bar{\sigma}_c$
CR-1	U.D.	100.4	57.4	1.0	6	0.338
CR-2	U.D.	101.8	65.6	6.0	2	0.456
CR-3	U.D.	97.9	42.4	1.0	45	0.210
CR-4	U.D.	100.2	56.3	1.0	108	0.136
CR-5	U.D.	98.3	44.8	6.0	2	0.327
CR-6	U.D.	109.5	100.0	1.0	40	0.214
CR-7	U.D.	107.7	97.5	6.0	23	0.156
CR-8	R.	105.7	87.0	1.0	48	0.267
CR-9	U.D.	106.3	90.2	6.0	20	0.175
CR-10	U.D.	97.0	36.7	1.0	6	0.280
CR-11	U.D.	96.6	34.2	1.0	14	0.240
CR-12	U.D.	100.7	59.2	6.0	11	0.242
CR-13	U.D.	100.9	59.1	1.0	184	0.219
CR-14	U.D.	99.0	49.1	6.0	48	0.145

TABLE 2.5-14 (Continued)

Test† Number	Sample* Condition	Dry Unit Weight, pcf	Relative ** Density, % (ASTM D-2049)	Consolidation Pressure, σ_c ksf	Number of Cycles To 5% Strain	Stress Ratio $(\sigma_1 - \sigma_3)_{cy} / 2\sigma_c$
CR-15	R.	99.6	52.7	1.0	10	0.215
CR-16	U.D.	106.0	88.2	1.0	12	0.231
CR-17	R.	97.0	36.7	1.0	2	0.229
CR-18	R.	99.9	54.5	1.0	39	0.125
CR-19	R.	101.2	62.1	1.0	34	0.186
CR-20	R.	98.1	43.6	1.0	11	0.183
CR-21	U.D.	102.8	71.2	6.0	55	0.167
CR-22	R.	108.6	100.0	1.0	10	0.198
CR-23	U.D.	99.0	49.1	6.0	4	0.288
CR-24	R.	96.2	31.7	1.0	25	0.236
CR-25	R.	101.6	64.4	1.0	10	0.302

*Note: U.D. = Undisturbed Sample
R. = Remolded Sample

**Relative Density Determined by

$$D_d = \frac{\gamma_{\max} (\gamma - \gamma_{\min})}{(\gamma_{\max} - \gamma_{\min})} \times 100, \quad \begin{array}{l} \gamma_{\max} = 108.2 \text{ pcf} \\ \gamma_{\min} = 91.5 \text{ pcf} \end{array}$$

† The boring numbers and sample depth for each CR test is given in Table V of Reference 2.5-102

SSES-FSAR

TABLE 2.5-15DESIGN PARAMETERS FOR SPRAY POND LINER

<u>Thickness (ft)</u>	<u>Liner</u>		<u>Total Seepage Loss*</u>		<u>Elevation of Ground Water Mound Beneath Center of Pond</u>
	<u>Permeability (ft/yr)</u>		<u>(ft³/yr)</u>	<u>Gal/30Days</u>	
1.0	0.20		8.4×10^5	5.2×10^5	670
1.0	0.12		4.8×10^5	3.0×10^5	660
1.0	0.04		1.9×10^5	1.2×10^5	650

*Liquefaction design requirements require a seepage loss rate of less than 6.7×10^5 cubic feet per year (4.1×10^5 gal/30 days). The liner is designed for a seepage loss of no more than 3.0×10^5 gal/30 days.

TABLE 2.5-16

SPRAY POND
SUMMARY OF LIQUEFACTION ANALYSES

Profile 1 (West End of Pond)

Depth Ft.	Avg. Induced Cyclic Stress psf		Cyclic Shear Strength psf		Factor of Safety	
	GWT 650'	GWT 640'	GWT 650'	GWT 640'	GWT 650'	GWT 640'
1	12	12	149	149	12.4	12.4
3.5	43	43	206	206	4.8	4.8
6.5	80	80	273	273	3.4	3.4
10.5	128	128	359	359	2.80	2.80
15.5	186	186	460	460	2.47	2.47
23	267	267	558	601	2.09	2.25
33	370	371	651	732	1.76	1.97
44	478	480	746	820	1.56	1.71
56	590	594	840	908	1.42	1.53
69.5	705	710	938	997	1.33	1.40
85	806	816	1034	1085	1.28	1.33

TABLE 2.5-16 (Continued)

Profile 2 (Central Section, Pumphouse, etc.)

Depth Ft.	Avg. Induced Cyclic Stress psf			Cyclic Shear Strength psf			Factor of Safety		
	GWT	GWT	GWT	GWT	GWT	GWT	GWT	GWT	GWT
	665'	660'	650'	665'	660'	650'	665'	660'	650'
1	18	12	12	162	149	149	9.0	12.4	12.4
3.5	49	43	43	207	206	206	4.2	4.8	4.8
6.5	80	80	80	239	273	273	3.0	3.4	3.4
10.5	128	128	128	282	334	359	2.20	2.61	2.80
15.5	185	185	186	337	388	460	1.82	2.10	2.47
23	265	266	267	418	465	558	1.58	1.75	2.09
33	367	368	370	519	565	651	1.41	1.54	1.76
43	464	466	470	615	657	738	1.33	1.41	1.57
52.5	553	555	560	700	739	815	1.26	1.33	1.46

TABLE 2.5-16 (Continued)

Profile 3 (East End of Pond)

Depth Ft.	Avg. Induced Cyclic Stress	Cyclic Shear Strength	Factor of Safety
	<u>psf</u> GWT 665'	<u>psf</u> GWT 665'	<u>GWT</u> 665'
1.5	18	162	9.0
4	49	207	4.2
6.5	80	239	3.0
10.5	128	282	2.20
15.5	185	337	1.82
19	223	375	1.68

Note:

1. Avg. Induced Cyclic Stresses = 0.65 Maximum Induced Cyclic Stresses (Ref. Seed and Idriss, 1971)
2. GWT = Ground Water Table, MSL.
3. Factor of Safety = Cyclic Shear Strength/Avg. Induced Cyclic Stress.

TABLE 2.5-17

EFFECT OF VARYING STANDARD RELATIONSHIP* OF EFFECTIVE
STRAIN WITH DAMPING AND MODULI FOR PROFILE 2, GWT-665'.

Depth Ft.	Std. Rela- tion	30% Increase in Modulus			No Change in Modulus		30% Decrease in Modulus		
		30%	No	30%	30%	30%	30%	No	30%
		Decrease In Damping	Change In Damping	Increase In Damping	Decrease In Damping	Increase In Damping	Decrease In Damping	Change In Damping	Increase In Damping
Average Induced Cyclic Shear Stress, psf.									
1.5	18	18	18	18	18	18	18	18	18
4	49	50	50	49	50	49	49	49	49
6.5	80	80	80	80	80	80	80	80	79
10.5	128	129	129	128	128	127	127	126	125
15.5	185	188	187	186	185	184	182	181	179
23	265	271	270	268	266	263	259	258	258
33	367	376	374	372	368	368	357	355	355
43	464	476	474	475	466	461	448	445	441
52.5	553	570	567	564	556	549	522	519	516

Depth Ft.	Shear Strength psf		Factor of Safety Against Liquefaction							
1.5	162	9.0	9.0	9.0	9.0	9.0	9.0	9.0	9.0	9.0
4	207	4.2	4.1	4.1	4.2	4.1	4.2	4.2	4.2	4.2
6.5	239	3.0	3.0	3.0	3.0	3.0	3.0	3.0	3.0	3.0
10.5	282	2.20	2.19	2.19	2.20	2.20	2.22	2.22	2.24	2.26
15.5	337	1.82	1.79	1.80	1.81	1.82	1.83	1.85	1.86	1.88
23	418	1.58	1.54	1.55	1.56	1.57	1.59	1.61	1.62	1.62
33	519	1.41	1.38	1.39	1.40	1.41	1.41	1.45	1.46	1.46
43	615	1.33	1.29	1.30	1.29	1.32	1.33	1.37	1.38	1.39
52.5	700	1.26	1.23	1.23	1.24	1.26	1.28	1.34	1.35	1.36

*Seed, H. B. and Idriss, I. M., "Soil Moduli and Damping Factors for Dynamic Response Analysis," EERC Report No. 70-10, U. C. Berkeley, 1970.

GWT = Ground Water Table, MSL.

Factor of Safety = $\text{Shear Strength} / \text{Average Induced Cyclic Stress}$.

TABLE 2.5-18

SPRAY POND

FACTOR OF SAFETY AS OBTAINED USING DIFFERENT EARTHQUAKES
 (ALL 3 PROFILES AND AT DIFFERENT GROUND WATER LEVELS)

Profile 1 (West End of Pond, 93' Overburden Below Bottom of Pond)*

Factor of Safety at Corresponding Depth

<u>EARTHQUAKE</u>								
<u>Depth Below Pond Bottom Ft.</u>	<u>Bechtel Synthetic</u>		<u>Golden Gate</u>		<u>Helena</u>		<u>Parkfield</u>	
	Ground Water Elevation, Ft. (MSL)							
	650**	640	650**	640	650**	640	650**	640
1	12.4	12.4	11.5	11.5	12.4	12.4	11.4	11.4
3.5	4.8	4.8	4.5	4.5	4.9	4.9	4.6	4.6
6.5	3.4	3.4	3.3	3.3	3.5	3.5	3.2	3.2
10.5	2.80	2.80	2.74	2.69	3.0	3.0	2.65	2.63
15.5	2.47	2.47	2.44	2.39	2.95	2.95	2.30	2.30
23	2.09	2.25	2.08	2.15	2.89	3.0	1.90	2.04
33	1.76	1.97	1.79	1.90	2.37	2.79	1.58	1.78
44	1.56	1.71	1.67	1.71	2.17	2.41	1.43	1.58
56	1.42	1.53	1.63	1.64	2.19	2.36	1.39	1.50
69.5	1.33	1.40	1.68	1.64	1.98	2.22	1.42	1.50
85	1.28	1.33	1.79	1.72	1.91	2.05	1.48	1.52

TABLE 2.5-18 (Continued)

Profile 2 (Central Section, Pumpouse, etc.,
57' Overburden below Bottom of Pond)*

Factor of Safety at Corresponding Depth

EARTHQUAKE

Depth Below Pond Bottom Ft.	<u>Bechtel Synthetic</u>			<u>Golden Gate</u>			<u>Helena</u>			<u>Parkfield</u>		
	Ground Water Elevation, Ft. (MSL)											
	665**	660	650	665**	660	650	665**	660	650	665**	660	650
1	9.0	12.0	12.4	8.1	12.4	11.5	8.1	12.4	11.5	8.1	11.5	11.5
3.5	4.2	4.8	4.8	4.0	4.5	4.5	4.1	4.7	4.8	4.0	4.6	4.6
6.5	3.0	3.4	3.4	2.85	3.4	3.4	2.95	3.4	3.5	2.92	3.3	3.3
10.5	2.20	2.61	2.80	2.16	2.57	2.78	2.27	2.63	2.80	2.13	2.53	2.72
15.5	1.82	2.10	2.47	1.79	2.09	2.46	1.96	2.19	2.54	1.75	2.04	2.39
23	1.58	1.75	2.09	1.59	1.79	2.12	1.84	1.96	2.26	1.48	1.69	2.02
33	1.41	1.54	1.76	1.51	1.64	1.87	1.80	1.96	2.04	1.35	1.49	1.74
43	1.33	1.41	1.57	1.52	1.62	1.79	1.81	1.96	2.03	1.33	1.47	1.61
52.5	1.26	1.33	1.46	1.59	1.67	1.79	1.91	2.01	2.05	1.37	1.44	1.55

TABLE 2.5-18 (Continued)

Profile 3 (East End of Pond, 20' Overburden below Bottom of Pond)*

Factor of Safety at Corresponding Depth

EARTHQUAKE

<u>Depth Below Pond Bottom Ft.</u>	<u>Bechtel Synthetic</u>	<u>Golden Gate</u>	<u>Helena</u>	<u>Parkfield</u>
Ground Water Elevation = 665 Ft. (MSL)**				
1.5	9.0	8.5	8.1	9.0
4	4.2	4.1	4.1	4.4
6.5	3.0	3.0	2.95	3.0
10.5	2.20	2.26	2.31	2.27
15.5	1.82	1.92	2.10	1.87
19	1.68	1.84	2.13	1.71

*See Figure 2.5-48 for Soil Profile

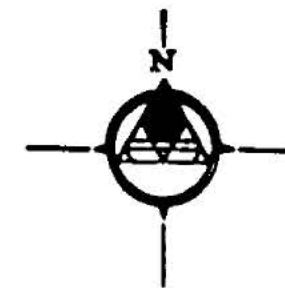
**Maximum Water Table

SEES - PSAR

TABLE 2.5 - 19

PROBABLE SETTLEMENT DURING EARTHQUAKE

RESULTED FROM COMPACTION OF DRY SOILS					RESULTED FROM RECONSOLIDATION OF SATURATED SOILS						
Depth Ft.	Thickness Ft.	Ave. Induced Cyclic Strain %	Probable Vert. Strain %	Probable Vert. Settlement 10 ⁻² , ft.	Stress Ratio Developed	Cycle Ratio, t/t_1	Preo Pressure Ratio, $\Delta u/\sigma_{3c}$	Volumetric Strain (Dr=50%), %	Vol. Strain Corrected to Dr=60%, %	Vertical Strain %	Probable Vert. Settlement 10 ⁻² , ft.
PROFILE 1 (East End of Pond, Ground Water Table = 650')											
1	2	.0033	.0001	.0002	.026	.005	0 - .01	0	0	1	0
3.5	3	.0009	.0008	.0024	.066	.005	0 - .01	0	0	1	0
6.5	3	.0016	.0011	.0033	.032	.005	0 - .01	0	0	1	0
10.5	5	.0024	.0016	.0090	.110	.005	0 - .01	0	0	1	0
15.5	5	.0031	.0025	.0125	.121	.005	0 - .01	0	0	1	0
23	10	.0042	.0035	.0350	.139	.025	.02 - .19	0 - .12	0 - .096	1 - .048	0 - 0.48
33	10	.0056	.0045	.0450	.161	.17	.15 - .41	.02 - .32	.016 - .256	.008 - .128	.080 - 1.28
44	12	.0065	.0055	.0660	.175	.18	.16 - .42	.02 - .33	.016 - .264	.008 - .132	.096 - 1.58
56	12	.0072	.0062	.0744	.185	.25	.22 - .49	.04 - .40	.032 - .320	.016 - .160	.192 - 1.32
69.5	15	.0073	.0063	.0945	.190	.25	.22 - .49	.04 - .40	.032 - .320	.016 - .160	.240 - 2.40
85	16	.0071	.0061	.0776	.187	.25	.22 - .49	.04 - .40	.032 - .320	.016 - .160	.256 - 2.56
Total	93 ft.			.004399 ft (0.05 in)							.009 - 0.10 ft (0.1 - 1.2 in)
PROFILE 2 (Central Section, Pump House, etc., Ground Water Table = 665')											
1.5	3	.0004	.0001	.0003	.036	.005	0 - .01	0	0	1	0
4	2	.0011	.0009	.0018	.075	.005	0 - .01	0	0	1	0
6.5	3	.0010	.0011	.0033	.107	.005	0 - .01	0	0	1	0
10.5	5	.0027	.0020	.0100	.142	.062	.06 - .23	.01 - .17	.003 - .136	.004 - .068	.020 - 0.34
15.5	5	.0030	.0023	.0140	.170	.17	.15 - .41	.02 - .32	.015 - .256	.008 - .128	.040 - 0.64
23	10	.0050	.0030	.0300	.191	.26	.23 - .51	.04 - .41	.032 - .328	.015 - .164	.160 - 1.64
33	10	.0062	.0049	.0490	.207	.33	.30 - .57	.05 - .40	.040 - .384	.020 - .192	.200 - 1.92
43	10	.0074	.0064	.0640	.214	.36	.32 - .60	.05 - .52	.040 - .416	.020 - .208	.200 - 2.08
52.5	9	.0076	.0065	.0535	.221	.42	.33 - .65	.06 - .53	.048 - .464	.024 - .232	.216 - 2.08
Total	57 ft.			.002389 ft (0.03 in)							.005 - .087 ft (0.1 - 1.0 in)
PROFILE 3 (West End of Pond, Ground Water Table = 665')											
1.5	3	.0004	.0001	.0003	.036	.005	0 - .01	0	0	1	0
4	2	.0011	.0009	.0018	.075	.005	0 - .01	0	0	1	0
6.5	3	.0010	.0011	.0033	.107	.005	0 - .01	0	0	1	0
10.5	5	.0027	.0020	.0100	.142	.062	.06 - .28	.01 - .17	.008 - .136	.004 - .068	.020 - 0.34
15.5	5	.0030	.0020	.0140	.170	.17	.15 - .41	.02 - .32	.016 - .256	.008 - .128	.040 - 0.64
19	2	.0045	.0036	.0072	.191	.23	.20 - .47	.04 - .37	.032 - .312	.016 - .156	.032 - 0.31
Total	20 ft.			.00366 ft (0.01 in)							.009 - .013 ft (0.01 - 0.2 in)



REFERENCE:

THIS MAP WAS PREPARED FROM PORTIONS OF THE FOLLOWING
USGS TOPOGRAPHIC MAPS: WILLIAMSPORT, PENN., 1972,
SCRANTON, PENN., N.Y., N.J., 1:50,000, 1972,
AND NEWARK, PENN., N.J., 1974.

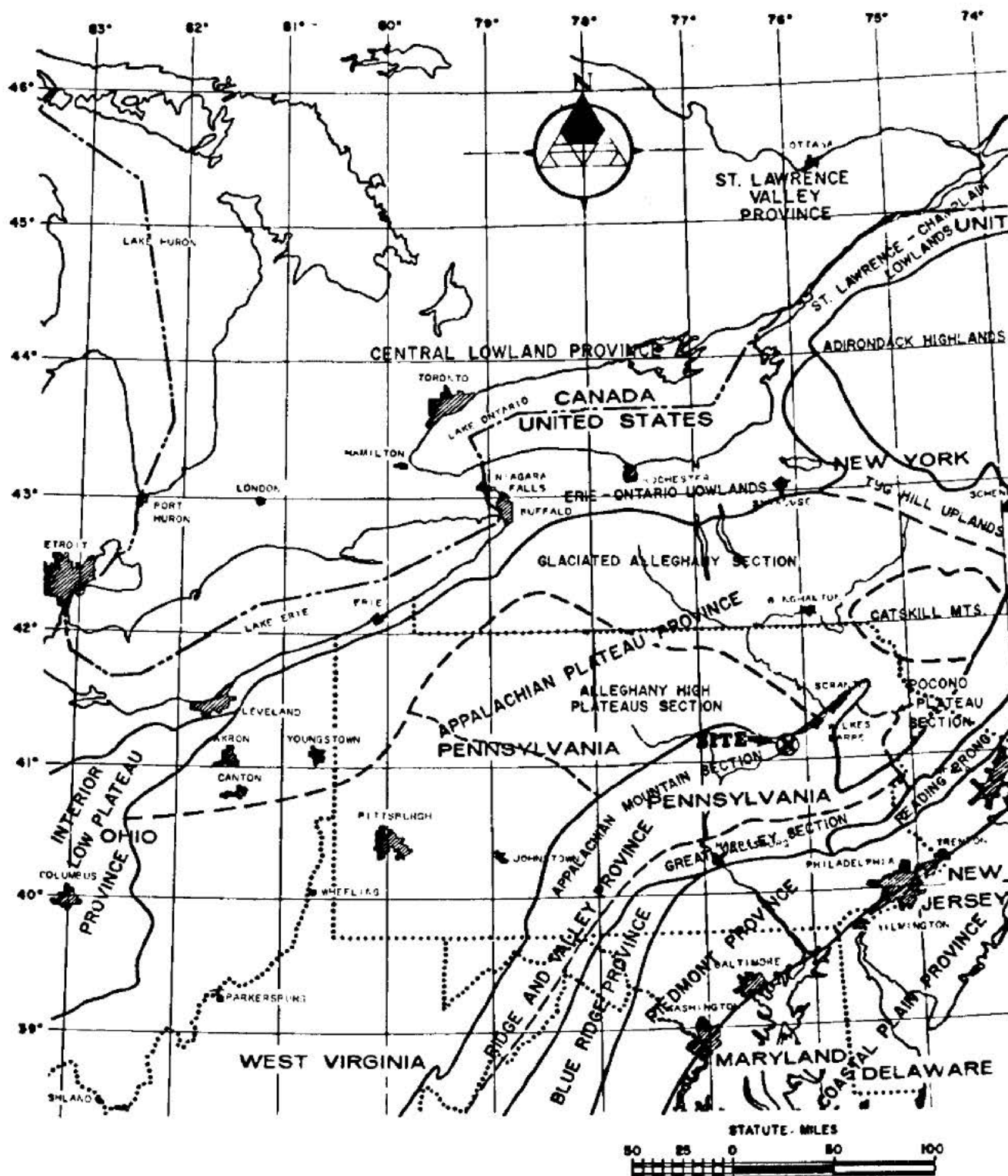
FSAR REV. 65

SUSQUEHANNA STEAM ELECTRIC STATION
UNITS 1 & 2
FINAL SAFETY ANALYSIS REPORT

SITE LOCATION

FIGURE 2.5-1, Rev 47

AutoCAD: Figure Fsar 2_5_1.dwg



FSAR REV. 65

SUSQUEHANNA STEAM ELECTRIC STATION
UNITS 1 & 2
FINAL SAFETY ANALYSIS REPORT

REGIONAL PHYSIOGRAPHIC MAP

FIGURE 2.5-2, Rev 47

AutoCAD: Figure Fsar 2_5_2.dwg

REFERENCE:

THIS MAP WAS PREPARED FROM A PORTION OF THE
U.S.G.S. "IFR WALL PLANNING CHART, EAST AND
WEST, 1968".

PHYSIOGRAPHIC DIVISIONS TAKEN FROM PHYSIOGRAPHY
OF EASTERN UNITED STATES BY N.M. FENNEMAN, 1938.



KEY:

- QUATERNARY
- TERTIARY
- CRETACEOUS
- TRIASSIC SEDIMENTARY ROCKS
- TRIASSIC IGNEOUS ROCKS
- PERMIAN
- PENNSYLVANIAN
- MISSISSIPPIAN
- DEVONIAN
- SILURIAN
- ORDOVICIAN
- CAMBRIAN
- PRECAMBRIAN

REFERENCE:
MODIFIED AFTER THE GEOLOGIC MAP OF THE UNITED STATES, 1974

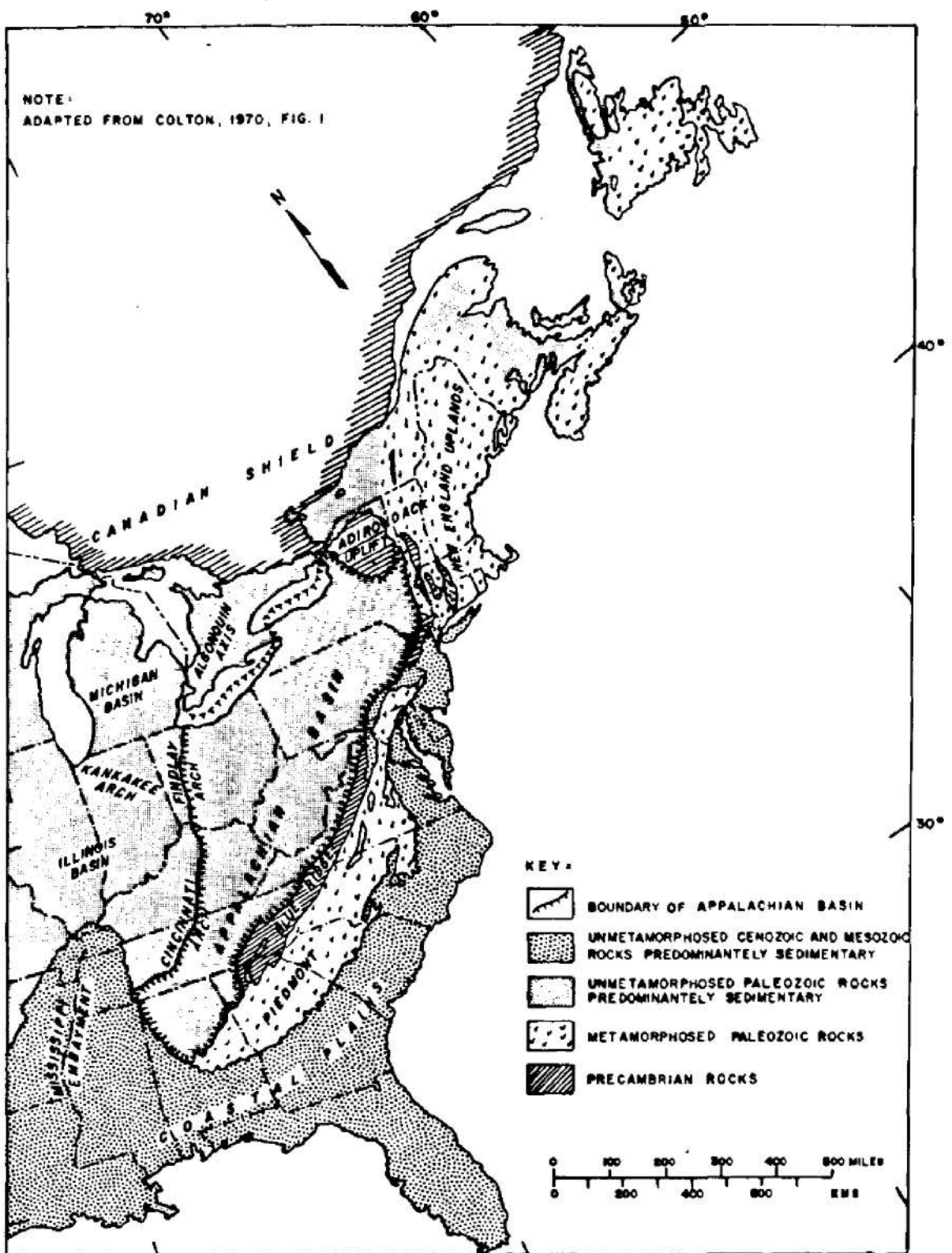
FSAR REV. 65

SUSQUEHANNA STEAM ELECTRIC STATION
UNITS 1 & 2
FINAL SAFETY ANALYSIS REPORT

REGIONAL GEOLOGIC MAP

FIGURE 2.5-3, Rev 47

AutoCAD: Figure 2.5_3.dwg



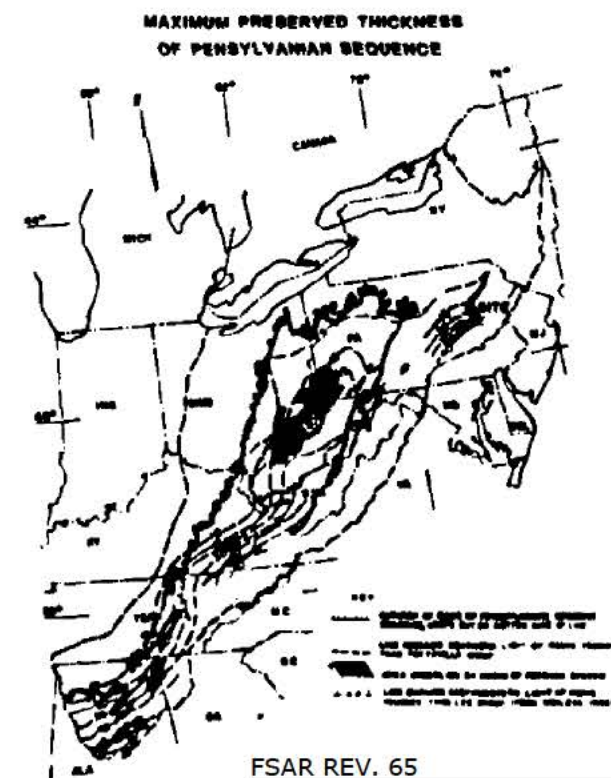
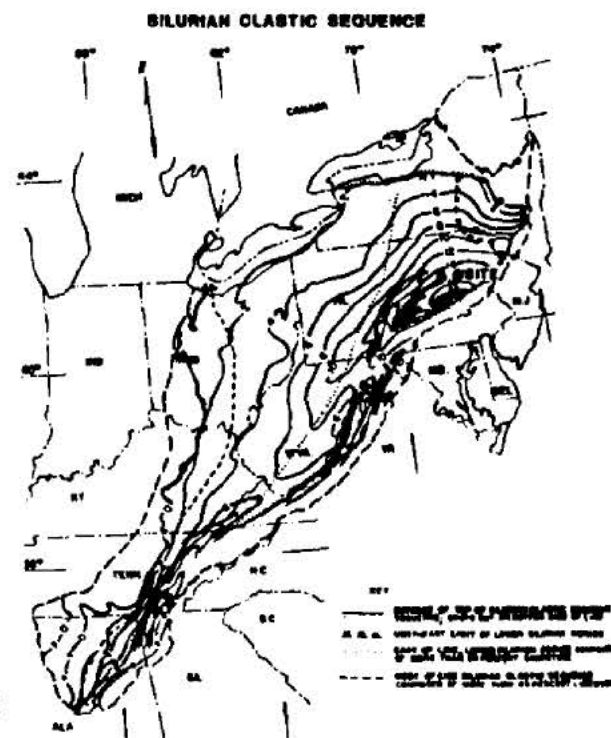
FSAR REV. 65

SUSQUEHANNA STEAM ELECTRIC STATION
UNITS 1 & 2
FINAL SAFETY ANALYSIS REPORT

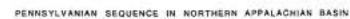
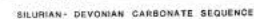
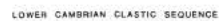
LOCATION OF THE
APPALACHIAN BASIN

FIGURE 2.5-4, Rev 47

AutoCAD: Figure Fsar 2_5_4.dwg



AutoCAD: Figure Fsar 2_5_5.dwg



NOTES:
BRACKETS BETWEEN COLUMNS INDICATE UNCERTAINTY OF LATERAL RELATIONSHIPS;
SOLID BARS INDICATE RELATIVE THICKNESS OF SECTIONS

ADAPTED FROM COLTON, 1970, FIGURES 9, 10, 12, 14, 15, 17, 19, 21, 23, 25 & 26

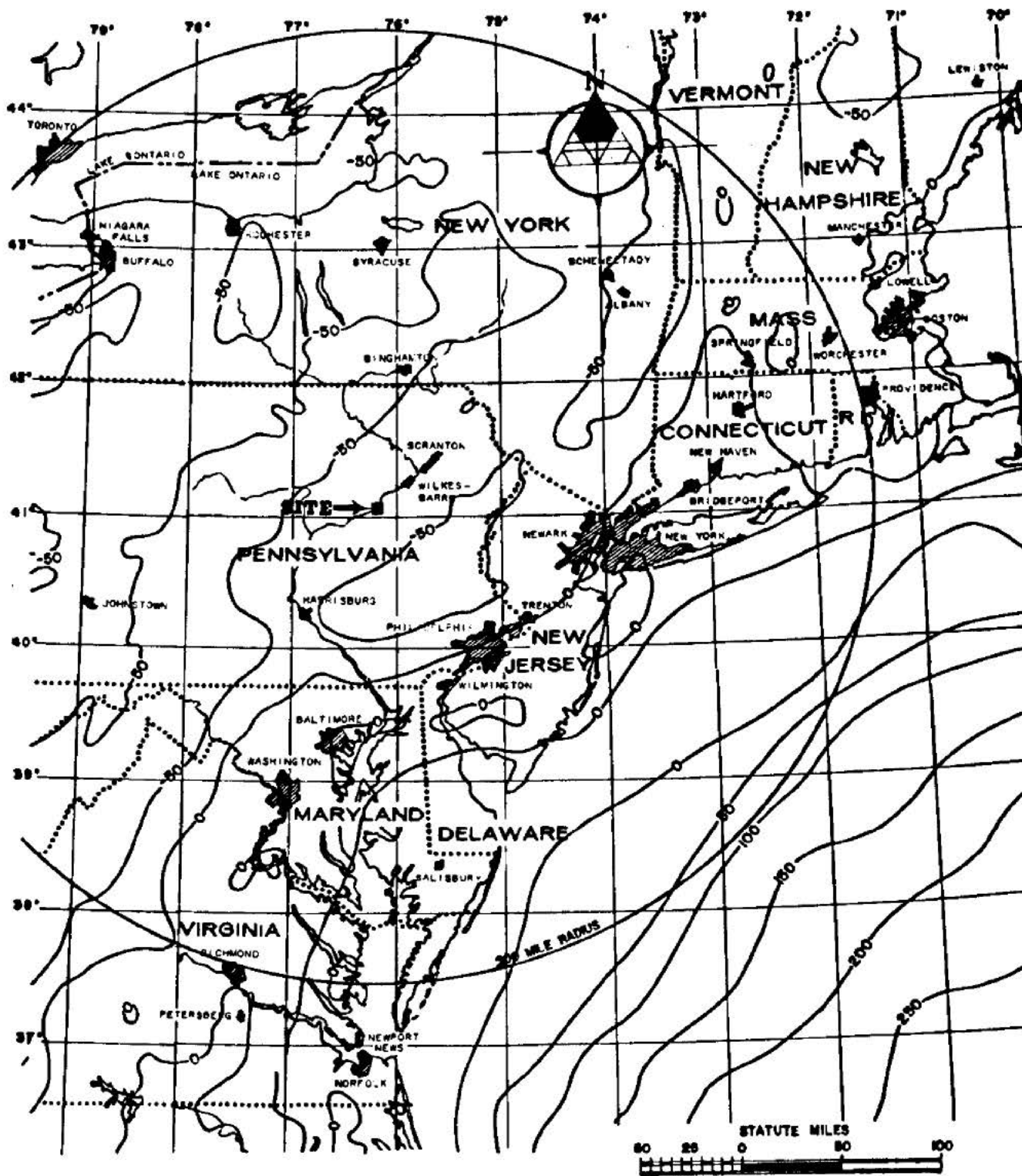
FSAR REV. 65

SUSQUEHANNA STEAM ELECTRIC STATION
UNITS 1 & 2
FINAL SAFETY ANALYSIS REPORT

STRATIGRAPHIC COLUMNS

FIGURE 2.5-6, Rev 47

AutoCAD: Figure Fsar 2_5_6.dwg



CONTOUR INTERVAL = 50 MILLIGALS

REFERENCE:

THIS MAP WAS PREPARED FROM A PORTION OF THE U.S.G.S.
"IFR WALL PLANNING CHART, EAST AND WEST, 1968".

THE "BOUGUER GRAVITY ANOMALY MAP OF THE UNITED STATES"
BY THE AMERICAN GEOPHYSICAL UNION AND THE U.S.
GEOLOGICAL SURVEY.

FSAR REV. 65

SUSQUEHANNA STEAM ELECTRIC STATION
UNITS 1 & 2
FINAL SAFETY ANALYSIS REPORT

BOUGUER GRAVITY
ANOMALY MAP

FIGURE 2.5-9, Rev 47

AutoCAD: Figure Fsar 2_5_9.dwg






LEGEND:

-  **DIT TRIMERS ROCK PH.**
-  **Dm MANTLE PH.**
-  **Dm PARCELLUS PH.**
-  **Dm CHANDLER / OLD PORT PH.**

-  **S1 TUNDRA PH.**
-  **S2 WILLIAMS PH.**
-  **S3 CHANDLER PH.**

SYMBOL:

-  **OUTCROP WITH STATION NUMBER BEDDING- INCLINED**
-  **APPROXIMATE STRATIGRAPHIC CONTACT**
-  **BEDDING - INCLINED**

REFERENCE: THE DATA FOR THIS MAP WAS PREPARED FROM THE FOLLOWING U.S. MAPS:
U.S.G.S. TOPOGRAPHIC QUADRANGLES: BLOOMSBURG, PA., 1940, 1:250,000; BERWICK, PA., 1940, 1:250,000.

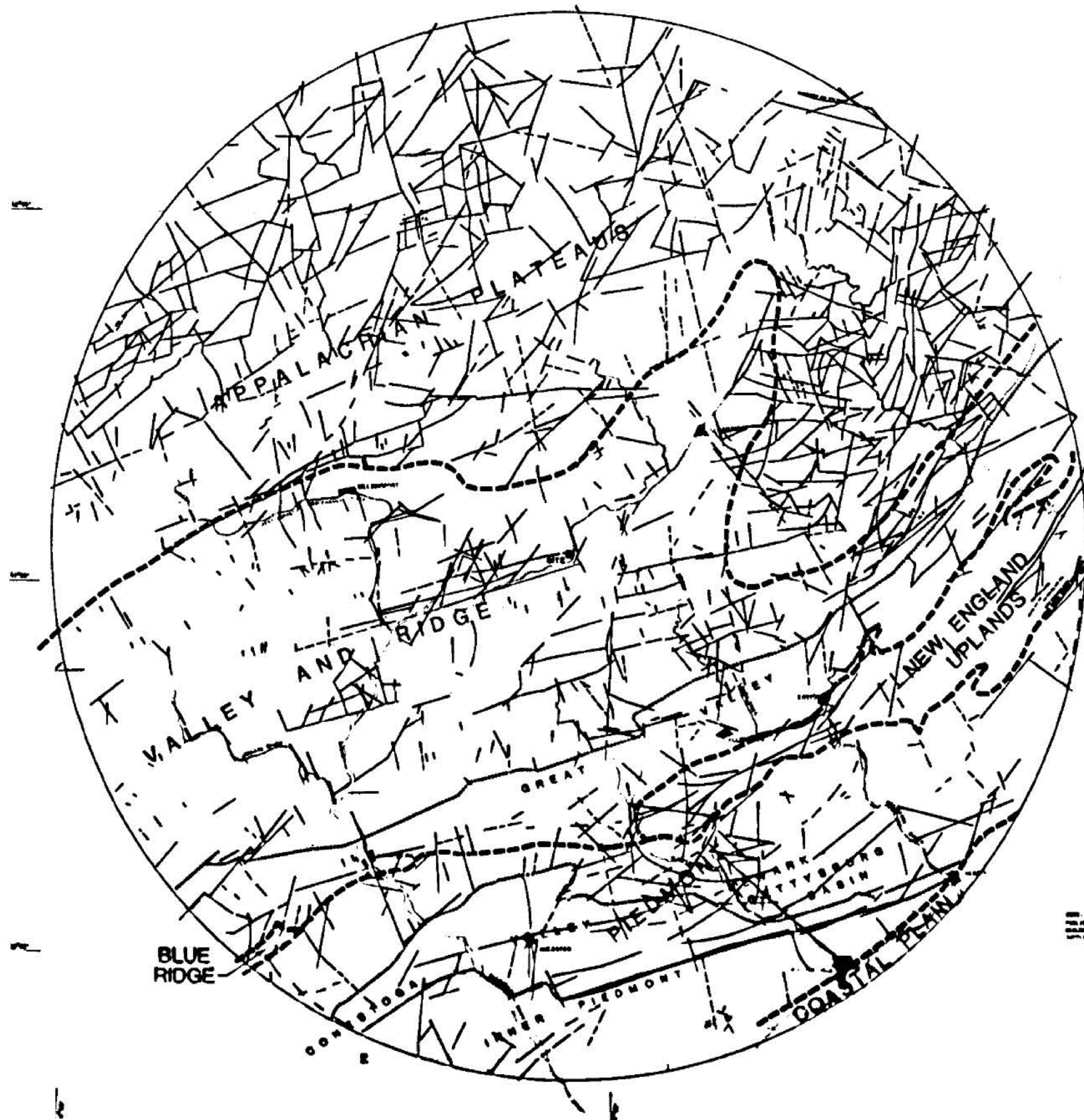
FSAR REV. 65

SUSQUEHANNA STEAM ELECTRIC STATION
UNITS 1 & 2
FINAL SAFETY ANALYSIS REPORT

GEOLOGIC MAP OF THE
BLOOMSBURG-BERWICK AREA

FIGURE 2.5-10, Rev 47

AutoCAD: Figure Fsar 2_5_10.dwg



REGIONAL LANDSAT LINEAMENTS
 SUSQUEHANNA STEAM ELECTRIC STATION
 UNITS 1 & 2
 FINAL SAFETY ANALYSIS REPORT
 REGIONAL LANDSAT LINEAMENTS
 FIGURE 2.5-11, Rev 47

FSAR REV. 65

SUSQUEHANNA STEAM ELECTRIC STATION
 UNITS 1 & 2
 FINAL SAFETY ANALYSIS REPORT
 REGIONAL LANDSAT LINEAMENTS
 FIGURE 2.5-11, Rev 47



FSAR REV. 65

SUSQUEHANNA STEAM ELECTRIC STATION
 UNITS 1 & 2
 FINAL SAFETY ANALYSIS REPORT

SITE GEOLOGIC MAP

FIGURE 2.5-12, Rev 47

AutoCAD: Figure Fsar 2_5_12.dwg



Looking south into large pothole in Unit 1 turbine area.
Workmen performing final clean-up operations provide scale.

FSAR REV. 65

SUSQUEHANNA STEAM ELECTRIC STATION
UNITS 1 & 2
FINAL SAFETY ANALYSIS REPORT

PHOTOGRAPH OF GEOLOGIC
FEATURE FOUND IN TURBINE
BUILDING EXCAVATION

FIGURE 2.5-13, Rev 47

AutoCAD: Figure Fsar 2_5_13.dwg

ERA	PERIOD	FORMATION	THICKNESS IN FEET	LOCATION OF SURFACE EXPOSURE	TECTONIC SIGNIFICANCE
CENOZOIC	HOLOCENE		10 - 20		
	PLEISTOCENE		0 - 300		
PALEZOIC	PENNSYLVANIAN	LLEWELLYN OR "POST POTTSVILLE" POTTSVILLE CONGLOMERATE	1800 ± 500 ±	ANTHRACITE REGION	UPPER PORTION GREATLY FOLDED, FAULTED
	MISSISSIPPIAN	HAUCH CHUNK SHALE POCONO SANDSTONE	2000 ± 600 ±	ANTHRACITE REGION	FOLDED, THRUST FAULTS
	DEVONIAN	UPPER CATSKILL SHALE AND SANDSTONE TRIMMERS ROCK SANDSTONE	1700 ± 2100 ±	VALLEY AND RIDGE AND PLATEAU VALLEY AND RIDGE AND PLATEAU	COMPETENT, LARGE OPEN FOLDS, FEW FAULTS
		MIDDLE MAHANTANGO SHALE INCLUDING: MARRELL AND TULLY EQUIVALENTS, SHERMAN CREEK AND MARCELLUS SHALES	2000 ±	VALLEY AND RIDGE AND PLATEAU VALLEY AND RIDGE AND PLATEAU	DECOLLEMENT (?) IN MARCELLUS, GENERALLY TIGHT FOLDS, FAULTED
		LOWER ONONDAGA LIMESTONE OLD PORT SANDSTONE KEYSER LIMESTONE	165 ± 100 ± 200 ±	VALLEY AND RIDGE VALLEY AND RIDGE VALLEY AND RIDGE	MODERATELY COMPETENT, GENERALLY LONG OPEN FOLDS
	SILURIAN	UPPER TONOLOWAY LIMESTONE	100 ±	VALLEY AND RIDGE	DECOLLEMENT UNDER PLATEAU IN EQUIVALENT SALINA GROUP
		MIDDLE WILLS CREEK SHALE	350 ±	VALLEY AND RIDGE	
		CLINTON SANDSTONE	500 ± 640 ±	VALLEY AND RIDGE VALLEY AND RIDGE	MODERATELY COMPETENT, GENERALLY LONG OPEN FOLDS
	CAMBRO-ORDOVICIAN	LOWER TUSCARORA SANDSTONE	250 ±	VALLEY AND RIDGE	
		CAMBRO-ORDOVICIAN CLASTICS AND CARBONATES	8000 - 12000	GREAT VALLEY ANTICLI- NAL CORES ALONG PA. CULMINATION	DECOLLEMENTS IN UPPER PORTION (MARTINSBURG) AND LOWER CAMBRIAN
PRE- CAMB- RIAN	PRECAMBRIAN BASEMENT	APPROXIMATELY 30,000 FEET BELOW SURFACE AT SITE			NOT INVOLVED IN VALLEY AND RIDGE AND PLATEAU TECTONICS

FSAR REV. 65

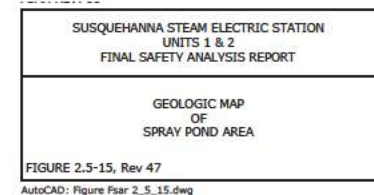
SUSQUEHANNA STEAM ELECTRIC STATION
UNITS 1 & 2
FINAL SAFETY ANALYSIS REPORT

SITE VICINITY GEOLOGIC COLUMN

FIGURE 2.5-14, Rev 47

Security-Related Information

Figure Withheld Under 10 CFR 2.390



THIS FIGURE HAS BEEN
INTENTIONALLY LEFT BLANK

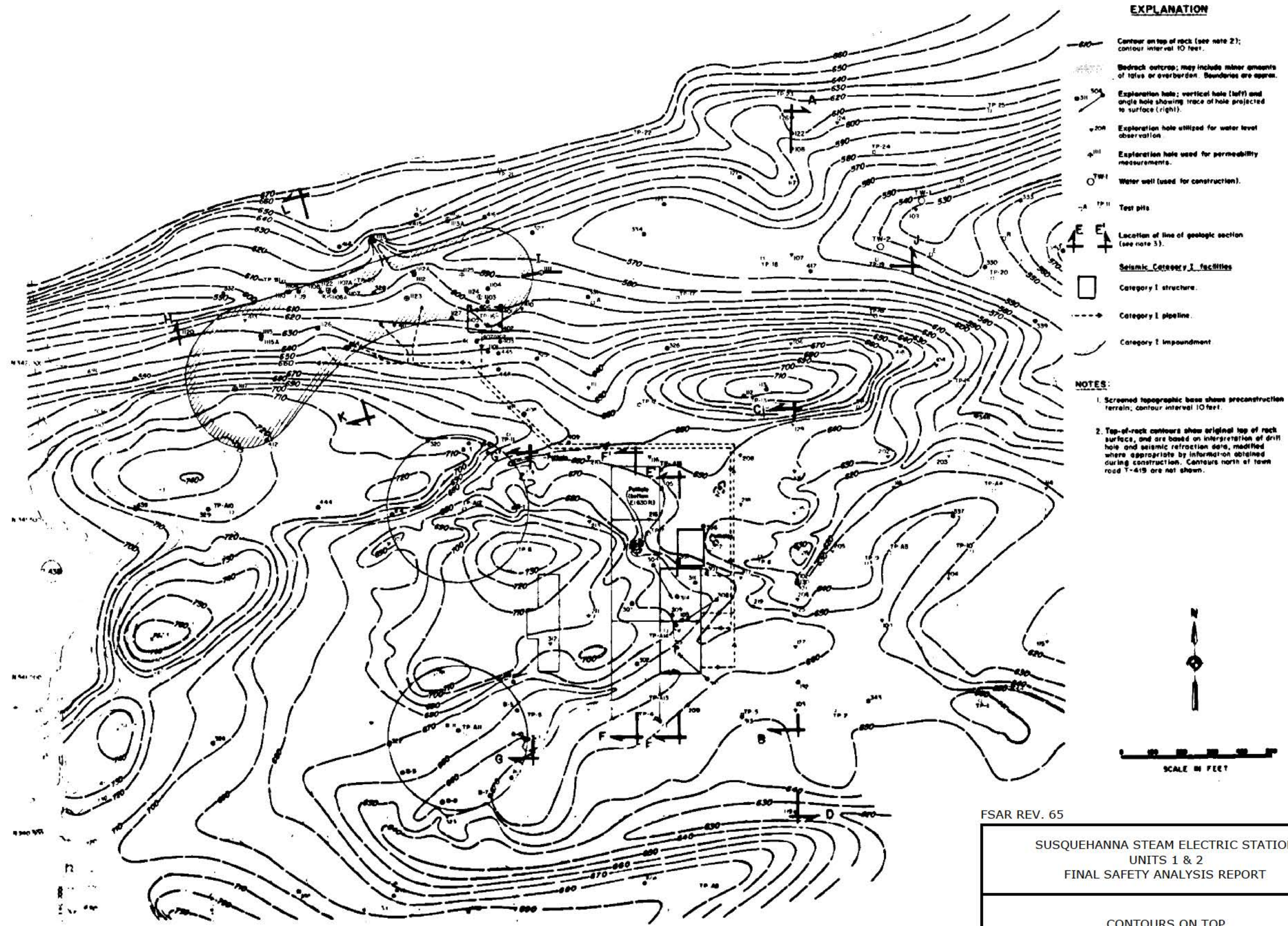
FSAR REV. 65

SUSQUEHANNA STEAM ELECTRIC STATION UNITS 1 & 2 FINAL SAFETY ANALYSIS REPORT

Figure intentionally left blank

FIGURE 2.5-16, Rev. 47

AutoCAD Figure 2_5_16.doc



FSAR REV. 65

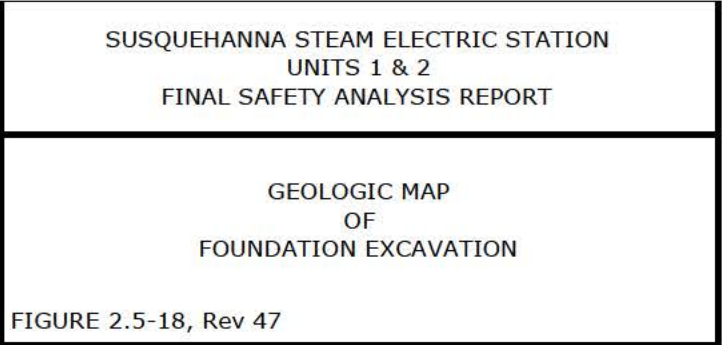
SUSQUEHANNA STEAM ELECTRIC STATION
UNITS 1 & 2
FINAL SAFETY ANALYSIS REPORT

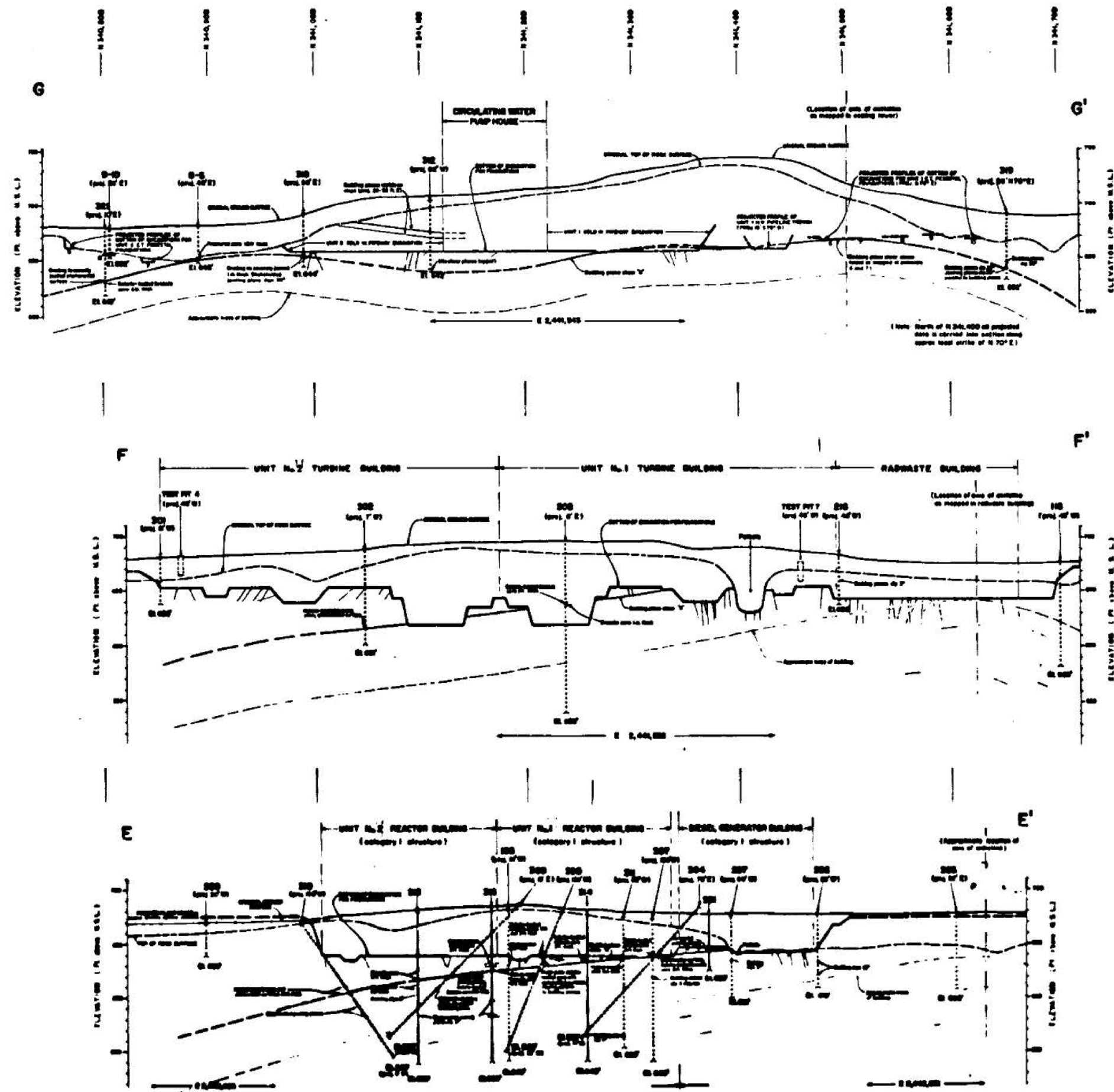
CONTOURS ON TOP
OF
BEDROCK SURFACE

FIGURE 2.5-17, Rev 47

AutoCAD: Figure Fsar_2_5_17.dwg

Security-Related Information
Figure Withheld Under 10 CFR 2.390





EXPLANATION

- Original ground surface
- Original top of bedrock surface
- Bottom of excavation for foundations (dashed line indicates finished grade). Mapped points are shown projected into the subsurface.
- Mapped bedding plane shear, dashes indicate inferred trend
- Drill hole, boring numbers and elevation of bottom of hole indicated. Projected holes denoted by dashed lines. Trace of projected angle holes shown in Section E-E' (see notes 1 and 2)

NOTES:

1. Data is projected into plane of Section along approximate local strike of 89° E, except as noted
2. Inclined drill holes shown projected into section E-E' were all based on an angle of 45 degrees
3. Elevations adjusted to trace of bedrock are taken from original drill hole logs for to approximately 2.5 ft.
4. Bedrock is a hard, fractured silty sandstone of the Middle Devonian Mahoning Formation

SCALE IN FEET
VERTICAL AND HORIZONTAL

FSAR REV. 65

SUSQUEHANNA STEAM ELECTRIC STATION
UNITS 1 & 2
FINAL SAFETY ANALYSIS REPORT

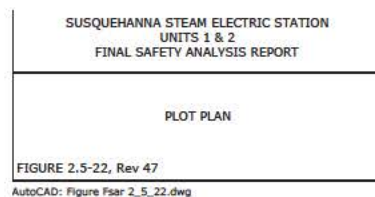
GEOLOGIC SECTION
THROUGH
FOUNDATION EXCAVATIONS

FIGURE 2.5-19, Rev 47

AutoCAD: Figure Fsar_2_5_19.dwg

Security-Related Information

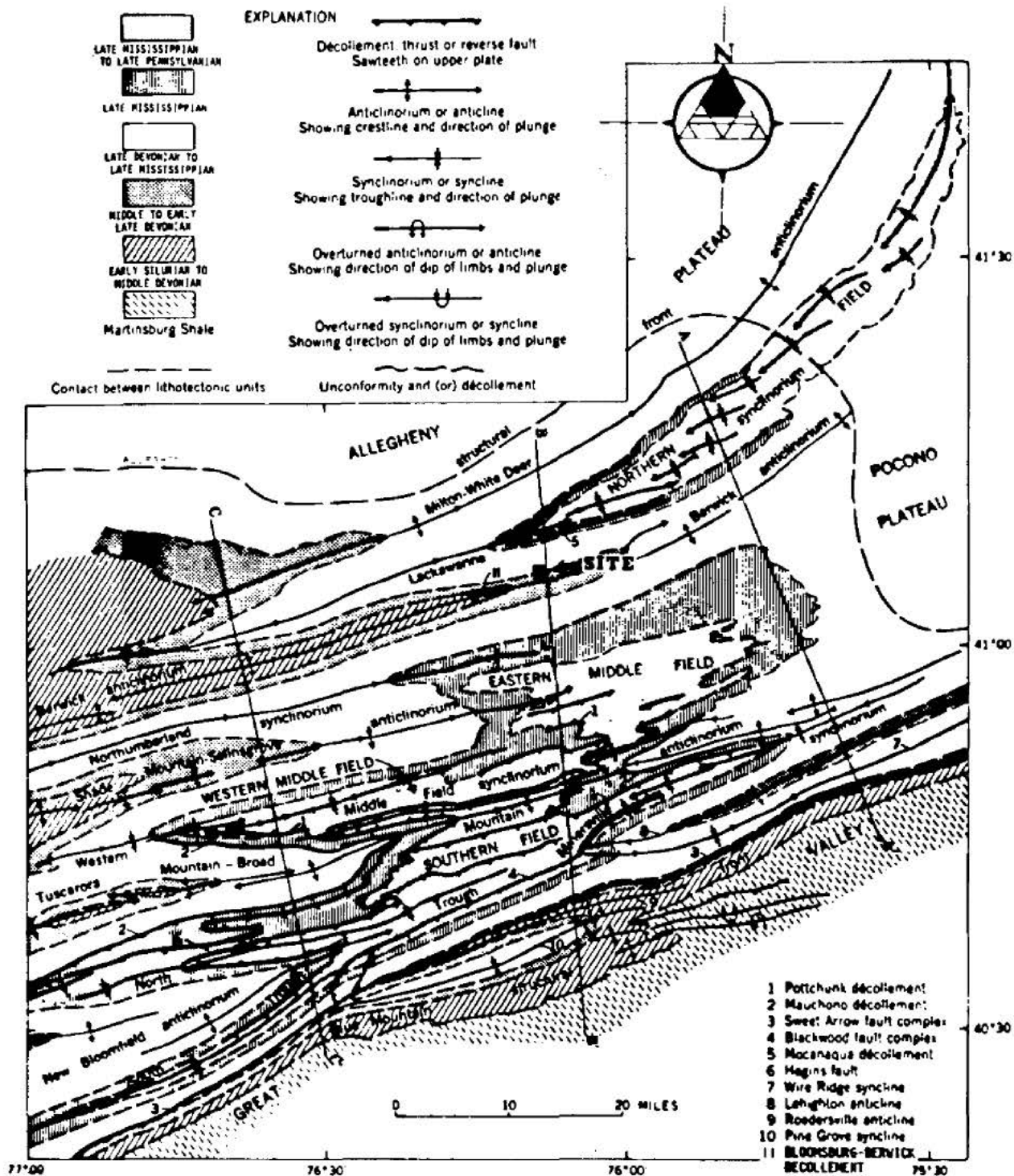
Figure Withheld Under 10 CFR 2.390



Security-Related Information

Figure Withheld Under 10 CFR 2.390

SUSQUEHANNA STEAM ELECTRIC STATION UNITS 1 & 2 FINAL SAFETY ANALYSIS REPORT
FINAL PLANT GRADES
FIGURE 2.5-24, Rev 47 AutoCAD: Figure Fsar 2_5_24.dwg



FSAR REV. 65

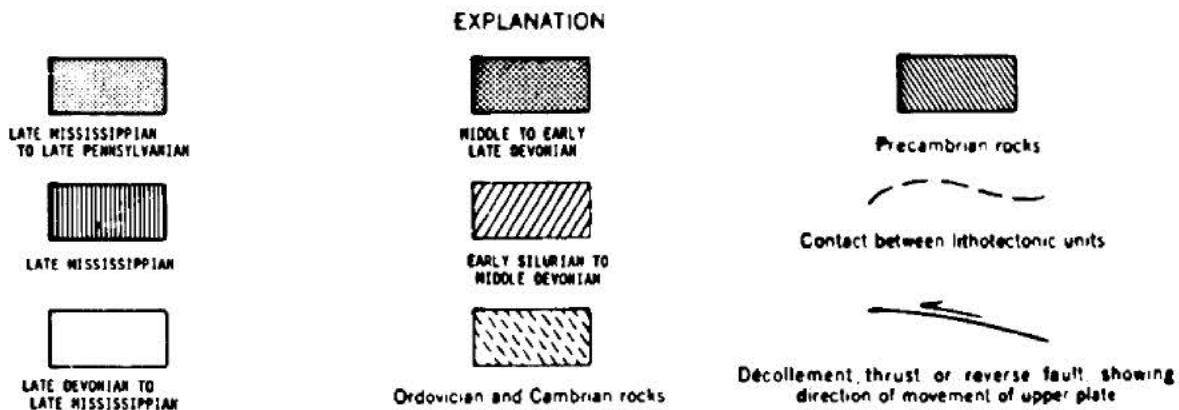
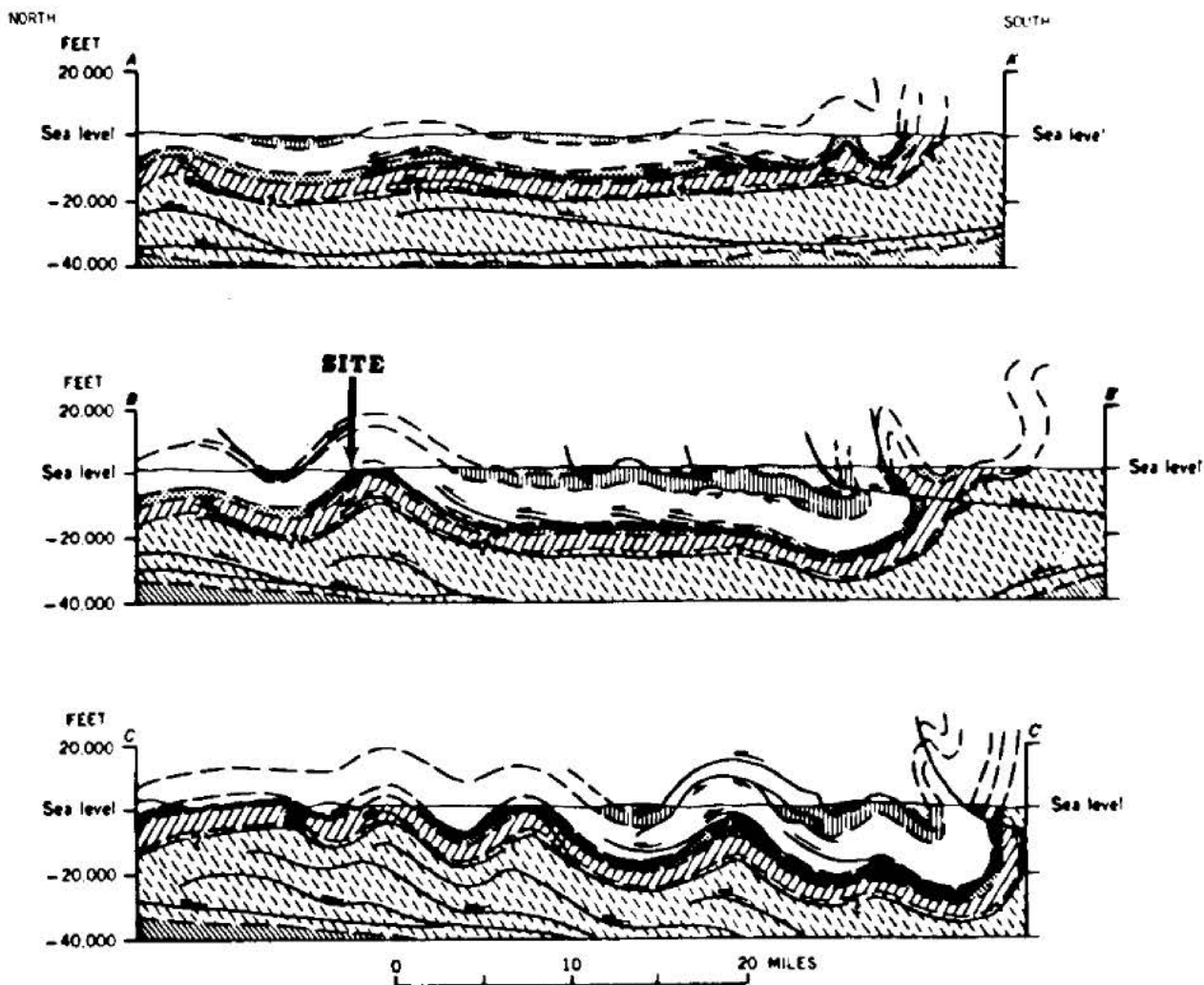
SUSQUEHANNA STEAM ELECTRIC STATION
UNITS 1 & 2
FINAL SAFETY ANALYSIS REPORT

TECTONIC MAP OF
ANTHRACITE REGION

FIGURE 2.5-25, Rev 47

AutoCAD: Figure Fsar 2_5_25.dwg

REPRODUCED WITH PERMISSION FROM STUDIES OF
APPALACHIAN GEOLOGY CENTRAL AND SOUTHERN:
JOHN WILEY AND SONS, 1970.



REPRODUCED WITH PERMISSION FROM STUDIES OF APPALACHIAN GEOLOGY CENTRAL AND SOUTHERN: JOHN WILEY AND SONS, 1970.

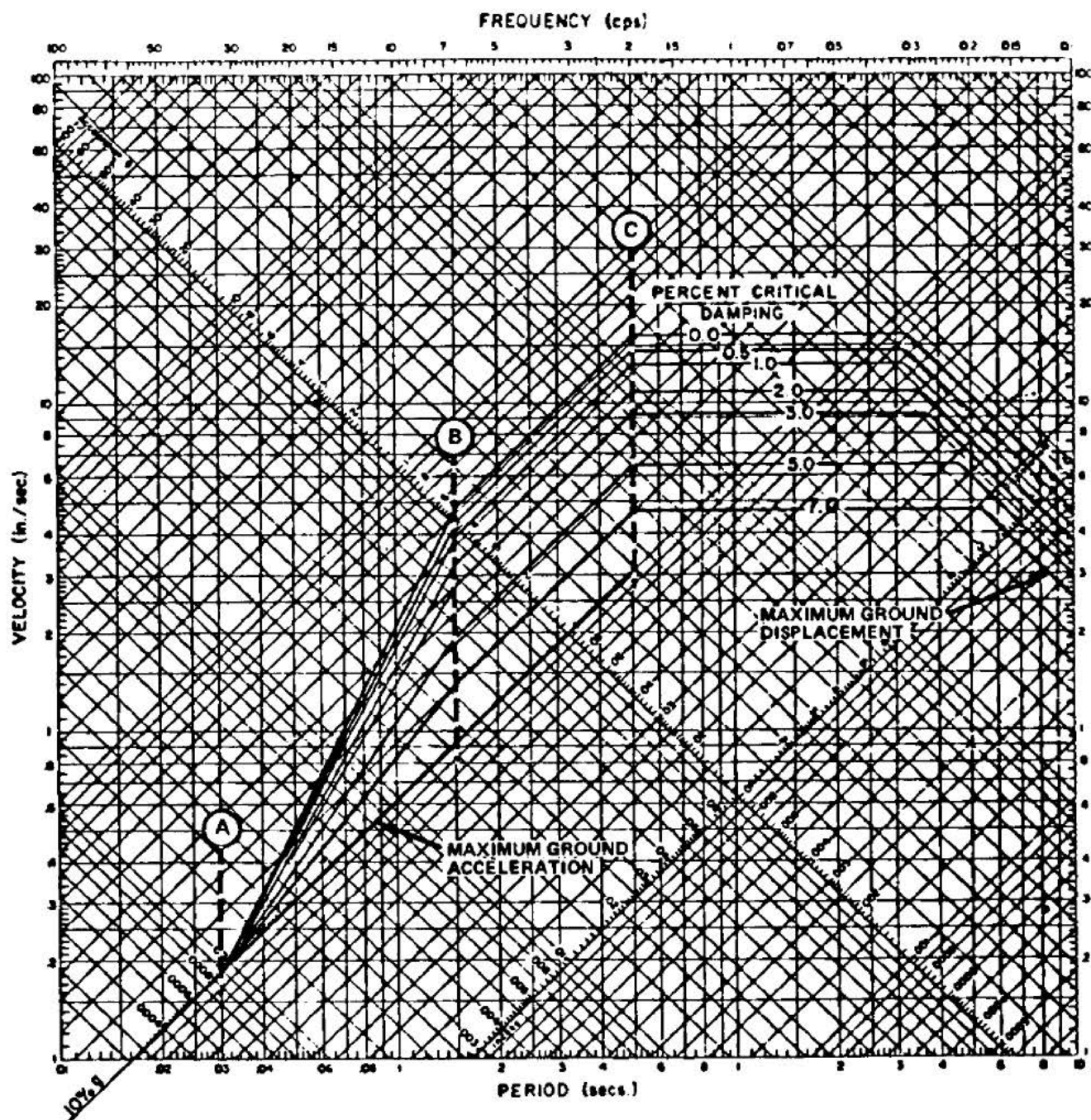
FSAR REV. 65

SUSQUEHANNA STEAM ELECTRIC STATION
UNITS 1 & 2
FINAL SAFETY ANALYSIS REPORT

GEOLOGIC SECTION OF
ANTHRACITE REGION

FIGURE 2.5-26, Rev 47

AutoCAD: Figure Fsar 2_5_26.dwg



* FOR ALL ROCK FOUNDED SEISMIC CATEGORY I
STRUCTURES EXCEPT THE DIESEL GENERATOR 'E' BUILDING.
FOR THE DIESEL GENERATOR 'E' BUILDING SEE FIGURE 3.7B-2A.

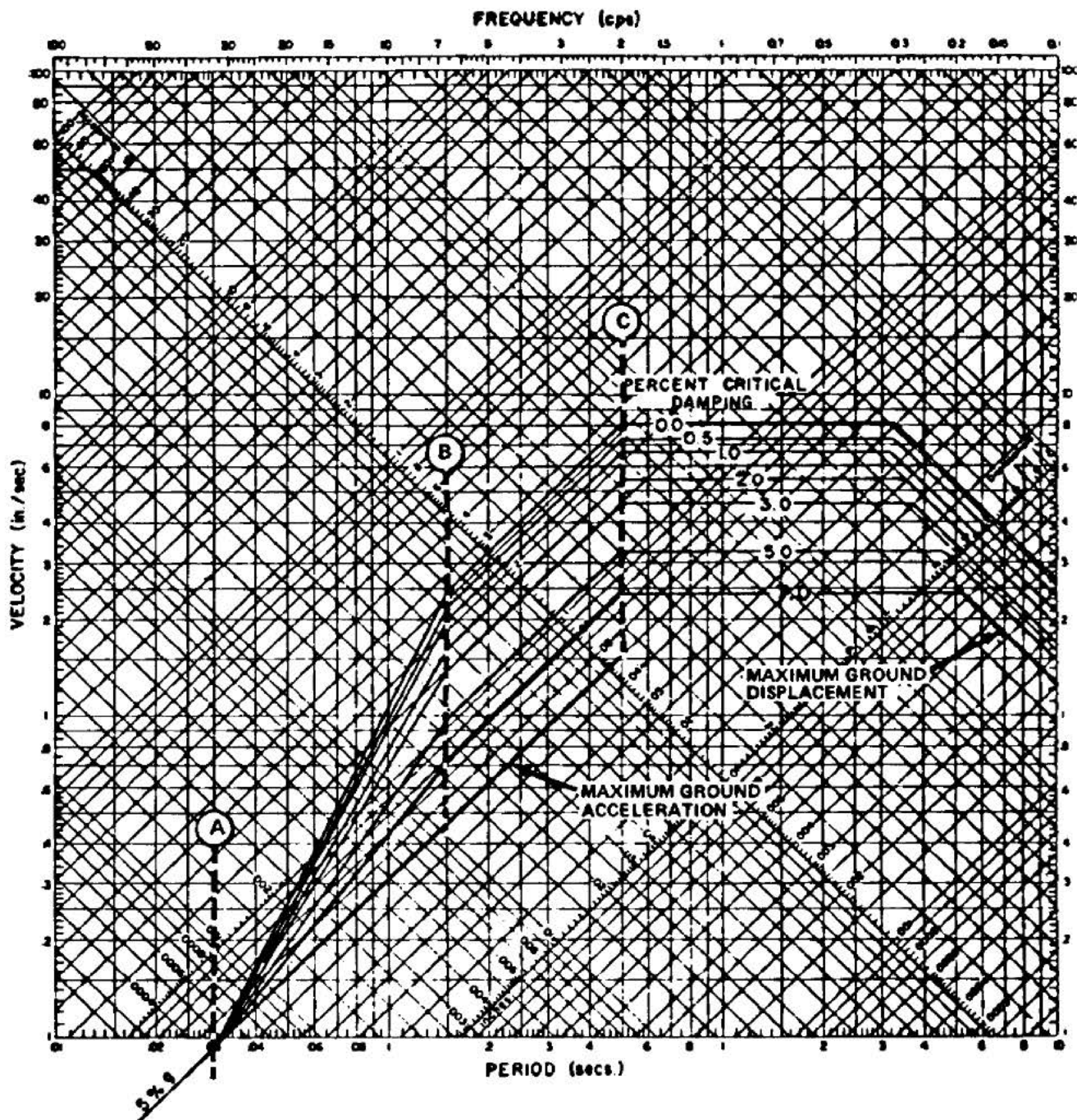
FSAR REV. 65

SUSQUEHANNA STEAM ELECTRIC STATION
UNITS 1 & 2
FINAL SAFETY ANALYSIS REPORT

DESIGN RESPONSE SPECTRA-
SAFE SHUTDOWN EARTHQUAKE
HORIZONTAL COMPONENT

FIGURE 2.5-27, Rev 47

AutoCAD: Figure Fsar 2_5_27.dwg



* FOR ALL ROCK FOUNDED SEISMIC CATEGORY I
STRUCTURES EXCEPT THE DIESEL GENERATOR 'E' BUILDING.
FOR THE DIESEL GENERATOR 'E' BUILDING SEE FIGURE 3.7B-1A.

FSAR REV. 65

SUSQUEHANNA STEAM ELECTRIC STATION
UNITS 1 & 2
FINAL SAFETY ANALYSIS REPORT

DESIGN RESPONSE SPECTRA -
OPERATING BASIS
EARTHQUAKE

FIGURE 2.5-28, Rev 47

AutoCAD: Figure Fsar 2_5_28.dwg

Security-Related Information

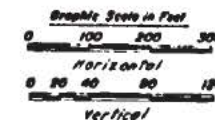
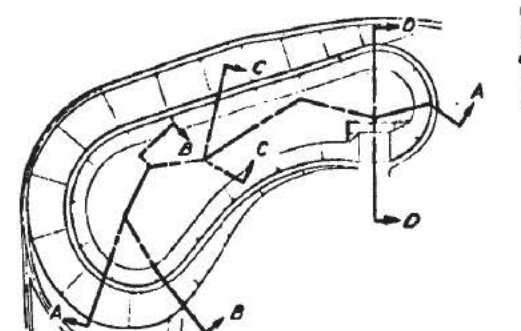
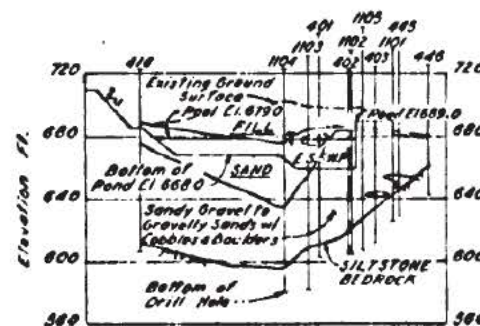
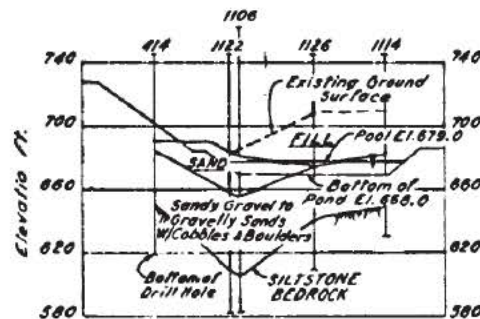
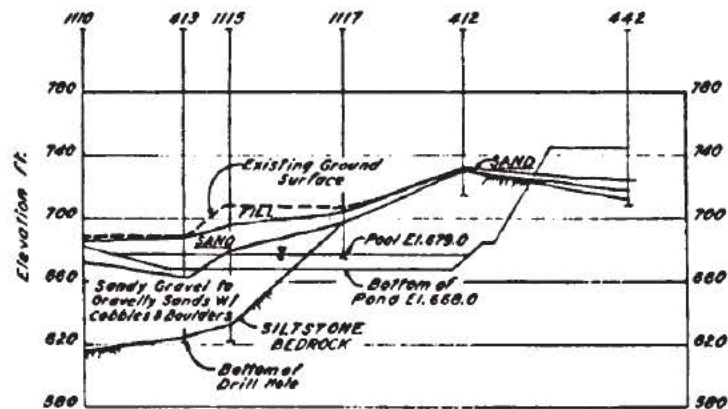
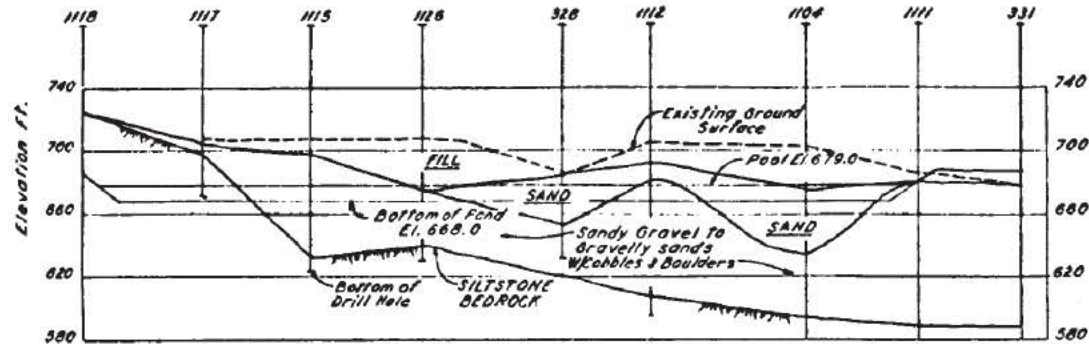
Figure Withheld Under 10 CFR 2.390

FSAR REV. 65

SUSQUEHANNA STEAM ELECTRIC STATION UNITS 1 & 2 FINAL SAFETY ANALYSIS REPORT
GEOPHYSICAL SURVEYS

FIGURE 2.5-29, Rev 47

AutoCAD: Figure Fsar 2_5_29.dwg



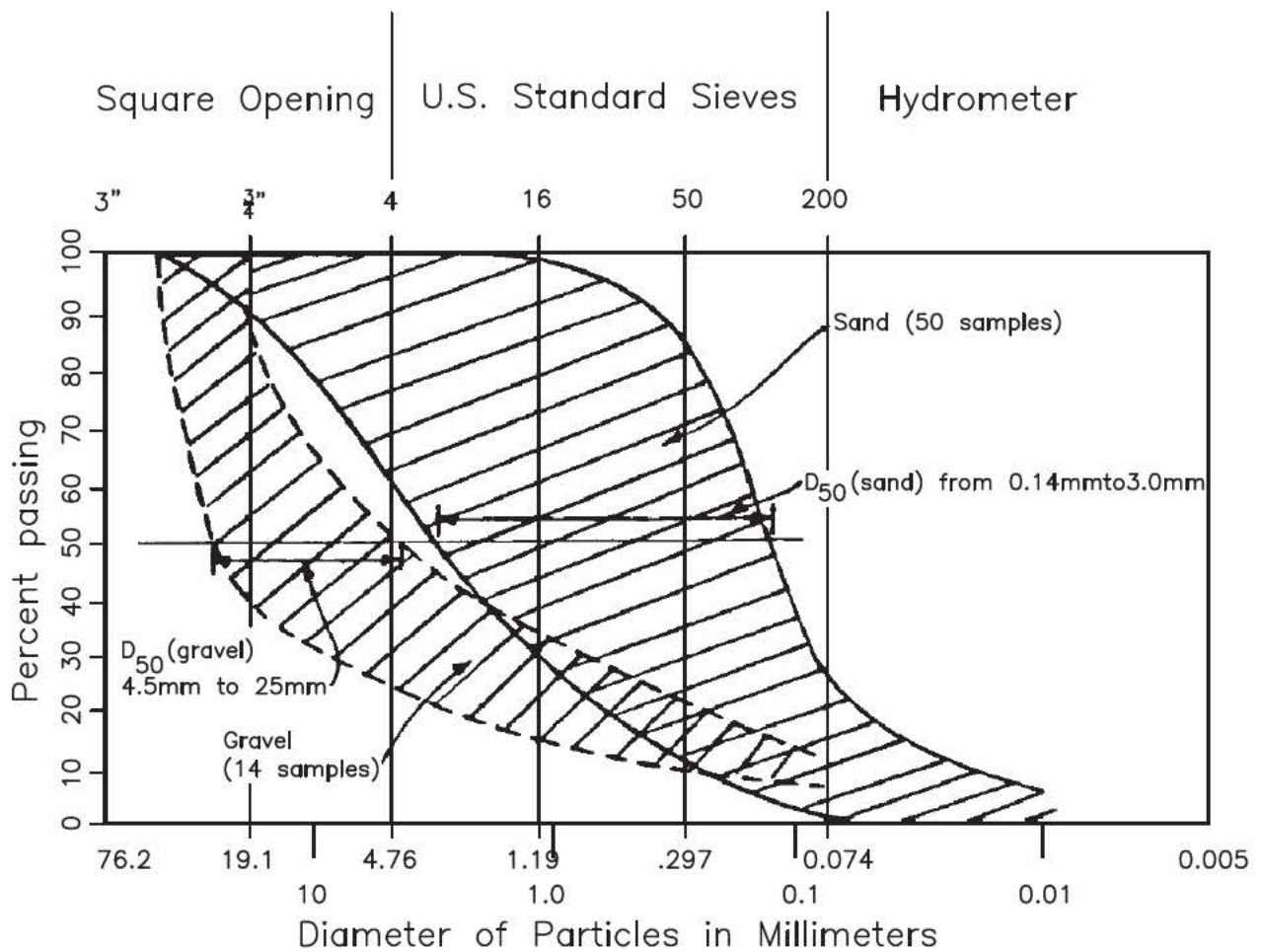
FSAR REV. 65

SUSQUEHANNA STEAM ELECTRIC STATION
UNITS 1 & 2
FINAL SAFETY ANALYSIS REPORT

SPRAY POND, GENERALIZED
CROSS SECTIONS

FIGURE 2.5-30, Rev 47

AutoCAD: Figure Fsar 2_5_30.dwg



Gravel		Gravel			Silt to Clay
Coarse	Fine	Coarse	Medium	Fine	

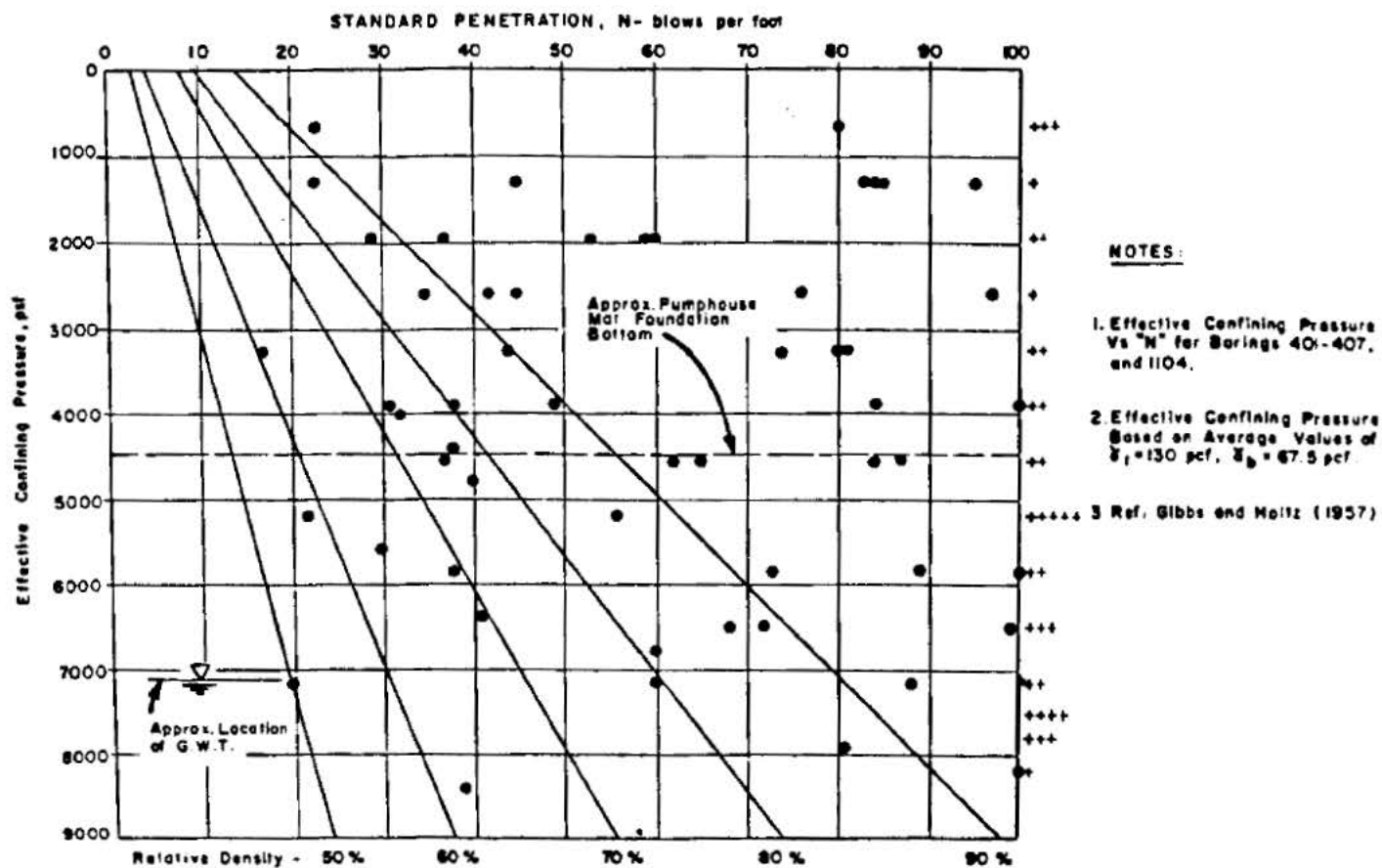
FSAR REV. 65

SUSQUEHANNA STEAM ELECTRIC STATION
UNITS 1 & 2
FINAL SAFETY ANALYSIS REPORT

SPRAY POND,
RANGE OF GRAIN
SIZE CURVES

FIGURE 2.5-31, Rev 47

AutoCAD: Figure Fsar 2_5_31.dwg



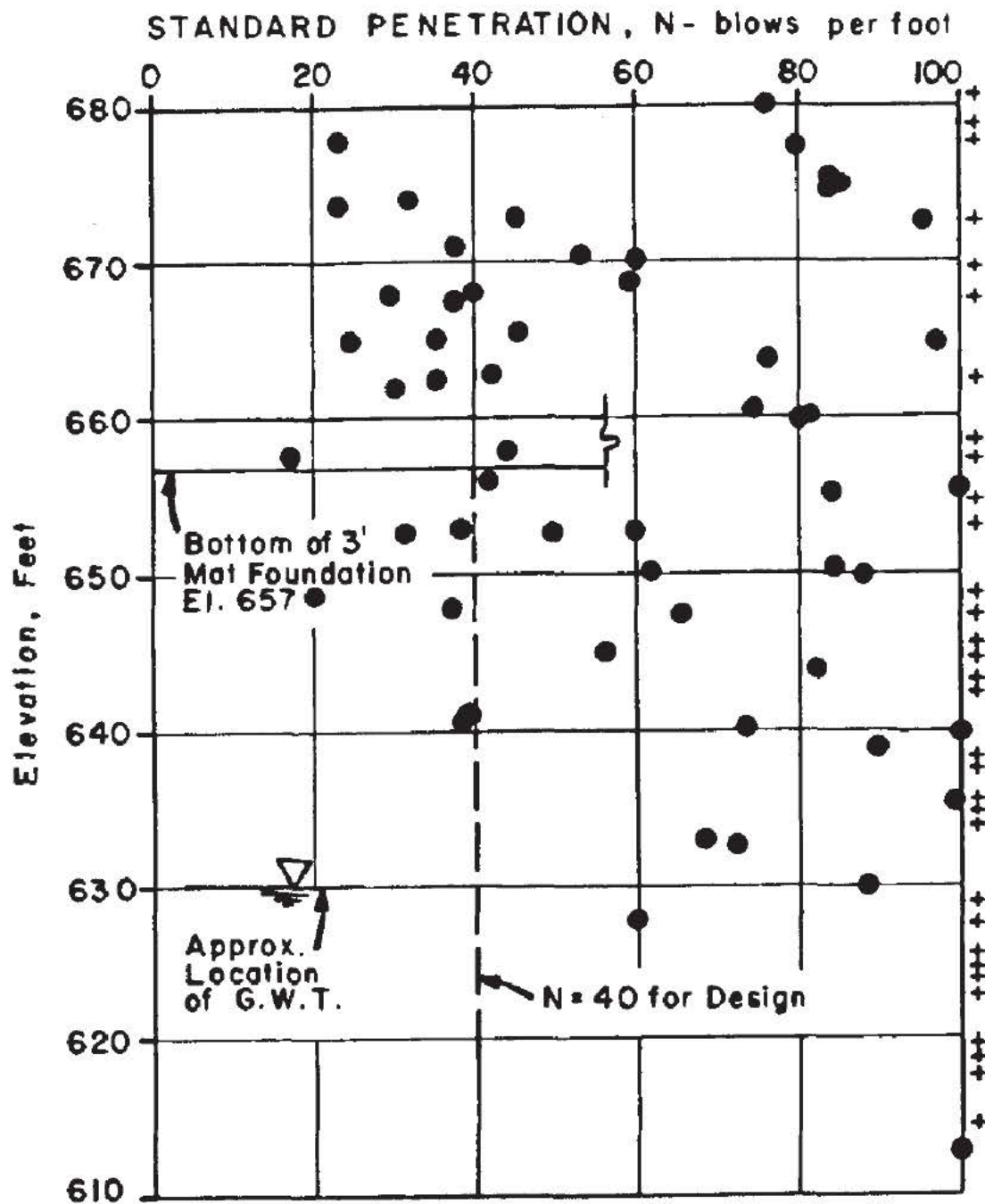
FSAR REV. 65

SUSQUEHANNA STEAM ELECTRIC STATION
UNITS 1 & 2
FINAL SAFETY ANALYSIS REPORT

RELATIVE DENSITY RELATED
TO N VALUE AT
ESSW PUMPHOUSE SITE

FIGURE 2.5-32, Rev 47

AutoCAD: Figure Fsar 2_5_32.dwg



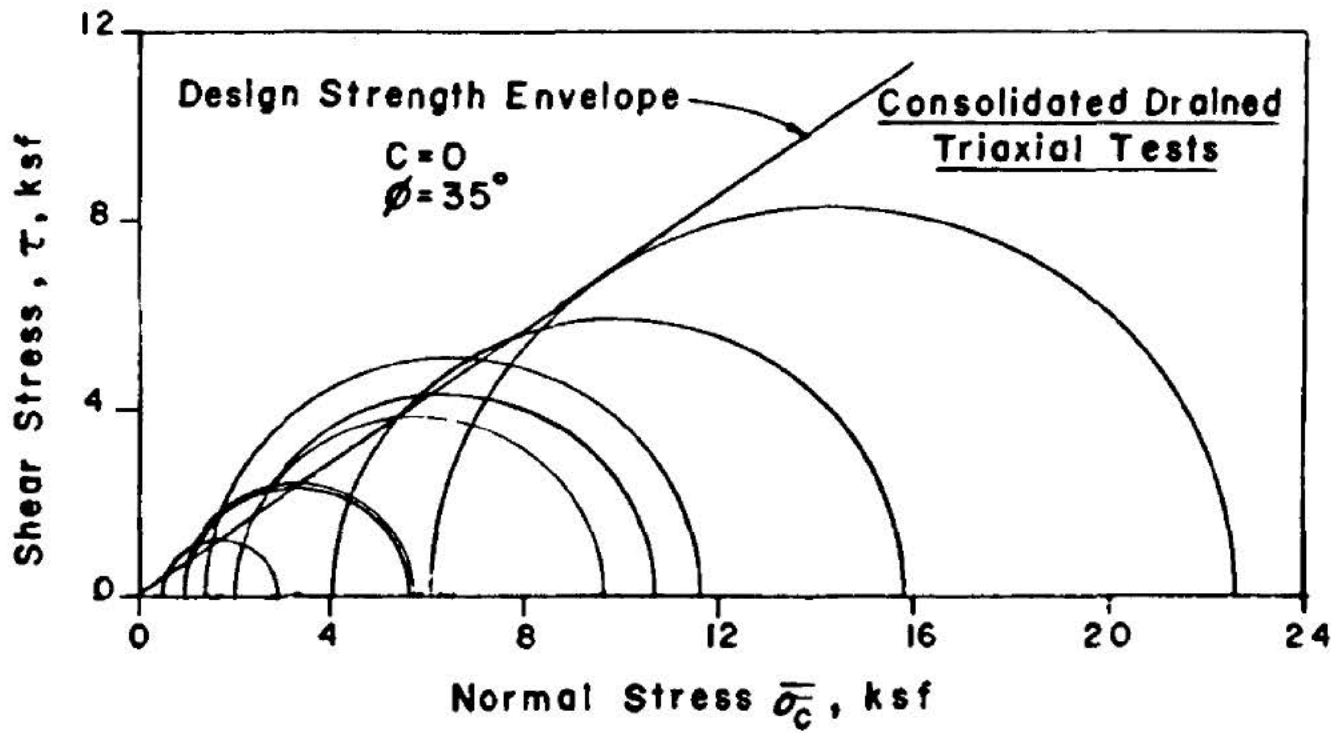
FSAR REV. 65

SUSQUEHANNA STEAM ELECTRIC STATION
UNITS 1 & 2
FINAL SAFETY ANALYSIS REPORT

"N" VALUE VERSUS
ELEVATION AT ESSW PUMPHOUSE SITE

FIGURE 2.5-33, Rev 47

AutoCAD: Figure Fsar 2_5_33.dwg



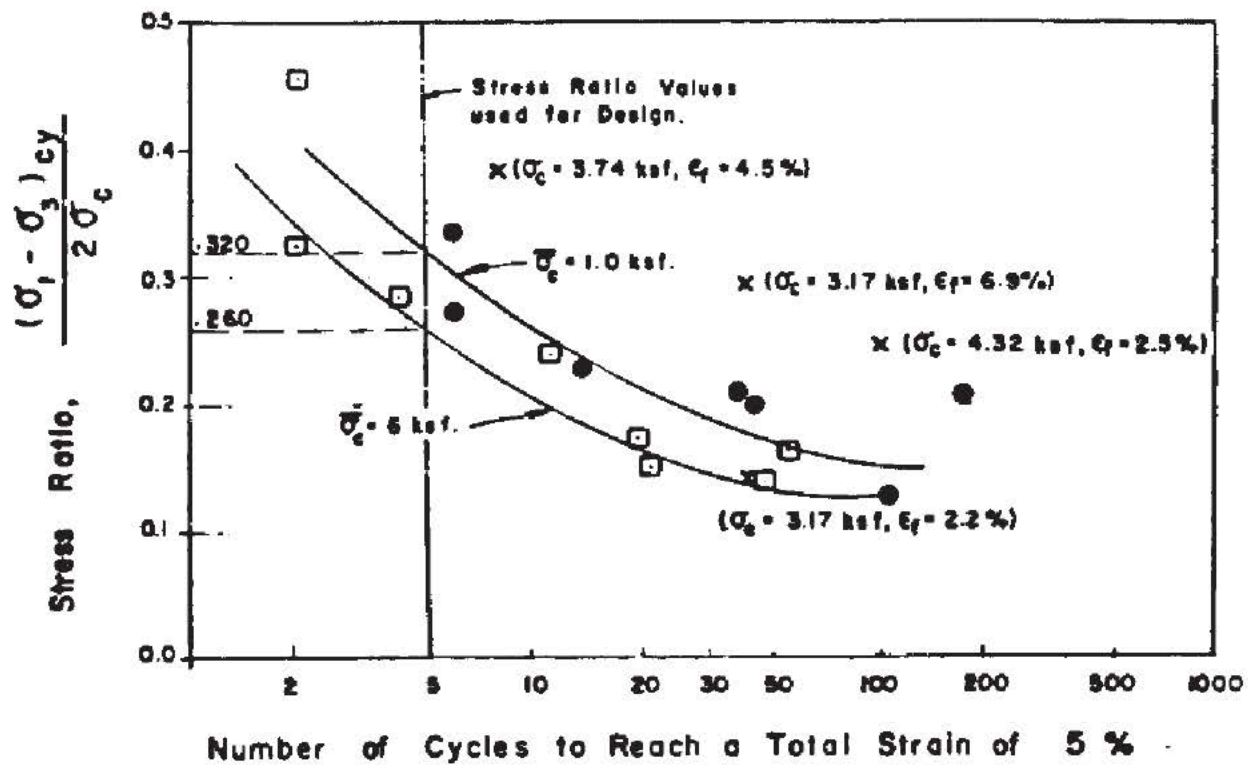
FSAR REV. 65

SUSQUEHANNA STEAM ELECTRIC STATION
UNITS 1 & 2
FINAL SAFETY ANALYSIS REPORT

SPRAY POND,
CONSOLIDATED DRAINED TRIAXIAL
TEST - MOHR CIRCLE DIAGRAM

FIGURE 2.5-34, Rev 47

AutoCAD: Figure Fsar 2_5_34.dwg



LEGEND

□ Undisturbed Test @ $\bar{\sigma}_c = 5 \text{ ksf}$

● Undisturbed Test @ $\bar{\sigma}_c = 1 \text{ ksf.}$

$\bar{\sigma}_c$ = Effective Consolidation Pressure

$(\sigma_1 - \sigma_3)_{cy}$ = Cyclic Deviator Stress.

× Test conducted by Dames & Moore with confining pressure ($\bar{\sigma}_c$) and failure strain (ϵ_f) shown in the parentheses

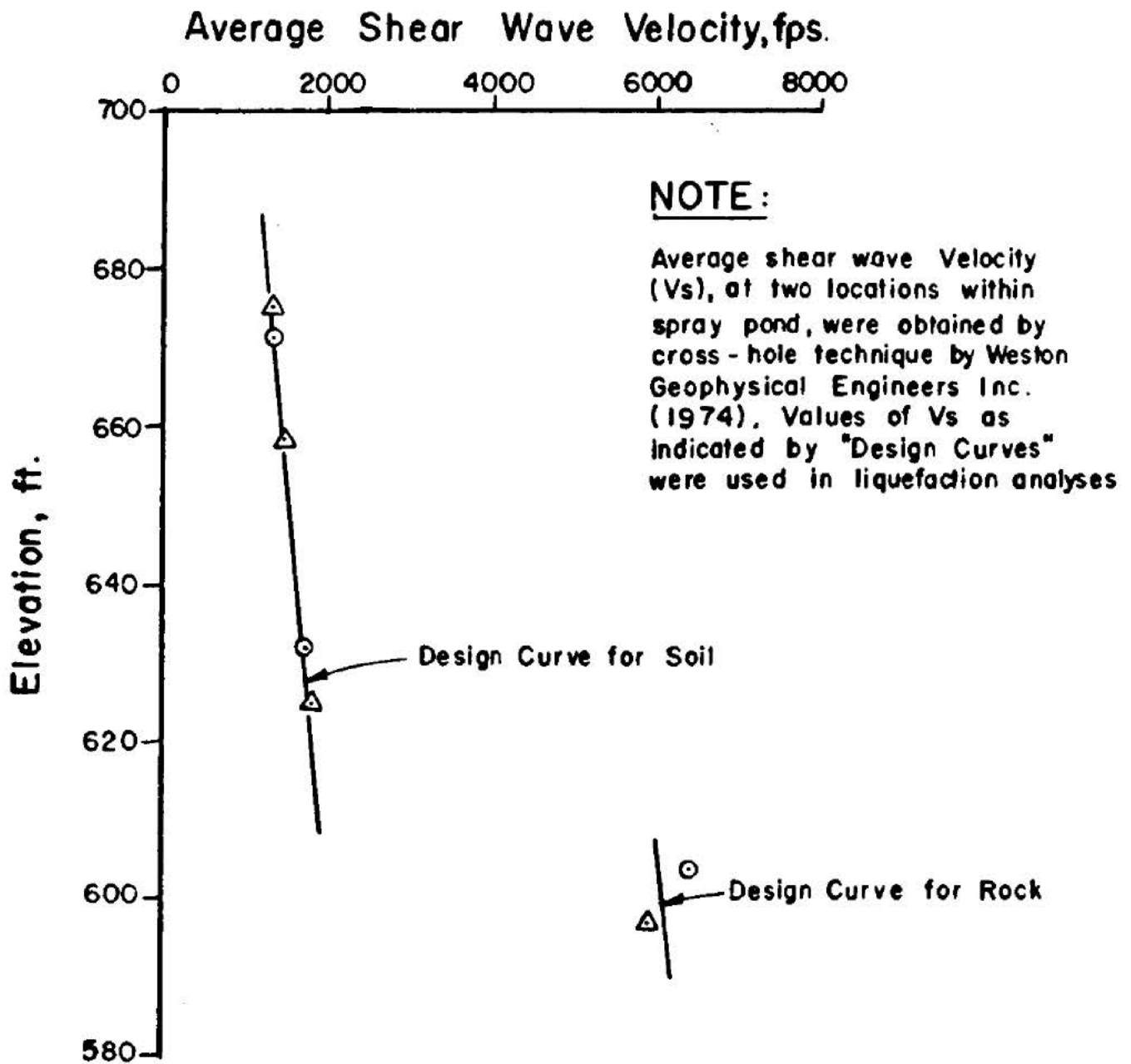
FSAR REV. 65

SUSQUEHANNA STEAM ELECTRIC STATION
UNITS 1 & 2
FINAL SAFETY ANALYSIS REPORT

SPRAY POND,
SUMMARY OF CYCLIC SHEAR TEST RESULTS

FIGURE 2.5-35, Rev 47

AutoCAD: Figure Fsar 2_5_35.dwg



LEGEND

- Boreholes 1101 - 1105
- △ Boreholes 1106 - 1110

FSAR REV. 65

SUSQUEHANNA STEAM ELECTRIC STATION
UNITS 1 & 2
FINAL SAFETY ANALYSIS REPORT

SPRAY POND,
SHEAR WAVE VELOCITY
DESIGN CURVES

FIGURE 2.5-36, Rev 47

AutoCAD: Figure Fsar 2_5_36.dwg

Security-Related Information

Figure Withheld Under 10 CFR 2.390

SUSQUEHANNA STEAM ELECTRIC STATION
UNITS 1 & 2
FINAL SAFETY ANALYSIS REPORT

LOCATION AND LIMITS OF
EXCAVATION FILL AND BACKFILL
FOR CLASS 1 STRUCTURES

FIGURE 2 5-37, Rev 47

AutoCAD: Figure Fsar 2_5_37.dwg

EXPLANATION

610 Contours for estimated ground water table, incorporating seepage loss from spray pond having liner such that seepage loss does not exceed 1.2×10^3 gallons in 30 days.

600 Water table contours in the pond site area are based on measurements taken on June 30, 1971. Measurements in the pond area were taken on August 6, 1974.

E E Location of section line.

60 Contour on top of rock (see note 2); contour interval 10 feet.

Bedrock outcrop; may include minor amounts of talus or overburden. Boundaries are approx.

Exploration hole; vertical hole (left) and angle hole showing trace of hole projected to surface (right).

Exploration hole utilized for water level observation.

Exploration hole used for permeability measurements.

Water well (used for construction).

Test pits.

Spray pond ground water observation well.

Systems Category I facilities

Category I structure.

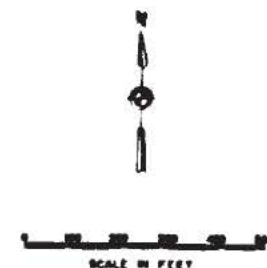
Category I pipeline.

Category I impoundment.

NOTES:

1. Screened topographic base shows preconstruction terrain. Contour interval 10 feet.

2. Top-of-rock contours show original top of rock surface based on interpretation of drill hole and seismic refraction data, modified, where appropriate, by information obtained during construction. Contours north of town road T-419 are not shown.



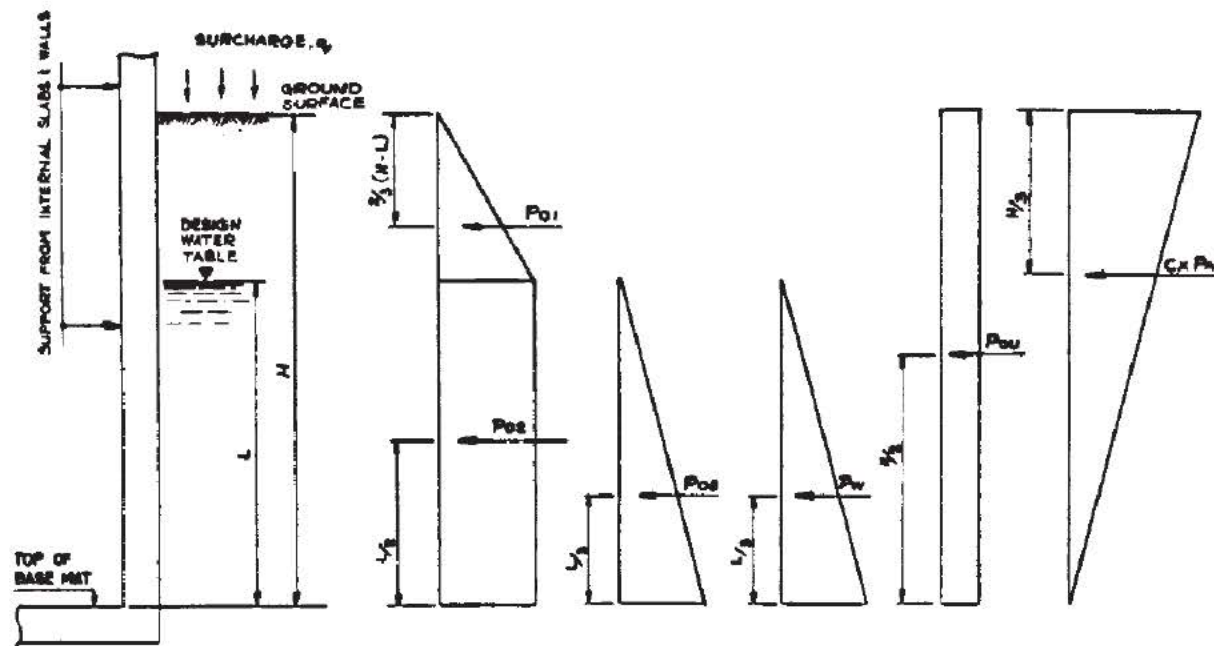
FSAR REV. 65

SUSQUEHANNA STEAM ELECTRIC STATION
UNITS 1 & 2
FINAL SAFETY ANALYSIS REPORT

LOCATION OF SPRAY POND
WITH CONTOURS ON TOP OF
ROCK AND WATER TABLE

FIGURE 2.5-38, Rev 47

AutoCAD: Figure Fsar 2_5_38.dwg



NOTES:

P_{o1} , P_{o2} , P_{o3} = THRUST RESULTING FROM SOIL IN THE "AT REST" STATE
 P_w = THRUST RESULTING FROM HYDROSTATIC PRESSURE
 P_{o4} = THRUST RESULTING FROM SURCHARGE PRESSURE
 P_{o5} = THRUST RESULTING FROM DYNAMIC ACTION OF SOIL & WATER (SEED-WHITMAN FORMULA, 1970)

$$\begin{aligned}
 P_{o1} &= \frac{1}{2} K_o \gamma_b (H-L)^2 \\
 P_{o2} &= K_o \gamma_b (H-L) L \\
 P_{o3} &= \frac{1}{2} K_o \gamma_b' L^2 \\
 P_w &= \frac{1}{2} \gamma_w L^2 \\
 P_{o4} &= K_o q_s H \\
 P_{o5} &= \frac{1}{2} \gamma_b H^2 K_h
 \end{aligned}$$

WHERE:

K_o = COEFFICIENT OF EARTH PRESSURE "AT REST" - 0.70
 γ_b = BULK UNIT WEIGHT - 125 p.c.f.
 γ_b' = BUOYANT UNIT WEIGHT - 77.5 p.c.f.
 γ_s = SATURATED UNIT WEIGHT - 140 p.c.f.
 γ_w = DENSITY OF WATER - 62.5 p.c.f.
 q_s = SURCHARGE PRESSURE - 250 p.c.f.
 K_h = HORIZONTAL ACCELERATION/g
 - 0.05 FOR OBE REACTIVE BUILDINGS
 - 0.10 FOR SSE
 - 0.05 FOR OBE E.S.S.W.
 - 0.15 FOR SSE PUMPHOUSE

C = COEFFICIENT

= 1.0 FOR STRUCTURES ON SOIL
 & 3.0 FOR STRUCTURES ON ROCK

SECTION THROUGH EXTERNAL WALL

SOIL AND WATER PRESSURE DIAGRAM

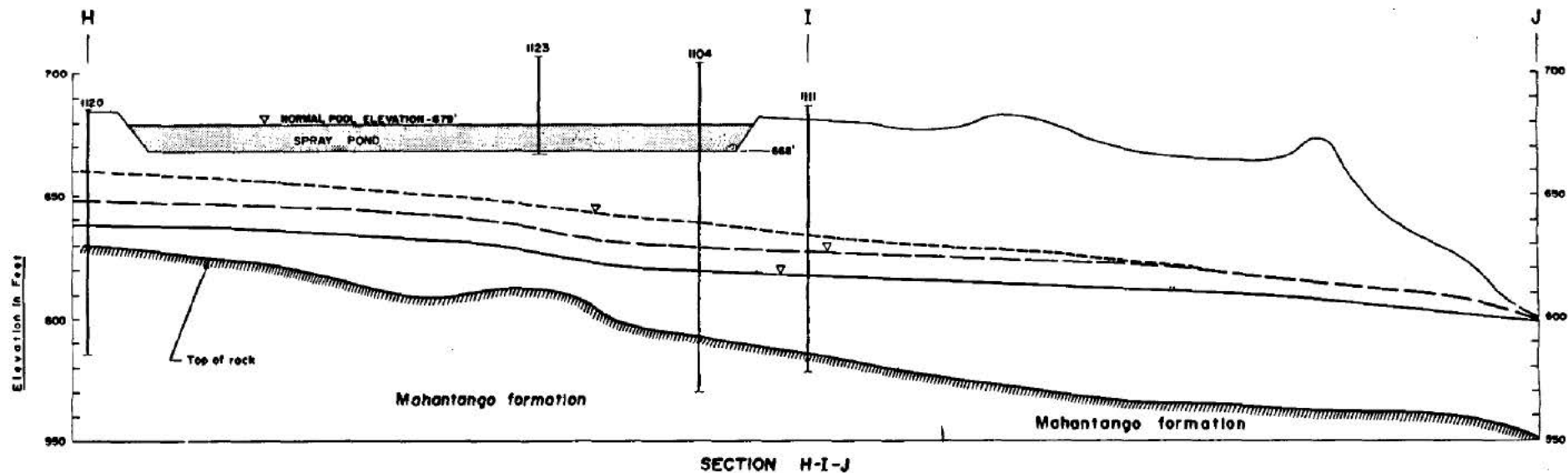
FSAR REV. 65

SUSQUEHANNA STEAM ELECTRIC STATION
 UNITS 1 & 2
 FINAL SAFETY ANALYSIS REPORT

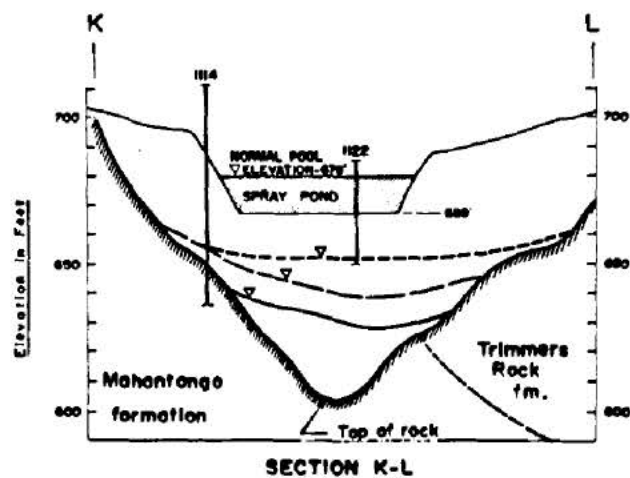
LATERAL SOIL PRESSURE DIAGRAMS

FIGURE 2.5-39, Rev 47

AutoCAD: Figure Fsar 2_5_39.dwg



0 100 200 300
HORIZONTAL SCALE IN FEET



EXPLANATION

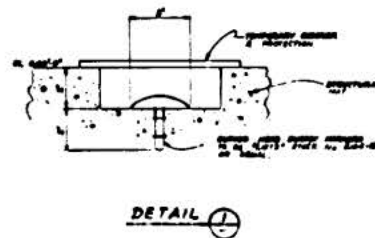
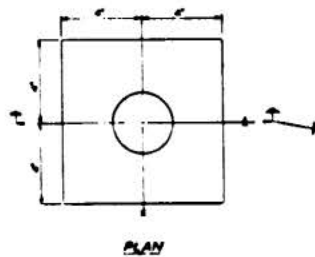
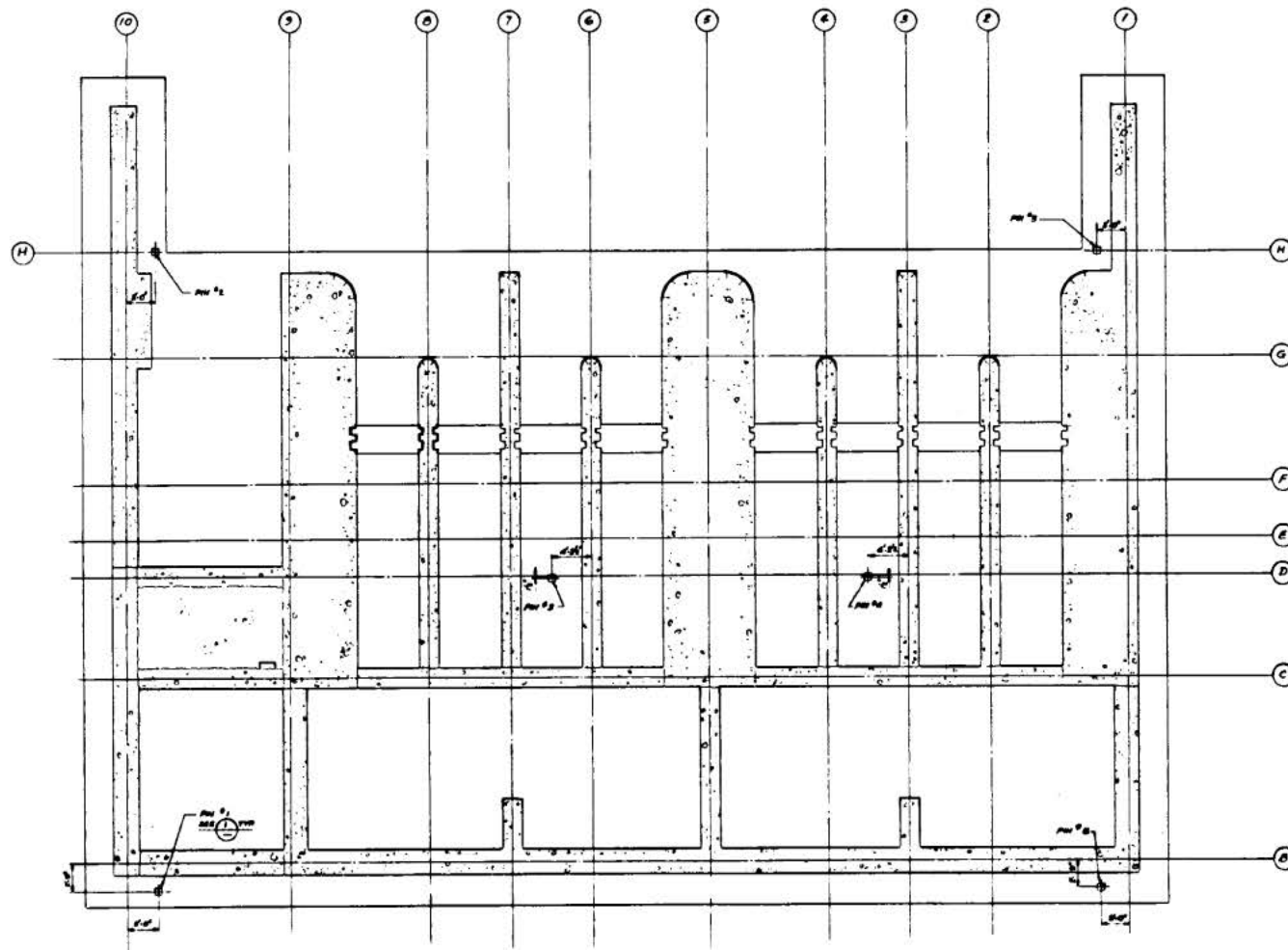
- Top of rock
- Undisturbed water table measured on 8-6-74
- Normal operating water level elevation assuming fluctuation of 10 ft. above measured water table level on 8-6-74
- Estimated ground water table, incorporating seepage loss from spray pond having WTR such that seepage loss does not exceed 1.2×10^6 gallons in 30 days
- Exploration drill hole

FSAR REV. 65

SUSQUEHANNA STEAM ELECTRIC STATION
UNITS 1 & 2
FINAL SAFETY ANALYSIS REPORT

SPRAY POND
MEASURED & PROJECTED
WATER LEVELS

FIGURE 2.5-40, Rev 47



FSAR REV. 65

SUSQUEHANNA STEAM ELECTRIC STATION
UNITS 1 & 2
FINAL SAFETY ANALYSIS REPORT

DETAILS OF SETTLEMENT PINS
CAST IN ESSW PUMPHOUSE BASEMAT

FIGURE 2.5-41, Rev 47

Security-Related Information

Figure Withheld Under 10 CFR 2.390

SUSQUEHANNA STEAM ELECTRIC STATION UNITS 1 & 2 FINAL SAFETY ANALYSIS REPORT
SPRAY POND, EARTHWORK PLAN
FIGURE 2.5-42, Rev 47 AutoCAD: Figure Fsar 2_5_42.dwg

THIS FIGURE HAS BEEN
REPLACED BY DWG.
C-63, Sh. 1

FSAR REV. 65

SUSQUEHANNA STEAM ELECTRIC STATION UNITS 1 & 2 FINAL SAFETY ANALYSIS REPORT

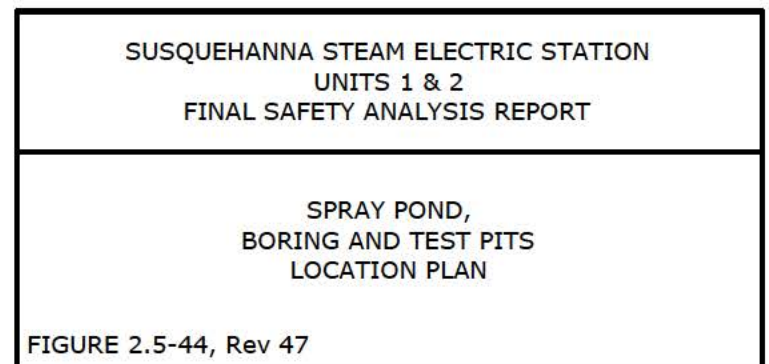
Figure 2.5-43 replaced by dwg. C-63, Sh. 1

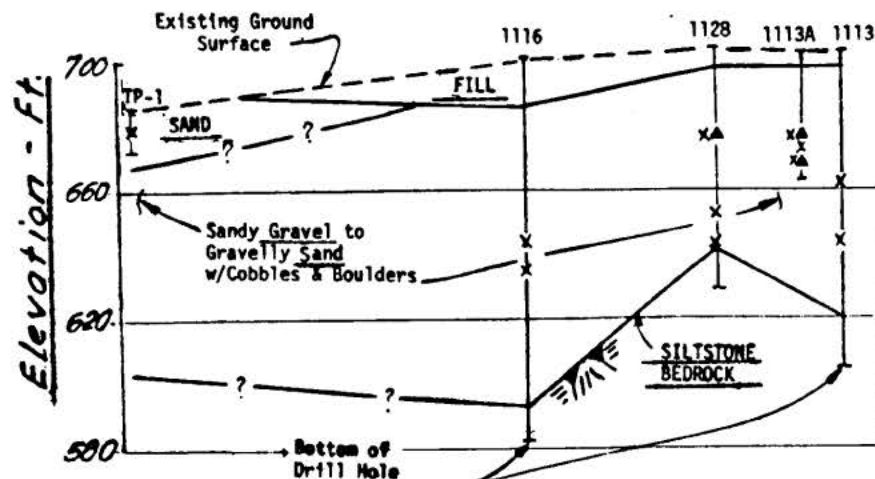
FIGURE 2.5-43, Rev. 48

AutoCAD Figure 2_5_43.doc

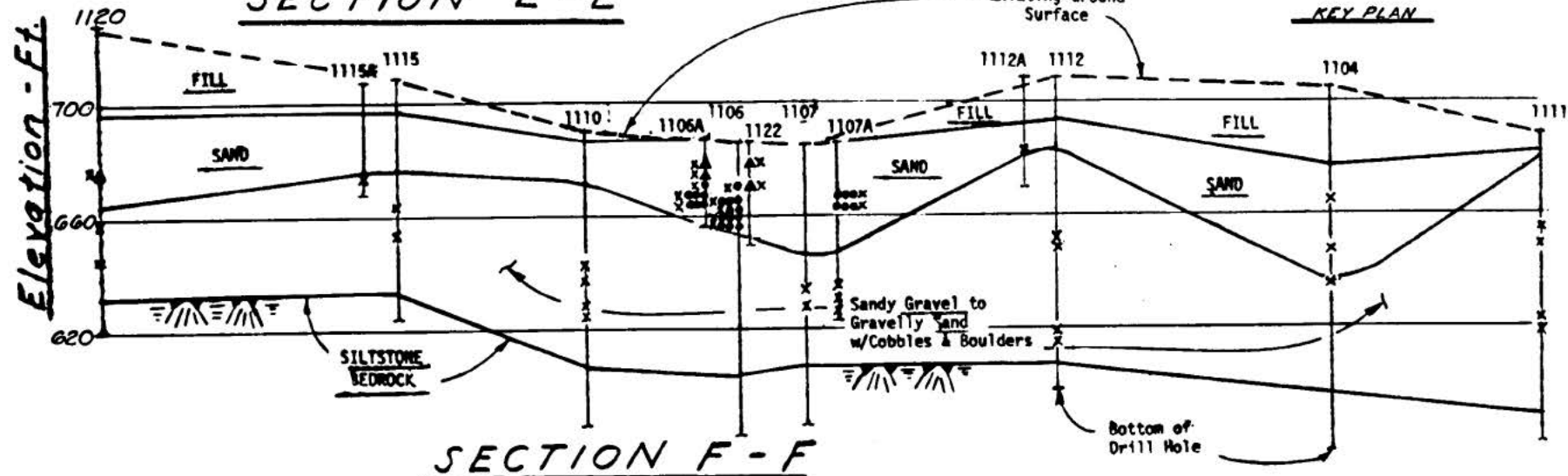
Security-Related Information

Figure Withheld Under 10 CFR 2.390





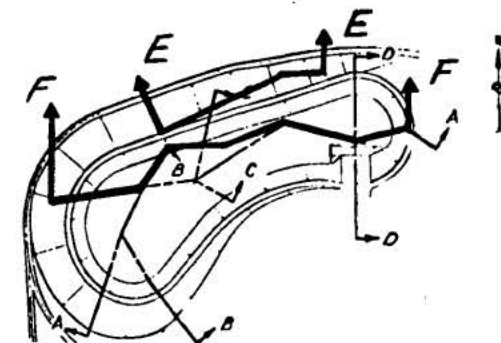
SECTION E-E



SECTION F-F

LEGEND:

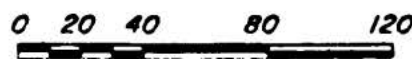
- CR (Cyclic Triaxial Test)
- ▲ S (Consolidated-Drained Triaxial Test)
- X Grain Size Distribution



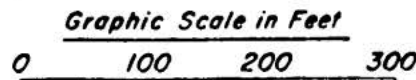
KEY PLAN

NOTES:

1. For details of laboratory tests refer to the Geotechnical Engineers, Inc. Report, dated Oct. 11, 1974. The locations of soil test samples are also shown on the boring logs.
2. Borings with A-designation were drilled adjacent to the borings with the same number. The locations of these borings shown on this drawing are approximate.



Vertical



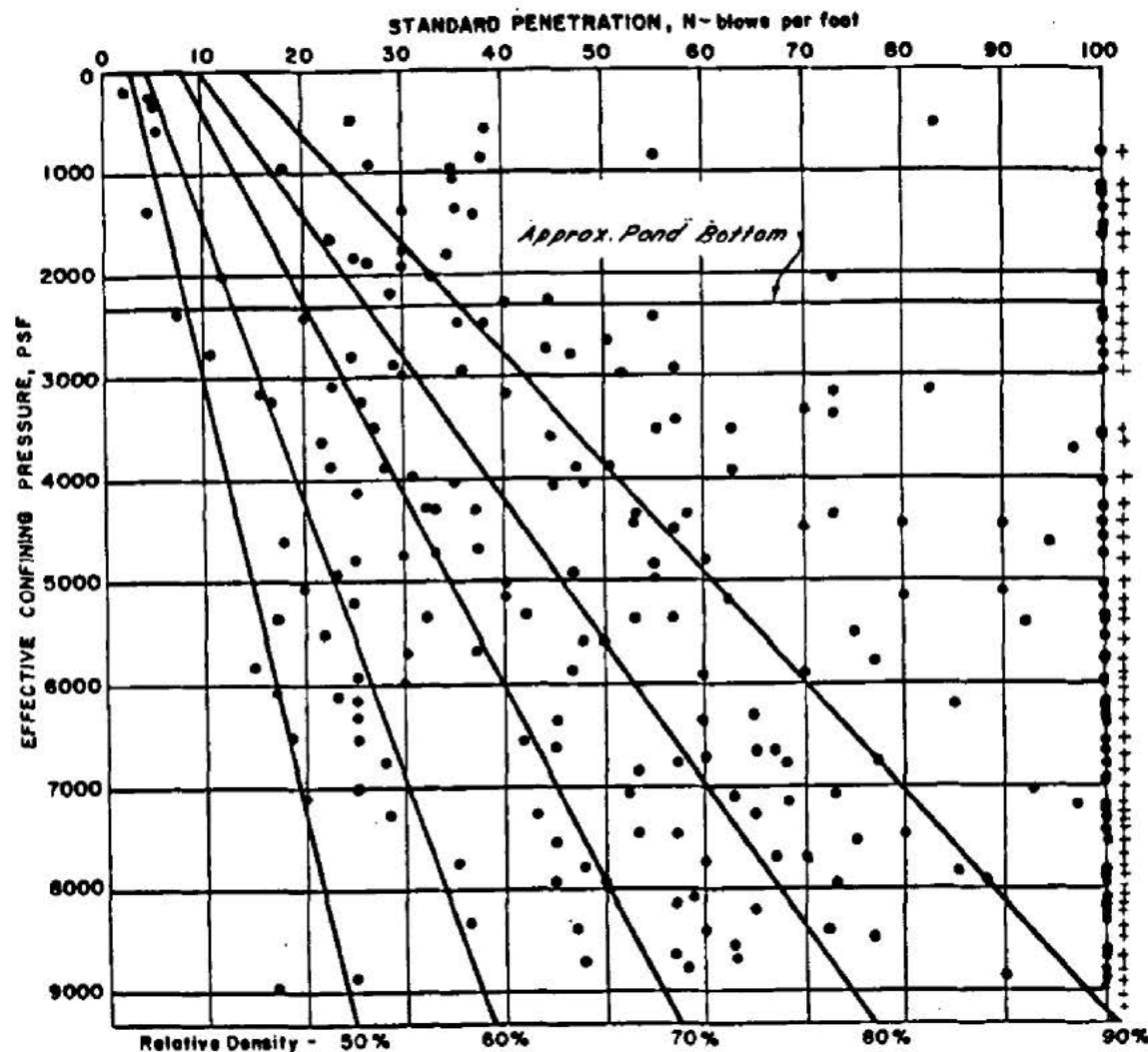
Horizontal

FSAR REV. 65

SUSQUEHANNA STEAM ELECTRIC STATION
UNITS 1 & 2
FINAL SAFETY ANALYSIS REPORT

SPRAY POND, GENERALIZED
CROSS SECTION WITH
LABORATORY TEST LOCATIONS

FIGURE 2.5-45, Rev 47



NOTES:

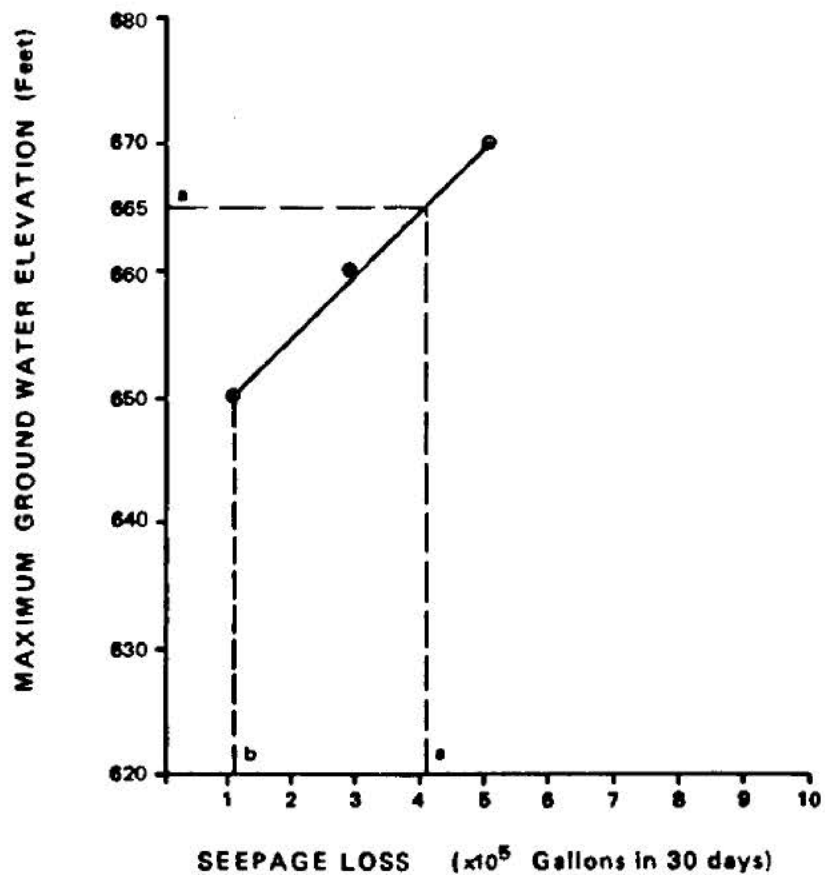
1. Effective Confining Pressure VS. "N" Shown by Symbol •
2. Effective Confining Pressure Based on Average Values of $\delta_c = 130 \text{ pcf}$, $\delta_b = 67.5 \text{ pcf}$.
3. Ref: Gibbs and Holtz (1957)

FSAR REV. 65

SUSQUEHANNA STEAM ELECTRIC STATION
UNITS 1 & 2
FINAL SAFETY ANALYSIS REPORT

SPRAY POND, RELATIVE DENSITY
RELATED TO "N" VALUE

FIGURE 2.5-46, Rev 47



NOTES:

- a. ELEVATION 665 IS THE MAXIMUM GROUND WATER LEVEL AT WHICH THE FACTOR OF SAFETY AGAINST LIQUEFACTION IS AT LEAST 1.2. THIS CORRESPONDS TO A SEEPAGE LOSS OF APPROXIMATELY 4.1×10^5 GALLONS IN 30 DAYS.
- b. THE POND LINER IS DESIGNED TO LIMIT THE SEEPAGE TO LESS THAN 1.2×10^5 GALLONS IN 30 DAYS TO PROVIDE AN ADDITIONAL MARGIN OF SAFETY.

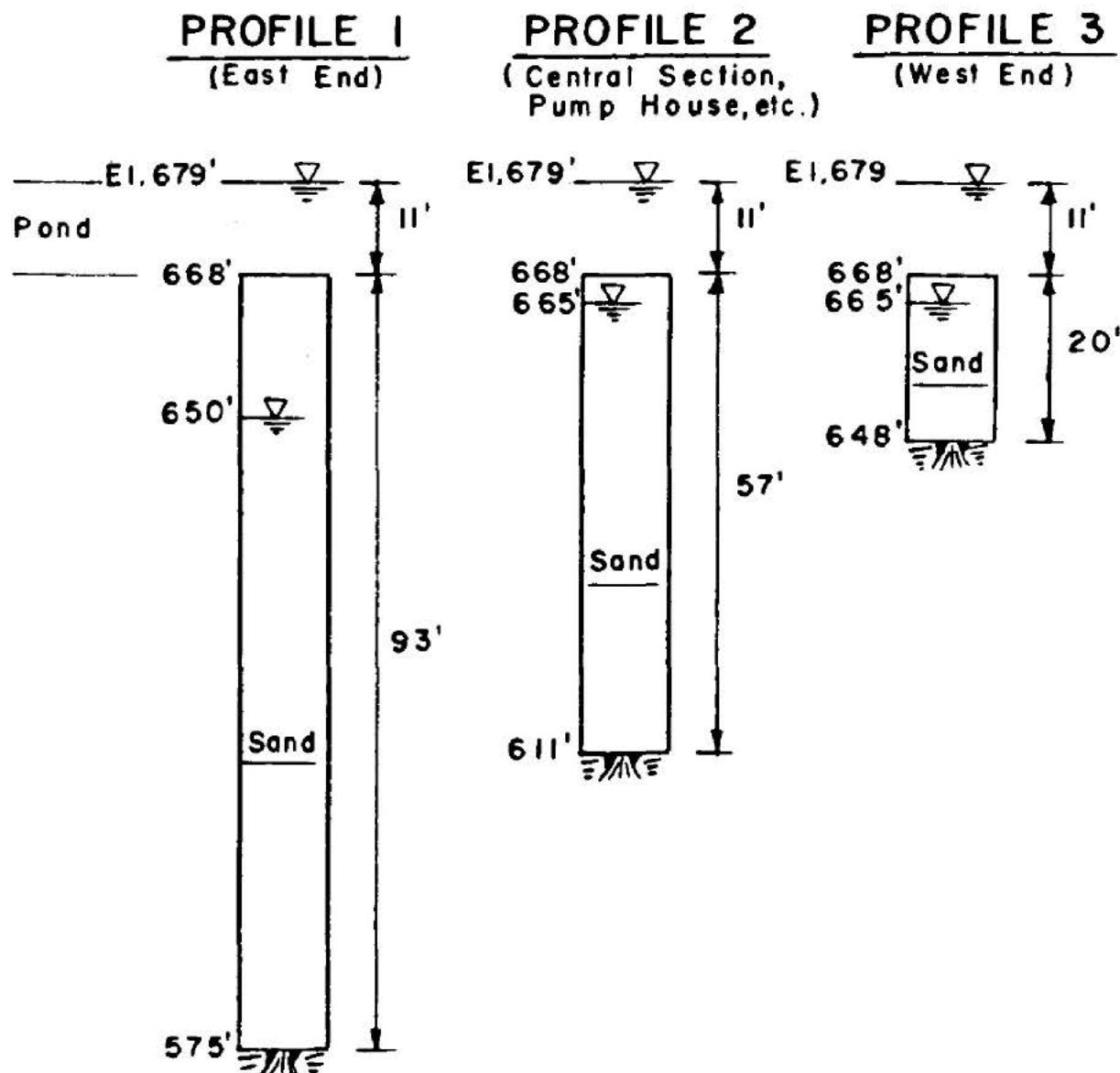
FSAR REV. 65

SUSQUEHANNA STEAM ELECTRIC STATION
UNITS 1 & 2
FINAL SAFETY ANALYSIS REPORT

SPRAY POND,
RELATIONSHIP BETWEEN SEEPAGE
LOSS & MAXIMUM GROUND
WATER ELEVATION

FIGURE 2.5-47, Rev 47

AutoCAD: Figure Fsar 2_5_47.dwg



NOTES:

1. Soil profiles were conservatively assumed to consist only of Sand.
2. Saturated Unit Weight of Sand = 130 pcf
Buoyant Unit Weight of Sand = 67.5 pcf.
3. Ground water tables shown in the profiles are the maximum level used in liquefaction analyses.

FSAR REV. 65

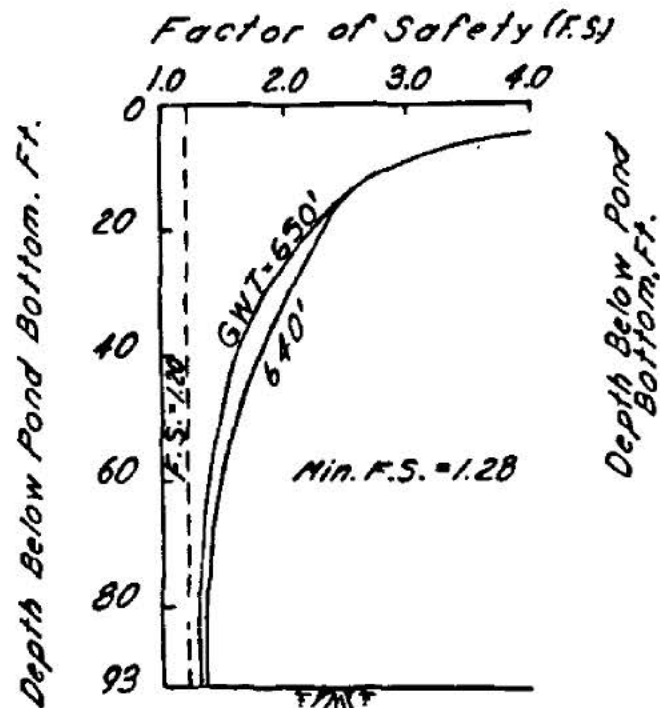
SUSQUEHANNA STEAM ELECTRIC STATION
UNITS 1 & 2
FINAL SAFETY ANALYSIS REPORT

SPRAY POND,
SOIL PROFILES USED IN
LIQUIFICATION ANALYSIS

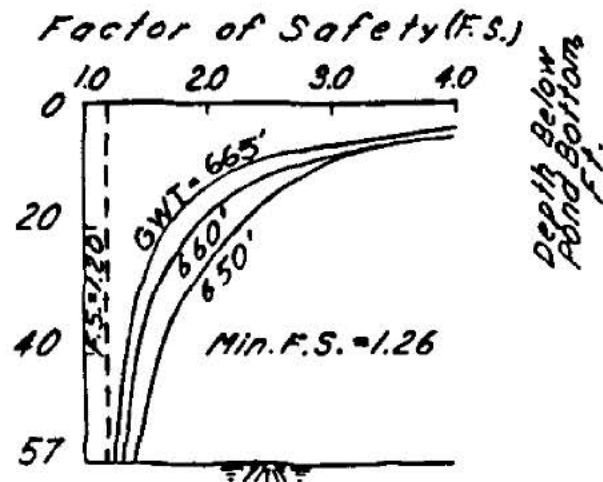
FIGURE 2.5-48, Rev 47

AutoCAD: Figure Fsar 2_5_48.dwg

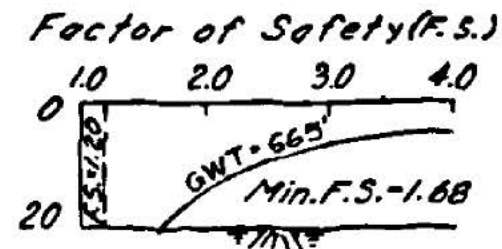
PROFILE 1
(East End of Pond)



PROFILE 2
(Central Section, Pump House, etc)



PROFILE 3
(West End of Pond)



NOTES:

1. Earthquake - Bechtel Synthetic (Ref: FSAR, SECTION 3.7.1.2)
2. SSE of 0.15 g.
3. G.W.T. - Ground Water Table
4. Pond bottom at El. 668'
5. Acceptable F.S. = 1.20.

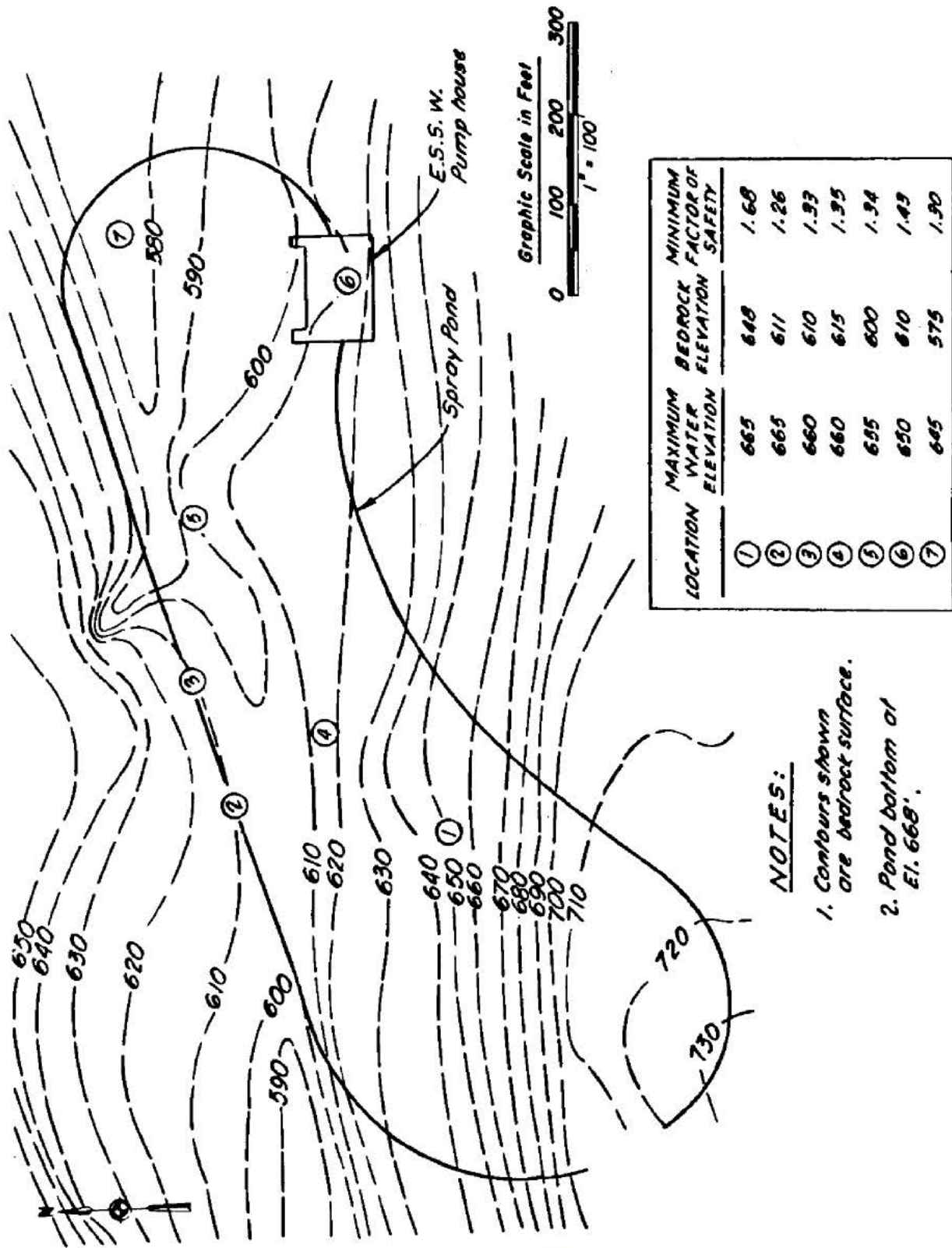
FSAR REV. 65

SUSQUEHANNA STEAM ELECTRIC STATION
UNITS 1 & 2
FINAL SAFETY ANALYSIS REPORT

SPRAY POND, FACTOR
OF SAFETY VARIATION WITH
GROUNDWATER TABLE & DEPTH

FIGURE 2.5-49, Rev 47

AutoCAD: Figure Fsar 2_5_49.dwg



FSAR REV. 65

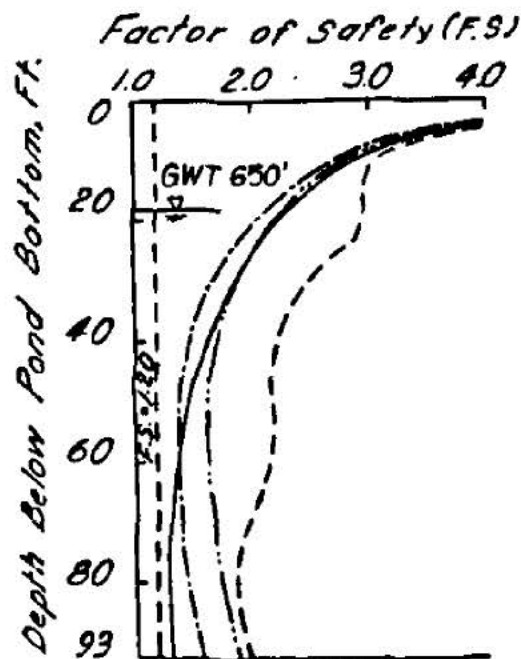
SUSQUEHANNA STEAM ELECTRIC STATION
UNITS 1 & 2
FINAL SAFETY ANALYSIS REPORT

SPRAY POND, MINIMUM FACTOR
OF SAFETY AGAINST
LIQUIFICATION AT SELECTED LOCATIONS

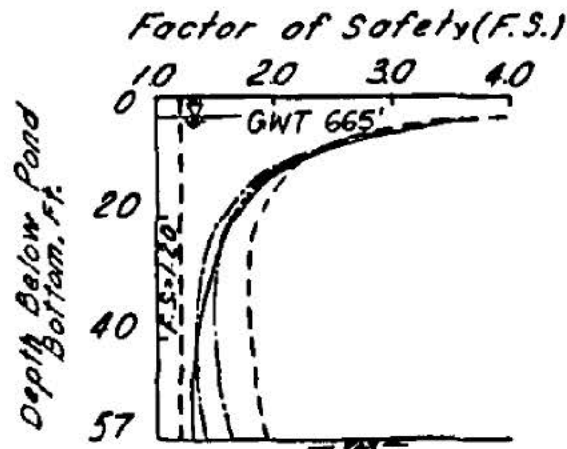
FIGURE 2.5-50, Rev 47

AutoCAD: Figure Fsar 2_5_50.dwg

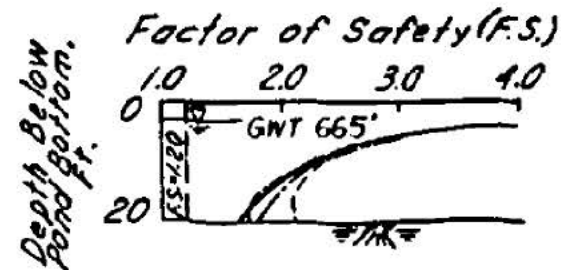
PROFILE 1
(East End of Pond)



PROFILE 2
(Central Section, Pump House, etc)



PROFILE 3
(West End of Pond)



NOTES:

1. Comparison shown only for the profiles with the maximum ground water table (GWT). Comparison of profiles with lower ground water table. See Table 10.
2. Pond bottom at El. 668'
3. Acceptable F.S. = 1.20.

LEGEND:

- Bechtel Synthetic (Design Earthquake) —————
- Golden Gate Earthquake - - - - -
- Helena Earthquake - - - - -
- Parkfield Earthquake - - - - -

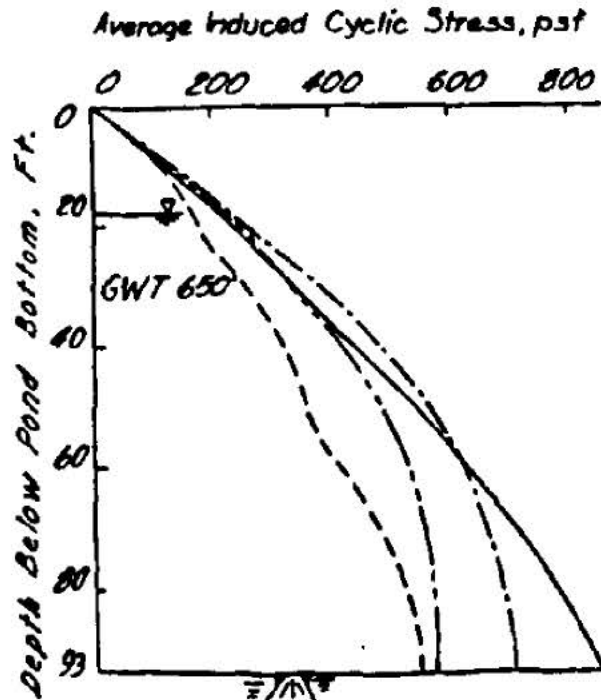
FSAR REV. 65

SUSQUEHANNA STEAM ELECTRIC STATION
UNITS 1 & 2
FINAL SAFETY ANALYSIS REPORT

SPRAY POND, COMPARISON OF FACTORS
OF SAFETY FOR LIQUIFICATION FOR THE
DESIGN EARTHQUAKE AND SOME REAL EARTHQUAKES

FIGURE 2.5-51, Rev 47

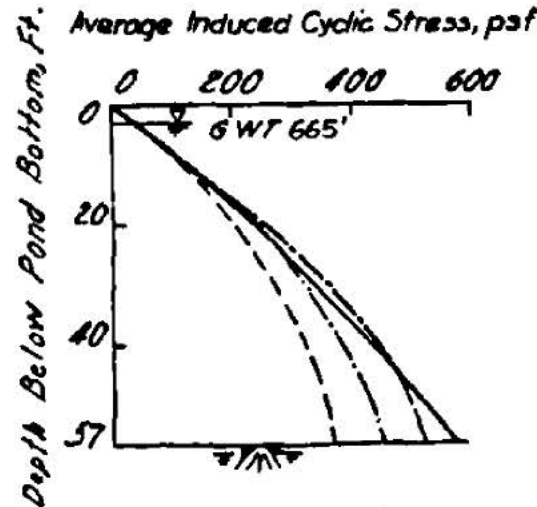
PROFILE 1
(East End of Pond)



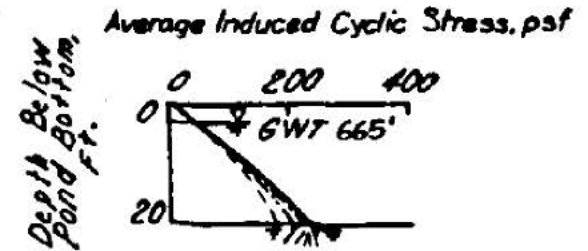
NOTES:

1. Comparison Shown for the profiles with the maximum ground water table (GWT)
2. Pond bottom at El. 668'

PROFILE 2
(Central Section, Pump House, etc)



PROFILE 3
(West End of Pond)



LEGEND:

- Bechtel Synthetic (Design Earthquake) ———
- Golden Gate Earthquake (dotted)
- Helena Earthquake — · — · — (dash-dot)
- Parkfield Earthquake - - - - - (dashed)

FSAR REV. 65

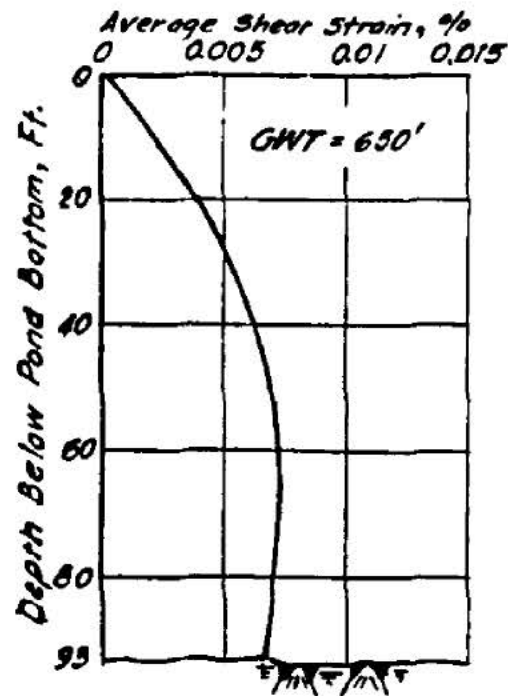
SUSQUEHANNA STEAM ELECTRIC STATION
UNITS 1 & 2
FINAL SAFETY ANALYSIS REPORT

SPRAY POND, COMPARISON OF AVERAGE
CYCLE STRESS AS INDUCED BY DESIGN
EARTHQUAKE AND SOME REAL EARTHQUAKES

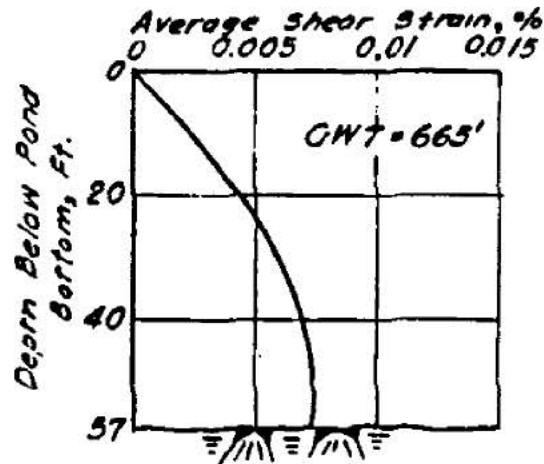
FIGURE 2.5-52, Rev 47

AutoCAD: Figure Fsar 2_5_52.dwg

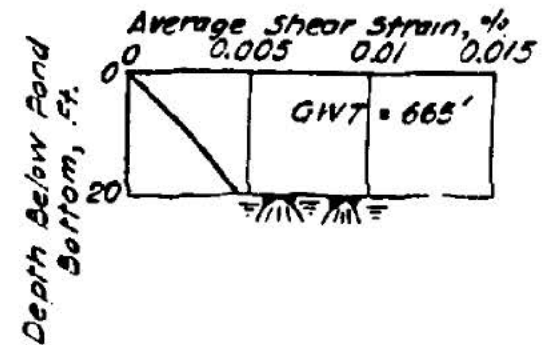
PROFILE 1 (East End Of Pond)



PROFILE 2 (Central Section, Pump House etc.)



PROFILE 3 (West End Of Pond)



NOTES:

1. Shear Strains Shown on the Drawings were induced by the SSE of 0.15g. The values were obtained from the SHAKE 3 Computer program.
2. Average Shear Strain = 0.65 Maximum Shear Strain.
3. GWT - Ground Water Table

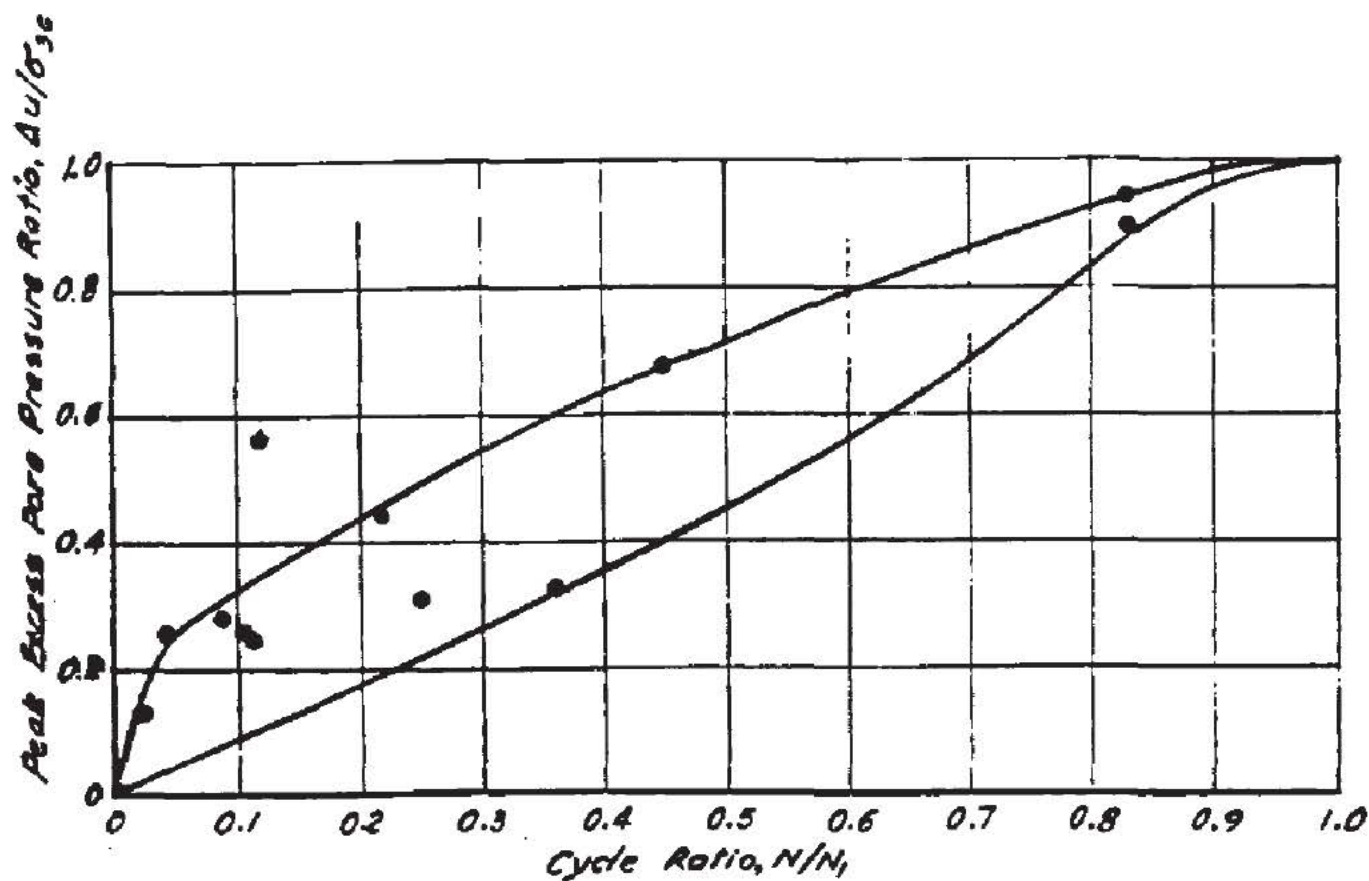
FSAR REV. 65

SUSQUEHANNA STEAM ELECTRIC STATION
UNITS 1 & 2
FINAL SAFETY ANALYSIS REPORT

SPRAY POND,
AVERAGE SHEAR VARIATION
WITH DEPTH

FIGURE 2.5-53, Rev 47

AutoCAD: Figure Fsar 2_5_53.dwg



NOTES:

1. This drawing was prepared following the procedure given in Lee, K. L., and Albaisa, A., "Earthquake Induced Settlements in Saturated Sands," Journal of the Geotechnical Engineering Div., ASCE, Vol. 100 No. GT4, pp 387-406, April 1974.

Where: N = the number of equivalent uniform cycles for design purposes ($N = 5$)

N_1 = the number of cycles required for the test sample to reach a total axial strain of 5%,

Δu = the induced excess pore pressure at the end of 5 cycles.

σ'_{vc} = effective consolidation pressure.

2. The points shown represent the actual test data of 12 cyclic triaxial tests on undisturbed samples. (Reference: Geotechnical Engineers, Inc. Report, dated October 11, 1974.

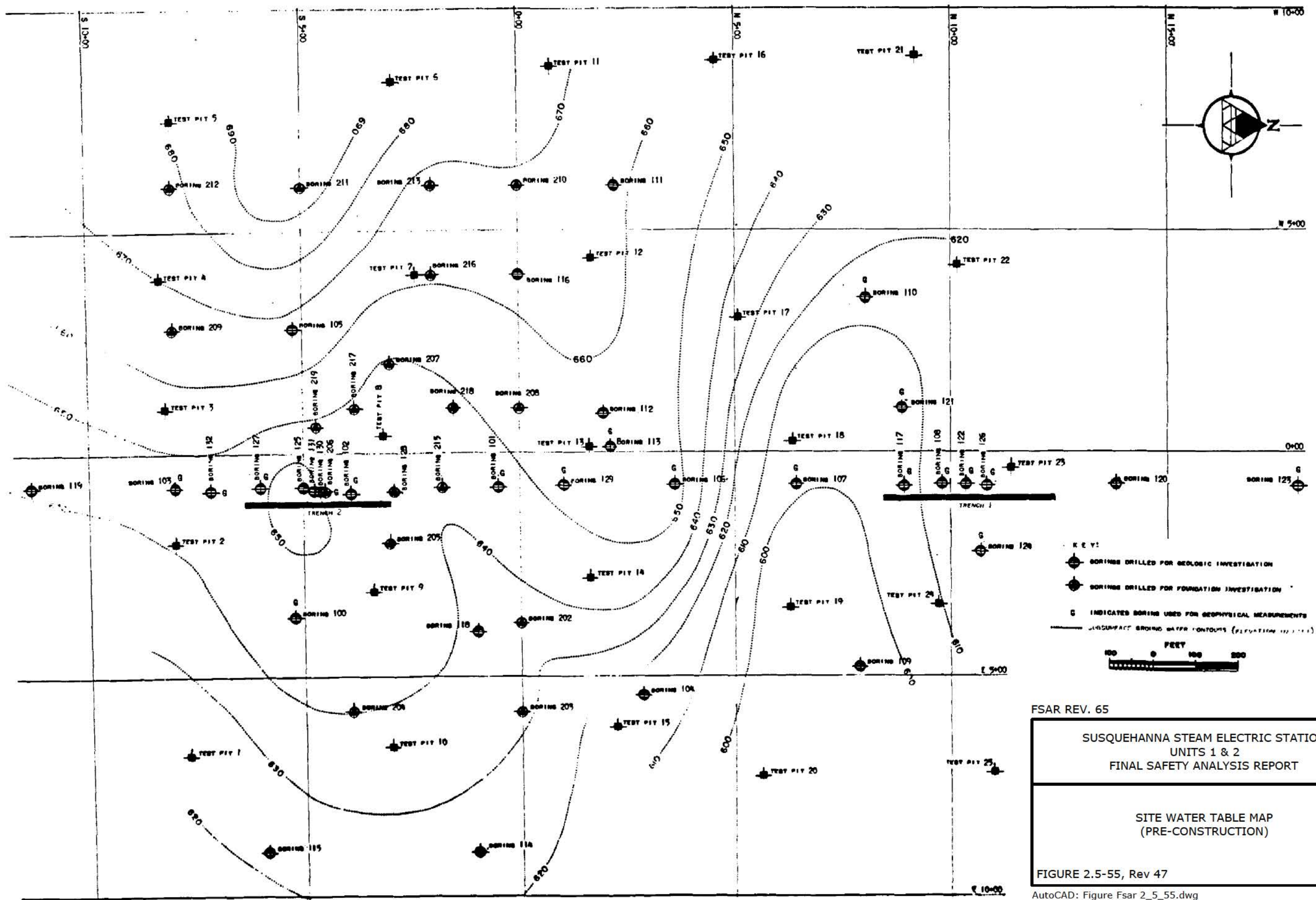
FSAR REV. 65

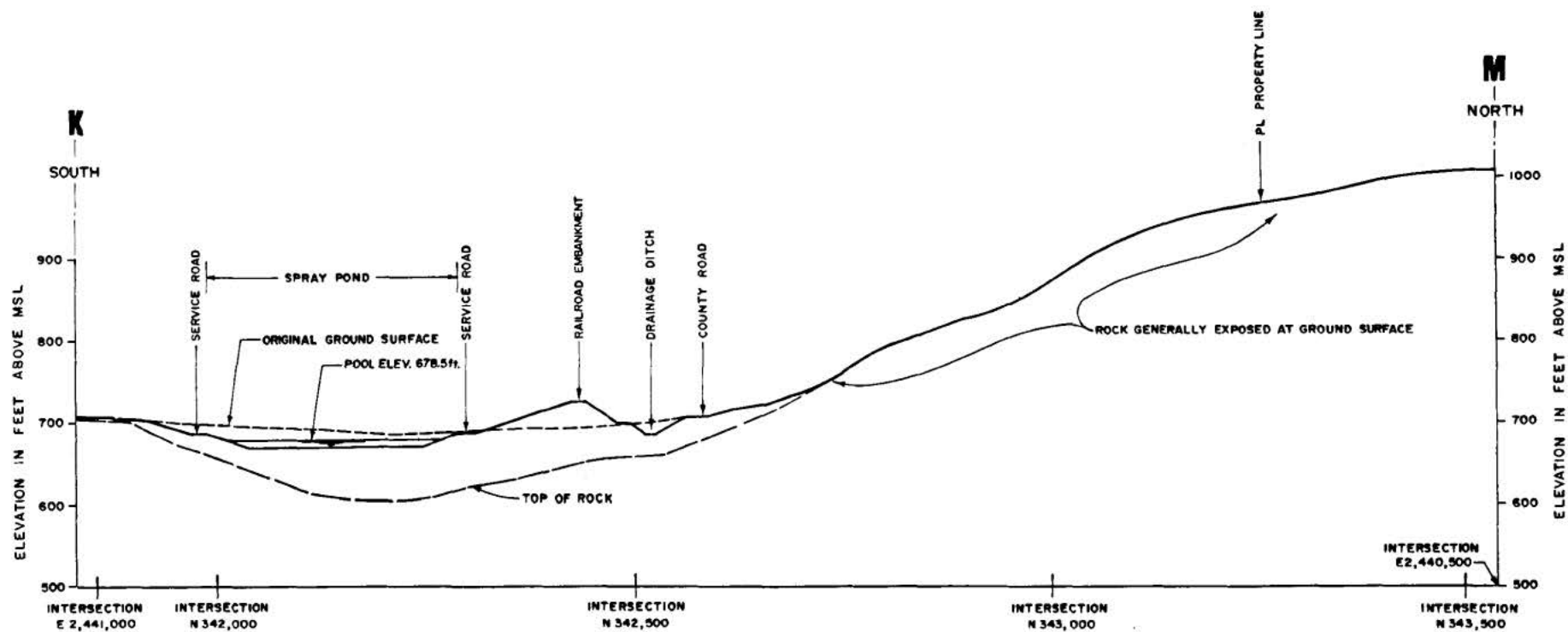
SUSQUEHANNA STEAM ELECTRIC STATION
UNITS 1 & 2
FINAL SAFETY ANALYSIS REPORT

SPRAY POND,
SUMMARY OF PORE
PRESSURE BUILDUP

FIGURE 2.5-54, Rev 47

AutoCAD: Figure Fsar 2_5_54.dwg





NOTES:

1. Location of profile is shown in Figure 2.5-22.
2. Excavated grades in spray pond area are shown in figure 2.5-42; final plant grades are shown in Figure 2.5-24.
3. Contours of slope north of county road are shown in Figure 2.1-2.

0 50 100 200
HORIZONTAL AND VERTICAL
SCALE IN FEET

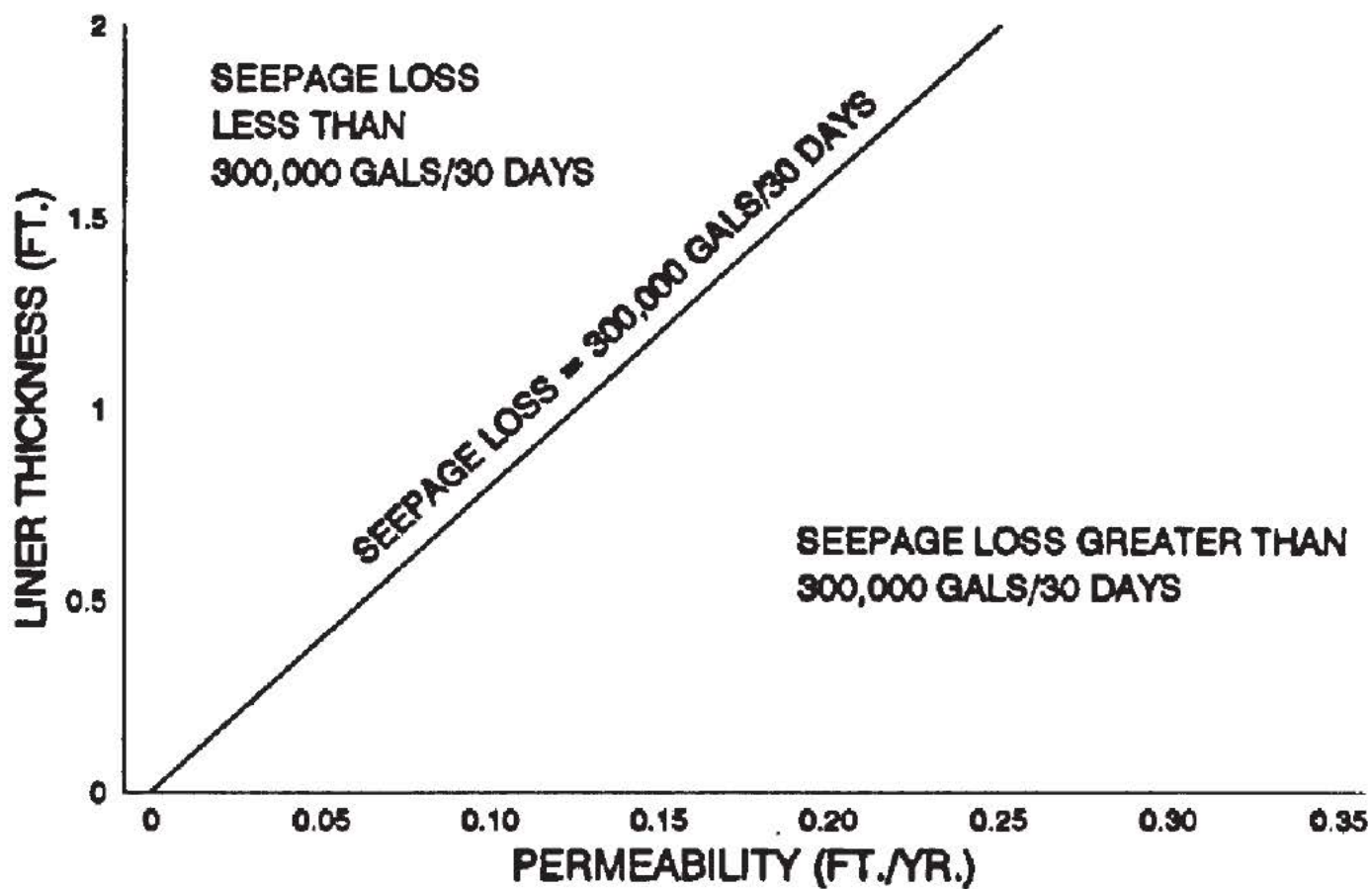
FSAR REV. 65

SUSQUEHANNA STEAM ELECTRIC STATION
UNITS 1 & 2
FINAL SAFETY ANALYSIS REPORT

PROFILE OF SLOPE
NORTH OF SPRAY POND

FIGURE 2.5-56, Rev 47

AutoCAD: Figure Fsar 2_5_56.dwg



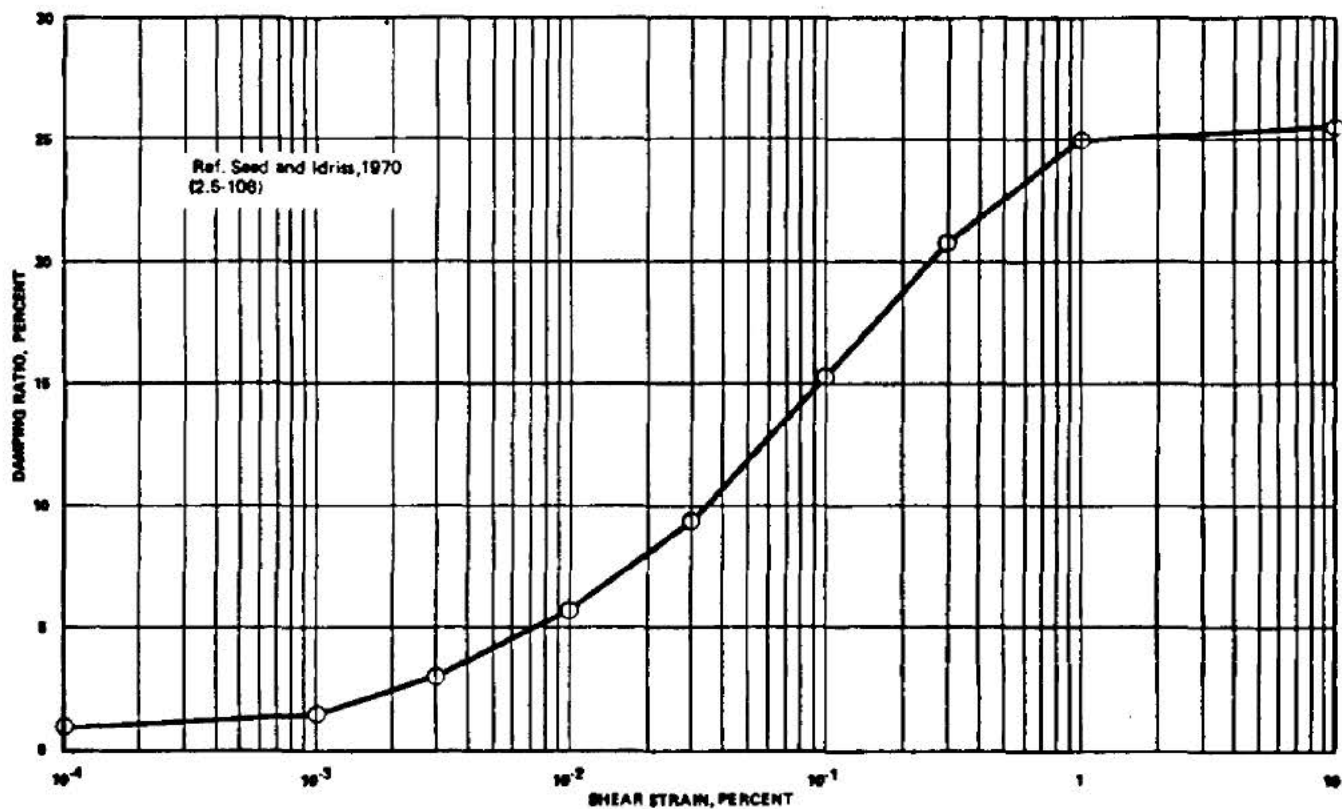
FSAR REV. 65

SUSQUEHANNA STEAM ELECTRIC STATION
UNITS 1 & 2
FINAL SAFETY ANALYSIS REPORT

SPRAY POND,
RELATIONSHIP BETWEEN LINER THICKNESS,
LINER PERMEABILITY AND SEEPAGE LOSS

FIGURE 2.5-57, Rev 47

AutoCAD: Figure Fsar 2_5_57.dwg



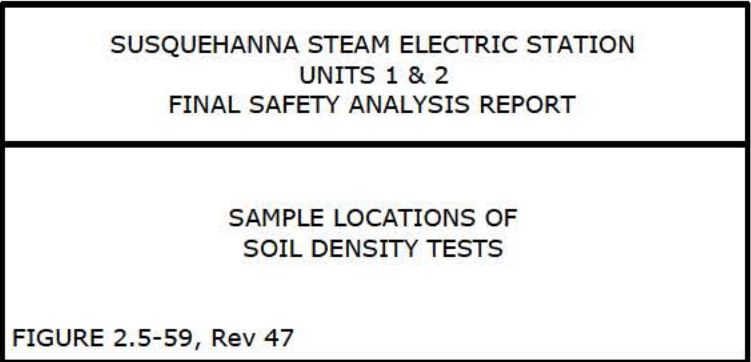
FSAR REV. 65

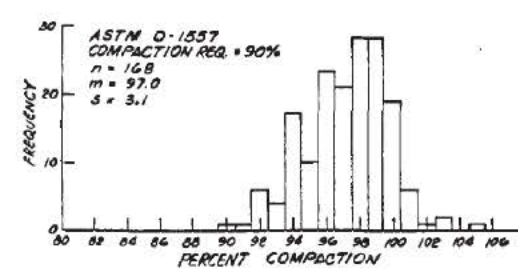
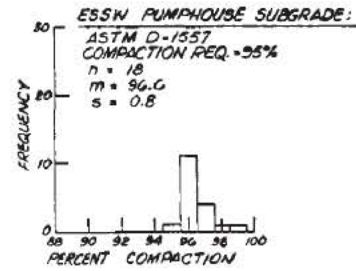
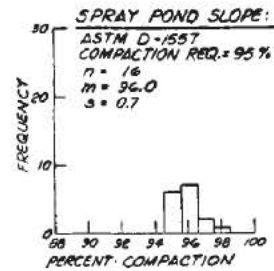
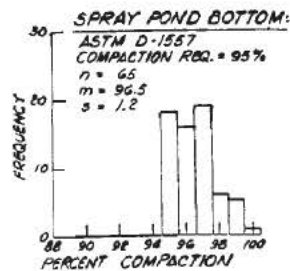
SUSQUEHANNA STEAM ELECTRIC STATION
UNITS 1 & 2
FINAL SAFETY ANALYSIS REPORT

DAMPING RATION vs. SHEAR STRAIN
OF SAND IN
LIQUIFICATION ANALYSIS

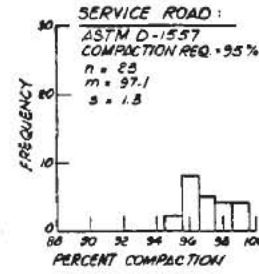
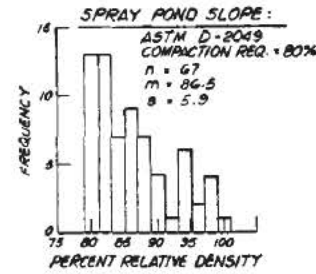
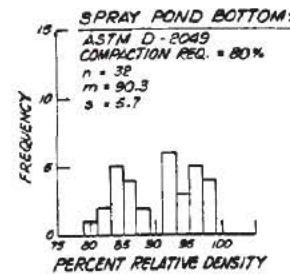
FIGURE 2.5-58, Rev 47

Security-Related Information
Figure Withheld Under 10 CFR 2.390





FILL TO EAST AND SOUTH EAST OF ESSWP



NOTE:

1. FIELD DENSITY TESTS REPORTED IN U.S. TESTING CO. REPORT BUT NOT INCLUDED IN THIS STATISTICAL ANALYSIS:
 - a.) IN-SITU SOIL DENSITY BEFORE COMPACTION AT ESSW PUMPHOUSE.
 - b.) TESTS FOR THE EFFECTIVENESS OF COMPACTION EQUIPMENT ON SPRAY POND SLOPE.
 - c.) FAILURE TESTS WHERE SOIL WAS FURTHER COMPACTED AND TESTED TO INDICATE A SATISFACTORY COMPACTION.
2. THIS DRAWING TO BE READ IN CONJUNCTION WITH FSAR QUESTION 562.18 AND SECTION 2.5.4.5.3

LEGEND:

- n = NUMBER OF TESTS
m = ARITHMETIC MEAN
s = STANDARD DEVIATION

HISTOGRAM FOR SUBGRADE PREPARATION

	COMPACTION CRITERIA		NUMBER OF TESTS	MEAN	STANDARD DEVIATION	(U.S. TESTING CO. REPORT NOS.)
	ASTM DESIGNATION	DENSITY REQUIREMENT				
<u>SUBGRADE PREPARATION</u> (REFERENCE FSAR 2.5.4.5.2.2)						
SPRAY POND - BOTTOM BOTTOM SLOPE SLOPE	D-1557	95% OF δ_{dmax}	65	96.5	1.2	25, 27-34, 38-40
	D-2049	80% RD	38	90.3	5.7	28, 34, 38-40
	D-1557	95% OF δ_{dmax}	16	96.0	0.7	6, 8, 11, 20, 38-40
	D-2049	80% RD	67	86.5	5.9	6-9, 11-15, 17, 19-21, 38, 39
ESSW PUMPHOUSE	D-1557	95% OF δ_{dmax}	18	96.6	0.8	2, 3
SERVICE ROAD AND THE SLOPES ABOVE ROAD	D-1557	95% OF δ_{dmax}	23	97.1	1.8	1
SPILLWAY	D-1557	95% OF δ_{dmax}	3	99.5	-	40
PIPELINE TRENCH	D-1557	95% OF δ_{dmax}	2	95.6	-	16
	D-2049	80% RD	2	89.3	-	38, 39
<u>FILL</u> (REFERENCE FSAR 2.5.4.5.3)						
FILL TYPE "B" TO SOUTH AND SOUTH EAST OF ESSWP	D-1557	90% OF δ_{dmax}	168	97.0	3.1	41

TABULAR SUMMARY

FSAR REV. 65

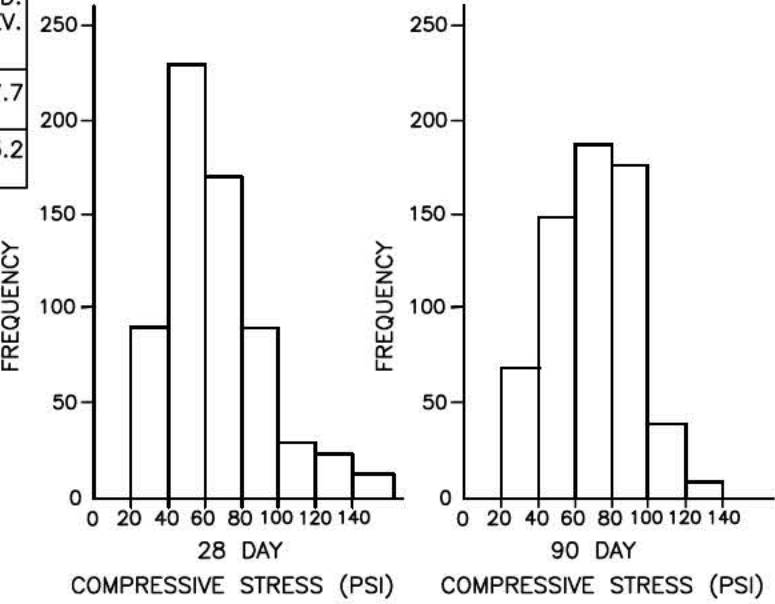
SUSQUEHANNA STEAM ELECTRIC STATION
UNITS 1 & 2
FINAL SAFETY ANALYSIS REPORT

STATISTICAL ANALYSIS OF
FIELD DENSITY TEST RESULTS

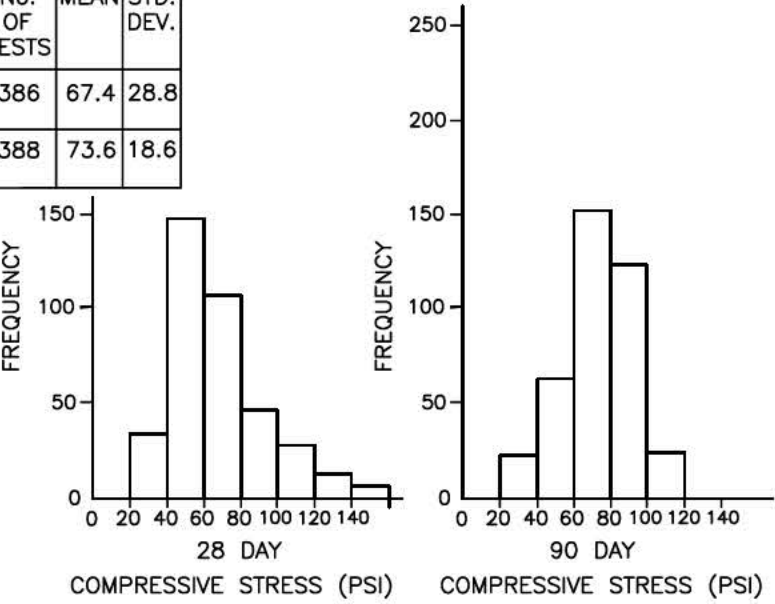
FIGURE 2.5-60, Rev 47

AutoCAD: Figure Fsar 2_5_60.dwg

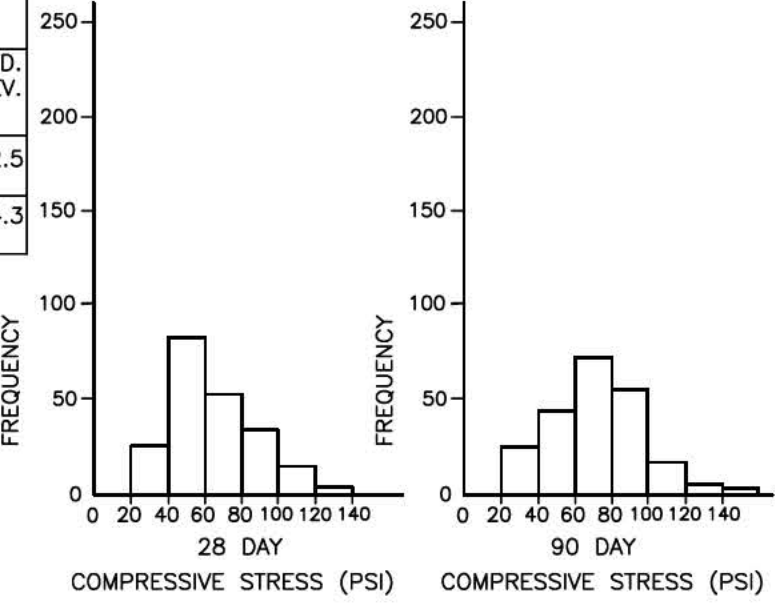
AREA EAST OF REACTOR BUILDING				
SPECIFICATION REQUIREMENT COMP. STRENGTH		No. OF TESTS	MEAN	STD. DEV.
28 DAY	40 PSI MIN.	637	66	27.7
90 DAY	100 PSI MAX.	635	71	23.2



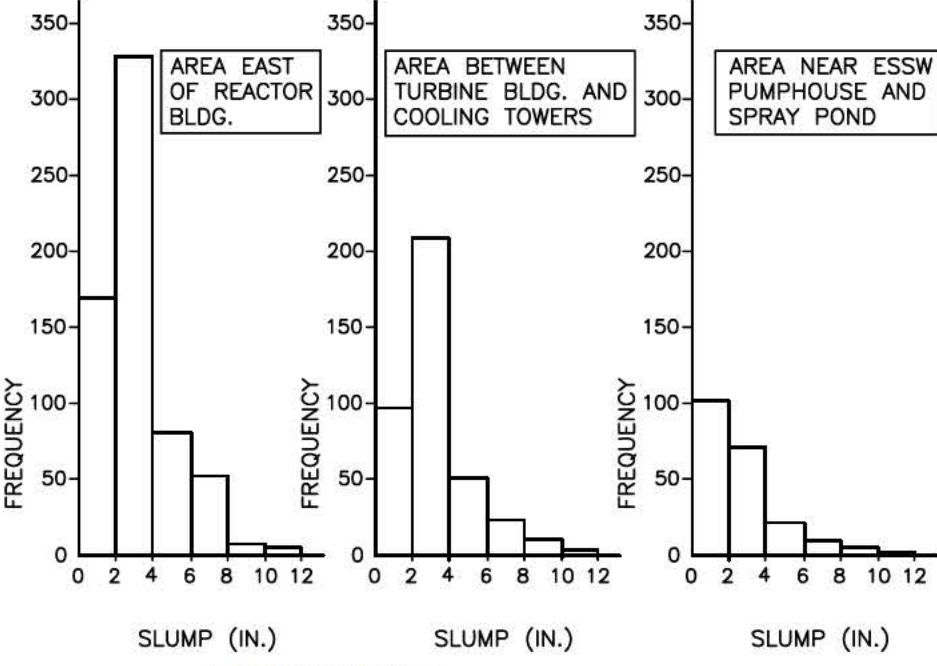
AREA BETWEEN TURBINE BUILDING AND COOLING TOWERS				
SPECIFICATION REQUIREMENT COMP. STRENGTH		No. OF TESTS	MEAN	STD. DEV.
28 DAY	40 PSI MIN.	386	67.4	28.8
90 DAY	100 PSI MAX.	388	73.6	18.6



AREA NEAR ESSW PUMPHOUSE AND SPRAY POND				
SPECIFICATION REQUIREMENT COMP. STRENGTH		No. OF TESTS	MEAN	STD. DEV.
28 DAY	40 PSI MIN.	212	64.9	22.5
90 DAY	100 PSI MAX.	212	71.8	24.3



SPECIFICATION REQUIREMENT FOR SLUMP	
3 IN. MIN.	6 IN. MAX..



NOTES:

1. SLUMP - THE SLUMP REQUIREMENTS OF 3 INCH MINIMUM AND 6 INCH MAXIMUM WERE FOR RANDOM WORKABILITY DURING FIELD POURING OPERATIONS AND AS ONE OF THE REQUIREMENTS TO ENSURE THAT A SUFFICIENT COMPRESSIVE STRENGTH WOULD BE OBTAINED. THEREFORE A DEVIATION FROM THE SPECIFICATION REQUIREMENT DOES NOT CONSTITUTE UNACCEPTABILITY SINCE THE ONLY BASIS WOULD BE AN ALTERED COMPRESSIVE STRENGTH AND THESE ITEMS HAVE THEIR OWN ACCEPTABILITY LIMITS.

2. 90 DAY COMPRESSIVE STRENGTH - THE REQUIREMENT FOR THE 100 PSI MAXIMUM STRENGTH WAS A CONFORMANCE ITEM ONLY. THE PURPOSE FOR THIS UPPER LIMIT WAS TO FACILITATE BASE OF FOUNDATION IN AREA PERMANENTLY BACKFILLED

WITH SAND-CEMENT-FLYASH MATERIAL. A DEVIATION FROM THE SPECIFICATION REQUIREMENT IN THIS AREA IN NO WAY LIMITS THE INTENDED USE OF THE MATERIAL.

3. 28 DAY COMPRESSIVE STRENGTH - THE REQUIREMENT FOR MINIMUM COMPRESSIVE STRENGTH WAS CHOSEN SUCH THAT THE COMPRESSIVE STRENGTH WOULD BE IN THE SAME RANGE AS THE BEARING VALUE OF COMPACTED GRANULAR BACKFILL. THE 30 PSI STRENGTH CONVERTS TO 2,100 LB/IN² WHEREAS COMPACTED GRANULAR BACKFILL HAS BEARING VALUES ON THE ORDER OF 2,000 TO 2,500 LB/IN². HOWEVER, SINCE THE SAND-CEMENT-FLYASH MATERIAL HAS NOT BEEN USED FOR FILL

ANY STRUCTURE, THEREFORE THE HIGHER BEARING VALUE IS NOT REQUIRED. THE SAND-CEMENT-FLYASH BACKFILL HAS BEEN USED ONLY AS GENERAL BACKFILL FOR PIPES, CONDUITS, AND ALONG THE SIDES OF BUILDINGS. IT HAS BEEN DETERMINED THAT THE 20 PSI (1,400 LB/IN²) MINIMUM VALUE THAT MAY BE FOUND IN SOME AREAS IS COMPLETELY ADEQUATE TO SATISFY THE CONDITIONS FOR WHICH IT IS BEING USED.

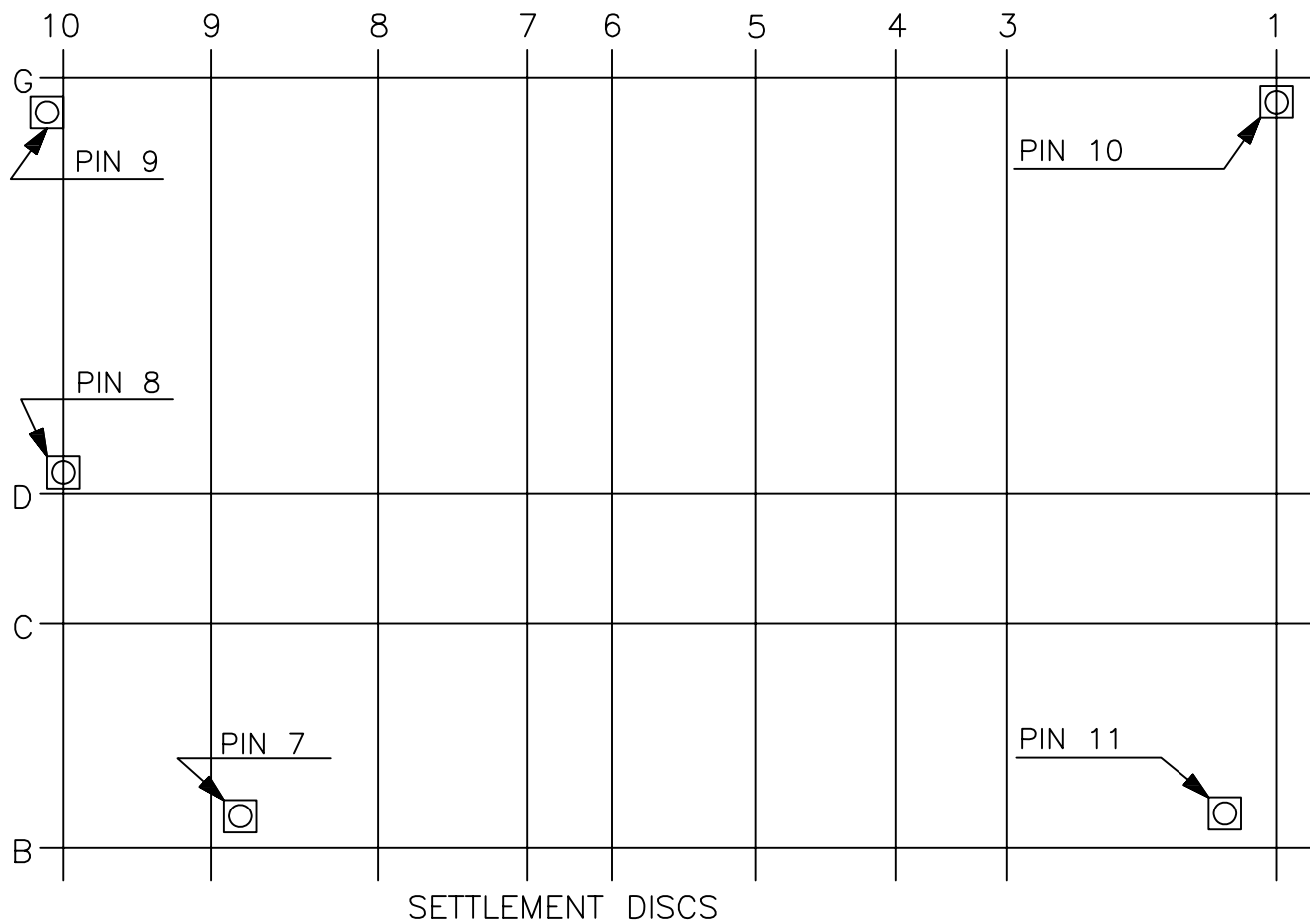
4. THIS DRAWING IS TO BE READ IN CONJUNCTION WITH PEAR QUESTIONS 002.0 AND 205.00 SECTION 2.5.6.5.5

FSAR REV. 65

SUSQUEHANNA STEAM ELECTRIC STATION
UNITS 1 & 2
FINAL SAFETY ANALYSIS REPORT

STATISTICAL ANALYSIS OF
SAND-CEMENT-FLYASH
BEDDING & BACKFILL

FIGURE 2.5-61, Rev 47



FSAR REV. 65

SUSQUEHANNA STEAM ELECTRIC STATION
UNITS 1 & 2
FINAL SAFETY ANALYSIS REPORT

ESSW PUMPHOUSE
FLOOR PLAN EL. 685'-6"

FIGURE 2.5-62, Rev 47

AutoCAD: Figure Fsar 2_5_62.dwg

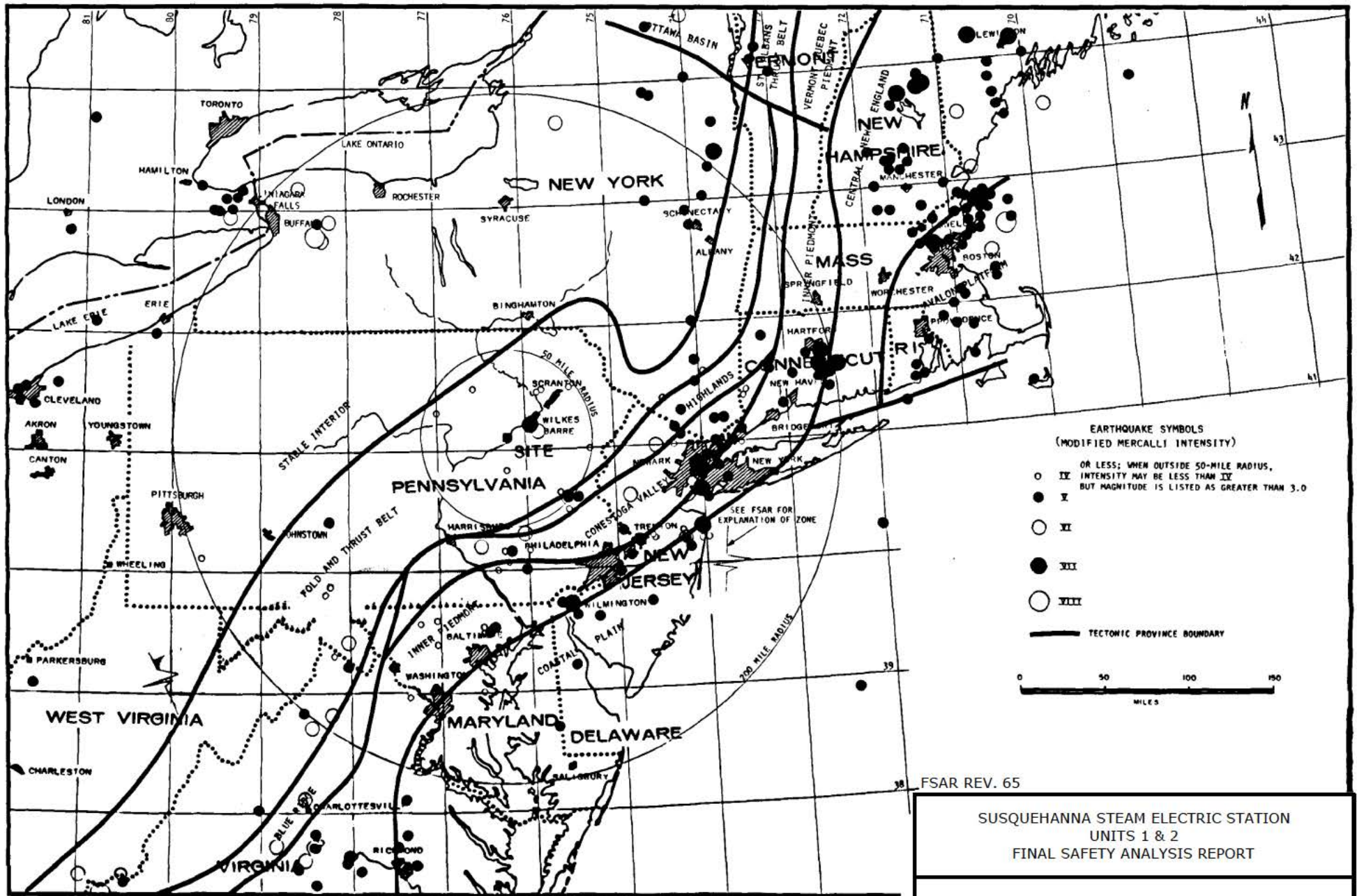
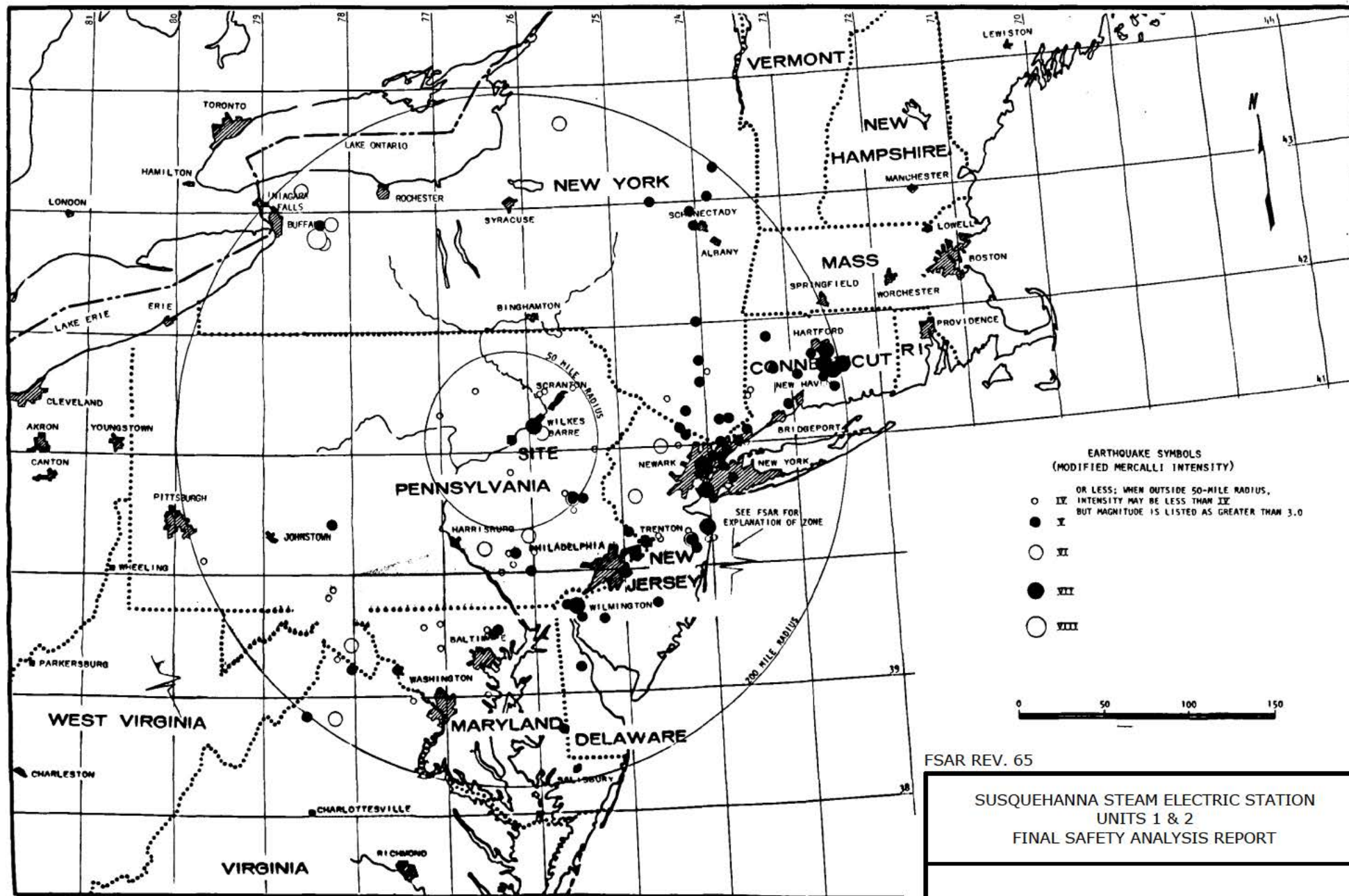


FIGURE 2.5-8A, Rev 47



FSAR REV. 65

SUSQUEHANNA STEAM ELECTRIC STATION
UNITS 1 & 2
FINAL SAFETY ANALYSIS REPORT

EARTHQUAKE EPICENTERS
WITHIN 200 MILES OF THE SITE

FIGURE 2.5-8B, Rev 47

AutoCAD: Figure Fsar 2_5_8B.dwg

Security-Related Information
Figure Withheld Under 10 CFR 2.390

SUSQUEHANNA STEAM ELECTRIC STATION
UNITS 1 & 2
FINAL SAFETY ANALYSIS REPORT

EXTENT OF ROCK AND SOIL
FOUNDATIONS

FIGURE 2.5-17A, Rev 55

AutoCAD: Figure Fsar 2_5_17A.dwg



Mahantango slaty siltstone exposed in west slope of Unit 2 cold water pipe trench adjacent to circulation water pumphouse, at approximate N340,995,E2,441,510. The exposure which is viewed northwest, displays prominent fracture cleavage here dipping 30 degrees southeast. Bedding planes, observable to both above and below the pick head, dip very gently south. The vertical, east-west oriented joint face is a natural surface forming top of rock, eroded by stream and ice scour.

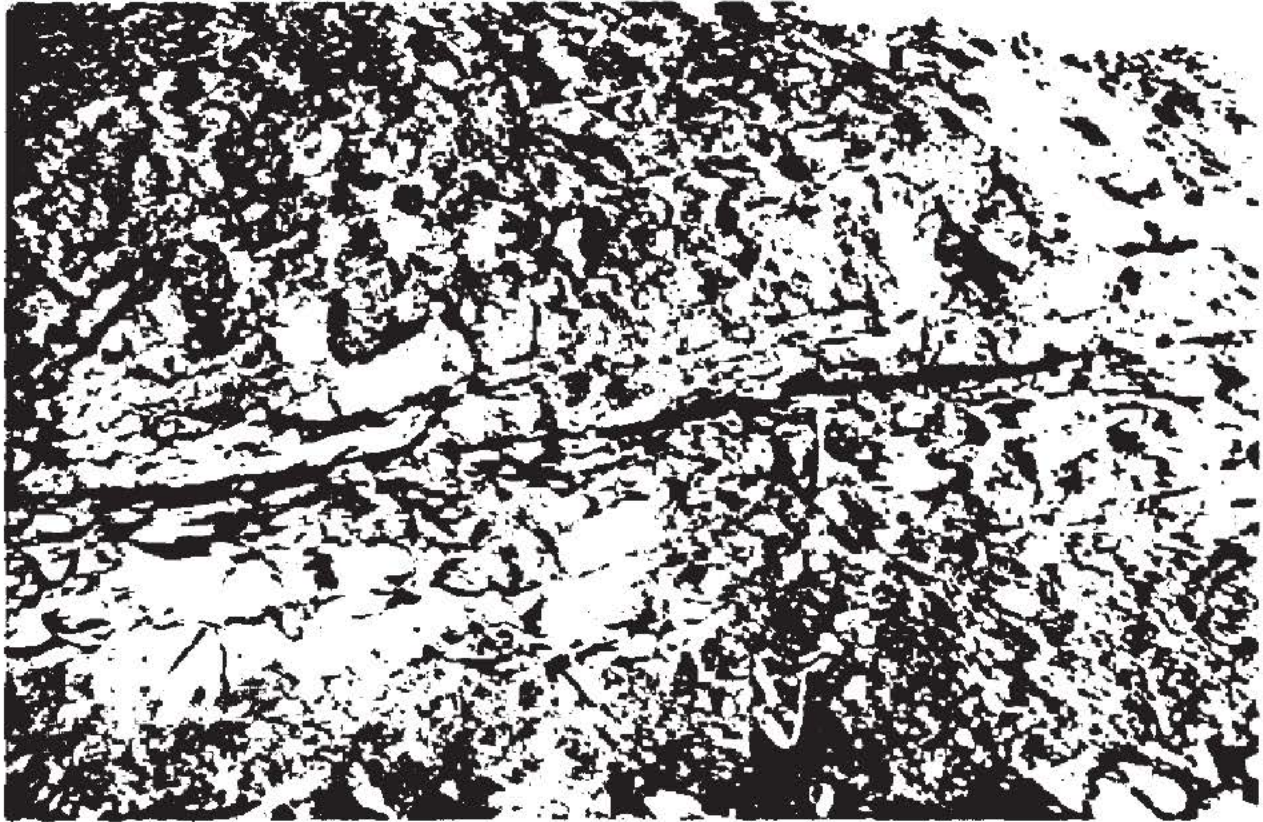
FSAR REV. 65

SUSQUEHANNA STEAM ELECTRIC STATION
UNITS 1 & 2
FINAL SAFETY ANALYSIS REPORT

PHOTOGRAPH OF GEOLOGIC
FEATURES EXPOSED IN
EXCAVATIONS

FIGURE 2.5-20A, Rev 47

AutoCAD: Figure Fsar 2_5_20A.dwg



Weathered shear plane (bedding plane shear A) exposed in rock slope at N341,360,E2,441,935. View is to the west. The shear plane parallels bedding, which here dips seven degrees south. Weathering has accentuated visibility of the shear, which is here 1/2 to 1 inch wide, containing leached quartz and brown-weathered siltstone fragments. There is no sign of brecciation along the shear plane. Photo taken April 22, 1974.

FSAR REV. 65

SUSQUEHANNA STEAM ELECTRIC STATION
UNITS 1 & 2
FINAL SAFETY ANALYSIS REPORT

PHOTOGRAPH OF GEOLOGIC
FEATURES EXPOSED IN
EXCAVATIONS

FIGURE 2.5-20B, Rev 47

AutoCAD: Figure Fsar 2_5_20B.dwg



Looking west at an excavated slope which shows the intersection of the weathered shear plane, bedding plane A, with the eroded rock surface. The intersection of these two surfaces is slightly above and to the left of the top of the hammer, as indicated in the photograph on the right. Scale is 8 inches long.

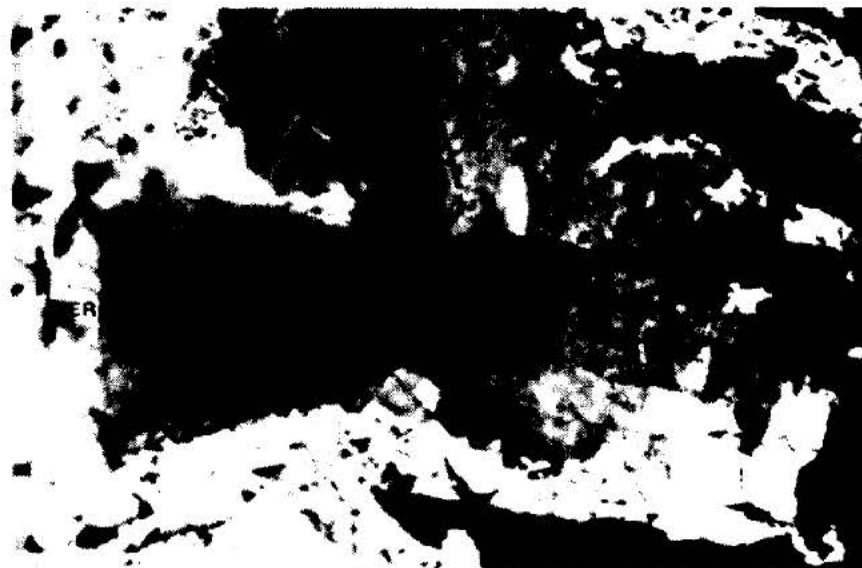
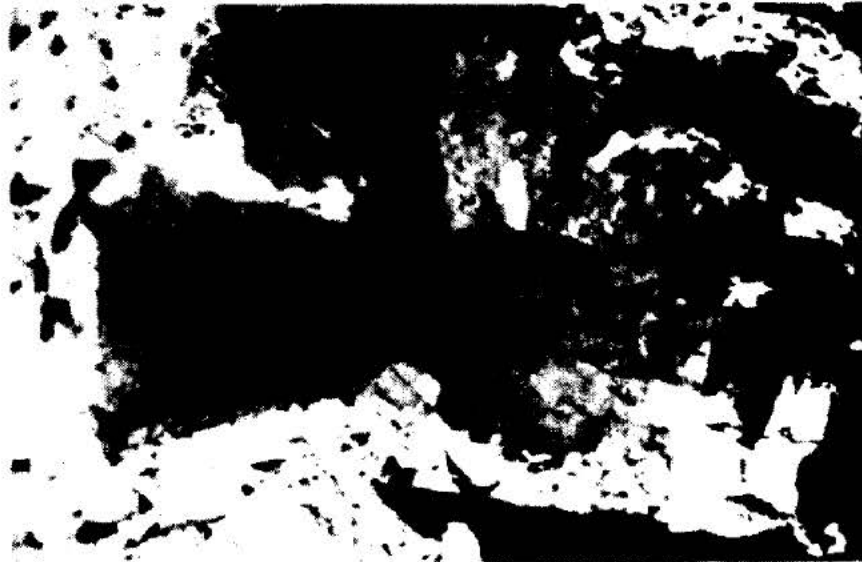
FSAR REV. 65

SUSQUEHANNA STEAM ELECTRIC STATION
UNITS 1 & 2
FINAL SAFETY ANALYSIS REPORT

PHOTOGRAPH OF GEOLOGIC
FEATURES EXPOSED IN
EXCAVATIONS

FIGURE 2.5-20C, Rev 47

AutoCAD: Figure Fsar 2_5_20C.dwg



Looking east at an excavated slope which shows the intersection of bedding plane A with the erosional rock surface, as outlined in the lower photograph. The erosional rock surface is essentially vertical. Mahantango siltstone at right, bouldery glacial drift on left. Location is about 30 feet from preceding photograph (at the approximate intersection of column line N and N341,375). Photo taken May 15, 1974.

FSAR REV. 65

SUSQUEHANNA STEAM ELECTRIC STATION
UNITS 1 & 2
FINAL SAFETY ANALYSIS REPORT

PHOTOGRAPH OF GEOLOGIC
FEATURES EXPOSED IN
EXCAVATIONS

FIGURE 2.5-20D, Rev 47

AutoCAD: Figure Fsar 2_5_20D.dwg



View south of a calcite veinlet crossing a slickensided bedding-plane shear (flat surface near observer) in Unit 1 turbine excavation (intersection of column lines 6 and 19. Note the calcite veinlet is not displayed above the shear plane. Photo taken May 22, 1974.

FSAR REV. 65

SUSQUEHANNA STEAM ELECTRIC STATION
UNITS 1 & 2
FINAL SAFETY ANALYSIS REPORT

PHOTOGRAPH OF GEOLOGIC
FEATURES EXPOSED IN
EXCAVATIONS

FIGURE 2.5-20E, Rev 47

AutoCAD: Figure Fsar 2_5_20E.dwg



A closer view of the same exposure described in the preceding photograph. Compass is oriented parallel to slickenside lamination which trends S3°E. If movement represented by the slickenside had occurred subsequent to formation of the calcite veinlet, the vein would have been offset. Photo taken May 22, 1974.

FSAR REV. 65

SUSQUEHANNA STEAM ELECTRIC STATION
UNITS 1 & 2
FINAL SAFETY ANALYSIS REPORT

PHOTOGRAPH OF GEOLOGIC
FEATURES EXPOSED IN
EXCAVATIONS

FIGURE 2.5-20F, Rev 47

AutoCAD: Figure Fsar 2_5_20F.dwg



Detail of excavation in condensate pump pit, Unit 2 turbine area. This photograph shows typical foundation excavation in the hard, unweathered Mahantango siltstone at the site. Here the slopes were presplit along closely spaced, line-drilled blast holes. View it to south. Photo taken July 3, 1974.

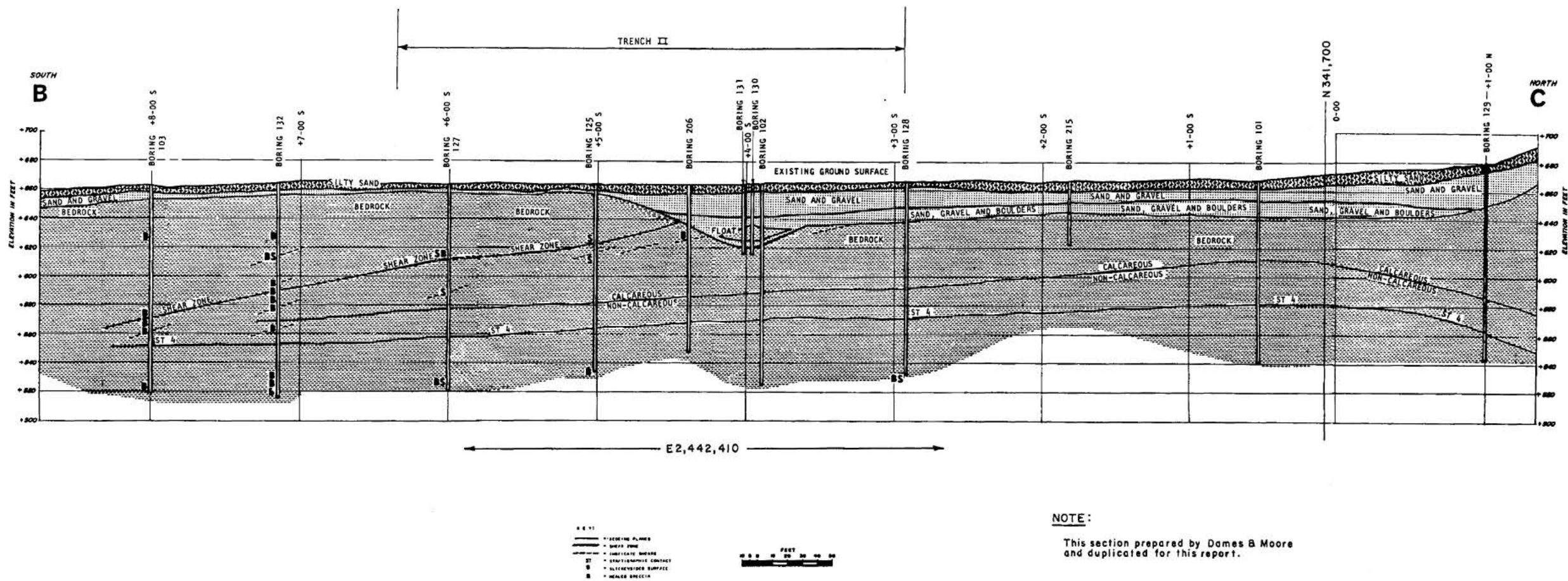
FSAR REV. 65

SUSQUEHANNA STEAM ELECTRIC STATION
UNITS 1 & 2
FINAL SAFETY ANALYSIS REPORT

PHOTOGRAPH OF GEOLOGIC
FEATURES EXPOSED IN
EXCAVATIONS

FIGURE 2.5-20G, Rev 47

AutoCAD: Figure Fsar 2_5_20G.dwg



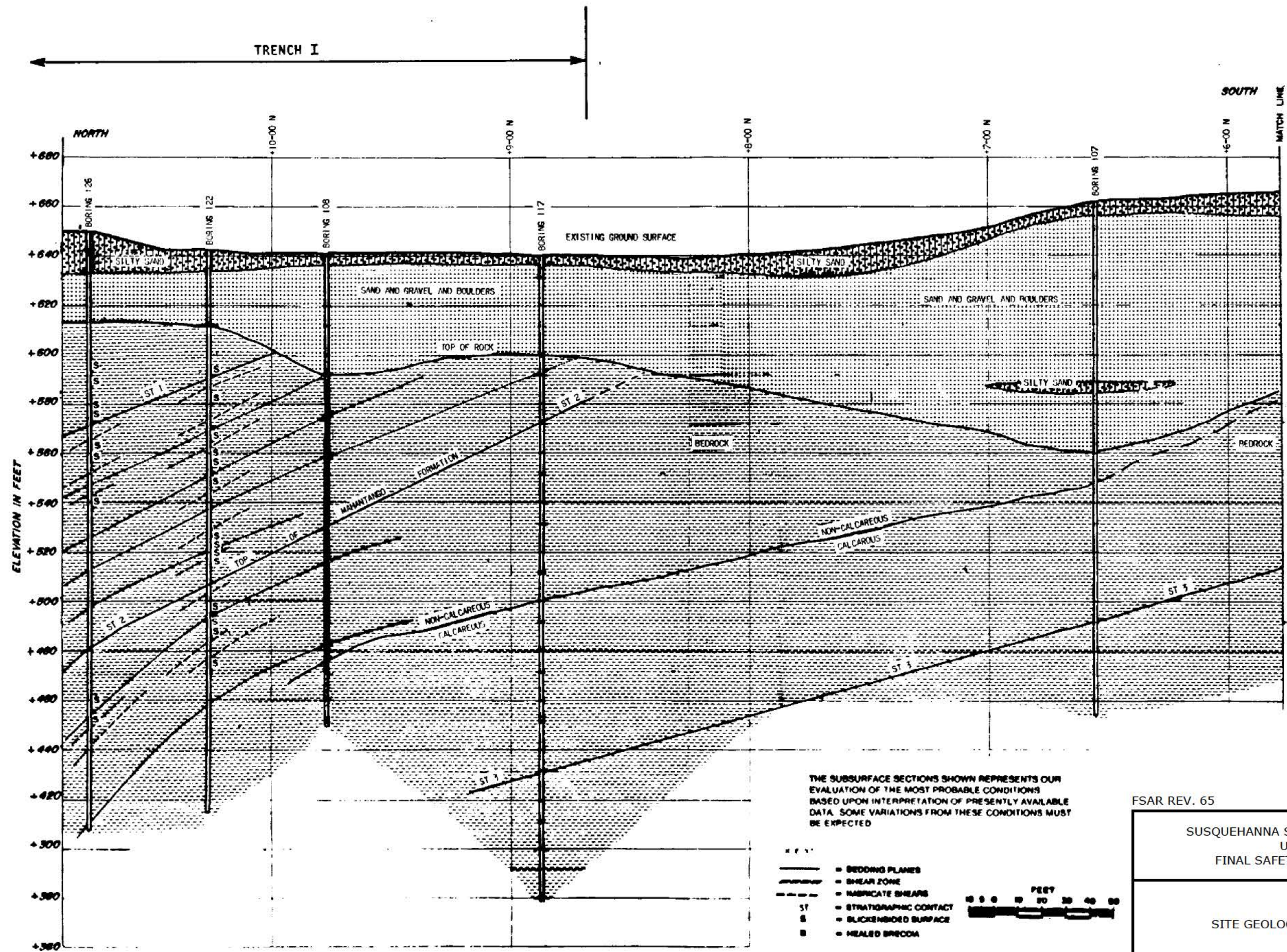
FSAR REV. 65

SUSQUEHANNA STEAM ELECTRIC STATION
UNITS 1 & 2
FINAL SAFETY ANALYSIS REPORT

SITE GEOLOGIC CROSS SECTIONS

FIGURE 2.5-21A, Rev 47

AutoCAD: Figure Fsar 2_5_21A.dwg



FSAR REV. 65

SUSQUEHANNA STEAM ELECTRIC STATION
UNITS 1 & 2
FINAL SAFETY ANALYSIS REPORT

SITE GEOLOGIC CROSS SECTIONS

FIGURE 2.5-21B, Rev 47

AutoCAD: Figure Fsar 2_5_21B.dwg

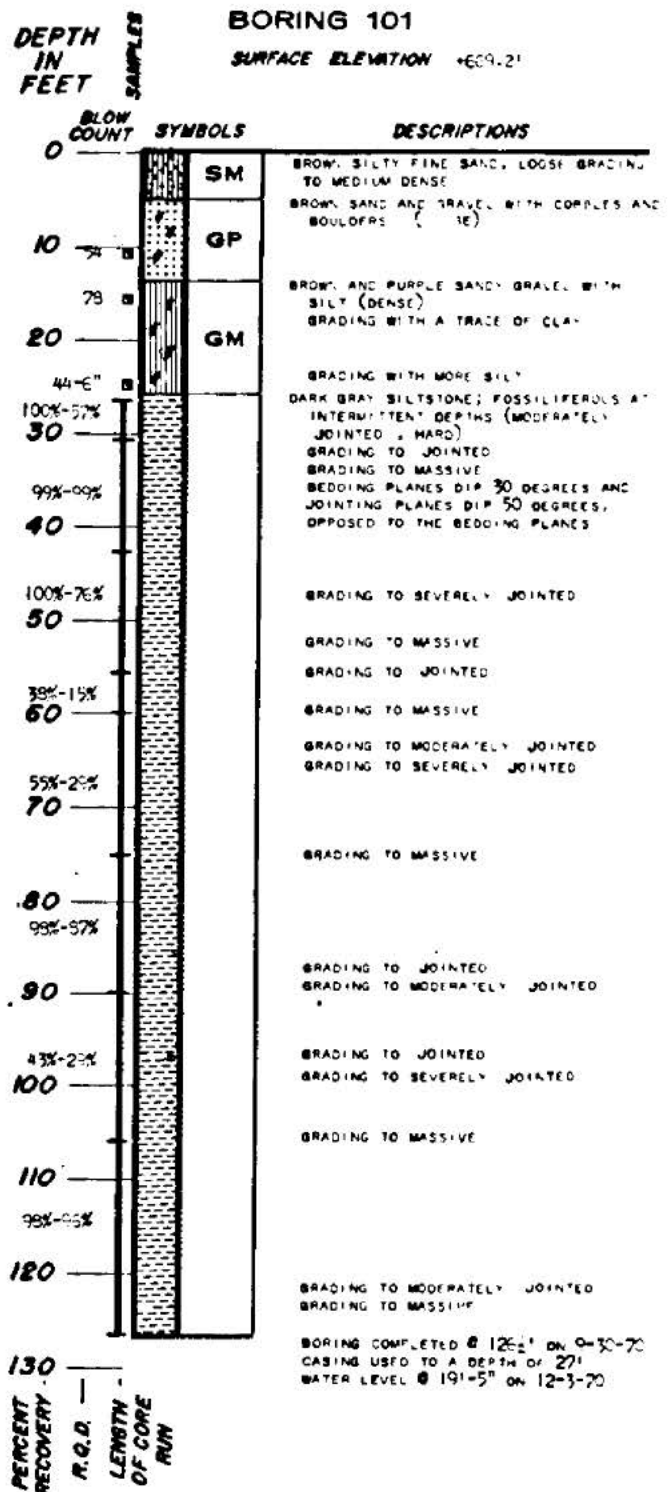
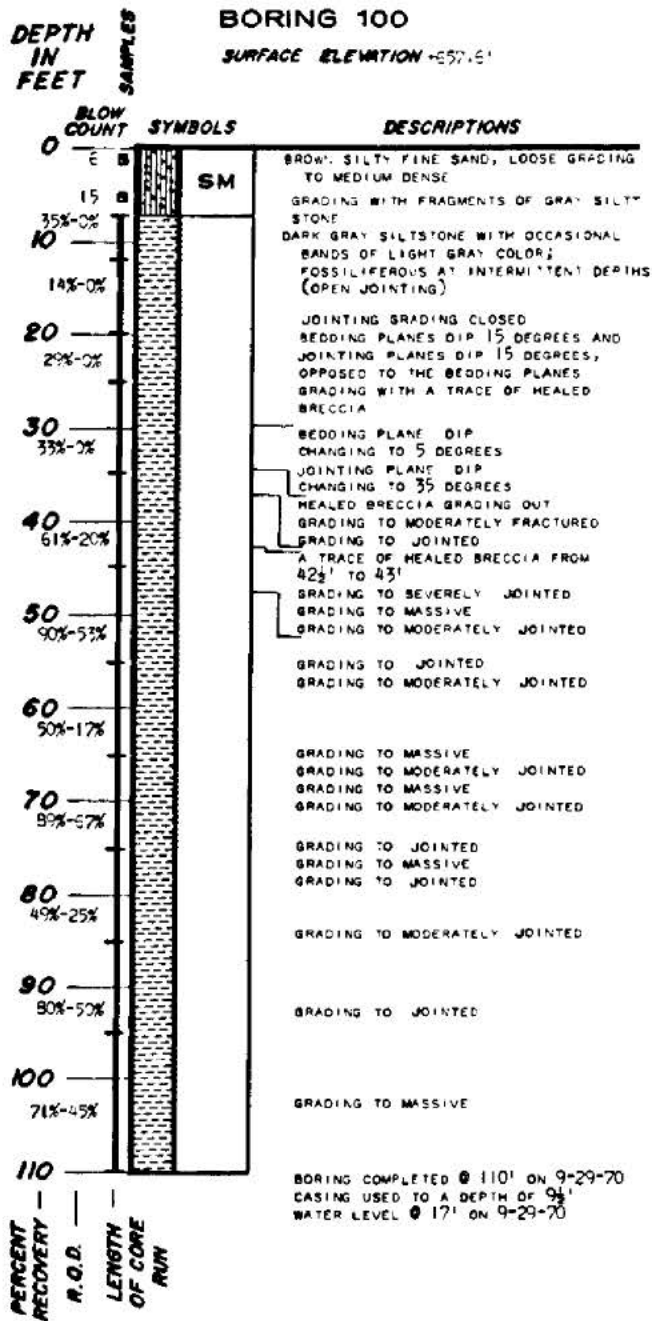
Security-Related Information

Figure Withheld Under 10 CFR 2.390

FSAR REV. 65

SUSQUEHANNA STEAM ELECTRIC STATION UNITS 1 & 2 FINAL SAFETY ANALYSIS REPORT
PLOT PLAN DETAILS
FIGURE 2.5-22A, Rev 47

AutoCAD: Figure Fsar 2_5_22A.dwg



NOTE: 1 THE FIGURES IN THE COLUMN LABELED "BLOW COUNT" REFER TO THE NUMBER OF BLOWS REQUIRED TO DRIVE THE DAVES & MOORE SOIL SAMPLER A DISTANCE OF ONE FOOT USING A 300-POUND HAMMER FALLING 18 INCHES, OR A STANDARD SPLIT-SPOON SAMPLER A DISTANCE OF ONE FOOT, USING A 140-POUND DRIVE WEIGHT FALLING 30 INCHES. THE DAVES & MOORE SAMPLER IS 3/4" O.D. AND APPROXIMATELY 2 1/2" I.D. THE STANDARD SPLIT-SPOON SAMPLER IS 2" O.D. AND 1-3/8" I.D.

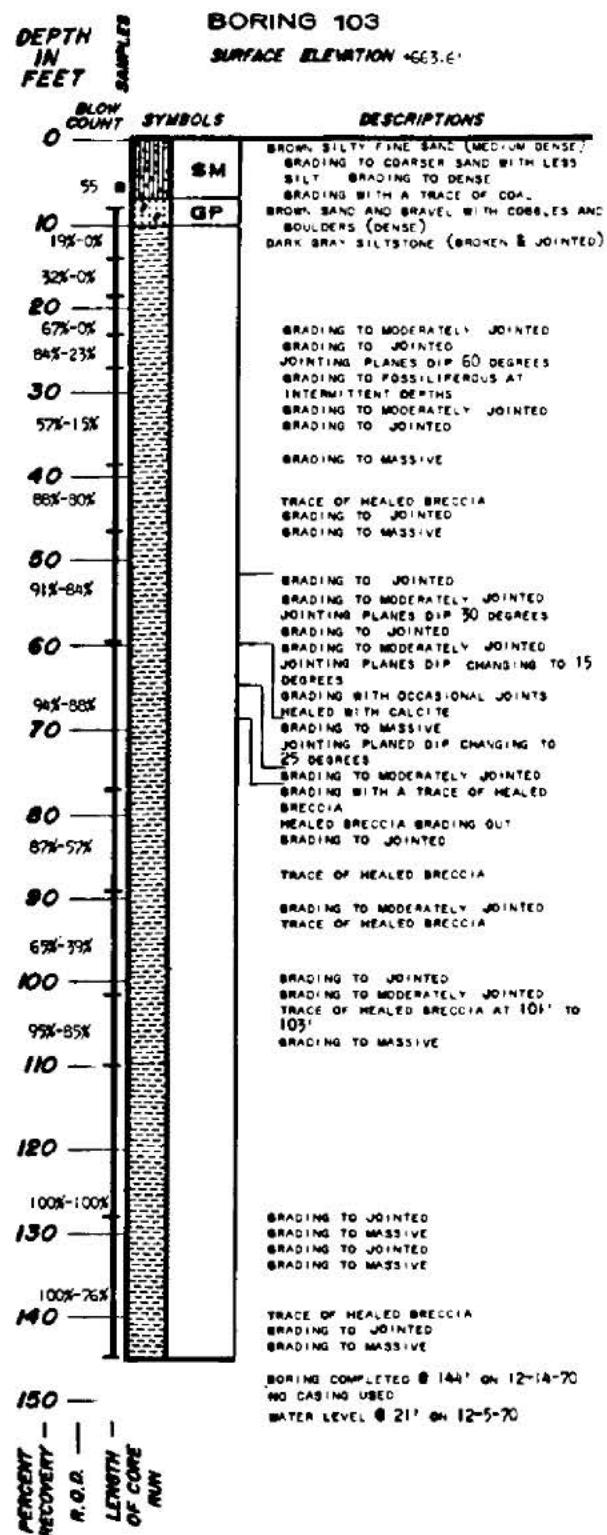
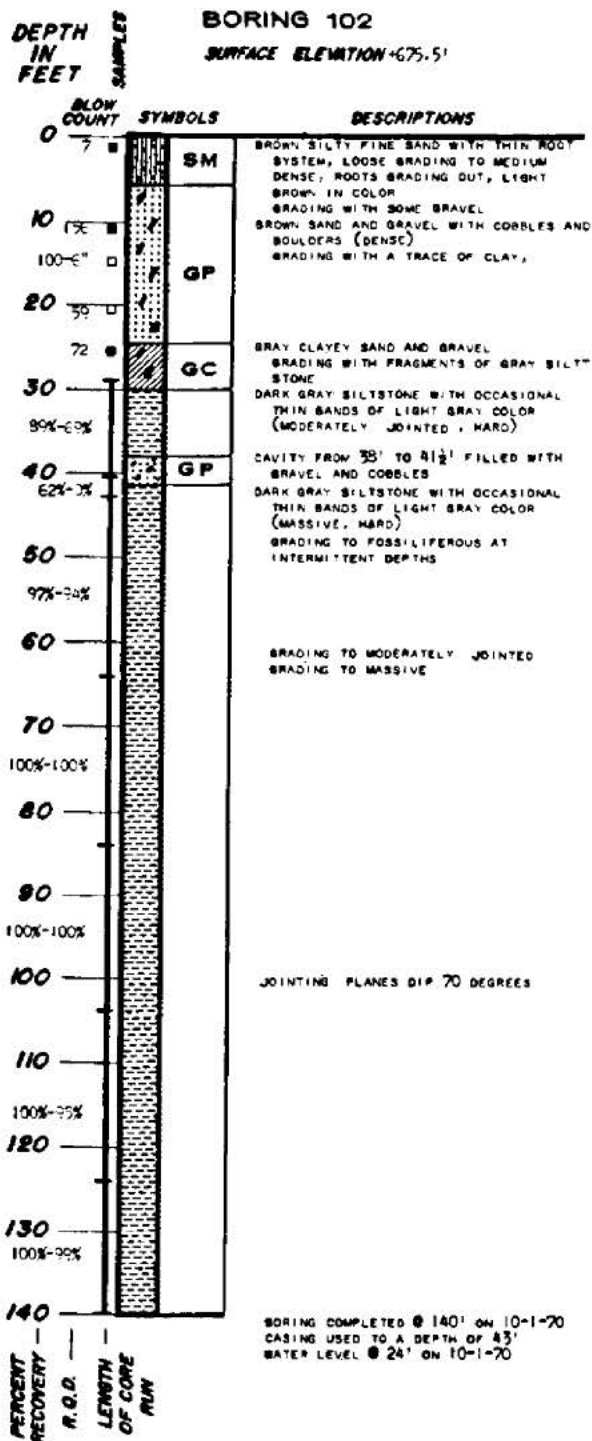
FSAR REV. 65

SUSQUEHANNA STEAM ELECTRIC STATION
UNITS 1 & 2
FINAL SAFETY ANALYSIS REPORT

LOG OF BORINGS

FIGURE 2.5-23A, Rev 47

AutoCAD: Figure Fsar 2_5_23A.dwg

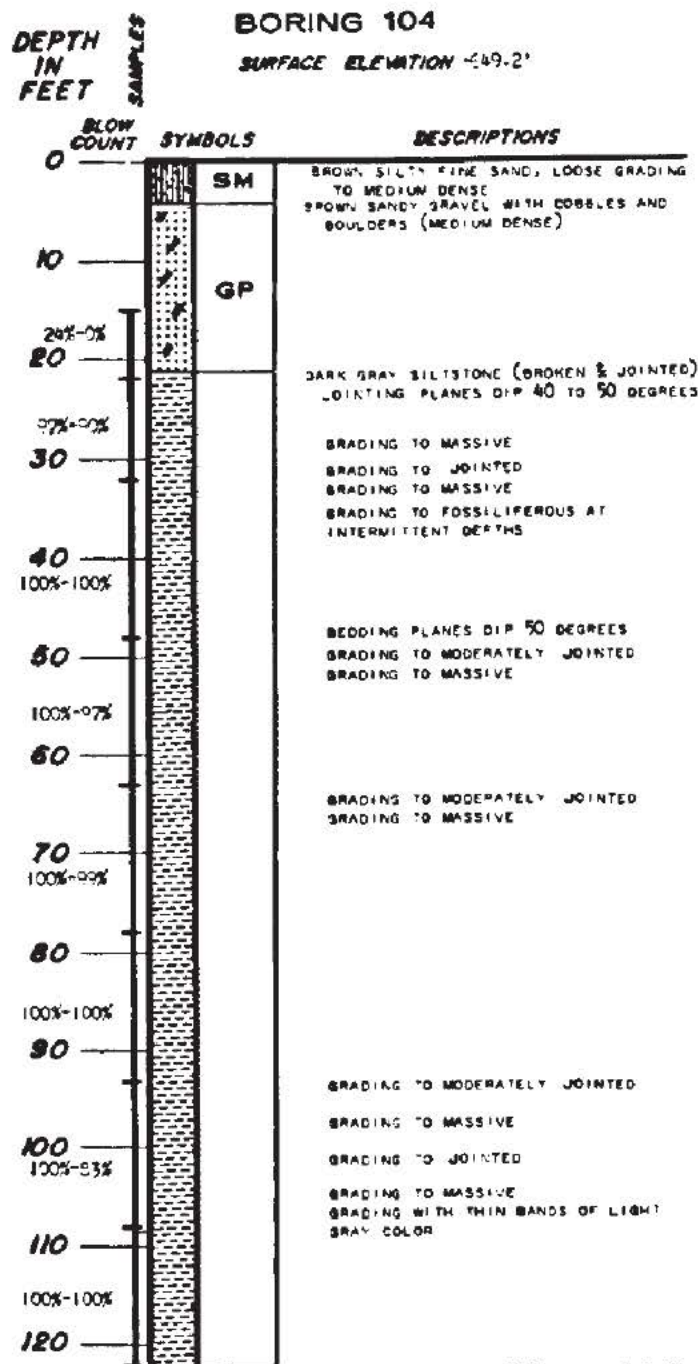


FSAR REV. 65

SUSQUEHANNA STEAM ELECTRIC STATION
UNITS 1 & 2
FINAL SAFETY ANALYSIS REPORT

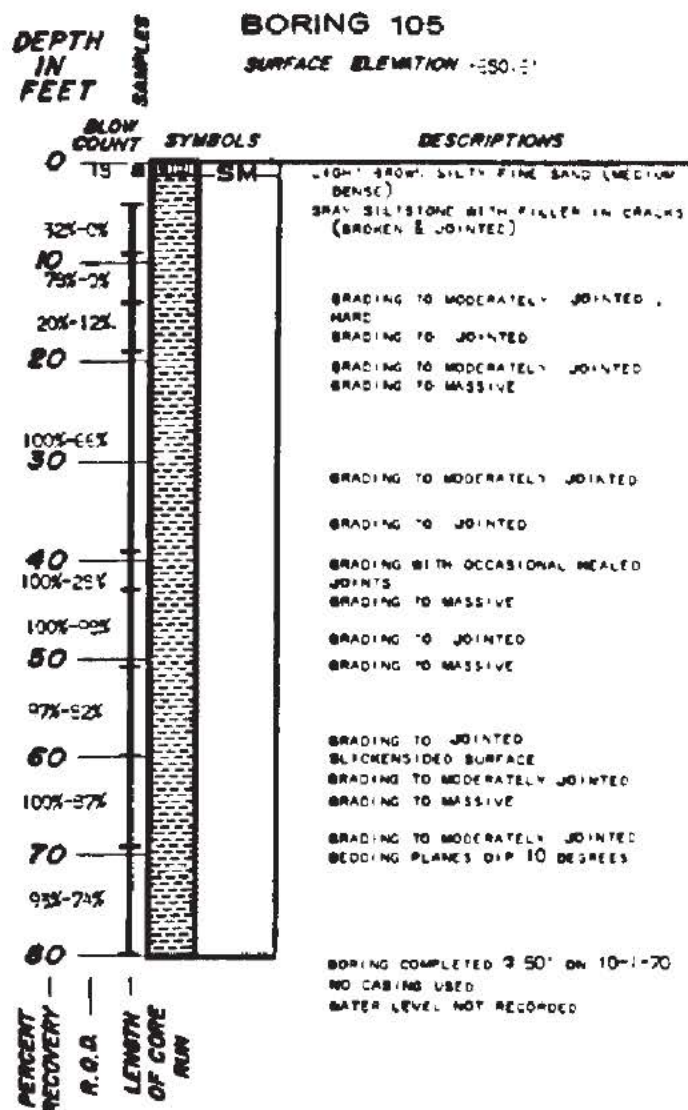
LOG OF BORINGS

FIGURE 2.5-23B, Rev 47



BORING COMPLETED @ 122' ON 10-6-70
CASING USED TO A DEPTH OF 20'
WATER LEVEL @ 31'-2" ON 12-3-70

130
PERCENT RECOVERY
R.O.D.
LENGTH OF CORE OF CORE RUN



BORING COMPLETED @ 50' ON 10-1-70
NO CASING USED
WATER LEVEL NOT RECORDED

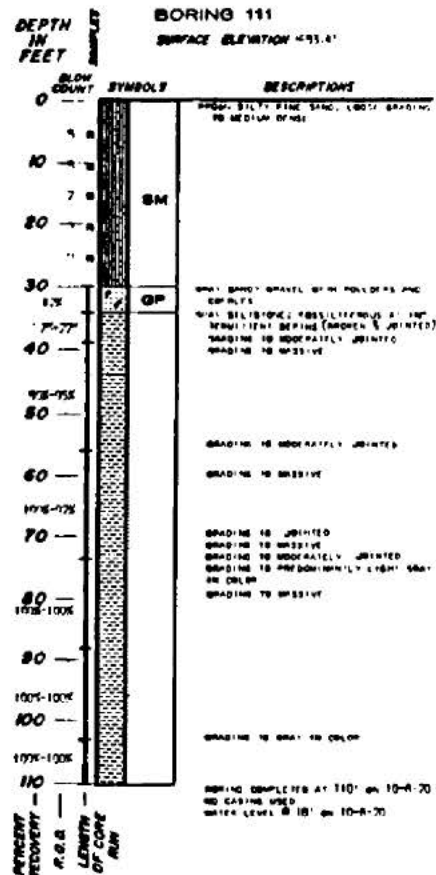
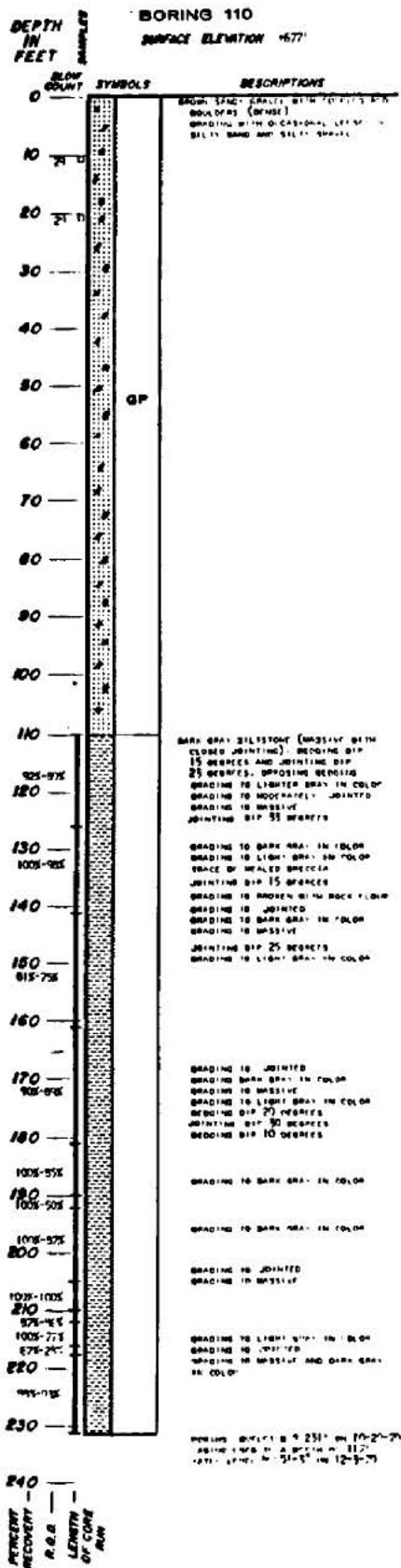
PERCENT RECOVERY
R.O.D.
LENGTH OF CORE OF CORE RUN

FSAR REV. 65

SUSQUEHANNA STEAM ELECTRIC STATION
UNITS 1 & 2
FINAL SAFETY ANALYSIS REPORT

LOG OF BORINGS

FIGURE 2.5-23C, Rev 47

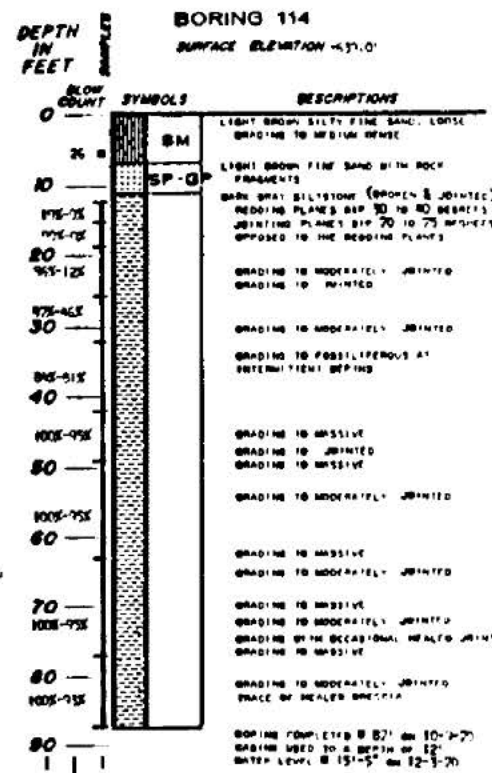
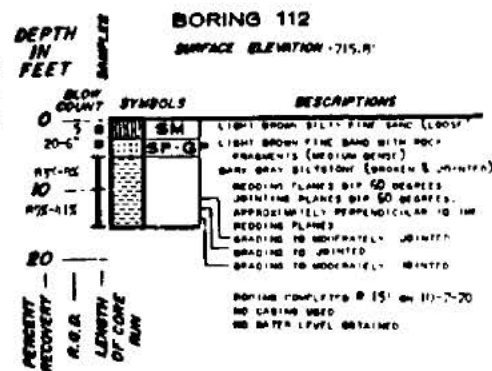
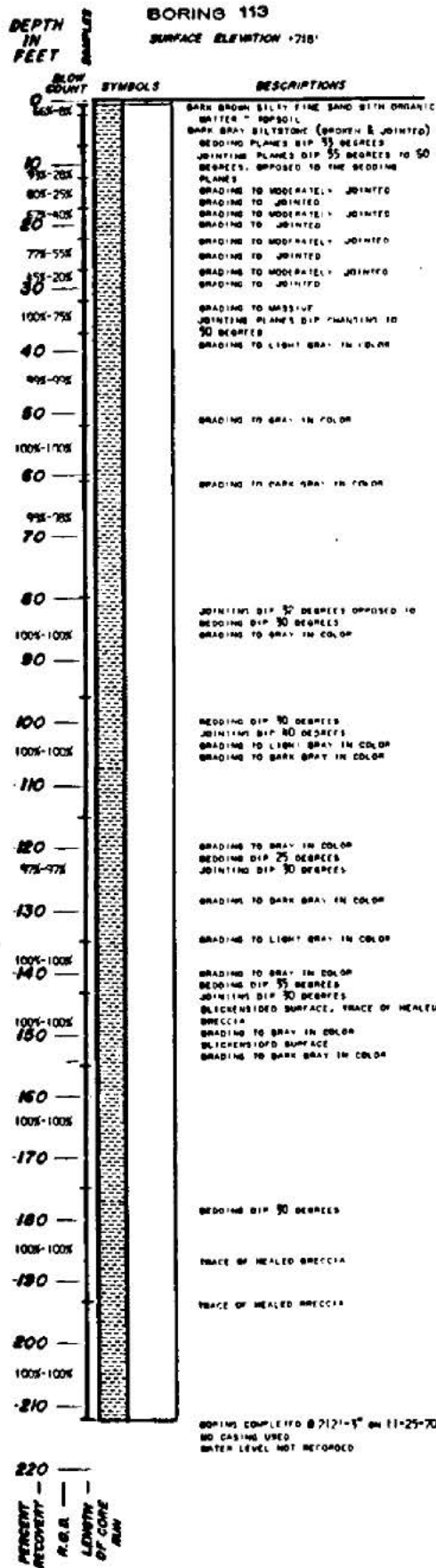


FSAR REV. 65

**SUSQUEHANNA STEAM ELECTRIC STATION
UNITS 1 & 2
FINAL SAFETY ANALYSIS REPORT**

LOG OF BORINGS

FIGURE 2.5-23F, Rev 47

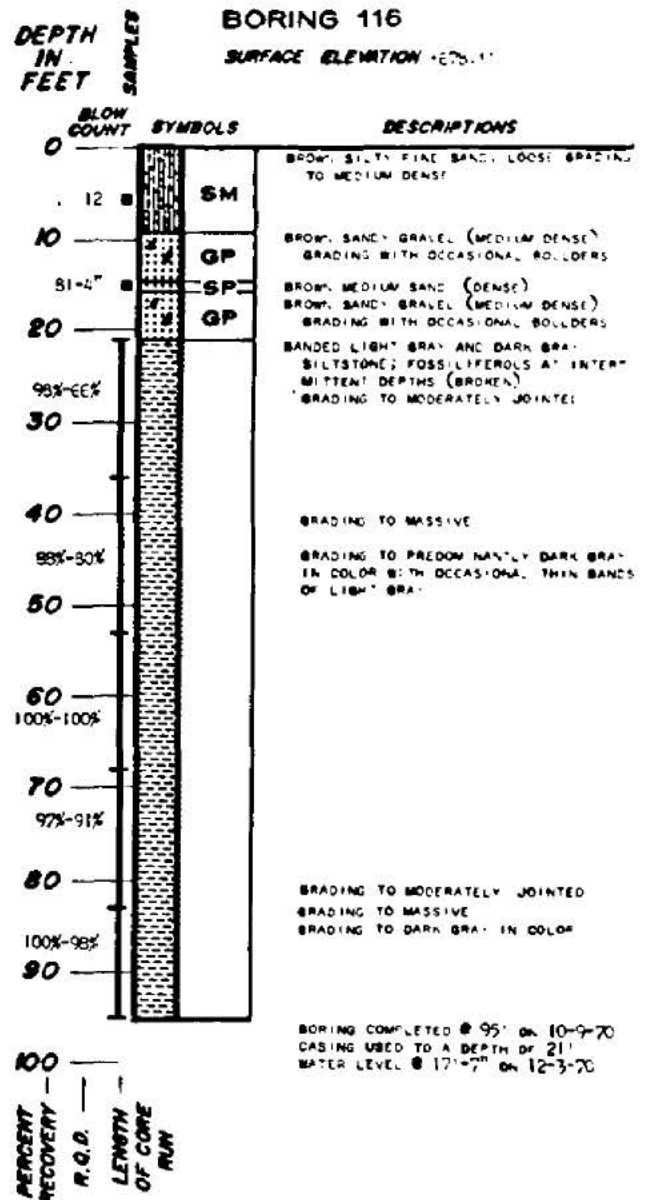
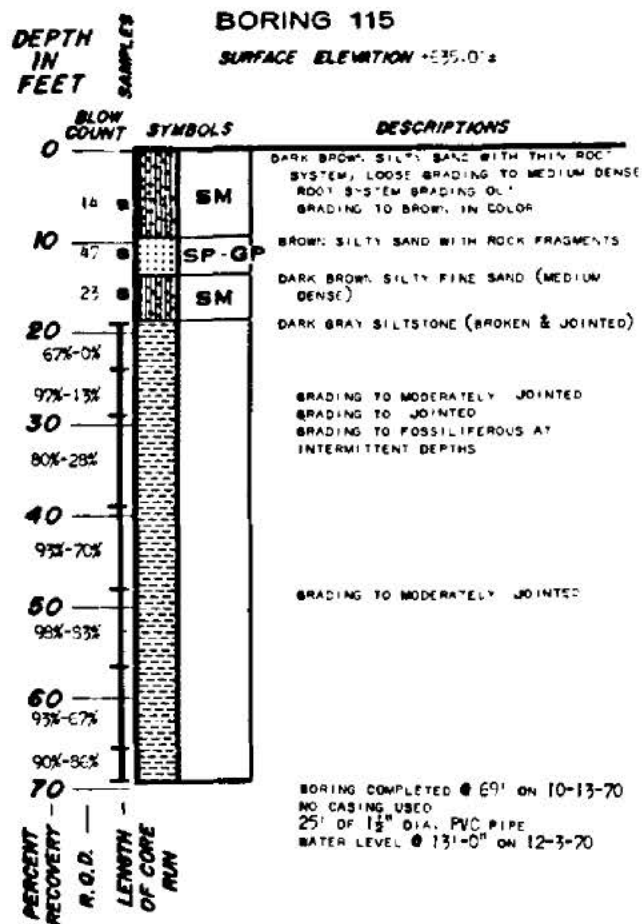


FSAR REV. 65

SUSQUEHANNA STEAM ELECTRIC STATION
UNITS 1 & 2
FINAL SAFETY ANALYSIS REPORT

LOG OF BORINGS

FIGURE 2.5-23G, Rev 47

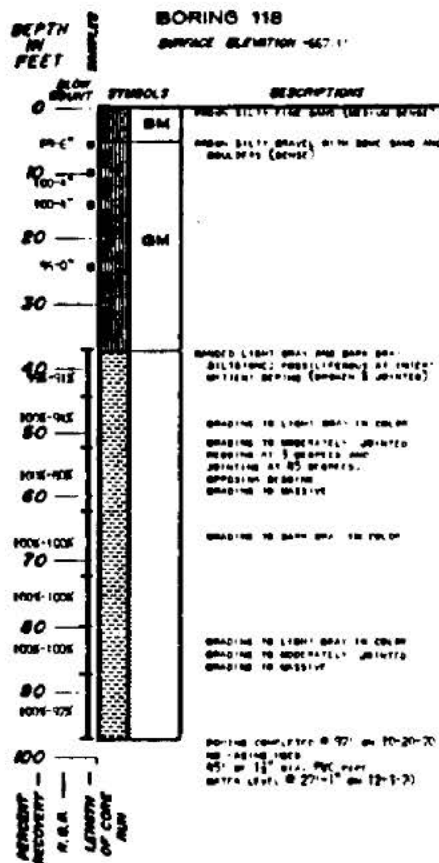
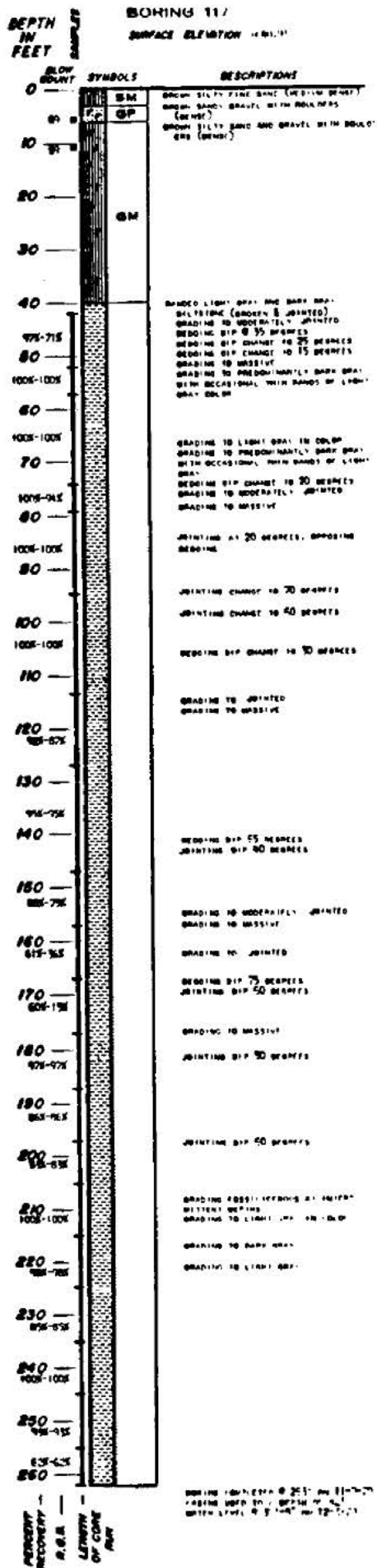


FSAR REV. 65

SUSQUEHANNA STEAM ELECTRIC STATION
UNITS 1 & 2
FINAL SAFETY ANALYSIS REPORT

LOG OF BORINGS

FIGURE 2.5-23H, Rev 47

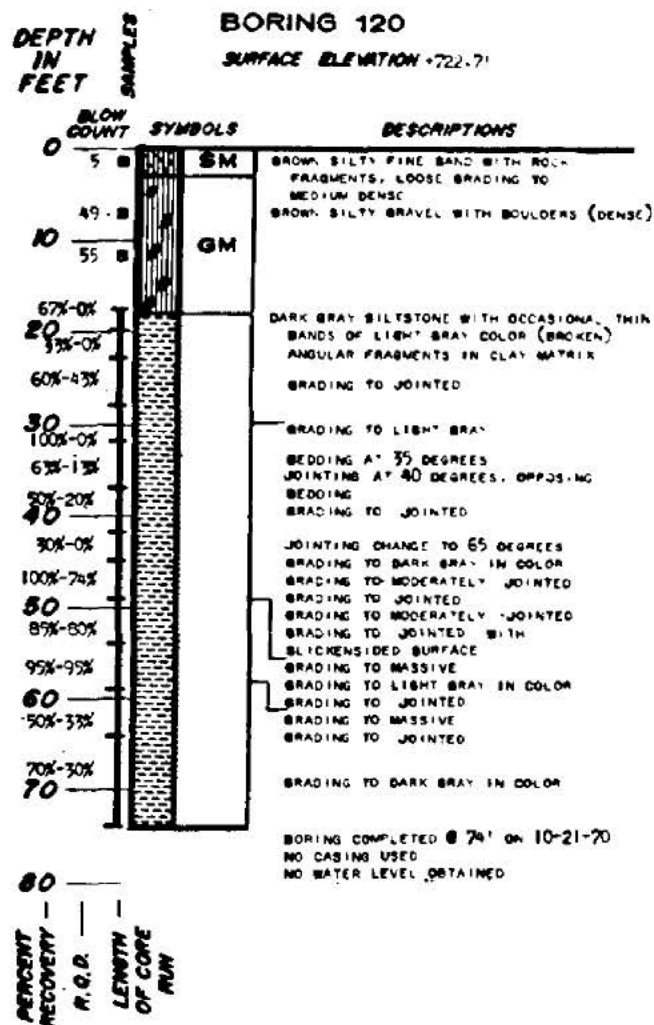
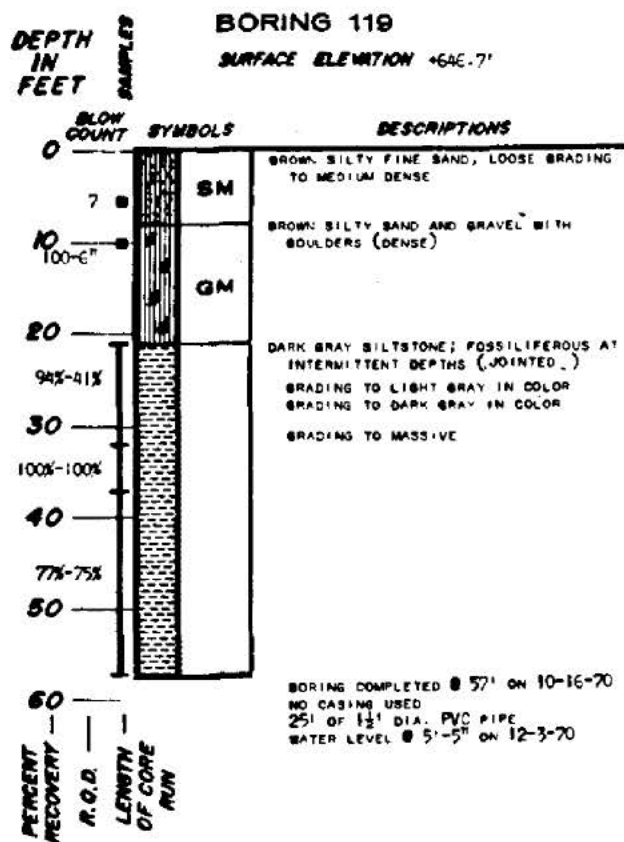


FSAR REV. 65

SUSQUEHANNA STEAM ELECTRIC STATION
UNITS 1 & 2
FINAL SAFETY ANALYSIS REPORT

LOG OF BORINGS

FIGURE 2.5-23I, Rev 47



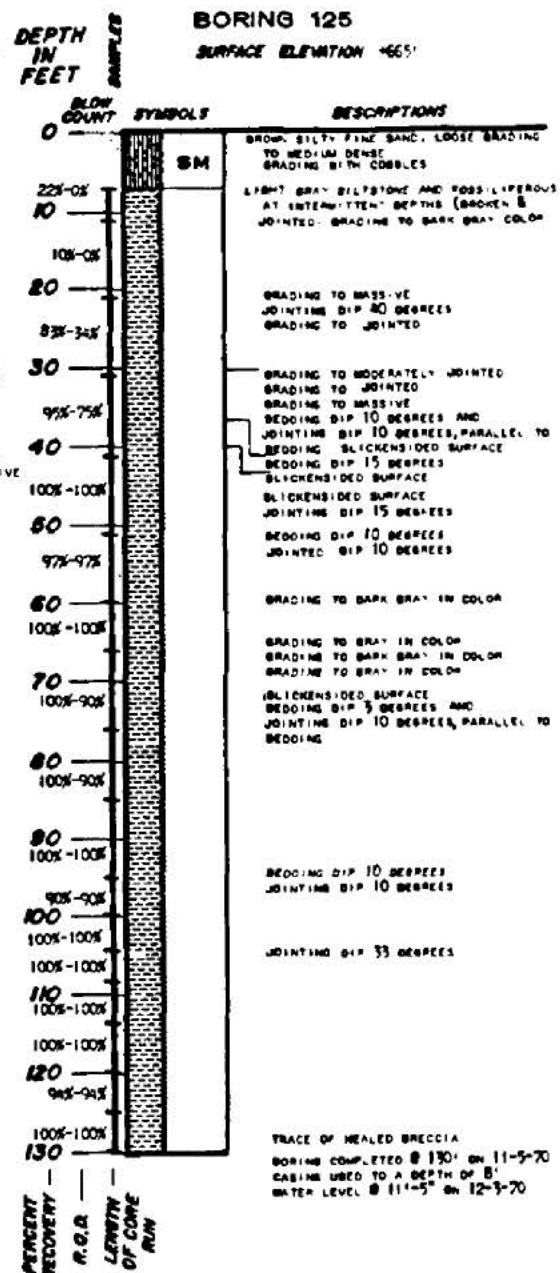
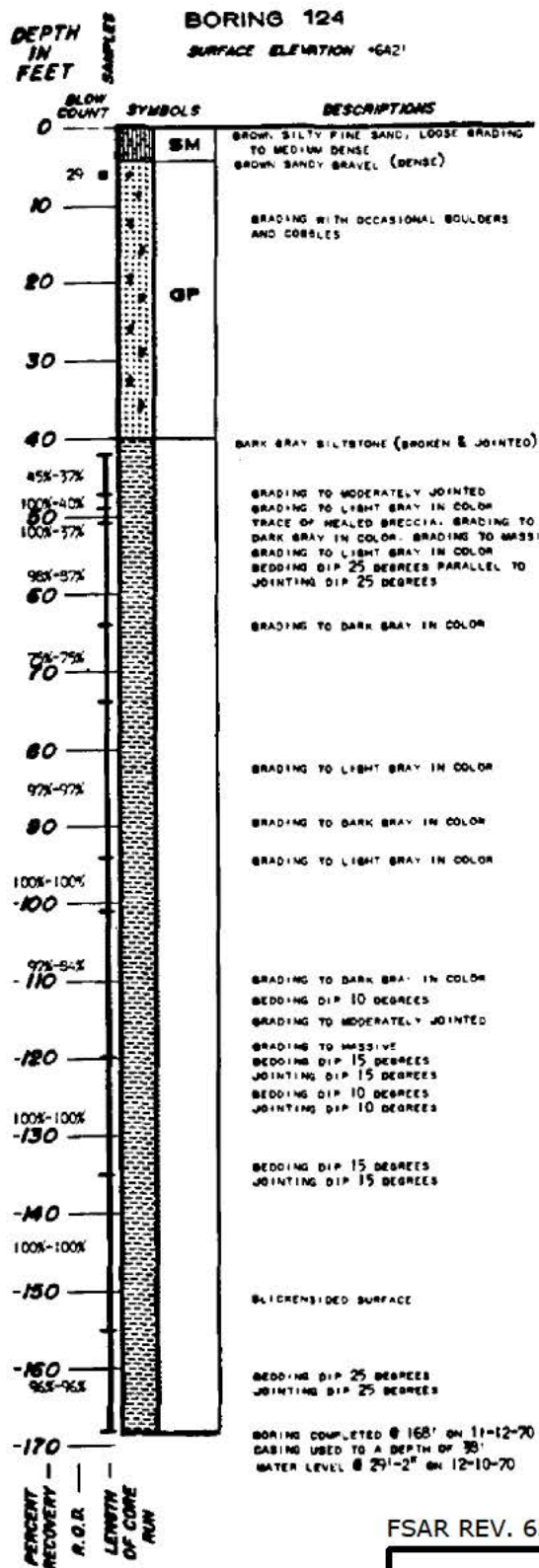
FSAR REV. 65

SUSQUEHANNA STEAM ELECTRIC STATION
UNITS 1 & 2
FINAL SAFETY ANALYSIS REPORT

LOG OF BORINGS

FIGURE 2.5-23J, Rev 47

AutoCAD: Figure Fsar 2_5_23J.dwg

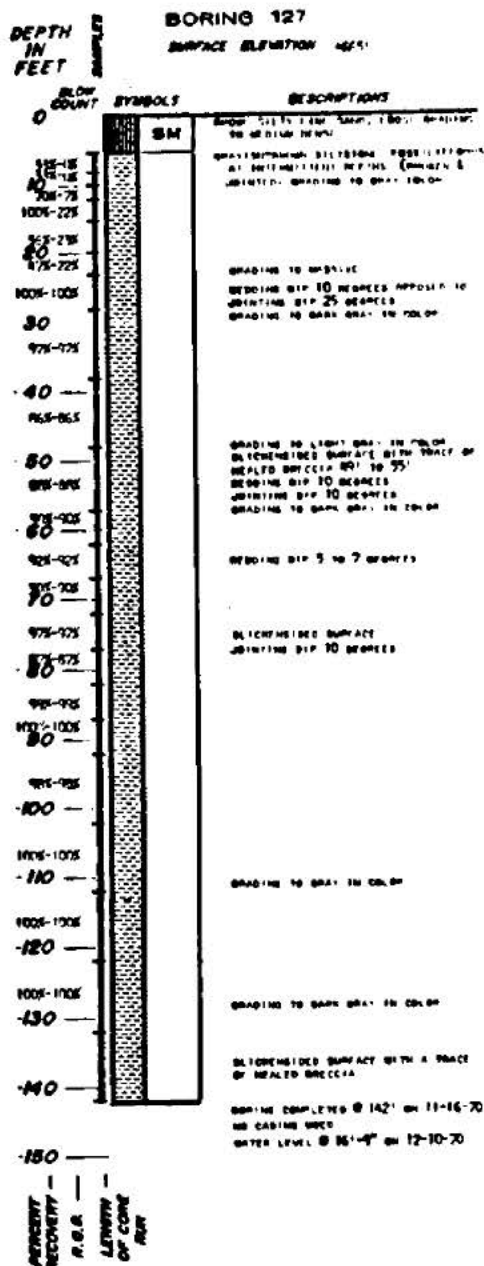
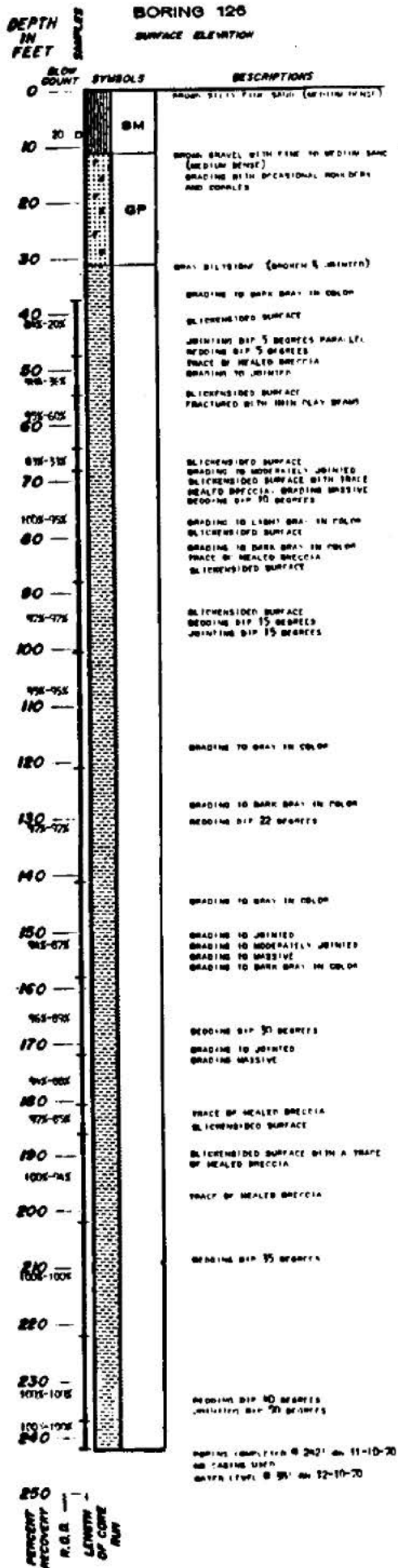


FSAR REV. 65

SUSQUEHANNA STEAM ELECTRIC STATION
UNITS 1 & 2
FINAL SAFETY ANALYSIS REPORT

LOG OF BORINGS

FIGURE 2.5-23M, Rev 47



FSAR REV. 65

SUSQUEHANNA STEAM ELECTRIC STATION
UNITS 1 & 2
FINAL SAFETY ANALYSIS REPORT

LOG OF BORINGS

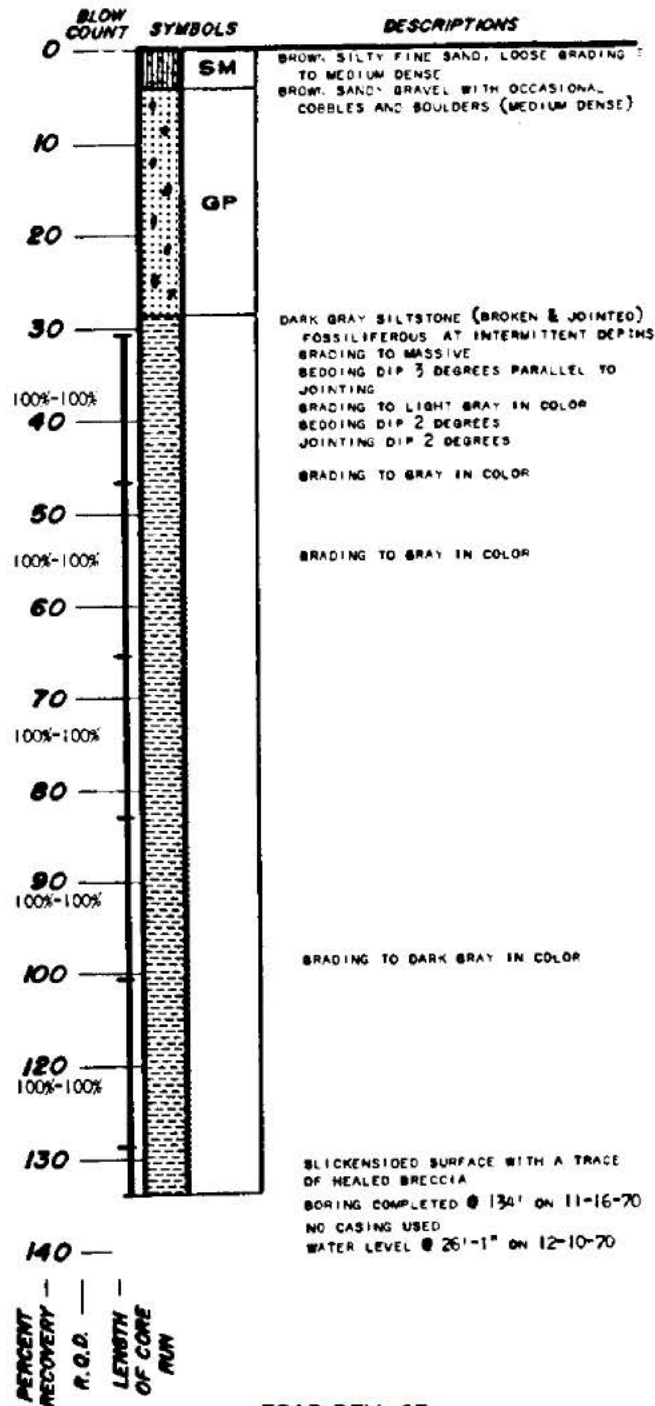
FIGURE 2.5-23N, Rev 47

AutoCAD: Figure Fsar 2_5_23N.dwg

DEPTH
IN
FEET

BORING 128

SURFACE ELEVATION +667'



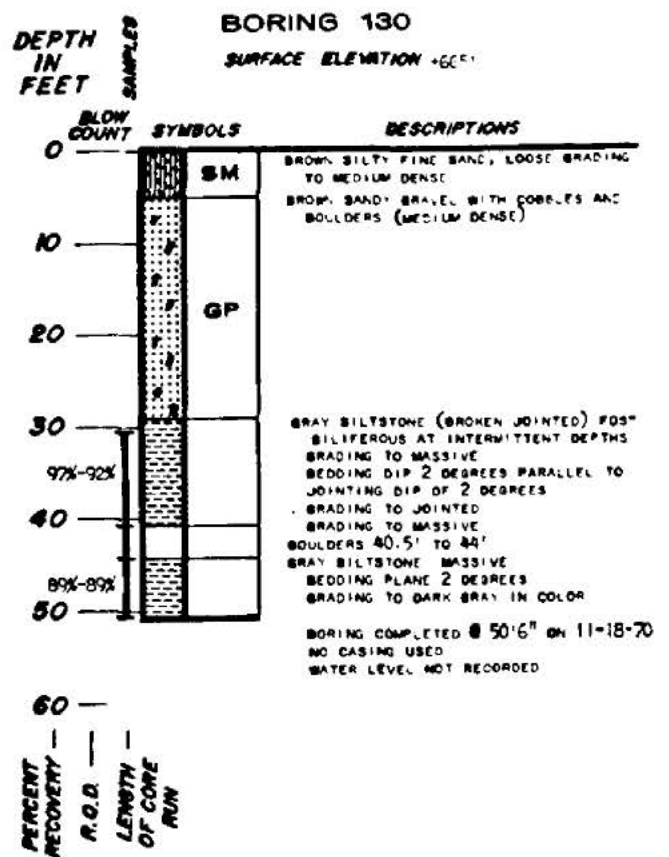
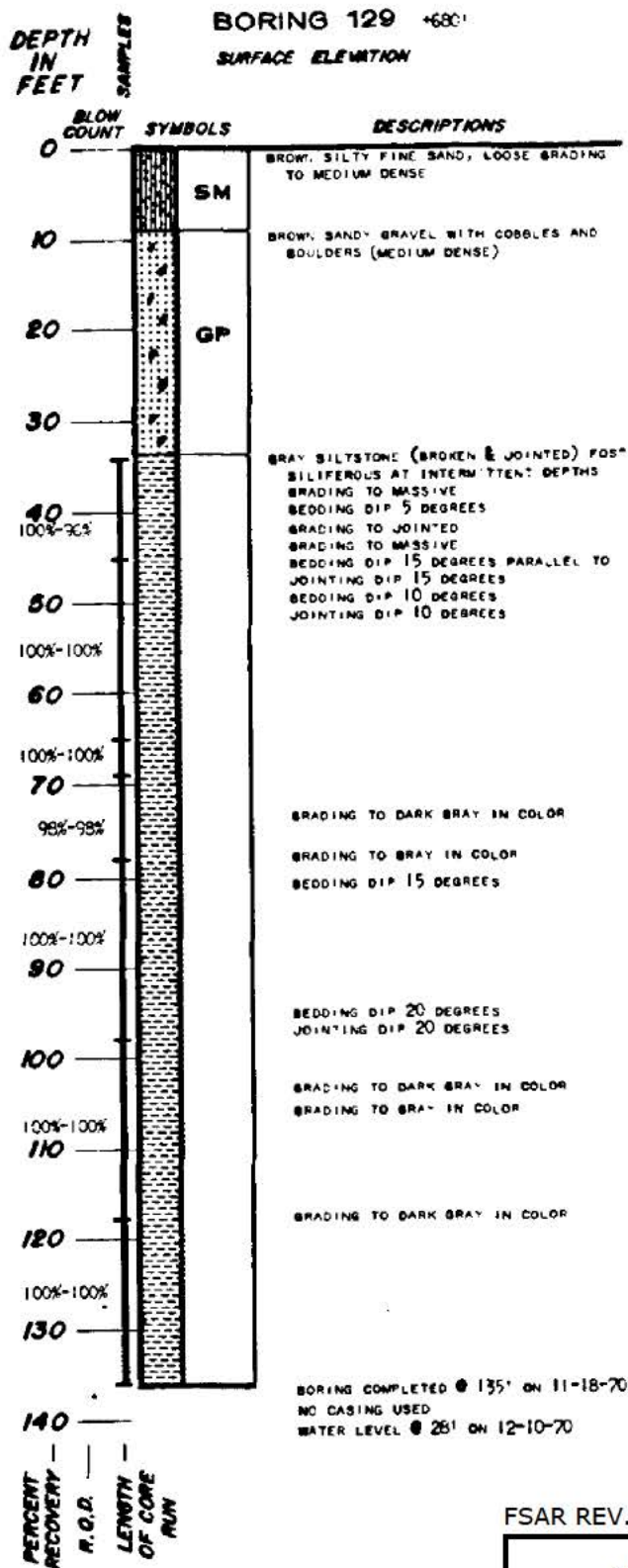
FSAR REV. 65

SUSQUEHANNA STEAM ELECTRIC STATION
UNITS 1 & 2
FINAL SAFETY ANALYSIS REPORT

LOG OF BORINGS

FIGURE 2.5-230, Rev 47

AutoCAD: Figure Fsar 2_5_230.dwg

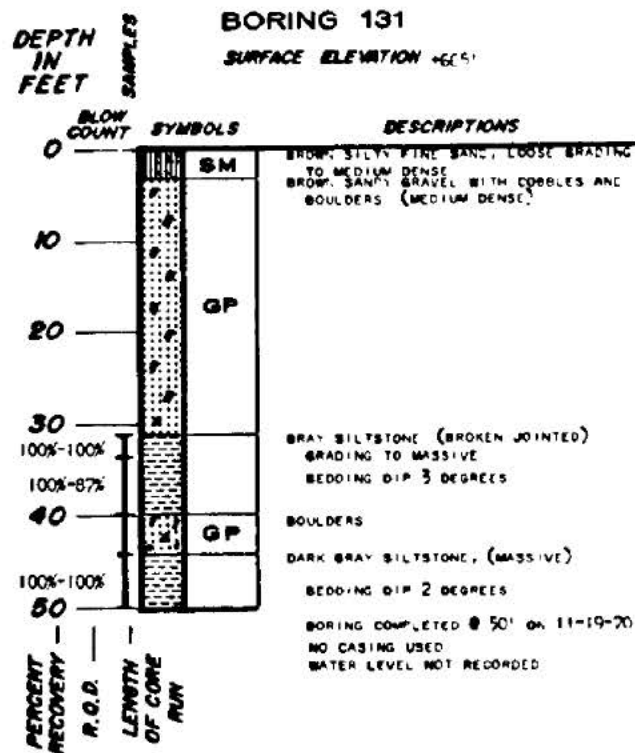
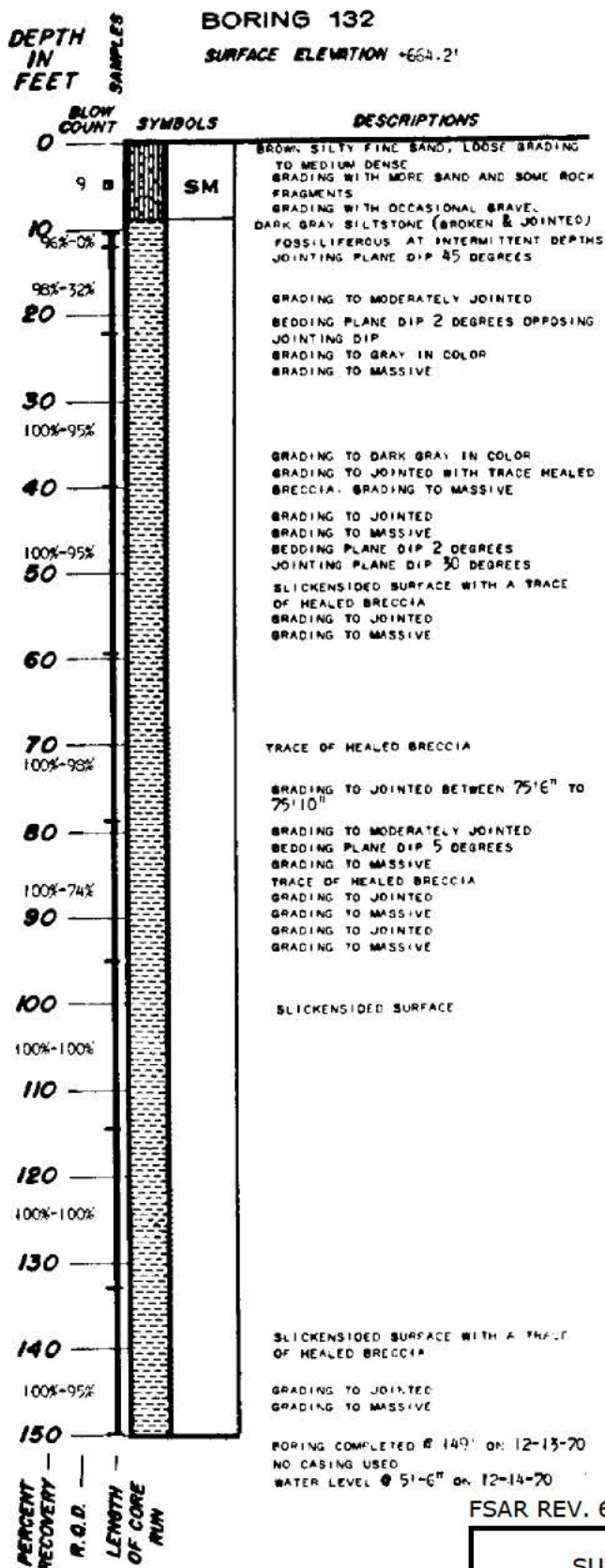


FSAR REV. 65

SUSQUEHANNA STEAM ELECTRIC STATION
UNITS 1 & 2
FINAL SAFETY ANALYSIS REPORT

LOG OF BORINGS

FIGURE 2.5-23P, Rev 47

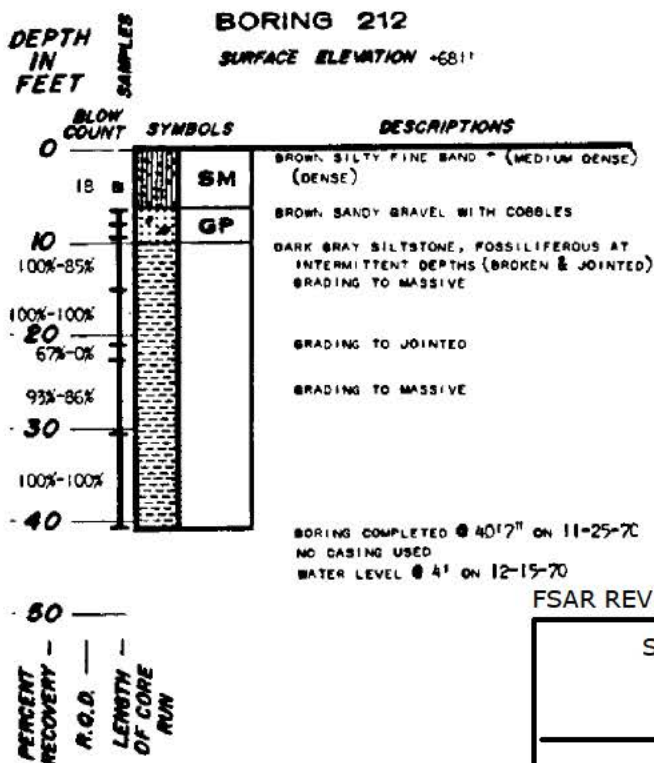
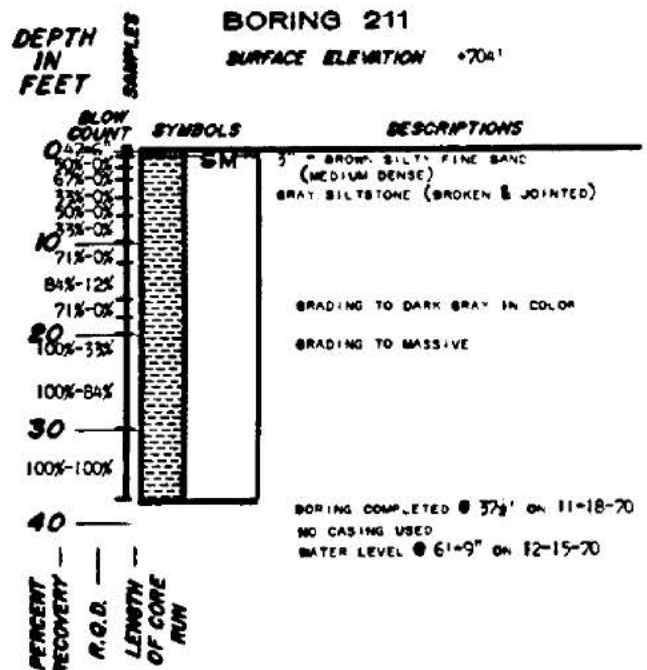
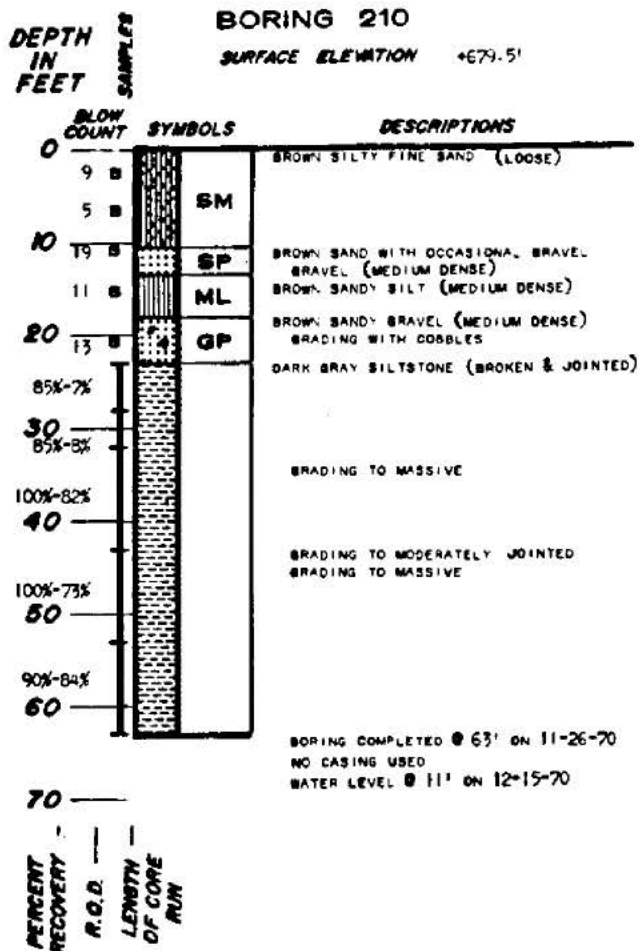


FSAR REV. 65

SUSQUEHANNA STEAM ELECTRIC STATION
UNITS 1 & 2
FINAL SAFETY ANALYSIS REPORT

LOG OF BORINGS

FIGURE 2.5-23Q, Rev 47

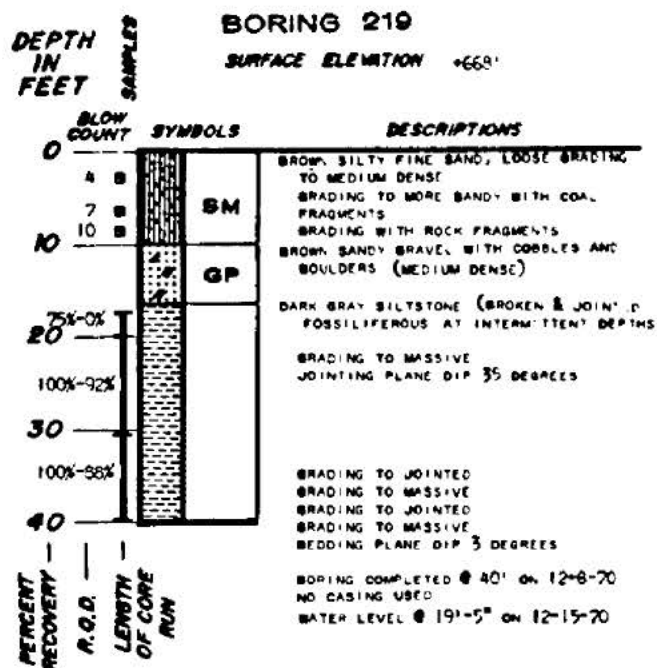
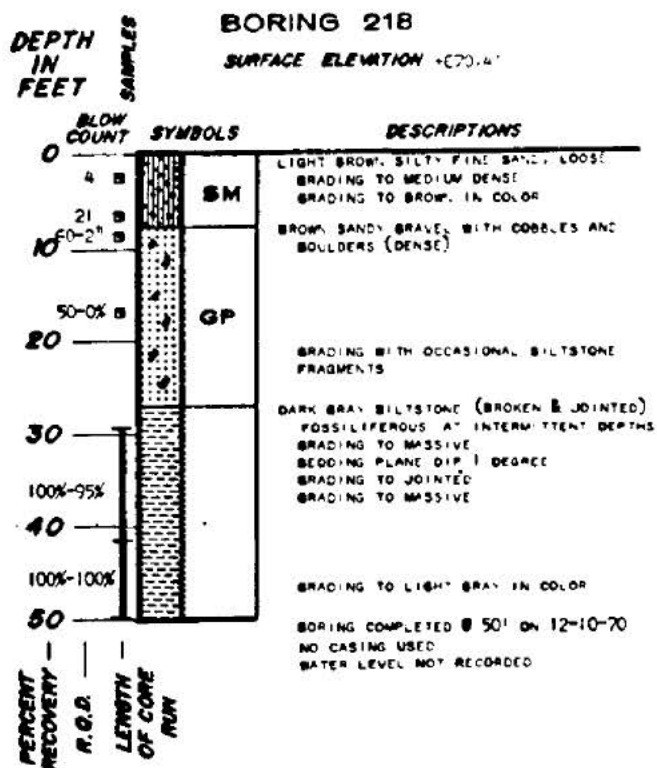
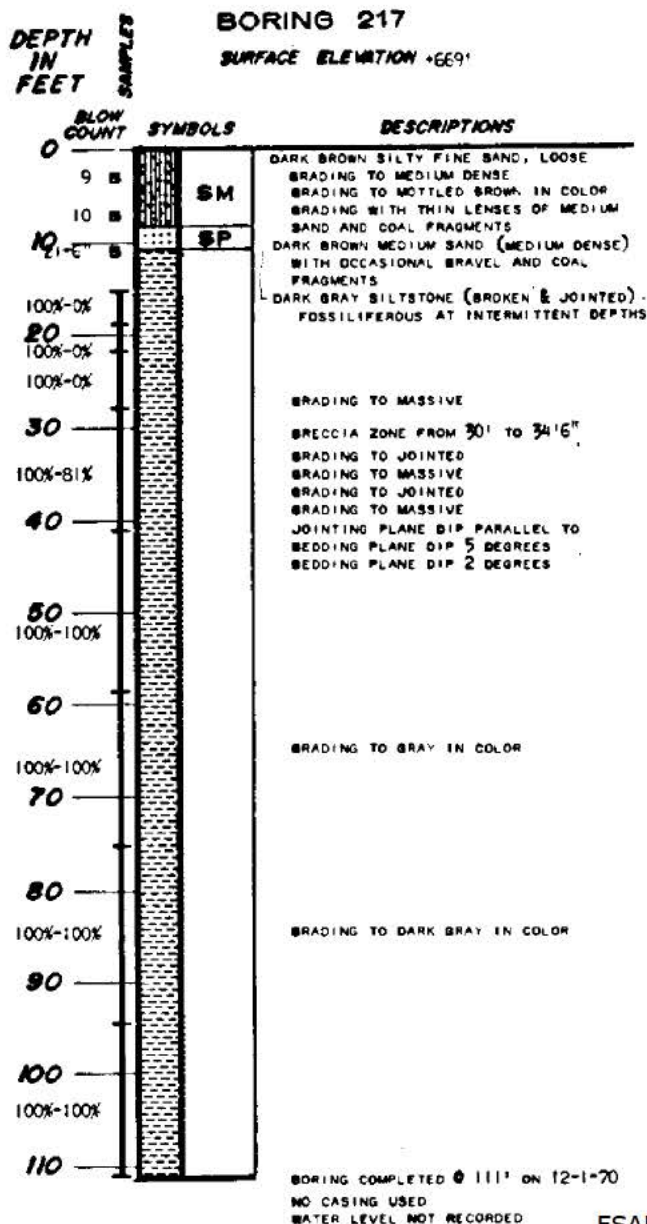


FSAR REV. 65

SUSQUEHANNA STEAM ELECTRIC STATION
UNITS 1 & 2
FINAL SAFETY ANALYSIS REPORT

LOG OF BORINGS

FIGURE 2.5-23R, Rev 47

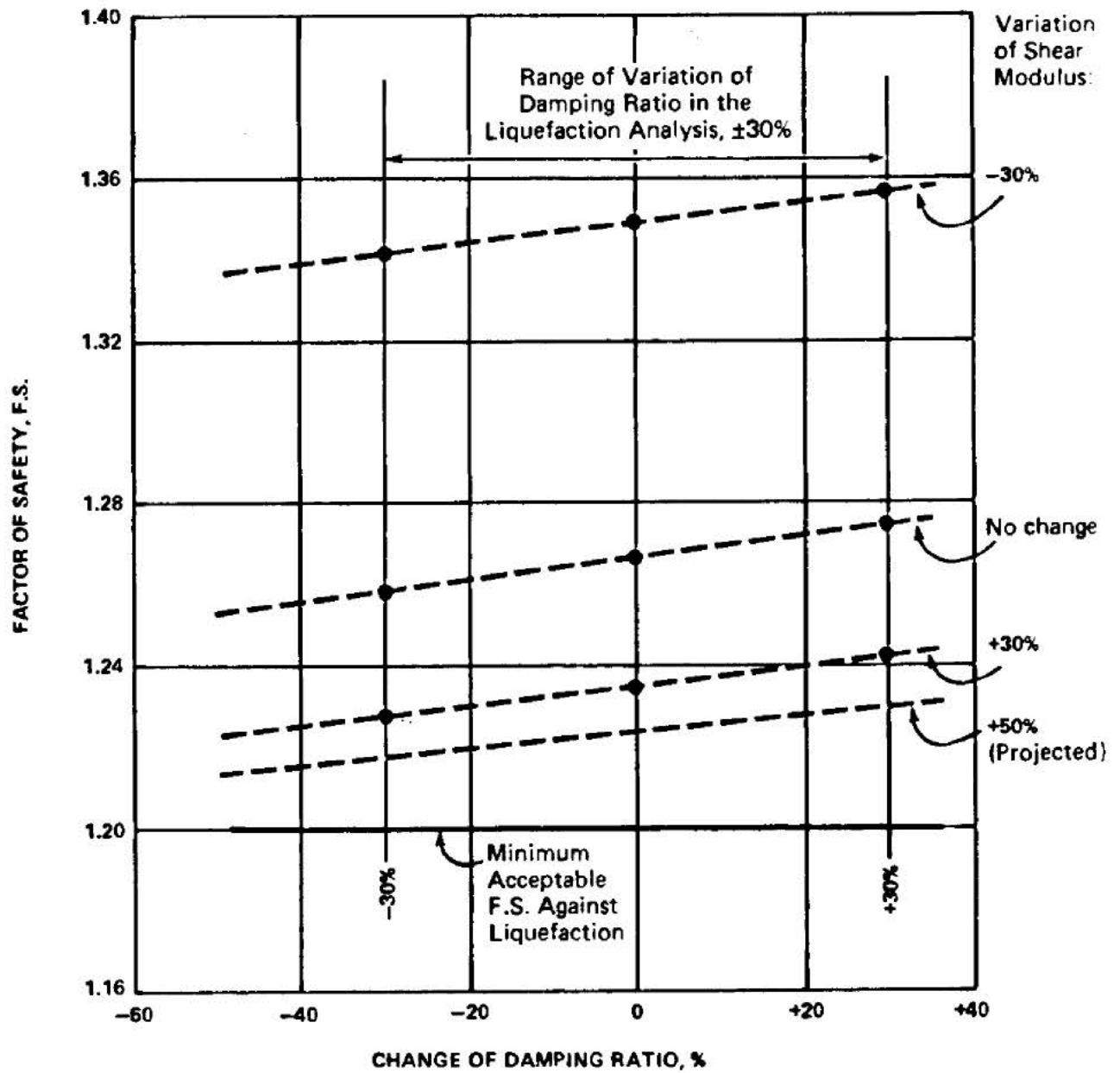


FSAR REV. 65

SUSQUEHANNA STEAM ELECTRIC STATION
UNITS 1 & 2
FINAL SAFETY ANALYSIS REPORT

LOG OF BORINGS

FIGURE 2.5-23T, Rev 47



FSAR REV. 65

SUSQUEHANNA STEAM ELECTRIC STATION
UNITS 1 & 2
FINAL SAFETY ANALYSIS REPORT

VARIATION FACTOR OF
SAFETY (F.S.) VERSUS
CHANGE OF DAMPING RATIO

FIGURE 2.5-50A, Rev 47

AutoCAD: Figure Fsar 2_5_50A.dwg

THIS FIGURE HAS BEEN
DELETED

FSAR REV. 65

SUSQUEHANNA STEAM ELECTRIC STATION UNITS 1 & 2 FINAL SAFETY ANALYSIS REPORT

Figure 2.5C Deleted

FIGURE 2.5C, Rev. 49

AutoCAD Figure 2.5C.doc

9 3 2 5 6 7 8 9 0 1 2 3 4 5 6 7 8 9 0

9067-0407

9067-0407

9 3 2 5 6 7 8 9 0 1 2 3 4 5 6 7 8 9 0

9 3 2 5 6 7 8 9 0 1 2 3 4 5 6 7 8 9 0

9 3 2 5 6 7 8 9 0 1 2 3 4 5 6 7 8 9 0

9 3 2 5 6 7 8 9 0 1 2 3 4 5 6 7 8 9 0

9 3 2 5 6 7 8 9 0 1 2 3 4 5 6 7 8 9 0

9 3 2 5 6 7 8 9 0 1 2 3 4 5 6 7 8 9 0

9 3 2 5 6 7 8 9 0 1 2 3 4 5 6 7 8 9 0

9 3 2 5 6 7 8 9 0 1 2 3 4 5 6 7 8 9 0

9 3 2 5 6 7 8 9 0 1 2 3 4 5 6 7 8 9 0

9 3 2 5 6 7 8 9 0 1 2 3 4 5 6 7 8 9 0

9 3 2 5 6 7 8 9 0 1 2 3 4 5 6 7 8 9 0

0
7
0
-
7
6
5
4
3
2

Thorough inspection of the workings in the Abbott, Kidney, and Hillman veins in the affected area was delayed pending the removal of methane that had accumulated therein as a result of disrupted ventilating facilities. Reestablishment of ventilation permitted inspection of workings in the Kidney vein on February 27 and in the Abbott vein on March 13. Dangerous roof conditions in the Hillman vein have prevented persons from advancing far enough into the workings in the affected area to repair the ventilating facilities; consequently a thorough inspection of the Hillman workings was not possible at the time this report was prepared. Inspection of the Five Foot and Lance veins showed conditions therein to be normal.

1. The vein in the affected area (known as the 38 slope section) was in the form of a trough, the main axis of which pointed east and west. The basin of the trough was beneath Lafayette Street, the crest of the trough on the south side was under and roughly paralleled Charles Street, and the crest of the trough on the north side was under and roughly paralleled Old River Road.
2. Recent spalling of coal off the pillar ribs was most pronounced near the crests of the trough on both the north and south sides.
3. Evidence of lateral movement of the strata was noted in the basin; 2" X 4" stringers installed to suspend trolley wire along gangways driven in the basin were generally bowed--some as much as 12 inches.
4. Generally, props and timber sets showed no evidence of weight, except that chambers No. 100 to No. 107, driven on the north side of the trough and the gangway (No. 573) between them, could not be inspected because of fresh, heavy roof falls and bad roof--evidence of a recent disturbance.

SSES-FSAR

5. Accumulations of methane were found by means of a flame safety lamp at the faces of chambers No. 110 to No. 121 off gangway 573.
6. Mining was conducted properly, and due precautions were taken to assure adequate surface support.

Inspection of the Abbott vein workings on March 13 revealed the following significant information:

1. The Abbott vein in the affected area was in the shape of a trough, similar in shape and position to that in the Kidney vein described previously.
2. The faces of the chambers driven up the pitch on the south side of the basin of the trough had encountered solid rock, indicating a faulted area. Inspection of the maps of the mine workings showed evidence of a displacement fault in all the strata in the area--the main axis of which pointed approximately east and west--and extended through the Woodward and Lance colliery workings.
3. Only slight fresh spalling of coal off the pillars was observed in the Abbott vein, and generally the props and timbers showed no signs of weight. However, almost continuous fresh falls of roof and brows were observed along gangway No. 511, but, as stated before, little or no spalling of coal was seen.
4. Careful examination of the faces of the chambers that had encountered the rock wall at the crest of the trough on the south side showed evidence of downward slipping of the strata along the line of fault.
5. Careful examination of concrete stoppings in the affected area revealed that:
 - (a) A very definite lateral movement of the strata from south to north along the south side of the trough and an upward thrust of the strata along the north side of the trough had occurred. The roof had moved recently as much as one inch away from the tops of some concrete stoppings (set parallel to the axis of the trough), and door frames set perpendicular to the axis of the trough showed evidence of lateral pressure. Concrete stoppings installed along the north side of the trough showed no indication of lateral movement of

SSES-FSAR

the strata, but they all looked as though they had been struck from the bottom with a strong, sudden blow that caused the bottom portions thereof to be splintered.

6. Methane was not found by means of a flame safety lamp during this inspection of the Abbott vein.
7. Mining was conducted properly, and due precautions were taken to assure adequate surface support.

Cause of the Earth Disturbance

According to official reports made by certified fire bosses employed by the Glen Alden Coal Company, following their regular, routine examination of workings in the subsequently affected area, conditions were normal during such inspections on the morning of February 21, 1954.

The charts on the continuous pressure-recording gages at main fans at the following locations showed that an unusual and sudden movement of the recording needle had occurred around 11:30 a.m. on February 21, 1954:

<u>Colliery</u>	<u>Fan</u>	<u>Degree of needle movement</u>		
		<u>Strong</u>	<u>Medium</u>	<u>Weak</u>
Woodward	#1	X		
Woodward	#2	X		
Lance	Baltimore	X		
Lance	Red Ash	X		
Nottingham	#5			X
Nottingham	#6			X
Avondale				X
South Wilkes-Barre	#5		X	
Inman	#21			X
Loomis	#2			X
Loomis	#4			X
Loomis	#39			X
Hollenback				X
Huber	#5	X		
Huber	#8	X		

93259710410

SSSES-FSAR

Sugar Notch	#5		X
Truesdale	#26		X
Truesdale	#1		X
Truesdale	#1 & #2		X
Truesdale	Askam	X	
Bliss	#1		X
Auchincloss	#3	X	

The chart of the cycle stormograph located at South Wilkes-Barre colliery showed an unusual and sudden movement of the recording needle at 11:30 a.m. on February 21, 1954.

This evidence, together with the upward buckling of surface sidewalks and roadways and the appearance of cracks in the ground in the disturbed area, seemed to point to the occurrence of an earth tremor. Upon further investigation of such a possibility, it was found that officials of the Seismology Branch, Geophysics Division, Coast and Geodetic Survey, Department of Commerce, Washington, D. C., had reported the occurrence of an earthquake at 11:20 a.m. on February 21, 1954. This "quake" was recorded on the seismographs at Fordham University and at Columbia University in New York City--but it was also recorded by many other seismographs located throughout the world, and, according to the official Federal report, the earthquake that was recorded on the seismographs at 11:20 a.m. on February 21, 1954, occurred definitely in the Aleutian Islands. No other evidence of earth tremors was recorded by official seismographs for the remainder of February 21, 1954.

Insofar as the seismograph records for February 21, 1954, are concerned, they did not indicate an earth tremor in the vicinity of Wilkes-Barre on that date. However, according to officials of the Seismology Branch, Department of Commerce, Washington, D. C., it is possible for an earth movement to occur at Wilkes-Barre and be too weak to be recorded on seismographs in New York City. Therefore, evidence of a localized earth movement was sought, and, we feel, was found.

Careful study of all the evidence gathered during the investigation of this earth disturbance caused the undersigned Federal investigators to deduce as follows:

1. Around 11:30 a.m. on February 21, 1954, a slight but sudden downward movement of the strata occurred along the displacement fault that exists in the strata beneath the south side of the affected area. We believe it was this sudden jolt that caused the aforementioned needles of the various gages to be moved out of normal position.

11-10-17-1954

SSES-FSAR

2. The powerful forces of the downward movement of the strata along the fault plane were pent up in the adjacent strata until they were suddenly released in an adjusting upward thrust of strata at the weakest point, which seemed to be along the crest of the trough on the north side directly beneath the area where the first buckling and cracking of the surface was observed.
3. Subsequent continued movement of the surface over a gradually extended area was caused by adjustment of the heavy alluvial deposits, which very likely were water logged and in a semi-fluid condition.
4. Whether downward movement of the strata along the fault plane caused failure of the coal pillars and strata under the affected area or whether failure of the coal pillars and strata under the affected area caused downward movement of the strata along the fault plane could not be definitely and positively determined.

Recommendation

Under the circumstances, we cannot offer any recommendation that may prevent recurrence of a similar earth movement.

S/ Frank Retzel
Federal Coal-Mine Inspector

S/ W. T. Torrance
Federal Coal-Mine Inspector

S/ H. F. Weaver
Chief, Coal-Mine Inspection Branch

9 3 2 5 9 7 1 0 4 1 2

SSES-FSAR

APPENDIX 2.5B

CITY OF WILKES-BARRE
REPORT ON AN EARTH DISTURBANCE

This appendix consists of the conclusions and a discussion of the disturbances in the mined area by John C. MacCartney and F. Edgar Kudlich, Consulting Engineers, who were commissioned by the City of Wilkes-Barre, Pennsylvania to investigate the earth disturbances which occurred in the southerly section of that city on February 21 and 23, 1954.

CONCLUSIONS OF MAC CARTNEY AND KUDLICH

"Many theories have been propounded as to the cause of the surface disturbances, which exclude mining as the possible cause. These have been investigated and considered by Dr. Warren J. Mead, Consulting Geologist, and us and have been discarded as unacceptable.

Our conclusions with respect to the disturbances, supported by discussions with Dr. Mead, are as follows:

1. That downward movements occurred at certain points in the southerly section of Wilkes-Barre City on and after February 21, 1954. Reactions from the downward movements resulted in some upward movements, giving to the whole the appearance of an undulation. This combination of movements caused damage to improvements on and under the surface. The magnitude of these movements is not accurately measurable due to the normal lack of references prior to the date of the disturbances.
2. That the disturbances of the surface were caused by a vertical movement in the consolidated strata underlying the area. This movement was transmitted upward through the wash, but not necessarily vertically.
3. That the movement which had its inception in and directly above the Hillman vein would not have occurred had there been no mining.
4. That the Glen Alden Coal Company, in the extraction of coal from the Hillman vein, adopted accepted practices of mining with the intention of supporting the overlying strata, if for no other reason than to protect its mine from the hazard of inundation, but the execution of the accepted practices extended to the removal of top coal and, affected by the presence of faults and a basin, set up stresses which resulted in failure and subsequent movement."

SSES-FSAR

Respectfully submitted,

(Signed) John C. MacCartney
Consulting Engineer

(Signed) F. Edgar Kudlich
Consulting Engineer

Wilkes-Barre, Pennsylvania

April 30, 1954.

(SEAL)

9 3 2 5 9 7 1 0 4 1 4

DISCUSSION OF DISTURBANCES IN MINED AREAS

"Our examinations of the mine workings indicated clearly that conditions in the uppermost five veins of coal that had been mined were abnormal, as evidenced by caving of the top rock and spalling of the pillars. The disturbed condition in the Five Foot and the Lance veins were resultants of movements in the upper veins rather than contributory causes to the disturbances of the surface.

Our references in this report to spalling of ribs and falls of top coal and rock are confined to recent occurrences except where specifically noted to the contrary. Naturally, we had no occasion to examine these mines prior to the February 21, 1954, disturbances. We judged the recency of the spalling and falls of top by the freshness of the exposed surfaces, which opinion was confirmed in many instances by reference to the inspection reports of those company employees whose duty it is to make daily or periodical examinations of active and abandoned workings as required by law. Furthermore, we were accompanied on our tours by individuals who had made inspections of many of the areas between February 21, 1954, and the times of our examinations and who pointed out locations where disturbances had taken place during the intervening period.

In order to portray graphically the conditions encountered in the various veins, transparent overlays were made for each, showing the areas examined and the conditions found. When superimposed in the geologic order of the occurrence of the veins, the overlays revealed a series of unusual coincidences in respect to the disturbances observed in the mines.

For example, the heavy cave previously referred to in the Hillman vein at the foot of No. 34 Slope was found to be directly beneath the heavy falls of top rock beyond which we could not penetrate in Roads 573 North and 573 South in the Kidney vein which lies 80 feet above the Hillman. Approximately at the same point and about 180 feet above the Hillman was the heaviest fall of top rock encountered and crossed in the Abbott vein in Road 511 South. This was also the point where the two ventilation walls were cracked in the Abbott.

Conversely, where the pillars in the Hillman Slope were spalled but the top coal and top rock remained intact there was spalling in the underlying Five Foot Vein.

Again, we were unable to penetrate the area in the Hillman vein lying between the Lance-Woodward barrier pillar and No. 34 Slope because of heavy falls. Although we also were unable to examine the overlying Kidney vein where worked in this vicinity, it was reported to us by both Federal and State Mine

SSES-FSAR

Inspectors that there were breaks in the bottom rock of the Kidney vein and that one portion of the Kidney near the Hillman No. 34 Slope was completely caved. Our own inspection of the Abbott vein in this same area revealed heavy spalling and some caving of top rock and a crack in the roof which was admitting water at the time of our visit.

We were stopped in the Hillman vein at the perimeter of the easterly surface disturbance by heavy falls of top coal and rock. In the Kidney vein above, just west of our point of penetration in the Hillman, we found spalling of the ribs and top falls. In the Abbott vein above and in the general line of the disturbances in the Hillman, there were spalling of the ribs and falls of top.

We noted also that near the center of the eastern disturbances, about at Academy Street, there were heavy spalling of the ribs and falls of top in the Kidney vein and lesser spalling and falls of top in the Abbott. The Hillman in this area was impenetrable.

In the Kidney vein, under the Lafayette Gardens area, there were spalled ribs and one top fall and a reputedly caved area which we could not examine, and spalling and heavy top falls in the overlying Abbott. The Hillman vein workings here also were impenetrable.

From the foregoing discussion it is evident that we were unable to examine the greater portion of the Hillman vein under the disturbed area. However, in several instances where we found caving and spalling in the Hillman vein we were able to observe similar conditions in the overlying veins. In other instances, where we were able to observe the overlying veins, we were unable to examine the Hillman vein. A comparison of the conditions at the latter points in the overlying veins with those where we were able to examine all three leads to a proper assumption that the conditions in the Hillman where not penetrated were just as bad as those observed where penetrated.

By measuring the mine workings as portrayed by the maps, we have found the normal extraction of coal in the Abbott vein had allowed 46.65% of the original vein area to remain as pillars, even after reserve pillars had been chambered; 49.49% remained in the Kidney vein and 51.35% in the Hillman vein.

No more than a cursory investigation was made of the size and strength of the pillars system in the Abbott and Kidney veins as the height of either vein, as well as the burden upon the vein, was less than the height of and burden upon the Hillman vein.

9 2 2 5 9 7 1 0 1 2 6 5 2 6 6

SSSES-FSAR

A computational investigation of the strength of the pillar system in the Hillman disclosed that the weight on the pillars, before the taking of the top coal, was slightly below the minimum calculated strength of the pillar under normal conditions.

By reference to the stratigraphic plates, it will be noted that the Hillman vein carries a bench of top coal which in ordinary practice is not mined during the first extractive operation unless it is structurally so weak that it fails during the first mining. It has been found that the top bench of coal is more stable than the immediate roof of the vein and therefore reduces the cost of maintaining the mine openings.

In the greater part of this area the operator has removed the top coal prior to the abandonment of the area, and accepted practice in the region, thereby increasing the height of the original pillars.

The ability of a coal pillar to support overlying strata is affected by the height of the vein. As a pillar increases in height its ability to support decreases. Consequently, the removal of the top coal of the Hillman vein tends to weaken the pillar system.

In this instance, the increased height of the pillars and the consequent weakening of the pillar system creates a condition which is further compounded by the presence of a series of faults. The geological definition of a fault is "a break in the continuity of a body of rock." Here, however, we use the word in the generally accepted application in the Anthracite district, e.g., an abrupt change in the plane of either the top or bottom rock, or of both, accompanied by a change in the thickness of the vein. The word also is commonly applied to structural irregularities in the rock above or below the vein. Where these faults occur the rock and vein strata are weaker than normal.

In addition to the removal of the top coal and the presence of faults in this area, there is a third condition which tends to rob the pillars of their normal efficiency and that is the occurrence of a syncline or basin centered beneath the disturbed area. The decrease in pillar efficiency is brought about by the fact that the force of gravity is not perpendicular to the plane of the vein.

In spite of the presence of faults and a basin, the strata were in equilibrium before mining. Had it not been for mining, the strata would have remained in equilibrium. It is a fact that the creation of voids, regardless of extent, sets up stresses in the surrounding strata. When the stresses created exceed the strength of the strata, failure must occur and it follows

7
1
0
1
2
6
5
2
3
9

SSES-FSAR

that the equilibrium is disturbed. Movement and redistribution of the stresses follow until equilibrium is re-established.

Many theories have been advanced as to the causes of the surface disturbances. No matter how vague or tenuous these theories may have been, we have investigated them and brought them to the attention of Dr. Warren J. Mead and discussed them with him.

Dr. Mead, former head of the Department of Geology, Massachusetts Institute of Technology, and now Professor Emeritus of the same department, is an internationally known geologist and a consultant in economic engineering and geology. Dr. Mead made a personal inspection of surface of the disturbed area, has reviewed carefully the reports of our findings in the mines, has examined the mine maps and cross sections of the Glen Alden Coal Company and has studied the overlays and other exhibits prepared by us."

01401266266

APPENDIX 2.5C

BORING LOGS

2.5C.1 Summary of Field Density Test Results

This summary is divided into four parts as follows:

- 1) Introduction
- 2) Specification Requirement
- 3) Explanation of Results
- 4) Conclusion

1) INTRODUCTION

The terminology used by U.S. Testing to identify the soils does not agree exactly with specification wording and the wording used in Subsection 2.5.4. Further, there are some inconsistencies on the "U.S. Testing Co." reports regarding elevations and/or coordinates. This condition is clarified later in this summary.

As explained in Subsection 2.5.4 the basic intent of the soil testing was to check the recompaction of the natural soil beneath the concrete liner and check the compaction of all soil fill used.

2) SPECIFICATION REQUIREMENT

The specification governing the work in the spray pond and vicinity addressed two types of soil fill (as well as recompaction of the existing soil under the concrete liner addressed in Section 2.5.4.5.2.2), classified as follows:

a) USAGE:

Fill Type A

This will be used for backfill behind concrete retaining walls, concrete cut-off walls and backfill where any make-up is required in soil beneath the concrete liner, spillway or service road.

Fill Type B

This will be used for embankment fill in the immediate vicinity of the spray-pond and ESSW Pumphouse.

0
2
7
0
4
7
9
10
14
15
6

General

Fill Type A

Fill Type B

c) PLACEMENT :

The finished grade of all fills shall be within \pm 2 inches of elevation specified or shown.

Fill Type A

Fill Type A shall be placed in a 6 inch maximum uncompacted layer thickness, moisture conditioned to obtain the required compaction, and compacted to at least 80 percent relative density as determined by ASTM D2049.

Fill material placed within 2 feet of structures and in areas where large construction equipment cannot be used shall be compacted to the specified density by hand operated equipment.

SSES-FSAR

Fill Type B

Fill Type B shall be placed in a 15 inch maximum uncompacted layer thickness, moisture conditioned to obtain the required compaction, and compacted to satisfy both of the following requirements:

- a) At least 80% relative density as determined by ASTM D2049 for material having not more than 12% passing the No. 200 sieve or 90% of maximum dry density as determined by ASTM D1557 for all other material.
- b) Irrespective of the compacting effort to satisfy part a) above, the fill shall be compacted in one of the following manners as a minimum effort:
 - i) Using a crawler tractor having a weight at least equal to that of a D8 Caterpillar tractor with bulldozer blade. Each track shall overlap the preceding track by not less than four inches. When the tractor has made one entire coverage of an area in this manner, it will be considered to have made one pass. Each fill lift shall be compacted with four passes.
 - ii) Using a vibratory roller of minimum weight 20,000 pounds having a roller width of approximately 78 inches and a diameter of approximately 60 inches. The roller shall have a vibrator frequency range of between 1100 and 1600 vibrations per minute and have a minimum vibratory dynamic force of 40,000 pounds. The roller speed shall not exceed 3 mph and each track shall overlap the preceding one by at least 4 inches. When the roller has made one entire coverage of an area in this manner, it shall be considered to have made one pass. Each fill lift shall be compacted with four complete passes.
 - iii) Using a hand controlled vibratory compactor in locations inaccessible by tractor or vibratory compactors will be

10426526

SSES-FSAR

on the basis of the demonstrated ability of the compactor to compact the material to the same density as the contiguous backfill.

d) TESTING

The Subcontractor shall engage the services of an independent soils laboratory to carry out the testing specified herein. Reports of results shall be made available to the Contractor immediately they are available, but not more than 7 working days following completion of the test. Whenever doubt exists as to whether the specified degree of compaction has been attained, density and compaction tests shall be promptly arranged by the Contractor to verify conformance with this specification. The Subcontractor will be responsible for the cost of this testing.

The Subcontractor shall be held responsible to remove and recompact, at his own expense, any fill that fails to meet the specified degree of compaction.

The in-situ density of Fill Types A and B shall be determined in accordance with ASTM D1556 and performed at a frequency of at least one test per lift and every 1000 square feet on plan for Fill Type A and every 10,000 square feet on plan for Fill Type B.

Tests in accordance with ASTM D2049 or ASTM D1557, as appropriate, shall be carried out on the same material extracted for the ASTM D1556 test. The frequency of this testing shall be carried out at least twice in each 8 hours during placing operations.

Gradation tests in accordance with ASTM D422 shall be carried out at least twice in each 8 hours during placing operations.

3) EXPLANATION OF RESULTS

Generally, limits of excavation, fill and backfill for Seismic Category I structures are shown on Figure 2.5-37. However, the test data reports furnished by the "U.S. Testing Company"

SSSES-FSAR

and included in the appendix are applicable to the spray pond area only (sand-cement-flyash mixture was used elsewhere). In order to clarify the locations of the samples identified in the "U.S. Testing Company" Reports, a new Figure 2.5-59 has been prepared showing wherever possible the distribution within the spray pond. Some traceability has been lost and not every test is plotted on this figure. It should be noted that the south west section of the pond was excavated in rock; soil sampling was therefore not applicable. Fill Type B was placed predominantly in the area to the south and south-east of the ESSW Pumphouse. However, there is a good distribution of tests overall for the soil areas; the results are discussed more closely under a following section dealing with statistical analysis. The correlation testing was carried out at a lesser frequency than specified. The good consistency of the material used, as indicated by the results of the compaction tests, permitted this to be acceptable.

In some cases, the test reports show that "failures" occurred. Whenever this was the case, the soil was recompact until satisfactory compaction was achieved. Accordingly, amended test reports #'s 7, 12, 17, 18, 20, 23, 32 and 33 are submitted. A copy of the SDDR (Supplier #46, Bechtel #52) is also submitted. A summary of the amendments is as follows:

- a) U.S. Testing Company Report No. 7 dated September 27, 1977 shows Test No. 1 failed with a relative density of 63.3% on August 29, 1977. After recompaction, Test Nos. 2, 3 and 4 were retested on August 30, 1979, for this same area, as per the field notes dated August 29, 1977, and August 30, 1977.
- b) U.S. Testing Company Report No. 12 dated October 4, 1978 shows Test No. 1 STA. 0 +90 failed with a relative density of 74.0%. Test No. 2 STA. 0 + 110 and No. 3 STA. 1 + 130 were retaken for this location with relative density results of 94.4% and 105.4% respectively, as per the field notes dated August 19, 1977, to August 24, 1977.

9 3 2 5 2 6 1 0 4 2 3

SSSES-FSAR

c) U.S. Testing Company Report No. 17 dated October 5, 1978 shows Test No. 3 was retaken (Relative Density 82.4%) because of failure of Test No. 2 (Relative Density 13.1%). See field notes dated September 12, 1977.

d) U.S. Testing Company Report No. 18 dated October 5, 1977 shows Test No. 1 (Relative Density 65.7%) and Test No. 2 (Relative Density 39.8%) taken on September 15, 1977, and Test No. 3 (Relative Density 74.0%) taken September 19, 1977, failed. Retest on September 30, 1977, shows satisfactory results, as per field notes dated September 15, 1977, September 19, 1977, and September 30, 1977.

e) U.S. Testing Company Report No. 20 dated October 6, 1977 shows Test No. 2 (Relative Density 13.6%) was an error in calculation. Should be 82.6%.

Test No. 4 (Relative Density 32.1%) was retaken after a recompaction and shown in Test No. 5 (Relative Density 83.4%). See field notes dated September 21, 1977.

f) U.S. Testing Company Report No. 22 dated October 7, 1977 shows retest done August 25, 1978, and reported on Test Report No. 43 dated September 7, 1978. See field notes dated September 15, 1977, and August 23, 1978.

g) U.S. Testing Company Report No. 23 dated October 7, 1977 shows retest taken September 21, 1977.

Note: Identification sheet attached to original report incorrectly shows S.16. Actual tests were done on S.14.

See field notes dated September 19, 1977, attached to Report No. 18 and dated September 21, 1977.

SSES-FSAR

- h) U.S. Testing Company Report No. 32 dated December 7, 1977 shows retest taken September 15, 1977, and reported on U.S. Testing Company Report No. 33. See field notes dated November 14, 1977, and November 15, 1977.

Statistical Distribution of Field Density Test Results

The field density test results given in the test reports were grouped for statistical study according to the test location and the compaction category (subgrade preparation or fill/backfill). The subgrade preparation for the spray pond liner was further divided into two groups -- pond bottom and pond slope.

The mean and standard deviation were computed for each group of data. Where additional compaction and density tests were made at the location where an initial test indicated too low a density, then only the final density result is included in the statistical study.

The results of the statistical distribution of percent compaction and relative density for all groups of data are summarized in Figure 2.5-60. For each group of data, the frequency histogram, number of tests, mean, standard deviation, and compaction criterion are shown. However, for small groups when the number of tests is only 2 or 3, only the mean is given.

Summary of Statistical Results

The statistical evaluation indicated the following:

- a) The distribution of relative compaction and relative density shown in the frequency histograms are generally skewed distributions with a concentration of test results close to the minimum compaction required by the specification.
- b) The exceptions to the above are exhibited in two groups of data:
 - i) Subgrade Preparation for spray pond liner at the pond bottom, when 80 percent relative density was required.
 - ii) Fill to the south and southeast of the ESSW Pump house.

2325971043

SSS-FSAR

Both sets of data show a mean much higher than the required compaction. The mean of the first group is 90.3 with minimum requirement of 80.0 (relative density). The mean of the second group is 97.0 with minimum requirement of 90.0 (percent of maximum dry density).

- c) Although standard deviation was computed as a matter of interest, it is not significant in this case because the specification minimum requirements were met.

4) CONCLUSION

The test results and statistical analysis demonstrate that the specification compaction requirement was met. The spray pond was constructed upon a sound foundation and will adequately serve its intended function.

An amendment is made to Subsections 2.5.4.5.2.2 and 2.5.4.5.3 to address the "filled" area to the south and south-east of the ESSW pumphouse, since some of the "U.S. Testing Co." reports cover the compaction of this area. Amended test reports are also included in this appendix.

9 3 2 5 9 7 1 0 4 3 0

SSES-FSAR

2.5C.2 Listings of Boring Logs

<u>Item</u>	<u>Sheets</u>
Key to Soil Boring Log Test Abbreviations For Borings 1101 through 1128	1
General Notes for Borings B1 through B-11	1
Boring Log 1101	1
Boring Log 1102	1
Boring Log 1103	1
Boring Log 1104	2
Boring Log 1105	1
Boring Log 1106	2
Boring Log 1106-A	1
Boring Log 1107	2
Boring Log 1107-A	1
Boring Log 1108	1
Boring Log 1109	1
Boring Log 1110	2
Boring Log 1110-A	1
Boring Log 1111	2
Boring Log 1112	2
Boring Log 1112-A	1
Boring Log 1113	2
Boring Log 1113-A	1
Boring Log 1114	2
Boring Log 1115	2
Boring Log 1115-A	1

SSS-FSAR

<u>Item</u>	<u>Sheets</u>
Boring Log 1116	2
Boring Log 1117	1
Boring Log 1120	2
Boring Log 1122	1
Boring Log 1123	1
Boring Log 1124	1
Boring Log 1125	1
Boring Log 1126	2
Boring Log 1127	2
Boring Log 1128	2
Boring Log B1	1
Boring Log B2	2
Boring Log B3	1
Boring Log B4	1
Boring Log B5	2
Boring log B6	1
Boring Log B7	1
Boring Log B8	2
Boring Log B9	1
Boring Log B10	1
Boring Log B11	1
Boring Log 1	2
Boring Log 2	2
Boring Log 3	2

SSES-FSAR

<u>Item</u>	<u>Sheets</u>
Boring Log 4	2
Boring Log 5	2
Boring Log 6	2
Boring Log 7	2
Seismic Velocity and Elastic Modul Measurements, Spray Pond, by Weston Geophysical Engineers, Inc.	11

NOTE: Holes 1118, 1119, and 1121 were planned but not drilled due to the bedrock out-cropping at borings 1118 and 1121, and heavy rock fill at boring 1119.

9 3 2 5 9 7 1 0 4 2 9

SSSES-FSAR

KEY TO SOIL BORING LOG TEST ABBREVIATIONS

FOR BORINGS 1101 THROUGH 1128

CR - Cyclic Consolidated - Undrained Triaxial Test

S - Consolidated - Drained Triaxial Test

Gs - Specific Gravity Determination

Grain Size - Grain Size Determination

9325710430

SSES-FSAR

GENERAL NOTES FOR BORINGS B1 THROUGH B11

1950 Chicago Building Code Soil Classifications are
Used Except Where Noted

DRILLING & SAMPLING SYMBOLS

SS : Split-Spoon - 1-3/8" I.D., 2" O.D. except where noted
ST : Shelby Tube - 2" O.D. except where noted
PA : Power Auger Sample
DB : Diamond Bit - NX: BX: AX:
CB : Carbide Bit - NX: BX: AX:
OS : Osterberg Sampler - 3" Shelby Tube
HS : Housel Sampler
WS : Wash Sample
FT : Fish Tail
RB : Rock Bit
WO : Wash Out

Standard "N" Penetration: Blows per foot of a 140 pound hammer falling 30 inches on a 2 inch OD split spoon, except where noted.

WATER LEVEL MEASUREMENT SYMBOLS

WL : Water Level
WCI : Wet Cave In
DCI : Dry Cave In
WS : While Sampling
WD : While Drilling
BCR : Before Casing Removal
ACR : After Casing Removal
AB : After Boring

Water levels indicated on the boring logs are the levels measured in the boring at the times indicated. In previous soils, the indicated elevations are considered reliable ground water levels. In impervious soils, the accurate determination of ground water elevations is not possible in even several days observation, and additional evidence on ground water elevations must be sought.

9 3 2 5 9 7 1 0 4 3 1

SSSES-FSAR

CLASSIFICATION

COHESIVE SOILS

If clay content is sufficient so that clay dominates soil properties, then clay becomes the principles noun with the other major soil constituent as modifier; i.e., silty clay. Other minor soil constituents may be added according to classification breakdown for cohesionless soils; i.e., silty clay, trace to some sand, trace gravel.

Soft	:	0.00 - 0.59 tons/ft ²
Stiff	:	0.60 - 0.99 tons/ft ²
Tough	:	1.00 - 1.99 tons/ft ²
Very tough	:	2.00 - 3.99 tons/ft ²
Hard	:	4.00 tons/ft ²

COHESIONLESS SOILS

"Trace"	:	1% to 10%	
"Trace to some"	:	10% to 20%	
"Some"	:	20% to 35%	
"And"	:	35% to 50%	
Loose	:	0 to 9 Blows	
Medium Dense	:	10 to 29 Blows	or
Dense	:	30 to 59 Blows	equivalent
Very Dense	:	60 Blows	